

Environmental Sciences Division

STATUS REPORT ON THE GEOLOGY OF THE OAK RIDGE RESERVATION

Robert D. Hatcher, Jr.¹
Coordinator of Report

Peter J. Lemiszki¹
RaNaye B. Dreier
Richard H. Ketelle²
Richard R. Lee²
David A. Lietzke³
William M. McMaster⁴
James L. Foreman¹
Suk Young Lee

Environmental Sciences Division
Publication No. 3860

¹Department of Geological Sciences, The University of Tennessee, Knoxville 37996-1410

²Energy Division, ORNL

³Route 3, Rutledge, Tennessee 37861

⁴1400 W. Raccoon Valley Road, Heiskell, Tennessee 37754

Date Published—October 1992

Prepared for the
Office of Environmental Restoration and Waste Management
(Budget Activity EW 20 10 30 1)

Prepared by the
OAK RIDGE NATIONAL LABORATORY
Oak Ridge, Tennessee 37831-6285
managed by
MARTIN MARIETTA ENERGY SYSTEMS, INC.
for the
U.S. DEPARTMENT OF ENERGY
under contract DE-AC05-84OR21400

MASTER

TABLE OF CONTENTS

| | |
|--|----|
| 1 INTRODUCTION | 1 |
| 1.1 History of Geologic and Geohydrologic Work at ORNL | 5 |
| 1.2 Regional Geologic Setting | 6 |
| 1.2.1 Physiography | 6 |
| 1.2.2 Geology | 7 |
| 2. AVAILABLE DATA | 9 |
| 2.1 Surface Geologic Data | 9 |
| 2.2 Core | 9 |
| 2.3 Geophysical Logs Database | 10 |
| 2.4 Seismic Reflection and Refraction Studies | 10 |
| 3. STRATIGRAPHY | 11 |
| 3.1 Introduction | 11 |
| 3.2 Rome Formation | 14 |
| 3.2.1 Introduction | 14 |
| 3.2.2 Previous Studies | 14 |
| 3.2.3 Lithologic Description | 15 |
| 3.2.4 Rome Formation Soils | 15 |
| 3.2.5 Rome Residuum | 16 |
| 3.3 Conasauga Group | 18 |
| 3.3.1 Introduction | 18 |
| 3.3.2 General Description | 18 |
| 3.3.3 Pumpkin Valley Shale | 19 |
| 3.3.4 Pumpkin Valley Shale Soil | 23 |
| 3.3.5 Pumpkin Valley Residuum | 24 |
| 3.3.6 Friendship Formation (Formerly Rutledge Limestone) | 25 |
| 3.3.7 Friendship Formation Soils | 27 |
| 3.3.8 Rogersville Shale | 27 |
| 3.3.9 Rogersville Shale Soils | 28 |
| 3.3.10 Rogersville Residuum | 28 |
| 3.3.11 Dismal Gap Formation (Formerly Maryville Limestone) | 29 |
| 3.3.12 Dismal Gap Formation Soils | 31 |
| 3.3.13 Dismal Gap Residuum | 32 |
| 3.3.14 Nolichucky Shale | 34 |
| 3.3.15 Nolichucky Shale Soils | 38 |
| 3.3.16 Nolichucky Residuum | 38 |
| 3.3.17 Maynardville Limestone | 39 |
| 3.3.18 Maynardville Limestone Soils | 40 |

| | | |
|---------|--|----|
| 3.3.19 | Maynardville Residuum | 41 |
| 3.4 | Knox Group | 41 |
| 3.4.1 | Introduction | 41 |
| 3.4.2 | General Description of Soils and Landforms | 42 |
| 3.4.3 | Copper Ridge Dolomite | 45 |
| 3.4.4 | Copper Ridge Soils | 46 |
| 3.4.5 | Chepultepec Dolomite | 47 |
| 3.4.6 | Chelpultepec Soils | 47 |
| 3.4.7 | Longview Dolomite | 48 |
| 3.4.8 | Longview Soils | 48 |
| 3.4.9 | Kingsport Formation | 49 |
| 3.4.10 | Kingsport Soils | 49 |
| 3.4.11 | Mascot Dolomite | 49 |
| 3.4.12 | Mascot Soils | 50 |
| 3.5 | Chickamauga Group | 51 |
| 3.5.1 | Introduction | 51 |
| 3.5.2 | Bethel Valley Section | 51 |
| 3.5.2.1 | Previous studies | 51 |
| 3.5.2.2 | Bethel Valley lithologic descriptions | 54 |
| | Blackford Formation and Eidson Member of the | |
| | Lincolnshire Formation | 54 |
| | Fleanor Member of the Lincolnshire Formation | 56 |
| | Rockdell Formation | 56 |
| | Benbolt Formation | 56 |
| | Bowen Formation | 57 |
| | Witten Formation | 57 |
| | Moccasin Formation | 57 |
| 3.5.3 | East Fork (Oak Ridge) Valley Section | 57 |
| 3.5.3.1 | Previous studies | 57 |
| 3.5.3.2 | East Fork (Oak Ridge) lithologic descriptions | 59 |
| | Stones River Group | 59 |
| | Pond Spring Formation | 59 |
| | Murfreesboro/Pierce Limestone | 59 |
| | Ridley Limestone | 60 |
| | Lebanon Limestone | 60 |
| | Carters Limestone | 60 |
| | Nashville Group | 60 |
| | Hermitage Formation | 61 |
| | Cannon Limestone | 61 |
| | Catheys and Leipers Formations | 61 |
| 3.5.4 | Chickamauga Group Soils | 61 |
| 3.5.5 | Chickamauga Residuum | 62 |
| 3.5.6 | Chickamauga Colluvium | 64 |
| 3.6 | Reedsville Shale | 65 |
| 3.7 | Sequatchie Formation | 65 |
| 3.8 | Rockwood Formation | 65 |
| 3.9 | Reedsville Shale, Sequatchie, and Rockwood Formation Soils | 66 |

| | |
|--|-----------|
| 3.10 Residuum | 66 |
| 3.11 Chattanooga Shale | 66 |
| 3.12 Fort Payne Formation | 67 |
| 3.13 Structural-lithic Unit Designations | 68 |
| 4 OAK RIDGE RESERVATION SOIL SURVEY | 69 |
| 4.1 Previous Investigations | 69 |
| 4.2 Surficial Geology and Geomorphology | 70 |
| 4.2.1 Geomorphology | 76 |
| 4.2.1.1 Geomorphic history | 76 |
| Modern geomorphic period | 77 |
| Holocene geomorphic period | 78 |
| Pleistocene geomorphic processes | 78 |
| Early Pleistocene and Late Tertiary | 79 |
| 4.2.2 Soil Genesis from Parent Rock in the Bear Creek Area | 80 |
| 4.3 Soil Classification | 81 |
| 4.3.1 Technical Approach to Soil Mapping | 83 |
| 4.3.2 Soil Legend Development | 84 |
| 4.4 Map Unit Descriptions | 84 |
| 4.4.1 Colluvium | 84 |
| 4.4.1.1 Rome colluvium | 84 |
| 4.4.1.2 Conasauga colluvium | 86 |
| Pumpkin Valley colluvium | 86 |
| Rogersville-Dismal Gap and Nolichucky colluvium | 87 |
| 4.4.1.3 Knox colluvium | 89 |
| 4.4.2 Doline Soils | 92 |
| 4.4.3 Reedsville Shale, Sequatchie Formation and Rockwood Formation | 94 |
| 4.4.3.1 Colluvium | 94 |
| 4.4.3.2 Alluvium | 94 |
| 4.4.4 Ancient Alluvium | 94 |
| 4.4.5 Holocene Alluvium | 98 |
| 4.4.6 Modern Alluvium | 99 |
| 4.4.6.1 Rome and Pumpkin Valley | 99 |
| 4.4.7 Conasauga Alluvium | 99 |
| 4.4.8 Knox Alluvium | 100 |
| 4.4.9 Chickamauga Alluvium | 101 |
| 4.5 Interpretations | 101 |
| 4.5.1 Drainage | 101 |
| 4.5.2 Hydrology | 102 |
| 4.5.3 Surface Water Infiltration and Near Surface Waterflow | 102 |
| 4.5.4 Water Flow Pathways Deeper in the Soil | 104 |
| 4.5.5 Soil Role in Hydrologic Discharge of Perched and Groundwater Tables | 105 |
| 4.5.5.1 Depth to restriction | 105 |
| 4.5.5.2 Disturbed soil erosion potential | 105 |

| | | |
|----------|---|-----|
| 4.5.5.3 | Undisturbed soil erosion potential | 106 |
| 4.5.5.4 | Suitability for pines | 106 |
| 4.5.5.5 | Ratings for hardwoods | 106 |
| 4.5.5.6 | Ratings for paved roads and streets..... | 106 |
| 4.5.5.7 | Ratings for unpaved roads | 106 |
| 4.5.5.8 | Ratings for waste disposal in trenches | 106 |
| 4.5.5.9 | Ratings for waste disposal in Tumuli | 107 |
| 4.5.5.10 | Source of fill materials | 107 |
| 4.5.5.11 | Source of cover materials..... | 107 |
| 4.5.5.12 | Septic tank drain fields | 107 |
| 4.5.5.13 | Suitability for low commercial buildings..... | 107 |
| 5 | STRUCTURE OF THE OAK RIDGE RESERVATION | 109 |
| 5.1 | Introduction..... | 109 |
| 5.2 | Copper Creek Fault | 112 |
| 5.2.1 | Regional Geometry and Displacement | 112 |
| 5.2.2 | Subsurface Fault Geometry..... | 114 |
| 5.2.3 | Fault Zone Characteristics | 118 |
| 5.2.4 | Hanging-Wall Deformation | 118 |
| 5.2.4.1 | Mesoscopic folds | 122 |
| 5.2.4.2 | Mesoscopic faults | 125 |
| 5.2.5 | Footwall Deformation..... | 127 |
| 5.3 | Whiteoak Mountain Fault | 128 |
| 5.3.1 | Regional Geometry and Displacement | 128 |
| 5.3.2 | Subsurface Fault Geometry..... | 129 |
| 5.3.3 | Hanging-Wall Deformation | 130 |
| 5.3.4 | Footwall Deformation..... | 133 |
| 5.4 | East Fork Syncline | 134 |
| 5.5 | Characteristics of the Fracture System in the Oak Ridge Reservation 136 | |
| 5.5.1 | Introduction | 136 |
| 5.5.2 | Previous Work | 138 |
| 5.5.3 | Method of Data Collection | 144 |
| 5.5.4 | Fracture Classification Scheme..... | 144 |
| 5.5.5 | Fracture System Geometry | 145 |
| 5.5.5.1 | Copper Creek thrust sheet..... | 147 |
| 5.5.5.2 | Whiteoak Mountain thrust sheet..... | 150 |
| 5.5.5.3 | Kingston thrust sheet and East Fork syncline | 150 |
| 5.5.6 | Changes in Fracture Orientation as a Function of Lithology.. | 154 |
| 5.5.7 | Fracture Type | 155 |
| 5.5.8 | Fracture Timing | 159 |
| 5.5.8.1 | Prethrusting fracture sets | 160 |
| 5.5.8.2 | Fold- and fault-related fractures | 161 |
| 5.5.8.3 | Post-thrusting fracture sets | 165 |
| 5.5.9 | Fracture Spacing Analysis | 168 |
| 5.5.9.1 | Field observations | 169 |
| 5.5.9.2 | Fracture spacing frequency distribution | 169 |

| | |
|---|-----|
| 5.5.9.3 Fracture spacing and bed thickness correlation analysis | 171 |
| 5.5.9.4 Fracture spacing results | 177 |
| 6 ISOTOPIC CHARACTERISTICS OF ROCK UNITS AND VEINS FROM THE OAK RIDGE RESERVATION: EVIDENCE FOR WATER-ROCK INTERACTION IN MIXED CARBONATE-SILICLASTIC ROCKS | 179 |
| 6.1 Introduction | 179 |
| 6.2 Isotopic Composition of Carbonates in Limestones and Shales | 182 |
| 6.2.1 Whole-Rock Limestone Analyses | 182 |
| 6.2.2 Individual Constituents of Oolitic Limestones | 183 |
| 6.2.3 Composition of Vein Calcites | 183 |
| 6.2.4 Diagenetic Carbonates in Shale Interbeds | 184 |
| 6.2.5 Isotopic Composition of Silicate Minerals | 184 |
| 6.3 Integration with Other Data | 184 |
| 6.3.1 Fluid Inclusion Data from Veins | 185 |
| 6.3.2 Time-Temperature Burial History Models | 185 |
| 6.4 Implications for Studies of Water-Rock Interaction | 186 |
| 7 OVERVIEW OF A NEW CONCEPTUAL MODEL OF THE HYDROLOGIC FRAMEWORK OF THE ORR | 189 |
| 7.1 Background climatological data for the ORR | 189 |
| 7.2 Stormflow Zone | 190 |
| 7.3 Vadose Zone | 191 |
| 7.4 Groundwater Zone | 191 |
| 7.5 Aquiclude | 194 |
| 8 CONCLUSIONS | 195 |
| 9 NEEDS AND RECOMMENDATIONS FOR CONTINUED INVESTIGATIONS | 197 |
| 9.1 Introduction | 197 |
| 9.2 Recommended Future Activities | 198 |
| REFERENCES CITED | 203 |
| APPENDIX 1 FIELD TRIP STOPS | 215 |
| APPENDIX 2 SOIL SERIES | 225 |
| APPENDIX 3 OAK RIDGE RESERVATION SOIL CODING LEGEND | 237 |

LIST OF FIGURES

| Figure | | Page |
|--------|--|------|
| 1-1 | Simplified tectonic map of the southern Appalachians showing the location of the Oak Ridge Reservation. | 2 |
| 1-2a | Simplified geological map of the Oak Ridge Reservation. | 3 |
| 1-2b | Geologic cross section based on seismic line on Tennessee 95. | 4 |
| 3-1 | Stratigraphic section in Bear Creek Valley, Chestnut Ridge, Bethel Valley, Haw Ridge, Melton Valley, and Copper Ridge. | 12 |
| 3-2 | Stratigraphic section in East Fork (Oak Ridge) Valley, East Fork Ridge and Pilot Knob, Pine Ridge, Bear Creek Valley, and Chestnut Ridge. | 13 |
| 3-3 | Regional facies relationships in the Conasauga Group in eastern Tennessee. | 21 |
| 3-4 | Geophysical logs - Pumpkin Valley Shale. | 22 |
| 3-5 | Geophysical logs - Rogersville Shale and Friendship formation (formerly Rutledge Limestone). | 26 |
| 3-6 | Geophysical logs - Dismal Gap formation (formerly Maryville Limestone). | 30 |
| 3-7 | Geophysical logs - Nolichucky Shale. | 32 |
| 3-8 | Geophysical logs - Maynardville Limestone. | 35 |
| 3-9 | Mascot Dolomite, Whiteoak Mountain thrust sheet, and Kerr Hollow quarry. | 43 |
| 3-10 | Copper Ridge Dolomite, Whiteoak Mountain thrust sheet, and sediment disposal basin near Y-12. | 44 |
| 3-11 | Map of part of the Ordovician carbonate sequence outcrop belt in the Whiteoak Mountain and Kingston thrust sheets showing areas of previous work. | 52 |
| 3-12 | Bethel Valley Chickamauga Group formation names, unit designations, and composite geophysical log. | 53 |

| | | |
|------|--|-----|
| 3-13 | Regional stratigraphic correlation of the Chickamauga Group in the Whiteoak Mountain thrust sheet. | 55 |
| 3-14 | Comparison of the dominant stratigraphic characteristics and stratigraphic nomenclature used between the Bethel Valley and East Fork Valley Chickamauga stratigraphy. | 58 |
| 5-1 | Location of the Oak Ridge Reservation in the southern Appalachian Valley and Ridge province of eastern Tennessee (from Hatcher 1987). | 110 |
| 5-2 | Location map for ridge and valley names on the Oak Ridge Reservation. | 111 |
| 5-3 | Equal-area lower hemisphere stereographic projections of poles to bedding from the hanging wall (left) and footwall (right) of the Copper Creek fault. | 113 |
| 5-4 | Stratigraphic separation diagram for the Copper Creek fault in Tennessee. | 114 |
| 5-5 | Balanced (and restored) cross section from the undeformed foreland of the Cumberland Plateau through the Oak Ridge area to the Beaver Valley fault. | 115 |
| 5-6 | Sketch of the map-view geometry of (A) the Copper Creek and (B) Whiteoak Mountain faults used to estimate displacement by the bow and arrow rule. | 116 |
| 5-7 | Line drawing of the seismic reflection profile that crosses the reservation along Tennessee 95. | 117 |
| 5-8 | Results of the three-point method to estimate the attitude of the Copper Creek fault at depth in Melton Valley. | 119 |
| 5-9 | Geologic map of the area surrounding the Copper Creek fault in the Bethel Valley quadrangle showing the trend and plunge of mesoscopic fold axes and the projection of imbricate fault branch lines. | 121 |
| 5-10 | Schematic longitudinal section parallel to the Copper Creek fault depicting the folding of the fault and bedding in the hanging wall by the accretion of imbricates in a duplex against a perturbation along the footwall flat. | 122 |

| | | |
|------|---|-----|
| 5-11 | (a) Near-surface cross section of some of the structures encountered in the Pits and Trenches area that are typical of those observed in the Conasauga Group in Melton Valley from Dreier and Toran (1989). | 123 |
| 5-12 | Mesoscopic fold styles in the hanging wall of the Copper Creek fault: (a) Nolichucky Shale in Melton Valley; (b) Dismal Gap formation in Melton Valley; (c-f) Rome Formation on Haw Ridge. | 124 |
| 5-13 | (a) Sketch of major structures, bedding, and lithologic units. | 126 |
| 5-14 | Stratigraphic separation diagram for the Whiteoak Mountain fault in Tennessee. | 128 |
| 5-15 | Equal-area, lower-hemisphere, stereographic projection of mesoscopic fold axes and poles to fold axial plains from the hanging wall and footwall of the Whiteoak Mountain fault. | 131 |
| 5-16 | Geologic map of the structures associated with the hanging wall and footwall of the Whiteoak Mountain fault in the Oak Ridge area. | 132 |
| 5-17 | Equal-area, lower-hemisphere, stereographic projection of all poles to bedding and related Kamb contour for the East Fork syncline | 135 |
| 5-18 | Map of previous fracture study sites on the reservation. | 139 |
| 5-19 | Equal-area contour plots of poles to fracture planes in the Pumpkin Valley Shale from (a) the Whiteoak Mountain thrust sheet and (b) the Copper Creek thrust sheet. | 140 |
| 5-20 | Fracture length vs number of fractures per meter in shale and siltstone beds of the Conasauga Group (from Sledz and Huff 1981). | 141 |
| 5-21 | Equal-area scatter plots and Kamb contour plots of poles to fracture planes from three different studies in the Conasauga Group in Melton Valley. | 143 |
| 5-22 | Definition of the orthogonal fabric axes used to describe the geometry of the fracture sets. | 144 |
| 5-23 | Brittle failure leading to the development of different fracture displacement modes that may be predicted by the relationship between the Coulomb-Mohr failure envelope and the stress circle (e. g., Price 1966). | 146 |

| | | |
|------|---|-----|
| 5-24 | Equal-area scatter and Kamb contour plot of poles to systematic fractures and equal-area rose plot of systematic fracture strikes for the ORR. | 148 |
| 5-25 | Equal-area scatter and Kamb contour plots of poles to fracture planes for the Rome Formation, Conasauga Group, and Knox Group in the Copper Creek thrust sheet. | 149 |
| 5-26 | Equal-area scatter and Kamb contour plots of poles to fracture planes for the Rome Formation, Conasauga Group, Knox Group, and Chickamauga Group in the Whiteoak Mountain thrust sheet. | 151 |
| 5-27 | Equal-area scatter and Kamb contour plots of poles to fracture planes for the Chickamauga Group, Reedsville Shale, Sequatchie Formation, Rockwood Formation, Chattanooga Shale, and Fort Payne Formation, which form the East Fork syncline. | 152 |
| 5-28 | Summary rose plots of fracture strikes recorded from each stratigraphic unit in the ORR. | 153 |
| 5-29 | The most common fracture sets in the study area: ac, bc, hk0 with an acute angle around a, and hk0 with an acute angle around b. | 154 |
| 5-30 | Rose plots of systematic fracture strikes from limestones and shales/siltstones of the Conasauga Group in the Copper Creek thrust sheet. | 155 |
| 5-31 | Changes in fracture orientation solely as a function of lithology, which can be explained by using a Mohr circle construction. | 156 |
| 5-32 | Fracture architectural styles observed on exposed bedding surfaces. | 157 |
| 5-33 | (a) Sketch of fractographic features indicative of an extension (Mode I) fracture (from Kulander and others 1979). | 158 |
| 5-34 | Sketch from a photograph of a sample of bedded chert from the lower Chickamauga Group in the Whiteoak Mountain thrust sheet. | 159 |
| 5-35 | Sketch of calcite veins from a limestone bed top in the Witten Formation in the Whiteoak Mountain thrust sheet. | 159 |
| 5-36 | Summary of results from previous fracture studies in the region. | 162 |

| | | |
|------|--|-----|
| 5-37 | Foreland fold–thrust belt structures, which can be used to infer the orientation of the regional stress field during their development. | 164 |
| 5-38 | Fracture sets that develop in folded layers. | 165 |
| 5-39 | (a) Structures formed during Mesozoic rifting, which can be used to infer the minimum principal stress orientation. | 166 |
| 5-40 | (a) Equal-area plot of poles to fracture planes that match those that should be produced from the inferred orientation of the Mesozoic and present-day stress fields. | 167 |
| 5-41 | Orientation of the present day maximum compressive stress in the southeastern United States based on overcoring, focal mechanisms, hydraulic fracturing, and borehole elongation tests, which is approximately N50°–N60E. | 168 |
| 5-42 | Possible fracture spacing frequency distributions (from Priest and Hudson 1976). | 170 |
| 5-43 | Fracture spacing frequency distribution. | 171 |
| 5-44 | (a) Fracture spacing vs bed thickness for all of the data. | 172 |
| 5-45 | Fracture spacing vs bed thickness for each lithology. | 174 |
| 5-46 | Fracture spacing vs bed thickness for each major stratigraphic unit. | 175 |
| 5-47 | Fracture spacing vs bed thickness for each lithology within each stratigraphic unit. | 176 |
| 6-1 | Decompacted burial curve for the Conasauga Group and younger strata in the Whiteoak Mountain thrust sheet. | 186 |
| 6-2 | Water–rock isotopic equilibrium diagram used to calculate fluid oxygen isotopic composition in equilibrium with host rocks and veins from the Nolichucky Shale and Pumpkin Valley Shale. | 188 |
| 7-1 | Generalized map of the ORR showing surface distribution of the Knox aquifer and the ORR aquitards. | 190 |
| 7-2 | Schematic vertical relationships of flow zones of the ORR, estimated thicknesses, water flow, and water types. | 192 |
| 7-3 | Schematic profile of the water table interval. | 193 |

| | | |
|------|--|-----|
| 7-4 | Common fracture orientation in the ORR. | 193 |
| A1-1 | Locations of field trip stops. | 216 |
| A1-2 | Geologic map in the vicinity of Dismal Gap, Powell quadrangle, Tennessee, modified from Beets (1985). | 218 |
| A1-3 | Lower hemisphere equal-area plots of structural data for the Rome Formation (a) and Conasauga Group (b) at Dismal Gap. | 219 |
| A1-4 | Sketch of structural features exposed in the hanging wall of the Copper Creek thrust at Haw Ridge at Stop 1a. | 220 |
| A1-5 | Lower hemisphere equal-area plot of structural elements at Stop 1a. | 221 |
| A1-6 | Geologic map of the area around Stop 2 at Bull Run Steam Plant. | 222 |

LIST OF PLATES

Plate

| | | |
|---|--|-------------------|
| 1 | Provisional geologic map of the Oak Ridge Area. | Inside back cover |
|---|--|-------------------|

LIST OF TABLES

| Table | Page |
|--|------|
| 3-1 Stratigraphic Thickness, Conasauga Group | 20 |
| 4-1 Categories of Soil Taxonomy in the Oak Ridge Reservation Soil Survey | 85 |
| 5-1 Tectonic events since the early Paleozoic have affected eastern North America and controlled the orientation and magnitude of the regional stress field | 137 |
| 6-1 Summary of oxygen and carbon isotopic compositions from limestones and calcite veins in Cambrian strata from the Oak Ridge Reservation (data from Haase et al. 1988) | 180 |
| 6-2 Carbon and oxygen isotopic analyses of oöids and interparticle matrix from Upper Cambrian Nolichucky Shale oölitic lime- stone, Bear Creek Valley core holes, Whiteoak Mountain thrust sheet, Oak Ridge Reservation (from Foreman 1991) | 180 |
| 6-3 Carbon and oxygen isotopic composition of Nolichucky Shale calcite veins from Bear Creek Valley core holes in the Whiteoak Mountain thrust sheet, Oak Ridge Reservation (from Foreman 1991) | 180 |
| 6-4 Calcite and dolomite isotopic compositions in Nolichucky Shale lithologies, determined from timed stepwise extractions of bulk shale samples | 181 |
| 6-5 Summary of isotopic compositions of silicate minerals from the Pumpkin Valley Shale and Rome Formation in the Oak Ridge Reservation (data from Haase et al. 1988) | 182 |

ACKNOWLEDGMENTS

An earlier draft of this report was considerably improved by reviews by R. C. Milici [Virginia Division of Mineral Resources (presently U.S. Geological Survey)], G. K. Moore (Oak Ridge National Laboratory), and R. E. Fulweiler (Tennessee Division of Geology). S. H. Stow and S. I. Auerbach provided valuable review of the section on history. The authors of the report remain culpable for all errors of fact or interpretation. We are also grateful for the time R. C. Milici spent guiding us through the Middle Ordovician stratigraphic section along nearby Watts Bar Reservoir. This section served as the basis for subdivision of the Chickamauga Group in East Fork (Oak Ridge) Valley. D. A. Lietzke acknowledges numerous informal field trips with Dick Ketelle and Richard Lee, without which it would not have been possible to establish relationships between surficial soils and the underlying geologic units.

Editorial and secretarial assistance by M. A. Drake and N. L. Meadows, and graphics and layout assistance by D. G. McClanahan (all University of Tennessee Science Alliance, Department of Geological Sciences) are very much appreciated.

EXECUTIVE SUMMARY

This report provides an introduction to the present state of knowledge of the geology of the Oak Ridge Reservation (ORR) and a cursory introduction to the hydrogeology. An important element of this work is the construction of a modern detailed geologic map of the ORR (Plate 1), which remains in progress. An understanding of the geologic framework of the ORR is essential to many current and proposed activities related to land-use planning, waste management, environmental restoration, and waste remediation. Therefore, this report is also intended to convey the present state of knowledge of the geologic and geohydrologic framework of the ORR and vicinity and to present some of the available data that provide the basic framework for additional geologic mapping, subsurface geologic, and geohydrologic studies. In addition, some recently completed, detailed work on soils and other surficial materials is included because of the close relationships to bedrock geology and the need to recognize the weathered products of bedrock units. Weathering processes also have some influence on hydrologic systems and processes at depth.

Major long-term goals of geologic investigations in the ORR are to determine what interrelationships exist between fracture systems in individual rock or tectonic units and the fluid flow regimes that are present, to understand how regional geology can be used to help predict groundwater movement, and to formulate a structural-hydrologic model that for the first time would enable prediction of the movement of groundwater and other subsurface fluids in the ORR. Development of a state-of-the-art geologic and geophysical framework for the ORR is therefore essential for formulating an integrated structural-hydrologic model. The groundwater systems of this area are similar to those of large areas of the humid eastern United States that are underlain by consolidated sedimentary rocks of low hydraulic conductivity. Partly because of their low water-yielding capabilities, but more because of their intractability to established mathematical representation, such systems have not been as extensively studied as have those that are more productive and more tractable. Now, with the emphasis on environmental protection and restoration, and in light of the enormous costs attached to corrective actions, it is essential that these systems be better understood and quantified so that conceptual models can be verified and suitable numerical models can be developed and applied. The Oak Ridge Hydrologic and Geologic Study (ORRHAGS) Project was begun in 1987 with the intent of coordinating these efforts and involves geoscientists from both the Environmental Sciences and Energy divisions at Oak Ridge National Laboratory (ORNL).

The bedrock geology exposed in the ORR is composed entirely of sedimentary rocks that range in age from Early Cambrian to early Mississippian. This stratigraphy formed as part of the early Paleozoic drift (ocean-opening) succession. The carbonate bank was developed, uplift and erosion of the carbonate bank occurred in early Middle Ordovician time forming the regional post-Knox unconformity, and the carbonate bank was reestablished during the Middle Ordovician only to be destroyed later in the Ordovician by development of a clastic wedge in the Late Ordovician and Silurian. This was followed by erosion and formation of another unconformity, then by the deposition of the Upper Devonian–Early Carboniferous clastic wedge.

Nine major stratigraphic units have been recognized previously in the ORR: Rome

Formation, Conasauga Group, Knox Group, Chickamauga Group, Reedsville Shale, Sequatchie Formation, Rockwood Formation, Chattanooga Shale, and Fort Payne Formation. Detailed studies of surface geology and core over the past decade have permitted, for the first time, subdivision of the Conasauga, Knox, and Chickamauga Groups. The Conasauga, and to a much lesser extent the Knox and Chickamauga Groups, have served as the principal units for disposal of radionuclides and other waste materials in the ORR, so this more detailed knowledge is very important in environmental restoration and related activities.

The ORR is located in the western part of the Valley and Ridge—at the narrowest part of the Appalachian foreland fold–thrust belt. Here the Valley and Ridge is dominated by several west-directed thrust faults that formed when the huge Blue Ridge sheet to the east pushed the Valley and Ridge sedimentary succession in front of it. The ORR contains a variety of geologic structures. The map-scale structure of the ORR is dominated by a uniform southeast dip of sedimentary layering interrupted only by the two large thrust faults, the Copper Creek and Whiteoak Mountain faults, and the East Fork Ridge (and Pilot Knob) syncline in the footwall of the Whiteoak Mountain thrust (Plate 1). The Whiteoak Mountain fault also has a very large displacement, compared with the Copper Creek fault, indicated by the character of facies changes occurring in the Middle Ordovician rocks northwest and southeast of it. Additional evidence for the greater displacement on the Whiteoak Mountain fault is derived from the preservation of rocks as young as Mississippian in footwall synclines, but nowhere in the vicinity of the ORR are rocks younger than the Middle Ordovician preserved in the footwall of the Copper Creek fault.

Outcrop-scale structures consist of inclined, faulted, and folded bedding, and joints. Joints (systematic fractures) are the most common structures present here, and several sets of joints with different orientations have been recognized. The dominant joint sets are oriented northeast and northwest, with lesser north–south and east–west sets. These structures are probably the most important in the ORR because they, along with bedding and local karst, form the conduit system that controls groundwater movement. Documenting joint attitude, timing, and evolution is one means of inferring the stress orientation history of a thrust sheet, but joint studies from the Appalachian Cumberland Plateau, Valley and Ridge, Blue Ridge, and Piedmont indicate that some joints developed in response to erosional unloading and the recent stress field, while others formed during Triassic–Jurassic extension related to the opening of the present Atlantic. Therefore, it is unwise to assume that all joints observed are a result of Paleozoic folding and thrust-sheet emplacement.

A number of criteria are being considered to aid in deciphering the history of joint formation within the ORR. Besides a more accurate portrayal of the stress history related to thrust-sheet emplacement by using only tectonic joints, further application of such an analysis involves an understanding of the control that joints have on groundwater flow paths in sedimentary rock and of how regional permeability is controlled by different joint sets.

The stable isotopic composition of minerals in sedimentary rocks can provide important insights into depositional and diagenetic processes affecting these rocks. Of interest to researchers studying the geology and hydrogeology of the ORR is the opportunity for stable isotopic studies of sedimentary rocks to provide basic information for identifying groundwater flow pathways, recording water–rock interaction, and under-

standing controls on groundwater chemistry. In deeper aquifers in particular, the chemistry of groundwater is strongly controlled by the composition of surrounding rocks as a result of longer groundwater residence times and increased opportunity for groundwater and rock to reach chemical and isotopic equilibrium. Characterizing the isotopic compositions of rocks and fracture-filling minerals (where significant groundwater flow may occur) and understanding controls on their compositions are crucial for future studies of groundwater flow and chemistry.

The relationship between the oxygen composition of interbedded limestones and vein calcites in the Nolichucky Shale reflects varying contributions of oxygen from two major sources: (1) formation water in near-isotopic equilibrium with interbedded silicate units and (2) formation water close to equilibrium with interbedded limestone. Similarities in the carbon isotopic composition of the veins and limestone are expected if the dominant carbon reservoir is the interbedded limestone. In the case of the Nolichucky, an intraformational source of oxygen and carbon could provide the necessary fluids to form calcite veins. From the isotopic data alone, large-scale migration of fluids into the Nolichucky Shale from other sources is not required to explain the occurrence and compositions of Nolichucky calcite veins, although large-scale fluid migration cannot be ruled out from the isotopic data alone.

In recent years, as a result of expanding environmental restoration activities, interest in hydrology of the ORR has escalated rapidly because groundwater is the primary medium for contaminant transport. Groundwater quality, and to a lesser extent the water-bearing properties of the geologic units in the vicinity of waste areas on the ORR, is now being studied intensively. Several recent contributions have been made for ORNL to develop conceptual models of groundwater occurrence and flow in systems of the Oak Ridge area through extensive acquisition, compilation, analysis, and interpretation of aquifer data, such as hydraulic conductivity, obtained mostly from the Chickamauga and the Conasauga Groups in the ORR. Intensive studies of shallow groundwater flow and modeling through aquifer tests and quantitative dye-tracing methods have documented geologic controls of flow.

The mantle of unconsolidated residual materials, or regolith, derived by in situ weathering of bedrock, is composed mostly of silt and clay. Water occurs in and moves through the regolith in pore spaces between particles or in voids created by the structure of the materials. The stormflow zone occurs at the top of the regolith; the water table is present in most places near the base. Wastes are buried in regolith in the ORR.

The carbonate rocks, deposited mostly by chemical precipitation, were formed without large interconnected pore spaces. Thus water in bedrock is present in secondary fractures or, in the carbonate rocks, in cavities formed along fractures. In the shales and sandstones, the abundance, the degree of openness, and the interconnectedness of fractures are spatially variable.

Near-surface water in the saturated zone is under unconfined or water table conditions. A transition to confined conditions occurs at deeper levels, particularly in the Chickamauga and Conasauga groups.

The water table typically is near the interface between regolith and bedrock. Depth to the water table is less in topographically lower locations—near or at ground surface along perennial stream channels or swampy areas—and greater in higher locations. Range in annual variation of water levels is topographically and geologically related—less in lower elevations, greater in higher. In a normal year, the water table is lowest

during September–October and highest during February–March. Perched water tables are common, especially in the Conasauga Group.

Groundwater systems here are local, as opposed to regional, with flow path lengths from recharge point to discharge point. All groundwater discharges in the Oak Ridge area are to the Clinch River or its tributaries.

Three general zones of groundwater flow exist in the ORR: the stormflow zone (or root zone), from ground surface to a depth of 1 to 2 m; the shallow zone, which includes the vadose, or unsaturated, zone, and the shallow saturated zone, extending generally to a depth of 20 to 60 m; and the deeper zone, to the base of fresh water at depths of about 150 m (may be deeper in Bear Creek Valley). Flow in the stormflow zone is transient, generated by rainfall events that lead to saturation. Only about 3 to 7 cm of water annually percolates through the vadose zone to enter the saturated flow system, and, of that, only about 5 percent enters and flows through the deeper zone, except in the Knox and Maynardville. Below the water table, water in the shallow zone moves through regions of interconnected fractures, or, in the case of carbonate beds, cavities, which are more or less enlarged by the circulating water, and water is present only in the matrix.

The Knox Group and the underlying Maynardville Limestone function as one hydrologic unit, the Knox aquifer. Most of the perennial springs and all of the larger springs in the area flow from the Knox aquifer and sustain almost all the natural base flow of perennial streams in the area. A significant difference between the Knox aquifer and other geologic units of the area is that areally extensive, locally large cavity systems occur to depths of nearly 100 m. While water-table divides correspond fairly closely to surface topography in other geologic units, those in the Knox aquifer may not.

1 INTRODUCTION

Robert D. Hatcher, Jr., and William M. McMaster

This report provides an introduction to the present state of knowledge of the geology of the Oak Ridge Reservation (ORR) (Plate 1; Figs. 1-1 and 1-2) and a cursory introduction to the hydrogeology. A detailed report on hydrogeology is being produced in parallel to this one (Solomon et al. 1992). An important element of this work is the construction of a modern detailed geologic map of the ORR (Plate 1) containing subdivisions of all mappable rock units and displaying mesoscopic structural data. Understanding the geologic framework of the ORR is essential to many current and proposed activities related to land-use planning, waste management, environmental restoration, and waste remediation. This interim report is the result of cooperation between geologists in two Oak Ridge National Laboratory (ORNL) divisions, Environmental Sciences and Energy, and is a major part of one doctoral dissertation in the Department of Geological Sciences at The University of Tennessee—Knoxville (Lemiszi 1992).

Major long-term goals of geologic investigations in the ORR are to determine what interrelationships exist between fracture systems in individual rock or tectonic units and the fluid flow regimes, to understand how regional and local geology can be used to help predict groundwater movement, and to formulate a structural-hydrologic model that for the first time would enable prediction of the movement of groundwater and other subsurface fluids in the ORR. Understanding the stratigraphic and structural framework and how it controls fluid flow at depth should be the first step in develop-

ing a model for groundwater movement. Development of a state-of-the-art geologic and geophysical framework for the ORR is therefore essential for formulating an integrated structural-hydrologic model.

This report is also intended to convey the present state of knowledge of the geologic and geohydrologic framework of the ORR and vicinity and to present some of the data that establish the need for additional geologic mapping and geohydrologic studies. An additional intended use should be for guided field trips or for self-guided tours by geoscientists (App. 1). This guidebook provides the following: (1) the geologic setting of the ORR in the context of the Valley and Ridge province, (2) general descriptions of the major stratigraphic units mapped on the surface or recognized in drill holes, (3) a general description of geologic structure in the Oak Ridge area, (4) a discussion of the relationship between geology and geohydrology, and (5) descriptions of localities where each major stratigraphic unit may be observed in or near the ORR. Appendices contain field trip stop descriptions and data on soils.

Several geologic maps have been published of the entire ORR (Fig. 1-2a) and surrounding eastern Tennessee (e.g., Rodgers 1953, McMaster 1962, Hardeman 1966), but none contain the detail needed to provide the kinds of data required for addressing the interrelationships between lithology, structure, and groundwater movement in an area as complex as the ORR. Rodgers (1953) described the geology of eastern Tennessee and outlined both the dominant structural style and the regional stratigraphic relationships.

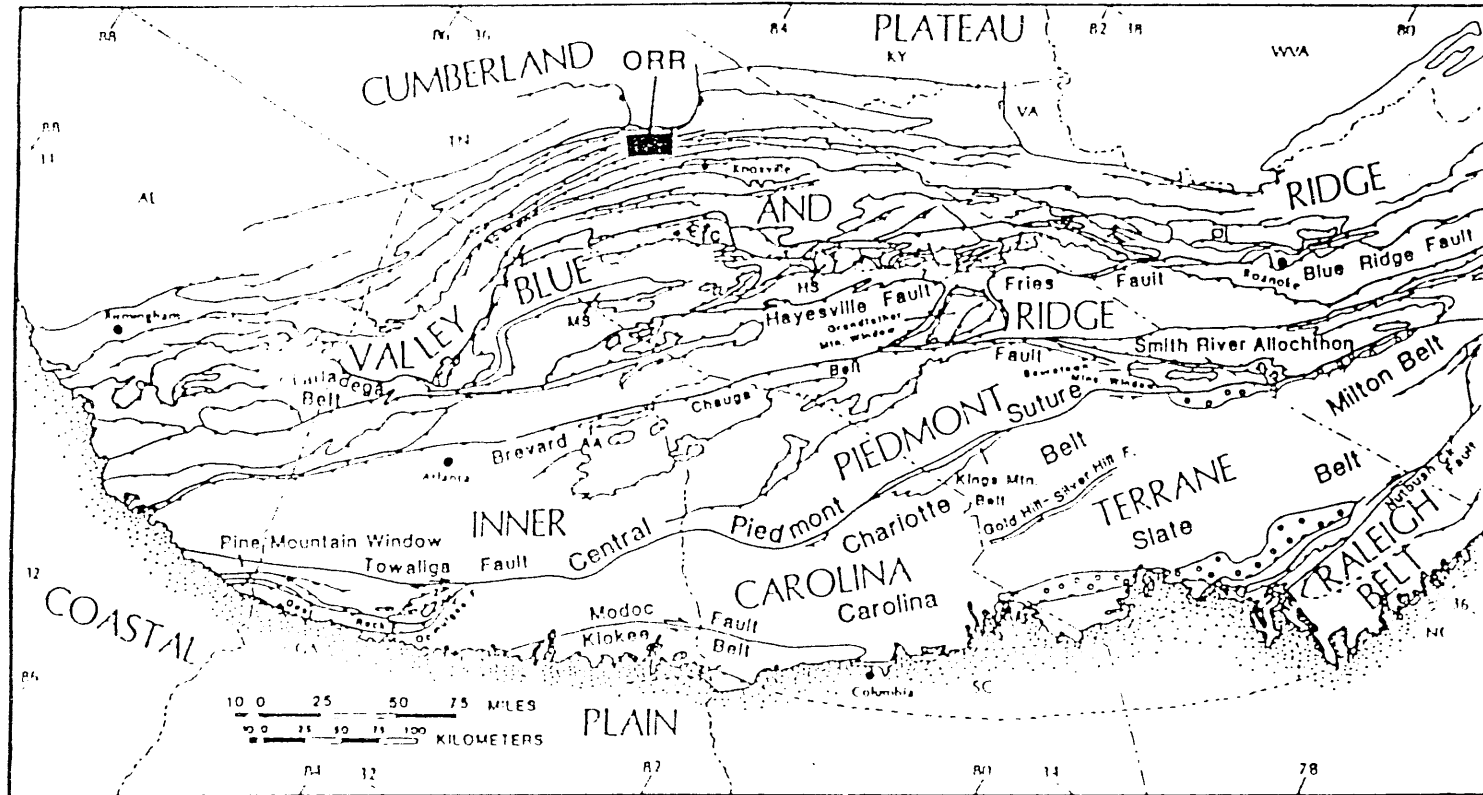


Fig. 1-1. Simplified tectonic map of the southern Appalachians showing the location of the Oak Ridge Reservation. MS - Murphy syncline. TC - Tuckaleechee Cove window. HS - Hot Springs window. AA - Alto allochthon. (After Hatcher 1987.)

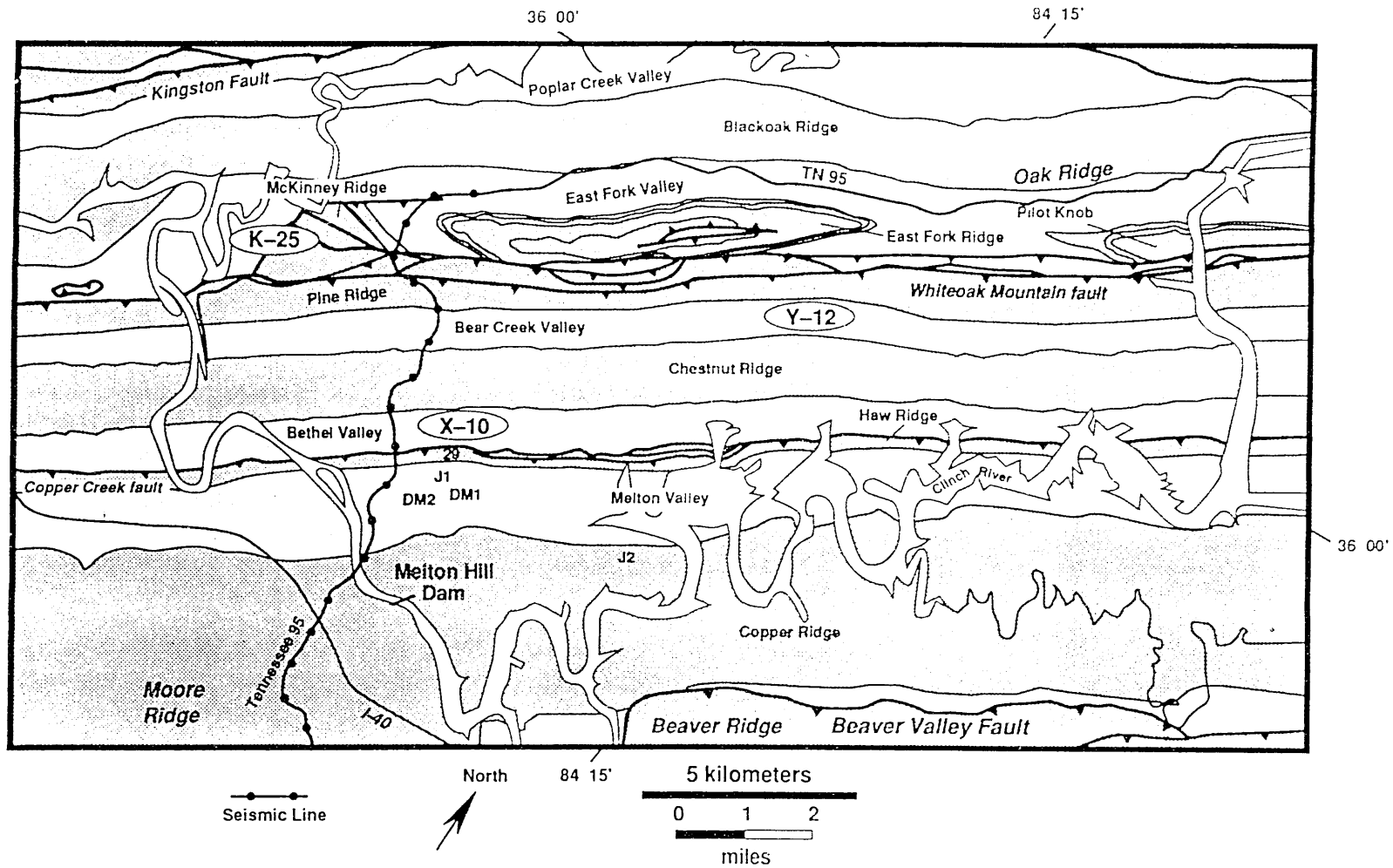


Fig. 1-2. (a) Simplified geologic map of the Oak Ridge Reservation. Dots along Tennessee 95 indicate the location of a seismic reflection profile that serves as the basis for the cross section in Fig. 1-2b. MHD - Melton Hill dam. J1, J2, DM1, DM2 are the locations of drill holes.

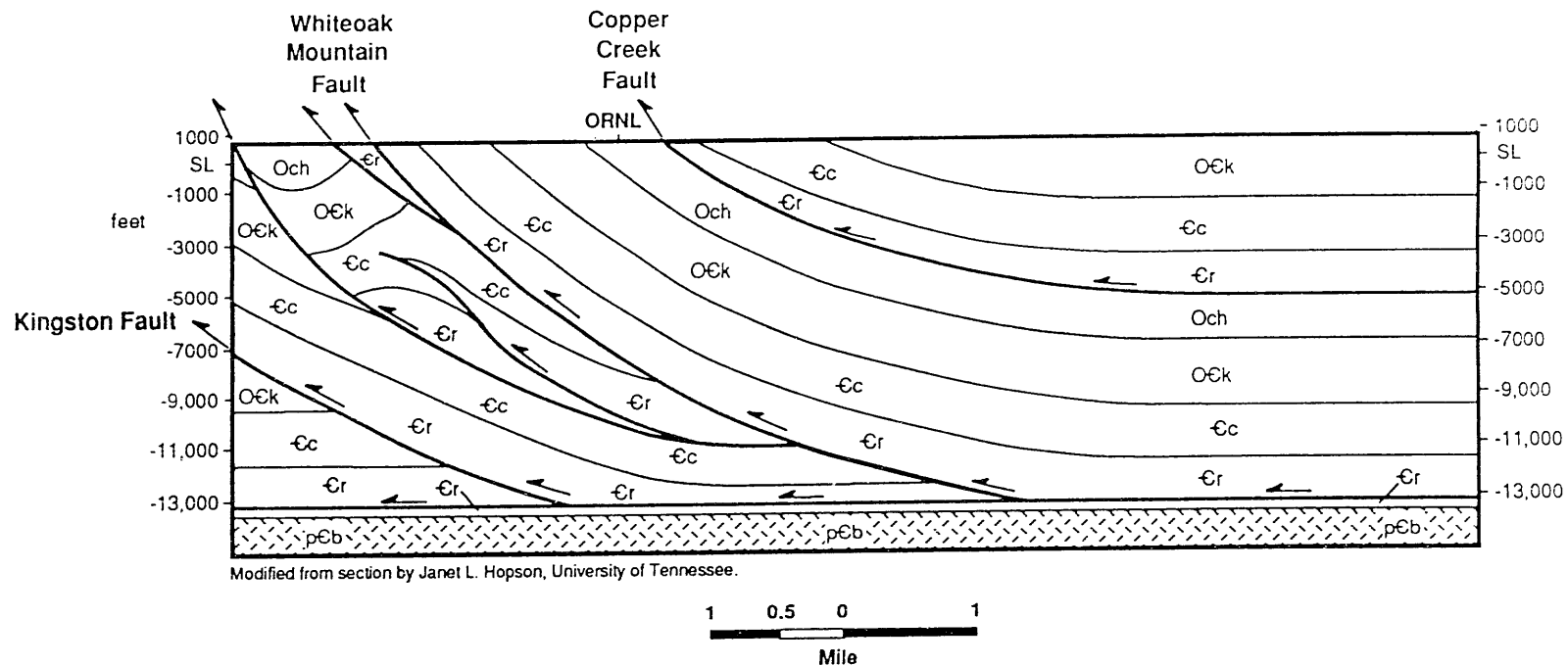


Fig. 1-2. (b) Geologic cross section based on seismic line on Tennessee 95. Modified from section by Janet L. Hopson, University of Tennessee. pCb - Precambrian basement. Cr - Rome Formation. Cc - Conasauga Group. OEk - Knox Group. Och - Chickamauga Group.

McMaster (1962) subsequently published a geologic map of the ORR that locates the boundaries of the major geologic units—Rome Formation, Conasauga Group, Knox Group, etc.—but lacks structural and stratigraphic detail needed for modern studies of structure and hydrogeology.

A number of site-specific geologic and hydrogeologic studies have been conducted by ORNL staff and contractors as part of past and proposed waste disposal activities. Most of the studies in Melton Valley have been summarized by Dreier et al. (1987); those in Bear Creek Valley have been summarized by King and Haase (1987) and Haase et al. (1989). These site-specific geologic investigations represent studies of small areas that have been conducted in great detail, but, until recently, little emphasis has been directed toward investigating the geology and hydrogeology of the entire ORR with the goal of synthesizing the existing data into a unified geologic and hydrogeologic framework. In order to develop a conceptual and quantitative geologic (and hydrogeologic) model of the ORR, it is necessary that the region studied be large enough to include the geologic processes responsible for the observed stratigraphic and structural characteristics. The Oak Ridge Hydrologic and Geologic Study (ORRHAGS) Project was begun in 1987 as a major effort to conduct these reservation-wide investigations.

1.1 HISTORY OF GEOLOGIC AND GEOHYDROLOGIC WORK AT ORNL

In 1948, P. B. Stockdale and H. J. Klepser, Department of Geology and Geography, The University of Tennessee, and G. D. DeBuchanne, United States Geological Survey (USGS), undertook the first detailed geologic and hydrologic investigations on the ORR, as consultants

to the U.S. Atomic Energy Commission (AEC) Office of Research and Medicine (Stockdale 1951). Detailed geologic mapping in the Chickamauga Group of the ORNL area was done by Klepser at a scale of 1 in. to 100 ft; the map was printed on a 10-ft contour interval topographic base at a scale of about 1 in. to 800 ft. The area mapped covered less than 6.5 km² (3 mile²) in Bethel Valley, in and around the main plant area and the area to the southeast and southwest to include what is now Waste Area Grouping (WAG) 3. The Chickamauga Group was divided into eight units designated as A through H from oldest to youngest. The trace of the Copper Creek fault and the contact between the Knox and the Chickamauga Groups were mapped. The text contained brief descriptions of the Knox and Conasauga lithologies. The first exploratory drilling for geologic and hydrologic purposes was done during this investigation, when 51 core holes 15 to 100 m (50 to 300 ft) deep were drilled in Bethel Valley to supplement surface information and to provide information on depths to the water table. DeBuchanne prepared a 5-ft contour interval water table map and performed hydraulic tests on several wells.

At about the same time, John Rodgers of the USGS was preparing the first modern map that included the entire ORR (Rodgers 1953). This was a generalized geologic map compiled from earlier sources (some field checking was done) of eastern Tennessee, published as a set of planimetric maps at a scale of 1:125,000 with explanatory text. G. D. DeBuchanne and R. M. Richardson used these maps as the base for showing locations of selected water wells and springs for a reconnaissance report on groundwater quantity and quality of eastern Tennessee (DeBuchanne and Richardson 1956). This report was formatted on a county-by-county basis and included Anderson and

Roane counties, where the ORR is located.

Field mapping for a reconnaissance geologic map of the entire ORR and the surrounding area was completed in 1958 by W. M. McMaster, U. S. Geological Survey. The map, assembled from Tennessee Valley Authority (TVA) 1:24,000-scale topographic quadrangles, was printed in 1962 at a scale of 1:31,680 by the Army Corps of Engineers, and the accompanying text (McMaster 1963) was issued as an ORNL publication in 1963. The map covers the same area as the 1987 topographic map of the Oak Ridge area prepared by TVA at a scale of 1:24,000.

Several subsurface drilling projects were begun during the 1980s by Martin Marietta Energy Systems, Inc. (Energy Systems) staff to better understand the lithologic and structural characteristics of units within the ORR, particularly the units used for waste disposal and those into which contaminants could migrate. Specifically, the Conasauga Group in the Copper Creek thrust sheet was described in detail and the group was subdivided into formations (Haase et al. 1985); additional subdivision and descriptions were made of parts of the Knox Group (Lee and Ketelle 1987) and the Chickamauga Group (Lee and Ketelle 1988). Additional investigations of the Conasauga Group in both Melton Valley and Bear Creek Valley were made by Dreier and Toran (1989) and Lee and Ketelle (1989). Also during this period, detailed fracture studies were begun on the surface in the Conasauga Group by Sledz and Huff (1981) and Dreier et al. (1987), along with detailed mapping of soils in the Conasauga and Knox groups in the ORR by Lietzke and Lee (1986) and Lietzke et al. (1988, 1989). Detailed geologic maps subdividing the Conasauga Group in Bear Creek Valley were made by King and Haase (1987) and reservation-wide cross sections were constructed from reprocessed seismic reflection data by

Dreier and Williams (1986) and from surface data as part of a University of Tennessee senior research project by C. L. Zucker (1987). A major effort to map the entire ORR in detail at 1:12,000, 1:24,000, or larger scale was begun in 1987 by R. D. Hatcher, Jr., The University of Tennessee and ORNL. This project will subdivide all major rock units and incorporate the previous detailed work on smaller parts of the ORR (Plate 1). P. J. Lemiszki has completed a 1:12,000-scale detailed map of the Bethel Valley quadrangle as part of a University of Tennessee Ph.D. dissertation (Lemiszki 1992).

Results of these investigations are discussed and summarized in other sections of this report.

1.2 REGIONAL GEOLOGIC SETTING

1.2.1 Physiography

The ORR is located in the western portion of the Valley and Ridge physiographic province in eastern Tennessee. The physiographic province extends from the St. Lawrence lowlands to Alabama and varies in width from 20 to 120 km (Fenneman 1936). The general features (Thornbury 1965) that distinguish this province from adjacent areas are (1) parallel ridges and valleys commonly aligned from northeast to southwest; (2) topography caused by erosion of interstratified weak and strong formations that are exposed at the surface by exhumation of a relatively strongly folded and faulted terrane; (3) a few major transverse superimposed streams with subsequent streams forming a trellis-like drainage pattern (actually, drainages are mostly dendritic in headwaters areas, trellis downstream); (4) many ridges with accordant summit levels suggesting former erosion surfaces (peneplanation—a largely outmoded concept); and (5) many

water and wind gaps through resistant ridges. The southern Valley and Ridge of Thornbury (1965) is similar to the northern section but differs from the central section by having (1) more thrust faults, (2) lower ridges, and (3) a more distinct longitudinal river drainage system. Four rivers—the Powell, Clinch, Holston, and French Broad—join to form the Tennessee River after flowing many miles in northeast–southwest-trending valleys. In Tennessee, the Valley and Ridge Province is bordered on the west by the Cumberland Plateau and on the east by the Blue Ridge. The ORR, located approximately 10 km east of the eastern Cumberland Escarpment (that separates the Valley and Ridge from the Cumberland Plateau), has an elevation ranging from 225 to 410 m.

1.2.2 Geology

The ORR is located in one of the classic foreland fold–thrust belts in the world, the Appalachian western Blue Ridge, Valley and Ridge, and Cumberland Plateau (Fig. 1-1). Several fundamental concepts of foreland deformation, e.g., the thin-skinned geometry of thrusting by Rich (1934), were based entirely on nearby structures in eastern Tennessee and southwestern Virginia. The basic structural style here has also been compared to that in the Canadian Rockies (Price and Hatcher 1983) and to the Moine thrust zone in Scotland (Hatcher 1986).

The Tennessee portion of the Appalachian Valley and Ridge is characterized by the presence of a number of northwestward-vergent southeast-dipping imbricate thrust sheets. About ten major northeast-striking thrust faults dominate the structure in the Valley and Ridge at the latitude of the ORR. Two of these major thrusts, the Copper Creek and Whiteoak Mountain faults, are traceable through the ORR (Plate 1). The contrasting geometry

and deformational style of these two faults provide a unique opportunity within the ORR for generic kinematic and mechanical studies of foreland thrusts.

The stratigraphic units in the ORR comprise a diverse assemblage of lithologies from the entire Cambrian and Ordovician section, as well as from several younger Devonian and Mississippian units (Fig. 1-2a). The total thickness of section in the ORR is on the order of 3 km (9500 ft). In general, the Cambrian–Ordovician Knox Group and part of the overlying Chickamauga Group form the competent units within the major thrust sheets in this area. Each major stratigraphic unit (and formations within those units), because of compositional and textural properties, possesses unique mechanical characteristics that responded differently to the deformation events affecting these rocks through time. Therefore, each has probably experienced a slightly different scheme of brittle deformation that produced fracture densities and spacings that affect the way fluids are transmitted through them.

2 AVAILABLE DATA

RaNaye B. Dreier

A wide variety of geologic data are available within the Oak Ridge Reservation (ORR). They range from surface geologic data to core samples, auger samples, and geophysical logs from holes drilled in the ORR to geophysical data. The purpose of this section is to summarize the locations and availability of these data.

2.1 SURFACE GEOLOGIC DATA

Geologic maps (e.g., Plate 1) have been constructed mostly from available exposures of bedrock, residual soils, and surficial deposits. Soils maps are constructed with the aid of augering to obtain information on near-surface soils. Outcrop exposure of bedrock units is variable, but much information can be obtained on the areal distribution of units and location of contacts in areas of poor exposure by making use of residual soils and float. Residual soils are commonly quite diagnostic of different rock units by color and texture, but that is particularly true where these soils contain fragments of the original rock material or of resistant rock types, such as chert or sandstone, that serve as stratigraphic markers. Quality of exposure ranges from generally poor in much of the Conasauga and Knox groups to excellent in parts of the Rome Formation, Chickamauga Group, Rockwood Formation, and Fort Payne Formation.

Structural measurements are gathered from exposed bedrock, weathered rock, and saprolite, where bedding, fracture surfaces, and rare cleavage are preserved. Exposure in the ORR is good enough to permit collection of several thousand

separate structural data stations that are represented by separate dip-strike symbols on the geologic map (Plate 1).

2.2 CORE

The core storage facility (Building 7042 at ORNL) contains approximately 15,000 m (45,000 ft) of core. Inventory of core in Building 7042, including well names, well reference, and storage location, was summarized by Dreier et al. (1990). Other core is being stored at various widely separated locations. A recommendation has been made to store future core samples at Beta-1 (the Oak Ridge Y-12 Plant).

Most studies of core have been directed at the units within the Conasauga Group because most waste disposal areas have been and continue to be sited in valleys underlain by the Conasauga Group. Therefore, more data are available from the Conasauga Group than from other units found in the ORR. The majority of core samples from the Conasauga Group are from Bear Creek Valley because of an extensive drilling project undertaken during the summer of 1986. Additional core is available from (1) the JOY-2 borehole (Knox Group through the Rome Formation in the Copper Creek thrust sheet and Moccasin Formation from the footwall); (2) various boreholes in Melton Valley (Conasauga Group) that are in the vicinity of White Oak Lake and Waste Area Groupings 5 and 7; (3) the Chickamauga Group in Bethel Valley (in ORNL area and near Rogers Quarry); (4) boreholes along Chestnut Ridge (East and West Chestnut Ridge sites), which provide core from the upper and lower

Knox Group (Lee and Ketelle 1987); (5) the crest and northern flank of Chestnut Ridge (Knox Group and Maynardville Limestone), which have been and are being cored as part of ongoing Y-12 Plant and environmental restoration projects; and (6) new drilling in support of the Advanced Neutron Source (ANS) facility which will provide additional Conasauga Group core.

2.3 GEOPHYSICAL LOGS DATABASE

Most boreholes (including core holes) that have depths greater than 30 m (100 ft) have been geophysically logged. Hence the data distribution is similar to that described above for core. The types of logs available from different boreholes vary considerably. The earliest suites of logs were small and primarily consisted of natural gamma-ray, spontaneous-potential, neutron, long-short normal resistivity, and caliper logs. With additional emphasis on borehole geophysics, the data have become more sophisticated, and a typical logging suite collected today contains caliper, temperature, deviation, compensated neutron, compensated density, natural gamma-ray, long-short normal resistivity, fluid resistivity, single-point resistance, spontaneous-potential, borehole televiewer, acoustic velocity, and full-waveform sonic logs. Since 1986 ESD has had the capability to collect borehole geophysical logs in-house, and a concerted effort is under way to maintain and upgrade logging capabilities.

As part of the Oak Ridge Hydrologic and Geologic Study FY 91 activities, a compilation of a historical geophysical log database was started. At present, the database is incomplete and continued work on the project is subject to future funding. The database is available from R. B. Dreier [Environmental Sciences

Division (ESD), ORNL]. In addition, all logs acquired in-house are archived electronically and maintained in a separate database; these are also available from R. B. Dreier.

2.4 SEISMIC REFLECTION AND REFRACTION STUDIES

The amount of other nonborehole geophysical data is limited, especially in comparison with other data types. In the early 1980s Amoco Oil Company acquired a vibroseis line along Tennessee 95 (Fig. 1-2a). The data were subsequently purchased by ESD and reprocessed at The University of South Carolina by Dreier and Williams (1986). A top-of-rock refraction survey has been acquired at the proposed ANS site in eastern Melton Valley (Davis et al. 1992) and at central Chestnut Ridge (Staub and Hopkins 1984). New seismic reflection surveys are proposed, however, at the ANS site and in Bear Creek Valley to investigate high-angle cross-strike lineaments.

3 STRATIGRAPHY

3.1 INTRODUCTION

Robert D. Hatcher, Jr., and Peter J. Lemiszki

The stratigraphic succession exposed in the Oak Ridge Reservation (ORR) ranges in age from Early Cambrian to the early Mississippian (Figs. 3-1 and 3-2). This stratigraphy formed as part of the early Paleozoic drift (ocean-opening) succession. The carbonate bank developed, then uplift and erosion of the carbonate bank occurred in early Middle Ordovician time (post-Knox unconformity), and the carbonate bank was reestablished during the Middle Ordovician, followed by destruction of the carbonate bank in the Middle and Late Ordovician development of a clastic wedge that persisted into the Late Ordovician and Silurian. This was followed by erosion and formation of another unconformity, then by the deposition of the Upper Devonian–Early Carboniferous clastic wedge.

Rodgers (1953) and McMaster (1957, 1962) mapped the contacts between the major stratigraphic units—Rome Formation, Conasauga Group, Knox Group, Chickamauga Group, Reedsville Shale, Sequatchie Formation, Rockwood Formation, Chattanooga Shale, and Fort Payne Formation—in the ORR. In addition, analysis of drill core in Melton and Bear Creek Valleys resulted in the subdivision of the Conasauga Group into the six formations previously described in the central part of the Valley and Ridge (Haase et al. 1985, Hasson and Haase 1988) despite the dominance of clastic rocks over limestones beneath the Maynardville Limestone. Furthermore, Stockdale (1951) and Lee and Ketelle (1988) mapped and

studied core in Bethel Valley in order to subdivide the Chickamauga Group into seven informal units based on differences in lithology.

One of the purposes of present surface work is to refine the previous stratigraphy and to subdivide the Conasauga, Knox, and Chickamauga Groups into the standard stratigraphic units recognized elsewhere in the region that are based on field criteria. In general, subdivision of the Conasauga Group has been most difficult because only a small portion of both valleys could be mapped in detail, exposure is poor, and lithologic contrasts between formations are not pronounced. There, additional data were obtained from the numerous wells that have been drilled into the Conasauga for waste disposal, monitoring, and other purposes. Subdivision of the Knox Group was easier because the characteristic marker units could be found and traced, even in the deep saprolite that commonly develops on this unit. Finally, subdivision of the Chickamauga Group in Bethel Valley was based on the appearance of distinctive redbed units that could be correlated with detailed stratigraphic analyses along strike; in East Fork (Oak Ridge) Valley, subdivision was based on bentonite layers and other criteria recognized in middle Tennessee (Wilson 1949) and correlated to eastern Tennessee (Milici and Smith 1969).

Soil descriptions for individual rock units are incorporated in Sect. 3. Details of how the soil surveys were made, numerical and other soil classifications, and

| | | Lithology | Thickness, m | Formation | | Structural Characteristics | Hydrologic Unit |
|------------|--------|-------------------------|--------------|-----------------------|--|--|-----------------|
| ORDOVICIAN | UPPER | Chickamauga Group (Och) | 100-170 | Omc | Moccasin Formation | Weak unit <i>Upper décollement</i> | Aquitard |
| | | | 105-110 | Owi | Witten Formation | | |
| | | | 5-10 | Obw | Bowen Formation | | |
| | MIDDLE | Chickamauga Group (Och) | 110-115 | Obe | Benbolt / Wardell Formation | Strong units <i>Ramp zone</i> | Aquifer |
| | | | 80-85 | Ork | Rockdell Formation | | |
| | | | 75-80 | Ofl | Hogskin Member Fleanor Shale Member | | |
| | | | 70-80 | Oe Obf | Eidson Member Blackford Formation | | |
| | LOWER | Knox Group (Ock) | 75-150 | Oma | Mascot Dolomite | Strong units <i>Ramp zone</i> | Aquifer |
| | | | 90-150 | Ok | Kingsport Formation | | |
| | | | 40-60 | Olv | Longview Dolomite | | |
| 152-213 | | | Oc | Chepultepec Dolomite | | | |
| 244-335 | | | Ccr | Copper Ridge Dolomite | | | |
| CAMBRIAN | UPPER | Conasauga Group (Cc) | 100-110 | Cmn | Maynardville Limestone | Weak units <i>Basal décollement</i> | Aquitard |
| | | | 150-180 | Cn | Nolichucky Shale | | |
| | MIDDLE | Conasauga Group (Cc) | 98-125 | Cdg | Dismal Gap Formation (Formerly Maryville Ls.) | | |
| | | | 25-34 | Crg | Rogersville Shale | | |
| | | | 31-37 | Cf | Friendship Formation (Formerly Rutledge Ls.) | | |
| | LOWER | Conasauga Group (Cc) | 56-70 | Cpv | Pumpkin Valley Shale | | |
| | | | 122-183 | Cr | Rome Formation | | |

Fig. 3-1. Stratigraphic section in Bear Creek Valley, Chestnut Ridge, Bethel Valley, Haw Ridge, Melton Valley, and Copper Ridge.

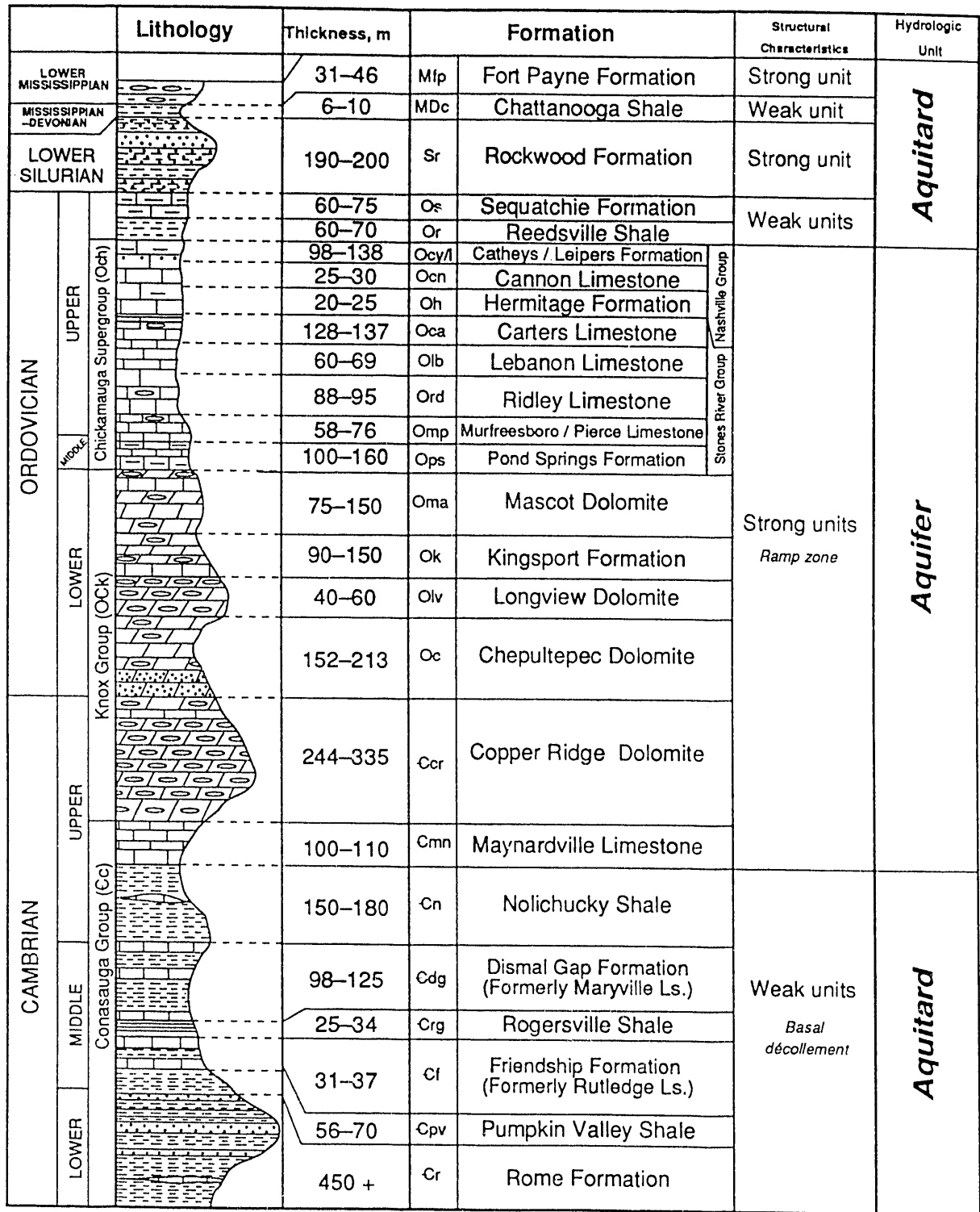


Fig. 3-2. Stratigraphic section in East Fork (Oak Ridge) Valley, East Fork Ridge and Pilot Knob, Pine Ridge, Bear Creek Valley, and Chestnut Ridge.

discussion of surficial depositions are discussed in Sect. 4.

3.2 ROME FORMATION

Peter J. Lemiszki, Richard R. Lee,
Richard H. Ketelle, and
David A. Lietzke

3.2.1 Introduction

The Rome Formation is the oldest rock unit exposed in the ORR and underlies Haw Ridge, Pine Ridge, and the valley and some small ridges northwest of Pine Ridge. From a distance, Rome topography is recognized by narrow, steep ridges broken by closely spaced wind and water gaps that give it a cockscomb appearance. The Rome Formation was named by Hayes (1891) for exposures at Rome, Floyd County, Georgia. Although no fossils were found in the ORR, Resser (1938) and Rodgers and Kent (1948) assigned an Early Cambrian age to the Rome Formation on the basis of faunal evidence, such as the trilobite *Olenellus*. The lower stratigraphic contact is not exposed in eastern Tennessee because it commonly is cut off by the basal décollement. The upper contact with the Pumpkin Valley Shale is located at the last thick sandstone bed below a consistent section of shale, thin sandstone, and silt-stone of the Pumpkin Valley. A thicker sequence of the Rome Formation is present within the Whiteoak Mountain thrust sheet than within the Copper Creek thrust sheet. The Whiteoak Mountain fault is located within the lower Rome (Apison) Shale and therefore brings to the surface a thicker section of the Rome. Although determining the stratigraphic thickness in the Rome is hampered by tectonic duplication and thinning, recent geologic mapping shows that the thickness in the Copper Creek thrust sheet is between 122

and 183 m; in the Whiteoak Mountain sheet, however, the Rome can be as much as 450 m thick (Plate 1). In the Copper Creek thrust sheet, Haase et al. (1985) reported a thickness of 188 m using the JOY-2 core, and McReynolds (1988) reported a true stratigraphic thickness between 90 and 125 m. Despite comparatively good exposures and topographic prominence, the Rome Formation is among the least studied formations in the ORR.

3.2.2 Previous Studies

During reconnaissance mapping of the ORR, McMaster (1962) recognized the existence of complex lithologic and structural relationships in the Rome Formation. He mapped the upper Rome Formation in the Copper Creek and Whiteoak Mountain thrust sheets and was further able to distinguish and map the lower Rome Formation in the Whiteoak Mountain thrust sheet on the basis of topography and float debris.

The Rome Formation in the Copper Creek thrust sheet was completely sampled by the JOY-2 core. A discussion of lithologic and structural features identified in core may be found in Haase et al. (1985). Because of unstable borehole conditions, however, a complete suite of geophysical logs was not obtained. In addition, core through the upper part of the Rome Formation was obtained during the course of other subsurface studies. All of the core is in storage in Building 7042, and geophysical logs are in the Oak Ridge National Laboratory (ORNL) Environmental Sciences Division (ESD) staff geophysical log database.

McReynolds (1988) studied the Rome Formation in the Copper Creek thrust sheet using surface exposures and the JOY-2 core. He identified a total of seven lithofacies consisting of three clastic, two

carbonate, and two mixed clastic-carbonate lithofacies. The sequence was interpreted to represent a mixed siliciclastic and carbonate depositional environment. Regional sedimentological studies of the Rome Formation conclude that it thickens and becomes more carbonate rock towards the southeast and was deposited in a tidal environment along the early Paleozoic North American passive margin (Rodgers 1953, Spigai 1963, Samman 1975, Harris and Milici 1977).

3.2.3 Lithologic Description

Exposures of the lower Rome in the Whiteoak Mountain thrust sheet are sparse, making contacts difficult to locate and detailed description of the unit difficult. A reasonably good exposure exists on the northeast face of Pine Ridge in the city of Oak Ridge near the intersection of LaFayette and Illinois Avenues. This section probably is similar to the Apison Shale Member of the Rome Formation (Hayes 1894, Wilson 1986). Micaceous shale is the most common lithology and is maroon, green, and yellow-brown. Sandstone and siltstone are interbedded with the shale and are maroon, brown, and gray. Thin to medium beds of light-gray argillaceous limestone and dolomite are also present. The shale is fissile and generally variegated. The unit weathers into soil containing shale and siltstone chips as well as small sandstone blocks. Fragments of bluish-white, tan-brown, and chalcidonic chert are derived from weathering of dolomite and limestone beds.

The upper part of the Rome Formation consists dominantly of interbedded maroon sandstone, siltstone, and shale, but the presence of distinctive dolomite and dolomitic sandstone intervals has proven useful for mapping the Rome stratigraphy in the Copper Creek thrust sheet (McReynolds 1988). The distinctive dolo-

mite and dolomitic sandstone intervals were not found in the Whiteoak Mountain thrust sheet. Similar dolomite was described by Rodgers and Kent (1948) northeast of Oak Ridge and has been used as a regional marker horizon (Harris 1964). Greenish-gray, yellowish-gray, pale-brown, and olive-green sandstones are interbedded with maroon sandstone. The sandstones are silica- and hematite-cemented, mostly fine- to medium-grained, quartzose, and occasionally glauconitic. Ripple bed forms, small-scale unidirectional and bidirectional crossbeds, flaser bedding, bioturbation, mudcracks, and local salt crystal casts are common sedimentary structures. Siltstones in the upper Rome are tan, gray, and greenish-gray. The siltstones are thin bedded and contain sedimentary structures similar to those in the sandstones. Shales in the upper Rome are olive green, light brown, green-gray, and maroon and are thin bedded. Shales are variegated in shades of maroon, pale green and greenish-gray, yellow, and black. Dolomite in the Rome is light to dark gray and massively bedded. Interbedded with the massive dolomite is thick-bedded dolomitic sandstones. Rome soils are sandy, silty, light-colored clay containing abundant siltstone and sandstone fragments. One of the most continuous exposures of the upper Rome Formation in the Copper Creek thrust sheet is along Pumphouse Road behind the Scarboro Facility in the ORR.

3.2.4 Rome Formation Soils

The Rome Formation consists of a wide variety of saprolite lithologies, including (1) a siliceous, yellowish-brown sandstone member; (2) a feldspathic, very fine grained, yellowish-brown sandstone member; and (3) a thin, fissile, dusky-red and gray shale member mappable only at 1:2400 on the crest and south side of Pine

and Haw Ridges. From the north side of Pine Ridge to the Whiteoak Mountain fault are (1) yellowish-brown, feldspathic siltstone; (2) pinkish, hard, micaceous sandstone; and (3) dusky-red mudstone interbedded with olive-gray siltstone and shale and very minor areas of carbonate soils. Haw Ridge has a similar assemblage of strata, but thin carbonate strata are more abundant, especially in the upper section. Larger areas of mappable carbonate soils are also more common on Haw Ridge, where they occur close to the top of the formation. Most of the soils in the Rome are defined on the properties of the parent rock. The feldspathic siltstone member is extensive enough in the Rome Formation so that two weathering groups have been established: the No. 001 soils occur only on slopes exceeding about 45 percent, have minimal soil development of genetic horizons, and depth to paralithic materials is generally less than 50 cm, while the No. 008 soils formed in similar materials, but on less steep slopes, and have well-defined and expressed argillic horizons. The No. 004 soils formed in interbedded dusky-red mudstone and greenish-gray shale saprolite. They have minimal genetic soil horization on slopes exceeding 45 percent, but have a better expression of horization on less steep slopes. The No. 009 soils occur only over carbonate rock, which is primarily a dolomitic limestone that is interbedded with a very fine grained feldspathic sandstone along the edges of these bodies. Fault breccia and highly fractured areas are extensive enough so that distinctive soils were mapped over these areas. The No. 005 and No. 006 soils are deeply weathered, with depth to paralithic materials exceeding 1 m. The Rome Formation generated large quantities of colluvium during the Pleistocene. Colluvial soils are identified by the source of their parent materials and by their soil morphology.

3.2.5 Rome Residuum

00051, 00061. The soils in these map units formed in the yellowish-brown saprolite residuum of fine-grained feldspathic sandstone that is assumed to have been mostly cemented by calcium carbonate. Most areas of these soils occur on the south side of Pine Ridge, where they occur on linear and convex side slopes between the summit knobs and the first bench landform. The soils on Haw Ridge have more common thin carbonate strata that have weathered out to form reddish clay seams. Rainfall infiltrates rapidly and percolates downward through the joint and fracture system. There is little evidence of overland flow from these soils.

00151, 00161. The soils in these map units formed in yellowish-brown saprolite residuum of feldspathic siltstone and very fine grained sandstone. Depth to the Cr (see Sect. 4 for explanation of all soil symbols) horizon is highly variable, but is mostly less than 50 cm. The upper 25 to 30 cm of these soils formed in creep and bioturbated materials. These soils occupy some of the steepest headwall and side slope areas of drainageways and have slopes of 45 percent to about 90 percent. Even though slopes are very steep, there is very little evidence of overland runoff, but infiltrated water flows laterally below the surface along the top of the Cr horizon or the rock contact. Some small areas show evidence of recent active creep or slumping.

00251. The soils in this map unit formed in multicolored yellowish-brown, yellowish-red, and light-gray fine- and medium-grained sandstone saprolite. Fragments of hard, light-gray or reddish sandstone typically litter the surface. These soils occupy the crestal knobs and crest shoul-

der areas of Pine Ridge. One sandstone unit is a yellow-red medium sand. Also included are bands of a hard, dusky-red sandstone interbedded with dusky-red and gray fissile shale and feldspathic fine-grained sandstone of the No. 000 soil as well as siltstone of the No. 001 and No. 008 weathering sequence. Rainfall infiltrates readily with little evidence of overland runoff. Water seems to readily percolate downward through the joint and fracture system, and the upper soil is well oxidized throughout. In low-resolution soil mapping at a scale of 1:12,000, the 002 soils are included with the 000 soils.

00323, 00341, 00343, 00351, 00361. The soils in these map units formed in saprolite from hard, light-red to red micaceous fine-grained sandstone that is cemented by iron oxides. These soils occur on upper and middle doubly convex or convex/plano side slopes on the first ridge north of the main crest. Depth to hard Cr horizon material is usually less than 20 cm, but can be as deep as 50 cm.

00441, 00451, 00461. The soils in these map units formed in surficial creep materials less than 50 cm thick and in the underlying interbedded dusky-red mudstone and olive-gray shale saprolite. These soils are more deeply weathered with depth to Cr materials usually more than 50 cm. The paralithic materials of the Cr horizon are also soft. These soils are on summits and on upper, middle, and lower side slopes with convex/plano slope configurations. These soils are more extensive on the north side of Pine Ridge, but some have been mapped on Haw Ridge.

00521, 00523, 00533, 00541, 00543, 00551, 00553. These soils formed in brecciated materials of mostly lower Rome origin, but are mapped only over fault breccia. Their largest extent is over the Whiteoak Moun-

tain fault, where their extent approaches a width of about 300 m (1000 ft). These soils also occur in the center of McNew Hollow over a fault, but most of the McNew Hollow fault breccia soils have been buried by colluvium and alluvium. A thin zone, commonly less than 16 m (50 ft) thick, occurs on the north side of Haw Ridge just above the Copper Creek fault. A wide range of colors are allowed in these soils ranging from 2.5YR to 10YR depending on whether the parent materials are dusky-red mudstones or yellowish feldspathic siltstones. The colors have a swirled appearance in the upper saprolite. Because of the more permeable underlying saprolite, these soils are deep to paralithic materials, usually more than 1.5 m thick. They also have well-developed soil morphology, including silty clay loam or clay Bt argillic horizons.

00631, 00633, 00641, 00643, 00651, 00661. The soils in these map units formed in highly fractured materials derived from the upper Rome Formation consisting of mostly sandstones and siltstones of the No. 001, 008, and 003 soils. Interbedded with these soils are areas of less brecciated No. 008 soils, which occupy ridge crests. Only one area of these soils was mapped along the Pine Ridge area in the Roane County portion of the soil survey. These soils are much more common on Haw Ridge, especially the western Roane County portion, which seems to be generally more highly fractured and has deeper soils.

00831, 00833, 00841, 00843, 00851. The soils in these map units formed in yellowish-brown saprolite residuum of feldspathic siltstone and fine-grained sandstone. Depth to paralithic materials or the Cr horizon ranges from less than 100 cm to more than 100 cm, with greater depth generally on less sloping landforms. The

saprolite is a light yellowish-brown. The Bt horizon has 10YR or 7.5YR hues, a texture of loam or clay loam and a moderate to strong grade of subangular blocky structure. Thicker Bt horizons tend to have higher clay content. Most areas of these soils occupy summits and upper side slopes of secondary ridges.

00943, 00951. These soils formed in the saprolitic residues of carbonate rock. The rock weathers to form a sticky clay saprolite that becomes plugged with additional translocated clay. The argillic horizon has a 7.5YR to 5YR hue, high clay content, and abundant black manganese coatings and zones. Only one mappable area of these soils was mapped on Pine Ridge. Several other areas, too small to be mapped, were identified in McNew Hollow. These soils are more common on Haw Ridge, where they occur on the southernmost ridge top. Carbonate rock outcrops generally occur on Haw Ridge only on very steep slopes and are commonly not visible from ridge tops or from drainageways. Two sinkholes have been identified on Haw Ridge. The first is on the ridge crest while the other is in a drainageway. The extent of the Rome carbonate unit that tree roots come into contact with is larger than that mapped on the surface. Where tree roots do contact the carbonate, there are excellent stands of white oak, beech, and northern red oak that respond to higher levels of fertility.

3.3 CONASAUGA GROUP

RaNaye B. Dreier, Robert D. Hatcher, Jr., and David A. Lietzke

3.3.1 Introduction

The Conasauga Group was named (actually as the Conasauga Shale) by

Hayes (1891) for exposures along the Conasauga River in Whitfield and Murray Counties, Georgia. It is a principal component of the Middle to Upper Cambrian portion of the stratigraphic sequence characterized by interlayered shale, limestone, and lime-rich shale. The Conasauga Group is repeated by Alleghanian faulting (see Sect. 5) and underlies both Bear Creek Valley (Whiteoak Mountain thrust sheet) and Melton Valley (Copper Creek thrust sheet). Because many historical and current ORNL and Y-12 Plant waste management areas are in Conasauga Group rocks, local geologic characterization studies have concentrated on these units. The descriptions presented below are taken from these studies, specifically from Haase et al. (1985), Dreier and Toran (1989), Lee and Ketelle (1989), and Foreman et al. (1991).

3.3.2 General Description

The Conasauga Group crops out throughout the southern Appalachian Valley and Ridge, but shows lithofacies transitions from clastics in the west to carbonates in the east (Rodgers 1953; Markello and Read 1981, 1982; Hason and Haase 1988). North to south changes in the amount of carbonate and clastic facies in the Conasauga Group have also been recognized (Rodgers 1953, Harris and Milici 1977). On the basis of the predominant lithology (carbonate, mixed carbonate-clastic, and clastic), Rodgers divided the Conasauga Group into three phases that occur in parallel, north-south or northeast to southwest-trending belts. The phases are subparallel and cross-structural strike. The central phase consists of six formations that represent interfingering of carbonate and clastic facies. To the west of the ORR, most of the carbonate formations are absent and only two formations are recognized. To the northeast, in the

eastern phase, the clastics are reduced in number and three formations can be identified.

The ORR lies near the western margin of the central phase of the Conasauga Group (Hasson and Haase 1988), where the group consists primarily of calcareous shale interbedded with shaly to silty limestone. The average thickness of the Conasauga Group is 567 m in Melton Valley to 557 m in Bear Creek Valley (Table 3-1). Six formations can be recognized within the group. They are, in ascending order, the Pumpkin Valley Shale, Friendship formation (Rutledge Limestone equivalent), Rogersville Shale, Dismal Gap formation (Maryville Limestone equivalent), Nolichucky Shale, and Maynardville Limestone (Fig. 3-3). All previous descriptions of the ORR Conasauga Group geology utilize the standard central phase terminology—Rutledge and Maryville Limestones instead of Friendship and Dismal Gap formations—but, because of rapid facies changes between the standard control phase sections (e.g., Thorn Hill) and the ORR (Fig 3-3), the traditional formation names are inappropriate. The Friendship and Dismal Gap formations are thinner than the Rutledge and Maryville Limestones farther east, as reported by Rodgers (1953) and Hasson and Haase (1988), and they contain 30 to 60 percent clastics. Nevertheless, the names Rutledge Limestone and Maryville Limestone are embedded in ORR geologic descriptions and regulatory directives. Hence, we suggest that future users of the names Dismal Gap formation and Friendship formation should note that they occupy the same stratigraphic positions as the Maryville Limestone and Rutledge Limestone. The use of the names Dismal Gap formation and Friendship formation is suggested for the first time in this report, and the names are to be treated informally. The type

section for the Dismal Gap formation is at Dismal Gap in the Powell quadrangle (in the same strike belt as the ORR); that for the Friendship formation is in a drill hole near Friendship Cemetery in the ORR. The type sections for these units have not been formally established and described in the literature.

3.3.3 Pumpkin Valley Shale

Regionally, the stratigraphy of the Pumpkin Valley Shale is not well known and formal stratigraphic members have not been defined (Rodgers 1953, Harris 1964, Hasson and Haase 1988). The formation was informally divided into upper and lower units in the Whiteoak Mountain thrust sheet by Law Engineering (1975).

Lithologic data and drill core descriptions of the Pumpkin Valley Shale are contained in Law Engineering (1975), Haase et al. (1985), King and Haase (1987), and Lee and Kettle (1989). The Pumpkin Valley Shale ranges from 90 to 109 m throughout the ORR, and the two informal units are of approximately equal thickness (Table 3-1). The informal members have not been mapped separately in surface exposures.

The contact of the Rome Formation and overlying Pumpkin Valley Shale is placed at the bottom of the shaly gray-brown siltstone of the Pumpkin Valley Shale and the top of the uppermost massive to evenly laminated gray-green sandstone in the Rome Formation. On geophysical logs, the contact between the Rome Formation and the overlying Pumpkin Valley Shale is easily recognized and is characterized by prominent anomalies in both the gamma-ray and neutron logs (point A in Fig. 3-4).

The lower Pumpkin Valley Shale consists of maroon-brown and gray to gray-green siltstone and mudstone that commonly is greatly bioturbated. The

Table 3-1. Stratigraphic thickness, Conasauga Group^a

BEAR CREEK VALLEY — WHITEOAK MOUNTAIN THRUST SHEET

| | Pumpkin Valley Shale through Dismal Gap Formation | | | | | | | | |
|------------------|---|--------------|-----------|----|-----|--------------|--------------|------------|--|
| | Lower €pv | Upper €pv | €pv | €f | €rg | Lower €dg | Upper €dg | €dg | |
| AVERAGE | 43 | 52 | 95 | 32 | 31 | 45 | 62 | 108 | |
| MIN | 36 | 39 | 90 | 28 | 21 | 41 | 53 | 95 | |
| MAX | 51 | 59 | 99 | 38 | 36 | 49 | 73 | 122 | |
| NO. OF VALUES | 4 | 4 | 4 | 5 | 6 | 4 | 3 | 2 | |

MELTON VALLEY — COPPER CREEK THRUST SHEET

| | Pumpkin Valley Shale through Dismal Gap Formation | | | | | | | | |
|------------------|---|--------------|------------|----|-----|--------------|--------------|------------|--|
| | Lower €pv | Upper €pv | €pv | €f | €rg | Lower €dg | Upper €dg | €dg | |
| AVERAGE | 41 | 61 | 101 | 38 | 36 | 61 | 63 | 126 | |
| MIN | 35 | 48 | 94 | 31 | 26 | 47 | 46 | 104 | |
| MAX | 46 | 67 | 109 | 45 | 48 | 85 | 75 | 158 | |
| NO. OF VALUES | 7 | 7 | 10 | 17 | 16 | 22 | 11 | 11 | |

BEAR CREEK VALLEY — WHITEOAK MOUNTAIN THRUST SHEET

| | Nolichucky Shale through Maynardville Limestone | | | | | | | | | | | |
|------------------|---|-----------|-------------|------------|--------------|--------------|--------------|------------|--------------|---------------|------------|--|
| | Lower €n | Mid €n | Upper €n | €n | Lower €lh | Upper €lh | Lower €cb | Mid €cb | Upper €cb | Upper U€cb | €mn | |
| AVERAGE | 55 | 90 | 20 | 170 | 38 | 21 | 28 | 10 | 22 | 5 | 121 | |
| MIN | 45 | 55 | 11 | 154 | 34 | 18 | 25 | 9 | 18 | 5 | 116 | |
| MAX | 65 | 105 | 36 | 183 | 43 | 26 | 29 | 11 | 27 | 6 | 127 | |
| NO. OF VALUES | 6 | 6 | 5 | 3 | 4 | 5 | 4 | 4 | 4 | 4 | 3 | |

MELTON VALLEY — COPPER CREEK THRUST SHEET

| | Nolichucky Shale through Maynardville Limestone | | | | | | | | | | | |
|------------------|---|-----------|-------------|------------|--------------|--------------|--------------|------------|--------------|---------------|-----------|--|
| | Lower €n | Mid €n | Upper €n | €n | Lower €lh | Upper €lh | Lower €cb | Mid €cb | Upper €cb | Upper U€cb | €mn | |
| AVERAGE | 55 | 78 | 54 | 187 | 20 | 15 | 15 | 6 | 22 | 0 | 79 | |
| MIN | 47 | 78 | 54 | 187 | 20 | 15 | 15 | 6 | 22 | 0 | 79 | |
| MAX | 63 | 78 | 54 | 187 | 20 | 15 | 15 | 6 | 22 | 0 | 79 | |
| NO. OF VALUES | 4 | 1 | 1 | 1 | 1 | 1 | 1 | 1 | 1 | 1 | 1 | |

TOTAL CONASAUGA GROUP THICKNESS

| | |
|-------------------------|------------|
| BEAR CREEK VALLEY (WOM) | 557 |
| MELTON VALLEY (CC) | 567 |

^aStratigraphic thicknesses measured in meters. Thicknesses calculated from measured downhole thickness, borehole deviation and estimated formation dip. Total formation thicknesses are shown in bold. €pv = Pumpkin Valley Shale; €f = Friendship Formation (formerly Rutledge Limestone); €rg = Rogersville Shale; €dg = Dismal Gap Formation (formerly Maryville Limestone); €n = Nolichucky Shale; €lh = Low Hollow member of the Maynardville Limestone; €cb = Chances Branch member of the Maynardville Limestone; €mn = Maynardville Limestone; U€cb = _____.

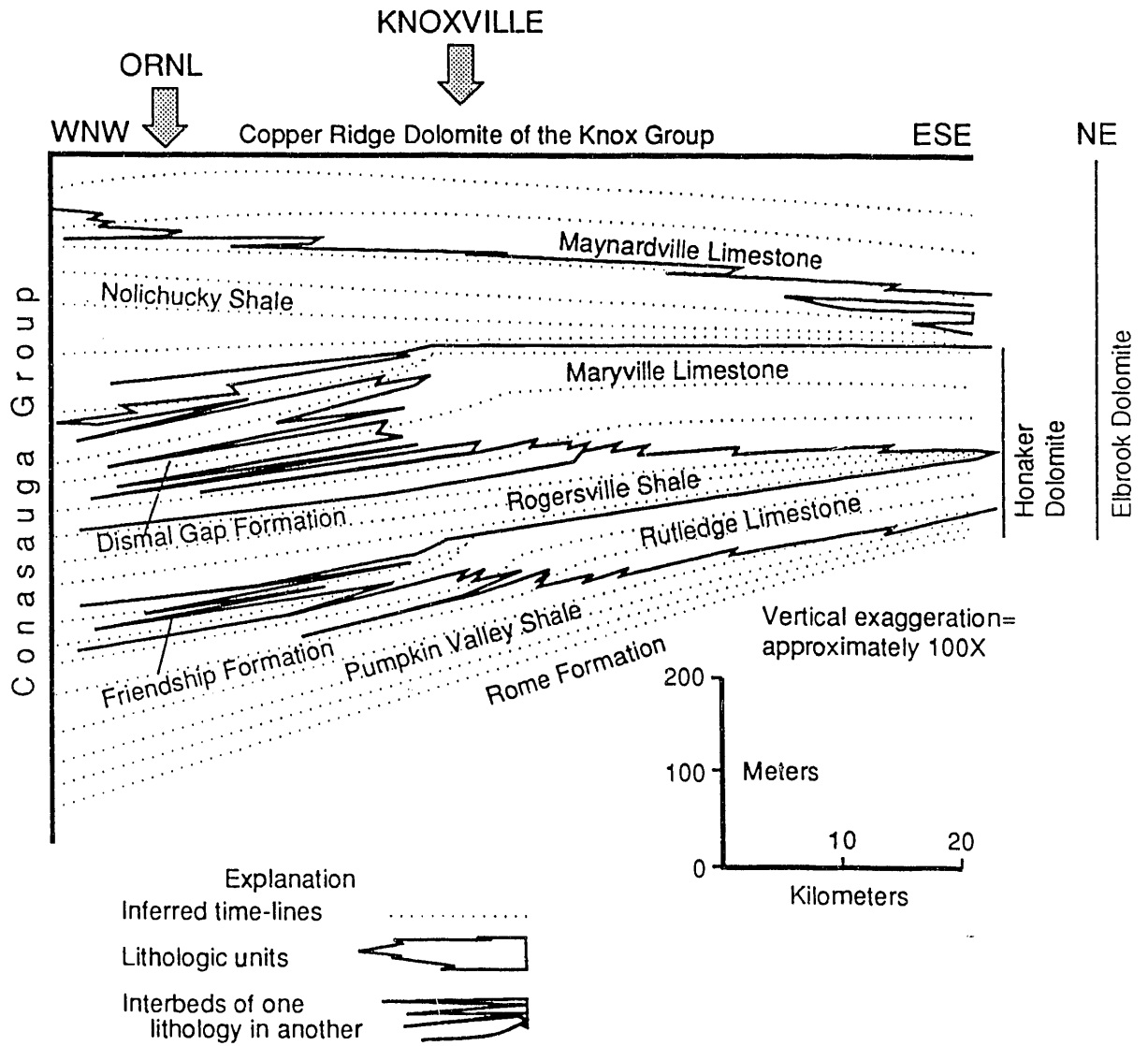


Fig. 3-3. Regional facies relationships in the Conasauga Group in eastern Tennessee. (Modified from Rodgers 1953 and Foreman 1991.)

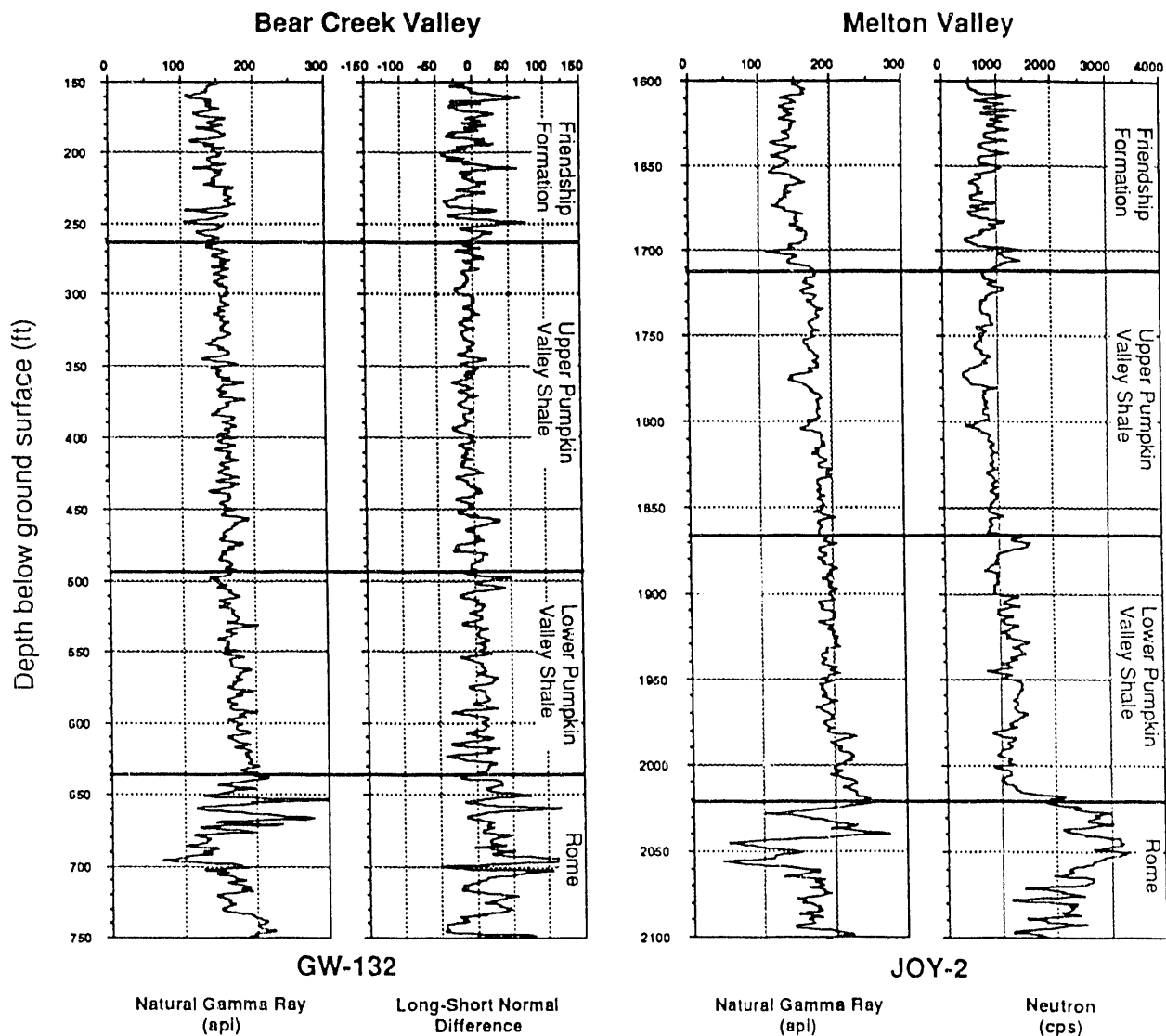


Fig. 3-4. Geophysical logs - Pumpkin Valley Shale.

mudstone is massive to thinly bedded and evenly to wavy parallel stratified. It ranges from pure mudstone to silty mudstone with thin 0.6- to 1.2-cm-thick stringers and disseminations of siltstone. Such disseminations locally coalesce to form discontinuous lenticular siltstone beds that occur throughout silty mudstone-rich intervals. Siltstone-rich horizons exhibit complex stratification patterns that range from thinly laminated to thinly bedded 0.6- to 1.2-cm-thick intervals with wavy to evenly parallel to nonparallel stratification. The bioturbated horizons, which are 0.15 to 1.5 m thick, are massive to mottled, and wavy or lenticularly bedded. Stratification within the lower unit is highly variable, with the massively bedded horizons being the most completely bioturbated and homogenized. Compositionally, the bioturbated intervals resemble simple physical mixtures of the siltstone and mudstone lithologies. Glauconite pellets are very abundant within bioturbated horizons and can compose as much as 40 percent of selected beds. The lower member of the Pumpkin Valley Shale is slightly more siltstone-rich than the upper member, as is reflected by the slight rightward shift of the trace of the neutron log (Fig. 3-4). In addition, at least locally (core hole GW-132), the long-short normal resistivity log differentiates the lower member from the upper member. The difference in long and short normal resistivity values can be an indication of the relative resistivity of the strata (or formation water). If the long normal is consistently more resistive than the short normal, as is the case for the upper Pumpkin Valley (Fig. 3-4), then the far field strata are more resistive (less saline) than strata in the immediate vicinity of the borehole. The Pumpkin Valley Shale exhibits an abrupt resistivity break at the informal contact between the upper and lower members.

The upper Pumpkin Valley Shale consists of red-brown, red-gray, and gray mudstone and shale interbedded with siltstone. Gray and maroon-gray silty mudstone is somewhat less common in the upper unit than in the lower unit, and the evenly laminated and crossbedded siltstone locally occurs in somewhat thinner beds than in the lower unit. Glauconite pellets are ubiquitous within siltstone intervals, occur as random disseminations throughout individual beds, or are concentrated into discrete laminae and bedding planes. Locally, 0.6- to 2.5-cm-thick horizons composed of 40 to 60 percent glauconite pellets are interbedded within siltstone and mudstone in the upper unit.

The contact of the Pumpkin Valley Shale with the overlying Friendship formation is characterized geophysically by conspicuous anomalies on the gamma-ray, neutron, and single-point resistivity logs (Fig. 3-4) described below. Beneath this contact is a slight rightward shift in the gamma-ray log baseline and a pronounced leftward shift in the neutron log baseline.

3.3.4 Pumpkin Valley Shale Soil

The No. 100, No. 101, No. 102, and No. 103 soils form a weathering sequence, ranging from highly weathered to least weathered, on the lower Pumpkin Valley, which contains a high content of interbedded glauconitic fine-grained sandstone and siltstone. These soils can be identified and easily mapped at a 1:1200 to 1:2400 scale, but only the soil of greatest extent (soil No. 102) was mapped at the 1:12,000 scale. The other soils of this sequence occur as inclusions at this map scale. The degree of weathering and amount of soil development is dependent on whether or not water flows off or infiltrates. Infiltration on these soils and their associated landforms is dependent not only on

the slope gradient but also on the width of the side slope and its convexity and on the joint and fracture network of the underlying rock. Even though slope classes of these soils overlap, the landform width and convexity are different. Most areas of the No. 101 soils are on slopes of generally 20 to 35 percent, while most of the No. 102 soils are on slopes of 35 to 45 percent. The No. 102 soils also occur on lower gradient landforms where interfluves are narrower and more convex. Most areas of the No. 103 soils are on slopes greater than 45 percent, but if areas are on less steep slopes, the landform, usually a spur ridge, is narrow and highly convex. The upper Pumpkin Valley Shale has a higher siltstone and shale content with less sandstone and has a high glauconite content that gives rise to a saprolite ranging from reds and violets to green. Because of the higher content of less permeable shale, the upper Pumpkin Valley weathers differentially, with more permeable strata more deeply weathered than less permeable strata. Soil No. 104 is mapped only over the upper part of the formation.

3.3.5 Pumpkin Valley Residuum

10043. These soils formed in glauconite-rich residuum of the lower Pumpkin Valley Shale of the Conasauga Group. Soils in this map unit are on broad-nose slopes with mostly doubly convex shapes. These soils typically have a uniform 5YR to 2.5YR hue in the upper Bt horizon, but, because of clay plugging in the BC, CB, C, and uppermost Cr horizon, the soil becomes increasingly mottled with depth. Depth to the Cr horizon or paralithic contact is more than 100 cm. Because these soils are severely eroded and have a clay-plugged upper saprolite horizon, they presently tend to generate high volumes of overland runoff and near-surface lateral

flow.

10141, 10151. These soils formed in interbedded glauconitic sandstone and siltstone saprolite of the lower Pumpkin Valley Shale and occur on broad convex landforms on the lower southern slopes of Pine and Haw ridges. The rock from which these soils are derived had a very small content of carbonate because the tree species, especially chestnut oak, that grow on these soils can tolerate acidic infertile soils and are evidently unable to tap into any calcium carbonate at depth. Very little white oak, poplar, hickory, dogwood, or ground cover that requires higher levels of natural fertility grow on any of the Pumpkin Valley soils. These soils produced colluvium during the Pleistocene whenever the upper horizons of the soil became so overly saturated that stability was lost.

10241, 10251. These soils formed in interbedded glauconitic sandstone-siltstone saprolite of the lower Pumpkin Valley Shale, where they occupy narrower, steeper, or more convex landforms on the lower slopes of Pine and Haw ridges. The argillic horizon contains well-developed structure and 5YR to 10YR hues. Depth to the Cr horizon is generally less than 50 cm, but can range to about 80 cm.

10361. These soils formed in less weathered glauconitic sandstone-siltstone saprolite of the lower Pumpkin Valley Shale. They occupy steep side slopes of drainageways cutting headwardly into and through the Pumpkin Valley Shale on the south side of both Pine and Haw Ridges. Overland runoff on these steep slopes has removed soil from the surface almost as fast as it has been added by rock weathering at the base of the soil. These soils have a very high erosion potential in their natural forested state. Clearing

would increase the erosion hazard as well as increase the rate of downslope movement of earthy material by gravity as creep or solifluction in a moist state or as mud or debris flows in a saturated state. Depth to paralithic materials averages about 50 cm, but ranges from about 75 to 120 cm. During the summer heat and drought of 1986, there was premature leaf drop from trees growing on these soils. These soils are hydrologically important because they generate rapid overland or near-surface lateral flow during storm events.

10422, 10432, 10441, 10442, 10443. These soils formed in the very dusky red shale and siltstone with thinner interbedded very fine grained glauconitic sandstone saprolite of the upper Pumpkin Valley Shale. Depth to the Cr horizon (paralithic materials) is less than 50 cm, but can be as much as 120 cm due to variable weathering of individual strata. Because of past erosion, these soils have lost most of their capacity to retain rainfall. Consequently, they probably now generate more overland or near-surface lateral flow than what percolates downward into deeper saprolite layers.

3.3.6 Friendship Formation (Formerly Rutledge Limestone)

Strata above the Pumpkin Valley Shale exhibit a rapid lithofacies transition in the vicinity of the ORR (Hasson and Haase 1988). Southeast of the ORR, the formation is dominantly ribbon-bedded carbonate with an upper unit of dolomite. In the ORR, the Friendship formation, named for a section cored in the Joy-2 core hole that crops out near Friendship Cemetery in Melton Valley, is dominantly clastic with some limestone. A good section of the Friendship is also exposed at Dismal Gap. West of the ORR, the clastic content of the Friendship formation continues to increase

and it becomes unrecognizable as a separate unit. Within the ORR, the Friendship formation varies in thickness from 21 to 48 m (Table 3-1).

The base of the Friendship formation is characterized by three coarse-grained limestone beds that range from wavy to lenticularly bedded and are locally mottled and bioturbated. The limestones are interbedded with distinctive maroon shale and mudstone. These lithologies combine to form a 6-m-thick sequence referred to as the "three limestone beds" (deLaguna et al. 1968) and produce a very distinct three-pronged pattern on gamma-ray and neutron borehole logs (Fig. 3-5). This pattern serves as an excellent stratigraphic marker throughout the ORR (Haase et al. 1985). The relatively clean, dark maroon shales in the lower Rutledge give way to dark-gray shale with thin calcareous siltstone interbeds. The siltstone interbeds in the upper part of the Friendship formation are generally thinner than those in the lower part of the formation, and lithologies coalesce more here. Limestone beds are commonly ribboned or wavy bedded, and some are greatly bioturbated and contain abundant glauconite pellets. Glauconite stringers commonly occur within the calcareous siltstone interbeds.

The Friendship formation consists of light-gray, micritic to coarsely crystalline thin- to medium-bedded limestone, commonly containing shale partings, that is interbedded with dark-gray or maroon shale beds. Bed thicknesses range from 0.6 to 1.5 m. The limestone is locally glauconitic, rarely fossiliferous, and evenly divided between wavy laminated and bioturbated lithologies with horizontal burrows.

The contact between the Friendship formation and overlying Rogersville Shale is abrupt and recognized by the absence of 0.3-m-thick limestone beds and the appearance of maroon shale. The contact is

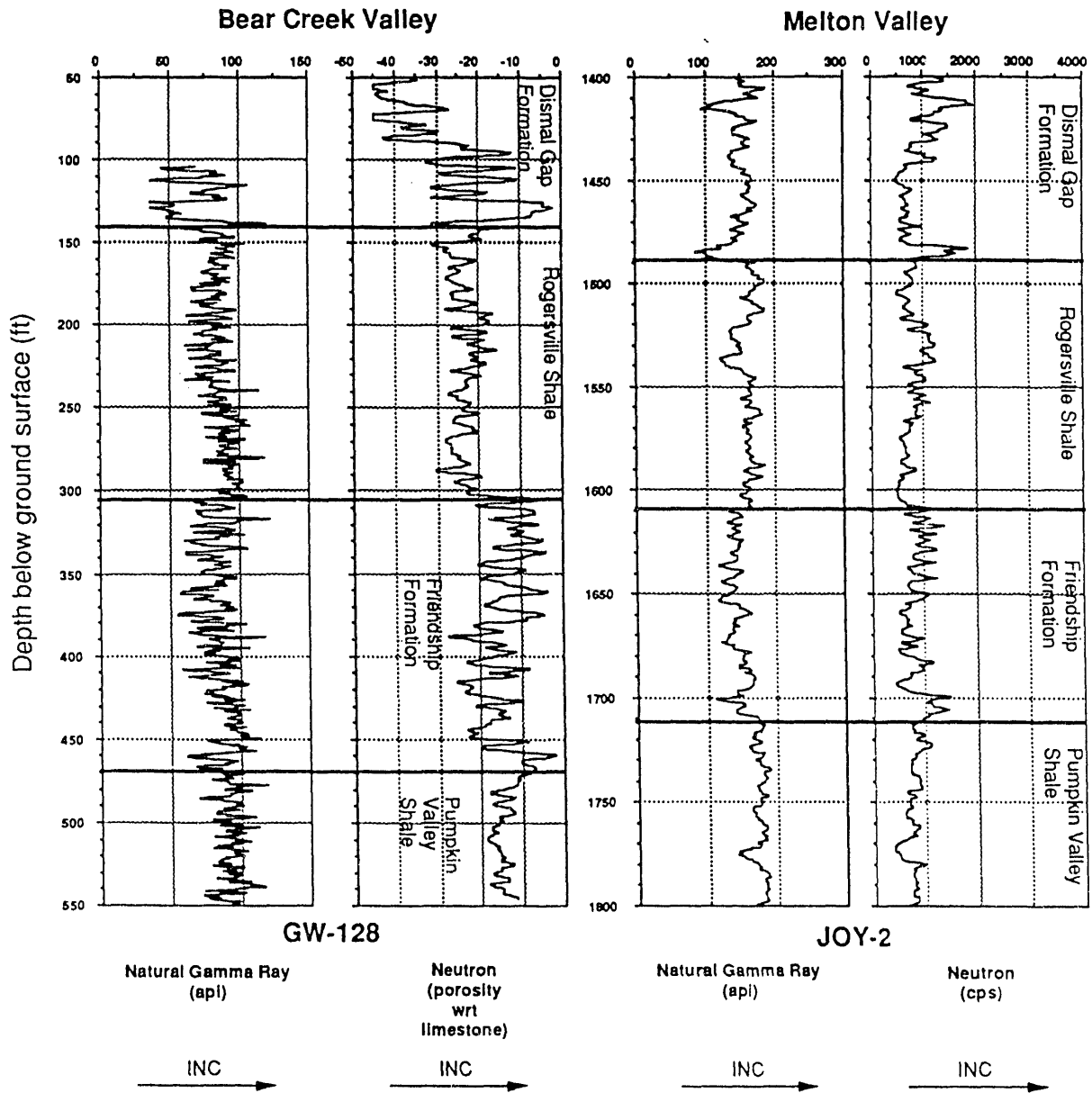


Fig. 3-5. Geophysical logs - Rogersville Shale and Friendship formation (formerly Rutledge Limestone).

placed at the top of the uppermost limestone bed. On geophysical logs, the contact is characterized by baseline shifts (locally pronounced) in both the gamma-ray and neutron logs (Fig. 3-5). These baseline shifts are associated with an increase in the limestone content of the Friendship formation relative to the Rogersville Shale. The spiked character of the gamma-ray and neutron logs suggests that limestones within the upper part of the Friendship formation occur within discrete beds, separated by more shaly intervals.

3.3.7 Friendship Formation (Formerly Rutledge Limestone) Soils

Most areas of the Friendship formation in the Bear Creek area are buried by either alluvium or colluvium. Weathering of the high calcium carbonate sections of the formation results in collapse of the residue, which is subsequently buried. The weathering of the siltstone and shale sections, with lower calcium carbonate content, forms saprolite, which has some surface exposure on low topographic highs. Friendship soils have sporadic distribution, an indication of the highly variable lithological nature of this formation in the area. The Friendship formation in Melton Valley is dominated by siltstone saprolite with thin to thick red clay seams that weathered from high carbonate content strata.

10522, 10523, 10532, 10533, 10543. These soils formed in silty and clayey saprolite that weathered from calcareous clastic rocks. The clay-enriched subsoil commonly has a 7.5YR to 5YR hue. The saprolite beneath has a wide range of colors. The loss of dusky-red saprolite and the appearance of red clayey strata mark the transition from the Pumpkin Valley to the Friendship. The disappearance of red

clayey strata and the appearance of thin shale strata mark the transition of the Friendship into the Rogersville. Coatings on fragment faces in less weathered saprolite is also utilized in formation boundary determinations in the field.

3.3.8 Rogersville Shale

The Rogersville Shale varies in thickness within ORR from 21 to 36 m (Table 3-1). Throughout much of the central belt in eastern Tennessee, a limestone-rich interval known as the Craig Limestone Member can be delineated within the upper portion of the Rogersville Shale (Rodgers 1953, Hasson and Haase 1988). The Craig Limestone Member, while recognizable in the Copper Creek thrust sheet has not been recognized in the Whiteoak Mountain thrust sheet in Bear Creek Valley (Lee and Ketelle 1989) and is not mappable on the surface as a separate unit.

The Rogersville Shale is characterized by massive to very thinly bedded non-calcareous mudstone and evenly to wavy bedded calcareous and noncalcareous siltstone. The mudstones are massively to very thinly bedded and exhibit parallel laminated to wavy to poor stratification. The lower part of the Rogersville Shale consists mostly of dark-gray mudstone. Where maroon shale occurs in the lower part of the formation, it is thinner and more chocolate-brown than the upper portion. Siltstone interbeds are gray to gray-green and exhibit wavy to lenticular to even parallel stratification that commonly contain crossbedding. Most siltstone intervals have upward-fining graded bedding with scour surfaces at the bottom and mud-draped tops. Amalgamation of two or more siltstone intervals is common. Siltstone is typically calcareous and contains abundant glauconite pellets. Glauconite partings also occur as bioturbated

beds several centimeters thick, in contrast to the much lower glauconite content of the siltstone beds in the overlying Dismal Gap formation. In the Dismal Gap, glauconite is rare, except for random disseminations in siltstones of the lowermost part of the formation. In portions of Bear Creek Valley, a medium-gray, medium-bedded limestone, which is typically glauconitic and is generally less than 0.6 m thick, may be present.

The upper part of the Rogersville Shale consists mostly of maroon shale that contains thin (less than 2.5 cm thick), wavy, light-gray, calcareous siltstone or argillaceous limestone lenses in varying amounts. Thin glauconitic partings are liberally incorporated within these lenses. The stacking of these variably colored lithologies gives the upper part of the Rogersville Shale an overall thinly laminated appearance. A distinctive reddish, massive- to thick-bedded mudstone occurs immediately below the contact between the Rogersville Shale and Dismal Gap formation. This lithology, which is 1 to 2 m thick, is persistent throughout the study area and serves as an excellent stratigraphic marker for the upper part of the Rogersville Shale.

The contact between the overlying Dismal Gap formation and the Rogersville Shale occurs at the bottom of the lowest comparatively thick limestone bed of the overlying Dismal Gap formation. Geophysically, the contact is characterized by a sharp anomaly on the gamma-ray and neutron logs (Fig. 3-5) that is associated with a prominent limestone bed. The lower part of the Dismal Gap formation is significantly more shale-rich than the upper portion (Haase et al. 1985) and resembles the underlying Rogersville Shale; thus no significant baseline shift would be expected in the logs.

3.3.9 Rogersville Shale Soils

The No. 200, No. 201, and the No. 202 soils form a weathering sequence on the Rogersville Shale, with the No. 200 soils in the least weathered class and the No. 202 soils the most weathered. The No. 200 and No. 201 soils occupy most of the surface area. The No. 202 soils have very limited extent because stable surfaces and low-gradient slopes are lacking.

3.3.10 Rogersville Residuum

20051, 20061. These soils occur almost exclusively on steep north and northeast aspects below Dismal Gap ridge tops. The saprolite beneath the soil solum ranges from light-gray to light-red siltstone and claystone and commonly contains glauconitic strata. These soils, because of the steep slopes on which they occur, generate overland flow, which removes surface soil material almost as fast as the underlying rock weathers to form soil.

20121, 20142, 20143, 20151, 20161. These soils make up the largest areal extent of soils that formed in saprolite from the Rogersville Shale. They occur on summits and side slope landforms. Severely eroded areas have lost most or all of their diagnostic morphologic features. Because of the shallow soil solum, these soils do not have much water-retaining capacity, so overland flow or near-surface flow is common, especially on dip slopes. The rougher rock surface of obsequent or scarp slopes allows for longer water residence time; therefore, more water tends to enter and move downdip along planar surfaces and gradually downward through joints and fractures.

20222, 20223. These soils formed in saprolite from steeply dipping Rogersville shales and siltstones. They have a continu-

ous Bt horizon, but of variable thickness. The Bt horizon has a yellow-brown to strong-brown color in 10YR and 7.5YR hues, in contrast to the 5YR and 2.5YR hues of Dismal Gap Bt horizons. Depth to the Cr horizon is also highly variable, ranging from less than 50 cm to more than 100 cm. These soils, of limited extent, occur only on gently sloping upland summits that were cultivated in the past.

3.3.11 Dismal Gap Formation (Formerly Maryville Limestone)

The Dismal Gap formation is informally defined here for exposures along Dismal Gap Road southeast of Eagle Bend on the Clinch River in eastern Anderson County, Tennessee (Powell quadrangle). The unit here consists of about 60 to 70 percent clastic material and 30 to 40 percent limestone. Intraclastic, oölitic, and wavy laminated limestone is interbedded with dark-gray shale. The shale typically contains wavy laminated, coalesced lenses of light-gray limestone and calcareous siltstone. The silty limestone produces a minor ridge along Dismal Gap Road as well as in Melton and Bear Creek valleys.

The Dismal Gap formation (or Maryville Limestone), is not subdivided into members throughout most of eastern Tennessee (Rodgers 1953, Hasson and Haase 1988), but a dolomite unit was recognized (Hatcher 1965) in the northeastern part of the Dumplin Valley fault zone that appears to be a western tongue of Honaker Dolomite. This dolomite occurs within the upper part of the Maryville. Within the Oak Ridge vicinity, however, the formation contains separate lithofacies that allow it to be divided, informally, into an upper and lower unit, at least within the immediate vicinity of the ORR. The Dismal Gap formation has a thickness of 95 to 158 m in the ORR (Table 3-1).

The lower unit of the Dismal Gap formation is composed of 0.15- to 0.5-m-thick beds of locally calcareous mudstone interstratified with pelloidal or oölitic calcarenite and calcareous siltstone. The mudstone is thinly bedded to thickly laminated with even to wavy parallel stratification that locally exhibits current-rippled structures and 1.5- to 5-cm-thick upward-fining siltstone-rich intervals. The limestone occurs in discrete 5- to 20-cm-thick beds in typically upward-coarsening cycles. Such cycles are similar to those observed in the overlying Nolichucky Shale except that the cycles in the Dismal Gap formation are thinner. The upward-coarsening cycles begin with calcareous mudstone. The mudstone is overlain by thinly bedded, locally calcareous siltstone and calcarenite that is evenly to wavy current-ripple stratified. Such lithologies typically comprise several amalgamated upward-fining sequences 1.5 to 5 cm thick. The upward-coarsening cycle is capped by massive to thinly bedded evenly to wavy stratified oölitic or intraclastic calcarenite. Within the lower part of the Dismal Gap formation, the upward-coarsening cycles exhibit a large amount of variability with one or more of the components of the cycle absent. A commonly observed variation is the absence of the coarse-grained oöid-bearing bed at the top of the cycle. Another commonly observed variation is the amalgamation of two or more upward-fining cycles that locally produce 0.15- to 0.5-m-thick wavy to evenly ribbon-bedded calcarenite or silty calcarenite horizons. The top of the cycle is marked by an abrupt change to calcareous mudstone. Glauconite pellets are common within the intraclastic calcarenites in the uppermost portions of many upward-coarsening cycles.

The gamma-ray and neutron logs of the lower unit have irregular baselines (Fig. 3-6). Several relatively limestone-rich

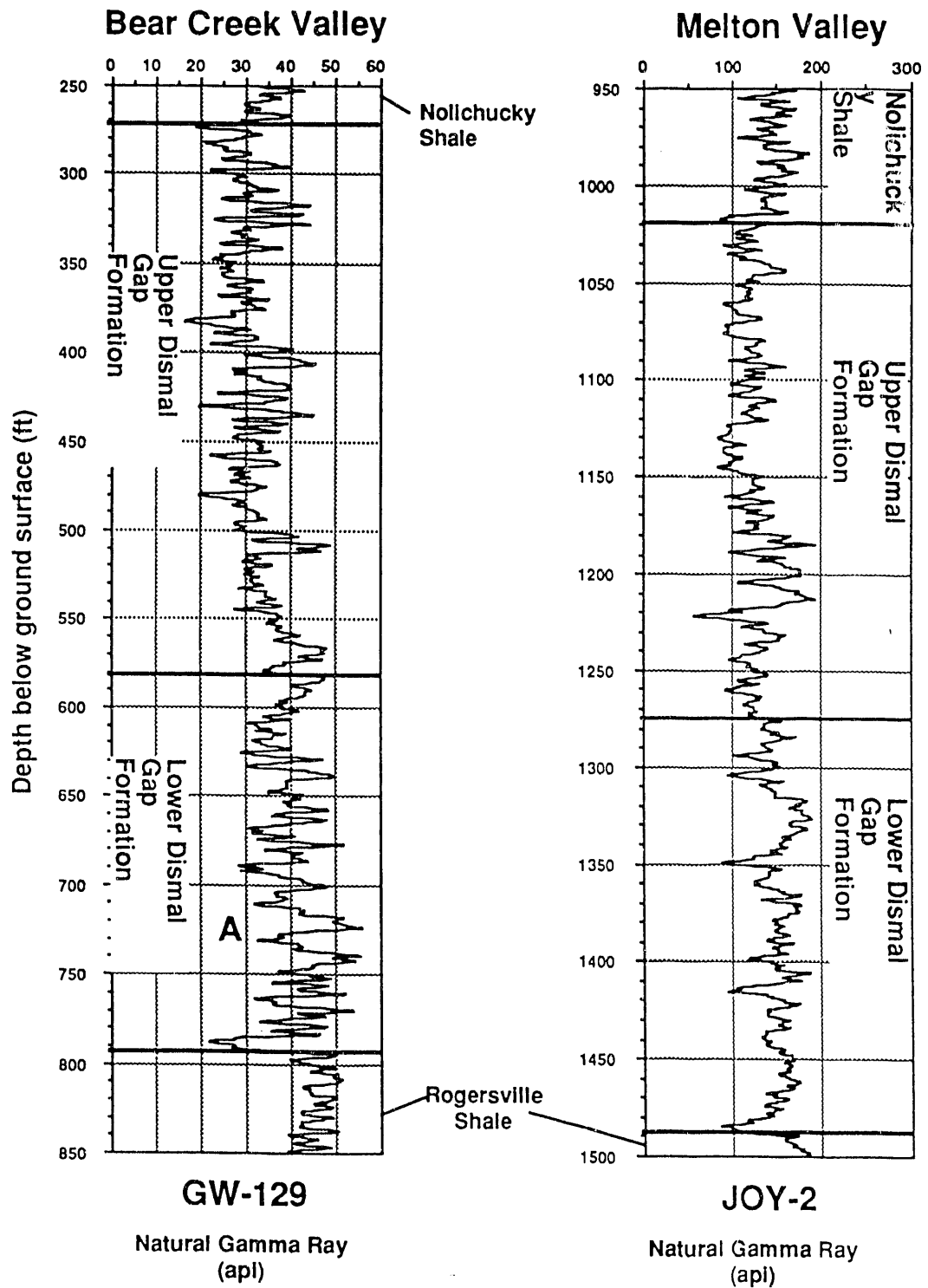


Fig. 3-6. Geophysical logs - Dismal Gap formation (formerly Maryville Limestone). Point A represents a prominent zone of limestone.

(Fig. 3-6). Several relatively limestone-rich horizons ranging from 6 to 12 m thick occur throughout the lower member (e.g., the two limestone beds at point A in Fig. 3-6). These occur throughout the study area and are a characteristic feature of the lower part of the Dismal Gap formation (Haase et al. 1985). The contact between the lower and the upper members occurs at the bottom of a slight baseline shift (Fig. 3-6). Above this horizon, the gamma-ray log shows a gradual leftward shift reflecting the greater limestone content of the upper part of the Dismal Gap formation.

The upper part of the Dismal Gap formation is characterized by the presence of distinctive flat-pebble limestone conglomerate. Such limestones are intraclastic and locally oölitic and glauconitic. Intraclastic limestones occur elsewhere in the Conasauga Group, but not in the abundance noted in the upper part of the Dismal Gap formation. Intraclastic limestones, which are locally glauconitic and rarely oölitic, typically exhibit continuous to discontinuous parallel to wavy stratification. Locally, they are wavy to lenticularly stratified. The limestones are medium gray and range from medium to thinly bedded. Interbedded with the flat-pebble conglomerate are siltstone, mudstone, and shale. The siltstone is locally calcareous and exhibits continuous parallel to wavy stratification, along with lenticular to mottled stratification patterns. The siltstone is very thinly bedded to laminated and ranges in color from gray to gray-green. The mudstone is locally calcareous and exhibits structureless to discontinuous parallel stratification. Locally the stratification becomes wavy to discontinuous parallel. Mudstone ranges from dark gray to black and is typically medium to very thinly bedded, although locally it becomes thickly bedded. Shale in the upper member is, like the mudstone,

locally calcareous. Shale stratification ranges from continuous parallel to wavy and wavy lenticular and is locally structureless. Shale ranges from very thinly to thinly bedded and is rarely thickly bedded. The shale is typically dark gray to gray-green and is occasionally black. A rare occurrence of gray to maroon-brown shale similar to that in the overlying Nolichucky Shale is present.

The upper contact of the Dismal Gap formation with the Nolichucky Shale is marked by a baseline shift to increasing gamma-ray log values (Fig. 3-6 and 3-7) and decreasing neutron log values. The contact between the formations is located where the baseline for the gamma-ray and neutron logs shifts from a constant position typical of the upper part of the Dismal Gap formation. Both the Nolichucky Shale and the Dismal Gap formation contain interbedded shale and limestone, and baseline shifts in the geophysical logs occur because the top of the Dismal Gap formation contains more limestone than the basal Nolichucky Shale (Haase et al. 1985).

3.3.12 Dismal Gap Formation (Formerly Maryville Limestone) Soils

The No. 203, No. 205, and No. 206 soils form a weathering sequence on the interbedded shale, siltstones, and limestones of the Dismal Gap formation. The No. 203 soils occupy gently sloping and stable landforms, are more highly weathered, have a deeper solum that has stronger horizonation, and a continuous clayey Bt subsoil horizon with a red 2.5YR hue. The moderately weathered No. 205 soils occur on steeper slopes or on landforms with more convexity. These soils have been periodically stripped of their upper soil horizons so that in an across-strike open trench sidewall, the Bt horizon is interrupted by either a cambic Bw horizon or

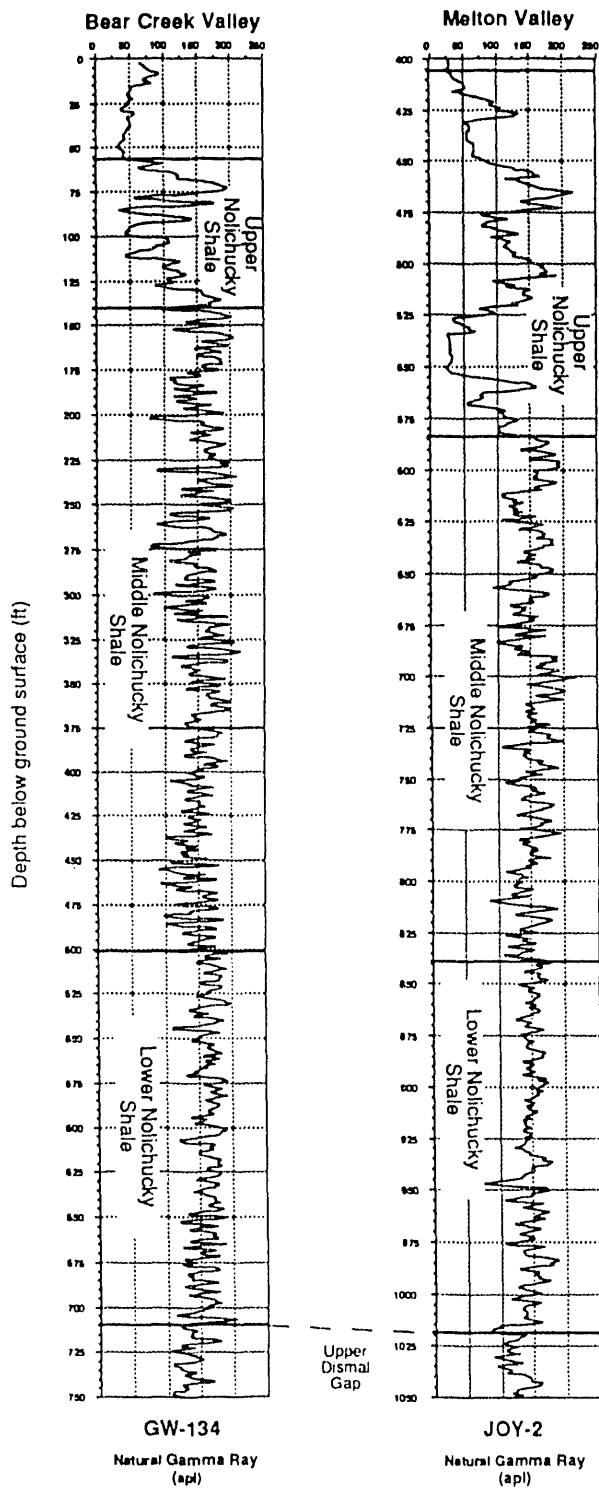


Fig. 3-7. Geophysical logs - Nolichucky Shale.

The least weathered No. 206 soils occur on the steepest and most convex landforms. They have no Bt horizon except in a few deep pockets, and soil solum thickness is usually less than 50 cm to as little as 10 cm.

The No. 204 and No. 207 soils occur only in the Solid Waste Storage Area 7 (SWSA 7) of Melton Valley. These particular soils occur on saprolite with a higher siltstone content, and have a loamy Bt horizon in contrast to the clayey Bt horizon of the No. 203 soils. The No. 207 soils are similar in morphology to the No. 206 soils but are deeper to paralithic Cr horizons and occur only on northeast to east aspects where there has been deeper penetration of water resulting in more weathering. The Dismal Gap formation contains more beds of calcium carbonate than the adjacent Rogersville and Nolichucky Shales.

3.3.13 Dismal Gap Residuum

20321. These soils formed in strongly weathered Dismal Gap saprolite. The soils have a Bt horizon with a 2.5YR hue, and the underlying upper saprolite horizons are tightly plugged by clay. These soils occur on broad upland summits with little convexity and on gentle, lower side slopes in areas of steeper topography. The saprolite under these soils is more weathered and softer than that under the adjacent No. 205 and No. 206 soils. Clay, iron, and manganese are being translocated downward in these soils. Clay plugging in the upper saprolite, however, reduces permeability so that water perches during prolonged storms and during the winter wet season. It is during these wet periods that the soil can become saturated, subsequently generating overland or near-surface lateral flow of water. These soils have limited extent.

20433, 20443, 20444. These soils formed in very acid saprolite weathered from calcar-

eous siltstone and very fine grained sandstone facies of the Dismal Gap formation. Thus far, in the mapping of the ORR, these soils only occur in SWSA 7 between the westernmost and easternmost drainage-ways that bound the site. They are similar to the No. 203 soils in morphology but lack clayey subsoil horizons. These soils occur on upland side slopes and are mostly well-drained. The Cr horizon occurs at depths of 50 to 100 cm, but is highly fractured and porous so that water does not perch except during periods of heavy rainfall. Cracks in the upper 5 to 10 cm of the Cr horizon are wide enough to admit clay-sized particles. Below this depth, only ions in solution can pass downward through the saprolite joint and fracture system into less weathered and oxidized saprolite beneath and finally into unweathered rock. Iron and manganese oxides and oxyhydroxides coat fracture and joint faces in the upper oxidized and leached saprolite zone. Three zones occur in this uppermost saprolite. The uppermost zone has a concentration of iron that coats fragment faces red or dark red. Below this is a mixed iron and manganese zone where iron coats upper surfaces of fragments and manganese coats lower surfaces. In the lower zone, manganese coats most fragments. Water flow zones in the upper saprolite can be readily identified by light grayish-brown streaks. The boundary between the uppermost oxidized and leached saprolite and the middle oxidized and partially leached saprolite seems to be the zone where the groundwater table fluctuates during the year. The middle saprolite zone may be several meters thick. The boundary between the oxidized and partially leached or unleached saprolite seems to coincide with the groundwater level below which there is little fluctuation. There are no visible coatings below the water table. The relationships between water tables, weathering properties, and refusal of split spoon

and both large- and small-diameter power augers have not yet been worked out.

These soils seem to have a high content of soil fauna, which appears to be responsible for the low bulk density and high porosity of the solum. Ants, termites, and other soil arthropods tunnel extensively throughout the soil solum. Worms seem to be absent due to very high acidity and low organic matter content.

Small areas of these soils are covered by a thin layer of colluvium, usually less than 50 cm thick. Other small areas have clayey subsoils, a reflection of the natural geologic variability in this section of the Dismal Gap formation.

20521, 20523, 20531, 20533, 20541, 20543, 20544, 20551. These soils occur on narrow summits and upper and middle side slopes with considerable convexity and are the most extensive soils underlain by the Dismal Gap formation. They formed in less weathered but highly interbedded siltstone and claystone with thin strata of argillaceous limestone and very fine grained sandstone saprolite of the Dismal Gap formation. These strata have undergone differential weathering, which increases soil variability, especially permeability in the upper saprolite. Depth to paralithic (Cr horizon) materials is highly variable, ranging from less than 10 cm to more than 100 cm over very short distances.

20641, 20643, 20644, 20651, 20661. These soils occur on steep side slopes of drainageways that are cutting headwardly through the Dismal Gap formation, or they are on highly convex shoulders and side slopes of narrow spur ridges. Most areas of these soils are located on northwest, west, and southerly aspects. These soils have a thin solum, usually less than 50 cm thick above paralithic materials. The saprolite directly beneath the solum

usually has a 2.5Y to 5Y hue, or if more weathered, has a 2.5Y to 10YR hue.

20751, 20761. The soils in these map units formed in saprolite weathered from highly fractured calcareous siltstone facies of the Dismal Gap formation. They are on steep and very steep northeast and easterly facing side slopes and have slope gradients ranging from 25 to 85 percent. Most slope shapes are doubly convex, but straight inclined segments occur between the break in the summit shoulder and the lower beginning of the foot slope. On some slopes with less past disturbance, white oak is the dominant tree species, indicating that roots of long-lived trees can extend through highly weathered and very acid saprolite into less weathered saprolite or rock that contains calcium carbonate. Calcium and other base cations are cycled to the surface by these long-lived deep-rooted trees.

The soils in these map units are similar to the No. 206 soils except that the depth to the Cr horizon ranges from about 50 cm to about 200 cm. The mid range is between 70 and 100 cm. The Cr horizon is not clay-plugged nor does it perch much water. Above the Cr horizon, shale fragments are silt- or occasionally clay-coated. Below the Cr, most paralithic, fragmented shale material is not coated with silt or clay particles but with either iron oxide (red) or manganese (black) plasma. The oxidized and leached saprolite zone is thicker beneath these soils than under the No. 206 soils. Nearly all areas of No. 207 soils are on obsequent slopes where the shale dips steeply into the slope.

3.3.14 Nolichucky Shale

The Nolichucky Shale is mappable throughout the eastern and central belts of the Conasauga Group in eastern Tennessee (Rodgers 1953). In the ORR, the

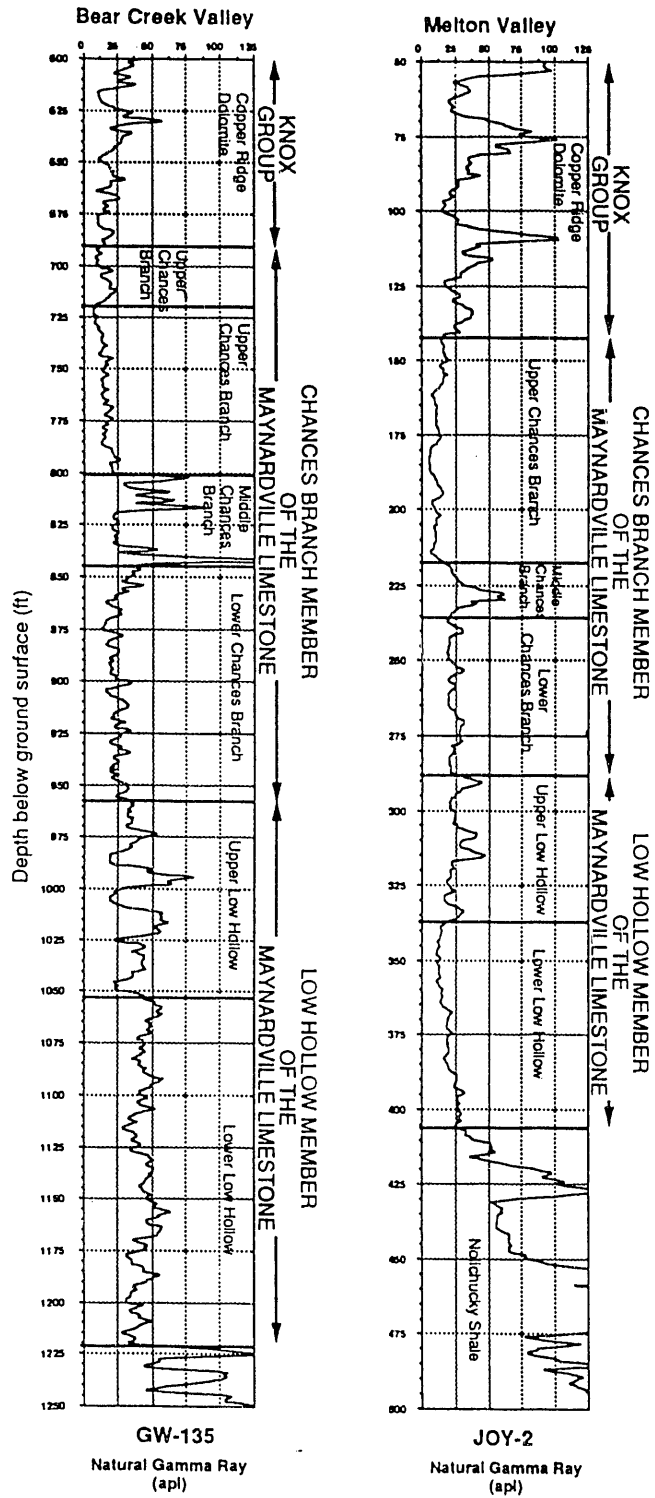


Fig. 3-8. Geophysical logs - Maynardville Limestone.

Nolichucky Shale can be informally divided into three units, based on core and geophysical log descriptions (Fig. 3-8). It ranges in thickness from 154 to 187 m (Table 3-1). Core descriptions are taken from Foreman et al. (1991), and the reader is referred to that article for a more detailed description of the Nolichucky Shale in the ORR. The subdivisions in Fig. 3-7 do not match those described from southwestern Virginia, where the Nolichucky Shale can be divided into the upper shale, Bradley Creek, and lower shale members (Markello and Read 1981). Typically, in southwestern Virginia, the Bradley Creek Member occurs toward the middle of the Nolichucky Shale and consists of shoaling-upward cyclic algal limestone. Within the ORR, however, lithologies typical of the Bradley Creek Member have not been identified. The absence of the Bradley Creek Member is interpreted to reflect a change in water depth during deposition. Nolichucky deposition in Tennessee occurred under water depths of several hundred meters (Foreman et al. 1991), whereas deposition in Virginia occurred under shallow water conditions (Markello and Read 1981, 1982).

Shale is the dominant lithology in the formation with an approximate shale-to-limestone ratio of 1:1.75. Shale intervals range from less than 2.5 cm to approximately 3 m thick. Thick shale intervals can be correlated with a high degree of confidence between wells in the Whiteoak Mountain and Copper Creek thrust sheets. Dark-gray shale is the most common, although black, dark-green, olive-green, and brown shale are also present. The darkest shale occurs in intervals where other lithologies are the least abundant. The shale has good fissility, especially in outcrop. Horizontal laminae are well preserved and are defined in thin section by the parallel alignment of clay mineral flakes and, less commonly, intercalated

glauconite and quartz-rich layers that are usually less than 1 to 2 mm thick.

Illite, chlorite, and kaolinite are the dominant clay minerals in the Nolichucky Shale (Lee et al. 1987, Weber 1988). Dolomite, the dominant carbonate mineral in the shale, occurs as euhedral rhombs with iron-depleted cores and iron-rich rims. The most common fossil debris observed in the shale consists of phosphatic, inarticulate brachiopods, as well as trilobite fragments.

The lower unit of the Nolichucky Shale is characterized by intraclastic (flat-pebble) limestone conglomerate interbedded with shale and calcareous siltstone. The conglomerate is typically less than 0.3 m thick, exhibits sharp upper and lower contacts with shale, and can be either clast- or matrix-supported. The conglomerate is polymictic at the base of the Nolichucky Shale and gradually becomes monomictic, with monomictic clasts similar to underlying interbeds of limestone or calcareous siltstone. Comparisons between the Copper Creek and Whiteoak Mountain thrust sheets show that intraclast beds are thicker in the Copper Creek thrust sheet, lime mudstone clasts and skeletal and peloidal clasts are more abundant in the Copper Creek thrust sheet, and calcareous siltstone clasts are almost nonexistent in the Copper Creek thrust sheet.

Calcareous siltstone is most common within the lower unit in the Whiteoak Mountain thrust sheet and is apparently absent in the Copper Creek thrust sheet. Siltstone beds are generally less than 10 cm thick with sharp tops and bases. This lithology occurs at the base of coarsening-upward sequences and is commonly overlaid by carbonate turbidite and intraclastic limestone debris flows. The siltstone is commonly misidentified because it is easily mistaken for laminated, fine-grained peloidal limestone. Scattered beds of fossiliferous and peloidal pack-

stone and wackestone occur in the lower unit, but they are not as prevalent as in the middle unit. Thicker beds (6 cm) of peloidal limestone in the lower unit commonly contain abundant glauconite.

The natural gamma-ray signature (Fig. 3-7) of the lower unit shows a slightly spiked character at the base that gradually becomes smoother with a relatively constant baseline. The contact between the lower and middle unit is marked by an abrupt change to greater frequency and higher amplitude spikes reflecting an increase in interbedded limestone beds. In addition, the middle unit is locally characterized by a gradually shifting baseline, possibly indicative of coarsening-upward sequences that are observed in core.

The middle unit of the Nolichucky Shale is characterized by allochthonous oölitic and skeletal packstone and grainstone interbedded with shale. The oölitic packstone is more common in the lower section of the middle unit and is usually part of a larger-scale coarsening-upward sequence. The oölitic limestone is the coarsest limestone in these sequences, with the exception of rare occurrences of intraclastic limestone. Oölitic packstone beds rarely exceed 0.3 m, and grading is generally poorly developed within these beds, although oölitic limestone may fine upward from intraclastic limestone to ripple-laminated wackestone caps. Oölitic packstone and grainstone are more abundant, and individual beds are thicker in the Copper Creek than the Whiteoak Mountain thrust sheet.

In the upper part of the middle unit, the portion of oölitic packstone (and coarsening-upward sequences) decreases and is replaced by fossiliferous and peloidal packstone and wackestone. These limestone beds range in thickness from 1 to 6 cm. In general, thicker beds are characterized by sharp tops and bases, whereas thinner beds have sharp bases

and diffuse tops.

The upper unit of the Nolichucky Shale is characterized by (1) laminated peloidal packstone, lime mudstone, and shale and (2) thrombolitic limestone overlying oölitic limestone and lime mudstone. The thickness of the upper unit can vary considerably, both along and across strike, and ranges from 11 to 54 m. Generally, an increase in thickness of this unit occurs at the expense of lower units within the Maynardville Limestone. A similar relationship between increase of shale in the upper Nolichucky and decrease in limestone in the lower Maynardville was noted in the Jefferson City and Morristown areas in the Dumplin Valley fault zone by Milici (1963) and Hatcher (1965).

Light- to medium-gray limy mudstone interbedded with shale is most common in the upper Nolichucky. Individual beds are less than 2.5 cm thick and have irregular tops and bases. The lime mudstone and shale exhibits a ribbon-rock appearance. Soft-sediment deformation features are common in the lime mudstone beds, exemplified by wavy and contorted bedding. The proportion of lime mudstone to shale increases toward the top of the Nolichucky Shale and increases from the Whiteoak Mountain to the Copper Creek thrust sheet. In addition, the lime mudstone grades up into a thrombolitic (clotted, non-laminated algal structure) limestone, indicating shallow-water deposition at the top of the Nolichucky Shale. The geophysical log signature of the upper unit is very distinctive from the middle unit (Fig. 3-7) and shows a gradual (GW-134) to abrupt (JOY-2) baseline shift to the left (more carbonate-rich) in the gamma-ray log. The baseline is punctuated by thick rightward deflections that mark the presence of shale beds.

The contact of the Nolichucky Shale with the overlying Maynardville Limestone has been described as gradational

because the abundance of carbonate-rich layers increases upward through the interval of the contact (Helton 1967, Haase et al. 1985). Examination of core data within the study area, however, reveals narrower transition. The contact can be placed directly below the lowermost massive 1.5- to 2-m-thick mottled limestone of the Maynardville Limestone, which also coincides with the uppermost occurrence of dark-gray shale containing light- to medium-gray, ribbon-bedded lime mudstone. Geophysically, this contact is placed immediately above the highest right deflection on the gamma-ray log and at the bottom of the fairly constant carbonate (Maynardville) baseline.

3.3.15 Nolichucky Shale Soils

The Nolichucky Shale in soil borings can be readily identified by the oxidized brownish-yellow or strong-brown color of the claystone and siltstone saprolite alternating with olive-hued saprolite from calcareous strata and reddish-yellow clay seams that weathered from limestone. In contrast to the adjacent and evidently more permeable Dismal Gap formation, geomorphic processes of erosion and denudation do not result in the formation of high hills and steep slopes in the less permeable Nolichucky Shale. The lower permeability of this unit may have allowed for higher overland runoff and consequently for more equal denudation over the entire landform; perhaps, freeze-thaw cycles during the late Pleistocene were more effective in reducing hilltop elevations. The combination of landform configuration and saprolite colors were the primary distinguishing characteristics used to locate the surface boundary zone between the Dismal Gap formation and Nolichucky Shale. The lower Nolichucky is interbedded with the upper Dismal Gap, and the boundary zone is identified by

interbedded olive-brown and strong-brown strata and increasing amounts of bright-red and black coatings on fragment faces. The upper Nolichucky is also interbedded with the lower Maynardville where the number and thickness of argillaceous limestone strata gradually increase.

The following No. 300, No. 301, and No. 302 soils form a weathering and drainage sequence.

3.3.16 Nolichucky Residuum

30021, 30023. These soils are on lower side slopes where overland and subsurface lateral waterflow from higher areas keeps the lower part of the soil wet during winter and spring. The upper part of Cr horizon is usually plugged by gray clay. They have a limited extent because they are usually covered by No. 221 colluvium, except at the base of long slopes where colluvial materials have been deposited farther up slope.

30122, 30123, 30133, 30143. These soils occupy summits and upper, middle, and lower side slopes. Because of favorable topography, they were cultivated in the past. Most areas, even on gentle slopes, were severely eroded. These soils have an intermittent Bt horizon with 10YR and 7.5YR hues. Clay flows in the underlying saprolite have similar colors. Fragments in the less weathered saprolite are thickly coated with black manganese or brownish-red iron compounds. Because of the relatively impermeable nature of the saprolite, the upper soil layers become saturated readily and, because of the high silt and clay content, tend to move downslope quite readily. The soils in these map units occupy the largest acreage in the area underlain by the Nolichucky Shale.

30222, 30223. These soils occur on very gentle slopes throughout the extent of the Nolichucky Shale, but they are most common in the upper portion, which contains a higher proportion of saprolite weathered from argillaceous limestone. These soils have a reddish-yellow Bt horizon. The saprolite beneath is soft, highly weathered, and clay-plugged in the upper part. Some to most areas of these soils were, at one time, covered by No. 995 alluvium and have been exhumed. A thin smear of alluvium, less than 50 cm thick, remains in some places where the elevation is less than 270 m (840 to 850 ft).

3.3.17 Maynardville Limestone

The Maynardville Limestone is recognized throughout eastern Tennessee and occurs within all three phases of the Conasauga Group (Hasson and Haase 1988). In the Valley and Ridge of northeastern Tennessee and southwestern Virginia, the Maynardville Limestone is divisible into upper Chances Branch limestone and lower Low Hollow dolomite members (Miller and Fuller 1954). In the eastern part of the central-phase Conasauga in the Rocky Valley and Dumplin Valley areas, the upper Maynardville is dominated by dolomite and the lower is limestone-rich (Bridge 1956, Hatcher 1965). Toward the southwest, in the ORR, the Maynardville is more uniformly dolomitic and exhibits more subtle vertical lithologic differentiation than that described at the type section. Thus, in the ORR, the contact between the Chances Branch and Low Hollow Members is not based on dolomite content. Within the ORR, the Maynardville Limestone varies in thickness from 79 m on the Copper Creek thrust sheet to 127 m on the Whiteoak Mountain thrust sheet. Because of waste management concerns about the influence of the Maynardville Limestone

on Bear Creek Valley groundwater flow systems, most Maynardville investigations have been—or are being—conducted in the Whiteoak Mountain thrust sheet and there are fewer Maynardville data from the Copper Creek thrust sheet (Haase et al. 1985).

The Maynardville is much better exposed on the surface in the Copper Creek thrust sheet than in the Whiteoak Mountain, possibly because of the shallower dip of the Copper Creek thrust sheet or greater dissection near the Clinch River drainage. Sections of the Maynardville Limestone with greater than 50 percent exposure are present along the northwest slopes of Copper Ridge. A particularly good section is exposed on the northwest side of Rainy Knob in the Freels Bend area of the ORR. In this area, the Maynardville consists dominantly of massively bedded fine-grained massive to ribboned limestone, some dolomitic, that in places contain a few shale partings. A 3- to 5-m section of fine-grained noncherty dolomite occurs at the top of the Maynardville beneath the contact with the Copper Ridge Dolomite.

The Low Hollow Member is generally a ribbon-bedded or mottled, fine- to medium-grained, dolomitic calcarenite with incipient stylolites and irregularly spaced beds of oölitic calcarenite. Thin lenticular beds and thin, wavy, pale-green to olive-gray shale partings commonly occur within the ribbon-bedded lithology, which imparts an overall clotted appearance to the member suggestive of an algal buildup origin. The oölitic sequences are more common at the top of the member, and the base is characterized by the massive limestone that commonly contains abundant stylolites. The natural gamma-ray signature of the Low Hollow Member reflects these distinctions (Fig. 3-8), with the lower part showing a rather stable baseline, and the upper part showing greater deflections. Generally, each leftward deflection on the gamma-ray log

corresponds to an oölitic sequence. As mentioned above, thicknesses within the lower Maynardville vary greatly, usually as a function of upper Nolichucky thicknesses. In the most extreme example observed in Bear Creek Valley, the entire Low Hollow Member is missing (Lee and Ketelle 1989).

The Chances Branch Member consists of medium to thinly bedded, buff and light-gray dolomite, ribbon-bedded dolomitic calcarenite and micrite, and medium-gray oölitic calcarenite. The uppermost Chances Branch Member consists of thickly to thinly bedded dolomite and intraclastic dolomitic calcirudite interstratified with irregularly bedded to mottled, bioturbated calcarenite that is locally dolomitic. Lenticularly to wavy laminated beds of dolomitic micrite occur throughout the mottled calcarenite. The middle section of the Chances Branch Member consists of alternating horizons of wavy to evenly ribbon-bedded calcarenite interbedded with dolomitic oölitic calcarenite. Locally, these units are also interbedded with thin (3 to 5 cm) shale beds, which are responsible for the strong rightward deflections of the gamma-ray log (Fig. 3-8). In Bear Creek Valley and Chestnut Ridge, in the Whiteoak Mountain block, the Chances Branch Member exhibits a consistently lower gamma-ray baseline than the Low Hollow Member (Fig. 3-8). This shift is not observed in the Copper Creek block and may reflect a subtle lithologic change, although, to date, these differences have not been investigated.

The contact of the Maynardville Limestone with the overlying Copper Ridge Dolomite, as mapped in the field, is gradational, occurring within the dolomite that occurs at the top of the unit. The contact in the field is marked by the sudden appearance of chert in the dolomite, particularly silicified algae and, farther up, the appear-

ance of concentrically ringed black and white oölitic chert. Also present is a thin (10 to 12 cm thick) sandstone to sandy dolomite that has been observed in a few places in the ORR.

The Maynardville–Copper Ridge contact in core and geophysical logs is identified over a 3-m-thick interval. The contact zone is marked by the appearance of mottled to irregularly bedded tan to light-brown calcarenite in the upper portion of the Maynardville Limestone. Within the contact zone, calcite content decreases from over 90 percent in the Maynardville Limestone to essentially zero in the lower Copper Ridge Dolomite, while the dolomite content increases progressively. The contact is marked principally by an abrupt change in dolomite content and in stratification patterns. There is no consistent geophysical marker that corresponds to the lithologically identified Maynardville–Copper Ridge contact. Rather, there is a change from a moderately spiked to a smooth signal either below the contact (GW-135, Fig. 3-8) or coincident with the contact (JOY-2, Fig. 3-8). The upper part of the Chances Branch Member includes both this spiked interval, where it occurs, and the interval with a smooth baseline (Fig. 3-8).

3.3.18 Maynardville Limestone Soils

The Maynardville Limestone in the ORR contains two major members. The lower member consists of argillaceous limestone interbedded with clay shale and may be considered to be part of the boundary zone between the Nolichucky and Maynardville. Distinctive soils (No. 303 and No. 304) of limited and sporadic distribution formed in this member. The upper member consists of thicker beds of noncherty carbonate that are separated by thinner strata of clayey saprolite weathered from interbedded shale and carbon-

ate. The No. 305 soils represent this upper part in the Bear Creek section, but most of the soils are buried under Bear Creek and Grassy Creek alluvium and low terrace soils. The upper member interbeds with the lowermost massive dolomite of the Knox Group Copper Ridge Dolomite. The upper part of the Maynardville Limestone is well exposed on steep lower slopes above Melton Hill Lake. In this area there are numerous rock outcrops and another soil (No. 306) was mapped.

3.3.19 Maynardville Residuum

30343, 30363. The soils in these map units formed in interbedded shale-siltstone and limestone saprolite. They also contain few to common limestone ledges. These soils are mapped only in the Melton Hill area of the ORR.

30423, 30433. These soils occur in the transition zone between the Nolichucky and Maynardville and in the lower Maynardville. They formed in acidic saprolite weathered from argillaceous limestone and calcareous claystone. The soils are deeply weathered and are more than 1.5 m to hard rock. The very sticky clay Bt horizon has a 5YR-7.5YR hue.

30521. These soils formed in thin residuum of high carbonate content limestone. The Bt horizon has a 10YR hue and high clay content. Depth to limestone is 50 to 100 cm, highly variable, with abundant pinnacles and ledges. These soils were deeply covered by alluvium in the past, but most has been removed by erosional processes of Bear Creek and its meander system.

30643, 30663. These soils formed in residuum of the upper Maynardville Limestone and are mapped only on the steep north side of Melton Hill. Ledges and rock

outcrops of limestone are abundant, but the soil between ledges formed from saprolite that contains a moderate content of highly weathered shale fragments. Most soil surfaces contain abundant chert fragments, but these fragments have been transported from higher areas. The clayey subsoil of these soils contains little if any chert. The subsoil chert content increases in the boundary zone to the Copper Ridge Dolomite.

3.4 KNOX GROUP

Robert D. Hatcher, Jr., Peter J. Lemiszki, and David A. Lietzke

3.4.1 Introduction

Safford (1869) named the Knox Group for exposures near Knoxville, Knox County, Tennessee. Ulrich (1911) was the first to subdivide the dolomite sequence. Oder (1934), Rodgers (1943), Oder and Miller (1945), Bridge (1945), Rodgers and Kent (1948), Rodgers (1953) and Swingle (1959) have refined the earlier subdivisions. Harris (1969) proposed a revision of the Ordovician Knox stratigraphy that redefined the upper Knox, raising the boundary of the Chepultepec Dolomite in the section, lowering the upper and lower boundaries of the Kingsport Formation, and eliminating the Longview Dolomite as a subdivision. Milici (1973) compared the Knox stratigraphy proposed by Harris (1969) and that of Bridge (1956), along with a detailed description of the units in nearby Knox County. Because of the ease of recognition of the standard five units in the field, we have chosen here to follow the earlier subdivisions of Bridge (1956) and Swingle (1959).

Faunal evidence indicates that the age of the Knox Group is Late Cambrian and Early Ordovician (Butts 1926, Oder 1934,

Resser 1938, Rodgers and Kent 1948). The Knox was deposited in a peritidal environment on the extensive Late Cambrian–Early Ordovician continental shelf, but the mechanism for widespread dolomitization is not clearly understood (Harris 1973, Rankin et al. 1989). It forms the principal strong (competent) unit to support the folding and low-angle thrust faulting that occurs throughout the Valley and Ridge and the Cumberland Plateau.

The Knox Group underlies Copper Ridge, Chestnut Ridge, Blackoak Ridge, and McKinney Ridge in the ORR. Surface differentiation of the Knox Group in the field is based primarily on the characteristics of weathered materials preserved in the residuum. The Knox Group in eastern Tennessee and adjacent states is divisible into five formations: the Cambrian Copper Ridge Dolomite and the Ordovician Chepultepec Dolomite, Longview Dolomite, Kingsport Formation, and Mascot Dolomite. Although complete exposures are relatively rare, the best exposure of the Knox Group in the ORR is along the CSX railroad tracks on the northeast side of Melton Hill Reservoir north of Edgemoor Road near Bull Run Steam Plant. This should be considered the standard section for the Knox Group in this area, because a nearly complete section of fresh rock is present here. All stratigraphic markers that characterize the different formations in the Knox Group have been recognized here, along with the Middle Ordovician unconformity at the base of the Chickamauga Group. (See Appendix 1, stops 2 and 3.) Total thickness of the Knox Group ranges from 700 to 1000 m (2000 to 3000 ft) in eastern Tennessee with the Copper Ridge Dolomite making up roughly one-third of the total. The thickness at the Bull Run section is approximately 720 m.

Lee and Ketelle (1987) studied the lower Knox Group rocks on Chestnut

Ridge southeast of the Oak Ridge Y-12 Plant, along with the upper Knox in the same belt toward the southeast, and were able to characterize some of the depositional environments of those parts of the Knox. A number of wells have been drilled in this part of the section, but geophysical logs in the Knox are difficult to correlate from hole to hole because of the composition of the unit (see Figs. 3-9 and 3-10 b). The lower amplitude of the gamma-ray log in the middle part of the Mascot [well GW 146 with a total depth of 70 m (220 ft), see Fig. 3-9] may indicate an increase in the limy character of the unit; in reality, the unit becomes more siliceous and dolomitic near the base. Logs in the Copper Ridge (well GW 158 with a total depth of 125 m, see Fig. 3-10) are also indistinct.

3.4.2 General Description of Soils and Landforms

Soils that formed in Knox Group residuum and are on slopes up to 25 percent seem to have thick enough clay-enriched subsoil Bt horizons and solum thicknesses to classify as Paleudults. Paleudults are soils with genetic horizons thicker than 1.5 m and are considered to be truly old soils on stable landforms. Knox Group residual soils on slopes exceeding 25 percent are mostly Hapludults. Hapludults are soils with genetic horizons less than 1.5 m thick. This reasoning is based on observations in trenches, even though laboratory data do not show much decrease in clay content. The presence of saprolite-yellow colors (a different shade of yellow than drainage-yellow mottles) and loss of most pedogenic soil structure within a depth of 1.5 m would indicate that the clay-enriched subsoil horizon terminates before the required depth for Paleudults, even though transitional BC and CB horizons beneath may be quite thick and extend for

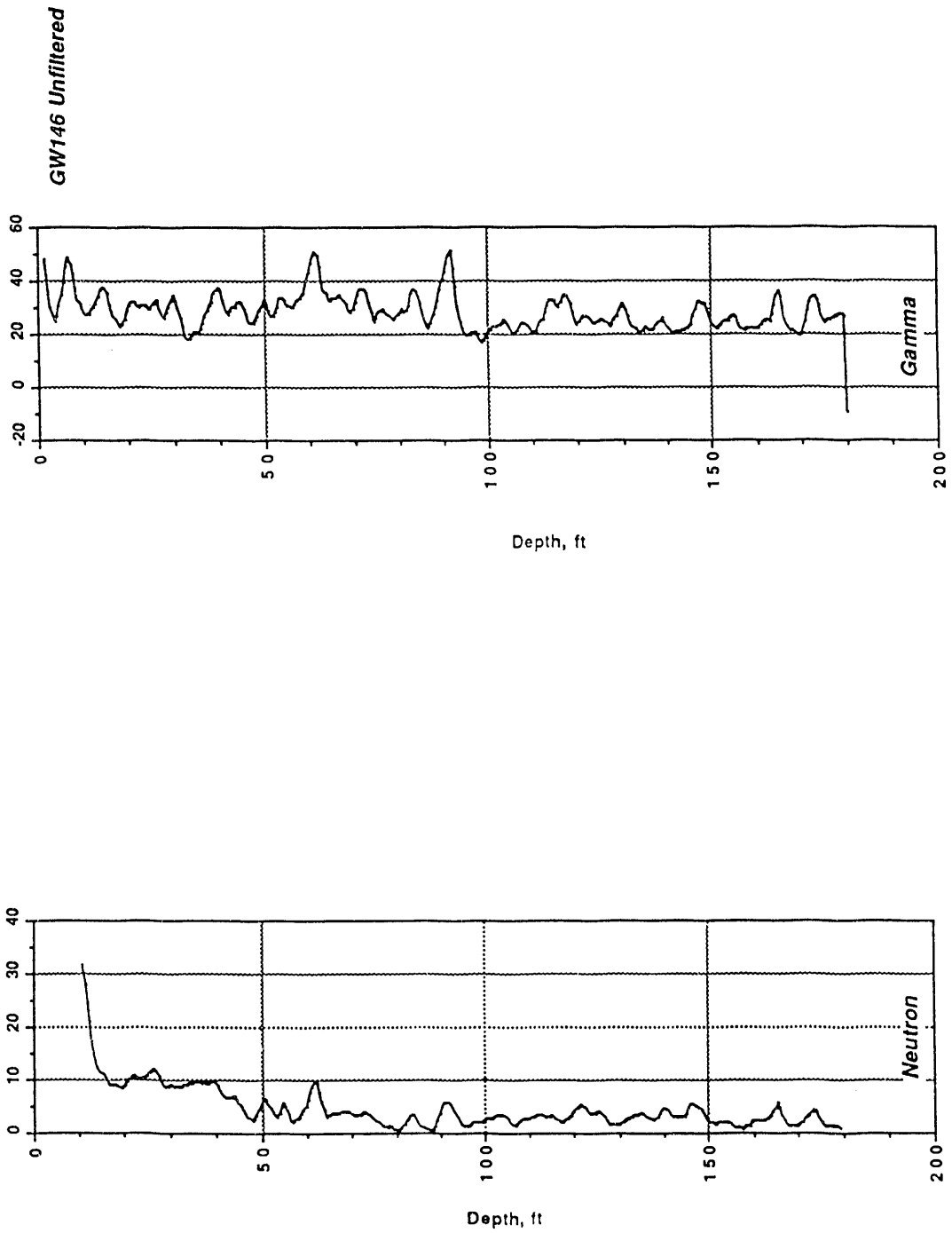


Fig. 3-9. Mascot Dolomite, Whiteoak Mountain thrust sheet, and Kerr Hollow quarry.

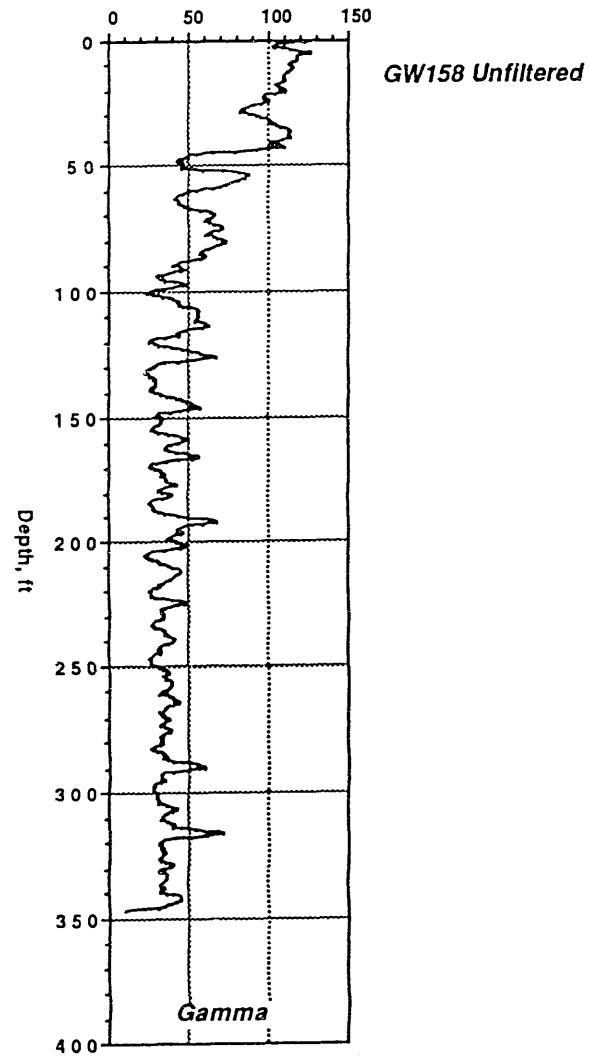
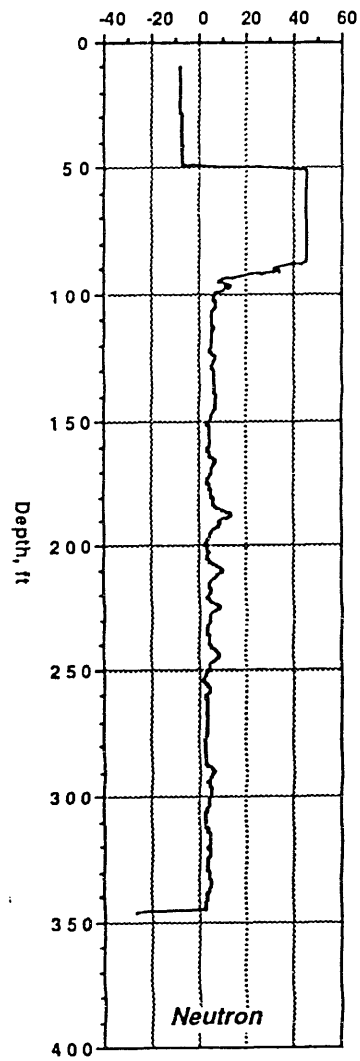


Fig. 3-10. Copper Ridge Dolomite, Whiteoak Mountain thrust sheet, and sediment disposal basin near Y-12.

many centimeters deeper. The relative thinness of genetic horizons on steeper slopes is an indicator of Pleistocene erosional processes that have partially stripped off upper soil horizons. This also explains the presence of the widespread colluvium on Chestnut Ridge and Melton Hill.

The Chestnut Ridge area encompasses all formations of the Knox Group. The Longview Dolomite, situated between the Chepultepec Dolomite and Kingsport Formation, is thin but contributes large blocks of chert, many dolomitic, which mantle the surface and have been let down as "lag" onto the uppermost Chepultepec and lowermost Kingsport. Commonly, the Longview can be identified by thick chert ledges, which have the greatest exposure on steeper west-facing slopes where drainageways have cut through. Some of the smaller chert fragments from the uppermost and lowermost Longview also have a distinctive appearance, identified by the presence of dolomolds. In the present geomorphic erosion cycle, the Longview Dolomite occupies ridge-top positions, although where ridge tops underlain by the Longview are broad enough, the surface is mantled with a thin layer of ancient colluvium, indicating that in a previous erosion cycle, the Longview was situated in a toe slope-drainageway landform. Topographic inversion occurred because the very high chert content of both the residuum and overlying colluvium preserved the soils beneath, while the adjoining less cherty soils, lacking any comparable armoring, underwent faster rates of denudation. There seems to be a higher concentration of dolines and rock ledges on Melton Hill than on Chestnut Ridge. Chestnut Ridge seems to have undergone more plastic deformation. The effects are seen in large trenches where chert strata and saprolite commonly have a swirled appearance. Doline distribution

on Chestnut Ridge appears to be more sporadic, with some areas having a high concentration and other areas having only a few dolines. Large dolines appear to be more widespread on Melton Hill, especially dolines that have orientation either parallel or perpendicular to strike. There are also more active sinkholes on Melton Hill. Large, high-elevation dolines are commonly associated with old or ancient colluvium and alluvium.

3.4.3 Copper Ridge Dolomite

The Upper Cambrian Copper Ridge Dolomite was named by Ulrich (1911) for exposures on Copper Ridge in northeastern Tennessee and southwestern Virginia. It consists dominantly of massively bedded cherty dolomite with beds ranging from 20 to 70 cm thick. The Copper Ridge Dolomite is characterized by medium- to coarsely crystalline, thick-bedded dark brownish-gray saccharoidal dolomite that gives off a fetid (petroliferous) odor on fresh surfaces. This lithology dominates the lower two-thirds of the unit, but, toward the top, the medium- to light-gray, fine-grained, medium- to thick-bedded dolomite typical of the entire Knox Group is more common. Chert is also more common in the upper part. Micritic algal limestone in minor amounts has been noted in the upper part of the Copper Ridge elsewhere in and southeast of the Mascot-Jefferson City zinc district (Bridge 1956, Hatcher 1965), but has not been encountered in either of the strike belts represented in the ORR or in core.

The Copper Ridge is a siliceous unit—a common ridge former in the Valley and Ridge—characterized by the presence of bedded oölitic chert, in which the oöids are concentrically banded with interlayered light-tan and dark-brown to black rings, with the dark rings dominant, and dark-gray to black algal cryptozoön chert that

has a waffle iron appearance on weathered bedding surfaces and resembles cabbage heads in cross section. Most of the oöids are spherical, but oval or flattened shapes are also present. Quartz sandstone beds up to 20 cm thick cemented by either quartz or dolomite are common in the upper part of the formation, particularly at the top, and a 10-cm-thick zone of sandstone may occur at the base. Other varieties of nodular and massive bedded chert may be present in the Copper Ridge that occur throughout the Knox Group. Soils commonly are cherty and colored orange to tan to light gray; noncherty soils are colored deep red. The contact with the Chepultepec dolomite is mapped at the base of a prominent sandy zone that produces abundant quartz sandstone float. The Copper Ridge is approximately 250 to 350 m (800 to 1100 ft) thick.

3.4.4 Copper Ridge Soils

40031, 40033, 40041, 40043, 40044, 40053. The soils in these map units formed in residuum of the Copper Ridge Dolomite. The residuum has high silt plus clay content and highly variable chert content. Soils of this unit are on doubly convex landforms. The A and E horizons are very cherty to extremely cherty due to lag chert left behind as fines were washed down-slope by overland flow. The underlying Bt horizons vary in chert content from about 5 to 30 percent. Some included soils that have more than 35 percent chert in the subsoil, and others are almost chert-free. The chert is commonly massive, but both oölitic and chalky types are present. The upper part of the subsoil has a uniform red (2.5YR) color and is free of yellow mottles. In some areas the lower subsoil becomes increasingly mottled in shades of dull yellow, presumably due to decreased permeability. Decreased permeability in the lower subsoil can result in the tempo-

rary perching of water and the development of gray colors along with reddish mottles.

Depth to rock is generally deep, probably more than 7 m (50 ft). Some drill holes have penetrated more than 30 m (100 ft) of saprolite before encountering rock, although, because of karst geomorphic processes in an acidic humid environment and the way carbonate rock weathers, pinnacles and ledges, either attached or detached, are a common feature of the underlying rock topography.

Surface depressions, generally referred to as sinkholes or dolines, are a common surface expression of underground collapse of caverns and solution channels. Some areas have a greater concentration of dolines than other areas. Most of the larger dolines occur on crestal landforms or at relatively high elevations with respect to ridge tops, evidence of their relatively great geomorphic age. Many of the larger high-elevation dolines are commonly associated with colluvium. They appear to be stable and do not exhibit evidence of recent activity. One or more layers of Pleistocene loess have been deposited in many broad, shallow dolines. Most dolines with active swallow holes and cave entrances seem to be situated on lower side slopes where surface and subsurface flow from higher landforms have been concentrated. More of these features are observed on Melton Hill than on Chestnut Ridge.

40151. These soils formed in residuum of the Copper Ridge Dolomite and in less than 50 cm of cherty surficial creep materials. They occur in protected shaded and cool northeast and east aspects on the north side of slopes. They have a thicker and darker A horizon and a darker and less distinct E horizon beneath than the adjacent No. 400 soils, which occur on southerly and westerly aspects. Rock

outcrops generally occur with a higher frequency in areas of these soils. The higher nutrient content of the No. 401 soils compared with the No. 400 soils is reflected in the composition of the forest vegetation, which includes canopy trees as well as the forest floor vegetation.

40951. These soils formed in residuum weathered from the lowermost Copper Ridge Dolomite and the boundary zone between the Copper Ridge Dolomite and the Maynardville Limestone. Because of the high carbonate content and lack of skeletal structure, saprolite does not commonly form. If saprolite does not form, red clayey residual material lies in nearly direct contact with rock with only a thin weathering zone 2 to 10 cm thick separating the soil from the rock. These soils occur on the lower third of the slope that forms the west side of Chestnut Ridge in Roane County and also on the lower side slopes of Melton Hill. Rock outcrops are common to dominant. The presence of long-lived red cedar is also a good indicator that carbonate rock is fairly close to the surface. Depth to rock is generally between 1 and 1.5 m, but is highly variable.

3.4.5 Chepultepec Dolomite

The Lower Ordovician Chepultepec Dolomite conformably overlies the Copper Ridge Dolomite. It was named for exposures near Chepultepec, Blount County, Alabama (Ulrich 1911). The Chepultepec is less siliceous than the Copper Ridge, and thus is a valley former between the more siliceous Copper Ridge and Longview dolomites throughout most of the Valley and Ridge of eastern Tennessee. Most of the Chepultepec is composed of light-gray, fine-grained, medium-bedded dolomite of the type found elsewhere in the Knox Group. Although other types of dolomite are present, they are less abun-

dant than the light-colored varieties.

In saprolite, the lower contact of the Chepultepec with the Copper Ridge Dolomite is marked by a change upward from a clay soil with large chert fragments to a sandy soil with large limonite-stained sandstone fragments and small oölitic chert blocks. The upper contact with the Longview Dolomite is located at the top of the less distinctive sandy soil containing occasional pieces of sandstone float and below massive float blocks of tan to white chalcedonic chert.

Dolomite weathers to orange- to red-colored clay soil with sandy streaks and scattered masses of white oölitic chert. The sandstone is composed of medium-grained quartz that upon weathering is friable, porous, and limonite-stained. The amount of limonite determines whether the color of the sandstone is white, tan, yellow, or reddish-brown.

Chert in the Chepultepec is less abundant and generally lighter in color than that in the Copper Ridge Dolomite. The Chepultepec is characterized by the presence of white oölitic chert beds, dolomoldic chert, and a prominent zone of quartz- and dolomite-cemented sandstone at the base. This sandstone ranges from 1 to 5 m thick in the ORR. Much of the chert found in float is light gray, cream, tan, and white. The chert ranges from dense to porous, and some is dolomoldic. The Chepultepec is approximately 165 to 225 m (500 to 700 ft) thick.

3.4.6 Chepultepec Soils

40221, 40222, 40231, 40233, 40241, 40243, 40251, 40253, 40261. The soils of these map units formed in thick saprolite weathered from the Chepultepec Dolomite. These soils are on upland summits and convex side slopes. Mapping units differ primarily by slope and past erosion classes. The A and E horizons of these soils have higher

chert content than subsoil horizons because of the lag gravel effect. The uppermost Bt horizon in uneroded soils has a 10YR or 7.5YR hue and a clay loam texture, but the lower clayey horizons become redder in 5YR and 2.5YR hues and the amount of bright yellowish or reddish colors from saprolite increases with depth.

40851, 40861. The soils in these map units formed in thin, very high chert content, in creep materials, less than 20 in. thick, and in the underlying residuum from Chepultepec chert beds. These soils occur only on south-facing dip slopes. Trees growing on these soils are tolerant of low fertility and drought. These soils were delineated in Walker Branch Watershed and only with high-resolution mapping. To date, only one delineation has been mapped on Melton Hill near the top of the formation.

3.4.7 Longview Dolomite

The Lower Ordovician Longview Dolomite was named by Butts (1926) for exposures near the town of Longview (now Algood), Shelby County, Alabama. It forms a prominent narrow ridge in the middle of the Knox outcrop belt in the ORR. It is the thinnest unit in the Knox Group (42 m along the railroad tracks northwest of the Bull Run Steam Plant) and is composed of medium- to light-gray, thin- to medium-bedded siliceous dolomite. The finer-grained dolomite is locally replaced by coarsely recrystalline dolomite. Bedded and nodular chert are commonly visible in fresh exposures, but the massive, porous, porcellaneous white chert that appears in weathered profiles is rare in fresh rock or core. These fragments of massive chert may be as much as 1 m or more thick and 2 to 3 m long. Rare fresh exposures also contain light-gray to white, concentrically banded chert nodules and lenses, as well as nodules of black, red,

blue, and tan chert. The base of the Longview is recognized by the appearance of tan to white oölitic chert beds (top of Chepultepec Dolomite). The Longview is approximately 40 to 65 m (130 to 200 ft) thick.

3.4.8 Longview Soils

40321, 40331, 40341, 40351, 40361. The soils of these map units formed in very cherty saprolite that weathered from the Longview Dolomite. Soils in these units occur only on narrow ridge tops and summit shoulders. The soils of the Longview Dolomite occupy a strip 16 to about 50 m (50 to 150 ft) wide. Their lateral extent cannot be mapped at a scale of 1:12,000, but they can be mapped at a scale of 1:1200. Small to large blocks of dolomoldic chert on the surface tend to help identify the presence of the Longview Dolomite, but other chert from the Kingsport Formation has also been let down onto the Longview and does not have dolomolds. Dolomoldic chert from the Longview has also been let down onto Chepultepec soils downslope, although in-place dolomoldic chert in substratum saprolite usually confirms that the soil formed in Longview residuum. Longview soils have redder upper subsoils than Chepultepec soils, while the Kingsport soils have highly weathered and soft white chert fragments in the upper red clayey subsoil. The lower subsoil of Kingsport soils is typically highly mottled. Colluvium that is derived from the Longview soils also has a very high chert content throughout, and the foot slope colluvial soils are loamy-skeletal with more than 35 percent chert by volume throughout the soil.

These soils have limited extent, but their identification can be important for some land uses where high surface and subsoil chert content is a limiting consider-

ation. Because of the high chert content, they have low water storage capacity. Trees tend to be subjected to several drought-stress cycles during the summer. Consequently, only trees that can tolerate drought stress will grow well on these soils. Longview soils have an additional problem concerning geohydrology. Chert beds tend to be zones where water moves rapidly downward. This was observed in deep soil cores and also at the large new borrow pit located on the west end of the Y-12 Plant. Chert pieces in the saprolite typically have one of three appearances: (1) the chert are surrounded by bright-red clay; (2) the chert are surrounded by highly crystalline black manganese oxides; or (3) the chert have both red clay and manganese oxides. The surrounding saprolite is yellowish-brown to olive-brown in color and has textures of silt to silty clay. In contrast, reddish saprolite always has a high clay content.

3.4.9 Kingsport Formation

The Lower Ordovician Kingsport Formation was named by Rodgers (1943) for Kingsport, Sullivan County, Tennessee, and was used first on a map of the Copper Ridge zinc district. The Kingsport Formation is composed of medium- to light-gray, fine- to medium-grained dolomite of the kind that occurs throughout the Knox Group; coarse-grained light-gray recrystalline dolomite; fine-grained, pale-pink to grayish-pink dolomite near the top; and massively bedded, mottled, calcilutite limestone near the base. Much less chert is produced from weathering of the Kingsport than from the other formations of the Knox Group. Nodular chert and some bedded chert as well as dolomite- to quartz-cemented sandstone occur in the Kingsport. Because of the amount of limestone present, however, it commonly forms a valley between ridges of Longview

Dolomite and the lower part of the Mascot Dolomite in this area. Gastropods were observed in chert float near the contact with the Mascot Dolomite. The Kingsport is approximately 100 to 165 m (300 to 500 ft) thick.

3.4.10 Kingsport Soils

40621, 40622, 40631, 40632, 40633, 40641, 40643, 40651, 40653, 40661. The soils of these map units formed in saprolite weathered from the Kingsport Formation. They have a variable chert content, although it is usually higher than 15 percent in the subsoil. Subsoil chert is quite soft and chalky and appears to be highly weathered. This chert is being transformed to kaolinite, which serves as an indicator for these soils and helps to separate them from the adjacent Longview soils. The Bt horizon is red (2.5YR hue) in the upper part and does not exhibit much evidence of degradation.

Most soils underlain by the Kingsport are generally deep to rock and have few if any outcrops. Ledges and pinnacles along with a concentration of depressions were mapped as Soil No. 407.

40751. The soils in this map unit formed in residual materials weathered from the upper Kingsport Formation. Ledges and pinnacles are close to or exposed above the surface. These soils were mapped only in Walker Branch Watershed. Except for higher chert content, they are very similar in morphology to the No. 406 soils described above.

3.4.11 Mascot Dolomite

The Lower Ordovician Mascot Dolomite was named by Rodgers (1943) for the Mascot zinc district northeast of Knoxville, Tennessee. The Mascot consists mostly of the same kinds of dolomite that occur in

the Kingsport, with greater amounts of mottled pale-pink to grayish-pink and greenish-gray dolomite in the upper part. Calcilutite limestone beds occur mostly in the upper part of the unit, but do not compose a large part of the Mascot section. Nodular and bedded chert are more abundant in the lower part of the Mascot than in the Kingsport, accounting for the tendency of the Mascot to form a ridge that is low and not as prominent as those formed by the Longview and Copper Ridge Dolomites. Jasperoid chert is also present here. Scattered white, gray, red, and tan chert nodules and pods occur throughout the unit. Thick beds of coarse-grained dolomite with scattered quartz sand grains also occur sporadically in the Mascot. Medium to thick, white chert beds occur in the lower part and near the contact with the Kingsport Formation. Dolomite- and quartz-cemented sandstone occur mostly in the lower part of the Mascot. One or more zones of chert-matrix sandstone occur at the base of the Mascot and these zones may serve as a marker that separates the Mascot from the Kingsport. Where the chert-matrix sandstone is not present, the combined unit is called the Newala Formation. The chert-matrix sandstone may locally be replaced by a quartz- or dolomite-cemented sandstone. The chert-matrix sandstone can be traced throughout the ORR, thus permitting separation of the two units.

The Mascot has the greatest variability in thickness of any in the Knox because of erosion on the Middle Ordovician unconformity. Thickness of the Mascot ranges from approximately 80 to 165 m (250 to 500 ft) in the ORR, indicating that the relief on the unconformity surface is a minimum of 70 m.

3.4.12 Mascot Soils

40431, 40432, 40433, 40441, 40442, 40443, 40451, 50453. The soils of these map units formed in residuum weathered from the Mascot Dolomite. These soils have a more intense red upper subsoil than the adjacent No. 406 Kingsport soils. In addition, the subsoil has a much more plastic consistency. The presence of sandstone fragments and chert-matrix sandstones on the surface and in the residuum serve as additional indicators that the soils are underlain by the Mascot Formation. Because of the sandstone fragments, these soils often have a higher sand content in the surface with loam or fine sandy loam rather than silt loam textures. These soils do not have any exposed rock outcrops, but carbonate rock is evidently close enough to the surface that lime-loving trees such as redbud tend to grow well. Areas with rock outcrops and exposed ledges were mapped into the No. 405 soils.

40531, 40541, 40551, 40561. The soils in these map units formed in saprolite weathered from the uppermost Mascot Dolomite. They are adjacent to soils of the lowermost Chickamauga Group. The type of chert in the Mascot (jasperoid and chalcedonic) served to identify these soils and was used to separate them from the No. 406 and 407 soils (soft chalky chert) to the north and the adjacent Chickamauga soils on the south, which contain blocky, tabular, brick-shaped chert fragments.

The presence of pinnacles and ledges, especially noticeable on steeper slopes, is a common surficial feature of the landscape. Karst depressions are a common landscape feature. The soils have a cherty or very cherty lag gravel surface and upper subsoil and highly variable chert content in the lower subsoil. Depth to rock is also highly irregular.

3.5 CHICKAMAUGA GROUP

Peter J. Lemiszki, Richard R. Lee,
Richard H. Ketelle,
Robert D. Hatcher, Jr., and
David A. Lietzke

3.5.1 Introduction

The Middle and Upper Ordovician Chickamauga Group in the ORR represents deposition on the regionally extensive disconformity at the top of the Knox Group. The Chickamauga Group underlies East Fork Valley (Oak Ridge Valley) in the Kingston thrust sheet and Bethel Valley in the Whiteoak Mountain thrust sheet (Fig. 3-11). Because stratigraphic characteristics of the Chickamauga Group differ between Bethel and East Fork Valleys, each stratigraphic section will be discussed separately. The sequences differ because displacement on the Whiteoak Mountain fault caused the juxtaposition of outer shelf against inner shelf stratigraphic sequences of the Chickamauga Group. Although the stratigraphic nomenclature used below is still provisional, these sequences have been studied in sufficient detail that the recording procedures required for proper stratigraphic classification will be accomplished in the near future.

3.5.2 Bethel Valley Section

3.5.2.1 Previous studies

Mapping of the Chickamauga Group in Bethel Valley was first performed by Stockdale (1951) in and around ORNL. In addition to field mapping, Stockdale's study included drilling 51 exploratory borings to depths of 15 to 76 m, with most holes drilled to 15 to 30 m. Most of the holes were drilled into the upper portion of the Chickamauga south of Central

Avenue. Core holes located within the ORNL security area and many of those located near roads have been destroyed. One well to the southeast of ORNL (Stockdale's well 50) and those wells between Building 1505 and SWSA 3 remain. Brief core descriptions from some of the borings accompany Stockdale's report, although the location of the recovered core is not known and the core is presumed to have been destroyed.

From October 1985 to January 1986, under the direction of R. H. Ketelle, a series of five core holes were drilled near Fifth Avenue at ORNL. Results of drilling activity were described by Lee and Ketelle (1988). The core holes formed a strike-normal transect to achieve stratigraphic overlap between holes and acquire a complete stratigraphic section. Composite geophysical logs were constructed from selected logs and combined with rock core information (Fig. 3-12), which closely approximates true stratigraphic thickness by assuming a uniform 35° dip. Borehole vertical deviation was not included in the approximation because geophysical logs indicate negligible borehole deviation from vertical.

As part of environmental restoration activities at ORNL, six core holes were drilled to nominal depths of 122 to 152 m at locations within and immediately outside the ORNL security area. The holes make up two incomplete transects, located to the west of the existing transect, to establish stratigraphic continuity. Core is in temporary storage in several locations on the ORR. Geophysical logs have been obtained from each core hole and include gamma, caliper, spontaneous potential, compensated density, neutron porosity, single-point and long-short normal resistivity, temperature, deviation, and borehole televiewer. Digital and analog copies of all geophysical logs will be provided to ORNL Environmental Sciences Division

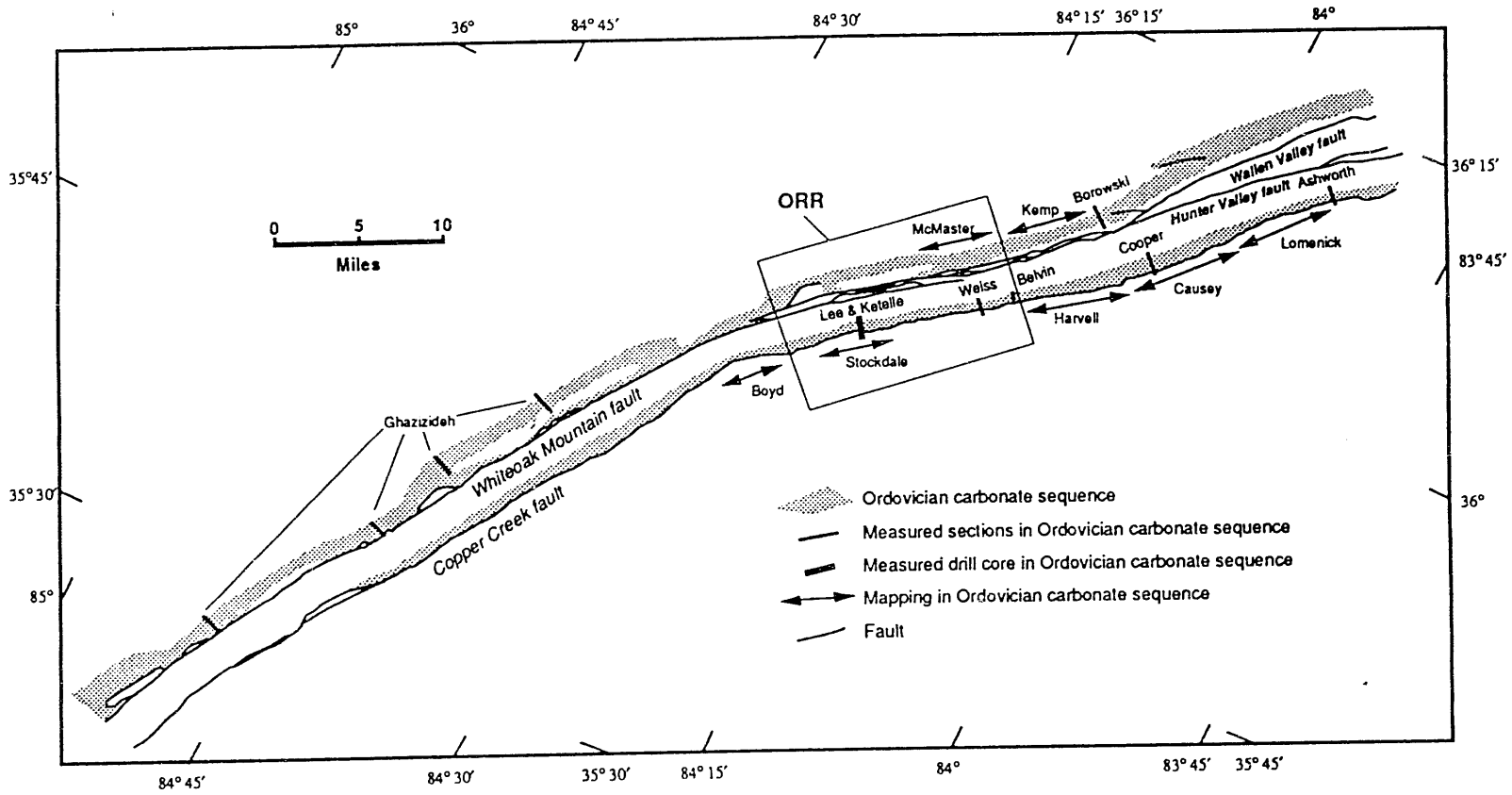


Fig. 3-11. Map of part of the Ordovician carbonate sequence outcrop belt in the Whiteoak Mountain and Kingston thrust sheets showing areas of previous work.

BETHEL VALLEY CHICKAMAUGA GROUP FORMATION NAMES,
UNIT DESIGNATIONS, AND COMPOSITE GEOPHYSICAL LOG

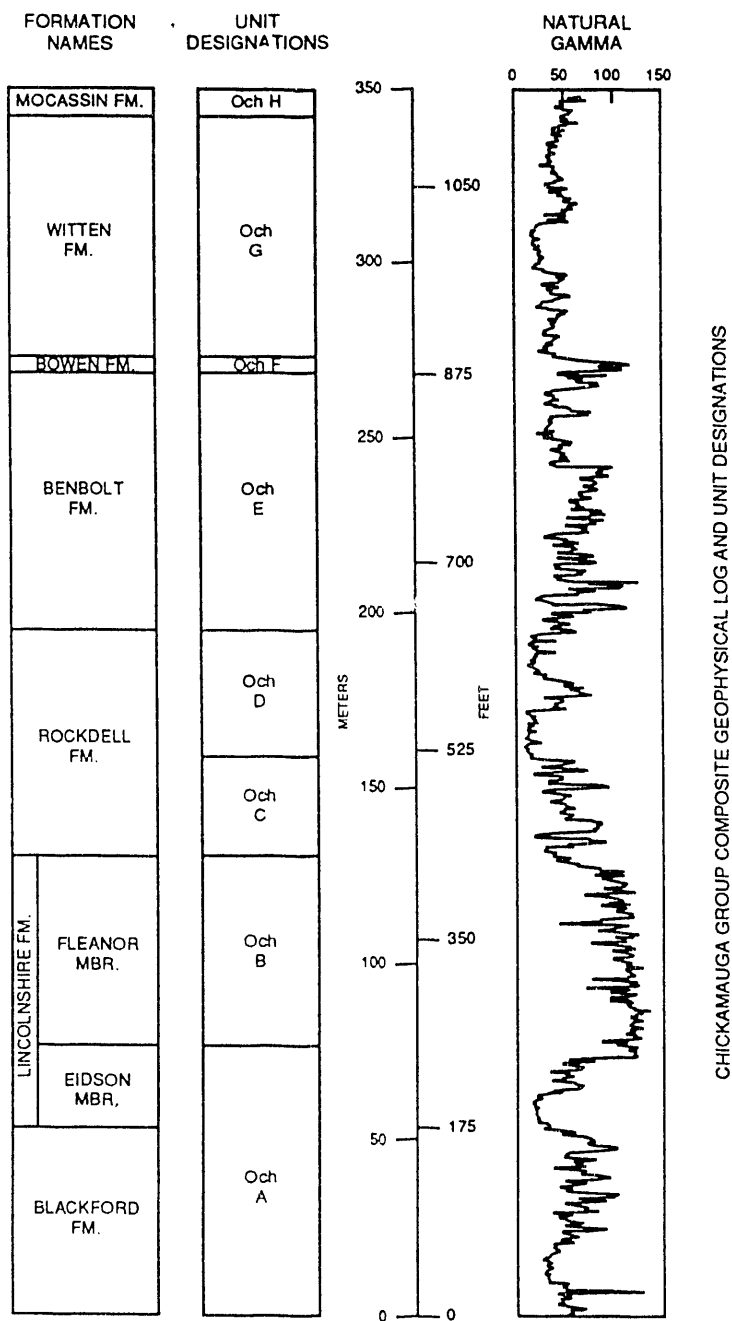


Fig. 3-12. Bethel Valley Chickamauga Group formation names, unit designations, and composite geophysical log.

staff for incorporation into the geophysical database.

As part of site characterization investigations related to the proposed Clinch River breeder reactor, core and geophysical logs from locations were obtained. Core descriptions and geophysical logs indicate that only the lower portion of the Chickamauga was studied. The core is stored in Building 7042, but despite being stored under cover, the condition of the core has deteriorated from handling. Because of undetermined quality assurance, it is likely that the core is unsuitable for use in further investigations. The location of the geophysical logs is unknown.

Lemiszki (1992) has compiled results from The University of Tennessee—Knoxville M.S. theses that studied the Chickamauga Group in Raccoon Valley, north of the Copper Creek fault and northeast of the ORR (Fig. 3-13). These theses include Harvell (1954), Boyd (1955), Causey (1956), Lomenick (1958), Fields (1960), Belvin (1975), Weiss (1981), and Ashworth (1982). Numerous other University of Tennessee—Knoxville theses dealing with Chickamauga Group rocks in adjacent strike belts provide useful insight into the lithologic variability of the units and complex paleodepositional setting, but are not included here. Walker et al. (1983) and Ruppel and Walker (1984) have also provided the regional paleodepositional context for the Bethel Valley Chickamauga Group. Results of the compilation and stratigraphic comparison indicate that, with minor lithologic and thickness variations along strike, nearly all are similar to the section in Bethel Valley.

Stockdale (1951) applied an alphabetic stratigraphic nomenclature (units A–H) to bedrock units of the Chickamauga Group in Bethel Valley similar to that adopted by Rodgers (1953) for exposures in upper eastern Tennessee and by Swingle (1964) for the Clinton quadrangle northeast of the ORR. Until recently, when attempts have

been made to adopt a formal, regional nomenclature, Stockdale's nomenclature has been used. Investigations performed on the ORR subsequent to Stockdale's have applied the alphabetic nomenclature. Recent efforts to apply regional stratigraphic nomenclature to the Chickamauga Group on the ORR have determined that nomenclature described in Virginia and eastern Tennessee may be reasonably applied to the Bethel Valley section.

3.5.2.2 Bethel Valley lithologic descriptions

Blackford Formation and Eidson Member of the Lincolnshire Formation

Butts proposed the name Blackford Formation for a series of conglomerates, redbeds, gray shales, dolomites, and chert beds that overlie the Knox Group at Blackford, Russell County, Virginia (Cooper 1956). The Blackford Formation consists of a very thin (1 m thick) purplish-maroon dolomitic limestone overlying a thin bed of pale-olive limestone, which in turn is overlain by a thick sequence of purplish to maroon siltstone. Both lower lithologies contain small, angular dolomitic intraclasts, presumably derived from the underlying Knox Group. Total formation thickness ranges from 70 to 80 m. In general, the lowermost lithologies of the Blackford are not mappable, but can be recognized in core and in a few exposures on the ORR. The bulk of the Blackford Formation consists of massive- to thick-bedded purplish to dark maroon and olive-gray calcareous siltstone interbedded with subordinate amounts of dark- and light-gray calcarenite. Dark maroon to purple, 5- to 10-cm-thick, bedded and blocky chert is diagnostic of the Blackford in the field.

In Virginia and elsewhere in eastern Tennessee, the Lincolnshire Formation is divisible into three members. In ascending

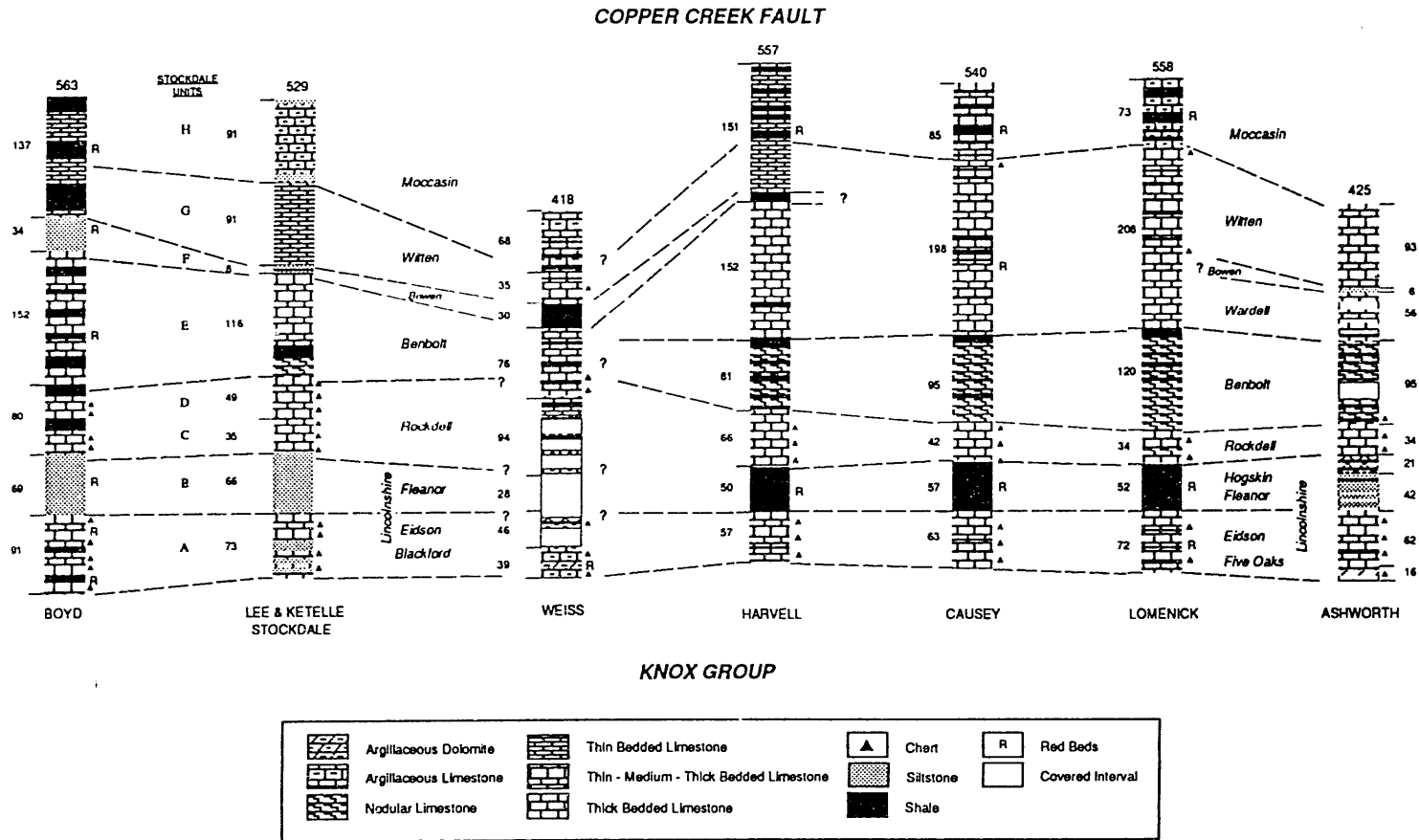


Fig. 3-13. Regional stratigraphic correlation of the Chickamauga Group in the Whiteoak Mountain thrust sheet.

order these are the Eidson, the Fleanor, and the Hogskin Members. Presumably because of lateral facies changes regionally, only the Eidson and Fleanor Members are recognized on the ORR. The Eidson type section is located north of Eidson, Kyles Ford, Virginia (Cooper 1956). The Eidson Member of the Lincolnshire Formation is a relatively minor limestone unit in the ORR with limited outcrop exposure, but it provides a sharp contrast to the maroon siltstones of the underlying Blackford Formation. In core, the Eidson Member is 20 m thick, but its thickness may vary laterally on the ORR. It consists of massive to nodular limestone with bedded and nodular chert near the top. The Blackford Formation and Eidson Member constitute Unit A in Stockdale's nomenclature.

Fleanor Member of the Lincolnshire Formation

The name Fleanor was proposed by Cooper and Cooper (1946) from exposures near Fleanor Mill near Heiskell, Tennessee. The Fleanor Member of the Lincolnshire Formation is a thick accumulation (75 to 80 m) of maroon, calcareous, and shaly siltstone with numerous light-gray limestone beds. Vertical burrows and general bioturbation are common. The lowermost and uppermost portions of the Fleanor consist of thick, olive-gray calcareous siltstone in contrast to the overall maroon siltstone that characterizes the unit. The introduction of thicker limestones and subordinate maroon siltstones higher in the section that constitute the Hogskin Member of the Lincolnshire Formation are not recognized on the ORR, and the entire maroon siltstone section is referred to as the Fleanor. The Fleanor corresponds to Unit B in Stockdale's nomenclature.

Rockdell Formation

The type section for the Rockdell Formation is near Elk Garden, Russell County, Virginia (Cooper 1945). A thick section of limestone, the Rockdell Formation, overlies the Fleanor. The Rockdell is 80 to 85 m thick and underlies the continuous low ridge near the middle of Bethel Valley. The lower portion of the Rockdell contains light-gray calcarenite, dark-gray calcareous siltstone, fossiliferous nodular limestone, and birdseye micritic limestone. Small chert nodules are common, and evidence of vertical burrowing has been observed. This lower lithology grades upward to dense calcarenite, which contains subordinate amounts of birdseye micrite and nodular limestone. The common occurrence of bedded and nodular chert is distinctive of the upper portion of the Rockdell. The lower and upper lithologies are of nearly equal thickness. The Rockdell limestone can be seen in old Rogers Quarry on the ORR. The lower and upper lithologies of the Rockdell are Units C and D, respectively, in Stockdale's nomenclature.

Benbolt Formation

This formation was defined by Cooper and Prouty (1943) for exposures in Virginia. The Benbolt Formation is a relatively heterogeneous formation that is 110 to 115 m thick. The Benbolt consists of thick interbeds of fossiliferous nodular limestone; unfossiliferous, amorphous micrite within a dark-gray siltstone matrix; dark-gray siltstone; and unfossiliferous calcarenite. A pale buff color is characteristic of weathered Benbolt rock fragments that are seen in vegetatively barren areas. Rock core and geophysical logs show that limestone content increases in the upper 23 m, which is indicative of the overlying Wardell Formation. The greater limestone content, however, is insufficient to be used

as a mappable unit. Therefore, although the Wardell may be present on the ORR, it is not mapped separately. The Benbolt corresponds to Unit E of Stockdale.

Bowen Formation

The Bowen Formation was named by Cooper and Prouty (1943) for exposures in Bowen Cove, Tazwell County, Virginia. The Bowen Formation is a maroon unit that overlies the lower thick limestone of the Benbolt and is a reliable marker for field and subsurface correlations. The Bowen is 5 to 10 m thick and consists of maroon calcareous and shaly siltstone and thin beds of light-gray to olive-gray limestone and argillaceous limestone. Vertical and horizontal burrows are prevalent throughout the unit. The Bowen underlies a very minor, discontinuous ridge in the southeastern portion of Bethel Valley. Stockdale referred to the Bowen as Unit F.

Witten Formation

The Witten Formation was proposed by Cooper and Prouty (1943) for limestones overlying the Bowen Formation in Virginia and eastern Tennessee. The uppermost limestone-dominated unit in the Chickamauga Group in Bethel Valley is the Witten Formation, which is 105 to 110 m thick. In many respects, the lower Witten resembles upper Benbolt, and, without the presence of the maroon Bowen between, the Witten and Benbolt might otherwise be mapped together. The Witten consists of interbedded nodular limestone; calcarenite; amorphous, thin-bedded limestone and siltstone; and wavy limestone. Extensively bioturbated beds and beds with numerous bryozoa are distinctive of the upper part of the Witten Formation. Much of the Witten is exposed along the interchange road cut connecting

Bethel Valley Drive with Edgemoor Road. The Witten constitutes Unit G of Stockdale.

Moccasin Formation

Because it was largely removed by the Copper Creek fault, the Moccasin Formation (Cooper 1956) is not fully represented on the ORR. For the same reason, its thickness varies from 100 to 170 m. Although Stockdale reported 104 m of the Moccasin on the ORR, subsurface investigations have not encountered a complete section of the formation. The Moccasin is recognized as olive- to light-gray and pale-maroon calcareous siltstone interbedded with light-gray, fine-grained limestone. Haase et al. (1985) described the upper 24.38 m of the Moccasin as interbedded maroon-gray, calcareous siltstone; gray to maroon-gray, shaly limestone; and maroon mudstone. Weiss (1981) described as much as 64 m of the Moccasin along the road cut on the southwest corner of Solway Bridge. The Moccasin represents Unit H of Stockdale.

3.5.3 East Fork (Oak Ridge) Valley Section

The Chickamauga Supergroup in the Kingston thrust sheet of East Fork Valley (Oak Ridge Valley) consists almost entirely of limestone-dominated lithologies and lacks the calcareous redbed units present in Bethel Valley (Fig. 3-14). Comparisons indicate that the East Fork Valley (Oak Ridge Valley) section is amenable to the application of the middle Tennessee Stones River and Nashville Groups and younger units stratigraphic nomenclature of Wilson (1949) to the eastern Tennessee-Northern Georgia region by Milici and Smith (1969).

3.5.3.1 Previous studies

The entire Middle to Upper Ordovician sequence is preserved in the footwall of

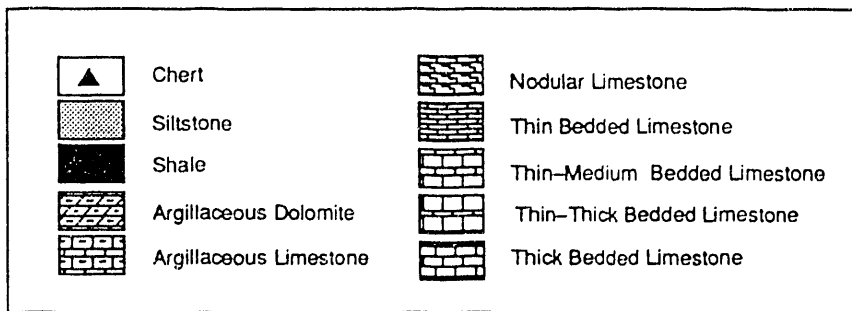
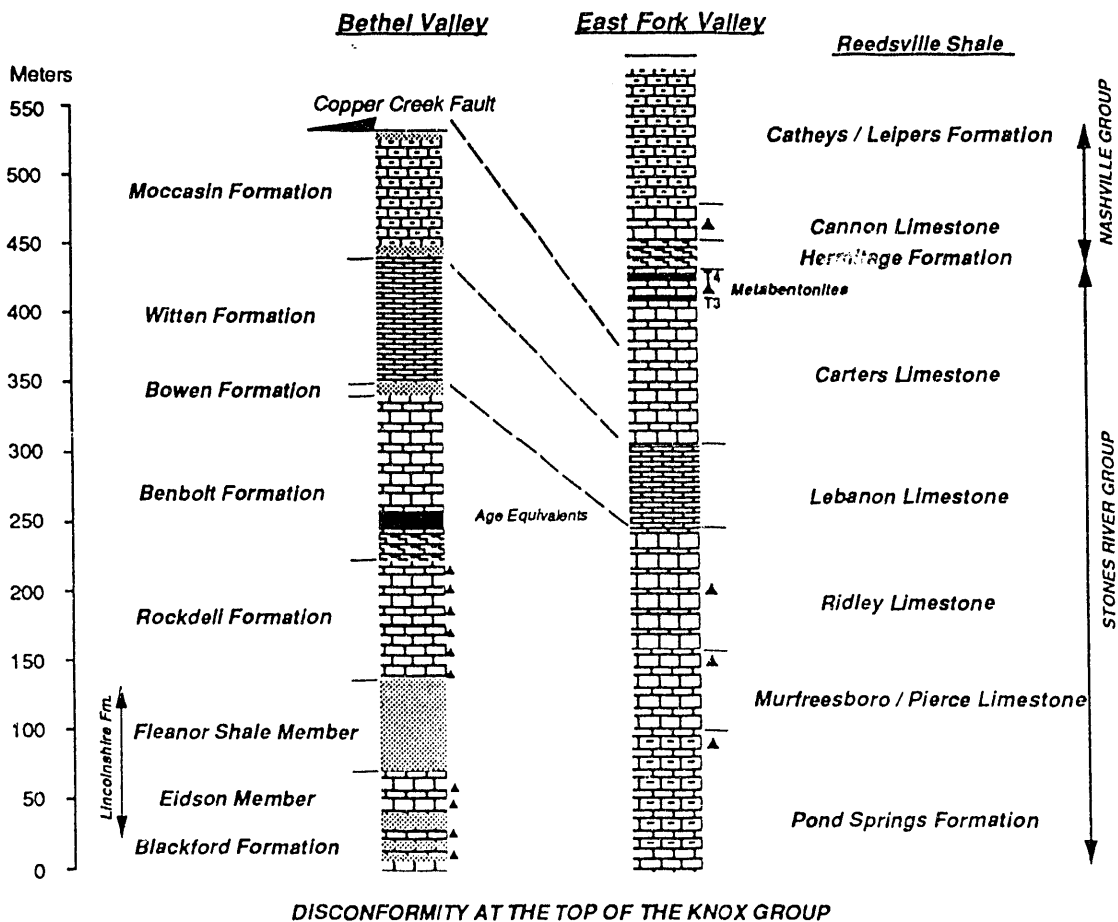


Fig. 3-14. Comparison of the dominant stratigraphic characteristics and stratigraphic nomenclature used between the Bethel Valley and East Fork Valley Chickamauga stratigraphy.

the Whiteoak Mountain fault and is approximately 575 m thick. Surprisingly, the sequence in this strike belt has not been as extensively studied as the belts towards the southeast where the sequence is often incomplete (Fig. 3-11). Previous workers in the area were able to subdivide the sequence on the basis of lithologic characteristics (Kemp 1954, McMaster 1957, Borowski 1982). Borowski (1982) described the metabentonites in the Carters Formation, but did not attempt to divide the section into formations. Ghazizideh (1987) applied middle Tennessee stratigraphic terminology to the units in four measured sections to the southwest of the study area, but did not describe the basis for the subdivision. His stratigraphic descriptions did not identify some of the major marker beds, such as the metabentonites. R. L. Wilson (1986) mapped the Ooltewah quadrangle farther to the southwest of the work of Ghazizideh and was able to identify the formations of the Stones River and Nashville Groups, which raises the Chickamauga to supergroup status in eastern Tennessee (Milici and Smith 1969). Milici (1991, Va. Geol. Surv., pers. comm.) mapped in the same strike belt on the Watts Bar Reservoir and was able to use middle Tennessee stratigraphic characteristics and marker beds to identify the formations of the Stones River and Nashville Groups. The same stratigraphic characteristics with little modification were used to identify the formations in East Fork Valley. Lithofacies analysis indicates that the carbonate sequence was deposited in a tidal flat and subtidal-lagoonal environment on a gently sloping platform-shelf environment (Ghazizideh 1987).

3.5.3.2 East Fork (Oak Ridge) lithologic descriptions

Stones River Group

The Stones River Group was named by Safford (1851) for exposures along the Stones River in Rutherford County, central Tennessee.

Pond Spring Formation. The Pond Spring Formation was named by Milici and Smith (1969) for exposures in northwestern Georgia. It was deposited on the Knox disconformity. A basal conglomerate of light greenish-red, fine-grained dolomite with thin- to medium-bedded, light greenish-gray, fine-grained limestone or lenses of shale and sandstone has been reported locally (Borowski 1982, Wilson 1986), but has not been observed to date during mapping of the ORR. The lower part of the formation is fairly well exposed in an abandoned quarry on the Reservation and consists of fine-grained, light-gray, thick-bedded, micritic limestone. The middle member of the Pond Spring is a thick-bedded micritic limestone. The upper part of the formation consists of greenish-gray, grayish-red, micritic limestone and mudstone. The limestone can range from thin to thick bedded, and the mudstone is commonly mottled. The lithologic sequence and general thickness of these members of the Pond Spring resemble the lower portion of the Chickamauga (Units A and B) in Bethel Valley. Thin beds of porcellaneous chert occur throughout the formation. The formation varies in thickness between 100 to 160 m (300 to 500 ft), because deposition occurred on the topographic highs and lows of the Knox disconformity.

Murfreesboro/Pierce Limestone. The Murfreesboro Limestone was named by Safford and Killebrew (1900) for exposures in and around Murfreesboro, Rutherford

County, Tennessee. The Murfreesboro Limestone has a gradational contact with the Pond Springs Formation that consists of thin to massive beds of maroon, green, and gray micrite. The rest of the unit is composed of well-defined thin to medium beds of micritic and fine- to medium-grained limestone. Some thick beds occur throughout the Murfreesboro, but they are not as abundant as in the overlying Ridley Limestone. The limestones are commonly medium to dark gray and fossiliferous. Some grayish-yellow argillaceous limestone and thin zones of greenish-gray calcareous shale are also present. The top is a persistent zone of nodular, ropy, and medium-bedded gray chert with silicified fossils. The Murfreesboro Limestone ranges from 58 to 76 m (180 to 250 ft) thick.

The Pierce Limestone was named by Safford (1869) for exposures at Pierce's Mill in Rutherford County, central Tennessee. It consists of fine-grained, gray, thin-bedded, flaggy to shaly limestone. Wilson (1949) indicated the thickness of the Pierce ranges from 6 to 9 m in several measured sections in central Tennessee. It occurs in East Fork Valley only as a thin shaly to flaggy interval at the top of the Murfreesboro or base of the Ridley Limestone that could not be mapped continuously. Consequently, it was mapped with the Murfreesboro Limestone (Plate 1).

Ridley Limestone. The Ridley Limestone was named by Safford (1869) for exposures in Rutherford County, Tennessee. The most distinctive feature of the Ridley Limestone is the predominance of medium to thick massive beds. Near the base the limestone is micritic and medium-grained, with occasional tan-brown dolomite splotches filling burrows. Coarser-grained, fucoidal limestone in thick beds is characteristic of the Ridley. The limestones are medium to dark gray and can give off a fetid (petroliferous) odor. Black, nodular chert is common. The Ridley

Limestone is approximately 88 m thick.

Lebanon Limestone. The Lebanon Limestone was named by Safford and Killebrew (1900) for exposures near Lebanon, Wilson County, Tennessee. The limestone is medium to dark gray and ranges from micrite to medium-grained. Very fossiliferous and bioturbated, thin to medium beds predominate with some thicker beds in the middle of the unit. Argillaceous or dolomitic fucoids are common, and brachiopods and bryozoa are abundant. The contact with the Ridley Limestone is drawn on a change from thick massive beds to thin to medium beds. The Lebanon Limestone is approximately 60 to 69 m thick.

Carters Limestone. The Carters Limestone was named by Safford (1869) for exposures along Carters Creek in Maury County, Tennessee. The Carters Limestone consists of upper and lower members separated by the T-3 metabentonite. The lower part of the Carters Limestone is medium- to dark-gray, thin- to thick-bedded, fossiliferous micrite. A prominent, dark-gray to black chert bed immediately underlies the T-3 metabentonite at the top of the lower member, and this chert bed serves as a reliable field indicator. The T-3 metabentonite occurs in a number of places as a fissile light-green to maroon shale. The upper member of the Carters is generally thin to medium-bedded calcilutite with minor amounts of calcisiltite and fine-grained calcarenite. The rocks weather to a light-gray to pale-buff color, and mud-cracks and burrows are common. Fauna are generally absent. The T-4 metabentonite occurs near the top of the Carters. The Carters Limestone is approximately 128 to 137 m thick.

Nashville Group

The Nashville Group was named by

Safford (1851, 1869) for exposures within the city of Nashville. The age of the Nashville Group is Late Ordovician.

Hermitage Formation. The Hermitage Formation was named by Hayes and Ulrich (1903) for exposures near the Hermitage community in Davidson County, Tennessee. It consists of argillaceous calcilutite to sandy argillaceous limestone to coarse-grained calcarenite in beds that are poorly defined due to bioturbation. It is olive-gray and light-gray, nodular, argillaceous micrite. The formation is poorly bedded and locally very fossiliferous. Faunal diversity is characteristic of the Hermitage. The Hermitage is approximately 20 m thick.

Cannon Limestone. The Cannon Limestone was named by Ulrich (1911) for exposures in Cannon County, Tennessee. A type section was designated by Bassler (1932) in Cannon and Rutherford counties, Tennessee. The Cannon is poorly exposed in the ORR, but where observed it is a thin- to medium-bedded, dark-gray calcilutite to calcarenite. It commonly consists of medium- to dark-gray, fossiliferous, medium-bedded limestone. Diverse fauna occur in some beds, and nodular and lenticular chert is common. The Cannon Limestone is approximately 27 m thick.

Catheys and Leipers Formations. The Catheys Formation was named by Hayes and Ulrich (1903) for exposures along Catheys Creek in Lewis and Maury counties, Tennessee. The Catheys Formation is argillaceous, yellowish-gray to medium-gray, fossiliferous, thin- to medium-bedded micrite and occasionally coarse-grained. Shale partings and float blocks of greenish-gray calcareous siltstone are common. It contains laminated to thin-bedded calcilutite and calcisiltite that weathers buff-colored and irregularly

bedded fossiliferous limestone with shale partings. The Leipers Formation consists of fossiliferous, thin- to thick-bedded, argillaceous, micritic limestone. It could not be mapped as a separate unit because exposures are rare. The Catheys and Leipers Formations range from 98 to 138 m thick.

3.5.4 Chickamauga Group Soils

The youngest group of rocks in the survey area is the Chickamauga Group. The soils are mostly Hapludalfs with some Hapludults. The brick-shaped tabular chert that litters the ground surface serves to differentiate this group from the uppermost Knox Group soils. The Fleanor member of the Lincolnshire Limestone consists of maroon mudstone and interbedded limestone but lacks chert. This unit has distinctive reddish, very shallow, and extremely eroded soils. Very severely eroded soils are Orthents, soils without diagnostic subsurface genetic horizons, while less eroded soils are mostly Hapludalfs. Vegetation is dominated by red cedar and Virginia pine. The Rockdell Formation consists of gray limestones and has shallow soils that classify as either Hapludalfs, Argiudolls, or Rendolls. These soils have high clay content in the subsoil and a dark surface layer. The Rockdell also contains cherty limestone that occurs in elongated landform knobs. The soils are deeply weathered and are Hapludults or Paleudults. The Benbolt Formation consists of a mixture of calcareous mudstones and limestones and occupies low topographic position in the broader landscape. Most outcrops of the Benbolt occur southeast of Bethel Valley and New Zion Patrol roads. The soils are mostly Hapludalfs and Argiudolls. Benbolt soils have been tentatively identified on the north side of Whiteoak Mountain fault. The Bowen Formation, although narrow and not mappable, can be located

because it occupies a slightly elevated ridge and has a reddish soil. The Witten and Moccasin Formations occur on the northwest lower slopes of Haw Ridge. The Copper Creek fault is visible along most of Haw Ridge, where it occurs quite high on the slopes. There is a sharp change in slope gradient from the steep Rome to the less steep Chickamauga at the fault contact. A thin veneer of Rome colluvium, commonly less than 30 cm (12 in.) thick, usually covers the actual location.

The Whiteoak Mountain fault marks the location where the Rome Formation has been thrust over the Chickamauga on the north side of the ORR. The fault zone in the Rome can be identified by the presence of fault breccia, in which soils with fairly thick clayey subsoils have formed and depth to paralithic saprolite is deep. The Chickamauga below the fault is different from the Chickamauga on the south side of the survey area. It seems to have a higher siltstone and shale content and commonly contains chert. Most of the soils are underlain by Cr horizons and not lithic limestone rock. The Pond Spring Formation in the Oak Ridge K-25 Site area is extremely heterogeneous. Depending on bed thickness and mapping scale, several distinctive soils are mappable. The upper Murfreesboro contains a thick chert bed that approaches 70 m (200 ft) in thickness. This northern slice of the Chickamauga appears to contain the Benbolt and younger formations of the Chickamauga. More definitive information will be available after soil mapping has been completed in the K-25 area.

3.5.5 Chickamauga Residuum

Residual soils in the Chickamauga are identified by their distinctive morphology and parent materials. They are further separated by whether they are underlain by hard rock or softer paralithic Cr materi-

als. Soils in this section are listed first, by which unit they are in, and second, whether they are underlain by hard rock at depths less than 1 m (40 in) or rock or paralithic saprolite at depths of more than 1 m (40 in). If the first symbol of the three-digit soil series is a "5" symbol, it designates soils shallow to hard rock, while the "6" symbol indicates deeper soils.

60041. The soils in this map unit formed in reddish clayey residuum of the Five Oaks Formation. These soils occur in ridge-top landforms close to the Knox contact. A mixture of lag chert from both the Knox and Chickamauga occurs on the soil surface. The subsoil is a red sticky clay or silty clay with very little chert. These soils are very similar to the No. 601 soils described below, but have much less lag chert in the upper soil horizons and less to none in the subsoil beneath. Soils in this map unit classify as Typic or Ultic Hapludalfs: fine, mixed and thermic. These soils have limited extent.

60141, 60143, 60151. The soils in these map units formed in cherty saprolite of the Five Oaks Formation. The chert in the Five Oaks Formation has a tabular shape, about the size of bricks, that helps in the identification of these soils and their separation from the uppermost Knox No. 404 and No. 405 soils. These soils usually have cherty or very cherty Five Oaks Formation and Benbolt Formation horizons. The clayey subsoil beneath has variable chert content and ranges in color from 2.5YR-hued reds to 5YR reddish yellows. Ledges and pinnacles of limestone are fairly close to the surface, but there are very few outcrops of rock except on very steep slopes.

50031, 50033, 50043, 50044. The soils in these map units formed in saprolite that weathered from the Fleanor Member of the Lincolnshire Limestone, which consists of

red or dusky-red calcareous shales and siltstones with red and dark-gray limestone strata. These soils have a dark loam or silt loam surface that usually contain some Five Oaks chert fragments. The Bt horizon is red or dark red and has a high clay content. The clay in these soils is also very sticky. Depth to Cr in the shaly material is extremely variable, ranging from less than 25 cm (10 in) to more than 1 m (40 in) over a very short distance. Where limestone occurs, a lithic contact is encountered. Some areas of these soils are severely or very severely eroded. In these areas there are many outcrops of rock and many gullies. The soils in these severely eroded areas classify as Udorthents, soils that have no diagnostic surface or subsoil horizons. There is one unit, located north of the ORNL Visitors Center, where soil material was removed and used as fill in and around the water reservoir. Severely and very severely eroded areas have the appearance of being natural "glades" with sparse red cedar and grasses, but the glades are mainly due to the effects of past activities that resulted in the removal of most of the soil and rooting medium for plants.

60731, 60741. These soils formed in deeply weathered dusky-red shales and siltstones of the Fleanor and have red or dark-red subsoil colors. They are mostly deeply weathered with paralithic or lithic contacts at depths more than 1 m (40 in.). These soils seem to fit the "Solway" soil series that was proposed for Anderson County but never correlated.

50121, 50131, 50141. The soils in these units formed in high-grade gray limestones of the Rockdell Formation. These soils have a dark clay loam or clay surface layer and a dark yellowish-brown heavy clay subsoil. Depth to hard rock (these soils have a lithic contact) is extremely variable, ranging from a few inches to

more than 1 m (40 in.) in a very short distance. Rock outcrops are numerous in all units. Vegetation ranges from mostly red cedar to mixed cedars and hardwoods to mostly hardwoods. Most areas of these soils had too many rock outcrops to cultivate, but most areas were probably cleared, planted to grass, and pastured. Most areas of these soils were identified as Gladeville-Rock outcrop complex in the Anderson County soil survey report.

60631, 60641, 60651. These soils formed in cherty, deeply weathered Rockdell Formation saprolites of the Chickamauga Group. These soils are mostly on elongated cigar-shaped ridges. The ORNL Visitors Center is located on a delineation of these soils. These soils have a cherty loam or silt loam surface layer and a yellowish-brown to yellowish-red cherty clay loam or clay upper Bt horizon. The middle cherty clay Bt horizon is yellowish red to red. Lower horizons become mottled in shades of red and yellow, with gray streaks.

60331, 60341. The soils in these map units formed in saprolitic materials weathered from argillaceous limestone of the Benbolt Formation in the Bethel Valley section. These soils are next to the cherty to very cherty Rockdell Formation No. 606 soils, but contain no subsoil or substratum chert. The surface commonly contains chert that has been let down from higher landforms. These soils have a bright-red to strong-brown clay upper Bt horizon, which becomes highly mottled with yellows and reds with depth. The lower BC, CB, and C horizons are mostly yellowish sticky clay. Gray wetness mottles occur in the lower Bt and horizons beneath. Depth to a lithic contact is more than 125 cm.

50522, 50531, 50533. The soils in these map units formed in clayey residues of Benbolt Formation in the Bethel Valley section of the Chickamauga. Depth to rock is 50 cm

to 1 m (20 to 40 in.). Rock ledges range from few to many.

50333. One delineation has been mapped thus far. It is located in Hot Yard Hollow and extends into Hot Yard from the east. This map unit is on the north side of Whiteoak Mountain Fault and formed in the Benbolt Formation. This soil formed from a high-grade limestone that probably contained some volcanic ash and interbedded clay shale. This soil has a dark clay loam or clay surface layer and a dark yellowish-brown subsoil with more than 60 percent clay. Depth to rock is more than 50 cm.

60223. These soils formed in the Benbolt Formation and younger units of the Chickamauga that are located below the Whiteoak Mountain fault. Only one unit has been mapped thus far. It is located in Hot Yard Hollow and extends into Hot Yard from the east. This soil has a dark clay loam or clay surface layer and a dark yellowish-brown clay subsoil. Gray mottles occur within the upper 25 cm of the Bt horizon. Depth to rock is 100 cm or more.

60531, 60533, 60543, 60544. Soils in these map units formed in shaly saprolite of the Benbolt. These soils are located in the Chickamauga located below the Whiteoak Mountain fault north of Pine Ridge. These soils formed in a yellowish-brown, very sticky saprolite that has the appearance of having weathered from a calcareous claystone-siltstone. Thin beds of chert fragments are in the saprolite. Some chert fragments are on the surface, while drainageway soils also contain few to common chert fragments.

50621, 50633, 50641, 50651. Soils in these map units formed in the clayey residue of the Bowen and the Moccasin formations.

Depth to rock is extremely variable, and ledges range from few to numerous.

50741, 50743, 50751, 50753. The soils in these map units formed in clayey residues of the Moccasin Formation. These soils have a reddish clay subsoil, with the red apparently inherited from the iron oxides of the rock beneath. Rock ledges are rare in these soils except on steep eroded areas.

Note: Soil mapping has just started in the K-25 area of the ORR. Rock units are different in the K-25 section of the Chickamauga from those in the Bethel Valley section. Bethel Valley soils will be used in the K-25 section where apparent morphology and properties are similar. New soils will be established as needed so that one soil series is not mapped over more than one formation unless the saprolitic residues are similar.

3.5.6 Chickamauga Colluvium

Most of the colluvium that occurs in the Chickamauga is derived from cherty colluvium that washed from higher areas of Knox soils. Within the Chickamauga, most colluvial soil materials are generated from the Five Oaks and Rockdell formations. Colluvial soils that formed wholly in Chickamauga colluvium are restricted to drainageways that head in the Chickamauga. Drainageways that head in the Knox and that cut through the Chickamauga contain a mixture of chert that is dominated by Knox soil materials. **54031, 54041.** These soils formed in colluvium derived from higher Chickamauga residual Five Oaks and Rockdell Formations soils. These soils typically have a 2.5Y hue in the upper Bt horizon. Lower horizons become increasingly mottled with gray. Some areas of these soils that are on low toe slopes next to alluvial soils show some evidence of having partially formed in old alluvium similar to the

No. 995 alluvium, but with higher clay content.

54141, 54151. These soils formed in cherty colluvium derived from both the Knox and Chickamauga and are underlain by Chickamauga residuum. These soils are in narrow drainageways consisting of a floodplain (Udifluvents) and colluvial side slopes. These soils are very similar in most characteristics to the No. 430 soils that are underlain by Knox residuum.

3.6 REEDSVILLE SHALE

The Upper Ordovician Reedsville Shale was named by Ulrich (1911) for exposures near Reedsville, Mifflin County, Pennsylvania (Rodgers 1953).

The Reedsville consists primarily of thin-bedded, often calcareous, orange-brown and gray-green shale and siltstone. The shale also contains black manganese stains. Near the lower contact with the Middle Ordovician Catheys Formation, thin, fossiliferous, limestone lenses are interbedded with the shale. Although no fossils were found during mapping, McMaster (1957) found brachiopods, gastropods, crinoid stems, and bryozoans in the limestones and a few bryozoans and brachiopods in the shales. The thickness of the Reedsville shale is approximately 60 m (180 ft).

3.7 SEQUATCHIE FORMATION

The Upper Ordovician Sequatchie Formation was named by Ulrich (1914) for exposures in Sequatchie Valley, Bledsoe County, Tennessee, and has a Late Ordovician age (Wilmarth 1938).

The Sequatchie Formation is composed of thin- to medium-bedded, gray to maroon-gray, argillaceous limestone; calcareous, maroon shales (sometimes

silty); and minor amounts of fine-grained limestone (Fig. 3-2). The argillaceous limestone is often mottled in shades of maroon and green. The formation is well exposed on the upper slopes on the northwest limb of the syncline. The southeast limb has relatively few exposures. The lack of exposure and the gradational nature of the contact between the Sequatchie Formation and Reedsville Shale make the contact difficult to pinpoint. Detailed sedimentologic studies of the Sequatchie Formation conclude a locally emergent tidal flat or deltaic depositional conditions (Thompson 1970, Milici and Wedow 1977). The best exposures of the Reedsville Shale and Rockwood Formation in the ORR are along Melton Lake Drive. The formation is approximately 60 m (180 ft) thick in the ORR.

3.8 ROCKWOOD FORMATION

The Rockwood Formation was named by Hayes (1891) for exposures at Rockwood, Roane County, Tennessee. The original Rockwood Formation included what is now known as the Sequatchie Formation. The Rockwood Formation is assigned a Lower Silurian age based primarily on brachiopod faunas (Wilmarth 1938, Berry and Boucot 1970). The contact between the Rockwood Formation and Sequatchie Formation is placed between sandstone, siltstone, and shale of the Rockwood overlying maroon, calcareous shale of the Sequatchie Formation.

The lower part of the Rockwood Formation contains shales and siltstones, but exposures commonly are medium- to thick-bedded and sometimes massive sandstones. The sandstones are iron-stained (brown, tan, maroon), fine- to coarse-grained, and contain a variety of sedimentary structures, such as cross-bedding, graded beds, load casts, and shale rip-up clasts. The shale pebbles are

maroon and sometimes calcareous, indicating that they may have been derived from the underlying Sequatchie Formation. The various sedimentary structures were useful for determining the facing direction in the fractured and overturned sandstones on the southeast limb of the East Fork syncline. Fossils in the lower part of the Rockwood consist of transported crinoid columnals and brachiopods. The middle and upper parts of the Rockwood contain interbedded thin to medium beds of brown, tan, olive, and gray shale and siltstone, and occasionally thick beds of sandstone. In addition, the upper half of the formation contains a few thin hematite beds that are commonly oölitic and very fossiliferous (McMaster 1957). Weathering of the Rockwood produces a shallow sandy and silty soil containing chips of shale and siltstone. Large boulders of sandstone are scattered along the ridge tops and slopes. Driese (1988) recently reviewed the Silurian depositional history in eastern Tennessee and concluded that the Rockwood Formation was deposited within a shoreface and shallow marine shelf environment. The Rockwood Formation is approximately 195 m (600 ft) thick.

3.9 REEDSVILLE SHALE, SEQUATCHIE, AND ROCKWOOD FORMATIONS SOILS

Residual and colluvial soils derived from the Reedsville and younger formations on ORR were encountered only along Hot Yard Hollow Road and, consequently, have very limited extent within present soil survey boundaries. Should the lands around K-25 be mapped, the soils from these formations will have more extent

and will require more extensive description of their classification, morphology, and distribution.

3.10 RESIDUUM

70051. The soils in this map unit classify as Typic Hapludults: clayey, mixed, and thermic. These soils formed in shale and sandstone residuum. They are on Sheet #1-254. To date, fewer than 2 ha (5 acres) have been mapped.

3.11 CHATTANOOGA SHALE

The Chattanooga Shale was recognized as a regionally distinctive unit by Troost (1835) and was named by Hayes (1891) as the "Chattanooga black shale," identifying a typical section in Hamilton County. A detailed stratigraphic study in central Tennessee by Conant and Swanson (1961) provided a type locality for the Chattanooga Shale in Dekalb County, Tennessee. More recently, Milici and Roen (1981) described the stratigraphy of the Chattanooga Shale in some detail northeast of the ORR, where the unit is much thicker and is divisible into four units. The exact age of the Chattanooga Shale is controversial. Various investigators have dated it as Late Devonian, Early Mississippian, or both (see review in Conant and Swanson 1961). Klepser (1937) interpreted the Chattanooga Shale as a time-transgressive unit that becomes increasingly younger to the south. A uranium-lead age for the upper member (Gassaway) of the Chattanooga Shale taken from core in the Youngs Bend area, Tennessee, resulted in an apparent age of 350 ± 10 Ma (early Mississippian) (Cobb and Kulp 1960). In the ORR, the Chattanooga Shale disconformably overlies the Rockwood Formation, and the contact is picked between the first appearance of black shale above fine-grained,

gray/tan/brown sandstone and shale of the Rockwood Formation.

The Chattanooga Shale is black to dark-gray, fissile, bituminous shale. The shale weathers to a dark-brown soil containing shale chips. Although no fossils were found, McMaster (1957) reported finding conodonts and the inarticulate brachiopods *Orbiculoiden* and *Lingula*. As reviewed by Conant and Swanson (1961), the presence of linguloid brachiopods provides evidence favoring shallow-water deposition of the Chattanooga Shale and supports a shallow flooding, transgressive/regressive depositional model related to the distal edge of the Acadian clastic wedge (Hasson 1982). The Chattanooga Shale is approximately 6 to 10 m (20 to 30 ft) thick in the ORR.

3.12 FORT PAYNE FORMATION

The Fort Payne Formation is the youngest stratigraphic unit exposed in the ORR. It was named by Smith (1890) for exposures at Fort Payne, DeKalb County, Alabama. Although comprehensive biostratigraphic studies are lacking, the Fort Payne is apparently no younger than middle Osagean (Early Mississippian) in northern Georgia and central Tennessee and no older than early Meramecian in southern Illinois (Wilmarth 1938, Ausich and Meyer 1990). The Fort Payne Formation conformably overlies the Chattanooga Shale; the contact is poorly exposed in the study area, however, because of the common occurrence on steep slopes and cover by cherty debris from the Fort Payne. The contact is located between the green shales and limestones of the lower Fort Payne and the distinctive black shales of the Chattanooga Shale. The Fort Payne Formation is approximately 31 to 46 m thick.

At the base of the Fort Payne Formation is a thin unit named the Maury Shale by Safford and Killebrew (1900) for expo-

sure in Maury County, Tennessee.

Although a widespread and distinctive unit in Tennessee, the Maury Shale in the area was included in the Fort Payne. The Maury was not mapped separately because it is only a few meters thick and only exposed in the strike valley northeast of Gum Hollow Road. The shale is dark green, indurated, and contains crinoid stems and plates. Associated with the shale are thin- to medium-bedded, sometimes mottled, fine-grained, gray sandstone and siltstone that contain phosphate nodules and white chert pods. In addition, thin- to medium-bedded chert occurs in the lower Fort Payne.

The middle to upper part of the Fort Payne Formation consists of a variety of lithologies including limestone, dolomite, siltstone, and chert. Limestone is medium-bedded, gray green, fine-grained, sometimes silty, and contains chert pods. The limestones weather deeply, leaving a very cherty soil with a few chert ledges projecting through. Siltstones are thin-bedded, gray green, and indurated. Dolomites are light gray, fine-grained crystalline, cherty, and contain geodes lined with calcite crystals. Chert is thin- to medium-bedded, chalcedonic, dark gray, and weathers to a milky white to tan-brown. Weathering of the Fort Payne produces a yellowish, sandy, silty clay soil with abundant chips and blocks of chert. The siliceous character of the Fort Payne makes it a ridge former, and, where outcrops are absent, the formation is mapped on the basis of cherty soil.

The Maury Shale and equivalents were deposited remote from source areas, at a slow rate in a low-energy environment favorable for the precipitation of phosphate. Facies characteristics, paleoecology, and taphonomy of the Fort Payne in south-central Kentucky and Tennessee support the hypothesis that the Fort Payne represents a progradational, shoaling-upward sequence (Sable and Dever 1990). Silica

content in the Fort Payne has been ascribed to either chemical precipitation, replacement during deposition and diagenesis, or secondary causes such as weathering (Bassler 1932). Detailed stratigraphic and sedimentologic reviews of the Fort Payne Formation can be found in Ausich and Meyer (1990), Lumsden (1988), and Macquown and Perkins (1982).

3.13 STRUCTURAL-LITHIC UNIT DESIGNATIONS

Rich (1934) was one of the first to recognize the control that stratigraphy has on the development of fold-thrust belt structures by observing that the angle a fault cuts through bedding changes as a function of lithology. He hypothesized that fault-bedding angles increase as material strength increases; therefore, a layercake stratigraphy will control the development of fault paths. The concept has been successfully applied in the Canadian and Idaho-Utah-Wyoming thrust belts (Douglas 1950, Bally et al. 1966, Dahlstrom 1969, Royce et al. 1975, Cook 1975). In addition, the concept has been further tested in the southern Appalachian fold-thrust belt (e.g., Harris and Milici 1977) and expanded upon by showing how a change within the stratigraphy along strike can control the structural style (Woodward et al. 1988, Hatcher and Lemiszki 1991). The term "structural-lithic unit" was originally coined by Currie et al. (1962) for layers controlling the style of a buckle fold and has been resurrected by Woodward et al. (1988) to designate mechanically significant stratigraphic units. An extensive discussion of the structural-lithic unit concept is the focus of the last chapter. The purpose here is to subdivide the stratigraphy in the study area into individual structural-lithic units.

A number of methods can be used to subdivide the stratigraphy into structural-

lithic units (Rutherford 1985): (1) Balanced cross sections can be used to interpret the different structural style of stratigraphic units; they tend to be somewhat subjective, however. (2) Fault-preference diagrams can be constructed (Dahlstrom 1970). Fault-preference diagrams are histograms that plot stratigraphic position against the distance a fault trace is from contact with individual units. For example, ramp-forming sections would typically show low fault-preference values, and flat-forming sections would be associated with high fault preferences. (3) Cutoff lines mapped on a palinspastic base provide a tool for showing aerial distribution of ramps and flats with respect to stratigraphy. For a given unit with a specified thickness, the horizontal spacing between the unit base and top cutoff lines will reflect the angle at which the fault passes through the layer. A narrow spacing indicates a steep angle (ramp), and a wide angle indicates a lower angle (flat) of fault-bedding cutoffs. (4) The dimensions of horse blocks may indicate a difference between strong and weak stratigraphic units. Helton (1979) pointed out that large single horses in the Valley and Ridge are typically composed of strong stratigraphic units such as the Knox and Chickamauga, but smaller horses are derived from sections of weaker rocks. (5) Stratigraphic separation diagrams indicate the angles and geographic positions of faults in stratigraphic units (Elliott and Johnson 1980). The structural-lithic unit designations shown in Fig. 3-1 are based upon stratigraphic separation diagrams for the Copper Creek and Whiteoak Mountain faults, a balanced cross section, mesoscopic observations of the structural style in some of the stratigraphic units, and previous work throughout the Valley and Ridge in Tennessee.

4 OAK RIDGE RESERVATION SOIL SURVEY

David A. Lietzke

4.1 PREVIOUS INVESTIGATIONS

Soils information for the Oak Ridge Reservation (ORR) is either obsolete for the Roane County portion or very generalized for the more recent Anderson County portion. The Roane County soil survey was published in 1942, with the soils map on a planimetric map base at a scale of 1:48,000 (Swan et al. 1942). The Anderson County soil survey was published in 1981 on a photographic base at a scale of 1:15,840 (Money-maker 1981). The Anderson County soil survey was made primarily for agricultural purposes and is quite generalized, with some soil series covering several geologic units.

With the need for more detailed soils information on which to locate waste burial sites, the first high-resolution soil survey at a scale of 1:2400 was made of the Solid Waste Storage Area 7 (SWSA 7) site (ORNL TM-9326) in 1982. This survey was made using standard National Cooperative soil survey methodology where geologic materials were not a criterion for defining soil series. Fortunately, most of the SWSA 7 site occurs within the Dismal Gap formation. After other high-resolution soil mapping had been completed and relationships between surficial soils and the underlying saprolite-rock had been worked out for the Conasauga Group, the original SWSA 7 mapping was reevaluated and changed to reflect the location and extent of other geologic formations when the site was expanded to its present size.

The West Chestnut Ridge site was mapped in 1984. This high-resolution soil survey at a scale of 300 ft/in. was the first

attempt to relate surficial soils and their morphologic characteristics with the underlying geologic formations. The results were published as ORNL TM-9361. This soil survey was later reevaluated and updated when the Bear Creek area of the ORR was mapped.

The next high-resolution soil survey was made of SWSA 6 and published as ORNL TM-10013. Accomplishments of this survey included the concept of weathering groups within a geologic formation and their relationship to landforms, along with slope shapes and gradients. The boundary between the Dismal Gap formation and Nolichucky Shale was also identified and mapped because of important soil differences and interpretations.

The next high-resolution soil mapping was completed on Pine Ridge northwest of the Oak Ridge Y-12 Plant waste disposal facility. Accomplishments of this survey made in 1986 (not published) included recognition of weathering groups in the Pumpkin Valley Shale and locating the Pumpkin Valley-Rome boundary.

In 1986 medium-resolution soil mapping of the Bear Creek section of the ORR was started at a scale of 1:10,000 and later changed to 1:12,000 scale. Knowledge from earlier high-resolution soil mapping was used to establish the initial mapping legend. Mapping Pine Ridge and the area north to the security fence provided the greatest challenge. Several soils were identified and related to the observed variability within the Rome Formation. Other, much different soils were related to the Chickamauga beneath the Whiteoak Mountain fault. A fault breccia soil of

Rome origin was mapped along this fault. Additional refinements of relating soils on Chestnut Ridge to the underlying Knox Group geologic units also were made. Soils related to Units A through E of the Chickamauga Group in Bethel Valley were also identified and mapped.

While the Bear Creek area was mapped at medium resolution, the Bear Creek low-level waste disposal development and demonstration (LLWDDD) project area was mapped at a high-resolution scale of 1:1200 and published as ORNL TM-10573. This soil survey area extended from the crest of Pine Ridge to Bear Creek and covered all formations of the Conasauga Group.

In 1989 high-resolution soil mapping was started in the East Chestnut Ridge area (ORNL TM-11364) and Walker Branch Watershed (ORNL TM, in press). Accomplishments from these surveys were an emphasis on karst features, especially doline soil stratigraphy, and development of the concept of a major topographic inversion that resulted in ancient alluvial and colluvial soils now occupying some of the highest elevations on Chestnut Ridge.

In 1991 medium-resolution soil mapping was started in the Oak Ridge National Laboratory (ORNL) area of the ORR at a scale of 1:12,000. This area includes all of the Whiteoak Creek drainage basin and Melton Hill. In 1992-93 the Oak Ridge K-25 site on the ORR will be mapped at the same scale and degree of resolution.

The location, elevation, and extent of both ancient alluvium and colluvium have brought forth the idea that there have been important inversions of topographic features. Geomorphic processes have produced all present-day landforms. The interrelationships between soils, bedrock formation variability, and geomorphic processes have resulted in the very complex assemblage of surficial soils in the

ORR. This complexity is reflected in the soil mapping legend and mapping unit descriptions that follow. As a result of continued interactions of geologists and hydrologists with soil scientists in interdisciplinary efforts, everyone involved will rise higher on the learning curve of ORR knowledge in the earth sciences.

4.2 SURFICIAL GEOLOGY AND GEOMORPHOLOGY

The ORR survey area is underlain by a complex assemblage of formations that have been faulted and folded. One major objective of the soil survey was to locate the surface boundaries between every geologic formation or member of a group. With the exception of most members of the Chickamauga Group and the Maynardville Limestone of the Conasauga Group, there were very few outcrops of hard rock. A few areas of ledges and pinnacles are exposed in the upper and lower Knox Group. Other rock outcrops occur in stream channels. Therefore, the characteristics of oxidized and weathered rock leached of its calcium carbonate, defined here as saprolite, and the surficial soil morphology were used to identify the approximate location of boundaries and the extent of each major geologic formation.

Bedrock is defined as unleached and unoxidized rock, and the oxidized, weathered zones above (which have not been transported) are termed saprolite. Saprolite is defined as isovolumetrically chemically weathered bedrock, a specific type of residuum. Where saprolite does not form due to collapse of the weathered soil material, this material is termed either regolith or residuum. The term "saprolitic materials" is used to describe highly weathered carbonate rock where there may have been partial and chaotic collapse

of saprolite because of insufficient framework strength of the silt and clay particles after removal of the carbonate. Depth to bedrock in the survey area is highly irregular because of the joint and fracture network and channelized flow of water at depth.

Characteristics of saprolite and saprolitic materials can be drastically different from the unoxidized and unleached parent rock. The upper saprolitic materials of the Knox Group, for example, consist of an acidic, high silt and clay content residue into which clay has been either translocated or neoformed. Iron and manganese oxides are a common but lesser component of most saprolites where they coat most fragment surfaces. Soil mapping located the boundaries and extent of the residual soils and underlying saprolite from all geologic formations wide enough to be mapped where they are exposed at the surface. Some areas are covered by alluvium and colluvium of more than one age of deposition.

The youngest group of rocks in the survey area belong to the Chickamauga Group. The discussion of these formations is based on mapping in Bethel Valley. Soil depth and depth of weathering ranges from very shallow to deep. Rock outcrops are absent for some of the more deeply weathered formations and are numerous for others. The slice of Chickamauga which occurs north of Pine Ridge near the boundary fence seems to be part of Unit E and perhaps younger units. Unit D consists of cherty limestones that occur in elongated landform knobs. The soils are deeply weathered. Unit C consists of gray limestones and has shallow soils with high clay content in the subsoil and a dark surface layer. Unit B consists of calcareous, very dusky red (10R) mudstones and limestones with very shallow to moderately deep soils that are mostly very severely eroded from past intensive agri-

cultural activities. Very severely eroded soils in this unit have saprolite or fairly hard, but oxidized rock exposed on the surface, while less eroded soils have some remaining genetic soil horizons. Except on the exposed, but weathered rock, vegetation is dominated by red cedar and Virginia pine. Unit A, the oldest, is a cherty limestone. Brick-shaped tabular chert that litters the ground surface serves to identify this formation from the uppermost Knox Mascot soils. The subsoil color also helps to distinguish Unit A soils from the uppermost Mascot soils of the Knox. The lowermost Unit A of the Chickamauga is separated by a disconformity or an ancient erosion surface from the uppermost formation of the Knox Group. This disconformity is not readily evident on the surface when it is covered by soil.

The Knox Group consists of five recognizable formations, which are commonly identified by their location with respect to formations above and below and, to some extent, by the type of chert they contain. When the western portion of Chestnut Ridge was mapped, criteria for distinguishing the Mascot and Kingsport soils had not been developed. Consequently, they were grouped together into the Newala Formation. Criteria for defining the Mascot and Kingsport soils were developed in 1989, when the high-resolution mapping of the Walker Branch Watershed and the East Chestnut Ridge Site was done (Lietzke, Ketelle and Lee 1989). The youngest formation in the Knox is the Mascot. This formation contains subrounded jasperoid and chalcedonous chert, which is a surficial visual clue used to separate it from the Unit A of the Chickamauga, with its tabular chert. Geomorphic processes, however, have scattered chert downslope across the landscape, so that one must be careful in mapping geologic formations using surficial float. In addition, the subsoil of

the Mascot Dolomite has its own distinctive reddish color and more plastic rheologic properties that help distinguish it from those of the Kingsport Formation. Areas of ledges and pinnacles commonly occur in the uppermost part of the Mascot Dolomite. The next older formation in the Knox is the Kingsport. This formation contains variable chert, much of which is oölitic. Rock outcrops are less common in the Kingsport than in the Mascot, and they are mostly confined to very steep slopes.

The Longview Dolomite typically contains abundant dolomoldic chert, which clearly distinguishes the formation. Because of its high chert content, the Longview Dolomite tends to form ridges. Because of the thinness of the Longview, it could not be identified on the 1:12,000-scale soil map without considerable distortion. The location and extent of the unit were resolved on 1:1200 to 1:2400-scale high-resolution soil maps of Walker Branch Watershed and East Chestnut Ridge.

The Chepultepec Dolomite occurs below the Longview. It has variable chert content and contains some very fine grained sandstone strata in the lower part, which contributes to a loam rather than silt loam surface and to a slightly lower subsoil clay content, although sometimes the presence of surficial loess masks the presence of higher sand content in the surface. Soils that formed in Chepultepec saprolite have 7.5YR and 5YR hues in the upper mottle-free subsoil. The Longview and Newala formations above and the Copper Ridge Dolomite below typically have 2.5YR hues in the upper mottle-free subsoil. Some soils from chert beds in the Chepultepec Dolomite were mapped in Walker Branch Watershed.

The Copper Ridge Dolomite is the lowest and oldest of the Knox Group. This formation also has variable chert content, but most of the chert is either massive or

öolitic. Copper Ridge residuum is characterized by a mostly reddish clay-plugged upper saprolite that grades irregularly downward into a yellowish high-silt material or reddish clayey material with red neoformed or translocated clay that fills voids in old fractures and voids. A thick lag gravel layer, thick E horizons, gradational E/B and B/E horizons, and red (2.5YR) upper subsoil horizons with much lower but highly variable chert content are common features of Copper Ridge soils. The lower Copper Ridge, including the transition to the underlying Maynardville Limestone of the Conasauga, is a massive dolomite that contains very little chert and/or other impurities. The residue collapses so the saprolite does not form. Instead, red clay is nearly in contact with hard rock with only a 1- to 5-cm weathering zone between. The soils are located only on the steep side slope of Chestnut Ridge above Bear Creek Road and on the north side of Melton Hill. Common rock outcrops, mostly ledges, are a surface feature of this part of the lower Copper Ridge Formation on Chestnut Ridge, while rock outcrops are very abundant on the northerly slopes of Melton Hill. A topographic bench partway up the slope marks the break between this lower chert-free part of the Copper Ridge and the upper cherty part of the Copper Ridge that forms saprolite or saprolitic materials on Chestnut Ridge. Rock outcrops are much more numerous on the steep slopes of Melton Hill where the lower Copper Ridge Dolomite and upper Maynardville Limestone are exposed.

The Conasauga Group is the next oldest group of diverse formations. This group is represented on the ground surface by the Maynardville, Nolichucky, Dismal Gap, Rogersville, Friendship, and Pumpkin Valley units. Each individual member has some surficial exposure. Transitional boundary zones between

some members are rather narrow [less than 8 to 14 m (25 to 50 ft)] and some 15 to 35 m (50 to 100 ft) wide or more depending on the dip and width of the boundary zone.

The transition zone between the Maynardville Limestone and the Copper Ridge Dolomite is a massive dolomite or dolomitic limestone that contains abundant impurities of silt and clay-sized particles and iron oxide, with increasing chert content. This transition zone is exposed on the steep slopes just south of Bear Creek Road but is mostly covered by thin to thick Knox colluvium or by Recent to Pleistocene alluvium and Knox colluvium. The Copper Ridge–Maynardville boundary is generally exposed on the steep north side of Melton Hill, but a thin layer of surficial cherty colluvium often masks the boundary.

The Maynardville Limestone is considered to be a relatively pure carbonate rock that contains clay and silt impurities. Soil mapping and exposures of weathered rock in gullies, however, indicate that the Maynardville Limestone on the ORR has a fairly high content of shale–siltstone strata. In the Bear Creek section of the Conasauga, most of the Maynardville occurs in the floodplain and present low terraces of Bear Creek and is covered. The lowermost part of the Maynardville Formation is a clay-rich or argillaceous limestone with interbeds of claystone in the transition zone where the Maynardville merges with the uppermost Nolichucky Shale. Rock weathering in this transition zone has produced a relatively thick saprolite, high in silt and clay, and very sticky. In the Melton Hill–Melton Valley section of the Conasauga, the Copper Ridge–Maynardville boundary is identified by the gradual disappearance of chert in the residual subsoil and underlying saprolite, with the Maynardville soils being more sticky and lacking chert in

subsoil and substratum layers in contrast to the presence of chert in the subsoil and substratum of Copper Ridge soils. Here, the upper Maynardville is a more pure high-carbonate rock. Numerous ledges are exposed at the surface, but the soil between ledges has a high shale content. The Maynardville–Nolichucky boundary in the field is identified by the presence of brownish shaly strata between thin carbonate strata.

Saprolite of the Nolichucky Shale consists predominantly of claystone, but contains lenses and strata of siltstone and very fine grained sandstone throughout. It also contains, in the uppermost and lowermost parts, more extensive lenses and strata of argillaceous limestone. In the Bear Creek section, the Nolichucky Shale commonly has a relatively low calcium carbonate content, when compared to the Dismal Gap formation below and the Maynardville Formation above. The Nolichucky Shale can be quite easily recognized at the surface by the mostly brownish saprolite colors that are sandwiched between olive-colored shale and siltstone saprolite. This brown, oxidized, saprolite color is derived from the darker brown of the less oxidized shale beneath. Nolichucky saprolite also has strata of olive-brown saprolite, characteristic of higher lime content, which increase in thickness near the Dismal Gap boundary zone. Because of the low carbonate content and the highly jointed and fractured nature of this formation, water has been able to percolate downward, allowing oxidation and hydrolysis reactions to proceed to considerable depth. The resulting chemically weathered and very acid materials form a thick saprolite which maintains a rather high bulk density, but tree roots are able to penetrate along planes, joints, fractures and reddish clay strata to considerable depth, exceeding 4 m.

The Nolichucky Shale, when compared to the Dismal Gap formation, has a relatively low iron content based on iron coatings on joint and fracture faces in the saprolite. However, manganese coatings on fragment surfaces in the saprolite are quite extensive. The soil that forms in the Nolichucky saprolite on stable landforms has a yellow-brown to strong-brown, clay-enriched subsoil.

An increase on the calcium carbonate content in the lowermost Nolichucky and increasing amounts of olive-hued saprolite strata marks the broad transition of the Nolichucky with the upper part of the Dismal Gap formation below. This transition zone, exposed in hillside gullies, is 15 to more than 35 m (50 to 100 ft) wide in Bear Creek Valley. In Melton Valley the transition zone is even wider because of the lower dip. The Dismal Gap formation consists of calcareous siltstones and argillaceous limestone. Thin strata of very fine grained calcareous sandstone also occur throughout, and glauconitic strata become common in the lowermost part of the formation. The Dismal Gap formation also has a relatively high iron oxide and manganese content, which is reflected by thick bright-red or dark-red iron oxide coatings in the upper saprolite, and thick, black manganese oxide coatings below the zone of iron oxide coatings. The Dismal Gap saprolite is easily recognized by the color of its oxidized and leached saprolite. The unoxidized rock has a very dark gray color, but as oxidation and hydrolysis proceed, the rock acquires a dark-olive color (5Y hue). With continued weathering, and nearness to the surface, the saprolite color changes to a light olive-brown (2.5Y) hue, and in the lower subsoil, saprolite fragments can have a yellowish-brown (10YR) hue.

The transition zone between the Dismal Gap formation and Rogersville Shale is usually less than 8 m (25 ft) wide. It is

marked by the increased presence of greenish, bluish, and pinkish claystone and siltstone saprolite strata and the lack of the abundant reddish iron coatings in the Dismal Gap. Also present in the lowermost Dismal Gap and throughout the Rogersville are very fine grained glauconitic sandstone strata. The Rogersville is typically less than 35 m (100 ft) thick and is exposed mostly on steep obsequent northeast facing slopes. There are other locations in the area, however, where the Rogersville is considerably thicker. Some of the increased thickness is evidently caused by local structure, or else there are locally thicker sections. Another reason for greater surface exposure of this formation in a few areas is that it occurs on dip slopes.

Saprolite of the Friendship formation has a high silt content. Most evidence of the Friendship formation is derived from Bear Creek Valley, which consists of a generally linear depression in which streams flow or which has been largely filled with colluvium and alluvium derived from the Rome Formation and Pumpkin Valley Shale. The Friendship formation in the Melton Valley section has much more exposure. Here, the surficial soils have formed in saprolite dominated by siltstone and claystone. Thin, high-lime, carbonate strata have weathered to red, sticky clay. Forest vegetation often provides assistance in locating the upper and lower boundaries of this formation, as the soils have higher fertility, and tree roots do not have to extend very deeply to encounter free carbonates.

Saprolite of the Pumpkin Valley Shale has two recognizable members that form distinctive soils. The upper member is an interbedded claystone and siltstone with abundant strata of very fine grained glauconitic sandstone. The saprolite has a distinctive color, which, along with the dark green of the glauconite, makes it

easily recognized. The lower Pumpkin Valley is dominated by still more permeable siltstone and very fine grained glauconitic sandstone. This saprolite can be identified by its higher sand content and colorful appearance, with colors ranging from reds, yellows, and browns to shades of green. Soils that formed from this saprolite, and which are on fairly stable landforms, have well-expressed morphology with reddish, clay-enriched, subsoil horizons.

The Rome Formation in the Bear Creek area occupies the upper third of the south side of Pine Ridge and continues on the north side of Pine Ridge to the Whiteoak Mountain fault. A bench landform or a change in slope gradient high on the south side of Pine Ridge marks the boundary between the Pumpkin Valley and Rome. The bench is formed by the presence of a thick, grayish-white to yellow-brown sandstone that contains abundant feldspars and some thin carbonate strata. This bench is usually covered with colluvium. Most drainageways on the south side of Pine Ridge have cut headwardly through the Pumpkin Valley until they impinged on this uppermost Rome sandstone unit. Some of these deeper drainageways contain springs, while others have only wet-weather seepage areas. Rome Formation saprolite on the south side of Pine Ridge is identified by the presence of a medium-grained sandstone unit that has a yellow-red oxidized color. Just below the sandstone unit is a unit composed of dusky-red and greenish-gray fissile shale. This fissile unit only occurs on the highest knobs of the ridge. Where this fissile unit occurs on side slopes and in saddles, however, it is commonly covered by colluvium that contains large quantities of hard, gray siliceous sandstone gravels and cobbles, part of the sandstone unit that holds up Pine Ridge. The crestal summit area is composed of a wide variety of

lithologies including a dusky-red ferruginous sandstone interbedded with an olive-gray and maroon fissile shale and strata of hard siliceous sandstone. As the softer shales and sandstones weather, the harder sandstone strata are exposed. The channels move downslope under the influence of gravity, and mantle the side slopes and saddles along the ridge crest.

The Rome Formation contains several members, which occur between the crest of Pine Ridge and the Whiteoak Mountain fault. One member is a feldspathic sandstone and siltstone, which weathers to form a yellowish-brown saprolite in which soils with strong-brown clay-enriched subsoil horizons have formed. Another member is a hard, reddish, fine-grained, micaceous sandstone that is mostly cemented by iron oxides. Soils are thin over this member. Another member is a red and dark-red mudstone interbedded with olive-colored siltstone. Most soils on the Rome Formation are thin, however, and do not have clay-enriched subsoil horizons. Only one area of Rome carbonate rock and the associated residual soils was mapped along Pine Ridge, but at least two other areas of Rome carbonate are known by the presence of rock outcrops. The Rome Formation also produced abundant colluvium of several ages from past geomorphic processes.

The Rome section on Haw Ridge has many similarities to the Pine Ridge Rome, but there are important differences. One major difference is the higher content of carbonate strata, often thin, that occur in the uppermost part of the formation. Another major difference is the presence of more numerous carbonate bodies (reefs) that occur along the first or southernmost ridge of Haw Ridge. Indeed, a fairly large sinkhole occurs within such a carbonate body along the crest. Other sinks, but lower on the south slopes of Haw Ridge, have been identified during soil mapping.

Another substantial difference between the Pine Ridge and Haw Ridge sections is the more highly fractured nature of the Haw Ridge section, with the lower sections being more highly fractured than the upper section. Other differences include more drainageways oriented parallel to the strike on Haw Ridge than on Pine Ridge. Because of the greater degree of fracturing and more abundant carbonate strata, soils are deeper to hand auger refusal on Haw Ridge than on Pine Ridge. Present-day forest vegetation is also of higher quality on Haw Ridge.

Two major faults cross the ORR. The Whiteoak Mountain fault marks the location where the Rome Formation that underlies Pine Ridge has been thrust over the Chickamauga. This fault zone in the Rome can be identified by the presence of fault breccia in which soils with fairly thick, clayey subsoils have formed and depth to paralithic saprolite is great. Saprolite from this fault breccia has a swirled appearance with a mixture of colors. The Chickamauga below the fault is lithologically different from the Bethel Valley Chickamauga. It seems to have a higher siltstone and shale content, low but usually some chert, and much lower limestone content. Most of the soils are underlain by paralithic Cr horizons of siltstone and shale saprolite and not by lithic limestone rock. The northernmost part of the survey area, north of the fault, is underlain by younger formations of the Chickamauga and other formations that occur above the Chickamauga. This part of the ORR has not yet been soil mapped. The Copper Creek fault is generally well-exposed along the north side of Haw Ridge, except where it has been covered by slump materials from the Rome. The location of the fault may be readily determined because there is a large change in slope gradient, with the Rome above being much steeper. The steeper slope gradient

of the Rome and the Chickamauga clays beneath have resulted in numerous slips and slumps along the fault on Haw Ridge. A thinner layer of fault breccia occurs at the base of the Rome on Haw Ridge when compared with the Whiteoak Mountain fault.

4.2.1 Geomorphology

4.2.1.1 Geomorphic history

The geomorphic history of the ORR survey area is long and complicated. Only a postulated and much simplified history, based on observations, starting with current conditions and extending back through the modern, the Holocene, and the Pleistocene epochs is attempted. The modern age of the Holocene Epoch is defined, for purposes of this report, as beginning about 300 years ago when the activities of European settlers resulted in large-scale deforestation, the beginning of agricultural activities, the onset of anthropogenic-accelerated erosion, and the burial of older Holocene alluvium by fresh sediments. The Holocene Epoch covers a time span starting at the end of the Pleistocene (approximately 12,000 years ago) and includes the modern age. In the southeast, the Holocene has often been thought to have been a benign period with little climate fluctuation. Holocene climate changes, however, have produced periods of geomorphic instability. A result is the burial of paleo-Indian habitations on low river terraces by younger sediments between about 2800 and 5000 years ago. There is only minimal evidence of paleo-Indian influence on the soils of the survey area. During the Pleistocene Epoch, which covers a period of at least 2 million years, important climate fluctuations occurred in the southeast resulting in significant landform alterations. There are also relict landforms in the ORR that are interpreted

to be of Tertiary age. Most of these relict landforms, once toe-slope colluvium and river terraces, have been topographically inverted and now occupy some of the highest elevations on Chestnut Ridge and Melton Hill.

Modern Geomorphic Period

In humid environments, the dominant geomorphic processes are those of denudation (the wearing away of topographic highs) and either the filling of low areas or the transport of sediment away from the local watershed system. These processes are driven by rainfall and the force of gravity. Soil particles are detached by raindrops or overland flow and then transported downslope to a depositional site or into a stream. This natural process will be a slow one whenever there is a vegetative cover on, and a tree canopy above, the soil surface. Deforestation and primitive agricultural management practices stripped the vegetative cover off the land and left bare soil exposed to the full force of raindrop impact and runoff. Agricultural fields were eroded rapidly by sheet and rill erosion and related transport processes. In areas where water coalesced, gullies formed and started their headwardly cutting activity into steeper landforms. Gullies are abundant in many areas of the ORR that were intensively farmed.

According to the 1941 United States Geological Survey (USGS) topographic maps of the area, about half of the ORR was open land. The open land was on the more gentle slopes. Only the steeper soils of the Conasauga and most Rome soils were evidently not cultivated. Steep areas and extremely cherty areas in the Knox were evidently not cultivated, but many areas were probably pastured. Most areas of the Chickamauga Unit A were evidently not cultivated because of the high chert content on the surface. Units B and E of

the Chickamauga were intensively cultivated. Most areas were extremely eroded or became gullied after takeover by the Atomic Energy Commission (AEC). Many of these severely eroded areas that are now under forest vegetation and that have a surface litter layer are no longer actively eroding. Most areas that were in agricultural land use can still be identified readily by (1) the present forest vegetation and (2) by the effects of plowing and erosion on soil morphology. Other areas of land, once cultivated or pastured, had been allowed to revert back to forest much earlier. These old fields do not show on the 1941 topographic maps, but their presence can often be identified in the woods on the basis of soil morphology.

Other evidence that modern-age erosion has occurred is revealed in drainageways and floodplains where 50 to 100 cm or more of modern-age sediment (mostly topsoil, derived from past agriculture and forestry land mismanagement) has covered older Holocene-age soils.

The presence of both modern and older multi-age colluvium on side slopes and foot slopes in the uplands indicates that there have been past cycles of accelerated geologic erosion during the Holocene and Pleistocene. Colluvium consists of soil particles and rock fragments that have been transported downslope under the influence of gravity, usually as a saturated mass, especially if the materials cover entire toe slopes. Other colluvium is a product of soil creep where moist soil materials move slowly downslope. Colluvium from creep processes usually occurs on steeper slopes with less concavity, is generally less than 50 cm to about 1.25 m thick, and is termed hillside colluvium. Colluvial deposits are readily identified by the lack of geologically oriented strike and dip or rock structure. The rock fragments in colluvium are mostly disoriented, with the exception that large flat fragments are

commonly oriented parallel to the slope. Colluvium has a distinctive appearance with commonly higher rock fragment content and other morphological clues that serve to identify it from either residuum or alluvium. The reworking and sorting of toe-slope colluvium by lateral stream cutting produces a deposit with characteristics of both colluvium and alluvium. The largest areas of young colluvium and alluvium are identified as modern alluvium. This soil material, in which genetic soil horizons have not yet formed, covers older soils and occurs as fans at the outlets of gullies and drainageways at the base of cultivated slopes throughout the area. Modern-age alluvium-colluvium also covers older soils in most flat-bottomed dolines on Chestnut Ridge and Melton Hill.

Holocene Geomorphic Period

Colluvium of Holocene age occurs (1) in doubly concave landform segments that occupy foot-slope and toe-slope positions at the base of slopes, (2) as fans at the out-lets of headwardly eroding drainageways, (3) on side slopes in doubly concave elongated landform segments and (4) in saddles between subwatersheds. Neoglacial Holocene colluvium can overlie (1) in-place saprolite, (2) the remnants of a truncated older colluvial soil of Holocene or Pleistocene age, or (3) the truncated remnants of older residual soils. Because there was only a slight reduction in temperature during this period, which was accompanied by wetter conditions, only highly geomorphically sensitive soils were destabilized. Colluvium of Neoglacial age was identified only on Conasauga Group soils and was mapped only on 1:1200-scale maps of the Bear Creek LLWDDD site.

Pleistocene Geomorphic Processes

The climate shifts of the Pleistocene produced significant changes not only in the types of geomorphic processes that were active in the area, but in the rates and intensity of these processes. Upland soils in the survey area underwent several cycles of denudation during the Pleistocene Epoch generally corresponding to periods of maximum glaciation. Some areas of geomorphically sensitive landforms and soils, especially those on steeper slopes, were periodically stripped down to hard rock or to hard saprolite, while other, less sensitive areas were hardly affected. The latest major episode of denudation occurred during the Wisconsinan, a time period of several thousand years that ended about 12,000 years ago. The longest period of unstable soil conditions occurred between 18,000 and 25,000 years ago, when glaciers extended to their maximum. Numerous freeze-thaw cycles along with periods of deep winter freezing and downward melting of the surface in the spring, which produced saturated conditions, destabilized many upland soils. Large volumes of soil flowed downslope as mud and debris flows, filling in topographic lows and choking stream valleys and river channels. The Clinch River may also have been unable to transport the increased sediment and may have aggraded its channel, producing a widening floodplain with a braided stream and damming Poplar Creek and other ORR tributaries. The evidence for an event described above is the presence of widespread alluvium and terrace remnants at an elevation of about 280 m (840 to 850 ft) in several tributary watersheds and on terrace remnants above the present Clinch river. Soil mapping in Melton and Bethel Valleys has located the presence of highly dissected terrace remnants along a bend of the Clinch River that are at an elevation of

about 280 m (840 ft) and a lower terrace that has an elevation of about 265 m (815 ft). The lower terrace corresponds to the elevation of an abandoned meander of the Clinch River.

When the Bear Creek floodplain in the Bear Creek LLWDDD site became choked with sediments, the stream was forced into other pathways through lower areas of the site. Evidence for this are chert gravels and other stream-rounded gravels lying on residuum that was part of the bed load. During the Pleistocene, at least three stream piracy events occurred within the Bear Creek LLWDDD site. One location is identified by the "E" symbol in the soils map of the site. Before piracy occurred, large amounts of sediment were deposited in ponded water as an alluvial or deltaic fan that extends to the present day Bear Creek floodplain. The deltaic fan material covers the underlying silty alluvium and was not covered by loess.

There are several sites in the area where loess of Pleistocene age has been preserved. One site is located in the Bear Creek LLWDDD area, where, on a nearly level old alluvium terrace landform, loess accumulated. Other places where loess has accumulated are on Chestnut Ridge. There, in shallow, flat-bottomed depressions, loess accumulated, burying the cherty lag gravel surfaces of older colluvial soils. The chert-free loess has, in turn, been buried by modern-age silty slope wash that contains a moderate content of chert fragments. In one wet depression on Chestnut Ridge, at least two episodes of loess deposition seem to have been preserved.

Early Pleistocene and Late Tertiary

The geomorphic events and processes that took place during the Wisconsinan were but repetitions of similar events that took place during the Illinoian and

Nebraskan glacial periods of middle and early Pleistocene. Remnants of old terraces from these earlier Pleistocene events are preserved on the ORR in areas underlain by permeable Knox soils. Permeable substrates and surface armouring by coarse fragments are two necessary requirements for the preservation of paleosols and also for topographic inversion.

There are several elevations on Chestnut Ridge and Melton Hill where ancient soils, either buried or not, have been preserved. At an elevation of approximately 350 m (1050 to 1060 ft) and extending to about 360 m (1100 ft) in places on Chestnut Ridge, ancient toe-slope colluvial and alluvial soils, of local origin, have been preserved on northeast and east aspects. On Melton Hill, ancient alluvium has been mapped at an elevation of nearly 450 m (1350 ft). Ancient main-channel alluvium has also been preserved at similar elevations. This main-channel alluvium is identified by the dark-red color, high clay content, and lack of chert fragments. Some well-rounded metaquartzite cobbles are observed in pit and trench excavations. Extremely cherty foot-slope/toe-slope colluvium has also been preserved on what are now broad ridge tops on Chestnut Ridge and Melton Hill. The chert in this ancient soil is quite soft and can easily be cut with a spade. Small areas of residual soils have been identified on Chestnut Ridge that occurred at a higher elevation than the ancient alluvium and colluvium. These truly old soils have very highly weathered chert fragments. Also on Chestnut Ridge, old alluvial soils occur at an elevation of approximately 290 m (875 to 900 ft). Most of the ancient colluvial and alluvial soils are interpreted to date from the late Tertiary to early Pleistocene. The Melton Hill area seems to have a preserved sequence of terrace remnants, but soil mapping has not yet been completed. Remnants of old alluvium are

preserved on the Conasauga in Melton Valley above White Oak Lake at elevations of approximately 290 m (875 to 900 ft) and at approximately 280 m (840 to 850 ft). An abandoned Clinch River meander occurs at an elevation of 265 m (800 to 815 ft). Present elevation of the Clinch River is about 247 m (741 ft). Younger terraces of the Clinch occur between about 265 m (800 ft) and present river elevation, but have not yet been mapped.

4.2.2 Soil Genesis from Parent Rock in the Bear Creek Area

In the Bear Creek area, parent materials, topography (geomorphic processes), and biota are diverse. Climate can be assumed to be similar for most of the area, except for north- and east-facing slopes. Present relationships between landforms and soils in the area are greatly related to the geohydrology of the underlying rock and surface water flow pathways produced by geomorphic processes of the past. On many geologic formations, as the slope gradient steepens or the convexity increases, there tends to be more overland runoff and less infiltration of rainfall.

The relationship between depth to unoxidized and unleached bedrock and the rate of soil formation is less evident because more recent Pleistocene and Holocene geomorphic periods of instability have resulted in the stripping of the upper soil horizons, especially on steeper slopes, while deep oxidation and leaching have continued. Therefore, soils with weakly developed genetic soil solums, on steep slopes, can have thick and highly weathered saprolite beneath.

The uppermost pedogenic soil horizons, of late Pleistocene and Holocene ages, are oriented parallel to the land surface. Relict paleosol soil horizons are commonly not oriented to present day landforms, an indication that there has

been alteration of landform shapes. However, in soils underlain by sedimentary rock with considerable dip, the lower genetic horizons tend to become oriented with respect to the geologic strike and dip. The reorientation of lower pedogenic horizons is due to differential subsurface water flow pathways. This differential water flow can result when harder, less permeable shale saprolite is interbedded with softer and more permeable sandstone and siltstone saprolite. Zones in the leached saprolite that have increased water flow also have higher rates of weathering and form soil horizons sooner than do less weathered areas. It is not uncommon, when making a vertical cut in a soil profile, with differential water flow and weathering rates, to have a Cr horizon of siltstone (paralithic materials) above a clayey Bt horizon that formed in a lime bed, a highly illogical pedogenic soil horization sequence. But, considering that water flow pathways are oriented to the strike and dip in the lower solum and in the underlying saprolite, genetic soil horizons would form first in more weathered saprolite zones.

Higher bulk density in underlying Cr horizons (leached saprolite) inhibits root penetration and proliferation and most other biotic activity except in water flow zones where fracture or joint spacing is closer together. Smaller pores and cracks preclude most clay particles. These surfaces, above the water table, are coated with red iron oxides or black manganese oxide. Zones with higher permeability weather faster and deeper into both the less leached saprolite and the rock beneath. Tree roots and other biotic activity can extend deeply into the saprolite along these water-flow zones. The higher bulk density at the boundary of the C horizon and the Cr horizon (paralithic saprolite materials) generally stops the hydraulic penetration of coring tubes, including

“shelby” tubes. Bulk density continues to increase with depth in the lower leached saprolite zone and in the upper oxidized but unleached saprolite zone. At some depth, however, bulk density becomes high enough to preclude the penetration of a split-spoon coring device, which may coincide with the leached to unleached saprolite zone; additional study and analysis are needed to confirm these preliminary observations. In the unleached saprolite-to-bedrock transition zone, where there is an oxidizing gradient, the decrease in weathering finally precludes the use of augering equipment with cutting bits that resemble steel fingers. Below this depth, drills with rotary bits are required to penetrate rock.

What must be stressed in the survey area is the gradational, extremely variable, and irregular nature of weathering processes and irregular thicknesses of the soil solum and underlying leached saprolite.

Limestone and dolomite, depending on the joint–fracture network, can have a different mode of weathering than most other sedimentary rocks. Limestone, because of its very slow permeability, tends to weather from the outside inward because water flows over joint and fracture surfaces rather than more or less through the rock as it does in sandstone, siltstone, and shales of the other sedimentary rocks. However, once carbonate has been removed, saprolite may or may not form. If a carbonate rock contains sufficient inert residue that forms a strong framework, saprolite will form. If a carbonate rock contains insufficient inert residue, collapse occurs without any formation of saprolite and red clay is commonly in direct contact with rock with only a very thin weathering zone. In between these two extremes are carbonate rocks that contain moderate, but variable, amounts of inert residue. Upon weathering and loss of soluble portions, saprolite will form in some places and not

in others. Commonly, there is sporadic collapse of these saprolitic materials. The weathering of carbonate rocks tends to produce pinnacles, ledges, and solution cavities and highly irregular depth to rock. Channels and caves form in some carbonates and are eventually filled with translocated or neoformed clay, or there is soil flow into surface depressions caused by collapse of underlying cave or solution channel roofs. Pinnacles and ledges, either attached or detached, are also a common feature of carbonate rock weathering. Weathering and geomorphic processes of carbonate rock in humid environments are sufficiently different from the weathering and geomorphic processes of other kinds of rock so that the process is termed “karstification.”

4.3 SOIL CLASSIFICATION

David A. Lietzke and Suk Young Lee

Each soil has a distinctive subset of morphologic properties that can include color, horizonation, soil structure, and soil texture. Some related properties are measured in the laboratory. Important diagnostic properties that soils have in common and that were produced by a soil forming process, i.e., soil genesis, are used to define conceptual classes for the purpose of classifying soils (Smith 1983). In the United States a hierarchical system of soil classification evolved to its current state with the development of *Soil Taxonomy* (Soil Survey Staff 1975) and the more recent amendments, which are a reflection of advancing knowledge of soil science and soil genesis. Soil taxonomy is based primarily on the morphologic properties of soil near the surface, properties that are the most direct result of a soil-forming process, but some deeper soil properties (at or near a depth of 2.0 m) are

used to define one or more high-level categories of the classification system. The highest category of soil taxonomy is the **Order**. There are presently ten orders and a provisional eleventh. The soil survey area has five of the ten orders: **Entisols, Inceptisols, Alfisols, Ultisols, and Mollisols**. **Entisols** are of two kinds: (1) very young, well- to poorly-drained soils of floodplains that have a thin A horizon over stratified alluvium or (2) very severely eroded steep slopes that have lost all evidence of past genetic horizons and that now exhibit very little evidence of soil genesis except for the formation of a thin A horizon over a C or Cr horizon of saprolite. **Inceptisols** are young soils that have a minimal soil horization sequence consisting of an A, Bw, C, and Cr horizon, but insufficient time has elapsed since the inception of soil formation for distinctive horization to have occurred.

Most Inceptisols will evolve with time into other soil orders that have more distinctive and contrasting horization. These three soil orders are (1) **Alfisols**, soils that have a clay-enriched subsoil Bt horizon (argillic horizon) and more than 35 percent base saturation at a depth of 1.8 to 2.0 m; (2) **Ultisols**, which are those soils that also have a clay-enriched subsoil Bt horizon (argillic horizon), but which are mostly highly weathered or have formed in low base status parent materials with less than 35 percent base saturation at a depth of 1.8 to 2.0 m below the surface; or (3) **Mollisols**, which are soils with (a) high base saturation throughout the soil and (b) a thick dark surface horizon. All Mollisols are underlain by high carbonate content rocks of the Chickamauga Group at depths commonly less than 50 cm.

All of the soils in an order must have at least one or more common properties that are the result of a common genetic pathway. Each order has one or more suborders. The suborder separates soils that

have more properties in common. In the order of **Entisols** there are three suborders present in the area. They are (1) *Fluventis*, well- and moderately well-drained soils of floodplains that have fine stratification throughout the upper soil; (2) *Aquents*, wet soils of floodplains and seepage areas; and (3) *Orthents*, soils of very severely eroded steep slopes, areas that have been stripped of their upper diagnostic soil horizons, or areas that have been filled by highly disturbed earthy materials. The order of **Inceptisols** is represented by one suborder. This is the suborder of *Ochrepts*. *Ochrepts* are well-drained and have a light-colored surface layer (ochric epipedon) and a subsoil horizon with minimal but significant evidence of a soil-forming process (cambic horizon) underway. The orders of **Alfisols** and **Ultisols** are represented by four suborders. They are *Aqualfs* and *Aquults* (alfisols), wet soils that have a light-colored surface layer (ochric epipedon) and a clay-enriched subsoil horizon (argillic horizon), and *Udalfs* and *Udults* (Ultisols), well-drained soils that have both an ochric epipedon and an oxidized subsoil argillic horizon. The order of **Mollisols** is represented by two suborders: *Rendolls* and *Argiudolls*. *Rendolls* have a dark surface layer over either hard or shattered limestone rock. *Argiudolls* have a dark surface layer more than 25 cm thick and a clay-enriched subsoil Bt horizon; they are underlain by limestone at depths of less than 50 cm to about 100 cm.

Each suborder has one or more Great Groups, with the soils in each Great Group having more commonality of properties. Great Groups are listed in Table 1. Each Great Group has one or more Subgroups. Those in the survey area are also listed in Table 1. Each Subgroup has one or more Families. Each category above the Family is conceptual. The Family category is represented by real physical and chemical

properties from a prescribed depth and thickness of soil.

The **soil series** is the lowest category of soil taxonomy. Each soil series is mostly defined by observable morphologic soil features. Each soil series in this report is identified by the first three digits of a five-digit number. The first three digits more specifically relate individual soils to individual rock types within a formation or to different kinds and ages of alluvium and colluvium.

4.3.1 Technical Approach to Soil Mapping

A basic premise in soil mapping is that residual soils and landforms are closely related. Geomorphic activities, including karst and erosional-depositional processes that have shaped landforms to their present state, have also affected the soil system by (1) additions to the soil system, (2) losses from the soil system, (3) translocations within the soil system, and (4) transformations within the soil system. A narrowly defined subset of these basic soil-forming processes gives rise, through time, to a soil with distinctive morphology and its associated landform.

Soil mapping in the ORR was accomplished by making traverses across landforms at fairly closely spaced intervals, the spacing depending on the observed or suspected spatial variability, map scale, and degree of resolution required. After mapping was completed, line transects were run with observations at 15- to 30-m (50- to 100-ft) intervals for purposes of verifying map quality and spatial variability. Observations of genetic soil horizons and the underlying saprolite or other parent materials were made with a 7-cm-diam hand auger. Soil parent materials, soil horizons, sequences of soil horizons, inherited and pedogenic colors, soil textures, and other observable morphologic

features were used to recognize each distinctive individual soil. These data were organized into conceptual taxonomic entities termed soil series. Each soil series is confined to a particular geologic unit, or to particular colluvial and alluvial deposits and to particular segments of landforms, and each has a certain sequence of genetic soil horizons, that have narrowly defined ranges in color, texture, and other morphological features.

Individual soil series and map units in the soil survey area were established within the hierarchical framework of *Soil Taxonomy* (1975). In the establishment of each soil, highest priority was given those variables and processes that define the soil system. Soil morphology of the genetic surficial horizons and of the underlying saprolite, which is related to and largely controlled by geology (parent materials), hydrology, geomorphic processes, and biotic processes, was used in conceptually defining distinctive soils. In the establishment of mapping units, each soil series was subdivided according to landform configuration and slope gradient, or wetness, and last by erosion class. Each individual delineation shown on the soils map represent some part of the "real" world. The total delineations of one kind, represented by a unique symbol, represent a mapping unit. The delineations that comprise a mapping unit should have more properties in common than those delineations that compose an adjacent mapping unit.

Soil observations were made to a depth of 1.5 m or to a paralithic contact (which precluded deeper observations) if shallower. Deeper observations were made in pits that were at least 3 m deep or to backhoe refusal if shallower than 3 m. All major soils were described according to methodology of the *Soil Survey Manual* (1984), Soils Staff. All major soils were

described from exposures in either backhoe pits or small hand-dug pits.

4.3.2 Soil Legend Development

Symbols that convey information are used to identify each soil series and phase(s) of each soil series on the soil map. Each identified soil series has been recognized and classified according to principles and criteria of *Soil Taxonomy* (Soil Survey Staff 1975). In addition, the properties of underlying geologic units were used as an additional criterion in the identification of residual soil series. Colluvium and alluvium of different geologic origins and ages as well as texture and degrees of wetness of alluvium were additional criteria used to identify and separate colluvial and alluvial soils.

Each soil series in the following legend is identified by a three-digit number that is related to the geologic unit, which defines, for the most part, the parent materials of each soil or is related to transported soil materials. Colluvial soils from each major geologic group or formation also have a commonality of parent material properties and are included as appropriate. Alluvial soils, which are defined on parent material properties of stratification, degree of wetness, and landform location, tend to occur over more than one geologic unit because geomorphic processes of alluvial transport and sedimentation mix materials. Soils of first- and second-order stream generally reflect their geologic parentage, while the soils in higher-order stream segments have a more diverse parentage. For example, the main Bear Creek floodplain soils are a product of contributions from the Rome, Conasauga, and Knox geologic materials, but the first- and second-order tributaries of Bear Creek have sediments derived from one or, at most, two geologic formations.

4.4 MAP UNIT DESCRIPTIONS

4.4.1 Colluvium

4.4.1.1 Rome colluvium

Because most residual Rome soils occur on steep slopes, geomorphic processes during the Pleistocene produced large quantities of colluvial-alluvial material. Most Rome colluvium-alluvium occurs at some distance from the steep source areas and is located on large coalesced fans, especially along and covering parts of the Whiteoak Mountain fault and some of the Chickamauga that occurs below the fault. The greatest extent of Rome colluvium from Haw Ridge also occurs on the north side, where fan terraces and mud flows cover Chickamauga residual soils. Elsewhere, Rome colluvium occurs locally on benches on the south side of Pine and Haw Ridges, and in drainage ways and hollows where flowing streams did not remove all of it.

The No. 010 and 011 soils are related to the colluvium source, while the No. 012 and 013 soils are separated on the basis of landform and soil morphology.

01041, 01051. These soils formed in colluvium more than 50 cm thick and often more than 100 to 200 cm thick. These soils occupy bench landforms high on the south side of Pine and Haw Ridges at the contact of the Rome Formation and the Pumpkin Valley Formation of the Conasauga Group, and on concave foot-slope positions at the base of slopes where the upland soils are the No. 001 or No. 008, or the No. 003 soils. These soils have well-expressed morphology with a well-defined loamy, very fine sand E horizon and a 7.5YR-hue loam or clay loam Bt horizon. These soils, because of their depth and particle size distribution, have the capacity to store considerable water and release it gradually into

Table 4-1. Categories of Soil Taxonomy in the Oak Ridge Reservation Soil Survey

| Order | Suborder | Great Group | Subgroup | Family |
|--------------|---------------------|--------------------------|---|---|
| Entisols | Aquents | Fluvaquents | Typic Fluvaquents Aeric Fluvaquents | fine-silty, coarse-silty, fine-loamy, or loamy-skeletal |
| | Fluvents | Udifuvents | Typic Udifuvents Aeric Udifuvents | fine-silty, coarse-silty, fine-loamy, or loamy-skeletal |
| Intceptisols | Ochrepts | Dystrochrepts | Typic Dystrochrept Ruptic-Ultic Dystrochrepts | loamy-skeletal or fine-loamy |
| Alfisols | Aqualfs | Ochraqualfs | Typic Ochraqualfs Aeric Ochraqualfs | fine or fine-loamy |
| | Udalfs | Hapludalfs | Typic Hapludalfs Ultic Hapludalfs | fine |
| Ultisols | Aquults | Ochraquults | Typic Ochraquults Aeric Ochraquults | clayey or loamy-skeletal |
| | Udults Ochreptic | Hapludults Hapludults | Typic Hapludults | clayey, fine-loamy, or loamy-skeletal |
| | | Paleudults | Typic Paleudults | fine-loamy, loamy-skeletal or clayey |
| Mollisols | Udolls | Argiudolls | Typic Argiudolls | fine |
| | Rendolls | ————— | Lithic Rendolls | |

lower horizons and into the joint–fracture system that controls summer stream base flow. These soils also generate little overland runoff. They and other Rome colluvial soils in the survey area are hydrologically important.

01131, 01141. These soils formed in colluvium derived from the micaceous red sandstone and the dusky-red mudstone of the Rome, where they contain reddish fragments. The argillic horizon is 5YR or redder and is a clay loam. These soils occur on doubly concave foot slopes below delineations of No. 003 and No. 004 soils.

01231, 01241. These soils formed in Rome-derived colluvium–alluvium and are mostly situated near and over the Whiteoak Mountain fault, but some areas are mapped on the north side of Haw Ridge. These soils are probably some of the oldest of the Rome colluvium-derived soils that have undergone topographic inversion. They formed in several layers of mudflow deposits.

01321. The soils of this map unit formed in Rome-derived colluvium on the north side of the Whiteoak Mountain fault and are underlain by clayey Chickamauga residuum. Most areas of these soils occur below delineations of the No. 012 soils. These soils have a younger colluvial cap of Rome materials overlying a gray, clayey, buried, residual soil. A fragipan has formed in the contact zone. No areas of these soils have been mapped near Haw Ridge.

4.4.1.2 Conasauga colluvium

Pumpkin Valley colluvium

The following sequence of No. 120, No. 121, and No. 122 soils constitutes a time- and litho-sequence. The No. 120 soils are

the oldest and formed primarily in Pumpkin Valley colluvium. The No. 120 landforms have undergone topographic inversion, so most areas of the No. 120 soils occupy topographically high landform positions that are now erosional rather than depositional. The younger No. 121 soils still occupy recognizable foot-slope and toe-slope depositional landforms, although younger drainageways are already starting to incise some of them. The present activity represents the beginning of a new cycle of localized topographic inversion. The No. 121 soils formed in a mixture of Pumpkin Valley and Rome colluvial materials, but the harder fragments are dominated by Pumpkin Valley materials. They occupy the largest extent of the Pumpkin Valley colluvial units. The youngest No. 122 soils formed in young surficial colluvium more than 50 cm thick that is dominated by Rome fragments. Most areas of these soils blanket the No. 121 soils. They also occupy young fan landforms of drainageways that have been actively headward cutting into the Rome. Some areas of the No. 122 soils probably have a thin younger layer of recent sediment eroded from agricultural areas or from forest clear cutting, but, based on soil morphology and degree of horizonation, the bulk of the surficial material was probably transported and deposited during the neoglacial period (about 2800 to 4000 years ago). The youngest age of the No. 26 soil is probably late Wisconsinan (about 18,000 to 25,000 years ago). Soil morphology and, more importantly, topographic inversion seem to indicate a large time hiatus between the No. 121 and No. 120 soils. The youngest age of the No. 120 soils is assumed to be middle or early Pleistocene (or about 1 to 2 million years).

12022. The soils in this map unit are the oldest of the Pumpkin Valley colluvial

soils. They are small in extent and can be delineated only on a scale of 1:2400 or larger in high-resolution mapping. Most areas of these soils are on broader uplands and are not related to present colluvial landforms. These soils have a Bt horizon with the reddest hues (5YR and 2.5YR) and highest clay content of any Pumpkin Valley colluvial soils and are probably some of the oldest and most highly oxidized Conasauga colluvial soils. These soils contain mostly Pumpkin Valley fragments, but usually have some Rome sandstone gravels. It is presumed that this old colluvium was deposited before headwardly cutting drainageways reached the Rome sandstones. Subsequent topographic inversion has placed most areas of these soils on what are now erosion surfaces. Some areas of No. 120 soils have been covered by younger side-slope colluvium of the No. 121 soils and are preserved.

12121, 12131, 12132, 12141, 12151. The soils of these map units formed in older colluvium, but younger than the colluvium of the No. 120 soils. Depositional landforms are still recognizable as doubly concave foot slopes, but many have been incised by drainageways or have been partially covered by the younger No. 122 soils. These soils have Bt horizons with 10YR and 7.5YR hues and textures of loam or clay loam. These soils have one or two discontinuities within a depth of 60 in. where No. 121 colluvium lies above a truncated No. 120 soil or above a truncated residual soil. Discontinuities in soils produce conditions for temporary water perching and, more importantly, for the lateral subsurface transmission of water.

12221, 12231, 12241, 12242, 12251. These soils formed in the youngest of the Pumpkin Valley colluvial units. The uppermost colluvial stratigraphic unit contains abun-

dant Rome fragments. These soils occur on typical toe-slope landforms and, if sufficiently thick, contain several discontinuities. Some lower areas are covered with modern alluvial, No. 970 soils. The underlying truncated paleosol is commonly the No. 121 soil. These soils tend to move water laterally because rock fragment orientation is generally parallel to the slope.

12333. The No. 123 soils consist of a sequence of strata where the uppermost strata, composed of young Pumpkin Valley colluvium–alluvium, is underlain by No. 995 old alluvium, which is underlain by residuum of No. 104 Pumpkin Valley glauconitic saprolite. The extent of these soils is not known, since its occurrence cannot be predicted with any certainty, and they can only be mapped at a 1:1200 scale. The identified delineations on the Bear Creek LLWDDD soil survey map have scientific interest in the geomorphic analysis of the area. A pit was dug in a delineation in the Bear Creek LLWDDD site that exposed all three parent materials, and samples were collected for characterization and comparison with similar soils that had not been buried. See pp. 73–76 in ORNL TM-10803 for the soil profile description and characterization data.

Rogersville–Dismal Gap and Nolichucky colluvium

Most colluvial soils could be separated easily according to their parent material origin. Rome and Pumpkin Valley colluvial soils have different rock fragment assemblages and low silt content. Most colluvium from the Rome and Pumpkin Valley Formations was intercepted by drainageways in the Friendship topographic low and did not extend onto and through the Rogersville, Dismal Gap, and Nolichucky with one exception: the

No. 222 deltaic fan or fan terrace in the Bear Creek LLWDDD site, which contains fragments and soil from the Rome and Pumpkin Valley. Soils that formed in Knox colluvium have a high chert content and are easily separated from the Rome, Rome–Pumpkin Valley, and colluvial soils derived from the Rogersville, Dismal Gap, and Nolichucky formations.

Colluvial soils derived from the Rogersville, Dismal Gap, and Nolichucky formations have similar morphologic characteristics, including shale and siltstone fragments, and high silt content. Therefore, they were grouped together in mapping.

22031, 22033, 22041. These soils occur mostly in heads of major drainageways, where smaller first-order drainageways coalesce. There is very little surface water flow across these soils. Most water flow is below the surface, either along horizon boundaries or lithologic discontinuities, and at the top of the Cr horizon. Because of the longer residence time of water in these soils, it also tends to move downward into the saprolite beneath these soils. Most slope shapes are doubly concave and have gradients of about 2 to about 25 percent. Lower slope gradients occur in the bottoms of drainageways and where these soils merge and interfinger with modern alluvial soils (No. 970 and No. 971). Areas of steeper slopes occur where these soils merge with steep residual soils of mid and lower side slopes. Parent materials in these soils is commonly of three kinds: the buried underlying residuum, the truncated and buried remains of an older colluvial soil (No. 225), and a younger uppermost colluvium that has a higher coarse fragment content and must be more than 50 cm thick. These soils tend to fill with water during winter and spring. Water perches at one or more depths after heavy

rains. The dominant flow of water in these soils is lateral.

22121, 22131, 22133, 22141, 22151. These soils are on toe slopes and fan terraces. They usually have one or more lithologic discontinuities, but there is little evidence of perched water at lithologic contacts unless the truncated remains of a clayey argillic horizon in the buried paleosol are present. Erosion during the Pleistocene epoch evidently stripped off most of the older soil before deposition of younger colluvium began. These soils are roughly equivalent to the Rome–Pumpkin Valley colluvial No. 121 soils in degree of soil development in the upper profile. Below the first lithologic-time discontinuity, there is either an older colluvium or the truncated remains of a residual soil. These soils are most common on the Dismal Gap formation. Most areas of these soils occur in first-order drainageways and side slopes of these drainageways. These soils have properties that permit infiltration and retention of rainfall, most of which percolates downward to where it flows laterally and contributes to stream base flow.

22222, 22231, 22232, 22233, 22241, 22242. These soils formed in paleo-Gum Hollow colluvial–alluvial deltaic fan materials that contain Rome and Conasauga fragments and have gravelly textures. They are similar to the No. 121 soils in terms of subsoil color and texture, but have a more strongly developed horizonation. These soils appear to be roughly equivalent in age to the Pumpkin Valley colluvial No. 120 soils and may have an equivalent age to the No. 225 soils described below. The source stream watershed that delivered the sediments was cut off by stream capture. Recent geomorphic investigations have revealed that the deltaic materials these soils formed in had buried the underlying No. 995 high-silt-content alluvium and loess soil, indicating that the

upper gravelly sediments were deposited into a body of standing or very slowly moving water.

22321. These soils formed in colluvium about the same age as the No. 221 soils, which overlay No. 995 Pleistocene alluvium that covers Nolichucky saprolite residuum. These soils occur adjacent to No. 995 soils in foot-slope and toe-slope landforms below long Dismal Gap side slopes, where the alluvium was subsequently buried by colluvium. Not all possible areas have been identified because of location problems in dense pine thickets. Larger areas that were identified are located on the soil map primarily for geomorphology studies. These soils were mappable only in high-resolution mapping at a scale of 1:2400 or larger in the Bear Creek LLWDDD project. They are included with other soils at a scale of 1:12,000 or smaller.

22441. These soils, of very limited extent, formed in colluvium similar to that of the No. 221 soils, but the underlying paleosol is commonly a clayey truncated residual soil that perches water. The fragipan has formed in the lower part of the youngest colluvium. In contrast, the No. 221 soils generally lie on weathered paralithic materials and do not perch water.

22521, 22523, 22531. These soils formed in old colluvium, primarily derived from surficial soils and saprolites of the Dismal Gap formation and Rogersville Shale. They are now on convex landforms (in contrast to the No. 221 soil concave landforms) and have undergone topographic inversion, or else they are perched toe slopes high above present drainageways. These soils seem to be related to, but younger in degree of development than, the Pumpkin Valley colluvial No. 120 soils. They seem to be about the same age as the

No. 222 soils in terms of age and landform location, but are older than the No. 995 soils in terms of age and landform relationships. The No. 225 landforms were probably the concave landforms during the time of No. 222 fan terrace deposition. Many small areas of these soils occur on side slopes in units of Rogersville No. 201 and Dismal Gap No. 205 soils, where their presence cannot be located or predicted by observable landform features. The Dismal Gap sampling pit dissected an old drainageway filled by the No. 225 soil (ORNL TM-10573). These old colluvium-filled drainageways deliver considerable water downslope since the Dismal Gap pit fills with water after each heavy rain and water can be seen seeping from the colluvium-residuum contact. These soils are of small extent, but are important in learning the past geomorphic history of the area and should prove useful in determining long-term rates of geologic erosion. They are also highly significant in the location of burial trenches and tumulus pads. Whenever a trench cuts through an old colluvium-filled drainageway, a hazard for "bath-tubbing" (development of water-filled areas) occurs.

4.4.1.3 Knox colluvium

Most Knox colluvium has a rather high chert content, ranging from about 15 to more than 50 percent throughout the soil. Colluvium is generated by several processes. One process occurs whenever the upper part of upland residual soils becomes saturated and loses stability. The saturated mass flows downslope as mud and covers the slope below, resulting in the lower foot slope being blanketed with a layer of colluvium. Another process is colluvium generated by bioturbation. Trees are overthrown, and the upturned roots bring soil above the surface. As the roots decay, soil is let down the slope.

This process produces a particular kind of micro-relief which is commonly called "cradle knoll." The colluvium generated by this particular process has a sporadic distribution on the landscape and accounts for the sporadic distribution of colluvial pockets in larger areas of residual upland soils. Another geomorphic process that generates colluvium is creep. Creep is a very slow process where soil material is very slowly transported downslope under the primary influence of gravity. Creep processes also move wind-throw soil mounds downslope. It is difficult to distinguish creep materials from bioturbated materials (soil disturbed by the growth of roots), but creep processes are more active on steeper slopes and the local colluvium has a more general and more uniform distribution over the hillslope, in contrast to local colluvium produced by tree tip-over bioturbation.

Knox colluvial soils were identified and separated in mapping according to several criteria including (1) soil morphology and chert content, (2) landscape setting, (3) age, and (4) minimum thickness. Colluvial soils were mapped only when the colluvium was more than 20 in. thick, a thickness that appears to affect subsurface water flow pathways. Colluvial soils were also separated depending on the presence or absence of fragic subsoil properties. Fragipan or subsoil layers with fragic properties that perch water occur only in some colluvial soils and never in residual soils. Colluvial soils with fragipans occur on low toe slopes but have a sporadic distribution and cannot be mapped at a scale of 1:12,000. Colluvial soils on doubly concave landscapes, commonly with fragic properties, were separated from colluvial soils on more convex landscapes which commonly did not have fragic properties. Knox colluvium spans a wide range in age from Tertiary to at least late Pleistocene. The

location of ancient Knox colluvium that now occupies some of the highest elevations on Chestnut Ridge indicates that topographic inversion has occurred. Ancient colluvium has no source area in the present-day landscape. Pleistocene colluvium occurs in saddles and other concave foot-slope and toe-slope landforms. Most Knox colluvium, especially on lower side slopes, has one or more time discontinuities, an indication of more than one major episode of geomorphic instability. The presence of fragic subsoil layers, fragipans, or glossic subsoil zones always marks such a discontinuity in these soils.

Loess has also been deposited throughout the Pleistocene with the latest significant deposition occurring about 12,000 to 25,000 years ago during the melting of the Wisconsinan glaciers. Most of the loess was washed downslope into depressions or onto gentle toe slopes, where it was partially mixed with, and then preserved beneath, younger cherty slope wash. Only at scales of 1:1200 to 1:2400 were loess-derived soils (Soils No. 438 and No. 439) mapped in bottoms of dolines and delineated only with high-resolution mapping.

43021, 43023, 43031, 43033, 43041, 43042, 43043, 43051. The soils of these map units formed in a minimum of 20 in. to several feet of colluvium derived from residual soils of the Knox Group. The No. 430 soils are similar in some respects to the ancient colluvium No. 436 soils, but the No. 436 soils are only mapped in the highest places on hilltops and have no present source of colluvium. The No. 430 soils generally have more than 15 percent chert by volume throughout the soil and can range to more than 50 percent in some areas depending on the chert content in the soils above. These soils occur in saddles and below saddles to the heads of drains, but have a colluvial source in residual soils above them. These soils also occur on

lower side slopes and commonly have a doubly concave slope configuration. Most areas of these soils have a restrictive layer that perches water during wet periods. This restrictive layer commonly occurs at a depth of 75 to 125 cm (30 to 50 in.) below the surface and is more pronounced where slope forms are doubly concave. The restrictive layer, identified by the presence of 10YR 6/3 mottles, locates a discontinuity and the presence of an older, often truncated, paleosol that formed in either an older colluvium or residuum beneath. Some areas of these soils have a fragipan, but the fragipan is intermittent in that it has a sporadic distribution and its presence is unpredictable. Most of the surficial colluvium is of late Pleistocene age, with the latest period of upland denudation and downslope mass movement occurring during the Wisconsin stage of glaciation. Buried beneath this younger colluvium are one or more older colluvial diamictos of probable mid and early Pleistocene. The No. 430 colluvial soils have not experienced topographic inversion. Where topographic inversion has occurred, the ancient late Tertiary or early Pleistocene colluvial soils are identified as No. 436 on the soil map.

The dominant subsurface water flow in these soils is lateral downslope. Water perches and flows above the fragic layer. During wet periods of late winter the soil above the fragic layer is often saturated. Shallow pits and drill holes fill rapidly under these wet conditions, but, during the summer, these soils dry out and become very dry as plants extract soil water from above the pan.

43121, 43131, 43141. The soils of these map units formed in modern deposits of slope wash and occur only in areas where there has been past agricultural activity. These soils occur in broader drainageways and in the bottoms of well-drained and moder-

ately well drained dolines, where surface soil, washed from higher slopes, has accumulated to a depth of more than 50 cm (20 in.). A buried soil always occurs in these soils within a depth of 40 in.

43221, 43231, 43241, 43251. These soils occur on alluvial fan terrace deposits of streams and intermittent drainageways that head in the Knox Group and drain into Bear Creek. The fan deposits have effectively kept Bear Creek from migrating down dip along the strike, but the Creek has impinged on the toes of these fans and redistributed chert fragments downstream. The No. 432 soils have a dark surface soil layer and yellowish-red cherty clay loam subsoil horizons beneath. Beneath the colluvium is Maynardville or Copper Ridge residuum. These fan terrace deposits are probably of late Wisconsinian age or about 25,000 years old. The Knox colluvial No. 432 soils, however, have the appearance of being much older than about 25,000 years because they formed in highly preweathered soil materials that came from the surface and uppermost horizons of very old Knox residual and colluvial soils.

43341, 43351, 43361. The soils of these map units formed in soil creep materials more than 50 cm (20 in.) thick and in the underlying residuum. They occur only on shaded east and northeast aspects underlain by the Knox Group formations. The surface layer is dark (10YR 2/1-3/2) from the high organic matter content and 7 to more than 10 in. thick. The clay-enriched subsoil that formed in creep materials has a yellowish-brown to yellowish-red color and a cherty to very cherty silt loam to silty clay loam soil texture. Cradle-knoll microrelief from past tree wind throws is a common surface feature of these soils. Included in mapping are small areas of soils with higher base saturation because

of the nearness of rock pinnacles or ledges to the surface.

43421, 43431, 43432, 43433, 43441, 43433, 43451. The soils of these map units formed in a layer of colluvium between 20 and 50 in. thick and the underlying clayey Knox residuum. These soils occur on landforms that are mostly convex in contrast to the No. 430 soils that occur on landforms with more concavity. The No. 434 soils have subsoil colors that are brighter and less yellowish than the No. 430 soils, and they have no evident subsoil layer that perches water. These soils have rapid infiltration of rainwater and also rapid subsurface lateral flow.

43551. The soils in this map unit formed in old toe-slope fan-terrace landforms that have partially undergone topographic inversion. Drainageway incision on either side has left these landforms elevated, and they now look like low upland hills. The subsoil has a yellowish-brown color and a high chert content. Texture is cherty or very cherty clay. Only one delineation of these soils was mapped on Chestnut Ridge. About half of the landform has been removed for use as fill materials elsewhere. The soils in this map unit were separated from other colluvial soils because this map unit represents an older mid to early Pleistocene stage of colluviation.

43621, 43631, 43641. The soils of these map units formed in ancient colluvium and local alluvium on toe-slope landforms that, through topographic inversion, now occupy upland summit landscapes. The soils in these map units are mapped only on broad, stable, high-elevation, upland summits on Chestnut Ridge and Melton Hill. They have a thicker and more strongly expressed E horizon than the younger No. 430 and No. 434 soils that

occur on recognizable colluvial landforms. The thickness of this ancient colluvium varies from less than 50 cm (20 in.) to more than 90 cm (36 in.). A paleosol that formed in residuum commonly occurs beneath the colluvium. The chert fragments in this old paleosol are also highly weathered; most are soft and easily broken by augering or cut with a spade, which indicates a long age of weathering. Chert fragments in the colluvium are also commonly impregnated with iron oxides. The presence of these iron-impregnated chert fragments is used as a clue in mapping the areal extent of these soils. Downslope from delineations of these No. 436 soils, it is common to find adjacent areas of the No. 990 and No. 994 soils that formed in ancient toe-slope-fan terrace colluvium-alluvium. Considering the time required for topographic inversion and reddening of the the No. 990 alluvium, it is probable that both these No. 436 soils and the related No. 994 and No. 990 soils have a late Tertiary age.

4.4.2 Doline Soils

Dolines on the ORR range in diameter from about 2 m to 50 m (6 to 150 ft). Dolines occur throughout the Knox Group, in some formations of the Chickamauga Group, a few in the Maynardville Limestone, and at least two in the Rome Formation. None have been observed in the Conasauga Group. Dolines or doline soils were not delineated at the 1:12,000 low-resolution soil mapping, but were delineated in the recent high-resolution soil mapping of Walker Branch Watershed and the East Chestnut Ridge site, where small dolines are shown with a diamond-shaped symbol. One of the larger dolines on the ORR is located in the East Chestnut Ridge site, where it is several hundred feet in diameter. Dolines have different bottom shapes. Dolines with funnel-shaped bottoms were probably more recently

active than dolines with broad, nearly level bottoms. Flat-bottomed dolines have collected sediments from surrounding higher landforms and from their own side slopes as slope retreat progressed. Because of this, a history of the past has been preserved in these flat-bottomed dolines. Soils of distinctive morphology also occur in flat-bottomed dolines. The soils of doline bottoms are described below. There are more active dolines and cave openings on Melton Hill than anywhere else on the ORR.

43731. The soils of this map unit formed in a layer of loess and high-silt-content slope wash that is 50 to 100 cm (20 to 40 in.) thick and in the underlying very cherty to extremely cherty colluvium. These soils occur in some dolines with broad, shallow bottoms and on broad, gently sloping hilltop dolines underlain by ancient colluvium. A well-developed but highly degraded fragipan occurs at the contact of the loess and the extremely cherty soil materials beneath. These soils have very limited extent, but are important in understanding the geomorphic history of Chestnut Ridge.

43821, 43831. The soils of these map units formed in loess that is 50 to more than 100 cm (20 to 40 in.) thick and occur only in the broad bottoms of well-drained and moderately well drained dolines. These soils are very similar to the No. 439 soils, but are better drained. They are also very similar to the No. 437 soils, but the underlying paleosol has a much lower chert content. The surface loess is commonly capped with a thin layer of slope wash consisting of loess with few to common chert fragments. The colluvial paleosol beneath generally has a completely preserved genetic soil horizon sequence. The buried A horizon has lost its organic component and now has a very pale

brown bleached-out appearance. At some depth below the loess, another paleosol occurs in cherty or very cherty colluvium. In some broad and stable doline bottoms, there are two or more layers of loess, commonly separated by a thin layer of silty slope wash that contains some chert fragments. Not all dolines that are shown on high-resolution surficial geology maps have loess deposits in them. Dolines with a funnel-shaped bottom generally have very cherty slope wash in the lowermost portions of them. These soils have very limited extent and can be mapped only at scales of 1:2400 or 1:1200. They are important in that a history of some past geomorphic events has been preserved. In contrast to the smaller dolines, the bottom of the very large doline on East Chestnut Ridge has soils with similar morphology, but with much higher clay content, a problem without an explanation.

43911, 43921. The soils of these map units formed in one or more layers of loess and the underlying cherty colluvium. (Two distinct layers of loess have been identified thus far.) Loess thickness is 50 to more than 100 cm (20 to 40 in.). These soils become increasingly gray with depth, although there are some places where surficial water is perched by paleofragipans that formed in the underlying colluvial paleosol before it was buried by the loess. These soils have very limited extent and can be mapped only at scales of 1:2400 or larger. They are important in acquiring an understanding of past geomorphic processes and events that have shaped the surrounding landforms. A large area of these poorly drained soils occurs in the large doline located on East Chestnut Ridge. These particular soils have a silty clay loam surface horizon and silty clay or clay upper subsoil horizons. At a depth of about 150 cm (60 in.), there is a stratum of fairly clean, pea-sized chert beneath which

is a layer of highly compacted gray silt with only a few pea-sized chert fragments. Below this compacted silt is a thick layer of extremely cherty colluvium. There is no apparent explanation for the higher clay content throughout the soil at present.

4.4.3 Reedsville Shale, Sequatchie Formation, and Rockwood Formation

4.4.3.1 Colluvium

75123, 75133. These soils formed in a mixture of sandstone, siltstone, and shale colluvium derived from East Fork Ridge. They have more than 100 cm of colluvium overlying shale residuum. Only 1.2 to 2 ha (3 to 5 acres) have been mapped on Sheet #1-254. Coarse fragments in the soil are mostly sandstone, but there are also some chert fragments, assumed to have been derived from the Fort Payne Formation.

75143. These soils formed in a thin layer of mostly sandstone-derived colluvium from East Fork Ridge. The colluvium is 50 to 100 cm (20 to 40 in.) thick and covers the Reedsville, Sequatchie, and part of the Chickamauga formations to the south. Only one delineation has been identified on Sheet #1-254.

75223, 75233, 75241. These soils formed mostly in siltstone- and shale-derived colluvium from the Reedsville Shale and Sequatchie Formation. These soils have been mapped on Sheet #1-254. These soils have a clayey Bt horizon and only a few sandstone coarse fragments.

4.4.3.2 Alluvium

Alluvium is defined as soil materials that have been transported by water and that have been sedimented from moving water.

4.4.4 Ancient Alluvium

Ancient alluvium is defined for purposes of this report as late Tertiary. The floodplains and low terraces of initial deposition have all been topographically inverted, and the ancient alluvium now occurs high on Chestnut Ridge and Melton Hill. Old alluvium is Pleistocene alluvium, which has been in place and stable long enough for well-defined genetic soil horizons to have formed and where most evidence for the original terrace landforms has been destroyed by erosion, or where high-level terraces have been stranded and preserved as rivers continued their down-cutting. Both old and ancient alluvium soils have thick, well-defined argillic horizons. Most classify as Paleudults. Both old and ancient alluvium soils have local and distant sources. Alluvium of local sources contains fairly abundant chert fragments, but the chert fragments are highly weathered and can easily be cut with a spade. In addition, many of these chert fragments are impregnated with iron oxides, and some iron oxides have been converted to maghemite, a visual clue to the identification of ancient alluvium. Main-channel ancient alluvium contains few, if any, chert fragments, but in a few places a rounded metaquartzite river cobble can be found on the soil surface and in pit sidewalls. Old alluvium soils have very few weatherable minerals in the sand or silt fractions, and the clay fraction is usually dominated by kaolinite or hydroxy-interlayered vermiculite (HIV). Some old and ancient alluvium has been covered by younger materials, including younger alluvium, colluvium, or loess.

99031, 99042, 99043, 99053. The soils in these map units formed in ancient alluvium of probable late Tertiary or early Pleistocene age. Today, these soils occupy some of the higher elevations on Chestnut

Ridge and Melton Hill. Most areas of these soils were preserved on southeast and south slopes, which tend to be more geomorphically stable, and are mostly underlain by residuum of the Copper Ridge Dolomite and the lower Chepultepec Dolomite. The No. 990 soils have a thick, dark surface layer and dark-red clayey subsoil horizons. Most areas of these soils have very few coarse fragments. Only fragments resistant to weathering remain. These are chert of local origin and metaquartzites from the Unakas that have been impregnated with maghemite and magnetite iron oxides. Another key indicator of these soils is the presence of numerous small, hard manganese-iron nodules throughout the soil, nodules that do not occur in adjacent residual or colluvial soils except in the No. 436 soils.

These soils are the alluvial remnants preserved from an earlier erosion cycle. Several questions remain as to how these soils became dark red, including: What is the source of all the iron oxide? Was the iron oxide translocated from higher landforms when these soils were in floodplain and terrace landforms? Today, except for the occasional rounded river cobble, it is difficult to imagine that these soils were once in low-lying but well-drained floodplain landscapes with hills rising from their edge. The present distribution of iron oxides and their color suggests that these soils were not subjected to a long period of fluctuating water tables. If they had, then the iron would have been organized into hard nodules, with a pale soil matrix between nodules. Typically, these soils are identified by the numerous iron (maghemite) shot that are about 1 to 2 mm in diameter. This soil feature would suggest that these soils were once in a fluctuating water table zone, a condition required for the migration of these oxides into hard nodules, but as rivers shifted course and continued to downcut, the soil would have

become better drained. It would seem that further additions of iron would be necessary to form the dark-red colors observed today. There are at least two sources for the additional iron that is now disseminated throughout these dark red soils. One source is deposition from the air; the other is from weatherable biotite and chlorite minerals carried from the Blue Ridge by an ancestral Tennessee River.

99121, 99122, 99131, 99132, 99141, 99143.

The soils in these map units formed in a layer of late Pleistocene yellowish-brown loess about 20 to 40 in. thick and in the underlying ancient reddish-yellow local alluvium. These soils typically have two clay-enriched subsoil horizons. The upper subsoil formed in loess-like materials. It is yellowish-brown and has a silty clay loam texture. The lower clay-enriched subsoil formed in the underlying alluvium. This particular subsoil layer has a redder, but often mottled color and a clay loam texture. Maghemite nodules are a common feature of the ancient alluvium and help to identify its presence. These soils occur on a bench landform close to the crest of the residual soil hills. They have undergone topographic inversion, an indication of their absolute age. The greater permeability of the alluvium compared to the surrounding clayey residual soils allowed for greater geomorphic stability, thus preserving these ancient soils. The permeability of the alluvium also allowed for the preservation of loess. The surficial loess, presumed to be of Wisconsinan age, or about 19,000 to 23,000 years before present, is based on the presence of abundant soil vermiculite, a highly reactive clay mineral lacking at a similar depth in older soils.

99221, 99231. These soils formed in main-channel alluvium of an ancestral Clinch (Tennessee) River. They are on an upland summit at an elevation of 280 m (840 to

850 ft) that is nearly level with 0 to 2 percent slopes, and on the shoulder and upper side slopes with slopes of 6 to about 20 percent. The summit is nearly level and 50 to 65 m (150 to 200 ft) wide. The shoulders around the summit are mostly doubly convex, while the side slopes are mostly inclined-linear.

The flat upland summit has a silty capping of loessal materials which results in the fine-silty family particle size class, while the side slope soils classify as clayey or fine-loamy. The southern side slopes are mostly clayey, while the westerly and northerly aspects have a higher sand content in the upper part of the soil and have a fine-loamy particle size class. All of the soils are only slightly to moderately eroded because of the relatively good permeability of the loess and the alluvium and of the fair permeability of the underlying shale.

It is most unusual to find old high-level alluvium lying on shale. Two factors appear to be responsible for its preservation: the rather permeable nature of the underlying shale and, probably the most important, the basal gravel zone in the alluvium, which would stabilize the side slopes by armouring the base of the alluvium, preventing slope retreat. The old alluvium occurs on one of the highest and broadest parts of the area around SWSA 6, although smaller doubly convex shale summits to the north are higher. The basal gravels contain chert from the Knox Group dolostones, rounded sandstone gravels from the Rome, and very hard and smooth-rounded quartzites gravels and cobbles from the metamorphic formations of the Great Smokies and Unakas. The border between the alluvium and underlying shale is marked by a change in slope, with the shale-derived soils having a steeper slope gradient.

99321, 99322, 99323, 99331. These soils occupy locations on two landforms separated by elevation and age, but have similar morphology. These soils are commonly associated with the No. 225 soils on higher parts of the landscape and are described as "old" No. 993 in the Bear Creek LLWDDD report. Some areas occur on lower parts of the landscape, where they are underlain by the Maynardville Formation and are referred to as "young" No. 993. Morphologically, the soils appear to be very similar, but might have significant chemical differences, and can be separated later, if necessary, should conditions warrant. These soils formed in alluvium. During early stages of soil formation, there were periods of fluctuating water tables, the cause for the formation of segregated iron and manganese compounds into hard nodules. These soils are now well-drained and highly oxidized due to continued downcutting of Bear Creek and its tributaries on that site. Small, hard manganese and iron nodules are required for positive identification. The Bt horizon has either a 7.5YR or 5YR hue and loam or clay loam texture. These soils are mapped only on the Conasauga Group and contain only fragments from the Rome Formation and Conasauga Group. (A similar No. 994 soil is mapped over the Knox Group, but contains abundant chert fragments.) Where the No. 993 soils occur over the underlying Maynardville Limestone, there has been better drainage and oxidation and the alluvial soil has redder hues. Thus these soils, at a lower elevation over limestone, have similar morphology to higher areas of these soils that are on shale even though they have a younger age. The differential rates of soil development seem to have resulted in soils of different absolute age having a same relative age based on morphological characteristics.

99421, 99431, 99441, 99443. These soils are on broad upland summit landscapes underlain by either Knox Group residuum or colluvial soils. They formed in a mixture of local cherty colluvium and alluvium and in the underlying Knox clayey residuum and were mapped whenever the surficial materials were more than 20 in. thick. These soils originally occupied low toe-slope-terrace landforms where alluvium and colluvium accumulated. Subsequent topographic inversion has transformed these once low landforms to where they are today. The soils in these map units have subsoils that contain less clay than nearby residual soils. Subsoil colors also tend to be redder than the adjacent residual soils, but less red and with lower clay content than the adjacent No. 990 ancient alluvial soils. A more important indicator of these soils is the highly weathered and iron-impregnated nature of the chert fragments. Maghemite is a common mineral in these soils and helps in their identification. Many chert fragments are quite soft and have been partially converted to kaolinite. Other chert fragments have a red rind. These soils occupy a transition zone between the No. 436 soils, which were stripped free of iron and manganese oxides, and the No. 990 soils, which have red and dark-red subsoils. Where these soils occur near the No. 436 soils, they have a higher chert content and less red colors, whereas areas near No. 990 soils have redder colors and less chert. As mapped on Chestnut Ridge and Melton Hill, the No. 994 soils represent at least two periods of erosion, downcutting of rivers and deposition of younger alluvium. Ridge-top areas of No. 994 soils represent the remnants of the oldest period of deposition. Other areas of No. 994 soils are mapped at lower elevation on Chestnut Ridge and Melton Hill on old fan-terrace landscapes, but still high above present areas of toe-slope and fan-terrace collu-

vium-alluvium deposition. The extent of the No. 994 soils is not large, but the age and geomorphic history of these soils and the associated No. 436 and No. 990 soils is important in the determination of the ages and stabilities of landform surfaces and in the development of karst topographic features.

99511, 99521, 99522, 99531, 99532, 99533, 99541. These soils formed in alluvium and surficial loess and have very high, fine sand content. A paleosol, also formed in alluvium, but with slightly higher clay content and less loess, commonly occurs within a depth of 40 in. There are few or no fragic properties at the discontinuity. Some areas have a fragipan. Fragipan areas have the old alluvium underlain directly by a clayey residual soil and are identified by the No. 996 symbol. These soils represent a time when Bear Creek, Poplar Creek, and most other creeks were probably dammed by the Clinch river and represent a backwater deposition. These soils occur at elevations of 215 m (840 to 850 ft) on nearly all ORR streams. One or more old Bear Creek channels have been identified in the Bear Creek LLWDDD site by the presence of chert fragments and well-rounded gravels. Because of the gentle topography, loess and dust also settled and were preserved. These soils typically have a 2.5Y hue in the upper Bt horizon. The upper solum has a high silt and very fine sand content. The lower Bt, which has better structure than the upper Bt, seems to be slightly older and has a mostly alluvial origin. This horizon and transition horizons beneath become more mottled with increasing depth. Small, hard manganese-iron nodules are a common feature in the upper subsoil, and large manganese or iron concentrations are commonly located in the lower Bt horizon. Most areas of these soils lie directly on 2C or 2Cr horizons of shale, but some areas

are underlain by Chickamauga soils. They were mapped whenever the thickness of alluvium exceeded 50 cm (20 in.). The No. 995 soils, wherever they occur on the ORR, have similar morphology, but can have differing textures and types and quantities of coarse fragments.

These soils have significant engineering problems. They cannot be compacted, and they have very low bearing capacity.

Note: Areas of No. 995 soils and very similar alluvium parent materials occur in Grassy Creek watershed, McNew Hollow, Hot Yard Hollow, Raccoon Creek watershed and Melton Branch, Bearden Creek, and other creeks that drain into the Clinch River. Large areas of the 995 soils should also occur in Poplar Creek watershed at an elevation of 280 m (840 to 850 ft).

99621. These soils occupy toe-slope positions between residual soils of the Nolichucky Shale and Dismal Gap formation and deeper alluvium of the No. 995 soils. These soils have a fragipan that occurs at a depth of 80 to 125 cm below the soil surface. Below the fragipan is a buried soil with a clayey argillic horizon that perches water. These soils have minor extent, but are significant for geomorphic studies in that a buried paleosol is preserved beneath younger surficial sediments.

99721, 99722, 99731, 997733. These soils were mapped on partially dissected terrace landforms that are not attached to the present-day terrace-floodplain landforms of the Clinch River. The largest extent of these soils occurs in an abandoned meander of the Clinch River at an elevation of 260 m (800 to 815 ft), but other areas have been mapped in the Melton Hill area at the same elevation. These soils have a yellowish-red clay loam subsoil that contains local chert plus other rounded quartzites and sandstones of more distant origin.

99821, 99831. The soils in these map units classify as Typic Paleudults: clayey or fine-loamy, siliceous, thermic (Etowah). These soils are on high river terrace landscapes. They formed in a mixture of old Clinch River alluvium from both local and distant origins. Continued downcutting by the Clinch River after deposition has resulted in the present higher elevation of these soils above the river. These soils have been mapped on an abandoned meander and on terraces of about 260 to 270 m (790 to 815 ft). They also occupy higher terraces adjacent to the No. 999 soils, which occur on lower elevation terraces.

4.4.5 Holocene Alluvium

Holocene soils have moderately well defined genetic soil horizons, but the argillic horizon has less thickness than in old alluvium soils. Holocene soils are all classified as Hapludults because of the thinness of genetic soil horizons. Holocene soils on the ORR are all river terrace soils, on well-defined and recognizable river terraces or on fan terraces or deltaic fans.

99922. These soils generally occur on wider low terraces along the Clinch River, but were mapped in alluvial floodplain sediments of an abandoned meander loop of the Clinch River and in Walker Branch Watershed. They are considered to have a late Pleistocene or early Holocene age. They have a high content of very fine sand throughout the profile, and a yellowish-brown Bt horizon with a loam or light clay loam texture. There are generally very few or no coarse fragments. They have segregated iron-manganese zones in the subsoil, but no hard nodules, an indication that the meander was abandoned in the late Pleistocene to Early Holocene, or about 30,000 to 18,000 years ago.

4.4.6 Modern Alluvium

Modern alluvium is defined as alluvium of less than 300 years old, the result of anthropogenic accelerated erosion from the clearing and agricultural activities of European settlers. Recent alluvium is stratified close to or to the surface and lacks any diagnostic subsurface horizon within a depth of 50 cm (20 in) below the surface.

4.4.6.1 Rome and Pumpkin Valley

96021. Where these soils occur along drainageways, they are highly stratified. Most of the sand fraction is very fine sand. Where they occur at the base of cultivated slopes, these soils consist of mostly topsoil that washed off higher slopes. Most areas of these soils in drainageways have a well-defined channel and are well or moderately well drained as a result. Most of the upper 100 cm of these soils consists of sediments eroded by the initial deforestation and subsequent agricultural and present-day forestry land uses. Most areas of these soils have a paleosol below a depth of 50 cm to more than 100 cm. These soils frequently flood for periods of short duration with storm events that produce overland runoff. Some small areas of these soils will qualify as wetland.

96211, 96221. These soils are on nearly level floodplains of drainageways that have their source in the Rome Formation and Pumpkin Valley Shale. Most of the sand fraction is very fine sand. Slopes range to 12 percent below springs. Most areas of these soils contain springs or seepage zones which keeps them wet most of the time, or they do not have a defined channel and water flows very slowly across the area keeping the soils wet. These soils usually contain large amounts of manganese brought by upwelling

groundwater. These soils qualify as wetlands.

4.4.7 Conasauga Alluvium

97011, 97021. These soils formed in Recent alluvium and have a much higher silt content than the Rome and Pumpkin Valley alluvial soils. They are in narrow drainageways in areas of Rogersville, Dismal Gap, and Nolichucky soils. These well- and moderately well drained soils are undifferentiated with respect to degree of wetness. Most areas of these soils have a well-defined and entrenched channel. The largest areas of these soils occur on the floodplain and low terraces of Bear Creek. Nearly all areas of these soils have a buried soil between a depth of 50 cm and 100 cm. Some small areas within these map units will have wetland soils.

97111. These somewhat nonsloping and poorly drained soils occur in nearly level drainageways within areas of Rogersville, Dismal Gap, and Nolichucky soils that contribute high-silt-content sediments to drainageways. Most areas of these soils overlie a buried soil between a depth of 50 to 100 cm (20 and 40 in.). Most areas of these soils contain springs or seepage zones or do not have a defined channel and remain wet most of the year. Present vegetation is hardwoods with a ground cover of water-tolerant plants. Most areas in these map units will qualify as wetlands.

97211. These are moderately well drained to poorly drained soils forming in modern alluvium over a wet (Typic Ochraqualf; fine, mixed or montmorillonitic, thermic) soil derived from the Nolichucky Shale and Maynardville Limestone. Most areas of these soils occur within the modern floodplain of Bear Creek southeast of Pine Ridge. Other areas occur in the

headwaters of Melton Creek. In some areas, remnants of an old cherty paleosol commonly occur just above the bedrock, especially close to the lowermost floodplain. Small areas in most map units will qualify as wetlands.

4.4.8 Knox Alluvium

98031, 98041. The landforms and soils in these units occur as a complex that comprises the coves and narrow drainageways of Chestnut Ridge and Melton Hill. The Udifluent soils occur in floodplains and narrow bottoms. They are stratified and show minimal evidence of soil genesis. Textures are cherty to extremely cherty silt loams and loams. The Fragiudult and Paleudult colluvial soils occur in narrow strips on toe slopes that are usually too small to delineate, but are important in hydrology and land use. Also included in the colluvial parts of the landscape are small alluvial fans from recently cut gullies, the results of past land mismanagement from both farming and forestry. Old farm or logging access roads are a common feature in areas of these soils, especially in wider drainageways. Most of the soils in these mapping units are well-drained, but some areas, where small seeps and springs occur, are wet. Knick points, entrenched channels, and over-washed zones occur throughout the Udifluent soil areas, giving rise to a complicated sequence and pattern of soils. Fragipans commonly occur in the colluvial soil areas, as well as in areas without fragipans or in areas that have fragic subsoil properties. Some toe-slope areas have been covered by modern slope wash from agricultural fields on the slopes above. Some areas of these soils have abundant cobble-sized and boulder-sized chert on the surface and in the soil. Most rainfall and run-on water from higher slopes infiltrates and flows downward and

laterally in these soils. Consequently, these soils have a tendency to become filled with water during wet periods. Water also perches at discontinuities, but these soils tend to be freely draining because of the low clay content, the slope, and the pipes that have formed from bioactivity.

98121, 98131. These well and moderately well drained soils formed in alluvium washed from residual upland and colluvial soils of the Knox Group. The upper part of these soils is derived from Modern-age sediments washed down into drainageways by land clearing and subsequent agricultural activities of European settlers. The thickness of this Modern-age sediment ranges from about 50 to more than 100 cm. The modern sediments commonly contain one or more buried surface layers, the effects of catastrophic, locally intense storms on bare soils. Buried soils beneath this Modern-age alluvium have a variety of morphologic expression ranging from weak cambic horizons to clay enriched argillic horizons. The largest area of these soils occurs along Ish Creek. Some areas occur along the lower reach of Walker Branch, but most areas of these soils occur in narrow drainageways and are mapped as a complex with low toe-slope colluvial soils and are identified by the No. 980 symbol.

98211. The soils in this map unit are located on wet floodplains, but are undifferentiated with respect to their morphology and classification. They are somewhat poorly drained to very poorly drained. Most of the delineations in this unit generally contain springs and seeps that keep the soils wet and saturated most of the time. In other areas that are wet, stream channels tend to be poorly defined or else they are very shallow. Only vegetation tolerant of wet conditions grows well

on these soils. Small areas of these soils occur as inclusions in larger areas of No. 980 soils.

98521. The soils in this map unit formed in dark reddish-brown sediments that were washed from higher areas of No. 990 and No. 994 soils. They have been mapped only on Melton Hill.

4.4.9 Chickamauga Alluvium

98321. The landforms and soils in this map unit occur as a complex. The soils that classify as Udifluvents occur on mostly narrow floodplains and second bottoms, usually with an entrenched channel. The soils that classify as Hapludults occur on foot-slope and toe-slope landforms that extend partway up the sides of drainageways. Small areas within this map unit will qualify as wetlands.

98411. The soil in this map unit formed in a thin mantle of alluvium and colluvium and in the underlying clayey residuum. Springs and seepage areas keep these soils wet for most of the year. They are identified by the wet-tolerant vegetation and gray subsoil colors. Most of the soils in this map unit will qualify as wetlands.

4.5 INTERPRETATIONS

The ability to predict the response of a particular type of soil to a change in land use needs to be known when land use is being planned. It is also important to know how the engineering properties of natural, in-place soil can be modified so that the site can be made more suitable for some specific use. Many predictions of interpretive behavior are based (1) on past observations, (2) on research on the same or similar soils, (3) on external and internal

forces and processes that influenced rock weathering and soil formation, and (4) on the physical, chemical, mineralogical, and hydrologic properties of the soil. Many of the interpretations of Table 3 were developed in accordance with the criteria in the National Soils Handbook (Soils Staff 1983). The rating criteria in the handbook allow soil scientists to make reasonable estimates of inferred soil properties on the basis of observable soil characteristics. The depth of soil observation for predicting soil behavior in the National Soils Handbook is confined to a depth of about 2 m (6 ft) in deep soils, or to hard rock or to dense weathered bedrock if these features occur at a shallower depth. Some of the interpretations in Table 3, however, require knowledge of soil properties for many meters beneath the surface. An understanding of the properties of deep soil layers (saprolite) is generally lacking on the ORR, but deep soil coring on the East Chestnut Ridge Site, Walker Branch Watershed, and new borrow pits located on Chestnut Ridge have provided a means for observation of spatial variability, and channelized saturated water flow at depth and observation of both vertical and lateral variations of saprolites in some parts of the Knox Group. Deep pits in some of the Conasauga Group have provided insight into the downward movement of water through saprolite in the Dismal Gap, Nolichucky, and Pumpkin Valley Formations. The interpretations in this section should assist in the preparation of environmental impact statements and in assessments for future land uses.

4.5.1 Drainage

Drainage classes are based on the frequency and duration of periods when the soil is saturated. Water may be either perched by some restrictive layer in the soil during wet periods or the soil becomes

saturated by the groundwater table as it rises during wet periods. Perched water or groundwater in the soil can usually be identified by soil color patterns. Soil colors are of two general kinds: (1) colors inherited from the parent materials (saprolite, colluvium, or alluvium) and (2) colors that are the result of soil formation. Most color in well-oxidized soil is due to (1) iron oxides, giving rise to yellows, browns, and reds, with less contribution from organic carbon (black in surface horizons), and manganese (black) and (2) deoxidized colors that result when water saturates the soil. These colors are those of uncoated mineral grains or of iron hydroxides. There are some areas where reduced iron accumulates in wet areas giving rise to soil colors in shades of greens and blues.

When water perches in a soil, the soil is usually not uniformly saturated. Instead there are areas with anoxic conditions where biologic activity removes oxygen from the soil. In these anoxic areas, manganese and iron are reduced, becoming much more mobile. Mobile iron ions migrate both laterally and downward to areas that have a higher redox potential, where they precipitate and form either coatings or nodules that have their own shades of reds and yellows. Manganese ions always move in front of iron compounds. Manganese will precipitate out at a lower level as black coatings on faces of fragments. The anoxic or reduced zones acquire the grayish color of uncoated mineral grains. In some reduced zones, where there is no water movement, reduced iron remains in the system, resulting in highly unusual soil colors of blues and greens. Perched zones commonly have a highly mottled color pattern, whereas the more oxidized unsaturated zone beneath does not. In those areas where the groundwater table intersects the surface, the upper soil can have a mottled color pattern, but the soil color becomes

increasingly gray and more uniformly gray with increasing depth. There are many small areas on the ORR where the groundwater table comes to the surface. These areas are down below springs and seeps and in very low drainageways that flow year around. The groundwater table that results in springs and seeps may also be perched in the rock or at the rock-soil contact.

Drainage conditions in soils have traditionally been interpreted for growing plants and other biologic activity in the soil. Drainage classes as defined in the Soil Survey Manual (1981) are based on shallow-rooted agricultural crops and for the season of plant growth. Drainage conditions are divided into five classes, ranging from excessively well drained to very poorly drained. Definitions of these classes are in the Revised Soil Survey Manual (Soils Staff 1981).

4.5.2 Hydrology

Soils and their associated landforms are rated for their capacity to allow the downward movement of water to recharge the groundwater or for their discharge potential. Once rainfall has infiltrated the soil surface, it tends to move downward rather uniformly through the surface layer and upper subsoil. With increasing depth in the subsoil, water tends to move in preferred, defined pathways, many of which were formed by biologic activity, including burrowing by soil fauna and deep rooting by trees.

4.5.3 Surface Water Infiltration and Near Surface Waterflow

Infiltration of rainfall, tree drip, or by stem flow into the soil is a dynamic process controlled by several factors including (1) slope gradient; (2) slope shape; (3) presence or absence of surficial organic

layers and their hydrophobicity; (4) surface layer soil texture, soil structure and aggregate stability, and macropores; (5) subsoil hydraulic conductivity, including pore size distribution and continuity; and (6) the layer in the soil with limiting hydraulic conductivity. Rainfall initially infiltrates at its highest rate in either dry or moist bare soil. The ability of a soil to sustain its high rate of infiltration depends on the ability of the soil to transmit this water downwards. Whenever the rate of rainfall exceeds the rate of infiltration, overland flow starts. As water moves downwards, the rate at which it does so decreases. Once a limiting hydraulic layer is encountered, water will tend to pile up and saturate the soil. Eventually the surface layer can become saturated. Once this happens, overland runoff starts. Saturated soil layers tend to lose much of their stability and tend to move downslope.

Surface litter can greatly affect the pathways that rainfall takes to eventually get into the mineral soil. Leaves and needles with high surface wax content tend to be hydrophobic. Water beads up on leaf surfaces and tends to puddle. Where the ground surface is covered with a thick layer of chestnut oak leaves, rainfall can puddle on the surface and flow off the site without much infiltration. The overlapping leaves act somewhat like a shingle roof. Often, rainfall that beads up on leaves will break through in random places and flow downward as saturated flow, while in other places the mineral soil does not become wetted. Tree stem flow, once it starts, results in considerable delivery of water into the soil. Stem flow water can penetrate quickly to considerable depth via saturated flow down existing root channels. Rainfall that initially ponds and flows on the surface litter can also impinge on old stump holes that are filled with leaves. The loose soil and leaves in the stump hole become saturated.

Water leaving old stump holes can also move rapidly downwards as saturated flow. This water, because it passes through a thick layer of decayed and decaying leaves, can pick up a load of dissolved organic carbon.

Water can perch in a soil, at any depth, whenever the saturated hydraulic conductivity of the soil layer beneath is exceeded. Perched water tends to pile up in the soil and has a tendency to flow laterally along a hydraulic gradient. In residual soils, water commonly perches during and after heavy rains within the E horizon because the Bt horizon beneath has much slower conductivity. Perched E horizon water also moves readily laterally downslope. Water that perches in the E horizon is responsible for both its generation and thickening over time. Specific kinds of chemical processes take place within an E horizon that is underlain by a Bt horizon. Water infiltrating through the organic surface layers and the carbon-enriched A horizon carry dissolved organics into the E horizon. These organic compounds plus anaerobic respiration results in the reduction of iron, destruction of clay minerals, and subsequent organic chelation of iron and aluminum. Iron and aluminum are carried downward into the Bt horizon. There, aluminum can recombine with silica neoforming kaolinitic clay minerals. In addition, downward streaming of water through the E horizon can also transport particulate clay particles into the Bt horizon. There, translocated clay and neoformed clay coats ped surfaces and lines pores. Both translocated and neoformed clay can occur many feet into saprolite where it eventually plugs water flow pathways.

The upper part of the clay-enriched Bt horizon has higher conductivity than the lower part. Water that gets into the Bt horizon tends to become confined to particular flow pathways in the lower part.

There again, water tends to perch whenever the conductivity of the more limiting layer below is exceeded. Once water has moved through the lower subsoil, it moves via saturated flow in defined pathways and also by unsaturated flow away from these pathways. Patterns of soil colors in the lower subsoil and saprolite visually defines these pathways of saturated water flow. Water usually perches at two or more depths in many residual soils in the survey area. Water commonly perches at the base of the E horizon at a depth between about 25 to nearly 75 cm (10 to 30 in.), the depth depending upon the thickness of the E horizon. Water commonly perches in the lower Bt horizon between depths of about 100 to 125 cm (40 to 50 in.). Water also perches at the upper Cr horizon and on top of hard rock.

The colluvial soils in the soil survey area have slightly different hydraulic conductivity properties than do the residual soils. First, the colluvial soil material was once saturated and flowed downslope as a saturated mass to a lower concave slope position, where it achieved some degree of geomorphic stability. Colluvium has undergone a partial sorting as it moved downslope. The clay content has been reduced, and considerable iron has been removed. Colluvium tends to have a higher hydraulic conductivity than the adjacent residual soils, and water tends to readily infiltrate and move downward. However, the contact between the more permeable colluvium and the less permeable soil beneath constitutes a limiting layer. There, water perches and then readily flows laterally downslope. If conditions are right, a fragipan having very limited conductivity forms at this discontinuity. Fragipans are not a common feature of most ORR colluvial soils, but lower colluvial subsoil layers have some properties of fragipans or show visual morphologic evidence of present or past perching

of water. Water usually perches in colluvial soils at the uppermost discontinuity that commonly occurs at a depth of 65 to more than 125 cm (24 to 50 in.).

Alluvial soils, because of their stratified nature, tend to transmit water laterally very easily because the fine strata act as water barriers for downward movement.

4.5.4 Water Flow Pathways Deeper in the Soil

Most saturated water movement in deeper soil layers and in saprolite is strongly confined along cracks and fractures and along bedding planes. Color patterns, including distributions of iron and manganese coatings in saprolite, can be used to show where water is moving via saturated and unsaturated flow. Water flows away from saturated zones via unsaturated flow mechanisms. Manganese is commonly reduced and mobilized in saturated zones, but is then transported laterally away via unsaturated flow. Some, but not all cherty zones and some chert beds in residual soils derived from the Knox Group tend to be zones where water moves downward quite rapidly. These water flow zones have bright-red iron oxide or red coatings of neoformed clay-iron oxide coatings. Manganese oxide, if present, occurs as well as a crystalline black mineral that has been occluded from the system by a thick iron oxide-clay coating. In areas where limestone pinnacles occur, water, once it reaches the pinnacle, can move downward very rapidly in the thin but very permeable weathering zone between hard rock and the clayey residuum.

4.5.5 Soil Role in Hydrologic Discharge and Recharge of Perched and Groundwater Tables

Rainfall that infiltrates the soil can move downward to recharge shallow perched water tables or the groundwater table, or it can move laterally at shallow depths, where it emerges at the surface as either a wet weather spring or seep. Most landforms underlain by residual soils tend to be recharge areas. However, most residual soils also generate overland flow or shallow subsurface lateral flow during periods of heavy rainfall. Some upland residual soils have much higher capacity to recharge groundwater than other soils. Residual soils that formed over feldspathic sandstones and siltstones of the uppermost Rome Formation appear to have a very high capacity to transmit water very quickly down dip to the groundwater because there is little evidence of overland flow. Many of the Knox Group residual soils can also transmit water downward quickly, although clay-plugged lower subsoil and upper clay-plugged saprolite slows down the rate. Knox Group soils also have the capability to transmit water laterally to lower landforms, a discharge of the ephemeral uppermost perched water table that forms in these soils during the winter and after very heavy rainfall.

Colluvial soils have the capability both to recharge and discharge shallow perched water. Laterally transmitted water from colluvial soils is discharged by upwelling in ephemeral "wet weather" seeps or discharged in seepy wet areas at the base of hills. Both colluvium and alluvium have a high capacity to move water laterally down slope. Groundwater recharge occurs readily in areas of karst, which allows for rapid movement of rainfall, overland flow, or near-surface lateral flow directly to the water table through dolines, pipes, or open swallow holes.

The only areas on the ORR where groundwater is discharged is at permanent springs. The soils downslope from these springs have the typical gray soil colors from ground that is constantly saturated. Stream reaches that flow only during periods of rainfall that generate overland flow tend to be areas of groundwater recharge. Stream reaches with permanent flow are areas of discharge.

4.5.5.1 Depth to restriction

Depth to a restriction refers to the location in the soil where there is a significant change in porosity or where a discontinuity results in a change in porosity. The potential for perched water conditions, the depth at which perching will occur, and its subsequent lateral downslope movement beneath the soil surface depend on the hydraulic conductivity of each soil layer and whether or not it is exceeded during periods of rainfall. Major subsoil and substratum restrictions are the following: (1) abrupt change in soil texture, (2) depth to weathered bedrock, (3) subsoil fragipan or subsoil fragic properties, (4) lithologic discontinuities, (5) clay-plugged zones, and (6) hard rock.

4.5.5.2 Disturbed soil erosion potential

The erosion potential of disturbed soils without surface vegetation cover or mulch is estimated. Erosion potential is rated from low to very high. Erosion is initiated by raindrop splash, which detaches soil particles. Overland flow transports soil particles downslope. Concentrated surface flow on bare, unprotected surfaces produces rills and gullies resulting in very high erosion potential. Disturbed soil erosion potential can be greatly reduced by adequate engineering design and installation of control measures before a site is disturbed and during site construction.

Maintenance of erosion control measures is needed until the site has been restabilized by permanently maintained vegetation.

4.5.5.3 Undisturbed soil erosion potential

The erosion potential (geologic rate of erosion) of undisturbed soils that are covered by grass or covered by a forest litter layer is estimated. Erosion potential is rated from low to medium.

Soil surface layers that have a high silt and clay content generally have a medium erosion potential, or less than 1 to 2 tons of soil per acre per year. In a forested area, soil particles are brought to the surface above the litter layer by ant and other soil fauna activity and then are subjected to downslope transport by overland flow. Periodic wildfires that destroy the litter layer result in pulses of increased erosion until the surface is protected again by litter.

4.5.5.4 Suitability for pines

Soils are rated for their suitability for growing tap-rooted pines. Soil depth for rooting activity is an important rating criterion. Ratings range from poor to good for short-rotation management of pines.

4.5.5.5 Ratings for hardwoods

Soils are rated for long-term management of hardwoods for saw logs. Different species of hardwoods have varying site requirements, including the ability of the soil to supply water and nutrients and potential rooting depth over the life span of the tree. Some hardwoods have the potential to extend their root systems deeply downward into saprolite and into hard rock fractures and joints where chemical weathering processes release quantities of calcium, potassium, and other

elements that trees need for sustained growth. Soils are rated from poor to good.

4.5.5.6 Ratings for paved roads and streets

Paved roads and streets are covered with an impermeable layer of asphalt or concrete, which covers a prepared subbase of natural soil materials that are modified by the additions of gravel to support a design load. Soils are rated for their suitability as a source for on-site subbase materials and for the ability of the natural undisturbed soil beneath the subbase to support the road and its designed dynamic load. Ratings range from very poor for soils with very high silt content, or that are saturated close to the surface, to good for soils that have good physical properties and that are well-drained.

4.5.5.7 Ratings for unpaved roads

Unpaved roads are those roads that rely on the properties of the natural soil for strength. Unpaved roads may be covered with gravel or cinders. Commonly, in construction, the surface, organic-enriched material is stripped off and the subsoil material from the ditches on either side is put onto the road bed, shaped to crown it, compacted to some extent, and covered with gravel. Therefore, on-site soils are rated for their suitability to support loads. Ditch and roadbank erosion potential is also considered in rating soils for this use. Ratings range from very poor to good.

4.5.5.8 Ratings for waste disposal in trenches

Soils are rated for their chemical capacity to retain cations and anions that may be released if the buried materials should become saturated. Soils are rated for depth, for sidewall stability, for their

permeability, for their potential to perch water (bathtubbing), and the likelihood of soils above the trench to transmit water laterally downslope to where it will intercept a trench. Soils are rated from very poor to good. Engineering design can overcome some soil problems. But it must be strongly emphasized that the properties of the natural, undisturbed, soil-saprolite-rock geohydrologic system beneath the trench must provide for the ultimate containment for the waste and any leachate that is produced. If this is not considered, then there can be a high probability of movement of hazardous materials away from the trench. Engineering modifications will only delay the onset of leachate production in the humid environment of Oak Ridge or elsewhere where there is excess rainfall available for deep soil penetration and soil leaching.

4.5.5.9 Ratings for waste disposal in tumuli

Soils are rated for their ability to support a concrete pad without differential settlement. Slopes and soil depth are important because cut-and-fill operations are necessary on sloping land to form suitable flat areas. The suitability and compactability of on-site fill in cut-and-fill sites are important. Ratings range from very poor to good.

4.5.5.10 Source of fill materials

Soils are rated for their potential as engineered modified properties. Thickness and extent of suitable materials is also important. Ratings range from very poor for soils with very high silt content or soils that are saturated, to good.

4.5.5.11 Source of cover materials

Cover materials are used for several different purposes. Some cover materials must be compacted to render them as impermeable as possible. However, compacted cover without surface protection has a very high erosion potential. Other cover, usually termed "final cover," must have suitable properties so that grass can be established and maintained. Cover materials are rated for covering trenches and tumuli. Ratings range from very poor to good, with depth of soil materials an important rating criterion.

4.5.5.12 Septic tank drain fields

In remote areas, sewage is commonly disposed of in subsurface drain fields after undergoing treatment in a septic tank. The soils are rated for their general suitability according to Tennessee Health Department guidelines. Ratings range from very poor (unsuitable for conventional drain fields) to good for conventional drain fields.

4.5.5.13 Suitability for low commercial buildings

Slopes, depth to rock, soil-bearing capacity for shallow footers, and potential for differential compaction under load are rating criteria for this land use. Ratings range from very poor for soils with very high silt content or soils that are saturated or subject to frequent flooding, to good.

5 STRUCTURE OF THE OAK RIDGE RESERVATION

Peter J. Lemiszki and Robert D. Hatcher, Jr.

5.1 INTRODUCTION

The ORR is located in the western part of the Valley and Ridge province—at the narrowest and most convex part of the Tennessee-salient part of the Appalachian foreland fold-thrust belt (Fig. 5-1). The Valley and Ridge is dominated by several thrust faults that formed either by a ramp-flat mechanism or by breaking the common limb between anticlines and synclines. The map-scale structure of the ORR is dominated by homoclinal southeast-dipping bedding interrupted by the Copper Creek and Whiteoak Mountain faults and by the footwall of the East Fork Ridge (and Pilot Knob) syncline (Plate 1). Figure 5-2 is a generalized geologic map of the study area. It indicates the location of the three plant sites, the ridge and valley names used throughout the text and the location of drill holes, the seismic reflection profile, and other figures associated with this report.

Mesoscopic structures in the area consist of inclined, faulted, and folded bedding, and fractures. Pressure-solution cleavage has been observed at a few localities, but is not a regionally penetrative structure. Tectonic stylolites have developed in some tightly folded limestones in the Nolichucky Shale and may be present elsewhere. Extensional, hybrid, and shear fractures are penetrative at map scale. Most fractures are open, but many are filled with either calcite or quartz. Carbonate rocks generally contain more filled fractures than other rock types because of the greater mobility of calcium carbonate in water. Fractures are probably the most important structure in the ORR

because, along with bedding and local karst, they form the conduit system that controls groundwater movement. Documenting fracture attitude, timing, and evolution is one means of inferring the stress orientation history of a thrust sheet, but fracture studies from the Cumberland Plateau, Valley and Ridge, Blue Ridge, and Piedmont indicate some fractures developed in response to erosional unloading and the recent stress field, while others formed during Triassic-Jurassic extension related to the opening of the present Atlantic. Therefore, it cannot be assumed that all fractures are a result of Paleozoic folding and thrust-sheet emplacement.

A number of criteria are being considered to aid in deciphering the history of fracture formation within the ORR, including abutting relationships, crosscutting relationships, variably rotated fracture orientations in conglomeratic blocks filling the post-Knox unconformity, fracture development isolated in chert pods in dolomite and other lithologic controls, fracture rotation by mesoscopic and map-scale folds, fracture reactivation, local fracture development and spacing in particular faults and folds, fracture mineral-filling geometry and crosscutting relationships, comparisons of local and regional systematic fracture patterns, and comparisons of fracture orientations to the present-day stress field. Such criteria are being utilized to separate tectonic, hydraulic, unloading, and release fractures to document the fracturing (stress) history of the ORR. Besides a more accurate portrayal of the stress history related to thrust-sheet emplacement by using only tectonic fractures, further application of

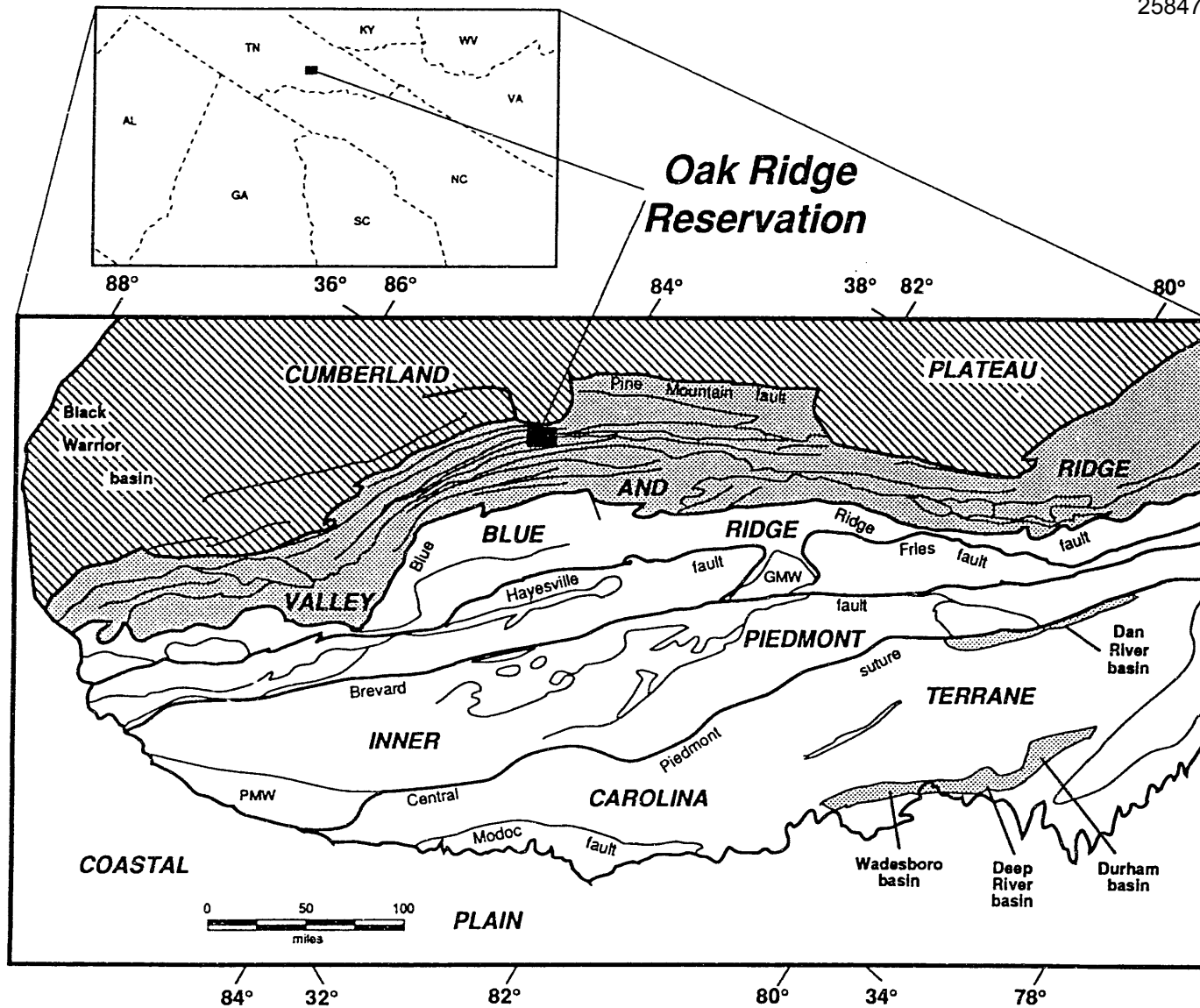


Fig. 5-1. Location of the Oak Ridge Reservation in the southern Appalachian Valley and Ridge province of eastern Tennessee (from Hatcher 1987). The Blue Ridge-Piedmont crystalline thrust sheet provided the stress that deformed the foreland fold-thrust belt (patterned). PMW - Pine Mountain window; GMW - Grandfather Mountain window. SME - Sauratown Mountain window.

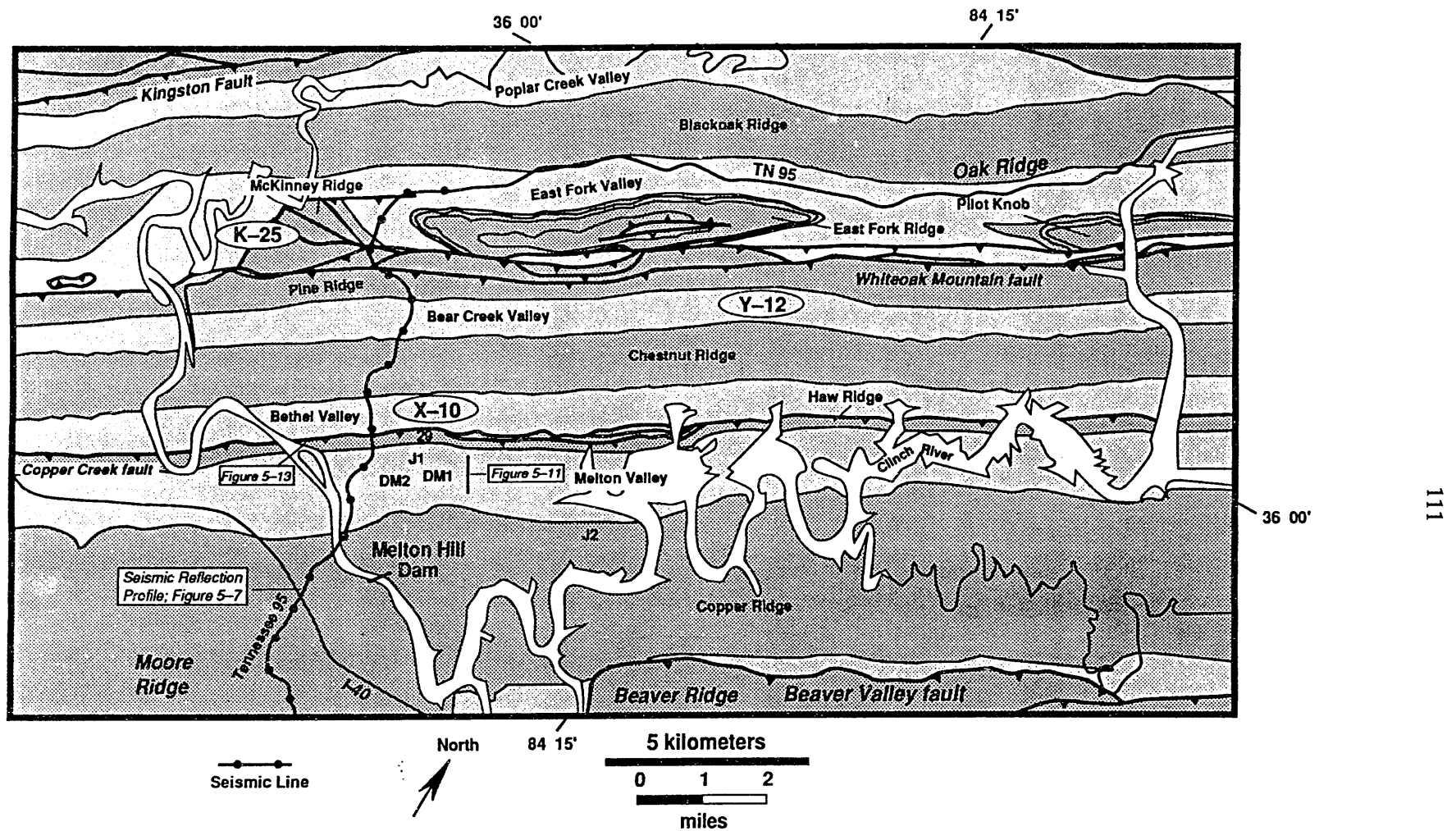


Fig. 5-2. Location map for ridge and valley names on the Oak Ridge Reservation. Map also marks the location of the main plant areas, drill holes, seismic reflection profile traverse, and other figures discussed in the text.

such an analysis involves an understanding of the control that fractures have on groundwater flow paths in sedimentary rocks and how regional permeability is controlled by different fracture sets.

5.2 COPPER CREEK FAULT

5.2.1 Regional Geometry and Displacement

The Copper Creek fault maintains a fairly consistent geometry in the study area as a hanging-wall flat in the Rome Formation and a footwall flat in the Moccasin Formation (Plate 1). The lower flat on the upper-flat geometry of the fault in map view is indicated by the consistent attitude of bedding across the fault zone (Fig. 5-3) and by the lack of stratigraphic cutoffs in either the hanging wall or footwall. A stratigraphic separation diagram for the Copper Creek fault footwall from the ORR northeastward into Virginia shows that the Moccasin Formation was utilized as an extensive décollement horizon (Fig. 5-4). The Virginia state geologic map (Milici et al. 1963) indicates that the fault location in the hanging wall is in the Honaker Dolomite, and in the footwall the fault cuts up section as displacement decreases and is accommodated by folding at the fault tip. Towards the southwest from the study area, the fault cuts down section in the footwall to the Rome Formation reducing the thickness of the Whiteoak Mountain thrust sheet to zero at the branch line (Fig. 5-4; Hardeman 1966). Approaching the southwest end, the fault bifurcates into a number of diverging and rejoining splays and into one connecting splay with the Whiteoak Mountain fault (Hardeman 1966, Wilson 1986). The splay geometry is similar to an A-type intersection map pattern (Milici 1975), although the splays may have

transferred displacement to the Whiteoak Mountain fault and to folds in northeastern Georgia (Butts 1948).

The restored, balanced cross section provides a minimum estimate of displacement along the fault because of erosion of the hanging-wall cutoffs in the Copper Creek thrust sheet (Fig. 5-5). Minimum displacement along the fault is approximately 12 km, which is in the range of previous estimates (Roeder et al. 1978, Woodward 1985). In addition, the "bow and arrow rule" was used to estimate the amount of displacement along the fault (Elliott 1976). This method requires joining the tips at either end of the trace of a thrust fault with a straight line and bisecting the line at the midway point (Fig. 5-6). Assuming that the line indicates the position of the fault prior to movement, then the length of the normal from the midpoint to the mapped position of the thrust fault will provide an estimate of the minimum displacement. The method works because most thrust faults are curved in map view, requiring the line joining the ends of the fault to pass behind the mapped position of the thrust fault. The midpoint of the line segment is chosen on the assumption that the fault began at a point and migrated at a constant rate in all directions. Although the curved trajectory of the thrust faults in the Appalachian fold-thrust belt matches those in Elliott's (1976) examples, application of the bow and arrow rule had not been previously attempted for any of the faults in the region. Application of the rule to faults that do not have the maximum displacement at the midpoint or to faults that curve around oroclinal bends (e.g., the Tennessee embayment) introduces errors into any attempt to use the rule for quantitative assessments.

Results for the Copper Creek fault indicate that the normal bisector is not the longest distance between the fault trace

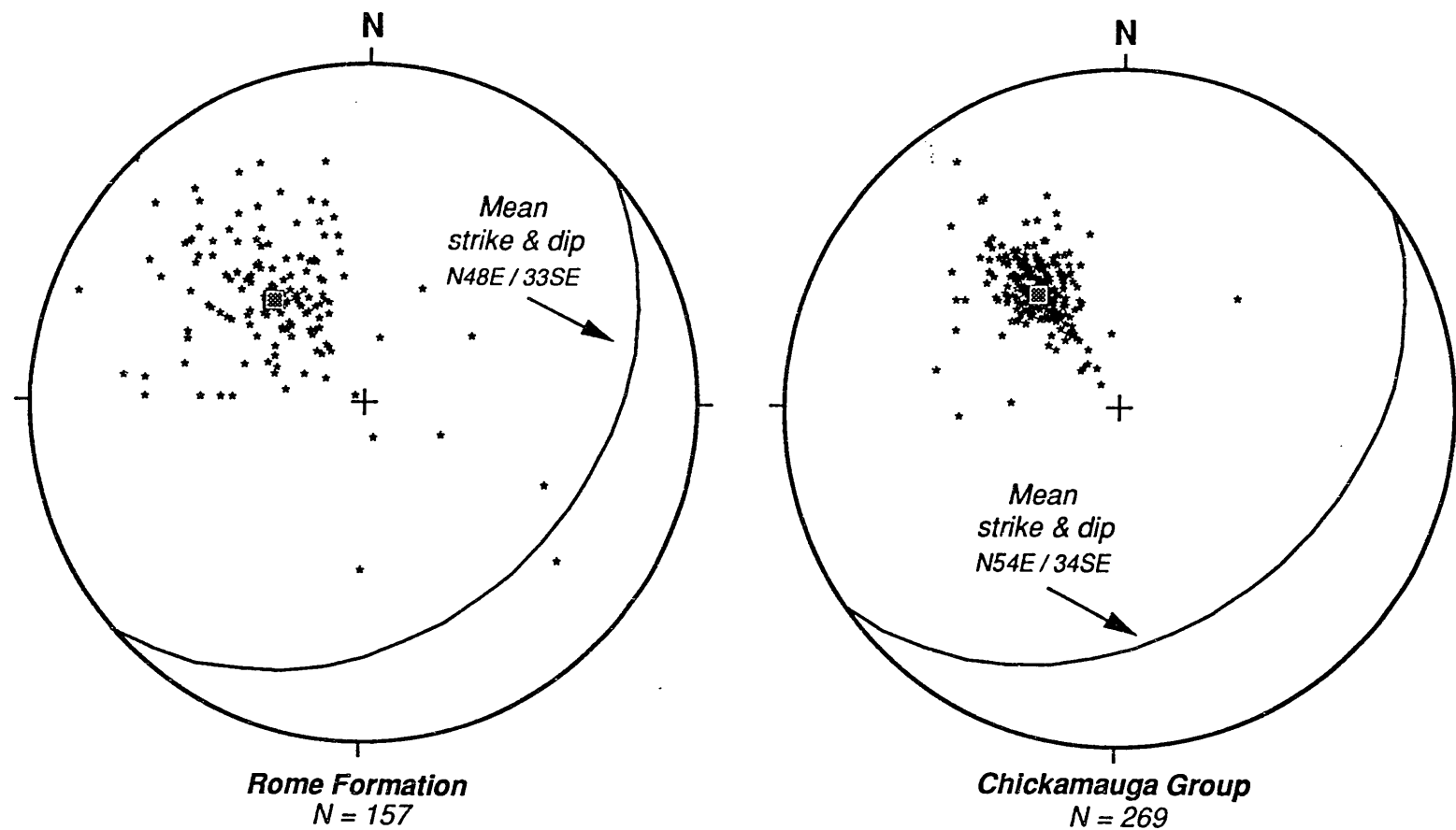


Fig. 5-3. Equal-area lower hemisphere stereographic projections of poles to bedding from the hanging wall (left) and footwall (right) of the Copper Creek fault. Box symbol is mean pole to bedding corresponding to the great circle.

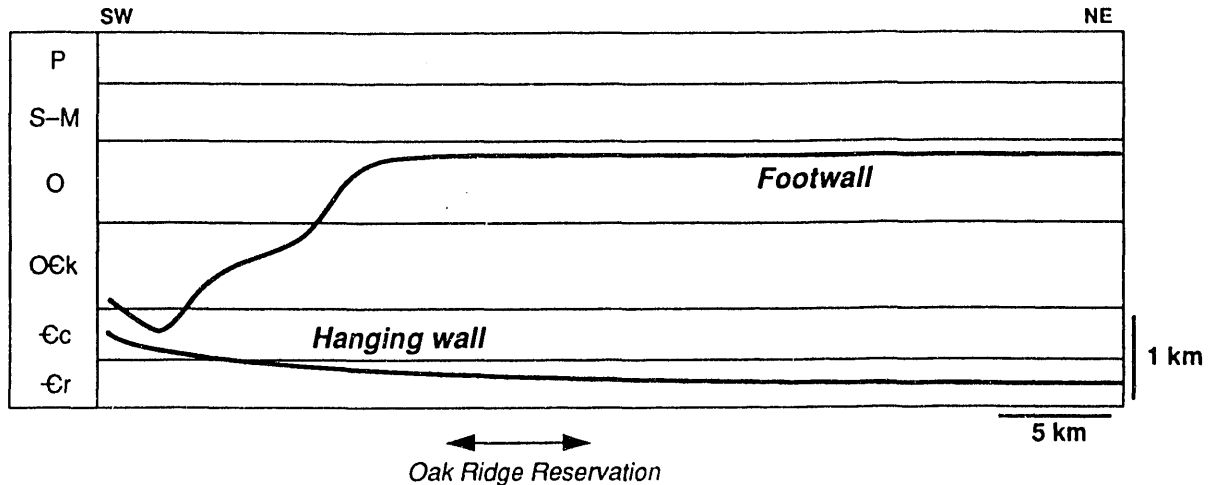


Fig. 5-4. Stratigraphic separation diagram for the Copper Creek fault in Tennessee. In the Oak Ridge area the fault is a hanging-wall flat in the Rome Formation and a footwall flat in the Moccasin Formation. Stratigraphic symbols not previously defined are: O - Ordovician, S-M - Silurian to Mississippian, and P - Pennsylvanian age rock units.

and the fault tip-line join. This suggests that erosion has cut back the amount of overlap on the flat in the Moccasin Formation, as substantiated by the lack of hanging-wall cutoffs. Using the midpoint results in 55 km of displacement along the Copper Creek fault, which is four to five times greater than the minimum amount of 12-km displacement required by the restored, balanced cross section. Relaxing the assumption that the fault began at a point and migrated at a constant rate in all directions, a length of 65 km is determined from the longest normal between the fault trace and the fault tip-line join. The amount of displacement would decrease if the curvature of the fault trace was less. The fault curvature may have been accentuated if either the rate of propagation and slip were substantially greater into the foreland vs along the strike of the fault (e.g., Thomas 1977) or the fault trace was modified by the movement of later faults. Although the bow and arrow rule still needs to be thoroughly tested, the results suggest that the amount of displacement

along the Copper Creek fault may be much greater than previous estimates.

5.2.2 Subsurface Fault Geometry

The hanging-wall flat on footwall flat geometry of the Copper Creek fault indicates that the fault is nearly parallel with bedding. Therefore, the change in bedding dip towards the southeast mimics the subsurface geometry of the Copper Creek fault. Bedding dip adjacent to the Copper Creek thrust sheet is approximately 34° southeast, but then gradually flattens towards the southeast where dip in the Knox Group is 5 to 15° southeast (Plate 1). The gradual flattening of bedding reflects the subsurface listric geometry of the fault. Bedding dip then begins to steepen towards the southeast in the Knox and Chickamauga groups near the Beaver Valley fault. The steepening of bedding dip is interpreted to occur above the subsurface position of the footwall ramp to the Copper Creek fault. The along-strike extension of the ramp was imaged on a

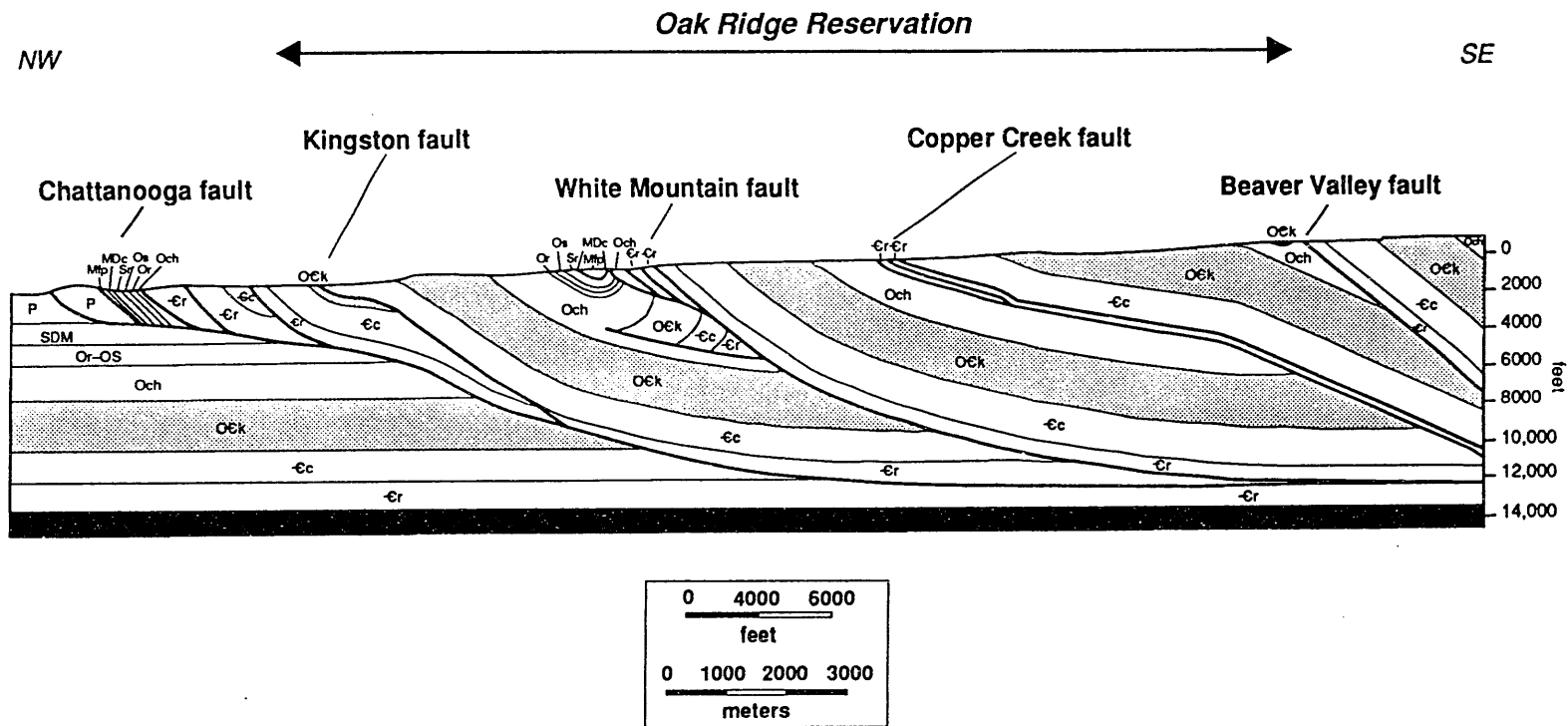


Fig. 5-5. Balanced (and restored) cross section from the undeformed foreland of the Cumberland Plateau through the Oak Ridge area to the Beaver Valley fault. Cr - Rome Formation. Ec - Conasauga Group. Ock - Knox Group. Och - Chickamauga Group (Supergroup). Or - Reedsville Shale. Os - Sequatchie Formation. Sr - Rockwood Formation. SDM - Silurian, Devonian, and Mississippian units. MDC - Chattanooga Shale. Mfp - Fort Payne Formation. P - Pennsylvanian units, undivided.

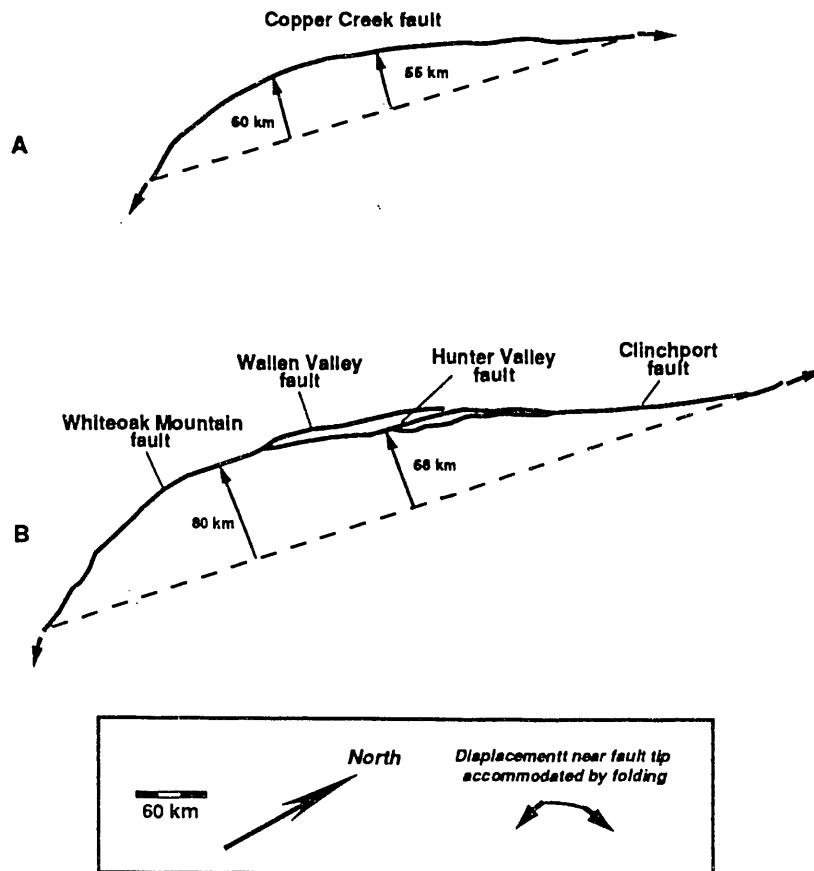


Fig. 5-6. Sketch of the map-view geometry of (A) the Copper Creek and (B) Whiteoak Mountain faults used to estimate displacement by the bow and arrow rule. Note that the length of the longest normal from the fault to the tip-line join results in greater displacement than if the middle of the tip-line join is chosen.

seismic reflection profile southwest of the ORR near Kingston (Harris and Milici 1977).

The subsurface geometry of the Copper Creek fault can also be determined from a seismic reflection profile that strikes along Tennessee 95 (Fig. 5-7, see Fig. 5-2 for location). The profile was reprocessed and migrated to provide an accurate depth section on which to base structural interpretations (Dreier and Williams 1986). Several observations are possible from the reflection profile: (1) The reflections on either side of the surface fault trace are subparallel to each other, which is indicative of a hanging-wall flat on footwall flat geometry. Although relatively sparse, most of the reflections

from within the Copper Creek thrust sheet mimic the changes in geometry of the reflections associated with the Whiteoak Mountain thrust sheet. (2) Discontinuous low-amplitude reflections are coincident with the surface trace of the Copper Creek fault. These reflections probably originated because of impedance contrasts produced by the juxtaposition of clastic lithologies of the Rome Formation and carbonate rocks of the Moccasin Formation. (3) The most prominent reflections in the Copper Creek thrust sheet occur downdip from the surface positions of the Rome Formation and upper Conasauga Group. The seismic style of the reflections is similar to that described from other surveys in the Valley and Ridge (Harris 1976, Tegland 1978, Christensen and

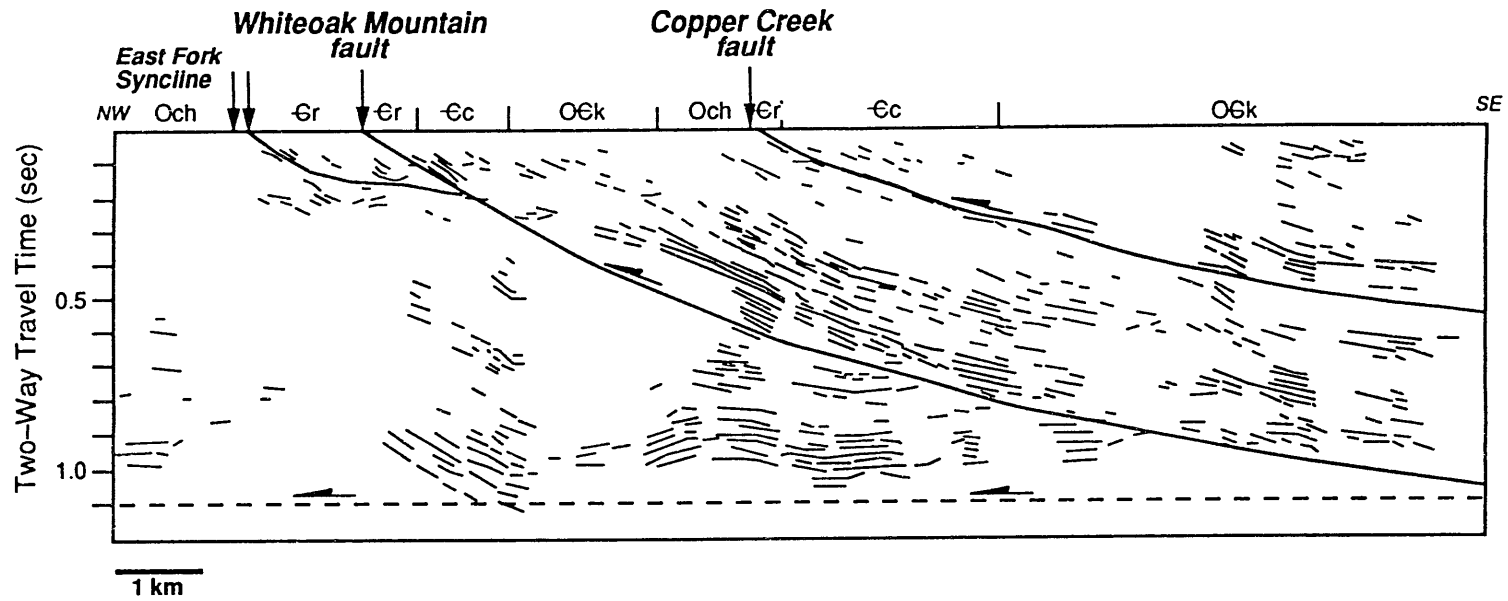


Fig. 5-7. Line drawing of the seismic reflection profile that crosses the reservation along Tennessee 95. Data from Dreier and Williams

Szymanski 1991). (4) Seismic reflection profiles that cross the fault to the northeast and southwest contain geometries that are similar to this profile (Harris and Milici 1977, Tegland 1978), which supports the interpretation that the Copper Creek fault is a regional hanging-wall flat on footwall flat.

The subsurface attitude of the Copper Creek fault towards the southeast can also be estimated by solving the three-point problem from the depths to the fault from three wells, JOY-1, DM1, and DM2 in Melton Valley (Fig. 5-8; see Fig. 5-2 for well locations). The result is a strike and dip of approximately N50E 8SE. Although it is a relatively small area, a decrease between the 34° southeast dip of the fault at the surface and the 8° southeast dip in Melton Valley supports the interpretation of an apparent listric fault geometry.

5.2.3 Fault Zone Characteristics

It is important to know the position, brittle mesostructure architecture, and gouge characteristics, such as thickness, porosity, and permeability of the Copper Creek fault zone when trying to deduce effects on groundwater flow paths. Although a few exposures of the fault have been found, weathering and incompleteness reduce their utility for deciphering subsurface characteristics. Subsurface fault zone characteristics have been reported from a study of the JOY-2 core hole (Fig. 5-2; Haase et al. 1985) and core hole 29 (Stockdale 1951). Core hole 29 is located on the top of Haw Ridge next to Melton Valley Drive and encountered a 21-m-thick deformed zone between 36 m and 57 m depth. The zone consists of a breccia of dolomite, quartzitic sandstone, and shale. The breccia ranges in color from gray, olive, buff, pink, to maroon with slickensided black partings and occasional thin zones of dark-gray gouge.

In the footwall, below the brecciated fault zone, the Moccasin Formation was not deformed like the rocks in the hanging wall.

The JOY-2 well encountered a deformed lower Rome section (44 m) consisting of a mixture of block lithologies bounded by both thrusts and high-angle faults (Haase et al. 1985). Deformation is primarily concentrated in several discrete zones interpreted as cataclasite and mylonite (Haase et al. 1985), although ductile deformation has not been confirmed here. The cataclasite matrix is fine-grained and the result of fragmentation of the host lithologies. Fragments of the host rock are randomly scattered throughout the cataclastic matrix. The mylonite is found within the cataclasite and consists of 1- to 5-mm-thick zones of cryptocrystalline material with a glass-like appearance (protomylonite?) (Haase et al. 1985). Haase et al. (1985) described the principal Copper Creek fault zone as a 6-m-thick breccia where calcareous siltstone and micrite of the Moccasin Formation are intensely brittlely deformed. This result is the major difference from Stockdale's (1951) observations, which do not describe extensive footwall deformation. In general, it appears that the increase in hanging-wall deformation towards the Copper Creek fault is similar to that described along strike and on other thrusts in the Valley and Ridge of Tennessee (Harris and Milici 1977, Wojtal 1986). The geometry of footwall mesoscopic structures along the Copper Creek fault, however, has neither been studied in detail nor been related to structural geometry in the hanging wall.

5.2.4 Hanging-Wall Deformation

Hanging-wall deformation is primarily confined to the Rome Formation and Conasauga Group (excluding the Maynardville Limestone) because they

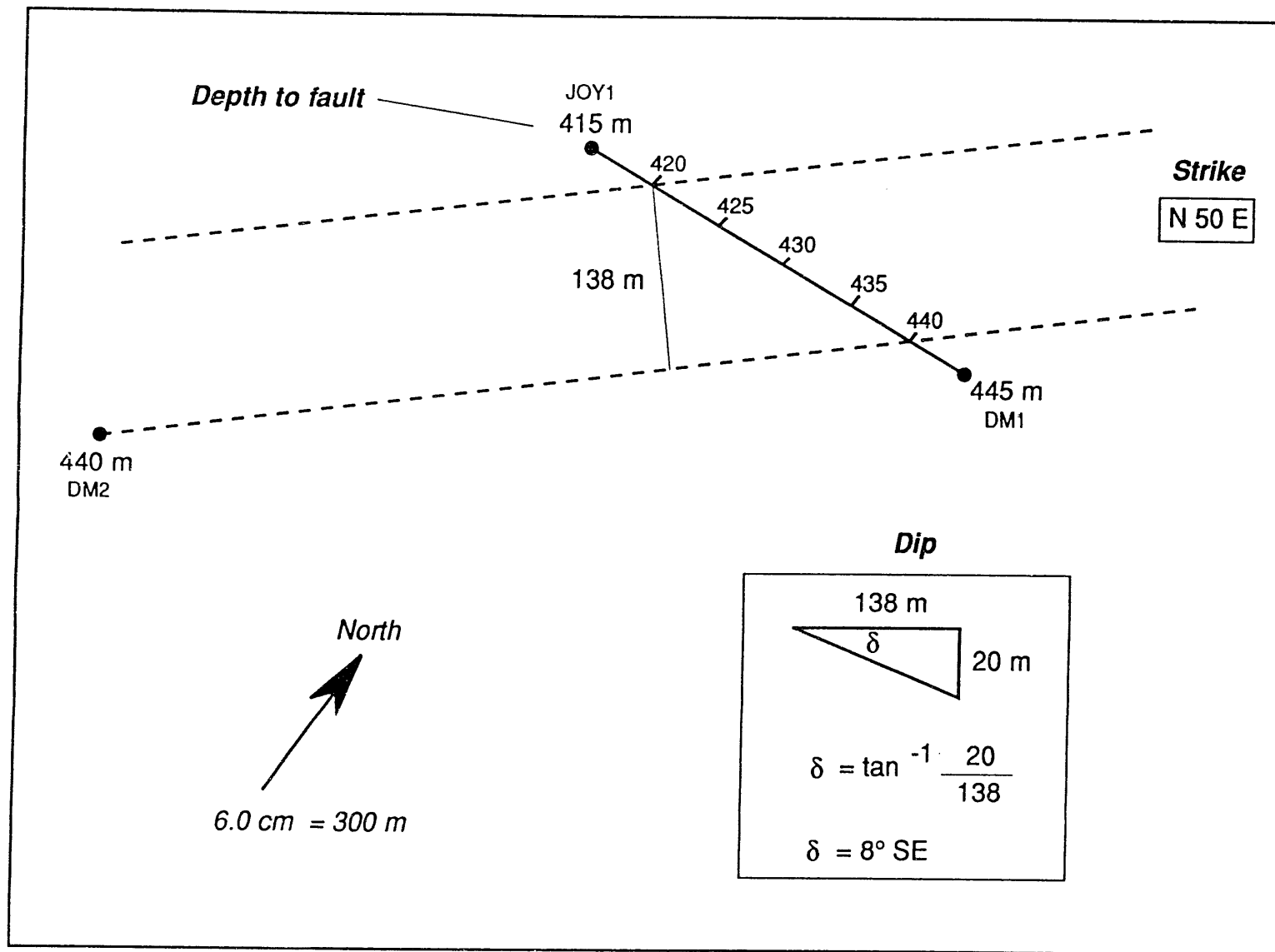


Fig. 5-8. Results of the three-point method to estimate the attitude of the Copper Creek fault at depth in Melton Valley. See Fig. 5-2 for well locations.

comprise the basal weak stratigraphic units. The strongest units are the Knox Group and Maynardville Limestone, which contain few mesoscopic structures besides fractures, although a zone of intense brecciation was found in the Copper Ridge Dolomite during excavation of Melton Hill Dam (Kellberg and Harrell 1964). In addition, Rodgers (1953) mapped a fault in Copper Ridge to the southwest of the study area that repeats the Knox and Chickamauga Groups, but this fault has not been located in the ORR. Finally, a klippe of the Copper Ridge Dolomite rests on the Chickamauga Group in the footwall syncline of the Beaver Valley fault. This klippe is related to folding of the Beaver Valley fault and is located in the southeastern part of the map area. It has not, as yet, been mapped in detail and is not the primary focus of this study.

Parts of the Rome Formation are repeated in two thin imbricates along Haw Ridge (Plate 1; Fig. 5-9). These imbricates may have been formed as part of a duplex involving the footwall (Boyer and Elliott 1982, McClay and Insley 1988), but a large amount of displacement would have been required to bring them into their present position. More likely, the hanging-wall flat on footwall flat geometry of the fault and the lack of intense deformation within the imbricates suggest that they were derived from the hanging wall, but still possess a duplex geometry. Mapping indicates that the frontal thrust fault did not follow a single stratigraphic horizon continuously along strike in the footwall, but cut up and down section in the Moccasin Formation. Perturbations along the fault may have restricted slip and caused the development of hanging-wall shortcuts by accretion of some hanging-wall imbricates in the manner suggested by Serra (1977) and Knipe (1985). The locations of the faults bounding the horses were identified by the change in topography

from a multiple- to a single-ridge crest, changes in bedding attitude, and a repeated Rome sequence. During the course of this study, detailed sedimentological work by McReynolds (1988) clearly resolved the Rome stratigraphy within the Copper Creek thrust sheet in the ORR, which aided identification of imbricate faults by repetition of a distinctive dolomite-sandstone-shale sequence. Furthermore, although the duplex geometry was unknown, Dreier et al. (1987) first hypothesized tear faulting in the Rome Formation using multiple ridge crests and well data. The interpreted downdip projection of the branch lines from the main thrust correlates with folding of the Copper Creek thrust sheet and indicates that the horses are widening and may thicken in the subsurface (Fig. 5-9). The downdip extent of the horses is suggested by the thickened Rome Formation encountered in the JOY-2 well below Copper Ridge (Haase et al. 1985). Folding of the Conasauga Group stratigraphic contacts at the southwest end of the duplex was first determined during detailed studies in the solid waste storage areas in Melton Valley (Dreier et al. 1987). In addition, drilling in the area encountered a "rubble zone" (Haase 1991, personal communication) indicating the presence of a more highly deformed zone in the vicinity. As shown in the longitudinal cross section (Fig. 5-10), the thrust sheet is interpreted to be draped over the duplex. Increased deformation within the drape fold and minor amounts of differential displacement across the branch line probably caused the intense fracturing. At the northeast end of the duplex, folding is more severe because of the occurrence of a second thin imbricate below the first that thickened the Rome section even more. Changes in strike in the Conasauga Group contacts are poorly resolved in this area, but, based upon the few bedding attitudes

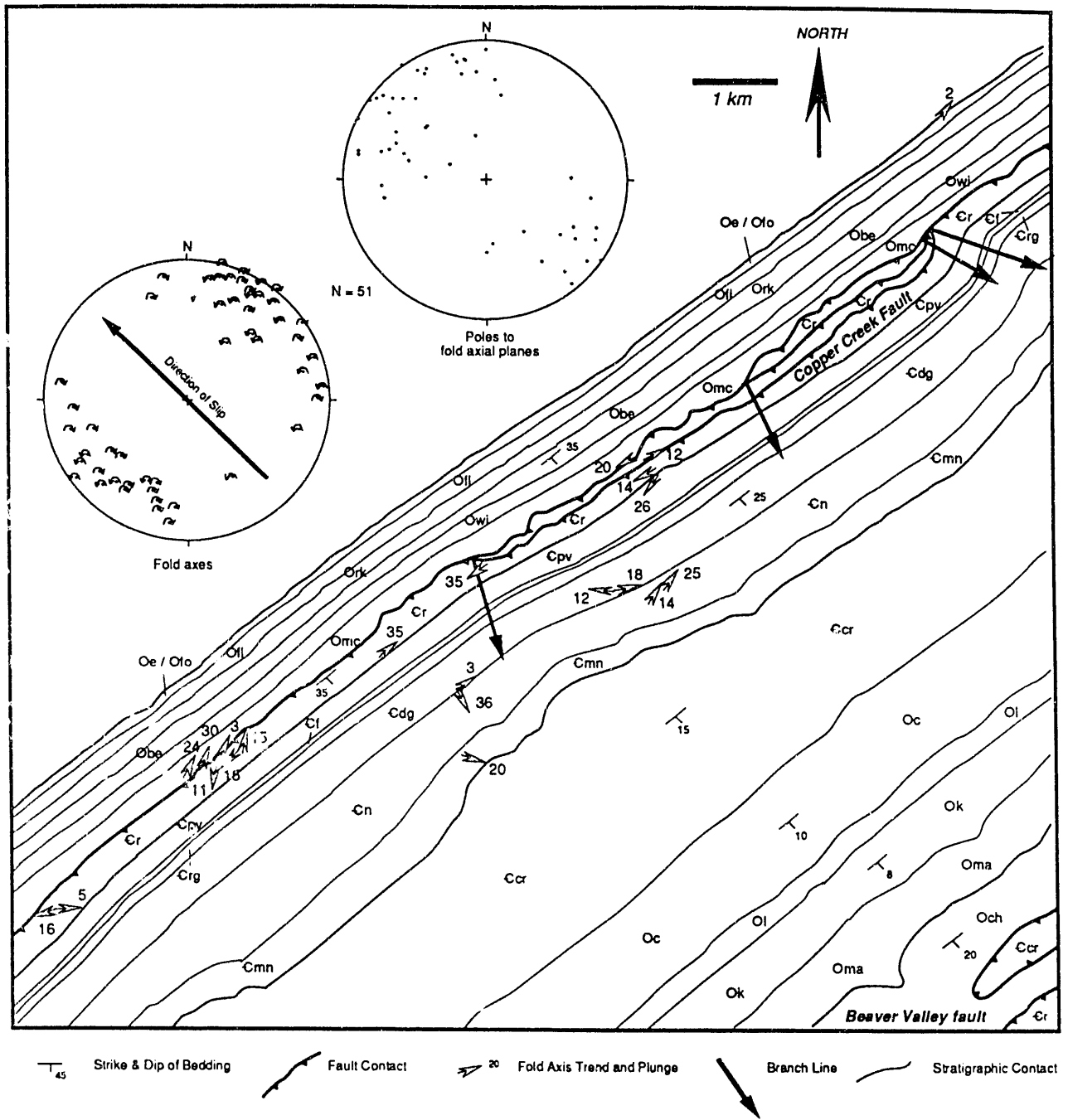


Fig. 5-9. Geologic map of the area surrounding the Copper Creek fault in the Bethel Valley quadrangle showing the trend and plunge of mesoscopic fold axes and the projection of imbricate fault branch lines. Included are equal-area, lower-hemisphere, stereographic projections of the same fold axes and their sense of vergence, and poles to fold axial planes. Curved open arrows indicate sense of vergence looking down the plunge of the fold axis. See Plate 1 for explanation of rock unit symbols.

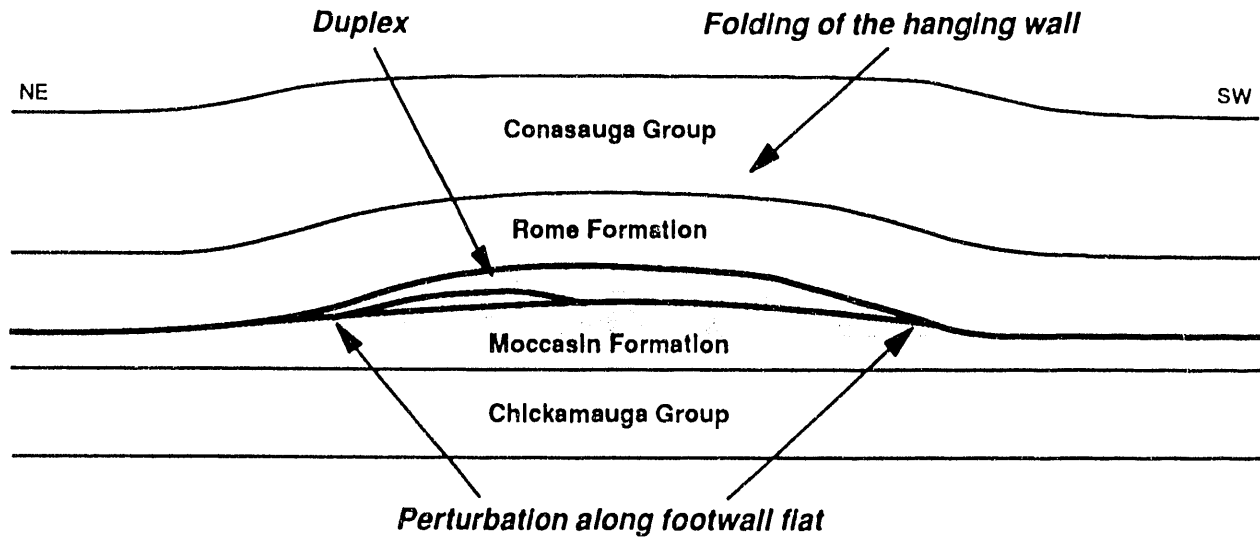


Fig. 5-10. Schematic longitudinal section parallel to the Copper Creek fault depicting the folding of the fault and bedding in the hanging wall by the accretion of imbricates in a duplex against a perturbation along the footwall flat.

available and the topographic expression, they are required.

Detailed structural and stratigraphic studies in the Conasauga Group have been conducted during extensive drilling and trenching programs in Melton Valley (Dreier and Toran 1989). These studies document abundant mesoscopic faults and folds throughout the interval and attest to the similarity in structural style with that observed in the better-exposed Rome Formation. This excludes the mildly deformed Maynardville Limestone, however, which responded to regional deformation like the Knox Group. The next strongest stratigraphic unit in the Conasauga Group is the Dismal Gap formation, which, based on well logs and drill core, has been interpreted to contain a number of intraformational thrust faults (Fig. 5-11a; Dreier et al. 1987). The thick and relatively strong limestone sequence within the Dismal Gap formation provided the strut needed for the growth of very small thrust sheets. This contrasts with the surrounding stratigraphic units that are

more pervasively folded and faulted because they are dominantly weak shale and siltstone. Geologic mapping did not resolve any of the minor thrust faults in the area because of poor exposure, although mesoscopic faults and folds are relatively common in outcrop. Strongly kinked folds with long limbs in the downdip direction and near-vertical short limbs would also account for these structures. Kinked mesoscopic buckle folds having this geometry are common in waste disposal trenches in the Conasauga Group (Fig. 5-11b); but small thrusts also occur here, although these tend to have steeper dip than bedding. Folds having this style are also present on the southeast side of Haw Ridge in a roadcut along the road through Haw Ridge at the northeastern end of the ORR.

5.2.4.1 Mesoscopic folds

Mesoscopic folds were observed in the Rome Formation, Pumpkin Valley Shale, Dismal Gap formation, Nolichucky Shale,

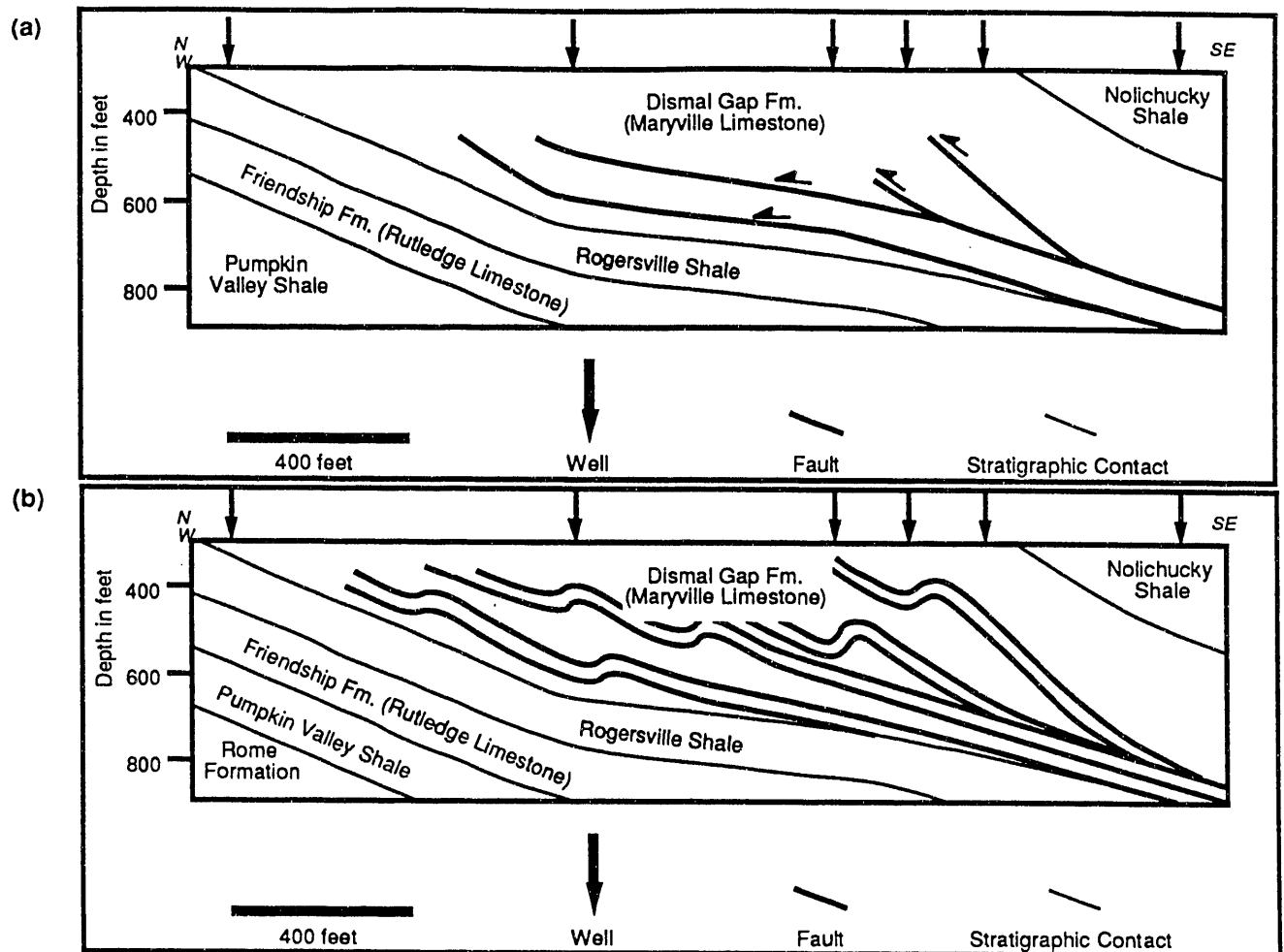


Fig. 5-11. (a) Near-surface cross section of some of the structures encountered in the Pits and Trenches area that are typical of those observed in the Conasauga Group in Melton Valley from Dreier and Toran (1989). (b) Alternative interpretation of Hatcher.

and Maynardville Limestone. Many of the folds are associated with mesoscopic thrust faults that may have either formed early and initiated folding at the tips or formed later and modified the final fold geometries (Fig. 5-12). The folds range from symmetric to asymmetric, plunge gently ($<30^\circ$), are open (70 to 120° interlimb angle), and are upright to steeply inclined (axial surface dip $>60^\circ$). Fold styles are parallel and range from concentric to chevron to kink geometries depending upon the mechanical characteristics of

bedding (e.g., Johnson 1977). For example, the folding of thin-bedded shale and siltstone without any interbedded strong mechanical unit, such as sandstone or limestone, commonly resulted in a chevron style. On the other hand, the presence of a strong layer interbedded in the shale and siltstone has in some cases resulted in concentric folds. Donath and Parker (1964) described parallel folds as flexural-slip folds, which form where beds slip past one another. The mechanical anisotropy of bedding planes and the low pressure and

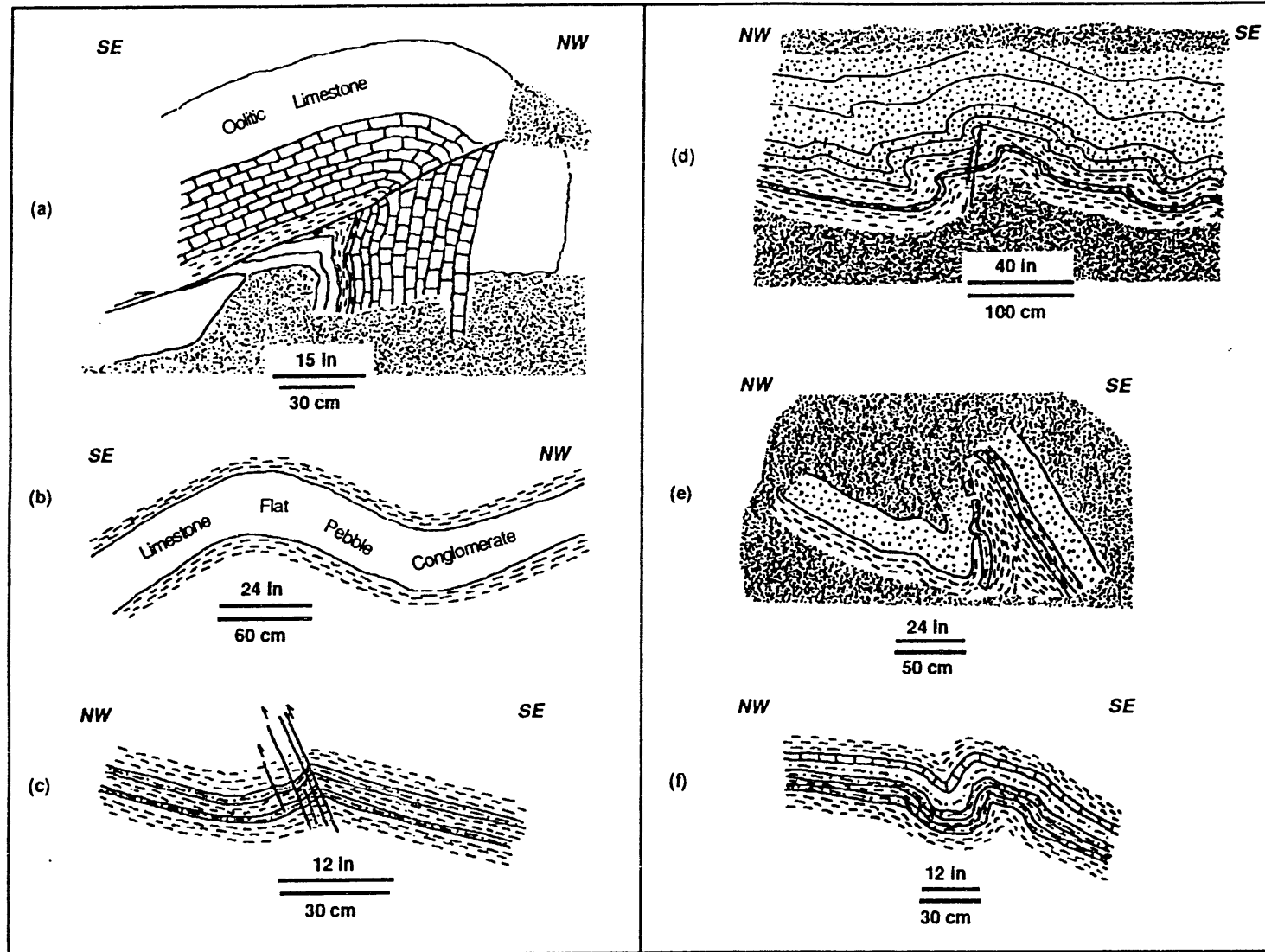


Fig. 5-12. Mesoscopic fold styles in the hanging wall of the Copper Creek fault: (a) Nolichucky Shale in Melton Valley; (b) Dismal Gap formation in Melton Valley; (c-f) Rome Formation on Haw Ridge. Symbols: brick - limestone; dashed - shale; stipple - sandstone; dashed-dot - siltstone.

temperature conditions of the deformation caused the preferential development of flexural-slip folds in the ORR. Bedding within the cores of some folds is pervasively fractured, faulted, and folded. These structures form because of the large compression induced by the inability for continued flexural slip in the tightened cores of folds—the room problem.

Most of the folds have northeast-trending axes that gently plunge to either the northeast or southwest (Fig. 5-9), indicating an overall southeast to northwest direction of regional maximum compressive stress during formation. This, in combination with a majority of northwest-verging folds, supports the interpretation that the Copper Creek thrust sheet was transported from the southeast to northwest. Two folds observed in the Conasauga Group have anomalous southeast-trending fold axes (Fig. 5-9). These folds occur above the subsurface position of the southwestern branch line of the duplex in the Rome Formation and may have formed in response to local reorientation of the regional stress field.

5.2.4.2 Mesoscopic faults

Mesoscopic faults were observed in most exposures containing mesoscopic folds. Large exposures in the Rome Formation typically contain a suite of bedding thrusts, high-angle thrusts, and high-angle extensional faults. Unfortunately, even the best exposure of the Rome Formation in the ORR is not suitable for a complete detailed structural analysis of the minor fault systems present and their relationships to the Copper Creek fault. A detailed description of the structures present was attempted for a small portion of the Rome Formation to provide a general picture of mesoscopic faulting patterns that may exist throughout the study area. The purpose here will be to describe some

of the observed structural relationships at this outcrop to provide a framework for discussing some of the deformational styles to be expected near the Copper Creek fault.

An interesting exposure was found in the Rome Formation near the crest of Haw Ridge near Jones Island at the southwest end of the ORR. The exposure is approximately 10 m wide and 5 m high, but contains numerous bends which allow the third dimension to be easily observed (Fig. 5-13). The outcrop contains a variety of mesoscopic faults and folds, which are less numerous in the moderately southeast-dipping beds exposed at the base of Haw Ridge. The Rome Formation was divided into five separate units, based on lithology. Unit 1 is the basal unit, which is tan, medium-grained, thin- to medium-bedded, relatively clean quartz sandstone approximately 1 m thick. Unit 2 is greenish-gray shale approximately 1 m thick that contains a 16-cm-thick siltstone bed located in the center of the unit. Unit 3 is a 2-m sequence of thin- to medium-bedded, maroon sandstone. Unit 4 is a 25-cm-thick, tan-brown, fine-grained dolomite. Unit 5, the uppermost unit, is approximately 2 m thick and is lithologically similar to the maroon sandstone of Unit 3. The N59E, 04NW bedding attitude is typical for the Rome Formation in this exposure.

Both contractional and extensional faults (Norris 1958) were found and are features common to exposures near the basal décollement in the Rome Formation (Harris and Milici 1977, Wojtal 1986). The contractional faults are thrusts that can be divided into two categories, based on the amount of bedding offset and continuity. The first category includes two major thrusts synthetic to the Copper Creek fault that can be traced throughout most of the outcrop with displacements ranging from 1 to 6 m. The second includes minor thrusts that branch from the major thrusts

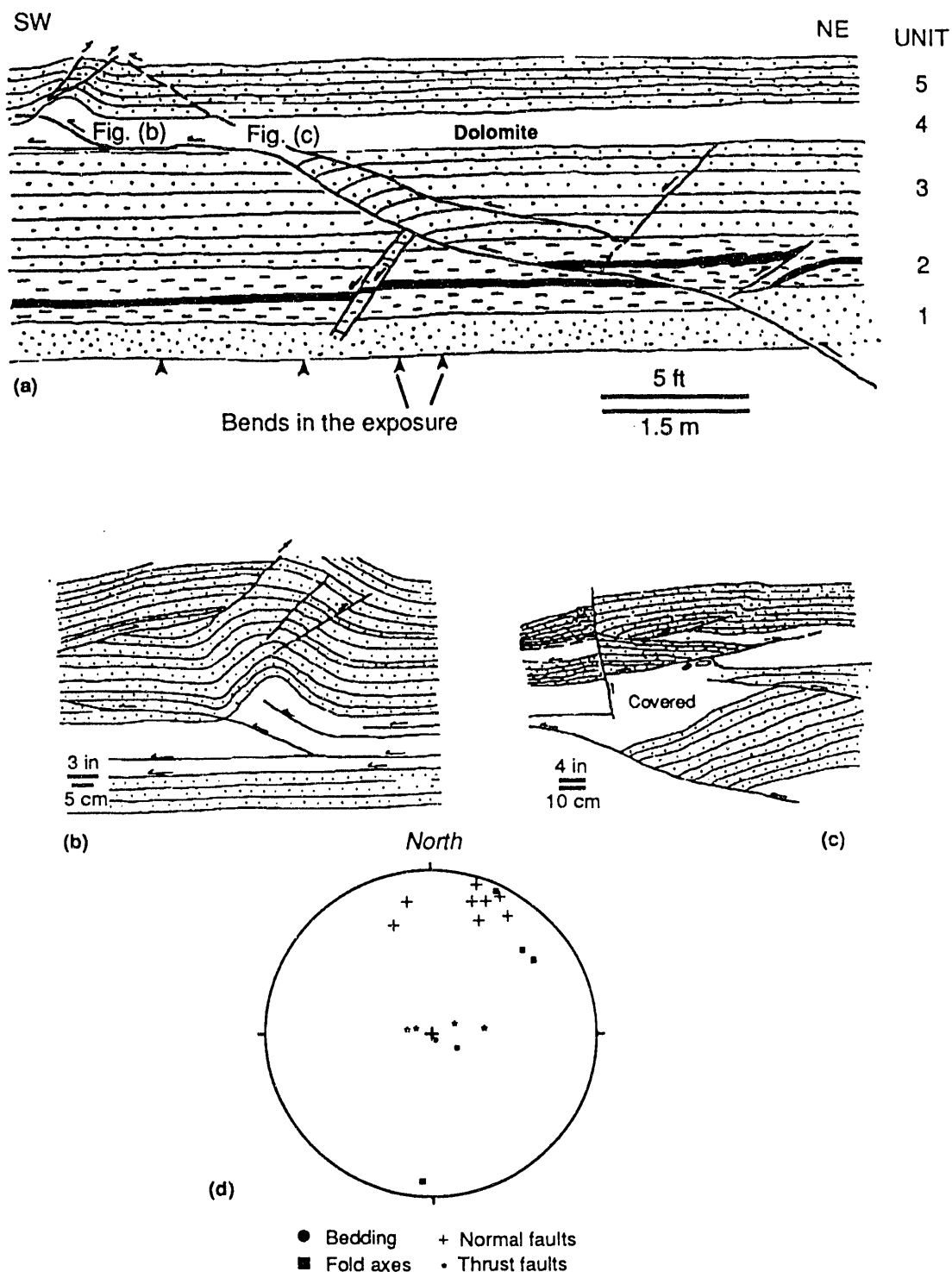


Fig. 5-13. (a) Sketch of major structures, bedding, and lithologic units. Note location of Figs. (b) and (c). (b) Detailed sketch of mesoscopic folds and faults in the southwestern part of exposure. (c) Detailed sketch of the complex geometry of mesoscopic folds and faults in the central part of the exposure. (d) Stereographic projection of poles to bedding, fold axes, and poles to faults.

and are associated with minor folds. The minor thrusts have displacements of less than 30 cm.

The major thrusts make up a ramp zone with minor displacement (Fig. 5-13). The lowermost thrust can be traced through Unit 1 at a relatively steep angle, flattens in the shale of Unit 2, and steepens again in the sandstone of Unit 3. The thrust parallels bedding in Unit 4, where displacement is transferred to minor splays and a minor fold at the northwest end of the exposure (Fig. 5-13b). The uppermost thrust begins near the base of Unit 3 and can be traced through Units 4 and 5 at a fairly constant angle to the top of the exposure. Both thrusts are separated in Unit 4 by approximately 1 m, and the region between them is a zone of folds and faults that are synthetic and antithetic to the major thrusts (Fig. 5-13c).

Extensional faults were observed in both the hanging walls and footwalls of the two major thrusts. Although some of the extensional faults cut and may slightly offset the uppermost of the two thrusts, none appear to offset the lower major thrust. This suggests that both the extensional and contractional faults formed during the same episode of deformation. The extensional faults have displacements ranging from 5 to 13 cm. The extensional faults in Unit 2 offset the siltstone bed stepwise by a number of very minor synthetic extensional faults.

Overall, the geometry of brittle mesostructures adjacent to the Copper Creek fault is typical of that described elsewhere (Harris and Milici 1977, Wojtal 1986). Even with only minor amounts of displacement along the major thrusts, a suite of structures developed that is beginning to accommodate the heterogeneous deformation.

5.2.5 Footwall Deformation

Footwall deformation was rarely observed except in exposures closest to the Copper Creek fault. A single mesoscopic fold was mapped in the Eidson Formation, however, based on opposing local bedding dip (Fig. 5-9). The lack of mesoscopic structures observed in the footwall is considered to be partly a function of exposure, because an excavation in the middle part of the Chickamauga Group in Bethel Valley exposed a variety of faults and folds. The structures in the excavation were not studied in detail, and the only available data pertain to bedding and fracture attitude. In addition, an excellent exposure of the Knox Group through a gap in Chestnut Ridge near the Bull Run Steam Plant contains only one apparent mesoscopic fold and one normal fault with approximately 2.5 m of displacement. Timing of movement on the normal fault is poorly constrained, although it does appear to be a reactivated strike-parallel extension fracture. Because the fracturing is interpreted to be prethrusting, the normal fault may have developed after the fracture was rotated to its present position, indicating syn- to post-thrusting displacement. Furthermore, because bedding was rotated by the Whiteoak Mountain fault after emplacement of the Copper Creek fault, the normal fault is not kinematically related to movement on the Copper Creek fault. Lastly, a thrust fault that repeats the Chepultepec Dolomite against the Longview Dolomite was mapped on Chestnut Ridge in The University of Tennessee Forestry Experiment Station (Plate 1). The short length of the fault and the small stratigraphic separation suggests that this is a thrust with small displacement.

The best exposure of mesoscopic folding and faulting in the footwall is in the Moccasin Formation on Haw Ridge near the

Clinch River across from Jones Island (Plate 1). At this locality, four imbricate thrust faults with minor displacement occur close to the Copper Creek fault. Three of the well-exposed faults have attitudes ranging from N19 to 50E and 35 to 45° SE, and the existence of the other faults (or possibly folds) is interpreted by changes in bedding dip. Poor exposure precluded determining whether the imbricate thrusts join a roof thrust and floor thrust in the manner of a duplex or if the thrusts simply decrease displacement and terminate up dip. The last exposure in the area towards the northwest, approximately 50 m from the Copper Creek fault, contains a fold. The fold is parallel-concentric and contains calcite slickensides on bedding surfaces that are consistent with a flexural-slip folding mechanism. The fold is open, moderately plunging, northwest-vergent, and contains minor fault arrays in the core of the anticline, as well as extension fractures in the hinge zone.

In summary, the Copper Creek fault is a major regional hanging-wall flat in the Rome Formation and footwall flat in the Moccasin Formation. Minimum displacement along the fault is 12 km, based on a

restored balanced cross section, but total displacement may be as great as 65 km. Much of the internal deformation related to the Copper Creek fault appears to be concentrated in the hanging-wall Rome Formation and Conasauga Group.

5.3 WHITEOAK MOUNTAIN FAULT

5.3.1 Regional Geometry and Displacement

In the ORR, the Whiteoak Mountain fault places a hanging-wall flat in the Rome Formation against a footwall ramp made up of various stratigraphic units (Plate 1). The footwall ramp geometry in map view is indicated by the presence of footwall synclines (some of which are overturned), imbricates, and numerous stratigraphic cutoffs against the fault. Evidence for the hanging-wall flat geometry is the lack of stratigraphic cutoffs and the consistent position of the fault in the Rome Formation. Because the Whiteoak Mountain fault consists of a number of fault strands, the stratigraphic separation diagram was constructed by choosing the fault with the greatest stratigraphic

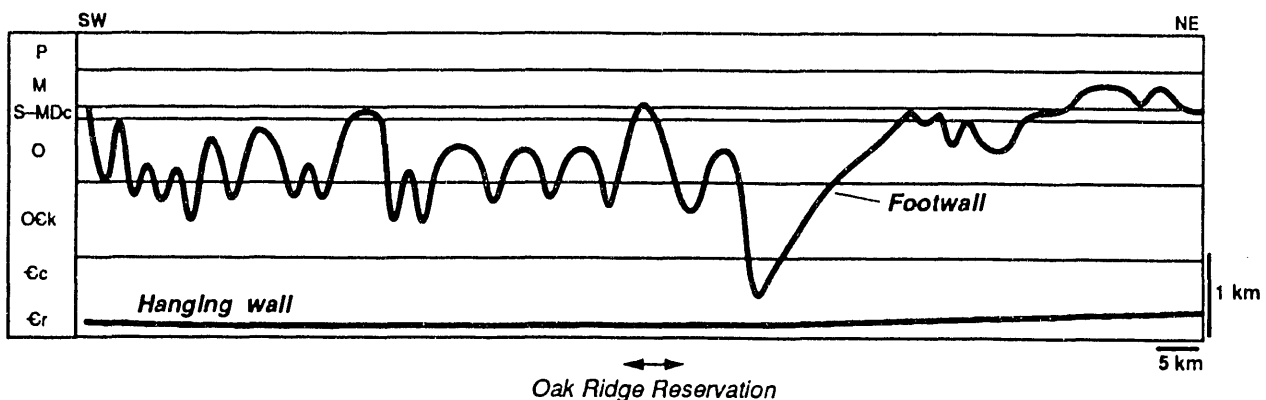


Fig. 5-14. Stratigraphic separation diagram for the Whiteoak Mountain fault in Tennessee. In the Oak Ridge area the fault is a hanging wall flat in the Rome Formation and a footwall ramp through all of the preserved stratigraphic units. See Plate 1 for explanation of map unit symbols.

displacement (Fig. 5-14). The footwall plot on the stratigraphic separation diagram has a much more jagged appearance than that of the Copper Creek fault because (1) the fault truncates a number of stratigraphic units that were probably initially folded before being faulted, and (2) horses of either the Knox Group, Chickamauga Group, or Rockwood Formation occur along the trace of the fault in Tennessee (Hardeman 1966). Along the strike northeast of the ORR, the fault is called the Hunter Valley fault, then Clinchport fault farther northeast (Rodgers 1953), but it carries the same rocks in the hanging wall that are indicative of a continuous thrust sheet. The footwall ramp geometry of the fault continues northeastward into Virginia and southwestward into Georgia (Butts 1948, Milici et al. 1963). The hanging-wall plot depicts the extensive flat in the lower Rome Formation, which was utilized all along the fault in Tennessee (Hardeman 1966). The exact stratigraphic position of the fault in the Rome, however, varies along the strike of the fault from the lower Rome to the middle Rome (Jones 1963, Swingle 1964, Beets 1985). In Virginia, the fault cuts up section as a ramp in the hanging wall as displacement decreases near the tip (Milici et al. 1963). Similarly, towards the southwest into Georgia, the fault ramps up section in the hanging wall as the displacement decreases and terminates in a syncline (Butts 1948).

As with the Copper Creek fault, displacement along the Whiteoak Mountain fault cannot be determined exactly because the hanging-wall cutoffs are not preserved. The balanced cross section indicates a minimum displacement of 10 km (Fig. 5-5). Applying the bow and arrow rule to the Whiteoak Mountain fault results in approximately 80 km of displacement (Fig. 5-6), a greater displacement than has ever been interpreted for the Whiteoak

Mountain fault. Such a displacement, which is on the same order of magnitude as that concluded by Woodward (1985) for the Saltville fault, greatly increases the total amount of shortening in the Valley and Ridge. Additional evidence of a large amount of displacement along the fault is found in the distinct differences in the stratigraphy of Chickamauga Group in the hanging wall and footwall. In the hanging wall, the Chickamauga Group closely matches eastern Tennessee stratigraphic characteristics and was deposited near the shelf-slope break, but in the footwall the Chickamauga consists of middle Tennessee formations and was deposited in a shallow-shelf setting (Milici and Smith 1969, Walker et al. 1980). As will be discussed later, however, the present continuous trace of the fault is interpreted to have formed late and to have truncated earlier faults in the ramp. Therefore, final movement may have acted to join numerous smaller displacement thrusts all along the fault trace bringing up a coherent hanging-wall sequence, making application of the bow and arrow rule inappropriate in this case.

5.3.2 Subsurface Fault Geometry

The geometry of the fault at depth is clearly imaged on the seismic reflection profile that crosses the Whiteoak Mountain thrust sheet and fault nearly perpendicular to strike (Fig. 5-7). Within the thrust sheet, southeast-dipping reflections characteristic of the Rome Formation and the upper Conasauga Group (Harris 1976, Tegland 1978, Christensen and Szymanski 1991) can be traced with little difficulty from near the surface down to the interpreted depth of basement. The geometry of the reflections in the thrust sheet follows a smooth curve indicative of the listric-ramp geometry of the Whiteoak Mountain fault.

The dip of the reflections near the surface is approximately 40 to 50° SE.

The seismic reflection traverse crosses the southwest end of an imbricate in the lower Rome Formation. Southeast-dipping reflections occur near the surface trace of the fault. The apparent flattening of the reflections in the subsurface is not indicative of a change in dip of the imbricate fault because the seismic line is parallel to the strike of the fault for a short distance. In general, relatively few reflections were recorded from within the imbricate which is consistent with it being composed dominantly of shales of the lower Rome Formation.

The mildly deformed bedding geometry near the base of the footwall is indicated by subhorizontal reflections between 0.6 to 1.0 s that terminate against the southeast-dipping reflections outlining the base of the Whiteoak Mountain thrust sheet. Subhorizontal reflections in the footwall can be traced southeastward to below the surface position of the Copper Creek fault. The reflections are interpreted to record the hanging-wall flat on footwall ramp geometry of the Whiteoak Mountain fault. Relatively few reflections occur near the upper part of the footwall. Structural complexity associated with the footwall syncline and the zigzag course of the seismic line most likely caused the lack of coherent reflections. The subsurface geometry of the Whiteoak Mountain fault in the study area is similar to that interpreted on a seismic reflection profile to the southwest near Kingston (Harris 1976). Finally, the subhorizontal reflections in the footwall towards the northeast are not indicative of a change in subsurface bedding dip, but instead are related to the seismic line orientation, which is nearly parallel to the strike of bedding in the footwall.

5.3.3 Hanging-Wall Deformation

Deformation within the hanging wall of the Whiteoak Mountain fault appears to be relatively minor. In contrast to the deformation in the hanging wall of the Copper Creek fault, macroscopic faulting is absent and mesoscopic folds and faults were rarely observed. For instance, a continuous Rome Formation to Knox Group sequence can be mapped from Pine Ridge to Chestnut Ridge in the Oak Ridge area (Plate 1). In addition, King and Haase (1987) were able to correlate well logs in the Conasauga Group throughout Bear Creek Valley without recognizing any macroscopic thrust faults. They did interpret the position of tear faults, however, when the stratigraphic contacts did not match along strike. The slight warping of contacts is interpreted here to be caused by folding of the entire thrust sheet by underlying horses and not by tear faults.

Mesoscopic fold axes in both the footwall and hanging wall of the Whiteoak Mountain fault trend generally to the northeast and southwest (Fig. 5-15). Since only fourteen mesoscopic folds were found in the area, all of the fold data are plotted together rather than divide by footwall and hanging-wall position. The fold styles are parallel concentric to chevron and are interpreted to have formed by flexural slip and buckling (Donath and Parker 1964). The vergence of minor folds is consistent with southeast to northwest thrusting.

The major change in the structure of the hanging wall from previous interpretations is the location of the Whiteoak Mountain fault in the Rome Formation (Plate 1). The fault has been located in the lower Rome Formation to the northwest of Pine Ridge, because no evidence has been found for a fault at the base of the ridge (McMaster 1962). In fact, a number of

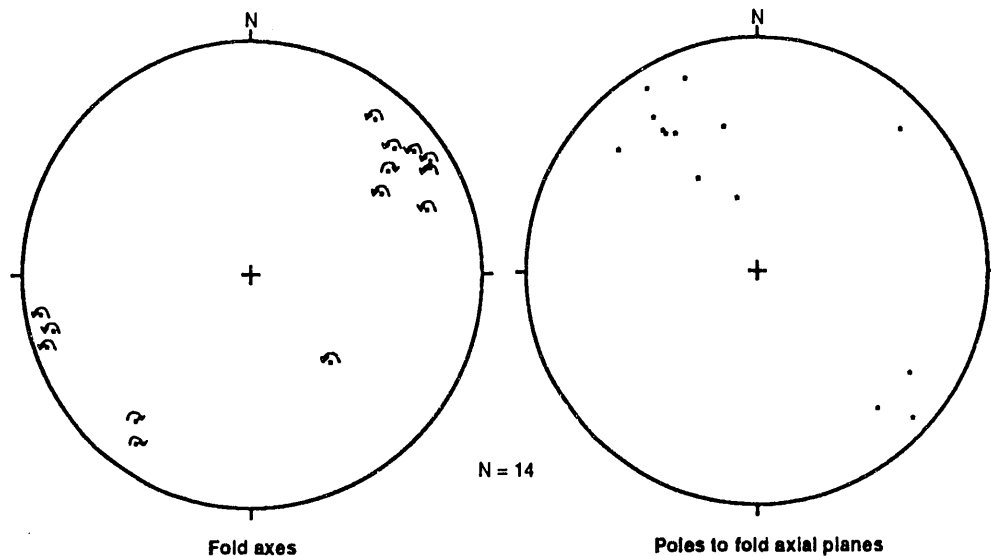


Fig. 5-15. Equal-area, lower-hemisphere, stereographic projection of mesoscopic fold axes and poles to fold axial planes from the hanging wall and footwall of the Whiteoak Mountain fault. Curved arrows indicate sense of vergence looking down the plunge of the fold axis.

observations support relocating the fault within the valley to the northwest: (1) The best exposure of the Rome Formation through Pine Ridge is located along Tennessee 95. At this locality, the sandstone-siltstone-shale sequence of the middle and upper Rome Formation contains none of the mesoscopic folds or faults that commonly occur adjacent to the main fault, for example, as observed in the Copper Creek thrust sheet. (2) McMaster (1962) interpreted the shale and siltstone that floor the valleys northwest of Pine Ridge to be part of the lower Conasauga Group, but they more closely resemble lower Rome shales mapped along strike to the southwest. Detailed paleontologic work is needed to resolve this important discrepancy in correlation. (3) Although structural analysis of a Rome exposure through Pine Ridge near the Clinch River did record some mesoscopic folds, no evidence was found for a fault at the base of the ridge (Zucker

1987). (4) The imbricate repeating the Rome Formation towards the northwest does not join Pine Ridge, but instead ends abruptly before reaching Pine Ridge. This suggests that the Rome sandstone holding up the small ridge is truncated by a fault located within the valley to the northwest of Pine Ridge. (5) Swingle (1964) located the fault in the Clinton quadrangle in the lower Rome Formation northwest of Pine Ridge. (6) Beets (1985) mapped the area of intersection between the Whiteoak Mountain, Wallen Valley, and Hunter Valley faults northeast of the ORR and observed only some minor faulting at the base of Pine Ridge. The Whiteoak Mountain fault, however, is interpreted to vary position within the lower Rome along the trace of the fault, suggesting that nothing was constraining the fault location in the thick sequence of shale.

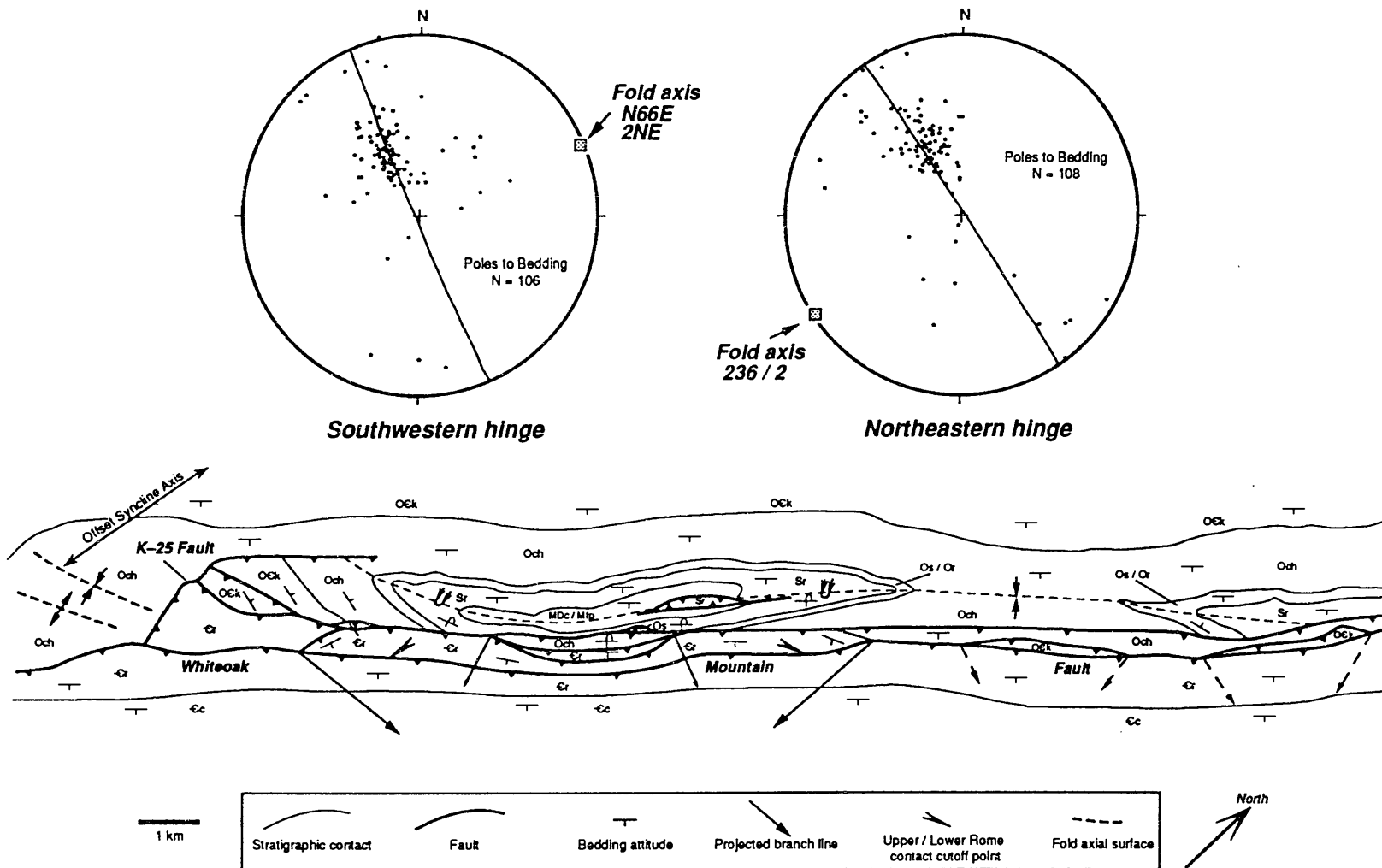


Fig. 5-16. Geologic map of the structures associated with the hanging wall and footwall of the White Oak Mountain fault in the Oak Ridge area. Equal-area, lower-hemisphere, stereographic projections of poles to bedding from the southwestern and northeastern hinges of the East Fork syncline. Each syncline hinge was plotted separately to properly determine the local fold axis orientation. Map symbols explained on Plate 1.

5.3.4 Footwall Deformation

Footwall structural geometry along the Whiteoak Mountain fault is indicative of a ramp position in a thrust system (Fig. 5-16). Repetition and the geometry of the Rome Formation northwest of Pine Ridge indicate a hinterland-dipping duplex (Plate 1; Boyer and Elliott 1982, Diegel 1986, Mitra 1986). The duplex consists of one long, thin imbricate composed of both the lower and upper Rome and a smaller imbricate of upper Rome. Ridge development associated with the upper Rome helped define the geometry of the imbricate. Bedding in the smaller imbricate is folded into a syncline. Accretion of the lower imbricate appears to have folded the upper imbricate and the overlying Whiteoak Mountain fault, which is the roof thrust of the duplex. The end of the duplex towards the southwest is indicated by the truncation of the Rome ridge and by a change in bedding strike towards the north in the lower Rome adjacent to the roof thrust (Plate 1). The lateral extent of the duplex to the northeast is less clear, but was inferred on the basis of a change in bedding strike towards the north and the termination of the upper Rome ridge against the roof thrust.

The subsurface projection of the branch lines of the imbricates with the roof thrust was determined by the folding of the roof thrust and overlying thrust sheet (Fig. 5-16). In addition, truncation of the upper Rome–lower Rome contact against the roof thrust indicates that the branch lines converge towards the center of the duplex in the subsurface (Fig. 5-16). The converging branch lines suggest that the imbricates of the duplex are thinning downdip, and therefore did not cause major folding of the Whiteoak Mountain thrust sheet. In addition, the roof thrust of the duplex is interpreted to cut up section within the lower Rome, which would also

reduce the amplitude of folding of the overlying thrust sheet.

Beginning near the intersection between the Whiteoak Mountain, Wallen Valley, and Hunter Valley faults, and continuing southwest all along the trace of the fault, are horses of predominantly the Knox and Chickamauga group rocks (Hardeman 1966). The horses are various sizes and shapes, but are composed of mechanically strong stratigraphic units (Helton 1979). Because exposure is often poor, many of the horses have been mapped on the basis of float and topography. Although the stratigraphic group involved can be inferred, the actual formation and bedding geometry is generally unknown. Some of the horses may be overturned if imbricate faulting occurred after folding of the footwall. The largest horse composed of the Chickamauga Group begins near the Whiteoak Mountain fault–Wallen Valley fault–Hunter Valley fault intersection and ends in the map area, but no data exist pertaining to bedding attitude (Beets 1985, Swingle 1964). A horse composed of the Chickamauga Group occurs in front of and may fold the previously described Rome Formation duplex (Plate 1). A few limestone outcrops were found in the horse, but the proper formation and facing direction of bedding could not be determined from them. A small imbricate of overturned Sequatchie Formation was mapped in front of the carbonate horse. The imbricate contains the distinctive maroon, argillaceous limestone and calcareous shale of the Sequatchie Formation. Because the geometry of bedding in the imbricates is poorly known, the subsurface projection of the branch lines cannot be accurately determined. In general, the imbricates appear to have originated from the footwall ramp, the Whiteoak Mountain fault acted as the roof thrust, and the imbricate faults have a relatively small amount of displacement compared to the roof thrust.

The southwestern end of the East Fork Ridge syncline is offset by an array of faults that project farther into the footwall than anywhere else along the Whiteoak Mountain fault. The faults record the progressive imbrication of the footwall and the relative timing of development of the major structures in the area. The most significant fault projects off the Whiteoak Mountain fault striking to the northwest and then changes direction towards the northeast where displacement decreases to zero at the tip line (Plate 1). For purposes of discussion, the fault is called the K-25 fault. In the hanging wall, the K-25 fault cuts at a steep angle through a horse of the lower Rome Formation, a horse of the Copper Ridge Dolomite, and then through a continuous sequence of upper Knox Group through lower Chickamauga Group. In the footwall, the fault cuts obliquely through bedding in the upper part of the Chickamauga Group and then strikes parallel to bedding in the Carters Limestone. The steep fault angle is indicated by the closely spaced stratigraphic cutoffs in both the hanging wall and footwall. The corresponding footwall cutoffs of the formations in the hanging wall are not evident in map view and therefore must exist in the subsurface. The type of displacement along the K-25 fault is interpreted to be towards the northwest, with the northwest-striking portion of the fault acting as an oblique ramp and the northeast-striking portion of the fault acting as a thrust. The fault offsets the axis of the syncline indicating that it formed after folding (Fig. 5-16). The fault may have formed as a means of accommodating differential shortening between the syncline and the area to the southwest. This fault probably continues northeastward for several kilometers in the Chickamauga, as possibly indicated by dip reversals in Carters Limestone on the Oak Ridge Country Club golf course (12th

hole), and by tight folding in Lebanon (?) Limestone in a recent excavation near the First Baptist Church in Oak Ridge. The point of intersection of the K-25 fault with the Whiteoak Mountain fault is not a branch line, but rather a point of truncation. Because displacement of the K-25 fault did not disturb either the Whiteoak Mountain fault or the thrust sheet, the fault must have formed prior to final movement on the Whiteoak Mountain fault.

Faults bounding the imbricates and horses of the lower Rome Formation and Knox Group are considered to have formed early in the development of the East Fork Ridge syncline because they are truncated on all sides by later faults. Variations in bedding attitude within the lower Rome Formation suggest that it is complexly deformed (Plate 1). The fault within the Knox Group is well exposed in an abandoned quarry northeast of K-25 off Blair Road near Poplar Creek and cuts steeply through folded beds. The horse of Copper Ridge Dolomite may also contain a continuous sequence into the upper Conasauga Group, but additional drilling is needed to test this hypothesis. Total displacement along the faults bounding the Rome Formation and Knox Group is considered minor because the faults are cutting steeply through units with little stratigraphic separation (i.e., Knox on Knox and Rome on either Knox or Conasauga).

5.4 EAST FORK SYNCLINE

The East Fork syncline is one of many synclines that developed in the footwall of the Whiteoak Mountain fault (Rodgers 1953, Hardeman 1966). Preservation of part of the lower Pennsylvanian Gizzard Group in a syncline to the southwest near Cleveland, Tennessee, (Hardeman 1966,

Wilson 1986) suggests that lower Pennsylvanian rocks were involved in the folding but have been mostly eroded. The folds involve rocks as old as the Knox Group. The Pilot Knob syncline extends into the northeastern portion of the ORR, but contains rocks only as young as the Rockwood Formation (McMaster 1957).

The East Fork syncline is doubly plunging, and the southeast limb is overturned to the northwest (Plate 1). Little to no change in stratigraphic thickness around the fold suggests a parallel fold style and a flexural-slip buckling fold mechanism. The southeastern limb of the syncline contains overturned beds of the Rockwood Formation that dip moderately to steeply southeast, with a few upright beds that dip northwest. In contrast, most exposures of the Fort Payne Formation in the southeastern limb have moderate

northwest dip, suggesting that near the core of the fold the southeastern limb is not overturned. Towards the southwest, detailed mapping of the footwall syncline forming Ten Mile Ridge also revealed an overturned southeastern limb (Zimmer 1964).

The doubly plunging geometry of the East Fork syncline in map view is indicated by closure of the stratigraphic contacts on the topographic surface (Plate 1). The asymmetric pattern of poles to bedding and the slightly spread-out distribution of the poles indicate that the fold is asymmetric and intermediate between a chevron and concentric geometry (Fig. 5-17). The orientations of the fold axes were determined for each hinge of the fold, using the cylindrical best fit of poles to bedding (Fig. 5-16). The northeastern hinge of the syncline has a fold axis oriented S54W / 02, and the

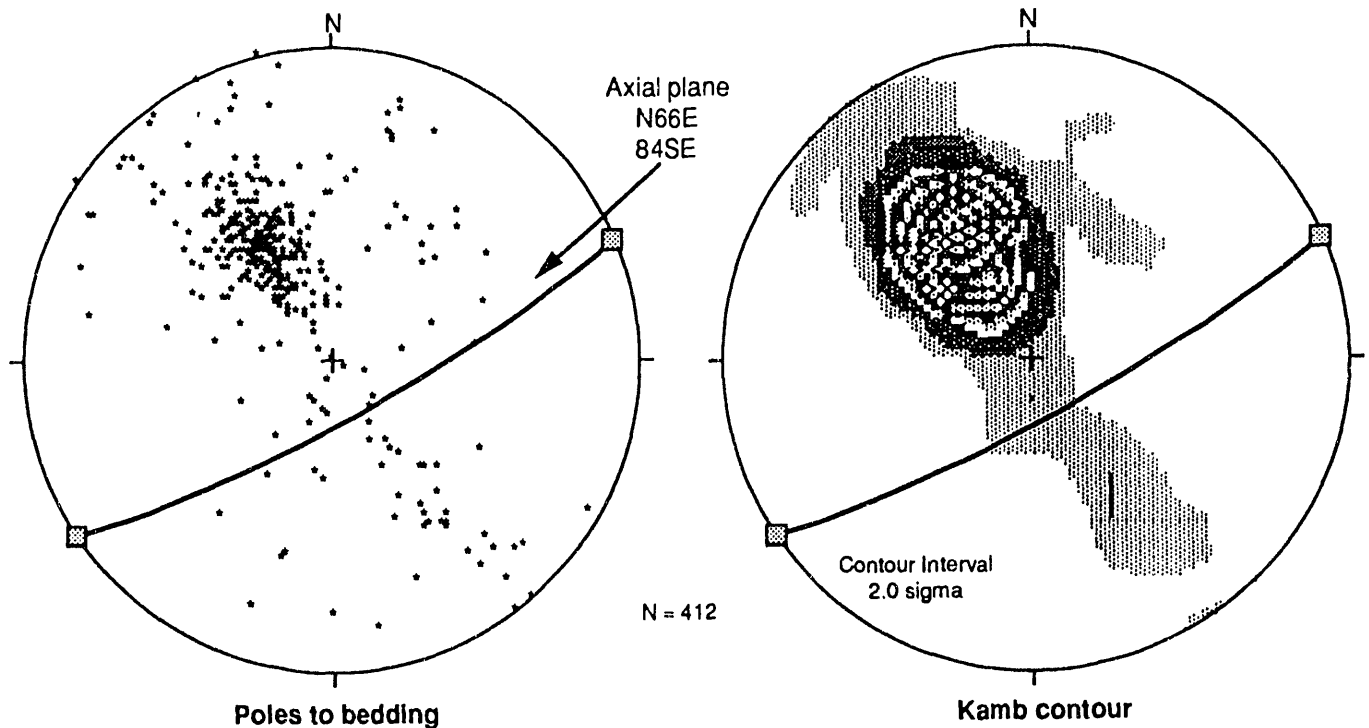


Fig. 5-17. Equal-area, lower-hemisphere, stereographic projection of all poles to bedding and related Kamb contour for the East Fork syncline. Axial plane chosen on the basis of the orientation of the fold axis at the southwestern and northeastern hinges.

southwestern hinge of the syncline has a fold axis oriented N66E / 02. The gentle plunge of the fold near the trace of the northeastern hinge is substantiated by the wide outcrop width of the Rockwood Formation. Although the results from the plot indicate that the plunge of the fold is similar around each hinge, the smaller outcrop width of the Rockwood Formation near the faulted southwestern hinge requires a steeper plunge. The axial plane of the syncline is oriented 66/84 SE, indicating an upright geometry with a slight northwest vergence to the fold (Fig. 5-17). Using the classification of Fleuty (1964), the interlimb angle is approximately 90°, indicative of an open-fold geometry. The fold is considered to have formed predominantly by flexural slip (Donath and Parker 1964). Evidence for flexural-slip buckle folding is the occasional preservation of downdip oriented quartz slickensides on bedding surfaces in the Rockwood Formation and the overall parallel geometry. Finally, strain within beds is relatively minor to nonexistent, as suggested by the lack of deformed crinoid columnals or shale pebbles in the Rockwood and Fort Payne Formations.

Two macroscopic thrust faults were mapped within the core of the syncline (Plate 1). McMaster (1962) identified part of a northwest-dipping fault by the offset and repetition of the Chattanooga Shale. The fault has been traced towards the southwest, where it juxtaposes the Rockwood Formation against the Fort Payne Formation within the core of the syncline. Further continuation of the fault towards the southwest is unknown, but it is considered to end within exposures of the Fort Payne Formation in the center of the syncline. The northeastern extent of the fault, however, is not so clear, but must end before reaching the undisturbed Rockwood Formation and Sequatchie Formation contact. The fault is interpreted

to repeat part of the Rockwood Formation because of the presence of an extra ridge composed of the Rockwood within the core of the syncline (Plate 1). A second southeast-dipping thrust fault was mapped towards the northwest, based upon the fact that the Rockwood Formation is juxtaposed against the Fort Payne Formation and the fact that the Chattanooga Shale upper and lower contacts are truncated. This fault has a minor lateral extent and rejoins the northwest-dipping fault. Faulting within the core of the syncline helped solve the room problem during folding. Furthermore, displacement along the K-25 fault may have affected the internal fold geometry towards the southwest, because the fold is curved clockwise and has a slightly steeper plunge than at the northeastern end.

5.5 CHARACTERISTICS OF THE FRACTURE SYSTEM IN THE OAK RIDGE RESERVATION

5.5.1 Introduction

Fractures are the most pervasive mesoscopic structure on the ORR and occur in all stratigraphic units. Fractures form during basin subsidence, folding, faulting, and basin uplift and can be used to infer the orientation of the regional stress field before, during, and after the development of the southern Appalachian fold-thrust belt. The fracture system consists of systematic and nonsystematic fractures (Hodgson 1961, Dennis 1972). Systematic fractures are defined as planar fractures having a common orientation and are typically regional in extent. Nonsystematic fractures are random, planar to curvilinear, and commonly terminate at systematic fractures. A fracture set consists of similarly oriented systematic fractures that also have a

similar origin. The systematic fracture sets were the focus of this study because (1) their regularity is indicative of a stress system that was regional in extent and (2) their regularity and connectivity is considered a major factor in controlling groundwater flow. Nonsystematic fractures were commonly encountered, however, either mixed with systematic fracture sets or alone, pervasively fracturing the host rock unit. Future studies are needed on the formation of nonsystematic fractures and how they relate to the systematic fractures and their effect on fracture permeability. The purpose of studying the fracture system in the area is multifold: (1) to provide data on the various fracture characteristics needed for groundwater modeling, (2) to relate the fracture system to the evolution of the

regional stress field, (3) to compare fracture characteristics between various fold-thrust belt structures, (4) to use fracture mechanics to model the development of the fracture system, and (5) to begin assembling a database on regional fracture characteristics.

The bedrock units in the area are all Paleozoic and have undergone a long and varied stress history that can lead to the development of different fracture sets (Table 5-1). The stress history is a result of changes in the regional tectonic framework of eastern North America. For example, the rock units that make up the Rome Formation through Knox Group were deposited on the early Paleozoic passive margin of the Iapetus ocean. These rock units have undergone a slightly longer and varied stress history related to passive

Table 5-1. Tectonic events since the early Paleozoic have affected eastern North America and controlled the orientation and magnitude of the regional stress field

| <i>Time Span</i> | <i>Tectonic Event</i> | <i>Factors Affecting Regional Stress Field</i> |
|------------------|---|--|
| 165–0 Ma | Neotectonic | North American plate drift Atlantic passive margin subsidence Foreland basin erosional unloading |
| 220–165 Ma | Mesozoic divergent margin tectonics | Middle Jurassic N-S dike swarm Early Jurassic NW dike swarm Late Triassic basin development |
| 470–245 Ma | Middle to late Paleozoic convergent margin tectonics | Folding and thrusting Forebulge migration Foreland basin subsidence |
| 570–470 Ma | Early Paleozoic passive margin development | Rome trough rifting Iapetus passive margin subsidence |

margin subsidence, Rome trough rifting, and early convergent margin tectonics (Rankin et al. 1989). The remainder of the stratigraphic section was deposited in the Appalachian foreland basin which developed after the Taconic orogeny. Stress provinces related to differential subsidence of the foreland basin and shortening during the Alleghanian orogeny appear to have formed clearly defined regional fracture sets. Subsequent Mesozoic divergent margin stresses produced dike swarms and fracture sets in the Blue Ridge and Piedmont, but it is still unclear if the stress field extended into the Valley and Ridge and Plateau provinces and caused the development of a new fracture set there (deBoer et al. 1988, Garihan et al. 1990). Finally, the present-day stress field related to North American plate drift and Atlantic passive-margin subsidence in conjunction with erosional unloading during isostatic rebound of the Appalachian foreland basin probably formed one or more recent fracture sets (e.g., Hancock and Engelder 1989, Gross and Engelder 1991). Considering the complicated stress history, information regarding changes in regional and local stress orientations needs to be determined from other structures or strain indicators to independently correlate the stress history interpreted from characteristics of the fracture system.

In addition to the regional stress provinces determined by lithospheric forces, local stresses developed during folding and thrust faulting associated with the Alleghanian orogeny. Structural analysis of the Copper Creek and Whiteoak Mountain faults in the area indicates that they represent different elements of a fold-thrust belt. The Copper Creek thrust sheet has been transported over a footwall ramp and onto an upper flat, but the Whiteoak Mountain thrust sheet sits on a footwall ramp. Because both faults are interpreted to have a differ-

ent kinematic emplacement sequence, fractures formed during deformation may differ between thrust sheets.

Groundwater studies have concluded that fractures are the major avenue for groundwater flow in the area, because rock matrix porosity and permeability are low (Smith and Vaughan 1985, Olsen et al. 1986, Dreier et al. 1987). Therefore, data pertaining to fracture characteristics, such as type, composition, and timing of mineral filling; geometry; aperture; connectivity; length; and spacing are needed for groundwater modeling (Hestir and Long 1990, Moreno et al. 1990, Olding and Webman 1991). Fracture geometry, spacing, mineral filling, and relative timing of development can be directly obtained from field mapping and core analysis. Predictions of fracture length, aperture, and connectivity, however, will also require knowledge of the timing of different fracture events, the physical conditions during fracture propagation, and the mechanical characteristics of the stratigraphy.

5.5.2 Previous Work

Previous fracture studies on the reservation have been conducted primarily in the Conasauga Group in both Melton and Bear Creek Valleys (Fig. 5-18). Sledz and Huff (1981) conducted a detailed fracture analysis in the Pumpkin Valley Shale at four exposures in Bear Creek Valley and at seven exposures in Melton Valley. The major purpose was to determine the relationships between fracture characteristics in shale and siltstone and to model fracture porosity and permeability. Fracture orientation, frequency, and length were measured in outcrop, and fracture aperture was measured in core. Orientation analysis indicated that northeast-striking and northwest-striking fracture sets are the most prevalent, especially in

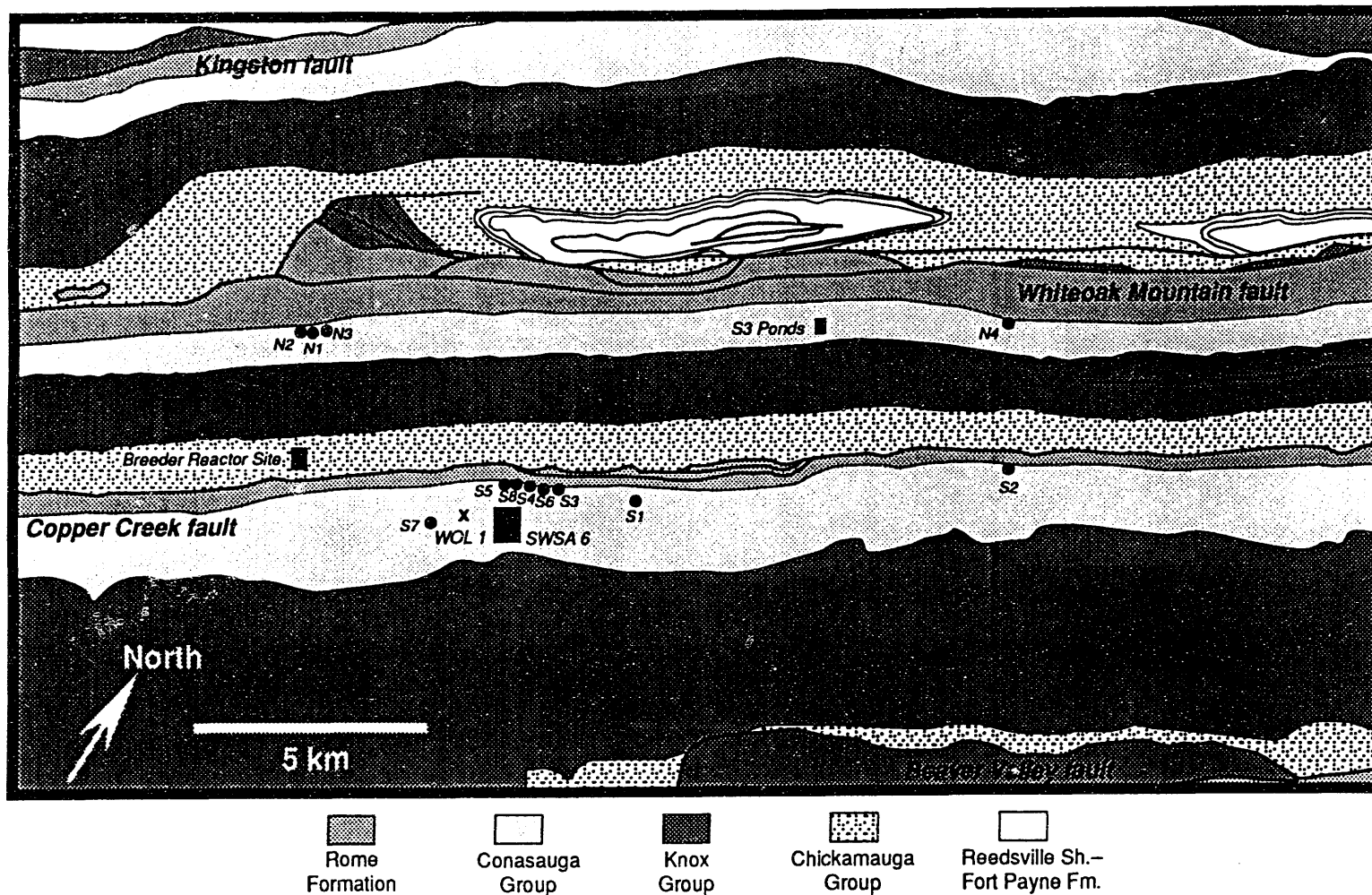


Fig. 5-18. Map of previous fracture study sites on the reservation.

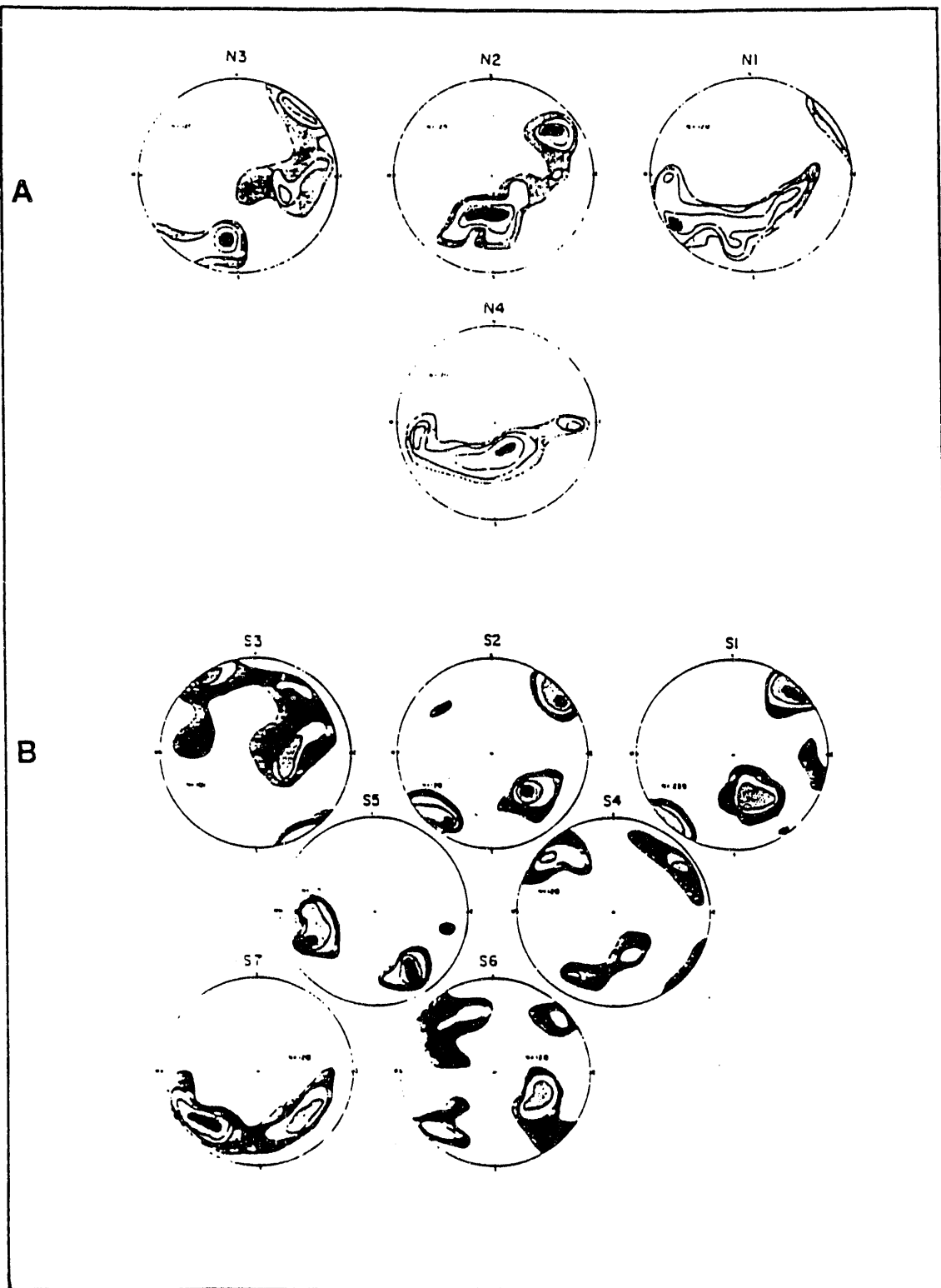


Fig. 5-19. Equal-area contour plots of poles to fracture planes in the Pumpkin Valley Shale from (a) the Whiteoak Mountain thrust sheet and (b) the Copper Creek thrust sheet. Contoured at 1, 3, 5, and 10 percent intervals (from Sledz and Huff 1981).

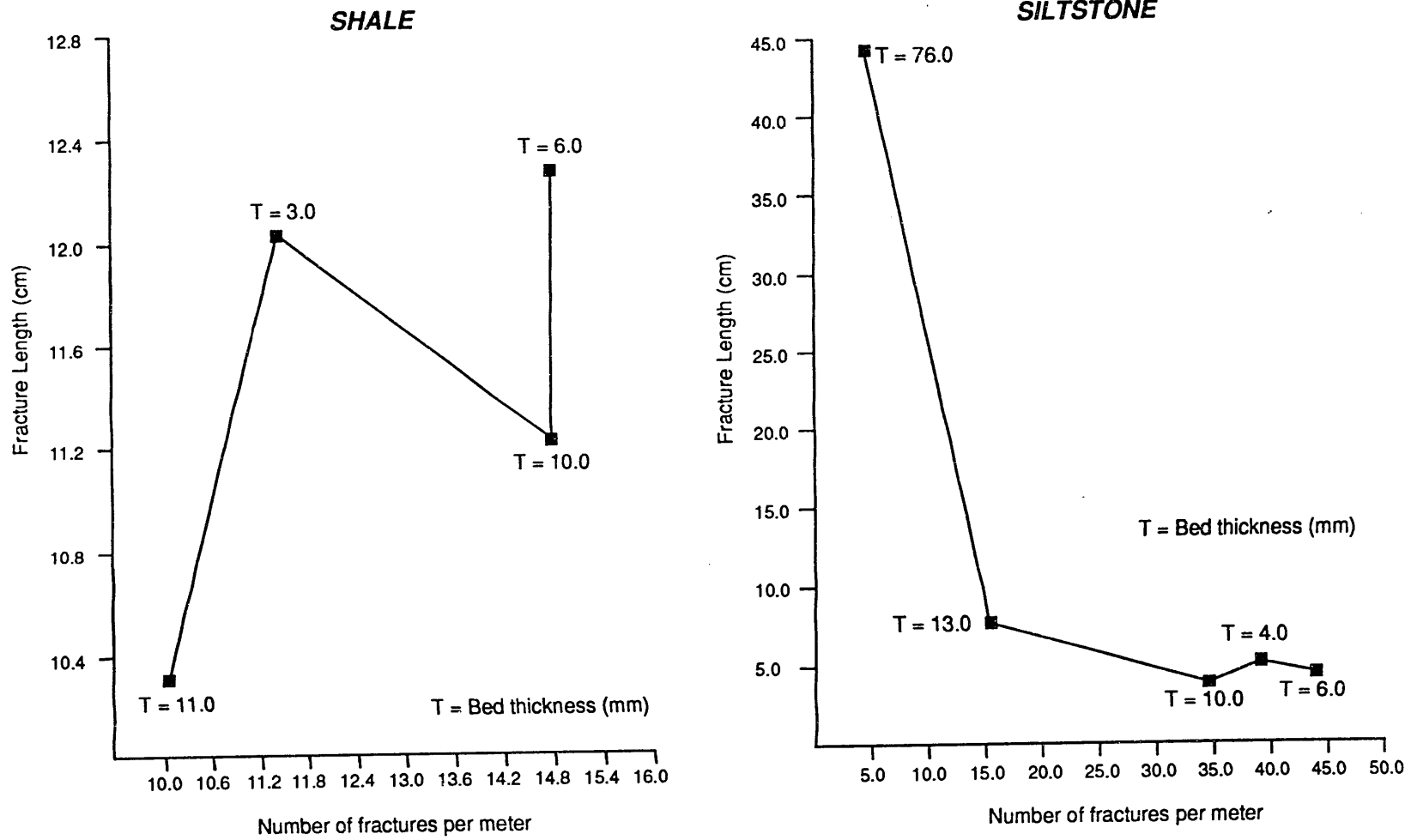


Fig. 5-20. Fracture length vs number of fractures per meter in shale and siltstone beds of the Conasauga Group (from Sledz and Huff 1981).

Melton Valley (Fig. 5-19). A linear regression analysis was used to develop mathematical relationships between the length and frequency of fractures and bed thickness, but resulted in little correlation between parameters (Sledz and Huff 1981). Fracture length and frequency were determined to depend on changes in bed thickness in siltstone, but not in shale (Fig. 5-20). In siltstone, as bed thickness increases, fracture frequency decreases and length increases. Factors considered to have affected the shale results are the precision of bed thickness measurements, weathering, and a combination of the data from different exposures (Sledz and Huff 1981).

In Melton Valley, the local fracture system was studied in trenches excavated in Solid Waste Storage Area (SWSA) 6, in trenches located on either side of Whiteoak Creek, and in core from drill hole Whiteoak Lake 1 (Fig. 5-18). In all of the studies the data were collected using the inventory method (Davis 1984) in which a large number of measurements are recorded and then fracture sets were assigned on the basis of using stereographic projections (Fig. 5-21). In SWSA 6, although northeast and northwest fracture sets are evident, there is a wide range in fracture orientation. The range of fracture orientation resulted from variations in local bedding attitude as a result of folding and faulting (Dreier et al. 1987). A similar interpretation can be made for the wide range of fracture orientation from the area surrounding Whiteoak Creek (Fig. 5-21). In addition to orientation changes in the SWSA 6 area, thin-bedded siltstone and shale had a slight increase in fracture frequency near folds and faults (Dreier et al. 1987).

Whiteoak Lake 1 is the only oriented core available in Melton Valley (Davis et al. 1987). A total of 91 fracture orientations were measured using a mechanical goni-

ometer. Fracture orientations cover a wide range, but the number of measurements are too few to constrain any preferred orientations (Fig. 5-21). Major fracture types observed in the core are mineralized fractures oblique to bedding and open bed-parallel fractures. In addition, the highest fracture densities were recorded in predominantly silty shales interbedded with limestones. Coarse, limestone breccia contained the lowest density of fractures (Davis et al. 1987).

Subsurface fracture data from the Conasauga Group in Bear Creek Valley are available from the S3 Ponds core transect (Fig. 5-18; Lutz, unpublished data). Although the cores were studied in detail, abundant fracture orientation measurements were either not made or not available. The average estimated strikes are N55E, N75W, N15E, and N20W. Foreman and Dunne (1991) estimated the orientation of 198 fractures in some of the same cores and interpreted the predominance of four bed-perpendicular fracture sets oriented N55E, N40W, E-W, and N15E. On the basis of crosscutting relationships, they concluded that the four fracture sets formed prior to thrust faulting; they were then able to use calcite fluid inclusions from the veins to infer the pressure and temperature conditions during the time of mineralization.

Available fracture data from other parts of the ORR are scarce (Fig. 5-18). Bedrock mapping for the Clinch River Breeder Reactor site located in the lower part of the Chickamauga Group in Bethel Valley listed four dominant fracture sets oriented N52E 37SE, N50E 58NW, N25W 80SW, and N65W 75NE (Kummerle and Benvie 1987). Enid Bitner (Dreier, personal communication) recorded the frequency and general orientation of all mesoscopic structures in core holes CH-1 through CH-5 in the Chickamauga Group from Bethel Valley. Fractures documented in

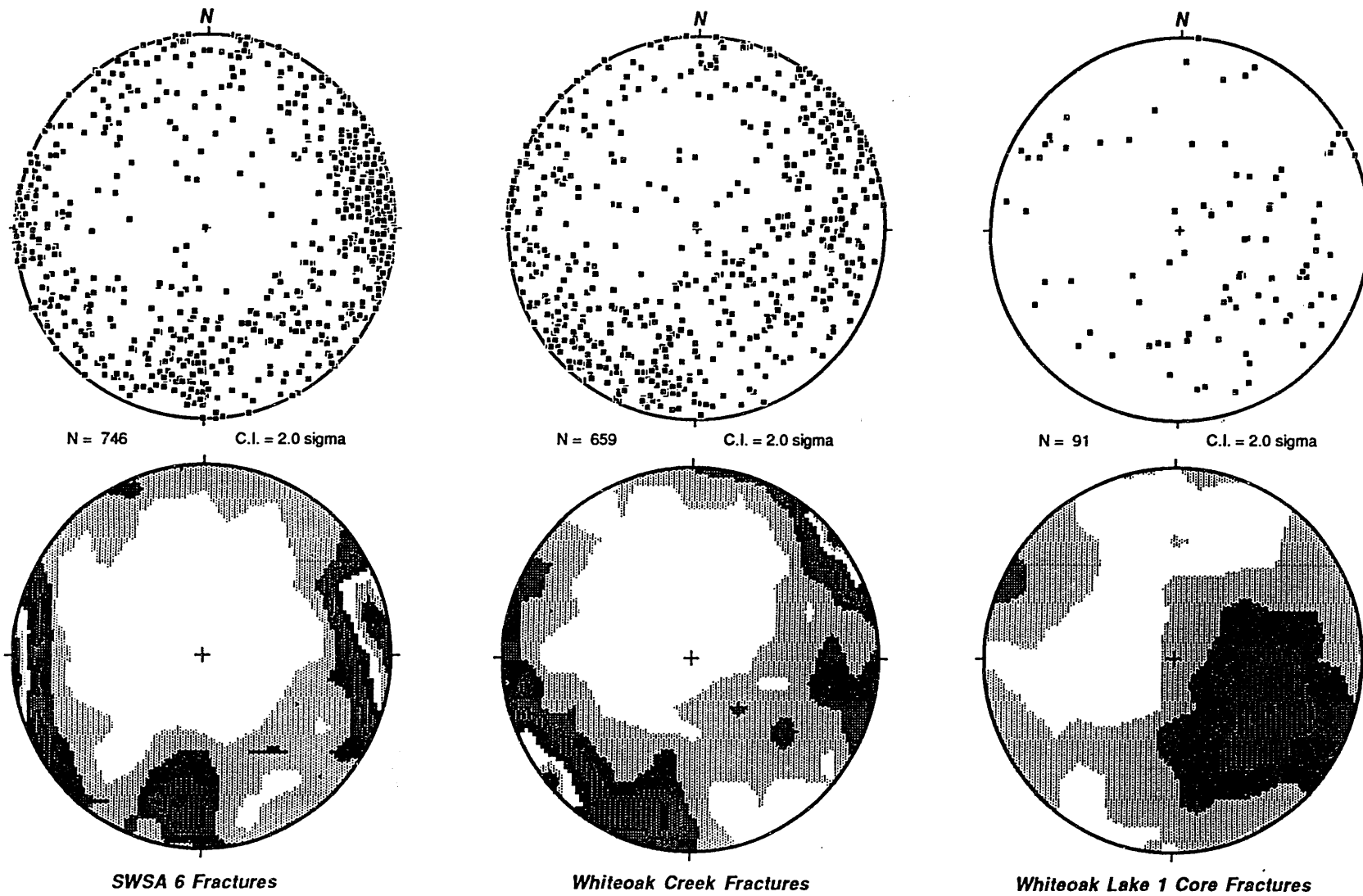


Fig. 5-21. Equal-area scatter plots and Kamb contour plots of poles to fracture planes from three different studies in the Conasauga Group in Melton Valley.

core consisted of bed-normal extension fractures parallel and perpendicular to bedding strike, bed-oblique shear fractures, and bed-parallel shear fractures.

In summary, most previous work on the fracture system on the reservation has been site specific, and little effort has been made to discuss the results with respect to other areas of the reservation or the regional geologic history.

5.5.3 Method of Data Collection

The data were collected in the field from observations made on road cuts, outcrops, and stream exposures. Measurements made include bedding and fracture orientation, bed lithology, bed thickness—using nomenclature of Ingram (1954)—minimum and maximum spacing between fractures in a set, features on the fracture surface, mineral filling, butting relationships, and local mesoscopic structures. All structural measurements were made with a Brunton compass. At outcrops where systematic fractures could be clearly identified, fracture measurements were collected by using the selection method (Davis 1984). The selection method involves measuring one orientation of a representative fracture from each set. From one to four measurements were recorded at each site. At small outcrops only a single fracture of a particular orientation was observed. In this case, although the selection method could not be applied, a measurement was recorded because the orientation of the fracture was similar to other sets in the area.

5.5.4 Fracture Classification Scheme

Fractures need to be classified both geometrically and genetically in order to relate their mechanical development within the context of the regional structural history. The geometric classification

is purely descriptive and may use geographic compass directions or terms related to regional strike, such as strike-parallel and strike-perpendicular fractures. A common method for describing fracture geometry that is not dependent on absolute orientation refers the orientation of the fracture plane to orthogonal fabric axes a , b , and c (Turner and Weiss 1963). Planes perpendicular to one axis, but containing the other two, are termed ab , ac , or bc , which refer to the axes the planes contain. Surfaces oblique to two axes, but containing one axis are in $0kl$, $h0l$, and $hk0$, and those oblique to all three axes are in hkl : h , k , and l refer to intercepts on the a , b , and c axes, respectively, and 0 indicates parallelism to an axis. A fabric axial cross-oriented with the a -axis parallel to bedding dip, b -axis parallel to bedding strike, and c -axis perpendicular to bedding is used to describe the orientation of each fracture set (Fig. 5-22). A genetic classification, on the other hand, is more difficult to apply because many of the fractures observed in the field do not contain evidence of their displacement mode. Therefore, the best approach is to combine the abundant

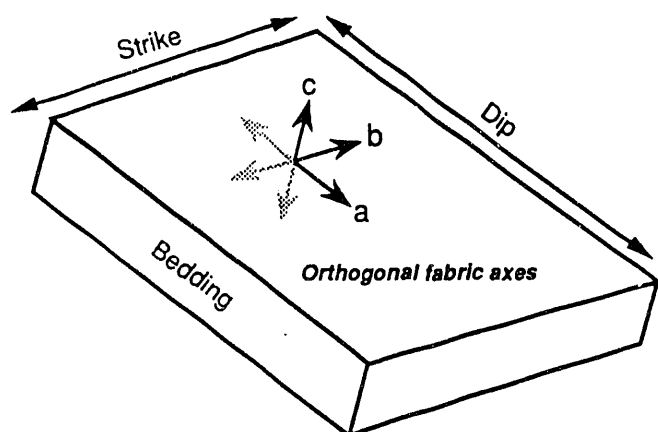


Fig. 5-22. Definition of the orthogonal fabric axes used to describe the geometry of the fracture sets.

fracture orientation data with available genetic information and assume a similar displacement mode for all of the fractures having the same geometric characteristics.

The presently accepted genetic classification of fracture types categorizes fractures as either extensional (Mode I), shear (Mode II), or hybrid (Combined Mode I & II) (Dennis 1972, Hancock 1985, Engelder 1987). With regard to present nomenclature, Pollard and Aydin (1988) proposed that the word "joint" be restricted to fractures with evidence for dominantly opening displacements; if the evidence for opening is not present, the term "fracture" should be used. In order to prevent ambiguity, the term fracture will be used here, and, where displacement mode is known, the appropriate modifier will be used, such as extension fracture and shear fracture. As shown in Fig. 5-23, brittle failure leading to the development of the different fracture displacement modes may be predicted by the relationship between the Coulomb-Mohr failure envelope and the stress circle (e.g., Price 1966). In the following discussion, s_1 , s_2 , and s_3 are the maximum, intermediate, and minimum principal stresses, respectively, and s_1' , s_2' , and s_3' are the maximum, intermediate, and minimum effective principal stresses, respectively. Extension fractures form normal to s_3 and in the s_1s_2 plane, provided that s_3' equals $-T$, where T is the tensile strength of the rock. An additional requirement* for extension fracturing is that $(s_1' - s_3')$ does not exceed $4T$ because, if greater, the Mohr circle will not fit beneath the failure envelope when s_3' equals $-T$. Conjugate shear fractures enclose an acute bisector parallel to the s_1 axis, an obtuse bisector parallel to the s_3 axis, and intersect parallel to the s_2 axis. Conjugate shear fractures develop provided that s_3' is zero or positive and $(s_1' - s_3')$ equals or exceeds $8T$. Such conditions permit the Mohr circle to be tangent to the failure envelope in its

straight-line part. The dihedral angle between the conjugate shear fractures will depend on the shape of the Coulomb-Mohr failure envelope, which is a function of the angle of internal friction, f . Hybrid fractures enclose an acute bisector parallel to the s_1 axis, an obtuse bisector parallel to the s_3 axis, and intersect parallel to the s_2 axis. There are two important characteristics of the failure envelope that lead to the development of hybrid fractures: (1) it slopes toward the tensile portion of the normal stress axis and (2) it becomes parabolic across the shear stress axis as it approaches the normal stress axis. A consequence of the slope to the Coulomb-Mohr failure envelope is that shear failure under conditions of decreasing confining pressure requires decreasing differential stress. A consequence of the parabolic shape is that shear failure will occur along conjugate planes with progressively smaller dihedral angles as the confining pressure decreases. Formation of hybrid fractures requires that s_3' is between $-T$ and zero and that $(s_1' - s_3')$ is between $4T$ and $8T$. In this case, the Mohr circle will be tangent to the parabolic sector of the failure envelope.

5.5.5 Fracture System Geometry

The present geometry of the fracture sets that make up the fracture system in the ORR is related to the timing of individual fracture events. Fracture sets that formed prior to regional thrust faulting are assumed to have formed in beds having a subhorizontal dip. Therefore, one factor affecting their present orientation, with respect to geographic coordinates, will be bedding attitude manifested as a result of regional thrusting and folding. Fracture sets formed during regional deformation will be related to structural position, as well as to the structural history of the different thrust sheets. Fracture sets that

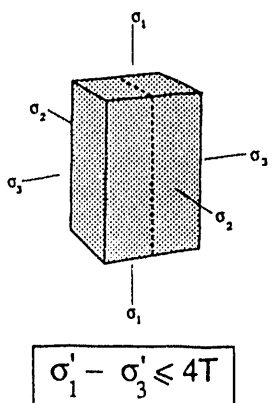
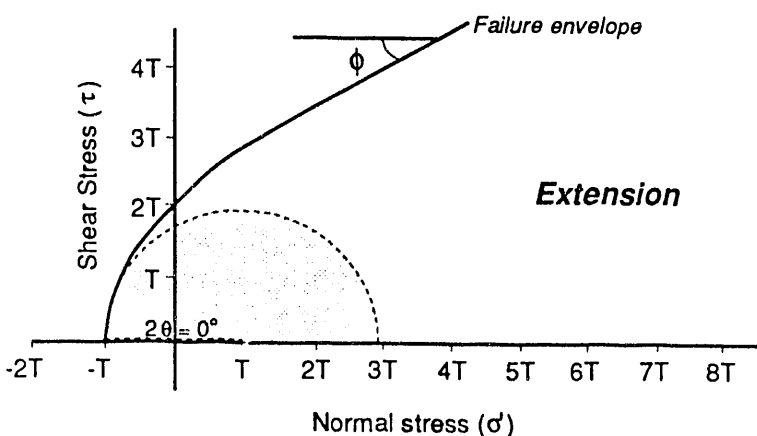
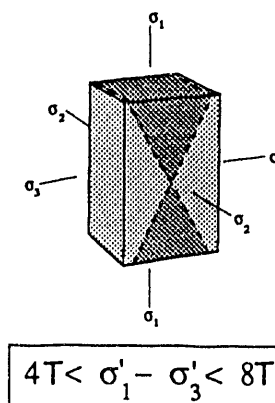
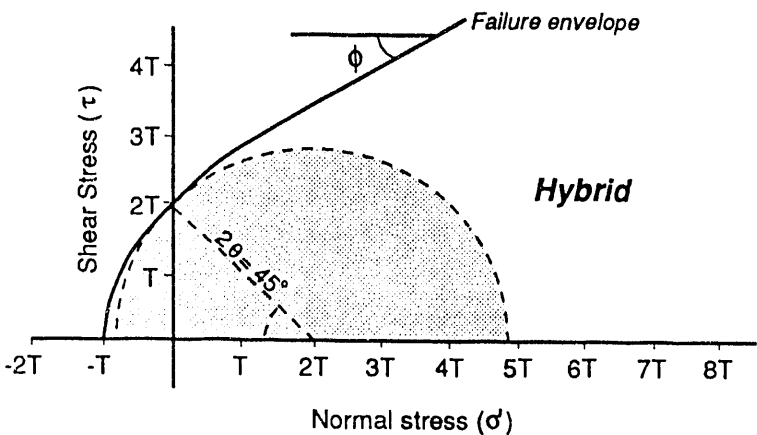
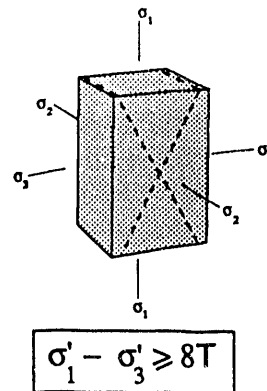
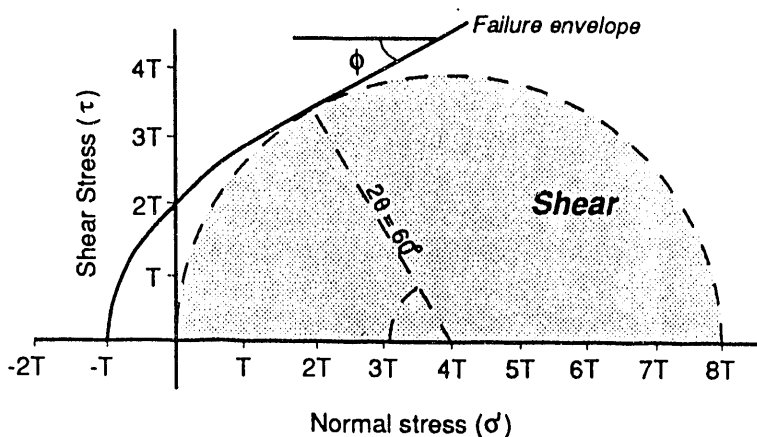


Fig. 5-23. Brittle failure leading to the development of different fracture displacement modes that may be predicted by the relationship between the Coulomb-Mohr failure envelope and the stress circle (e. g., Price 1966).

formed after regional deformation should have a geometry unrelated to bedding attitude or structural position, unless stress fields were affected by a residual stress or anisotropy related to bedding. In addition to the complex stress history through time, differences in fracture orientation can arise during any particular fracturing event by variations in mechanical properties between rock units, formation fluid pressure, and deviatoric stress.

The equal area stereographic projection of poles to systematic fracture planes for the ORR contains a wide range of fracture orientations (Fig. 5-24). Fracture attitudes span all geographic orientations and dip from 0 to 90°. Although the plot depicts a wide range of fracture orientations, it is misleading because the data were collected across an area where there is (1) a change in bedding dip, (2) a doubly plunging syncline, (3) a change in lithology, (4) macroscopic and mesoscopic faults, and (5) a difference in structural history between thrust sheets.

In order to evaluate the geometric aspects of the fracture system, the data need to be divided into homogenous structural and lithologic domains. First, the fracture data have been divided on the basis of thrust sheet. Because each thrust sheet is interpreted to have followed a different structural evolution, each sheet can be considered an individual domain. Second, within each thrust sheet the fracture data have been further subdivided on the basis of stratigraphic unit. Such a subdivision is useful because each unit occupies a fairly distinct structural position. For example, the major thrust faults are located within the Rome Formation, but only minor faulting is evident in the Knox Group. In addition, within the Copper Creek thrust sheet is a gradual change in the dip of bedding from 35 to 10° from the Rome Formation into the Knox Group. Changes in fracture orienta-

tion with respect to bedding dip can then be evaluated. Third, in order to examine the effects of lithology on fracture geometry, fracture data from the limestone and shale/siltstone units of the Conasauga Group were used because they occupy the same structural position.

5.5.5.1 Copper Creek thrust sheet

The Copper Creek thrust sheet covers the largest portion of the ORR studied to date and therefore has the greatest number of fracture stations. The 786 measurements have been separated by stratigraphic unit: Rome Formation, Conasauga Group, and Knox Group (Fig. 5-25). Although fabric axes are used to describe the geometry of the fracture sets within each stratigraphic unit, the geographic coordinates are included for reference in future discussions. All of the dominant fracture sets have a strike variance of 10 to 20° and a dip variance of approximately 10°.

The Kamb contour plot of 294 poles to fracture sets measured in the Rome Formation contains three point maxima related to bc (054 / 55 NW), ac (321 / 87 NE), and hkl (287 / 84 SW) extensional fracture sets. Between the point maxima is a wide girdle of fracture orientations. The range in fracture orientation is partly a function of variations in bedding attitude throughout the Rome Formation, as well as of some local fracture set development. The primary reason for the range in fracture orientation may be the development of hybrid and shear fracture sets symmetrically arranged with respect to the extensional fracture sets. The additional strike-parallel fracture sets include conjugate hk0 fractures enclosing an acute angle about b and conjugate h0l fractures enclosing an acute angle about c. Strike-perpendicular fractures consist of ac fractures, conjugate hk0 fractures enclosing an acute angle about a, and conjugate 0kl fractures enclosing

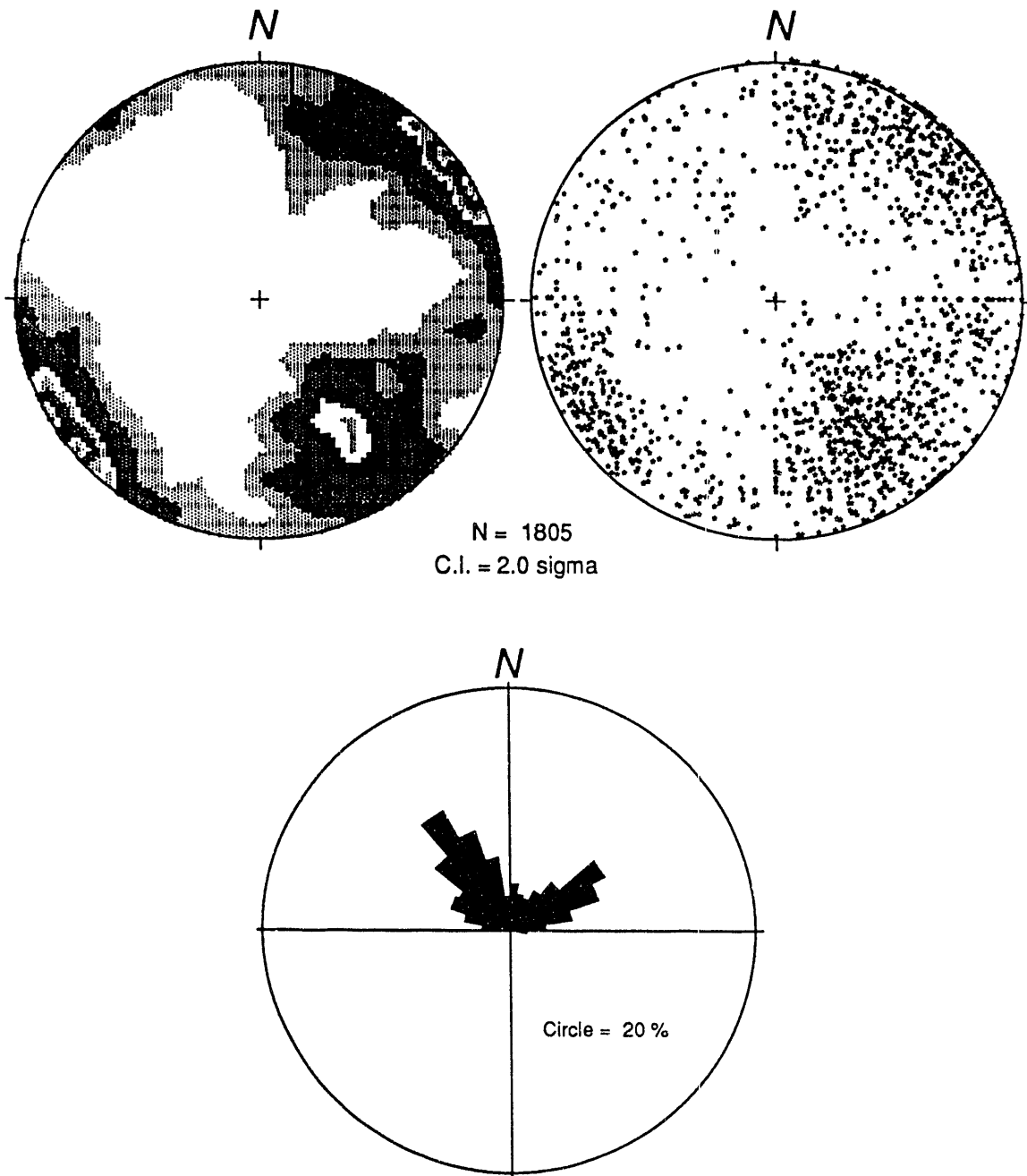


Fig. 5-24. Equal-area scatter and Kamb contour plot of poles to systematic fractures and equal-area rose plot of systematic fracture strikes for the ORR.

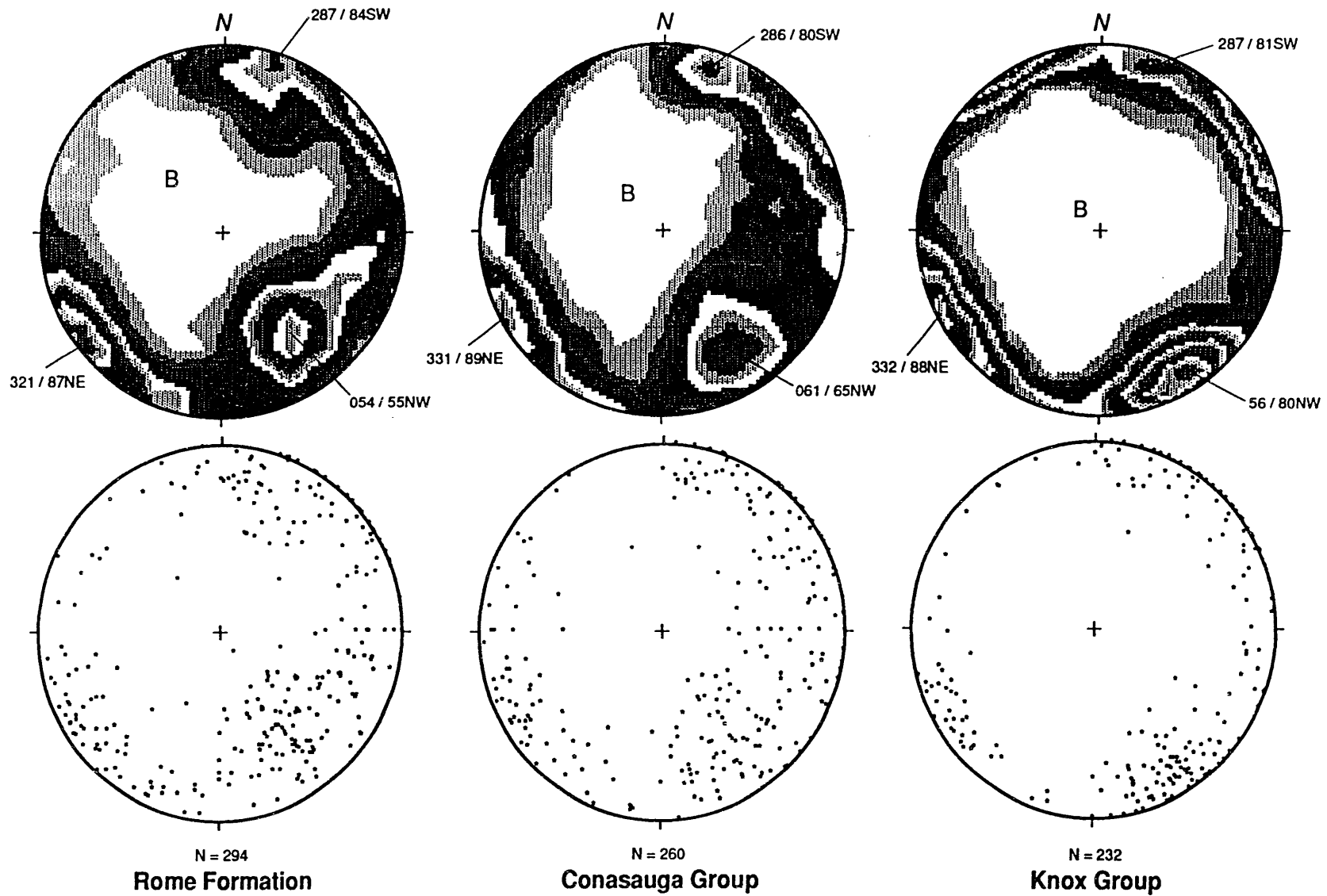


Fig. 5-25. Equal-area scatter and Kamb contour plots of poles to fracture planes for the Rome Formation, Conasauga Group, and Knox Group in the Copper Creek thrust sheet. Contour interval is 1.0 sigma; B = mean pole to bedding.

ing an acute angle about *c*. The acute angle enclosed by the conjugate fractures ranges from 10 to 60°. The conjugate *h0l* and *0kl* fractures, which enclose an acute angle about *c*, appear to be the least well developed of all the fracture sets. Criteria for determining the type of fracture set are discussed in the next section.

A total of 260 fracture set measurements were made in the Conasauga Group. A Kamb contour plot of poles to fracture planes depicts four point maxima related to *ac* (061 / 65 NW), *bc* (331 / 89 NE), and two *hkl* (286 / 80 SW & 06 / 88 NW) extensional fracture sets. Like the Rome Formation, the range of fracture orientations may be related to (1) development of hybrid and shear fracture sets symmetrically arranged around the extensional fracture sets, (2) slight variations in bedding dip, and (3) local development of fracture sets.

A total of 232 fracture set measurements were recorded from the Knox Group. The two point maxima on the Kamb contour plot belong to the *ac* (56 / 80 NW) and *bc* (332 / 88 NE) extensional fracture sets. In addition, the Kamb contour plot contains a minor point concentration representing an *hkl* (287 / 81 SW) extensional fracture set. Each set has associated hybrid and shear fractures, but the tighter concentration of fracture poles indicates a more consistent bedding attitude across the Knox Group outcrop belt. Furthermore, the tighter concentration of fracture poles in the Knox Group probably reflects the lack of local fracture development related to mesoscopic and macroscopic faulting and folding, which is common in the Rome Formation and Conasauga Group.

5.5.5.2 Whiteoak Mountain thrust sheet

A total of 596 fracture measurements were collected in the Whiteoak Mountain

thrust sheet (Fig. 5-26). Fracture measurements were collected in the Rome Formation, Conasauga Group, Knox Group, and Chickamauga Group. In general, fracture orientations in the Whiteoak Mountain thrust sheet are similar to the Copper Creek thrust sheet, but the range is less because bedding dip is relatively constant.

The Kamb contour plots of poles to fracture planes for each of the stratigraphic units contains two point maxima related to the *bc* and *ac* extensional fracture sets. Fracture sets in the Rome Formation are oriented 067 / 45 NW and 320 / 88 SW. Fracture sets in the Conasauga Group are oriented 041 / 40 NW and 306 / 54 SW. The different orientation of the point maxima for the *ac* and *bc* fracture sets in these units is probably related to the fewer number of data points. In the Knox Group, the two dominant fracture sets are oriented 068 / 56 NW and 321 / 87 SW. Finally, in the Chickamauga Group, the dominant fracture sets are oriented 053 / 55 NW and 328 / 89 SW. The *bc* and *ac* fracture sets in the Knox and Chickamauga Groups have similar orientations to those in the Copper Creek thrust sheet. Additional strike-parallel fracture sets comprise conjugate *hk0* fractures enclosing an acute angle about *b* and conjugate *h0l* fractures enclosing an acute angle about *c*. Strike-perpendicular fractures consist of *ac* fractures, conjugate *hk0* fractures enclosing an acute angle about *a*, and conjugate *0kl* fractures enclosing an acute angle about *c*. The acute angle enclosed by the conjugate fractures ranges from 10 to 60°. The conjugate *h0l* and *0kl* fractures that enclose an acute angle about *c* appear to be the least well developed of all the fracture sets.

5.5.5.3 Kingston thrust sheet and East Fork syncline

A total of 307 fracture set orientations

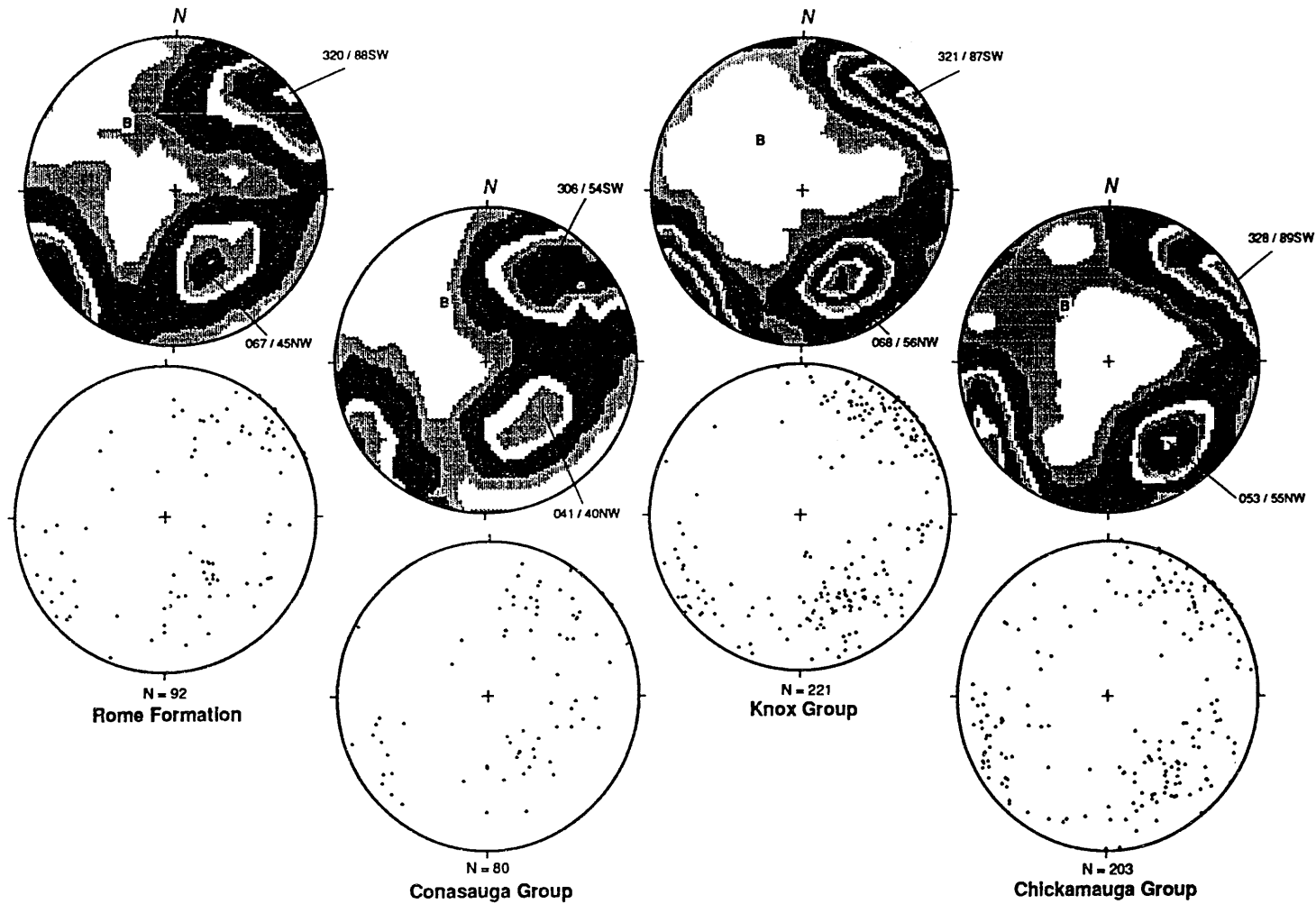


Fig. 5-26. Equal-area scatter and Kamb contour plots of poles to fracture planes for the Rome Formation, Conasauga Group, Knox Group, and Chickamauga Group in the Whiteoak Mountain thrust sheet. Contour interval is 1.0 sigma; B = mean pole to bedding.

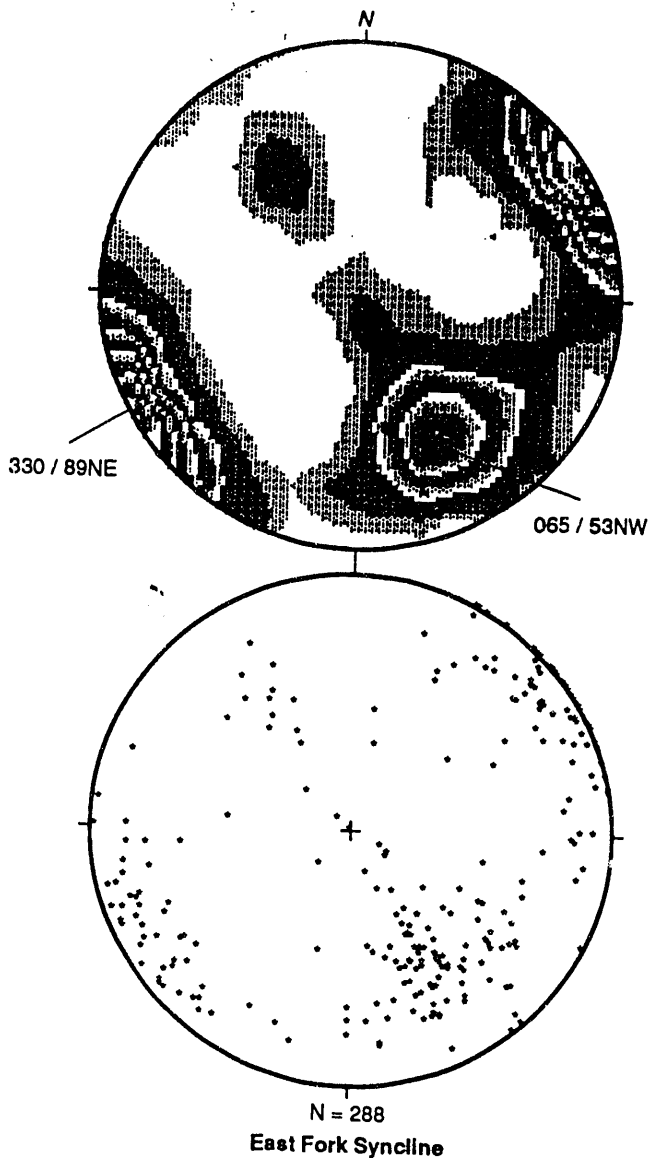


Fig. 5-27. Equal-area scatter and Kamb contour plots of poles to fracture planes for the Chickamauga Group, Reedsville Shale, Sequatchie Formation, Rockwood Formation, Chattanooga Shale, and Fort Payne Formation, which form the East Fork syncline. Contour interval is 1.0 sigma.

tion of proximity to the Kingston fault. The orientations of the fracture sets are similar within each stratigraphic unit composing the East Fork syncline and therefore have been combined to provide a suitable number of measurements for Kamb contouring. The Kamb contour plot contains three point maxima. Two of the point concentrations are related to bc (065 / 53 NW) and ac (330 / 89 NE) fracture sets developed in the southeast dipping beds of the syncline. The third point maximum is not related to the development of a new fracture set, but is the bc fracture set recorded from the northwest-dipping beds on the southeast limb of the syncline. The partial girdle of fracture poles oriented perpendicular to the

were measured in the Kingston thrust sheet. The majority of fracture measurements are from the Chickamauga Group, Rockwood Formation, and Fort Payne Formation, which compose the East Fork syncline (Fig. 5-27). A total of 19 fracture set measurements were recorded in the Conasauga and Knox Groups to the northwest of the syncline approaching the Kingston fault. Unfortunately, the measurements are too few to document changes in fracture orientation as a func-

fold axis is the bc fracture set fanning around the fold as bedding dip changes. Additional strike-parallel fracture sets comprise conjugate $hk0$ fractures enclosing an acute angle about b and conjugate $h0l$ fractures enclosing an acute angle about c . Strike perpendicular fractures consist of ac fractures, conjugate $hk0$ fractures enclosing an acute angle about a , and conjugate $0kl$ fractures enclosing an acute angle about c . The acute angle enclosed by the

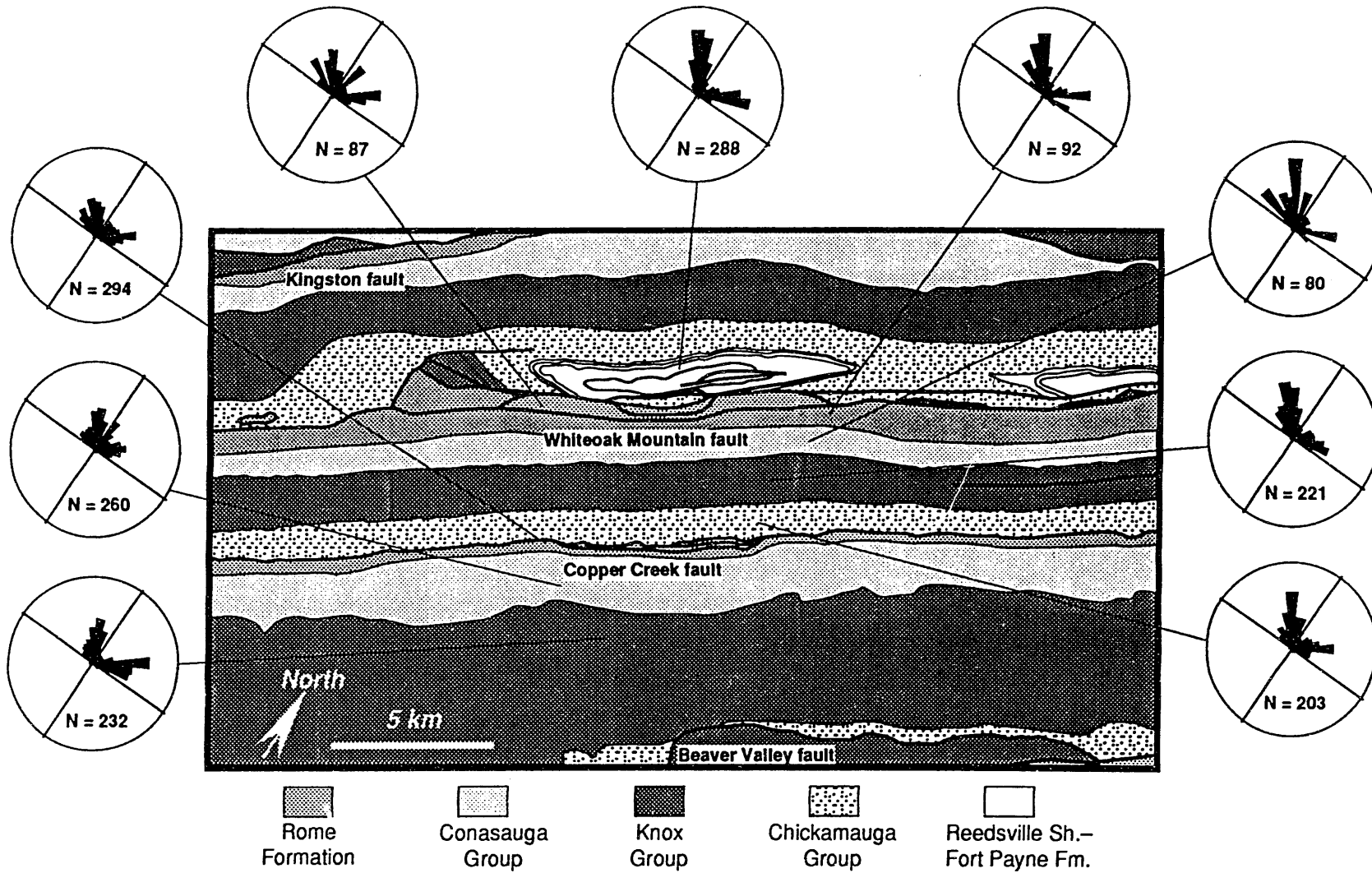


Fig. 5-28. Summary rose plots of fracture strikes recorded from each stratigraphic unit in the ORR.

conjugate fractures ranges from 10 to 60°. The conjugate $h0l$ and $0kl$ fractures, which enclose an acute angle about c , appear to be the least well developed of all the fracture sets.

In summary, fracture geometries are similar within each thrust sheet (Fig. 5-28). The most common fracture sets are ac and bc extensional fractures, as well as conjugate $hk0$ fracture sets with an acute angle around a and conjugate $hk0$ fracture sets with an acute angle around b (Fig. 5-29). Also present, but much less abundant, are conjugate $0kl$ fractures with an acute angle around c and conjugate $h0l$ fractures with an acute angle around c . The similar fracture geometries between each thrust sheet suggest that the stress field responsible for fracturing was consistent across the region. Furthermore, fracture geom-

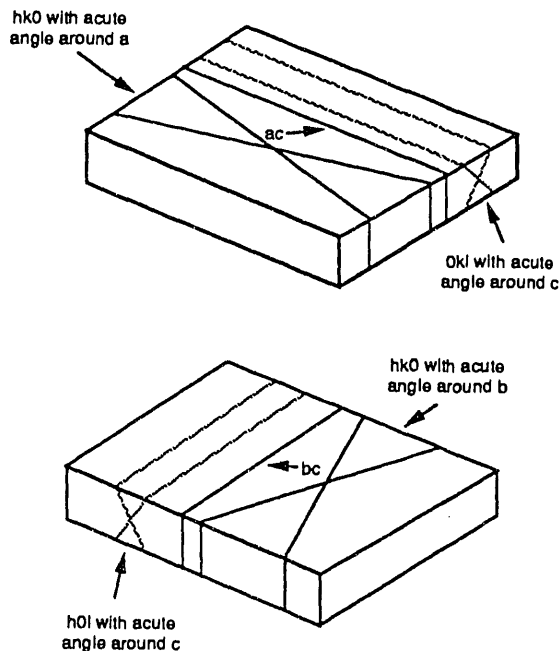


Fig. 5-29. The most common fracture sets in the study area: ac , bc , $hk0$ with an acute angle around a , and $hk0$ with an acute angle around b . Much less pervasive, but present: $0kl$ fractures with an acute angle around c and $h0l$ fractures with an acute angle around c .

etry combined with the mode of fracture opening (i.e., fracture type) can be used to infer the orientation of the principal stresses at the time of fracturing.

5.5.6 Changes in Fracture Orientation as a Function of Lithology

Mechanical analyses incorporating a Mohr circle construction of failure envelopes for various sedimentary rock types indicate that, given the same fluid pressure and deviatoric stress, fracture orientation and displacement mode will be a function of lithology. Data from the Conasauga Group in the Copper Creek thrust sheet were examined in order to test the influence of lithology on the formation of extension, hybrid, and shear fractures. The Conasauga Group contains a mixture of clastic (shale and siltstone) and carbonate (limestone and dolomite) lithologies. The rock units are approximately the same age and occupy the same structural position, suggesting that they have experienced a similar stress history.

A total of 144 fracture set measurements were made in limestone and 114 measurements were made in shale and siltstone (Fig. 5-30). The rose diagram of fracture strike directions for limestone indicates that the dominant fracture sets strike 5, 45, 325, and 285°. The dominant fracture sets in shale and siltstone strike 5, 35, 55, 335, and 300°. Except for the 5° set, the dominant fracture sets in each rock type differ by approximately 10°.

An explanation for the difference in fracture orientation between the clastic and carbonate lithologies can be shown schematically by constructing a Mohr circle diagram (Fig. 5-31). Assuming similar fluid pressure and deviatoric stress in each rock type, the hypothetical failure envelopes for limestone and shale will intersect the Mohr stress circle at different points. The stress circle intersects the

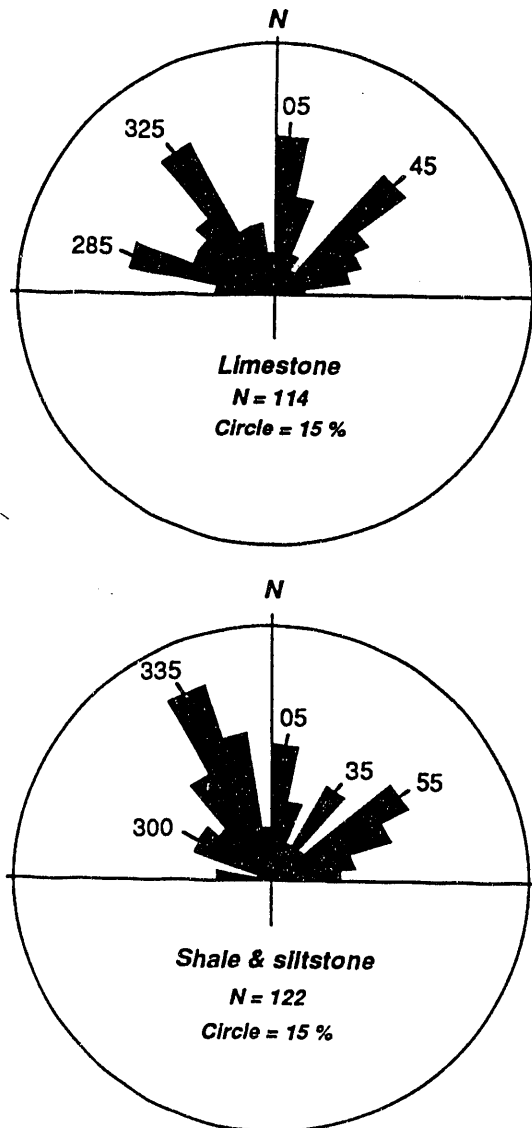


Fig. 5-30. Rose plots of systematic fracture strikes from limestones and shales/siltstones of the Conasauga Group in the Copper Creek thrust sheet.

limestone failure envelope in the tension field where extension fractures propagate normal to the minimum compressive stress, but the circle intersects the shale failure envelope in the hybrid fracture region. As a result, although the boundary stresses have the same orientation and magnitude, fractures in each rock type will

have a slightly different orientation.

On a larger scale, there are minor differences between fracture orientations in the dolomite of the Knox Group and the clastics of the Rome Formation and Conasauga Group (Fig. 5-28). For example, although the ac and bc fracture sets are similar, the minor hkl extensional fracture sets are not well developed in the Knox Group. In this case, conditions causing the formation of the minor hkl extensional fracture sets in the Rome Formation and Conasauga Group may not have been sufficient to cause fracturing in the stronger dolomite. Variations in bedding between the Rome Formation and Conasauga Groups vs the Knox Group, as well as differences in structural position of the stratigraphic units, may account for differences in fracture sets.

5.5.7 Fracture Type

A genetic classification requires assessing the displacement mode of the fracture walls to determine whether a fracture set comprises extension, hybrid, or shear fractures (Hancock 1985, Price and Cosgrove 1990). More than 90 percent of the measured fractures are unfilled, and, at the scale of observation possible in the field, there is no evidence of shear offset. The criteria used to determine fracture type were (1) fracture set architecture, (2) preserved fracture surface structures, (3) conjugate fracture dihedral angles, (4) symmetry of fracture orientations with respect to nearby kinematic indicators, and (5) microscopic analysis of mineral filling crystal growth patterns. Hybrid fractures were the most difficult to identify, but are considered part of the system because of the geometric relationship of fractures with a small dihedral angle surrounding known extensional fractures.

Architectural style proved to be a useful criterion for classifying extension

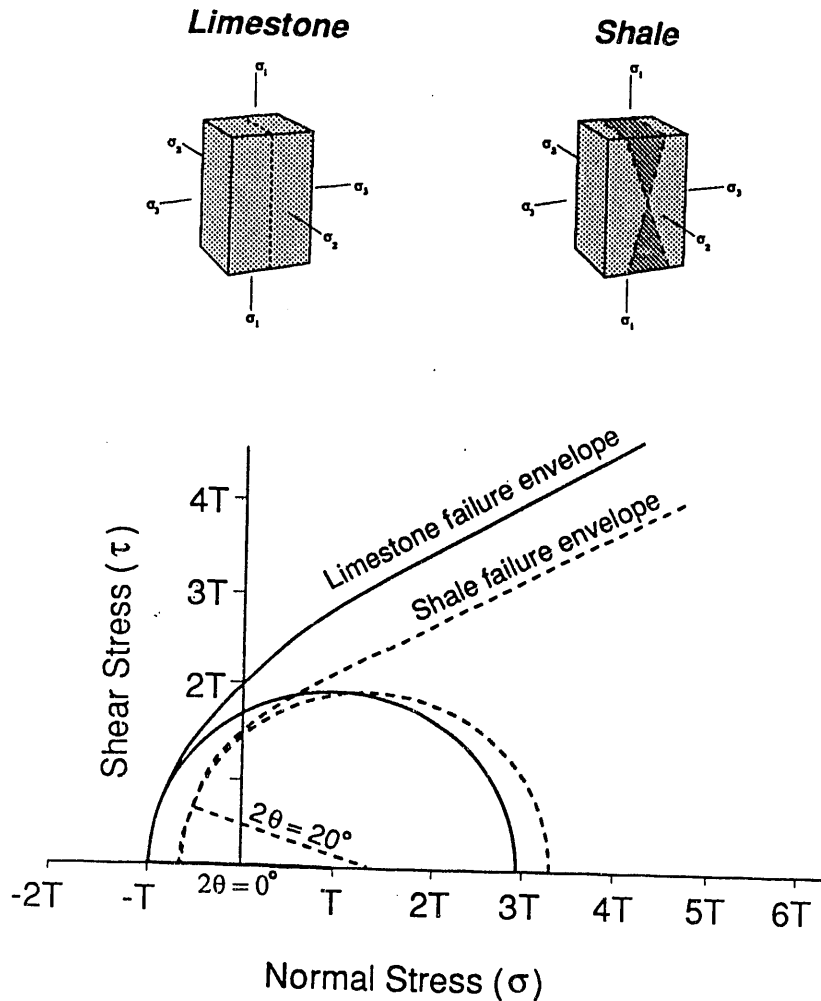


Fig. 5-31. Changes in fracture orientation solely as a function of lithology, which can be explained by using a Mohr circle construction.

fracture sets occur, the architectural style consisted of combinations of the above (Fig. 5-32f). The interpretations of fracture type based on architectural style are the most reliable when combined with other displacement criteria.

Fractography involves using the morphological features of fracture faces to infer the mode of fracture displacement and hence fracture type (Kulander et al. 1979). In the study

and conjugate fracture sets indicative of both hybrid and shear fractures (Hancock 1985). A number of exposures contained only a single fracture set, resulting in the I-shaped architectural style indicative of extension fractures. Exposures containing more than one fracture set commonly had the following types of architectural styles (Fig. 5-32): (1) orthogonal and continuous (+ or double I \geq extension); (2) nonorthogonal and continuous (X \geq conjugate); (3) orthogonal with one set continuous and the other discontinuous (H \geq extension); and, occasionally; (4) orthogonal or nonorthogonal with both sets being discontinuous (T \geq extension and Y \geq conjugate) (Fig. 5-32a-e). Where more than two

area, most visible fracture surfaces are featureless to slightly hackly, although a few preserve a poorly developed plumose structure. The best example of a plumose structure and associated twist hackle observed to date is in the Copper Ridge Dolomite in a CSX railroad cut north of the TVA Bull Run Steam Plant (Fig. 5-33). The photo contains an example of the ac fracture set, and the morphology of the plume indicates that the fracture is extensional and the front propagated from the southwest to the northeast (Bahat 1979, Engelder 1982, Bahat and Engelder 1984). Unfortunately, the paucity of preserved fracture face structures precluded using

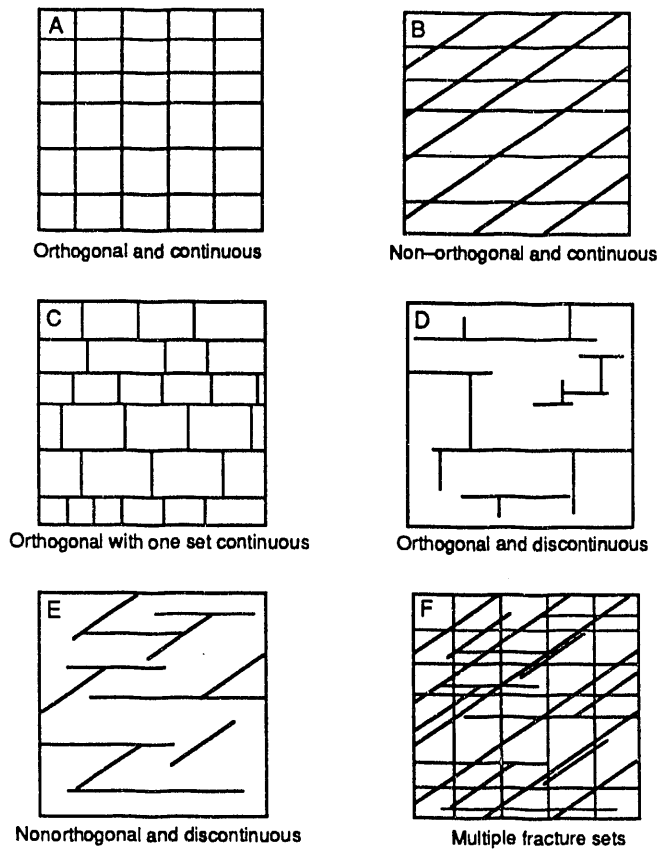


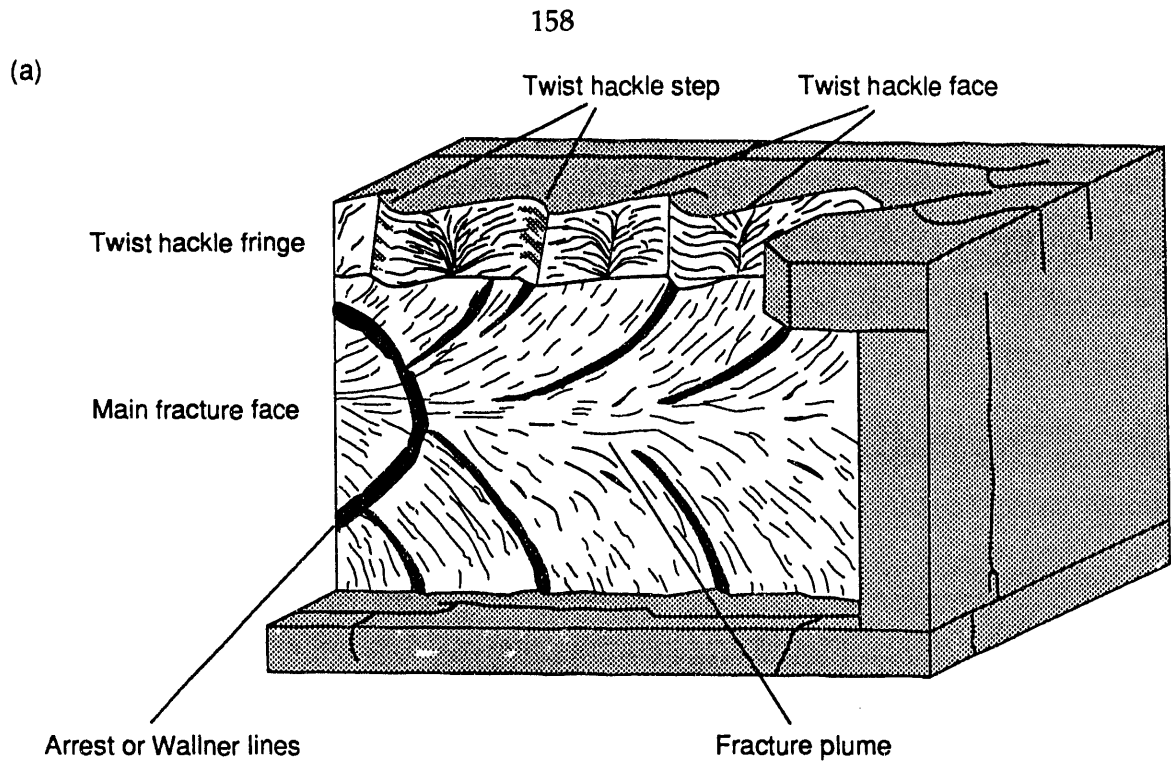
Fig. 5-32. Fracture architectural styles observed on exposed bedding surfaces.

fractography as an efficient means of determining fracture type.

The dihedral angle between conjugate fractures was used to interpret the occurrence of both hybrid and shear fractures in the area. Nonorthogonal conjugate fracture sets have dihedral angles ranging from less than 10 to 60°. Some exposures contain an extensional fracture set that bisects the dihedral angle between two conjugate fractures. Assuming that the fractures are approximately the same age, the three fracture sets can be interpreted to have formed under the same stress field orientation, but not magnitude. Fracture sets oblique to bedding are also interpreted to be either hybrid or shear fractures.

Other associated kinematic indicators, such as en echelon veins or fracture traces, pinnate fractures, and slickensides, have been used to interpret the shear origin of some fractures. For example, an exposure of bedded chert from the lower Chickamauga Group in the Whiteoak Mountain thrust sheet contains three fracture sets (Fig. 5-34). The two orthogonal sets are ac and bc extension fractures, which have a fairly continuous and planar geometry. The third set, however, consists of short en echelon fractures indicative of a shear origin. The shear fractures make up one set of the conjugate hk0 fractures with an acute angle around a and have been observed elsewhere. Although truncation relationships are a bit ambiguous, the latter set passes through the ac set of extension fractures, but is in places truncated by and merges with the bc extensional fracture set, suggesting it is contemporaneous with the latter extensional set. Conjugate fractures with a small dihedral angle, in conjunction with pinnate veins, have been used to infer a hybrid shear-fracture origin. For example, in the Witten Formation, pinnate veins and elongate calcite crystals occur with two sets of conjugate hk0 fractures that have a dihedral angle of 20° (Fig. 5-35).

Microscopic analysis was not intensively employed in this study because most of the fractures measured at the surface are unfilled. A few oriented samples were collected from the limestones in the Conasauga Group and sandstones in the Rome Formation in the Copper Creek thrust sheet and in limestones in the Chickamauga Group in the Whiteoak Mountain thrust sheet. Examples of the ac and bc fracture sets in both the Conasauga Group and Chickamauga Group contain twinned, equigranular calcite that truncate fossils and ooids and offset them parallel to the fracture walls. This observation is indicative of extensional fracturing



(b)



Fig. 5-33. (a) Sketch of fractographic features indicative of an extension (Mode I) fracture (from Kulander and others 1979). (b) Face of an ac fracture in a fine-grained dolomite from the Copper Ridge Dolomite containing plumose structure and twist hackle.

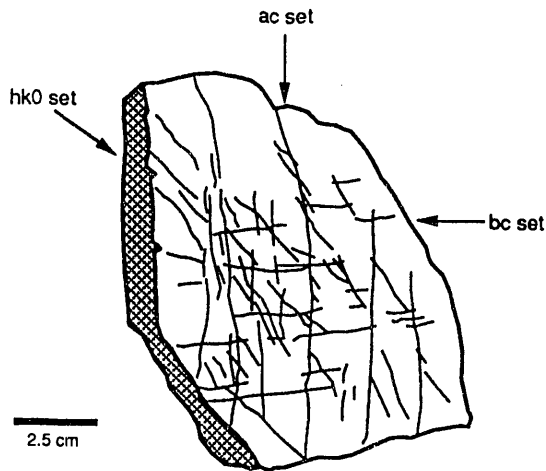


Fig. 5-34. Sketch from a photograph of a sample of bedded chert from the lower Chickamauga Group in the Whiteoak Mountain thrust sheet.

(Engelder 1982). Foreman and Dunne (1991) observed similar characteristics in fractures in the Nolichucky Shale in the

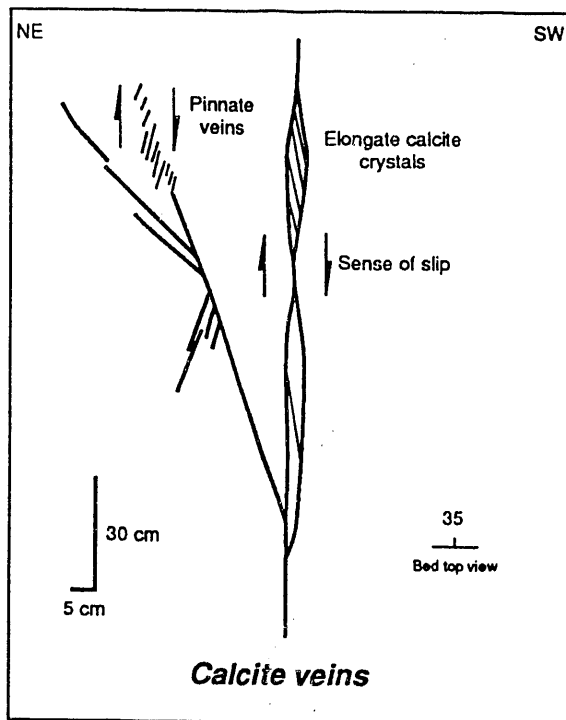


Fig. 5-35. Sketch of calcite veins from a limestone bed top in the Witten Formation in the Whiteoak Mountain thrust sheet.

Whiteoak Mountain thrust sheet and interpreted them to have formed by extension.

5.5.8 Fracture Timing

In areas of multiphase fracturing, abutting relationships can be used to determine the relative timing of propagation between fracture sets. Given two unfilled fracture sets, the most continuous fracture set is interpreted to have propagated first and the abutting set is considered to have formed later. Even where there are no more than two orthogonal fracture sets, however, there is commonly field evidence from butting relationships that each set formed contemporaneously. Therefore, it is rarely possible to state that a particular set contains fractures that are universally younger than those in another set (Hancock and Kadhi 1978, Engelder and Geiser 1980, Dunne and North 1990). A number of butting relationships in small bed-top exposures were recorded across the study area, but did not provide conclusive timing evidence between fracture sets. For example, both ac and bc fractures abut each other, as well as crosscut each other continuously, which suggests that they formed contemporaneously. Crosscutting orthogonal fracture sets without any disruption of the fractures near intersection points suggest that one fracture set may have been mineralized during the growth of the second set. If this were not the case, the intersection of a fracture perpendicular to an open fracture would tend to prohibit propagation and result in T-type architectural style. In addition, mineralized crosscutting fractures are rare, but indicated coeval development between the ac and bc fracture sets. The primary reason butting and crosscutting relationships were not a successful indicator of relative timing is that the extensive exposed bedding surfaces needed to record a

suitable number of timing relationships within one structural domain were not available.

The timing of fracturing events is best discussed in relation to regional thrust faulting associated with the Alleghanian orogeny. Displacement and rotation of bedding as a result of thrusting allows prethrusting fractures to be identified because they will change orientation as a function of bedding attitude. In addition, crosscutting relationships between fractures and thrust structures will date the fracture with respect to regional deformation. Fractures formed during the Alleghanian orogeny should have orientations consistent with the stress field needed for thrust faulting and may be preferentially developed on the basis of structural position. Post-thrusting fractures should have orientations irrespective of bedding attitude and crosscut structures related to thrust faulting. In addition, knowledge of changes in the regional stress field orientation subsequent to folding and thrusting can be correlated with the occurrence of different fracture sets.

5.5.8.1 Prethrusting fracture sets

The predominant fracture sets on the ORR are interpreted to have formed prior to regional thrust faulting related to the Alleghanian orogeny. The prethrusting fractures include extensional ac, bc, and associated hybrid fractures, as well as other hkl fracture sets. The following criteria were used to infer the prethrusting development of the fracture sets: (1) the fractures are symmetrical with respect to bedding so that their orientation is controlled by bedding orientation, (2) the fractures are crosscut by slickensided bed-parallel fractures formed during the Alleghanian orogeny, (3) calcite fracture fillings are commonly twinned, and (4) the

fractures are offset by mesoscopic faults. The relative timing of development between the prethrusting fractures, however, is uncertain. Butting relationships and mutual crosscutting relationships between filled fractures indicate that the sets may have formed coevally.

The present orientation of the prethrusting fractures is a function of bedding attitudes that were formed during the Alleghanian orogeny. The Copper Creek thrust sheet contains the best macroscopic example of the systematic rotation of fracture orientation as a function of bedding dip. Because the fractures are symmetrical with respect to bedding, the change in orientation of the fracture sets in each stratigraphic unit in the Copper Creek thrust sheet is related to the 15 to 20° decrease in dip of bedding towards the southeast away from the position of the thrust fault. As the dip of bedding decreases to zero, the northeast fracture set will change strike by a few, but the dip will steepen equal to the change in the amount of bedding dip. On the other hand, the northwest fracture sets will maintain a fairly constant dip, but the strike will rotate towards the north. The Kamb contour plots of poles to fracture planes clearly show how the dip of the northeast-striking fracture set increases from the Rome Formation into the Knox Group as the bedding dip decreases (Fig. 5-25). In addition, the 320° striking fracture set in the Rome Formation is rotated towards the north to become the 330° striking fracture set in the Conasauga and Knox Groups. Similar small-scale rotations of fracture sets in mesoscopic folds have been observed.

Microscopic analysis of fracture crosscutting relationships and fracture-filling characteristics of the bed-normal extension (ac, bc) and associated hybrid fractures, as well as other hkl fracture sets, can be used to document prethrusting fractures. Fore-

man and Dunne (1991) observed that 49 out of 50 of the bed-normal veins in the Nolichucky Shale are crosscut by bed-parallel shear veins and therefore concluded that they formed prior to the Alleghanian orogeny. In addition, most of the calcite filling from the same fracture sets is twinned. Because calcite twinning is the result of Alleghanian deformation (Wiltschko et al. 1985, Kilsdonk and Wiltschko 1988, Craddock and van der Pluijm 1989), the fractures are interpreted to be prethrusting. Furthermore, at a larger scale, mesoscopic thrust faults offset beds containing ac, bc, and associated fracture sets.

If the pervasive systematic fracture sets in the study area formed prior to the Alleghanian orogeny, similar sets may also be present throughout the region. There have been few regional fracture studies in the Tennessee Valley and Ridge and Cumberland Plateau provinces (Fig. 5-36; Slusarski 1979, Masuoka 1981, Kilsdonk and Wiltschko 1988). Fracture studies on the Cumberland Plateau are located in the southern portion of the Wartburg basin adjacent to Walden Ridge (Slusarski 1979) and in the northern portion of the Wartburg basin west of the Pine Mountain fault (Masuoka 1981). Both studies used rose plots to compare fracture orientations and air photo lineament orientations. The fracture data were collected in a reconnaissance manner from a total of 35 sites across the area and show a poor correlation between fracture and lineament orientations. In general, there are no consistently oriented fracture sets that can be traced across the region, although locally there are similar fracture orientations between adjacent sites. The variations in fracture orientation may be related to the way the studies were conducted: (1) the data were collected from various structural settings (e.g., adjacent to the thrust front, adjacent to the Jacksboro fault, and within the

undeformed regions of the plateau), and (2) the fracture data were not divided on the basis of either dip or type. Although the above studies do not provide a clear picture of the fracture system, there are similar orientations to those in the study area suggesting that the fractures formed sometime prior to thrust faulting.

Relatively few fracture studies have been conducted in the Tennessee Valley and Ridge Province. Kilsdonk and Wiltschko (1988) studied the deformation mechanisms in the Powell Valley anticline of the Pine Mountain thrust sheet and documented four bed-perpendicular fracture sets oriented N40W, N60E, E-W, and N-S (Fig. 5-36). The northwest and northeast sets were interpreted to have formed during the Alleghanian orogeny as a result of extension perpendicular to the thrust-shortening direction and by bending of the Pine Mountain thrust sheet over a ramp, respectively. The latter two sets were interpreted to have formed prior to the Alleghanian orogeny because they were only found in pre-Silurian rocks. In the ORR, however, similar prethrusting fracture sets are present in the oldest (Rome Formation) to the youngest (Fort Payne Formation) stratigraphic units. There appears to be no relationship between the age of a stratigraphic unit and the development of a particular fracture set. Therefore, the stress field that caused the fracturing may have been present during and certainly after the youngest stratigraphic unit was lithified. Therefore, the propagation of prethrusting fractures must have occurred before thrusting associated with the Permian Alleghanian orogeny.

5.5.8.2 Fold- and fault-related fractures

The development of the southern Appalachian foreland fold-thrust belt during the late Paleozoic Alleghanian

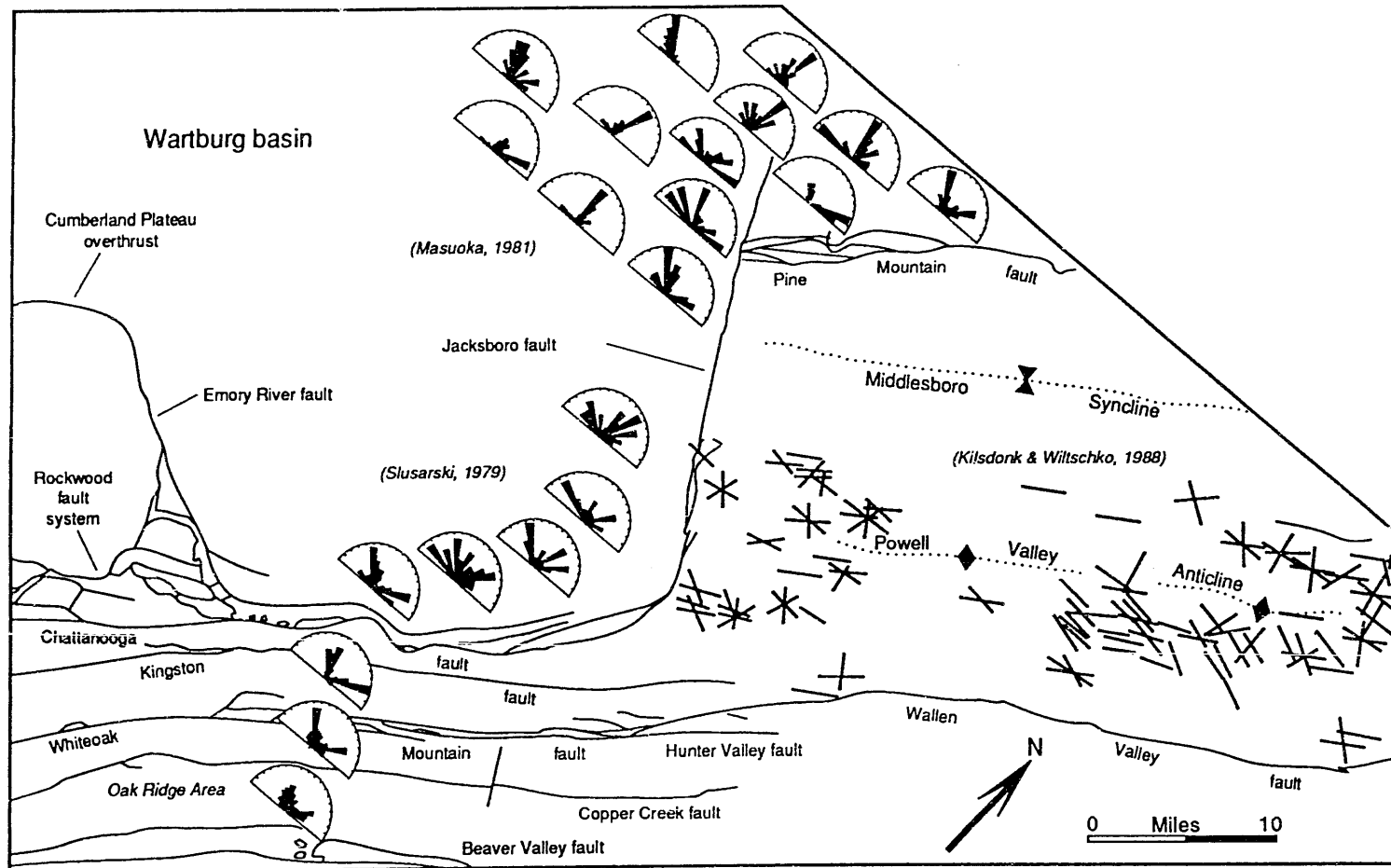


Fig. 5-36. Summary of results from previous fracture studies in the region. Rose diagrams in the Oak Ridge area correspond with the Copper Creek, Whiteoak Mountain, and Kingston thrust sheets.

orogeny was the primary deformational event to affect the region. Prior to active deformation in the area, the orientation of the principal stress axes may have remained nearly constant since the early Paleozoic transition of the eastern North America passive margin to a convergent plate boundary. The geometry of macroscopic and mesoscopic faults and folds indicates the approximate orientation of the regional principal stresses during deformation. Within the active thrust belt, orientations of the maximum, intermediate, and minimum principal compressive stresses would have been northwest, northeast, and vertical, respectively. Beyond the active thrust front, however, the intermediate and minimum principal stresses could have switched positions, reorienting the bulk extension direction from vertical to parallel to the strike of the thrust belt. Therefore, besides local reorientation of the stress field in folds and near faults, the orientation of the maximum principal compressive stress needed to produce the fold-thrust belt may have existed from the Taconic orogeny through the Alleghanian orogeny.

The Copper Creek and Whiteoak Mountain faults occupy different positions in a thrust system, thus providing the opportunity to study fracture development on hanging-wall and footwall flats, as well as along a footwall ramp expressed as the East Fork syncline. A number of bed-parallel and bed-oblique fractures occur proximal to the major thrust faults in both the hanging wall and footwall. Fractures associated with faults are generally related to the same stresses that caused the fault. Therefore, by knowing the attitude of the fault, the orientation of shear and extension fractures can be predicted. The orientation of the local stress field may be a transient phenomenon, however, as rock units undergo layer-parallel compression, faults propagate, thrust sheets slide, and

folde grow. In addition, new fractures may form as thrust sheets climb footwall ramps, depending on whether bedding acts as an efficient stress guide (Fig. 5-37).

Bed-parallel fractures are the most pervasive synthrusting fractures in the area. The bed-parallel fractures are most conspicuous in core as calcite veins with elongate mineral crystals parallel to bedding in the direction of thrust transport (Foreman and Dunne 1991). Exposures of bed-parallel veins are less common, but, when preserved, are slickensided. Some of the bed-parallel slickensides are minor faults, but others may have formed during bedding slip as a result of the passive folding of thrust sheets that were transported over a footwall ramp. Exposures of bed-parallel slickensides were never cut by bed-perpendicular fractures. In addition, low-angle bed-oblique fractures are interpreted to have formed as a result of thrust faulting. The stress orientations need to form these fractures are similar to the stress field needed to cause folding and faulting. Because exposures near faults are rare, what cannot be predicted at this time is the amount of fracturing and the width of the fractured zone adjacent to the fault.

There are a number of minor fracture sets that formed proximal to major thrust faults that cannot be satisfactorily explained. The development of a thrust fault, however, creates a heterogeneous stress field associated with the propagation of the fault tip. If propagation is hindered, a zone of deformation may form around the fault tip, which is manifested as a band of fractures adjacent to the fault. The remaining fracture sets may be related to a zone of fracturing that developed as the result of the propagation of the Copper Creek and Whiteoak Mountain faults. The remaining sets may have formed, however, in relation to mesoscopic structures that were close to, but not exposed in the

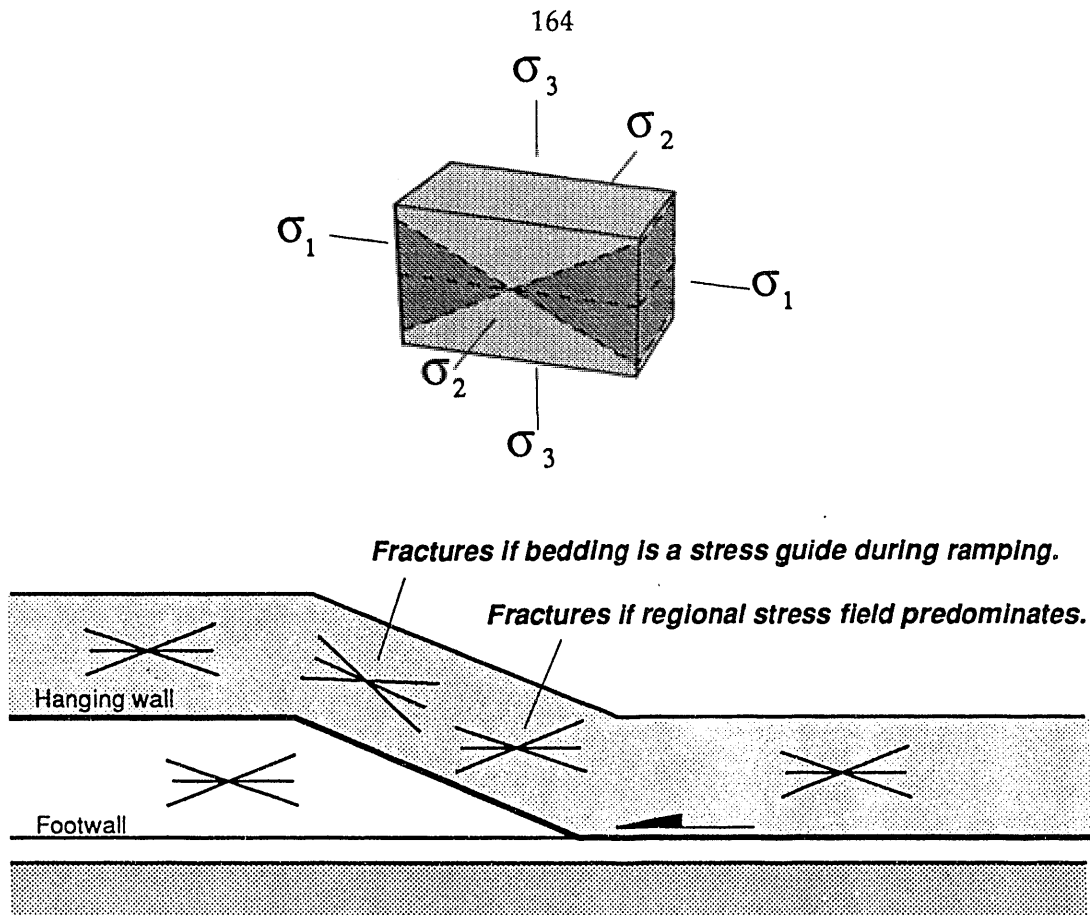


Fig. 5-37. Foreland fold-thrust belt structures, which can be used to infer the orientation of the regional stress field during their development. Shown are the orientations of the fractures that would form if the orientation of the regional stress field predominates across the thrust belt or if bedding acts as a local stress guide during ramping.

outcrop in which the fracture measurements were taken.

A surprising result of this study is that, although the Copper Creek thrust sheet, Whiteoak Mountain thrust sheet, and East Fork syncline have had different structural histories, the dominant fracture sets are relatively consistent across the study area and formed prior to thrusting. For example, the Copper Creek thrust sheet has been transported through a ramp, but the Whiteoak Mountain thrust sheet is located on the ramp, and the East Fork syncline is a macroscopic flexural-slip fold. In other thrust belts, different structural histories have caused the development of distinct fracture sets (Srivastava and Engelder

1990, Turner and Hancock 1990). For example, Srivastava and Engelder (1990) studied the conditions and timing of fracturing during fault-bend folding in the central Appalachian thrust belt of Pennsylvania. They concluded that strike-parallel veins formed during motion of the thrust sheet through fold hinges and strike-perpendicular veins formed when the thrust sheet was moving on the upper flat and is related to strike-parallel extension. Similarly, relationships between thrusts and fractures in the south Pyrenean thrust belt have been interpreted to indicate the geometry and evolution of the thrust sheets (Turner and Hancock 1990). Turner and Hancock (1990) concluded that strike-

perpendicular fractures formed during stretching of footwalls as a result of their loading by overriding thrust sheets, and strike-parallel fractures, which only occur in the undeformed foreland, are attributed to stretching above a basement flexure related to thrust loading. The contrasting interpretations of similar fracture sets in the same tectonic setting suggests that future work is needed to evaluate the discrepancies. Results from this study, however, do not indicate any differences in fracture geometry with respect to structural evolution of the various thrust sheets. Because the region is interpreted to have had a well-developed fracture system prior to thrust faulting, then possibly the preexisting fracture sets accommodated strain by additional displacements, thereby inhibiting the development of new fracture sets.

Fracture geometries associated with the East Fork Ridge syncline are similar to fold-related fracture sets reported in various tectonic settings (Price 1966, Stearns 1969, Hancock 1985). For example, Stearns (1969) identified extension and shear fractures in the Teton anticlines in Montana and inferred their age relationships on the basis of orientation. He inferred the principal stress directions by grouping three fracture orientations into an assemblage of two conjugate shear fractures and one extension fracture bisecting the acute angle and associated all of these fractures with one stress field. The relationship between extensional fracture patterns and fold geometry is very simple (Fig. 5-38a). Major extensional fractures are usually parallel and perpendicular to fold axes and normal to bedding. Shear and hybrid fracture relationships to fold geometry are more complex, with the most commonly observed orientations shown in Fig. 5-38b. East Fork Ridge syncline fracture geometries are consistent with such extensional and shear fractures, but are

interpreted to have been part of the preexisting regional systematic fracture sets. As previously stated, reactivation of preexisting fractures may have inhibited the development of new fracture sets by accommodating layer strains during folding.

5.5.8.3 Post-thrusting fracture sets

Following the Alleghanian orogeny, the orientation of the regional stress field has rotated as a result of rifting and divergent margin tectonics during the Mesozoic and the development of the present Atlantic passive margin. Structures related to Mesozoic rifting, such as extensional basins, dike swarms, and faults have been used to infer the temporal evolution of the regional stress field in the Blue Ridge and Piedmont Provinces (Fig. 5-39; e.g., deBoer et al. 1988). The geometry of Late Triassic rift basins requires a northwest-oriented minimum principal stress, which was

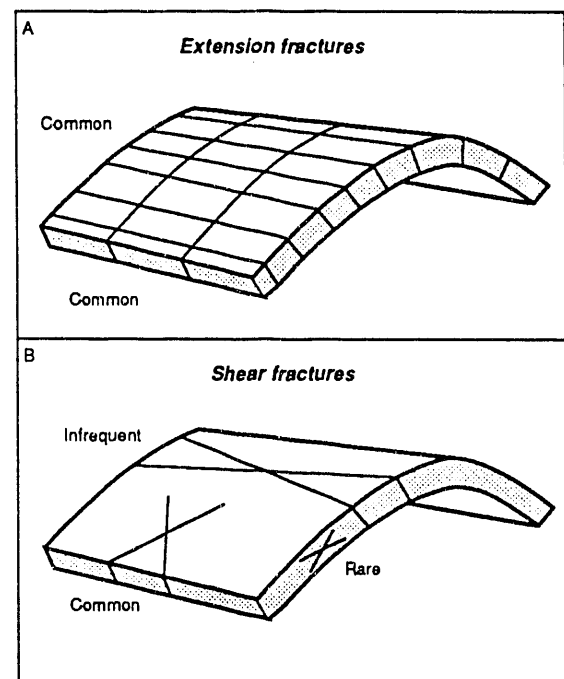


Fig. 5-38. Fracture sets that develop in folded layers. (a) Extension fractures. (b) Shear fractures. (From Price and Cosgrove 1990).

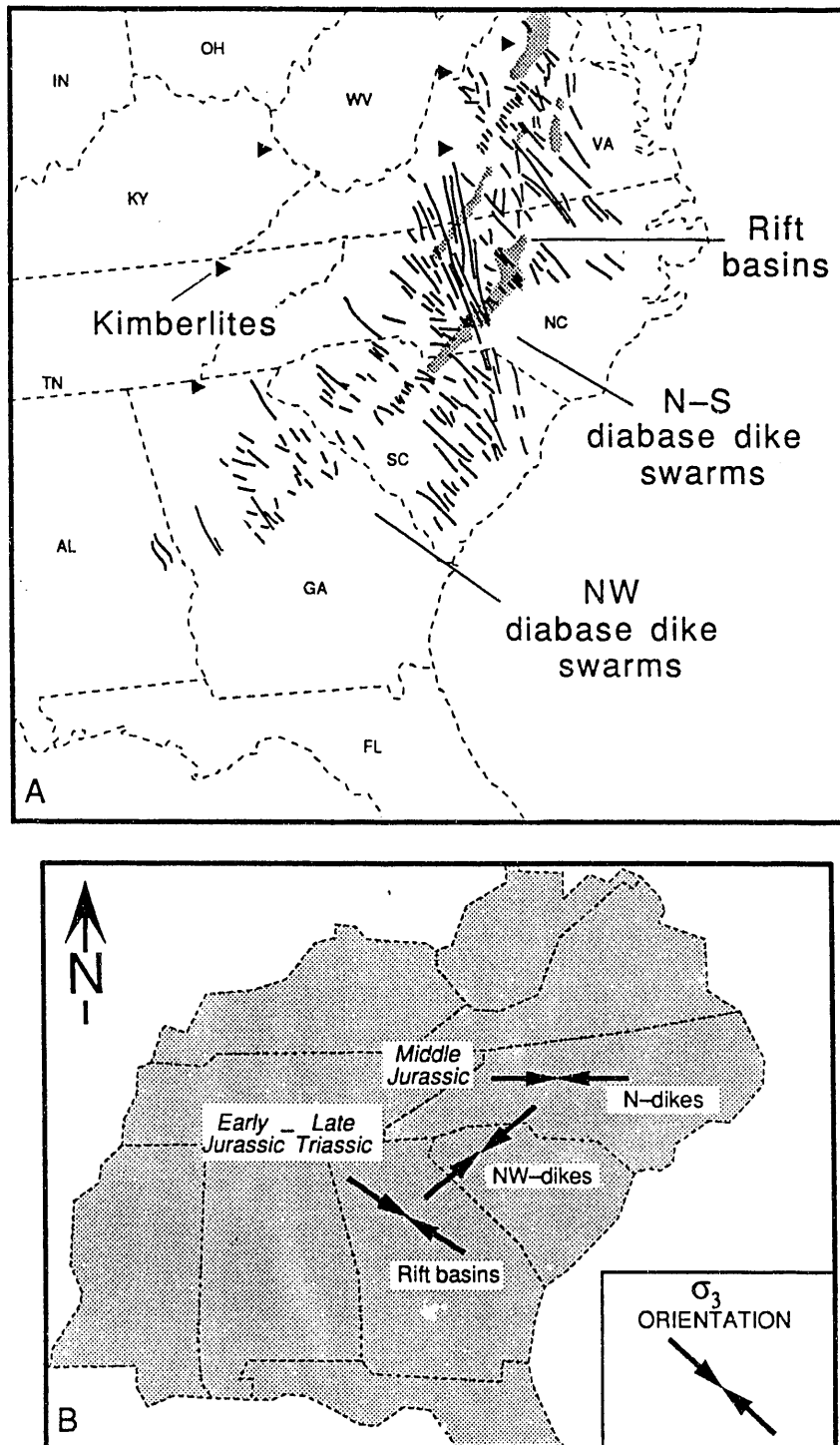


Fig. 5-39. (a) Structures formed during Mesozoic rifting, which can be used to infer the minimum principal stress orientation. Structures indicative of the orientation and extent of the stress field during divergent margin tectonics include rift basins, different generations of dike swarms, and kimberlites. (b) Inferred minimum principal stress orientations from structures in (a). (From deBoer and others 1988).

followed by the emplacement of north-west-striking diabase dike swarms indicating a northeast-oriented minimum principal stress in the Early Jurassic. Subsequently, in the Middle Jurassic a second set of north-striking diabase dike swarms was emplaced, indicating an east-west

stress inferred from them was used to correlate fracture orientations in the area. Fractures formed under the influence of regional Mesozoic stress fields should have a near-vertical dip and be perpendicular to the inferred direction of the minimum principal stress. Since the exact

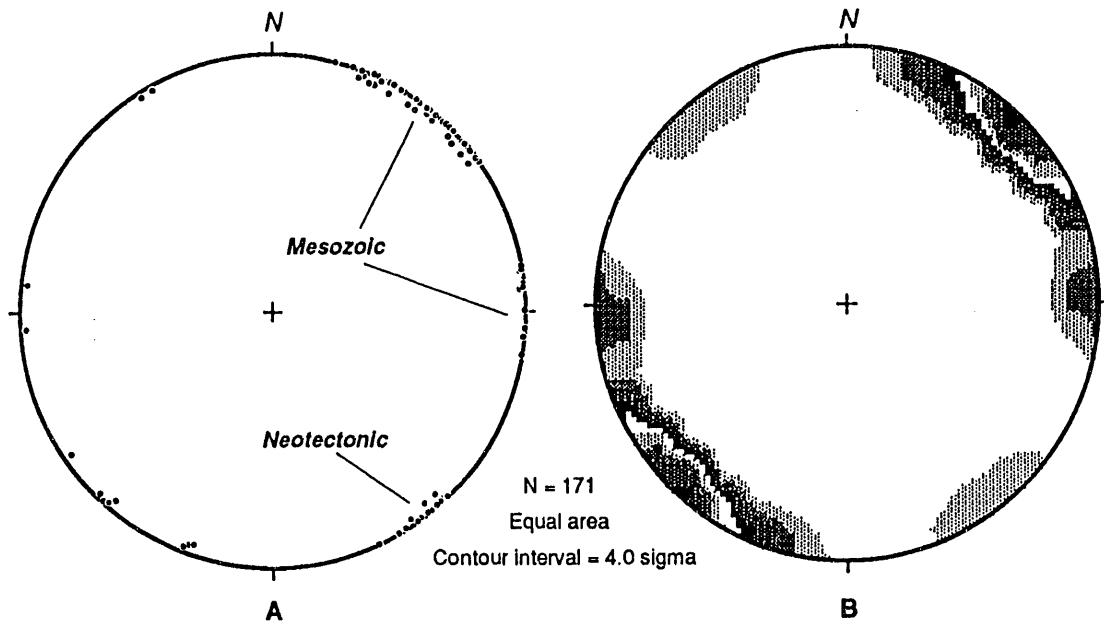


Fig. 5-40. (a) Equal-area plot of poles to fracture planes that match those that should be produced from the inferred orientation of the Mesozoic and present-day stress fields. (b) Equal-area Kamb contour plot of the same data.

minimum principal stress orientation. Although macroscopic structures related to Mesozoic extension did not develop in the Tennessee Valley and Ridge, kimberlites in the Appalachian basin suggest that the stress field related to rifting may have extended into the area.

The presence of the rift-related stress field during uplift and erosion of the Appalachian foreland basin may have influenced the development of new fracture sets. The Early to Middle Jurassic diabase dike swarms appear to have had the largest areal extent, and, therefore, the orientation of the minimum principal

orientation of the minimum principal stress is unknown, ranges of N35 to 55E and N10W to N10E were used for the northwest and north-striking diabase dike swarms, respectively. A number of fractures have orientations suitable to have formed under the prescribed stress fields (Fig. 5-40). Besides orientation, however, no other criteria have been observed to characterize the existence of younger fracture sets. The orientation of new fracture sets may have been controlled by (1) residual tectonic stresses from the Alleghanian orogeny and (2) the presence of bedding as a dipping anisotropy.

Furthermore, the growth of new fracture sets may have been inhibited by preexisting fractures accommodating the strains. Future work on subsurface fracture characteristics in core is needed to better address the existence of younger fracture sets.

The present-day stress field orientation for eastern North America has been determined using various stress measurement techniques (Plumb and Cox 1987, Zoback and Zoback 1989). Neotectonic fractures (Engelder 1982, Hancock and Engelder 1989, Gross and Engelder 1991) will have an orientation controlled by the present-day stress field. The orientation of the present-day maximum compressive stress in the area ranges from N50 to 60E and is located in the horizontal plane (Fig. 5-41).

If some of the fractures in the area are neotectonic and not influenced by a preexisting weakness, then they should strike 50 to 60° and dip near vertically. A small subset of fractures has the appropriate orientation, but additional timing criteria are needed to determine their origin (Fig. 5-40).

5.5.9 Fracture Spacing Analysis

Systematic fractures not only maintain a persistent orientation across a region, but have a spatial frequency that is controlled by the interaction of many variables. A number of studies have attempted to identify and model the variables that control the spacing of systematic fractures (Bogdanov 1947, Hodgson 1961, Sowers

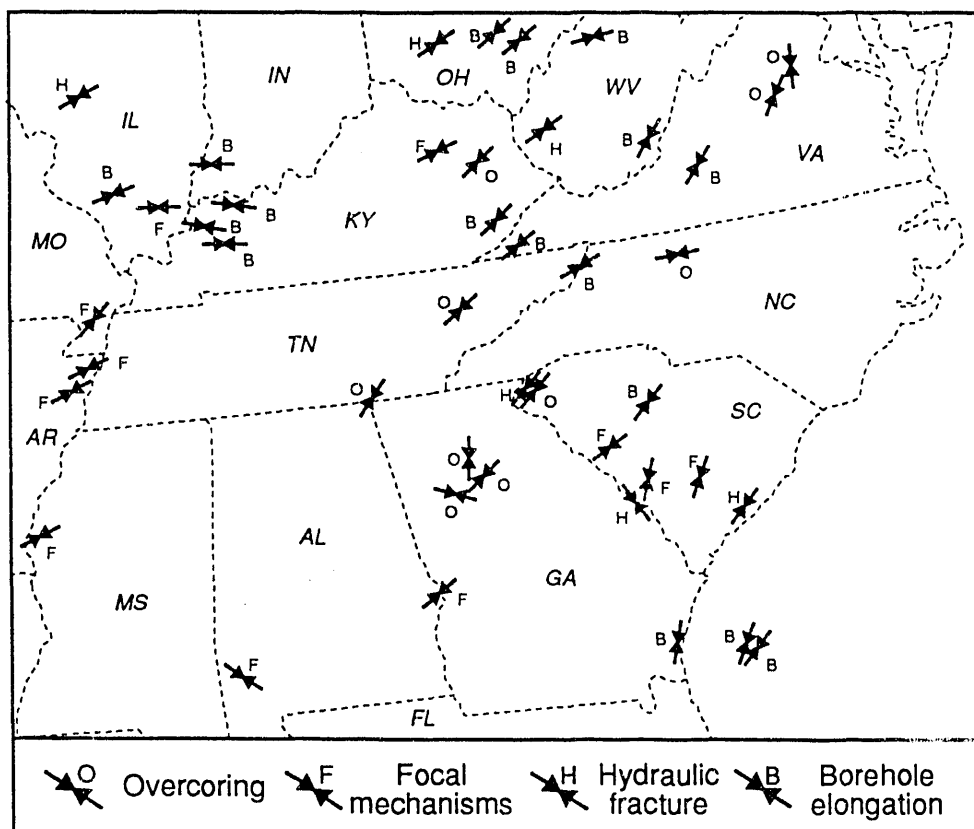


Fig. 5-41. Orientation of the present day maximum compressive stress in the southeastern United States based on overcoring, focal mechanisms, hydraulic fracturing, and borehole elongation tests, which is approximately N50-60E. (Compiled from Zoback and Zoback 1980, Plumb and Cox 1987).

1972, Stearns and Friedman 1972, McQuillan 1973, Ladeira and Price 1981). Knowledge of the change in fracture spacing (commonly termed fracture intensity and fracture frequency) is useful for structural analysis. For example, an increase in fracture frequency has been used to predict the location of hidden faults (Pohn 1981). Fracture frequency also affects the strength and slope stability of rock masses and is an important consideration in mine and excavation design. Furthermore, the frequency of fractures affects the ability of a rock mass to transmit and hold fluids such as groundwater, pollutants, oil, and gas. The purpose of estimating fracture spacing during field mapping was to assess the overall spacing distributions and to guide the direction of future work.

5.5.9.1 Field observations

In well-bedded sequences, changes in bed thicknesses often corresponded to a change in fracture spacing. Unfortunately, most outcrops are small and do not expose the range in bed thicknesses necessary to observe possible changes in fracture spacing. In addition, some exposures of only shale or dolomite make it difficult even to estimate bed thickness. The best exposures contained clearly defined bedding of different lithology and thickness and most often consisted of interbedded sandstone, siltstone, and shale. In general, exposures of thin interbeds of shale and siltstone contained closely spaced fractures not related to bed thickness. Chert pods, nodules, and beds surrounded by either limestone or dolomite commonly contain fractures spaced more closely than the surrounding beds. The change in fracture spacing could be caused either by the difference in elastic moduli between the carbonate and chert or by the thin bedding of the chert zones.

Mesoscopic faults and folds usually involve bedding that is intensely fractured. Fracture sets are commonly more closely spaced than the thickness of the bedding, but some fractures may be traced through a number of beds. Not only can the strain energy associated with these structures decrease the fracture spacing in a particular set, but also the strain around a fault or fold can change the orientation of the regional stress field, leading to the development of new fracture sets. Most mesoscopic folds involve thin to medium beds of shale, siltstone, limestone, and sandstone of either the Conasauga Group or Rome Formation. Although fold hinges have the greatest curvature, fracturing of the folded beds was usually very intense, regardless of the position in the fold.

5.5.9.2 Fracture spacing frequency distribution

Knowledge of the fracture spacing frequency distribution is useful for determining the best statistical analysis routine for the data (Priest and Hudson 1976). If the fractures are fairly evenly spaced with a normal distribution of spacing values, then the frequency distribution will peak at the mean spacing (Fig. 5-42a). If the fractures have a clustered distribution, then a high frequency of low spacing values occurs within clusters and a low frequency of high spacing values occurs between clusters (Fig. 5-42b). A random distribution of fractures will lead to a negative exponential frequency distribution (Fig. 5-42c). In general, evenly spaced, clustered, and random distributions will combine to form a negative exponential distribution (Fig. 5-42d, Priest and Hudson 1976). Because randomly oriented fracture spacing was not measured, a combination of the evenly spaced and clustered distributions best fits the fracture frequency distribution in the study area.

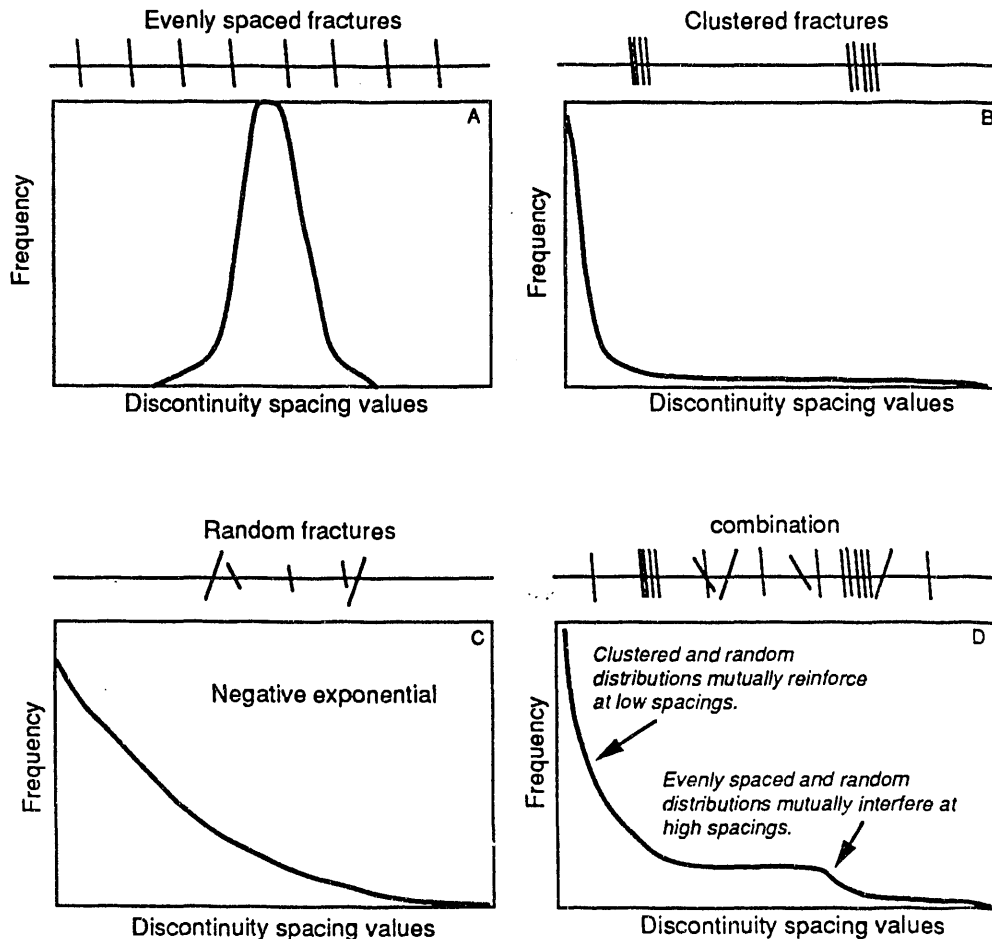


Fig. 5-42. Possible fracture spacing frequency distributions (from Priest and Hudson 1976).

The fracture spacing frequency distribution is not normally distributed and follows a trend similar to a combined distribution plot (Fig. 5-43). Unfortunately, many of the fracture spacing measurements were recorded as less than 2.54 cm (1 in.), resulting in the fact that all of the data were combined into the 1-in. category in the frequency distribution plot. Considering that fact, the fracture frequency reflects a combination of evenly spaced and clustered distributions. Visually reducing the frequency of the 1-in. (2.54-cm) beds and increasing the value of the less than 1-in. (2.54-cm) spacing measurement results in a negative exponential

distribution containing various spikes (Fig. 5-26). The greater frequency of closer fracture spacings is expected because small outcrops only expose the closely spaced fractures. Therefore, the frequency results are biased and will not closely correspond to the frequency distribution results from detailed scan line surveys used by engineers (Priest and Hudson 1976). A rigorous statistical analysis of the data set was attempted by Toran (personal communication), but correlation tests for log-normal and exponential distributions failed, which indicates the complexity of the fracture spacing data (Wheeler and Stubbs 1976, Wheeler and Holland 1978,

Wheeler and Dixon 1980). Since the data were not rigorously collected following prescribed scan line surveys, the simplest approach was to assume a normal distribution and determine the mean fracture spacing.

5.5.9.3 Fracture spacing and bed thickness correlation analysis

For each site, a mean fracture spacing was determined from the minimum and maximum fracture spacing measurements. The mean value from each site was then summed and averaged according to

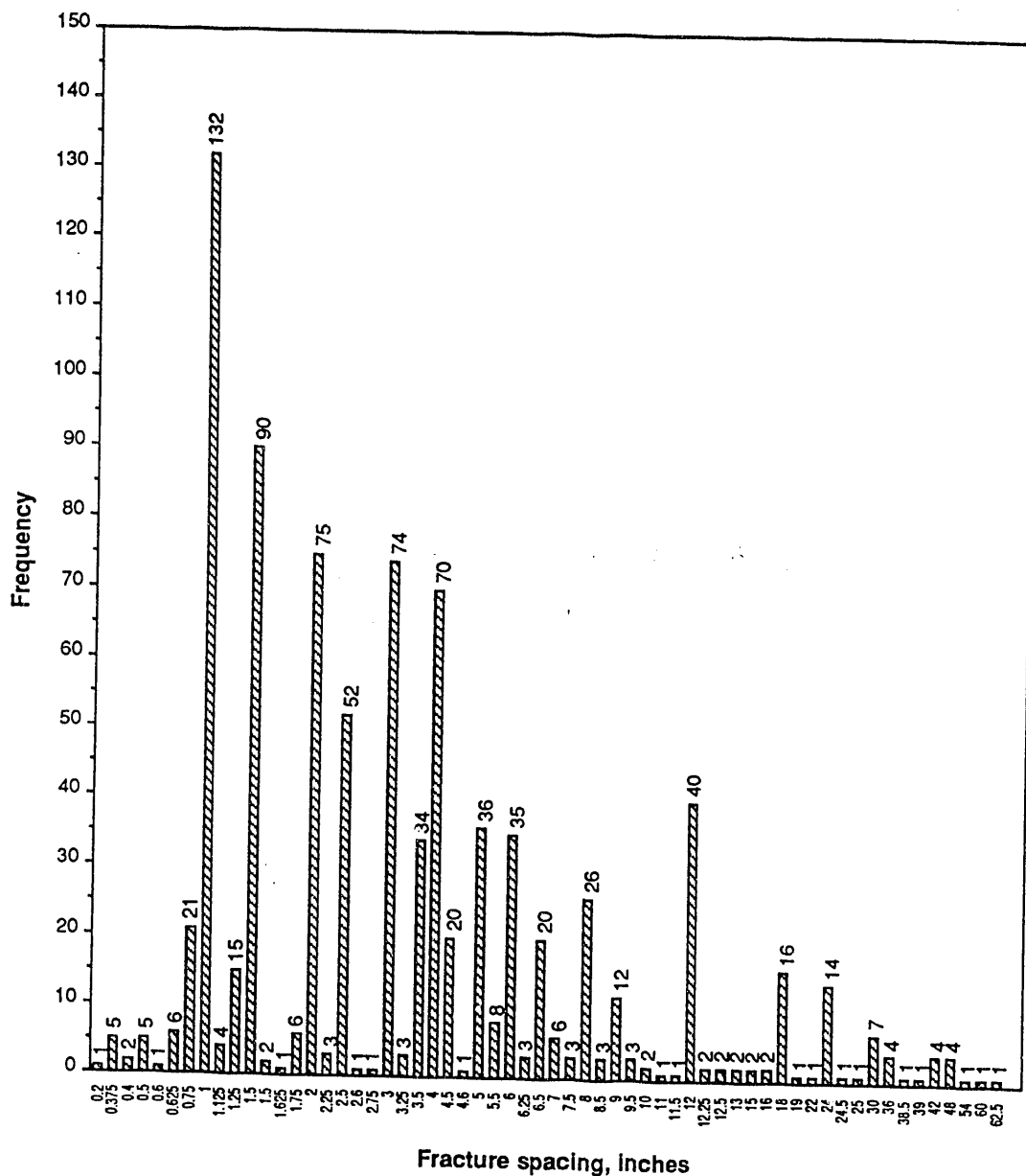


Fig. 5-43. Fracture spacing frequency distribution.

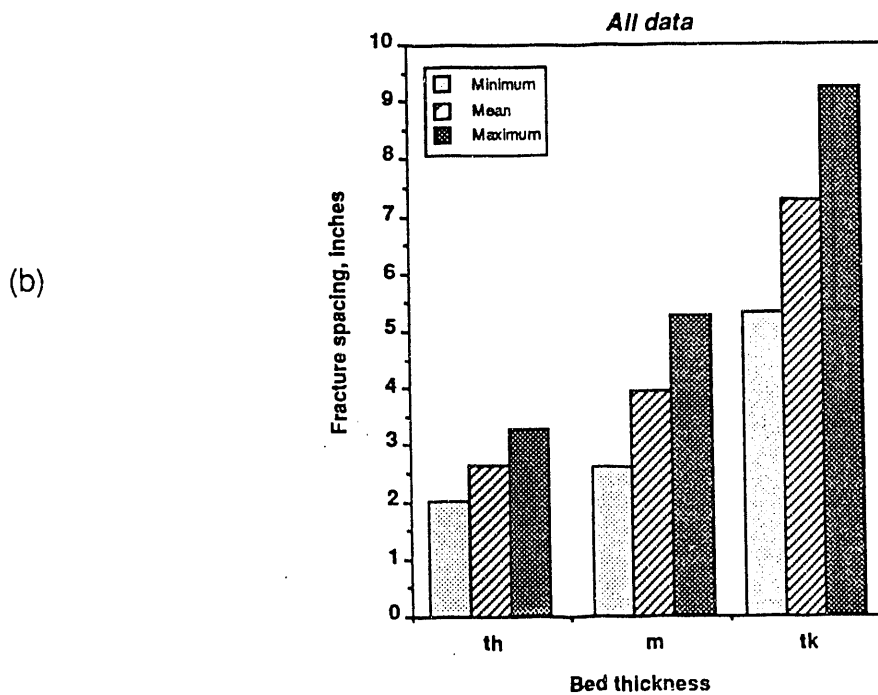
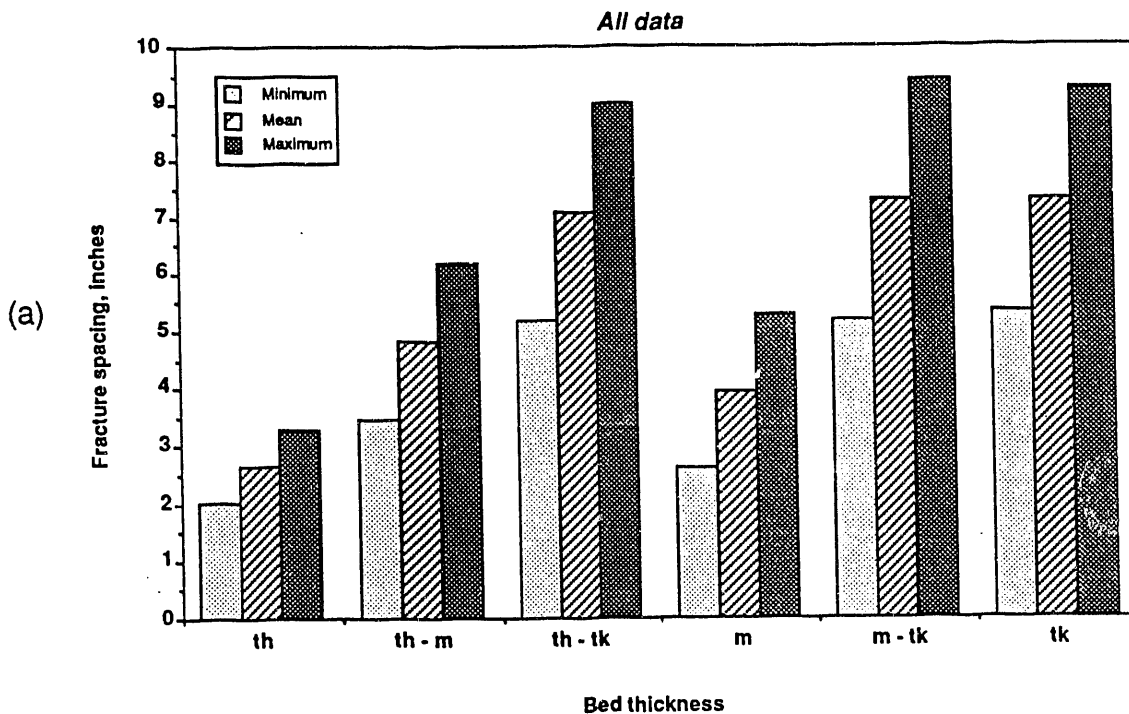


Fig. 5-44. (a) Fracture spacing vs bed thickness for all of the data. (b) Graph A, except only the three main bed thickness categories are plotted. Bed thickness nomenclature is th - thin; m - medium; tk - thick.

different categories, such as bed thickness and lithology. Since the data do not represent exact measurements, the following discussion does not concentrate on the absolute value of the results, but instead on the overall trends. When all of the data are plotted against bed thickness, there is no particular trend (Fig. 5-44a). Considering only the three main bed thickness categories, however, thin, medium, and thick, mean fracture spacing increases as bed thickness increases (Fig. 5-44b). The direct relationship between bed thickness and fracture spacing is disturbed by the thin-medium, thin-thick, and medium-thick categories. When the data are further divided, the reason becomes clear and will be discussed below.

The mean fracture spacing data were divided by lithology and plotted against bed thickness (Fig. 5-45). Except for limestone and dolomite, fracture spacing increases as bed thickness increases. The sandstone results contain a range of bed thicknesses and show the direct change in fracture spacing. Sandstone is generally well-bedded and surrounded by shale, which appears to have controlled the spacing of fractures. Fracture spacing in limestone decreases by approximately 1 in. as bed thickness increases from thin to medium. Grouping thin beds of limestone as one fracturing unit could cause an increase in the overall fracture spacing measured in each bed. Dolomite has the greatest variation in fracture spacing vs bed thickness with no clear trend. The variability of the spacing data may be related to the problem of determining bed thickness for small and weathered exposures of dolomite. In addition, although an exposure of dolomite may consist of only thin beds, the bonding between the beds may have been sufficient enough to allow them to fracture as one thick unit, resulting in a relatively large fracture spacing for each individual thin bed. The

spacing data from the dolomite beds are the reason for the fracture spacing vs bed thickness variations observed in the plot of all the measurements (Fig. 5-44). A consideration of only the thin, medium, and thick-bedded dolomite indicates a direct relationship between bed thickness and fracture spacing. Thus, an increase in fracture spacing vs bed thickness can be generally assumed regardless of lithology, but the thickness of the fracturing unit may be greater than bedding for the more massive carbonates.

Next, the fracture spacing measurements were plotted against bed thickness for each of the major stratigraphic units (Fig. 5-46). The purpose here was to determine if either age or structural position influenced fracture spacing. For example, the Rome Formation and Conasauga Group have a high fault preference and are usually adjacent to the major thrust faults. The Knox Group, however, occupies an internal position in the thrust sheets. The data indicate that the Rome Formation has a consistently closer fracture spacing for all bed thicknesses compared with the Knox Group. The closer fracture spacing in the Rome Formation could have resulted from factors such as an increase in strain energy close to the major thrust faults and differences in lithology. Overall, the data continue to show an increase in fracture spacing with bed thickness regardless of either stratigraphic unit or structural position. This is clearly evident when considering only the three main bed thickness categories in each plot. The variability is probably related to combining the data for different lithologies in each stratigraphic unit. The Rockwood Formation has a consistently wide fracture spacing, which is unusual considering it is folded. Although a comparatively well bedded clastic sequence, the thin to medium sandstone beds in the Rockwood

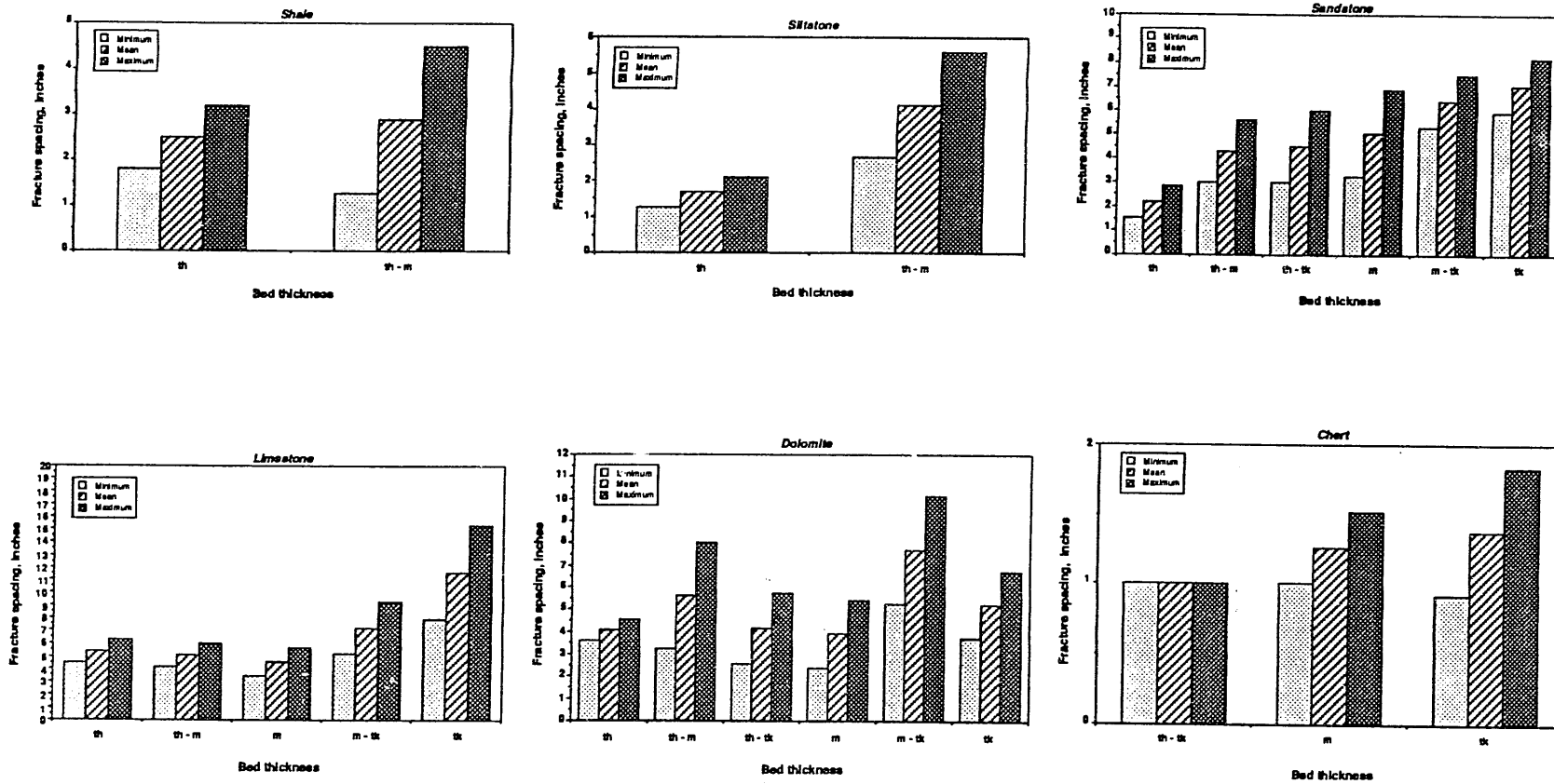


Fig. 5-45. Fracture spacing vs bed thickness for each lithology.

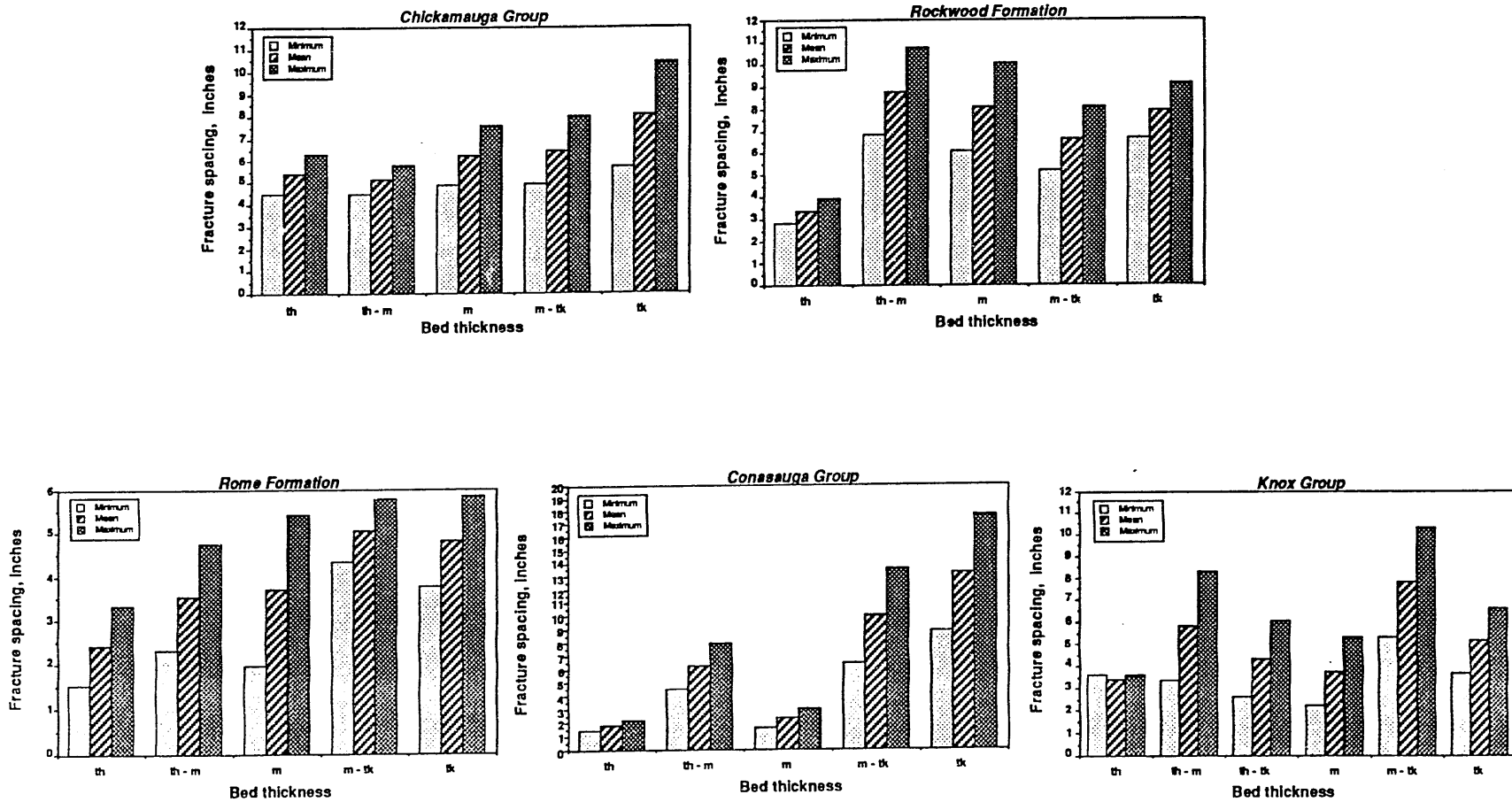


Fig. 5-46. Fracture spacing vs bed thickness for each major stratigraphic unit.

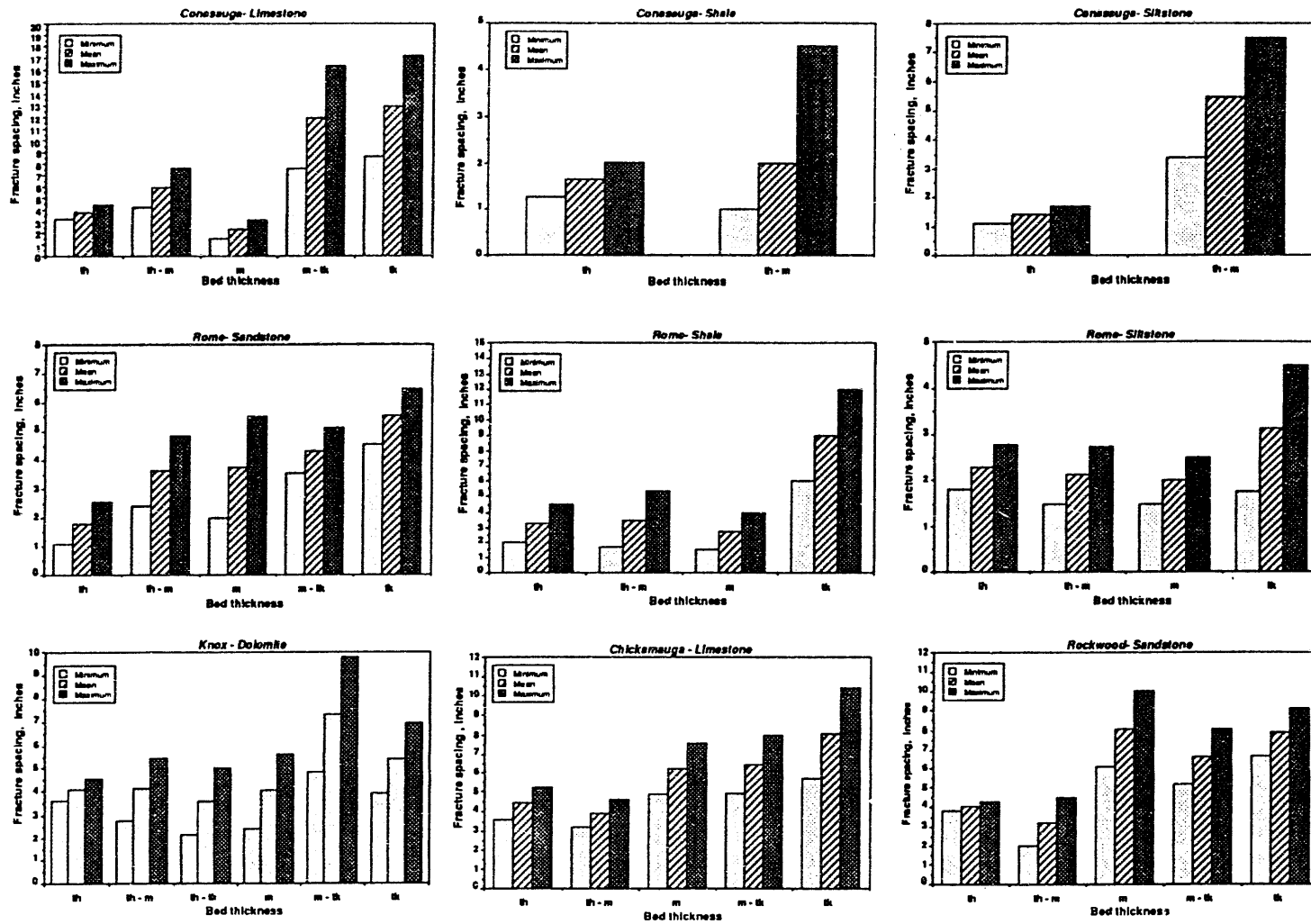


Fig. 5-47. Fracture spacing vs bed thickness for each lithology within each stratigraphic unit.

may have bonded and behaved like thick fracturing units.

Fracture spacing was plotted vs bed thickness for the individual lithologies in each stratigraphic unit (Fig. 5-47). As with the constant lithology histograms of all the data, the direct relationship of increasing bed thickness and fracture spacing is evident regardless of stratigraphic unit. A comparison of fracture spacing, for example, indicates that the average spacing is less for the sandstone beds of the Rome Formation than for those in the Rockwood Formation. The closer fracture spacing in the Rome Formation suggests a greater amount of deformation than in the Rockwood Formation. This is not surprising considering the amount of transport and strain along the major décollements located in the Rome Formation. In addition, the age difference between the two formations (Cambrian vs Silurian) could be a factor in the number of fracturing events affecting them; the older formation may have experienced earlier episodes of strain buildup and fracturing. A comparison of spacing between limestones of the Conasauga and Chickamauga groups indicates a closer spacing for the thin and medium beds in the Conasauga, but a closer spacing for the thick beds in the Chickamauga. The closer spacing for the thick beds is due to the fact that the thick bed measurements in the Conasauga Group are from the Maynardville Limestone, which has considerably thicker beds than the Chickamauga Group. Limestone beds in the Chickamauga Group have an overall wider fracture spacing, which may have resulted from either the sequence of beds fracturing as a coherent unit vs the more isolated limestone beds in the Conasauga or the greater amount of local folding and faulting in the Conasauga Group, although the upper Chickamauga is a fault zone in Bethel Valley.

5.5.9.4 Fracture spacing results

Most of the published fracture spacing studies are done in well-exposed areas where the rocks have only been mildly deformed into broad, open folds (Stearns and Friedman 1972, McQuillan 1973, Ladeira and Price 1981). The rocks are more highly deformed in the study area, where a number of other problems arise in trying to determine the variables that control the spacing of fractures. First, because exposures are generally small, accurately defining the thickness of the fractured unit is difficult when the fractures extend beyond the confines of one bed. In general, however, the bed thickness assumption appears to be satisfactory considering the results of the correlation analysis. Second, the effects of surrounding bed thicknesses and lithology on the fracture spacing in a particular unit is also hampered by the lack of large exposures. Finally, variables such as strain and elastic moduli are difficult to determine without extensive testing.

Comparison of the Conasauga Group shale and siltstone fracture spacing data with the previous work of Sledz and Huff (1981) from the Pumpkin Valley Shale indicates that the results fall within similar ranges. Their results also indicate a direct relationship between fracture spacing and bed thickness in siltstone. This is interesting because both the bed thickness and fracture spacing data were collected and analyzed differently. For example, Sledz and Huff (1981) determined a fracture spacing in thin-bedded siltstone (4- to 13-mm bed thickness ranges in Fig. 5-20) that ranges from approximately 2.5 to 5 cm (1 to 2.5 in.). Thin-bedded siltstone from the Conasauga Group has a fracture spacing range of 2.5 to 4.5 cm (1 to 1.75 in.) (Fig. 5-47). All of the siltstone data have a thin-bedded fracture spacing that ranges from 3 to 5 cm (1.25 to 2 in.) (Fig. 5-45),

and the Rome Formation thin-bedded siltstone has a fracture spacing range of 4.5 to 7 cm (1.75 to 2.75 in.). These results generally fall into similar ranges. Results for shale are not as similar between the two studies. For example, Sledz and Huff (1981) determined a fracture spacing in thin-bedded shale (3- to 11-mm bed thickness ranges in Fig. 5-20) that ranges from approximately 5 to 10 cm (2.5 to 4 in.). Fracture spacing results presented here for the thin-bedded Conasauga Group shale range from 3 to 5 cm (1.25 to 2 in.) (Fig. 5-47), which are below the minimum value determined by Sledz and Huff (1981). All of the shale data have a thin-bedded fracture spacing that ranges from 4.5 to 7.6 cm (1.75 to 3 in.) (Fig. 5-45), and the Rome Formation thin-bedded shale has a fracture spacing range of 5 to 11.4 cm (2 to 4.5 in.), which are similar to the ranges determined by Sledz and Huff (1981).

Fracture spacing models do not explain the existence of fracture zones that are defined as the localized development of numerous fractures. Fracture zones were evident in a number of outcrops. Considering the thickness of the fracturing unit, the fracture spacing in these zones is expected to be much less. Traced along strike, fracture zones contain individual fractures that terminate and step over to a new joint. Therefore, fracture zones may be regions of increased strain associated with the coalescence of individual fractures propagating along strike and may indicate a spacing phenomenon related to propagation rather than strain release. Unfortunately, in the field, the location and geometry of fracture zones is unpredictable, but these zones may be important pathways of enhanced groundwater flow.

6 ISOTOPIC CHARACTERISTICS OF ROCK UNITS AND VEINS FROM THE OAK RIDGE RESERVATION: EVIDENCE FOR WATER-ROCK INTERACTION IN MIXED CARBONATE-SILICICLASTIC ROCKS

James L. Foreman

6.1 INTRODUCTION

The stable isotopic composition of minerals in sedimentary rocks can provide important insight into depositional and diagenetic processes affecting these rocks. Of interest to researchers studying the geology and hydrogeology of the Oak Ridge Reservation (ORR) is the opportunity for stable isotopic studies of sedimentary rocks to provide baseline information for identifying groundwater flow pathways, recording water-rock interaction, and understanding controls on groundwater chemistry. In deeper aquifers in particular, the chemistry of groundwater is strongly controlled by the composition of surrounding rocks as a result of longer groundwater residence times and increased opportunity for groundwater and rock to reach chemical and isotopic equilibrium. Characterizing the isotopic compositions of rocks and fracture-filling minerals (where significant groundwater flow may occur) and understanding controls on composition are crucial for future studies of groundwater flow and chemistry.

In this section, a series of tables summarizes the stable isotopic composition of rocks and fracture-filling minerals from Middle and Upper Cambrian rocks in the ORR that were analyzed from 1986 to 1991 using either the stable isotope facilities of the Chemistry Division at Oak Ridge National Laboratory (ORNL) or the Department of Geological Sciences at The University of Tennessee (UT). The past emphasis on understanding water-rock interaction in Cambrian strata in the ORR

is clear from the number of analyses from these units and absence of isotopic data from the Ordovician limestones. Stable isotopic studies are currently underway on Ordovician limestones in the vicinity of Knoxville and northeast Tennessee by students at UT (Steinhaff, in progress; Tobin, in progress).

It is important to note that the stable isotopic data presented below are the result of several sample treatment methodologies. These include (1) "micro" bulk rock or whole rock analyses in which 50 to 150 mg are drilled out or powdered from a chip that was broken from a larger core or outcrop sample (the CO₂ analyzed by this method is a mixture of gas from both calcite and dolomite in the sample), (2) samples collected with a dental pick or microscope-mounted microdrill in which sample sizes are typically < 5 mg and may consist of a single depositional constituent or diagenetic phase, and (3) bulk rock samples containing calcite and dolomite in which the CO₂ from these phases is collected over a period of time during reaction with anhydrous phosphoric acid. This last method is particularly useful for extremely fine grained rocks, such as lime mudstones and shales, where physically isolating calcite from dolomite is otherwise impossible.

All isotopic analyses are measured relative to universally recognized standards [Pee Dee belemnite (PDB) or standard median ocean water (SMOW)] and experiments that can quantify potential fractionation effects with each method of extracting the CO₂ for analysis. As a

Table 6-1. Summary of oxygen and carbon isotopic compositions^a from limestones and calcite veins in Cambrian strata from the Oak Ridge Reservation (data from Haase et al. 1988)

| Formation | Category | $\delta^{13}\text{C}$ avg | std dev | $\delta^{13}\text{C}$ min | $\delta^{13}\text{C}$ max | $\delta^{18}\text{O}$ avg | std dev | $\delta^{18}\text{O}$ min | $\delta^{18}\text{O}$ max | N |
|-------------------|----------|------------------------------|---------|------------------------------|------------------------------|------------------------------|---------|------------------------------|------------------------------|----|
| Maynardville | matrix | 0.52 | 0.50 | 0.00 | 1.10 | 22.08 | 0.34 | 21.60 | 22.40 | 5 |
| Nolichucky | matrix | -0.73 | 0.63 | -1.50 | 0.40 | 22.02 | 0.61 | 21.10 | 23.30 | 28 |
| Dismal Gap | matrix | -0.57 | 0.37 | -1.40 | 0.20 | 21.45 | 0.88 | 19.80 | 23.30 | 17 |
| Friendship | matrix | -3.01 | 0.59 | -4.45 | -2.31 | 22.00 | 3.76 | 18.53 | 32.25 | 10 |
| Pumpkin Valley | matrix | -7.21 | 2.77 | -10.91 | -2.34 | 18.69 | 1.55 | 15.64 | 21.55 | 28 |
| Rome | matrix | -3.58 | 1.89 | -9.30 | -1.19 | 21.34 | 3.48 | 15.20 | 26.81 | 15 |
| Nolichucky | veins | -1.55 | 0.93 | -3.50 | -0.20 | 17.76 | 1.11 | 15.90 | 21.50 | 22 |
| Dismal Gap | veins | -0.81 | 0.55 | -1.90 | 0.30 | 18.22 | 0.96 | 15.60 | 20.40 | 18 |
| Friendship | veins | -3.32 | 1.73 | -10.00 | -2.03 | 18.31 | 0.90 | 15.86 | 19.76 | 19 |
| Pumpkin Valley | veins | -7.92 | 2.42 | -11.17 | -3.29 | 17.24 | 1.14 | 15.69 | 20.63 | 44 |
| Rome | veins | -4.37 | 2.67 | -8.77 | 1.72 | 17.58 | 2.76 | 15.26 | 23.89 | 14 |

^a Carbon isotopic compositions with respect to PDB standard; oxygen with respect to SMOW standard.

Table 6-2. Carbon and oxygen isotopic analyses^a of oöids and interparticle matrix from Upper Cambrian Nolichucky Shale oölitic limestone, Bear Creek Valley core holes, Whiteoak Mountain thrust sheet, Oak Ridge Reservation (from Foreman 1991)

| Formation | Well-footage | Category | $\delta^{13}\text{C}$ | $\delta^{18}\text{O}$ |
|------------|----------------------------|-----------------|-----------------------|-----------------------|
| Nolichucky | GW134-416.2 | unaltered oöids | -1.0 | 20.55 |
| Nolichucky | GW134-416.3 | micrite matrix | -0.9 | 21.48 |
| Nolichucky | GW134-434 | unaltered oöids | -0.7 | 21.58 |
| Nolichucky | GW134-440.1 | unaltered oöids | -0.6 | 21.38 |
| Nolichucky | GW134-440.2 | micrite matrix | -0.8 | 21.07 |
| Nolichucky | GW134-440.3 | unaltered oöids | 0.0 | 21.48 |
| Nolichucky | GW134-440 ARS ¹ | unaltered oöids | -1.1 | 20.35 |
| Nolichucky | GW139-266 | micrite oöids | -1.8 | 21.48 |
| Nolichucky | GW139-283 | micrite oöids | -1.5 | 20.45 |

^a Carbon isotopic compositions with respect to PDB standard; oxygen with respect to SMOW standard.

1. ARS-slab stained with Alizarin Red S stain in 0.25% HCl solution prior to sampling.

Table 6-3. Carbon and oxygen isotopic composition^a of Nolichucky Shale calcite veins from Bear Creek Valley core holes in the Whiteoak Mountain thrust sheet, Oak Ridge Reservation (from Foreman 1991)

| Well | ¹ Sample | ² Category | Wall rock | $\delta^{13}\text{C}$ | $\delta^{18}\text{O}$ |
|-------|---------------------|-----------------------|-----------|-----------------------|-----------------------|
| GW134 | 76 | bed perp vein | Shale | -0.6 | 18.9 |
| GW134 | 173.5A | bed perp vein | Shale | -1.4 | 18.9 |
| GW134 | 407 | bed perp vein | Shale | -0.7 | 18.7 |
| GW134 | 407A | bed perp vein | Shale | -1.2 | 18.5 |
| GW134 | 416-1 | bed perp vein | Limestone | -1.1 | 18.0 |
| GW134 | 416-2 | bed perp vein | Limestone | -1.6 | 17.8 |
| GW134 | 434-1 | bed perp vein | Limestone | -3.3 | 14.3 |
| GW134 | 440-1 | bed perp vein | Limestone | -1.0 | 18.6 |

| | | | | | |
|-------|--------|---------------|-----------|------|------|
| GW134 | 440-1 | bed perp vein | Limestone | -1.0 | 18.6 |
| GW134 | 440-2 | bed perp vein | Limestone | -1.1 | 17.8 |
| GW134 | 440-3 | bed perp vein | Limestone | -1.1 | 18.5 |
| GW134 | 440-4 | bed perp vein | Limestone | -1.1 | 17.8 |
| GW134 | 621.5 | bed par vein | Shale | -1.5 | 18.4 |
| GW134 | 621.5A | bed par vein | Shale | -2.0 | 18.2 |
| GW139 | 161-3 | bed perp vein | Siltstone | -1.3 | 18.6 |
| GW139 | 180-1 | bed perp vein | Siltstone | -2.0 | 16.6 |
| GW139 | 180-2 | bed perp vein | Siltstone | -2.0 | 17.0 |
| GW139 | 210-1 | bed perp vein | Siltstone | -1.3 | 18.4 |
| GW139 | 210-3 | bed perp vein | Siltstone | -1.3 | 18.3 |
| GW139 | 228 | bed perp vein | Limestone | -0.5 | 19.8 |
| GW139 | 229 | bed oblq vein | Limestone | -0.3 | 19.2 |
| GW139 | 230 | bed perp vein | Limestone | -0.4 | 19.0 |

^a Carbon isotopic compositions with respect to PDB standard; oxygen with respect to SMOW standard.

1. Sample numbers are equivalent to downhole footage. Samples with same footage indicate multiple veins.
2. Bed perp vein- bed perpendicular vein; bed par vein- bed-parallel vein; bed oblq vein- bed-oblique vein.

Table 6-4. Calcite and dolomite isotopic compositions^a in Nolichucky Shale lithologies, determined from timed stepwise extractions of bulk shale samples. Dolomite compositions shown in bold. Final three values are from core hole GW140, all others from GW134 (Foreman 1991)

| Well-Footage | ¹ Rxtn. time | ² ΣRxtn. time | ³ Phase | δ ¹³ C | δ ¹⁸ O |
|--------------|-------------------------|--------------------------|--------------------|-------------------|-------------------|
| GW134-197 | 140 | 140 | cc | -0.51 | 20.65 |
| GW134-197 | 295 | 435 | cc +dol | 0.07 | 21.61 |
| GW134-197 | 1405 | 1840 | dol | -0.03 | 22.15 |
| GW134-267 | 120 | 120 | cc | -2.10 | 20.55 |
| GW134-267 | 290 | 410 | cc +dol | -0.80 | 21.51 |
| GW134-267 | 1320 | 1730 | dol | -0.80 | 21.51 |
| GW134-297 | 120 | 120 | cc | -3.20 | 19.17 |
| GW134-297 | 300 | 420 | cc +dol | -1.30 | 20.55 |
| GW134-297 | 1305 | 1725 | dol | -0.40 | 21.93 |
| GW134-360 | 125 | 125 | cc | -0.78 | 19.81 |
| GW134-360 | 290 | 415 | cc +dol | -0.51 | 20.65 |
| GW134-360 | 1405 | 1820 | dol | -1.01 | 20.02 |
| GW134-436 | 120 | 120 | cc | -2.07 | 15.13 |
| GW134-436 | 320 | 440 | cc +dol | -1.46 | 15.77 |
| GW134-436 | 1510 | 1950 | dol | -1.13 | 18.53 |
| GW134-643 | 130 | 130 | cc | -3.36 | 16.51 |
| GW134-643 | 285 | 415 | cc +dol | -1.69 | 19.81 |
| GW134-643 | 1360 | 1775 | dol | -2.06 | 17.48 |
| GW140-1026 | 205 | 205 | cc | -3.30 | 19.38 |
| GW140-1026 | 360 | 565 | cc +dol | -0.60 | 21.40 |
| GW140-1026 | 1275 | 1840 | dol | -0.40 | 23.84 |

^a Carbon isotopic compositions with respect to PDB standard; oxygen with respect to SMOW standard.

1. Reaction time with phosphoric acid (minutes).
2. Cumulative reaction with phosphoric acid (minutes).
3. Probable carbonate phase being extracted, based on reaction time, cc - calcite, cc+dol - calcite+dolomite, dol - dolomite.

Table 6-5. Summary of isotopic compositions^a of silicate minerals from the Pumpkin Valley Shale and Rome Formation in the Oak Ridge Reservation (data from Haase et al. 1988)

| Formation | Class Mineral ¹ | $\delta^{18}\text{O}$ avg | std dev | $\delta^{18}\text{O}$ min | $\delta^{18}\text{O}$ max | N | δD avg | std dev | δD min | δD max | N |
|----------------|----------------------------|------------------------------|---------|------------------------------|------------------------------|----|-------------------------|---------|-------------------------|-------------------------|----|
| Pumpkin Valley | < 2 μm I>Chl | 14.87 | 1.11 | 12.84 | 16.49 | 15 | -43.5 | 17.05 | -66.9 | -10.2 | 13 |
| Pumpkin Valley | 2-45 μm Q>I>Chl | 13.75 | 0.63 | 12.81 | 14.19 | 4 | ** | ** | ** | ** | ** |
| Rome | < 2 μm I>Chl | 16.84 | ** | ** | ** | 1 | ** | ** | ** | ** | ** |
| Rome | 2-45 μm Q>I>Chl | 13.19 | ** | ** | ** | 1 | ** | ** | ** | ** | ** |
| Pumpkin Valley | vein Q | 8.41 | 2.94 | 5.78 | 13.58 | 5 | ** | ** | ** | ** | ** |
| Rome | vein Q | 11.79 | 5.65 | 7.68 | 15.91 | 2 | ** | ** | ** | ** | ** |

^a Oxygen and hydrogen values are with respect to SMOW standard.

1. I-illite, Chl-chlorite, Q-quartz. Pumpkin Valley mineralogy from S.-Y. Lee (pers. comm., 1991, ORNL) Rome mineralogy assumed to be equivalent to Pumpkin Valley.

result, the data in the following tables (Tables 6-1 to 6-5) can be compared directly, regardless of methodology used, though it must be realized that bulk rock analyses reflect an average isotopic composition (dominated by the isotopic composition of depositional grains in most limestones), whereas microsamples record values of individual constituents making up the whole rock.

6.2 ISOTOPIC COMPOSITION OF CARBONATES IN LIMESTONES AND SHALES

6.2.1 Whole-Rock Limestone Analyses

Summary statistics for stable isotopic analyses from whole-rock limestones (indicated as matrix) in Cambrian units from the ORR are presented in the upper part of Table 6-1. Limestones were sampled from both the Whiteoak Mountain thrust sheet and the Copper Creek thrust sheet. Reported precision for the data in Table 6-1 is ± 0.1 per mil for carbon and ± 0.2 per mil for oxygen (Haase et al. 1988), although it is not uncommon to find variations between similar carbonate depositional grains of ± 0.5 per mil in the

same sample.

The most obvious feature from these data is that the Pumpkin Valley Shale is the lightest in terms of carbon ($\delta^{13}\text{C} = -7.21$ per mil) followed by the Rome (-3.58) and Friendship (Rutledge) (-3.01). The carbon isotopic composition of the Dismal Gap (Maryville) and Nolichucky limestones more closely approximates that of the overlying Maynardville (Table 6-1).

With respect to oxygen, the Pumpkin Valley Shale is again the lightest or most depleted in ^{18}O ($\delta^{18}\text{O} = 18.69$ per mil). The remaining units have fairly similar oxygen isotopic compositions. Only one isotopic analysis of Ordovician limestone from the ORR has been made to date. A whole-rock analysis from the Moccasin Formation in the JOY-2 well yielded $\delta^{13}\text{C} = -2.23$ and $\delta^{18}\text{O} = 19.11$ per mil (Haase et al. 1988). Clearly, more data are needed from Ordovician limestones if controls on the isotopic composition of groundwaters flowing through them and the entire ORR are to be understood.

Intraformational compositional trends in the carbon and oxygen composition of interbedded limestones have been investigated by Foreman (1991) for the Nolichucky Shale. The carbon and oxygen isotopic compositions of interbedded

limestones show a statistically significant decrease with depth in the formation. Because of limited study of other Cambrian units on the ORR, it is not clear that similar variations with depth occur in them.

6.2.2 Individual Constituents of Oölitic Limestones

Isotopic analyses of depositional grains (calcite ooids) from Nolichucky oolitic limestone interbeds are presented in Table 6-2. Each analysis is actually a composite sample of 10–20 ooids (0.5 to 1.0 mm diam each) drilled from polished, slabbed core with the aid of a microscope (Foreman 1991). These data provide an indication as to the composition of depositional constituents in the limestone and are nearly identical to the average carbon and oxygen isotopic compositions determined from whole-rock analyses (depositional components + diagenetic cements) from oölitic limestones and other limestones in the Nolichucky Shale (Table 6-1 and 6-2, Haase et al. 1988).

It cannot be assumed that the compositions of the depositional constituents reflect their original preburial compositions considering the age of these limestones and the possibility for isotopic exchange in the burial diagenetic environment. Determining the original isotopic composition is important if isotopic exchange as a result of water–rock interaction is to be recognized. Though Recent unaltered shallow-water limestones have $\delta^{13}\text{O} = 30.0$ to 32.0 per mil, lower Paleozoic limestones were probably considerably lighter, with original compositions of about 23.0 to 25 per mil with respect to $\delta^{13}\text{O}$ (Popp et al. 1986).

A combination of petrographic and trace element data from ooids in Nolichucky limestones suggest the isotopic composition of these limestones is several

per mil lighter in terms of oxygen because of relatively early diagenetic alteration following burial (Foreman 1991). This isotopic exchange was the result of stabilization of originally high-magnesian calcite ooids to low-magnesian calcite in the presence of burial fluids modified by interaction with interbedded marine muds (Foreman 1991). It is possible that similar processes occurred following deposition of the other Cambrian mixed carbonate–siliciclastic units in the ORR, resulting in measured oxygen isotopic compositions that are several per mil lighter than original values. Fluids in equilibrium with silicate minerals similar to those in the Cambrian shales may have been as much as 5.0 to 10.0 per mil lighter in ^{18}O compared with fluids in equilibrium with Cambrian limestones (O'Neil et al. 1969, Friedman and O'Neil 1977, Eslinger et al. 1979). These shales provide a potential reservoir of isotopically light oxygen and are a viable alternative to meteoric waters, typically considered the most important light oxygen reservoir.

6.2.3 Composition of Vein Calcites

The stable isotopic composition of vein calcites from Cambrian strata on the ORR are summarized in the lower part of Table 6-1. Comparison of the vein isotopic data in this table with the matrix (whole-rock) data yields several interesting observations. First, the carbon isotopic composition of vein calcites closely approximates that of the whole-rock limestone values for each formation. Second, the oxygen isotopic compositions of vein calcites are at least 3.0 to 5.0 per mil lighter than the average whole-rock oxygen isotopic composition for interbedded limestones in each formation, with the exception of the Pumpkin Valley Shale (Table 6-1). In this unit, the oxygen isotopic composition of vein calcite is essentially identical to that

of interbedded limestones. Third, the isotopic composition of vein calcite remains fairly constant regardless of stratigraphic position in the Nolichucky Shale (Foreman 1991).

Formation-scale comparisons between interbedded limestone and vein calcite show a general similarity in isotopic compositions of these two groups, but this is not the case on a hand specimen scale. This is illustrated in Table 6-3 which shows the isotopic composition of Nolichucky Shale vein calcite for three different wall rocks (shale, limestone, or siltstone). From this table, it is clear that there is no systematic relationship between vein isotopic composition and the type of wall rock, even though the bulk oxygen composition of these wall rock lithologies is expected to vary by as much as 5.0 to 10.0 per mil (based on oxygen fractionation differences in carbonate and silicate minerals).

6.2.4 Diagenetic Carbonates in Shale Interbeds

The carbon and oxygen stable isotopic composition of carbonate disseminated in interbedded Nolichucky shale is presented in Table 6-4. Petrographic examination of polished thin sections from shale intervals in the formation indicates that nearly all the calcite and iron-rich dolomite (ankerite) is diagenetic rather than detrital (Foreman 1991). Therefore, the composition of these minerals should provide information on the mobilization of carbonate and nature of water-rock interaction in the shale during burial diagenesis. The carbon and oxygen isotopic compositions of both calcite and dolomite become more depleted in ^{13}C and ^{18}O with increasing distance from the overlying Nolichucky/Maynardville formation contact (Table 6-4). This behavior parallels the compositional variations with depth observed for interbedded limestone in the Nolichucky (Foreman 1991).

6.2.5 Isotopic Composition of Silicate Minerals

Extraction of oxygen and deuterium from silicate minerals using BrF_5 is a painstaking and time-consuming process, and, as a result, fewer of these analyses are available compared with analyses of carbonates. The oxygen and deuterium isotopic compositions for silicates from the Pumpkin Valley Shale and Rome Formation on the ORR are summarized in Table 6-5. This table includes the oxygen isotopic composition of the $<2\text{-}\mu\text{m}$ - (clay-)size fraction and the 2- to $45\text{-}\mu\text{m}$ size fraction. The $<2\text{-}\mu\text{m}$ fraction is generally considered to be dominated by diagenetic mineral phases, whereas the 2- to $45\text{-}\mu\text{m}$ fraction is more representative of the depositional or detrital minerals (S.-Y. Lee, pers. comm., 1991, ORNL). The $<2\text{-}\mu\text{m}$ fraction is isotopically heavier than the 2- to $45\text{-}\mu\text{m}$ fraction in both the Pumpkin Valley and Rome formations, whereas the oxygen isotopic composition of vein quartz is the most depleted of the three categories (Table 6-5). These data provide estimates of the isotopic composition of an important oxygen and deuterium reservoir in the Cambrian strata—interbedded siltstone and shale—and must be considered for studies of mass transfer between interbedded carbonates, and siltstones and shales.

6.3 INTEGRATION WITH OTHER DATA

The interpretation of stable isotopic data is severely hampered by two uncertainties: temperature during diagenetic reactions and isotopic compositions of diagenetic fluids. These are important variables because they provide the major controls for determining the isotopic composition of a mineral phase measured

in the laboratory and are key indicators of the diagenetic environment during mineral growth. If one of the variables is known, the other can be calculated, assuming the mineral grew under equilibrium conditions.

It is difficult to determine the temperature of precipitation from stable isotopic data alone, unless the isotopic composition of two coexisting minerals is known and it can be demonstrated that they formed at the same time from the same fluid. Two other approaches can provide either limits on precipitation temperatures (thermal burial history models) or nearly unique solutions to precipitation temperatures (primary fluid inclusions). These two techniques were used together to investigate mass transfer of oxygen and carbon during burial diagenesis of the Nolichucky Shale on the ORR (Foreman 1991) and are summarized below.

The isotopic composition of a trapped diagenetic fluid is extremely difficult to determine directly without the use of specialized techniques such as ion-microprobe analyses of frozen fluid inclusions, extraction of fluids from fluid inclusions by crush-leach techniques, or decrepitation methods. The precision associated with these methods is poor because of the small sample volumes. Back-reaction of the trapped fluid with the host crystal subsequent to trapping must be evaluated for the analyses to be of use. For these reasons, the direct determination of ancient diagenetic fluid isotopic compositions is rarely attempted, but is calculated instead using precipitation temperatures and published mineral-water fractionation equations.

6.3.1 Fluid Inclusion Data from Veins

Homogenization temperatures from two-phase fluid inclusions can provide minimum estimates of mineral precipita-

tion temperature, assuming the inclusions are primary (trapped during crystal growth). More accurate estimates of precipitation temperatures can be determined if the fluid pressure during inclusion trapping is known, either from depth estimates or other means. These corrected temperatures have been determined for calcite veins in the Nolichucky Shale from Bear Creek Valley and indicate precipitation temperatures of 80 to 110°C (Foreman and Dunne 1991, Foreman 1991). These temperature data provide fundamental information for interpreting the isotopic composition of the vein calcite with respect to sources of fluids and water-rock interaction during vein formation.

6.3.2 Time-Temperature Burial History Models

Burial history plots are used to show the time-temperature path a geologic unit makes during burial and subsequent uplift. As such, they can predict the ambient temperature of a unit at any time during its burial history and can be used to constrain the temperature and/or duration of an episode of diagenesis, such as precipitation of vein calcite or maturation of hydrocarbons. These plots are extensively utilized by the petroleum industry to understand the timing and migration of hydrocarbons. In order for these models to be at all reliable, they must be constrained by time-temperature indicators (TTI), such as conodont color alteration indices (CAI), illite crystallinity (WI), or vitrinite reflectance (r_0). The indicators must occur in some portion of the stratigraphic sequence being modeled, but they do not have to occur in the primary unit of interest.

A burial history model has been constructed for the Pumpkin Valley Shale and younger strata in the Whiteoak Mountain thrust sheet in the ORR (Fig. 6-1). This

burial curve is constrained by CAI values from Ordovician conodonts, illite crystallinities from Conasauga shale, and clay mineral assemblages from the same shales (Foreman 1991). The burial history model predicts maximum ambient temperatures of $<125^{\circ}\text{C}$ for the Nolichucky Shale (Foreman 1991). This interpretation is supported by Nolichucky vein calcite fluid inclusions, which exhibit little to no evidence of having been subjected to temperatures greater than the maximum

trapping temperatures of 110°C (Foreman and Dunne 1991, Foreman 1991).

6.4 IMPLICATIONS FOR STUDIES OF WATER-ROCK INTERACTION

The relationship between the oxygen composition of interbedded limestones and vein calcites in the Nolichucky Shale reflects varying contributions of oxygen from two major sources: (1) formation

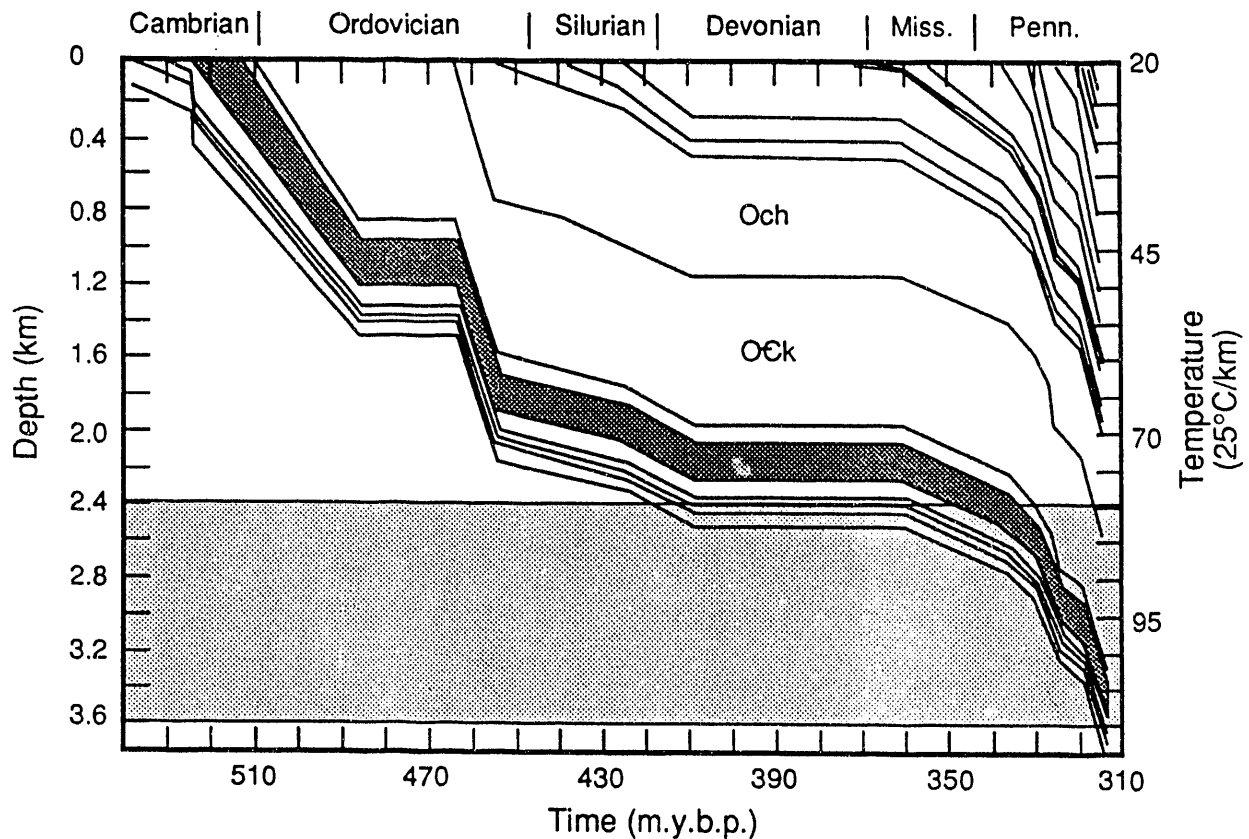


Fig. 6-1. Decompacted burial curve for the Conasauga Group and younger strata in the Whiteoak Mountain thrust sheet. Dark pattern - Nolichucky Shale, Ock - Knox Group, Och - Chickamauga Group, stippled band - range of temperature corresponding to calcite vein formation in Nolichucky Shale based on pressure-corrected fluid inclusion temperatures in vein calcite. See Foreman (1991) for additional details.

water in near-isotopic equilibrium with interbedded silicate units and (2) formation water close to equilibrium with interbedded limestones (Foreman 1991). Similarities in the carbon isotopic composition of the veins and limestones is expected if the dominant carbon reservoir is the interbedded limestones. In the case of the Nolichucky, an intraformational source of oxygen and carbon could provide the necessary fluids to form calcite veins. From the isotopic data alone, large-scale migration of fluids into the Nolichucky Shale from other sources is not required to explain the occurrence and compositions of Nolichucky calcite veins, although large-scale fluid migration cannot be ruled out from the isotopic data alone.

The whole-rock oxygen isotopic composition of a silicate-dominated sedimentary rock will generally be 5.0 to 10.0 per mil lighter in $\delta^{18}\text{O}$ compared with a limestone or dolostone. The fact that Nolichucky vein calcites have similar isotopic compositions regardless of the wall rock lithology, and are relatively constant with depth, indicates that there has been limited isotopic exchange between the immediately adjacent wall rock and diagenetic fluid during vein calcite precipitation (Foreman 1991). On the scale of a single vein and its immediately adjacent wall rock, the fluid composition, and calcite precipitated from the fluid, was not controlled by the surrounding wall rock; this situation is characteristic of a water-dominated system rather than a rock-dominated system. On a larger scale, however, the isotopic composition of the veins does reflect mixing of fluids that have compositions controlled by the composition of the interbedded limestones and shales (Foreman 1991).

The isotopic analyses of silicate minerals from the Pumpkin Valley Shale and Rome Formation (Table 6-5) are interesting in that they provide insight into isotopic

exchange in the host rock vs isotopic exchange during quartz vein formation. The <2- μm fraction in the Pumpkin Valley Shale is dominated by authigenic illite followed by authigenic chlorite, whereas the 2- to 45- μm fraction is mostly detrital quartz, followed by lesser detrital illite and chlorite (S.-Y. Lee, ORNL, pers. comm., 1991). We assume that similar mineralogies exist for the underlying Rome Formation.

The oxygen isotopic composition of calcite veins in the Nolichucky Shale are intermediate in composition to heavier interbedded limestones and lighter interbedded shales and siltstones. This relationship suggests that fluids mixed from these interbedded lithologies were the source of fluids responsible for the vein calcites (Fig. 6-2, Foreman 1991). The same can be said for calcite veins in the Pumpkin Valley Shale. In contrast, the quartz veins in the Pumpkin Valley Shale and Rome Formation are lighter than both the interbedded limestones and shales (Fig. 6-2) and suggest that a source of oxygen extraneous to these units must have contributed to the oxygen isotopic composition of the quartz veins. This interpretation assumes that the composition of the quartz veins reflects isotopic equilibrium with the fluid during quartz precipitation. The existence of isotopic equilibrium needs to be tested further before the interpretation can be accepted that fluids external to the Pumpkin Valley Shale were responsible for the formation of quartz veins.

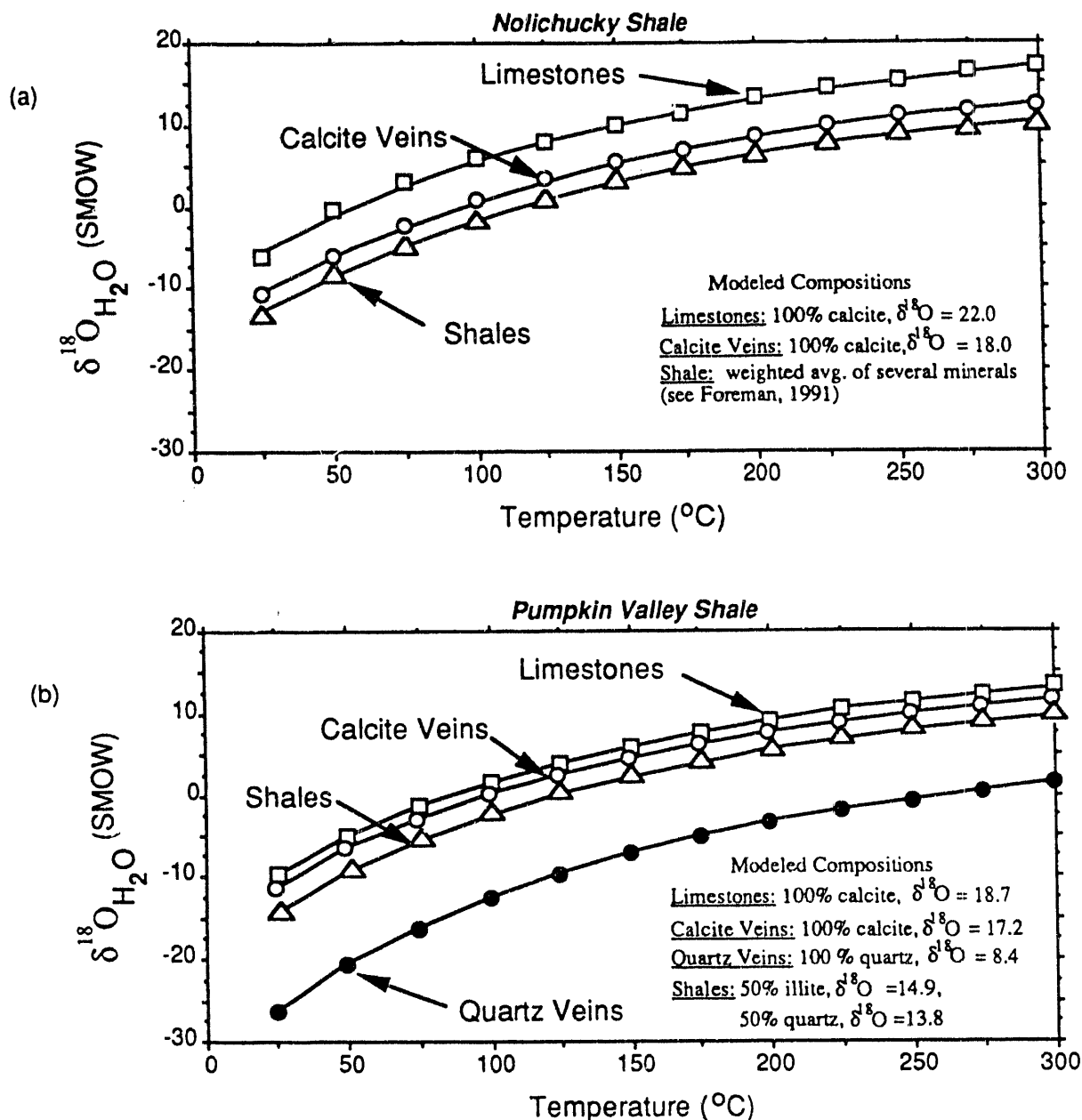


Fig. 6-2. Water-rock isotopic equilibrium diagram used to calculate fluid oxygen isotopic composition in equilibrium with host rocks and veins from the Nolichucky Shale and Pumpkin Valley Shale. (a) Nolichucky Shale showing position of calcite veins between interbedded limestones and shales. This demonstrates fluids for calcite veins could have been derived from these interbeds. (b) Pumpkin Valley Shale showing similar position of calcite veins with similar interpretation as for Nolichucky. Quartz veins are significantly lighter and suggest that an external fluid was required to explain the composition of these veins. See text for sources of fractionation factors and Foreman (1991) for additional details.

7 OVERVIEW OF A NEW CONCEPTUAL MODEL OF THE HYDROLOGIC FRAMEWORK OF THE ORR

7.1 BACKGROUND CLIMATOLOGICAL DATA FOR THE ORR

- Mean annual precipitation (1951–80 reference period) = 136 cm
- Mean annual evapotranspiration = 76 cm (56 percent of precipitation)
- Mean annual streamflow = 60 cm (44 percent of precipitation)
- Mean annual stream discharge = 19 L/s/km²
- Wettest quarter, normal year (January–March) = 46 cm precipitation
- Driest quarter, normal year (October–December) = 30 cm precipitation
- Mean annual air temperature = 15°C

This section is excerpted from Solomon et al. (1992), which presents a new conceptual model of subsurface flow and contaminant transport in the ORR. This model represents an integration of data, information, and concepts from many technical studies and is intended to describe, generically for the ORR, water flux and water chemistry as they vary in three dimensions and in time. The model is consistent with most but not all observations and measurements. Some parts of the model are limited by data availability. Because uncertainty exists in some parts, the model described here is a framework upon which to build as new data are obtained.

Two broad hydrologic units are identified in the ORR, each having fundamentally different hydrologic characteristics. The Knox Group and the Maynardville Limestone of the Conasauga Group constitute the Knox aquifer, in which flow is

dominated by solution conduits. The remaining geologic units constitute the ORR aquitards, in which flow is dominated by fractures. Figure 7-1 is a generalized map of surface distribution of the Knox aquifer and the ORR aquitards.

The subsurface flow system in both the Knox aquifer and in the ORR aquitards can be divided as follows: the stormflow zone; the vadose zone; the groundwater zone, which is subdivided into the water table interval, the intermediate interval, and the deep interval; and the aquiclude. These hydrologic subsystems are defined on the basis of water flux, which decreases with depth; the largest flux is associated with the stormflow zone and the lowest with the aquiclude. Note that these subsystems are vertically gradational and are not separated by discrete boundaries. Because a subsystem does not operate independently of the system as a whole, it is not possible to understand a given subsystem out of the context of interactions with the entire system. Although it is useful to simplify a system by subdividing it for the purpose of analysis, it is important to understand that major processes within a subsystem, as well as the interactions that occur between subsystems, are functions of the system as a whole.

The hydrologic subsystems description differs from the stratigraphic units description elsewhere in this report in that hydrologic boundaries do not coincide with stratigraphic boundaries in many cases. Hydrologic subsystems are defined in the vertical, superimposed on stratigraphic units. In other words, the hydrologic subsystems are continuous across the entire reservation, but the subsystem properties and boundaries are locally

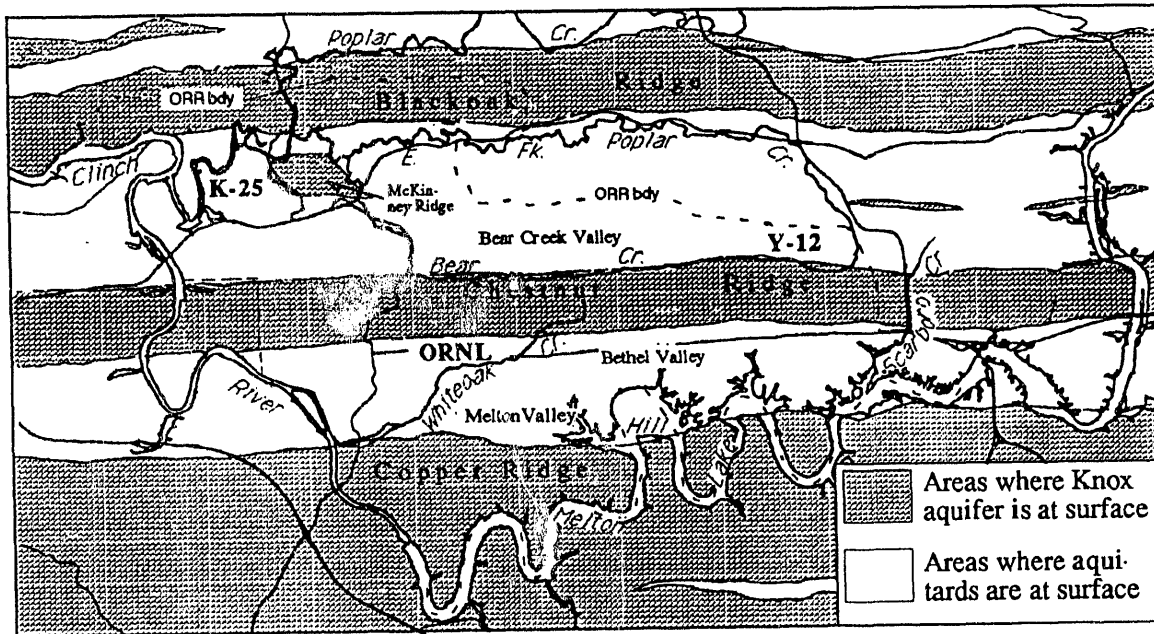


Fig. 7-1. Generalized map of the ORR showing surface distribution of the Knox aquifer and the ORR aquitards.

influenced by hydrostratigraphic units. Although many factors influence groundwater flow on the ORR, topography, surface cover, geologic structure, and lithology exhibit strong influence on the hydrogeology. Variations in these features result in water flux variations.

Because of substantial topographic relief and a marked vertical decrease in permeability, subsurface flow is predominantly shallow on the ORR. In addition to groundwater flow, contaminant migration rates are strongly influenced by geochemical processes, including ion exchange, sorption, and precipitation/dissolution of mineral phases. The retardation of contaminants on the ORR resulting from geochemical processes is specific to each contaminant. The rate of tritium migration, for example, is virtually the same as that of groundwater, whereas the migration of cesium through the ORR aquitards may be too small to detect. Although chemical processes constitute the dominant retardation mechanism for many

contaminants, the process of matrix diffusion is emphasized in this report because it is generic to all contaminants and provides the basis for a "worst case" scenario for contaminant migration.

7.2 STORMFLOW ZONE

Detailed water budgets indicate that approximately 90 percent of active subsurface flow occurs through the 1- to 2-m-deep stormflow zone. Natural areas of the ORR are heavily vegetated, and the stormflow zone approximately corresponds to the root zone. Infiltration tests indicate that this zone is as much as 1000 times more permeable than the underlying vadose zone. During rain events, the stormflow zone partially or completely saturates and then transmits water laterally to the surface-water system. During rain events, the stormflow zone can become completely saturated, in which case overland flow occurs.

Where such excavations as waste trenches penetrate the stormflow zone, a commonly observed condition known as bathtubting can occur in which the excavation fills with water. Between rain events, as the stormflow zone drains, flow rates decrease dramatically and flow becomes nearly vertical toward the underlying vadose zone. The transmissive capability of the stormflow zone is created primarily by root channels, worm holes, clay aggregation, fractures, etc., collectively referred to as large pores. Although highly transmissive, large pores make up only approximately 0.2 percent of the total void volume of the stormflow zone. Because most of the water mass resides within less transmissive small pores, advective-diffusive exchange between large and small pores substantially reduces contaminant migration rates relative to fluid velocities in large pores.

7.3 VADOSE ZONE

A vadose zone exists throughout the ORR except where the water table is at land surface, such as along perennial stream channels. The thickness of the vadose zone is greatest beneath ridges and thins towards valley floors. Beneath ridges underlain by the Knox aquifer (Copper Ridge, Chestnut Ridge, McKinney Ridge, and Blackoak Ridge), the vadose zone commonly is as much as 50 m thick, whereas beneath ridges underlain by the Rome Formation (Haw Ridge and Pine Ridge); the vadose zone is typically <20 m thick. In lowland areas near streams, a permanent vadose zone does not exist because the stormflow zone intersects the water table. The vadose zone consists of regolith composed mostly of clay and silt, most of which is derived from the weathering of bedrock materials and which has significant water storage capacity. Most

recharge through the vadose zone is episodic and occurs along discrete permeable features that may become saturated during rain events, even though surrounding micropores remain unsaturated and contain trapped air. During recharge events, flow paths in the vadose zone are complex and are controlled by the orientation of structures of the materials, such as relict fractures. Between recharge events, flow rates decrease dramatically and flow paths are toward the groundwater zone.

7.4 GROUNDWATER ZONE

A convergence of evidence indicates that most water in the groundwater zone is transmitted through a layer, approximately 1 to 5 m thick, of closely spaced, connected fractures near the water table, as shown below.

Many open fractures, which extend only a short distance into the rock, can be seen in outcrops, and the near correspondence of the water table with the top of weathered bedrock in the ORR is probably not coincidental. Regolith above this level has been formed by a large water flux, and the presence of unweathered bedrock at deeper levels apparently indicates a smaller water flux. Cyclic variations in water table elevation change the saturated thickness of the permeable layer. The resulting changes in transmissivity explain an order-of-magnitude fluctuation in groundwater discharge rates even though (1) contours of annual high and low water table elevations show little change in hydraulic gradient and (2) seasonal changes of water level in most wells are small compared with height of the water level above stream level. Opposite changes in hydraulic gradient and saturated thickness occur from one topographic location to another. The product of transmissivity and hydraulic gradient is

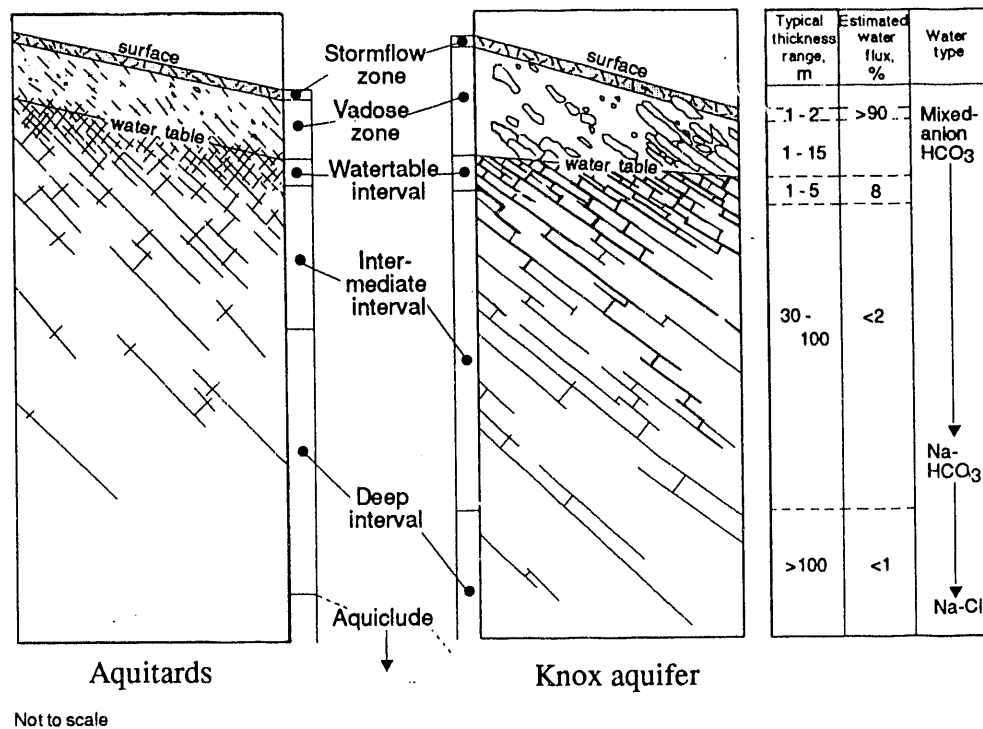


Fig. 7-2. Schematic vertical relationships of flow zones of the ORR, estimated thicknesses, water flow, and water types.

constant (or increases with recharge) along each flow path.

The range of seasonal fluctuations in depth to the water table and in rates of groundwater flow vary significantly across the reservation. In the areas of the Knox aquifer (Fig. 7-2), seasonal fluctuations in water levels average 5 m and the specific discharge through the active groundwater zone is typically 9 m per year. In the aquitards of Bear Creek Valley, Melton Valley, East Fork Valley, and Bethel Valley, seasonal fluctuations in water levels average 1.5 m and typical specific discharge is 5 m per year.

As in the stormflow zone, the bulk of water mass in the water table interval resides within porous matrix blocks between fractures, and diffusive exchange between matrix and fractures reduces contaminant migration rates relative to fracture fluid velocities. For example, the

leading edge of a geochemically non-reactive contaminant plume migrates along fractures at a typical rate of 1 m per day; however, the center of mass of a contaminant plume typically migrates at only 0.05 m per day.

Below the water table interval, fracture control becomes dominant in flow path direction. The base of the water table interval corresponds to the zone of transition from regolith to bedrock (Fig. 7-3). In the intermediate interval of the groundwater zone, groundwater movement occurs primarily in permeable fractures that are poorly connected in three dimensions. In the Knox aquifer a few hydrologically dominant cavity systems control groundwater movement in this zone, but in the aquitards the bulk of flow is through fractures, along which permeability may be increased by weathering.

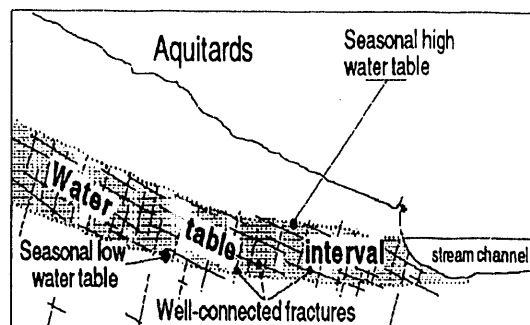


Figure 7-3. Schematic profile of the water table interval.

As described in detail in Sect. 5, fracture orientations measured in outcrop generally fall into three sets, as illustrated below (Fig. 7-4). One fracture set is parallel to and along bedding planes and thus parallel to strike. The dip of this fracture set varies with bedding plane dip, generally ranging between 10 and 50°. A second set is also parallel to strike but perpendicular to bedding planes. The dip of this set also varies with bedding plane dip and thus is a function of depth, inclined near the surface where bedding planes dip more steeply, then vertical at depth where bedding plane dip flattens. A third set is perpendicular to strike.

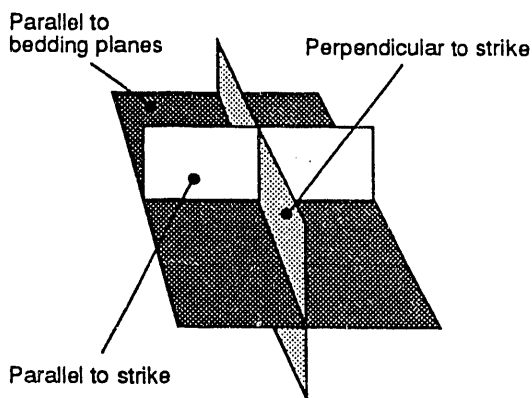


Figure 7-4. Common fracture orientation in the ORR.

Fracture orientations and converging groundwater flow paths in and near valley floors give rise to preferential groundwater movement along strike, toward cross-cutting tributary drainageways. Bedding-plane and strike-parallel fractures and their intersections are more permeable than the dip-parallel fractures, and flow paths are along valley toward crosscutting tributary streams.

The chemical characteristics of groundwater change from a mixed cation- HCO_3 water type to an Na-HCO_3 type in the ORR aquitards at depths ranging from 30 to 50 m. Although the geochemical mechanism responsible for this change in water types is not entirely quantified, it probably is related to water residence time. The transition from Ca-HCO_3 to Na-HCO_3 serves as a useful marker and is used in this report to distinguish the intermediate groundwater interval from the deep interval, a transition which is not marked by a distinct change in rock properties.

Below the intermediate interval, small quantities of water are transmitted through discrete fractures in the deep interval. The hydrologically active fractures in the deep interval are significantly fewer in number and shorter in length than in the other intervals, and the spacing is greater, partly because of less dissolution of fracture fillings. Fracture orientations are similar to those described earlier for the water table interval.

Wells finished in the deep interval of the ORR aquitards typically yield <0.1 L/min and thus have no potential for water supply. The specific storage of the bedrock aquitard is small, and as a result some hydraulic heads in the deep interval respond to precipitation events, even though the associated water flux is small. The chemical characteristics of groundwater in the deep interval are different from those of the water table interval and pro-

bably reflect longer water residence times. Although diffusive transfer between fractures and matrix blocks is an important process in the deep interval, the total matrix porosity is less than that of the water table interval, vadose and stormflow zones, thereby reducing the retarding effect on contaminant migration rates relative to more shallow zones.

7.4 AQUICLUDE

Saline water, having total dissolved solids ranging from 2000 to 275,000 mg/L, lies beneath the deep interval of the groundwater zone, delineating an aquiclude. Chemically, this water resembles brines associated with major sedimentary basins, but its origin and rate of movement are not known. The depth to the aquiclude is approximately 180 to 240 m in Melton and Bethel valleys and is believed to be >300 m in portions of Bear Creek Valley. Depth to the aquiclude in areas of the Knox aquifer is not known, but is believed to be >350 m.

8 CONCLUSIONS

1. A state-of-the-art geologic framework is emerging for the Oak Ridge Reservation (ORR) based on combined surface and subsurface geologic investigations. This knowledge of the bedrock and surficial geology should permit better generic understanding of the hydrogeologic framework of the ORR and should affect environmental remediation and land-use planning activities as well.
2. The bedrock geology exposed in the ORR is composed entirely of clastic and carbonate sedimentary rocks that range in age from early to late Paleozoic. These strata formed in a variety of depositional environments ranging from shallow to deep water, with clastic sources from both the west (Cambrian) and the east (Late Ordovician to Mississippian). Two major unconformities occur within this succession.
3. Nine major stratigraphic units were recognized previously in the ORR. A major result of this investigation is the subdivision of the Conasauga, Knox, and Chickamauga Groups. The Conasauga and, to a much lesser extent, the Knox and Chickamauga Groups have served as the principal units for disposal of radionuclides and other waste materials in the ORR, so this more detailed knowledge is very important in environmental restoration and related activities.
4. The map-scale structure of the ORR is dominated by uniform southeast dip of sedimentary layering interrupted only by the two large thrust faults, the Copper Creek and Whiteoak Mountain faults, and the East Fork Ridge (and Pilot Knob) syncline in the footwall of the Whiteoak Mountain thrust. The Whiteoak Mountain fault also has a very large displacement, compared to the Copper Creek fault, which is indicated by the character of facies changes occurring in the Middle Ordovician rocks northwest and southeast of it. Additional evidence for the greater displacement on the Whiteoak Mountain fault is derived from the preservation of rocks as young as Mississippian in synclines in the footwall, but nowhere in the vicinity of the ORR are rocks younger than Middle Ordovician preserved in the footwall of the Copper Creek fault.
5. Outcrop-scale structures consist of inclined, faulted, and folded bedding, and joints. Joints (systematic fractures) are the most common structures present here, and several sets of joints with different orientations have been recognized. The dominant joint sets are oriented northeast and northwest, with lesser north-south and east-west sets. These structures are probably the most important in the ORR because they, along with bedding and local karst, form the conduit system that controls groundwater movement.
6. Documenting joint attitude, timing, and evolution is one means of inferring the stress orientation history of a thrust sheet, but joint studies from the Appalachian Cumberland Plateau, Valley and Ridge, Blue Ridge, and Piedmont indicate that some joints developed in response to erosional unloading and the recent stress field, while others formed during Triassic-Jurassic extension related to the opening of the present Atlantic. Therefore it is unwise to assume that all joints observed are a result of Paleozoic folding and thrust-sheet emplacement.

7. The relationship between the oxygen composition of interbedded limestones and vein calcites in the Nolichucky Shale reflects varying contributions of oxygen from two major sources: (1) formation water in near-isotopic equilibrium with interbedded silicate units and (2) formation water close to equilibrium with interbedded limestones. Similarities in the carbon isotopic composition of the veins and limestones is expected if the dominant carbon reservoir is the interbedded limestones. In the case of the Nolichucky, an intraformational source of oxygen and carbon could provide the necessary fluids to form calcite veins. From the isotopic data alone, large-scale migration of fluids into the Nolichucky Shale from other sources is not required to explain the occurrence and compositions of Nolichucky calcite veins, although large-scale fluid migration cannot be ruled out from the isotopic data alone.
8. Groundwater systems here are local, as opposed to regional, with short flow path lengths from recharge point to discharge point. All groundwater discharges in the Oak Ridge area are to the Clinch River or its tributaries. The mantle of unconsolidated residual materials, or regolith, derived by in situ weathering of bedrock, is composed mostly of silt and clay. Water occurs in and moves through the regolith in pore spaces between particles or in voids created by the structure of the materials. The stormflow zone occurs at the top of the regolith; the water table is present in most places near the base. Wastes are commonly buried in regolith in the ORR.
9. The Knox Group and the underlying Maynardville Limestone function as one hydrologic unit, the Knox aquifer. Most of the perennial springs and all of the larger springs in the area flow from the Knox aquifer and sustain almost all the natural baseflow of perennial streams in the area.

9 NEEDS AND RECOMMENDATIONS FOR CONTINUED INVESTIGATIONS

9.1 INTRODUCTION

This status report of the geology of the Oak Ridge Reservation (ORR) provides much of the basic geologic framework of the reservation. A number of unknowns remain, however, which, when pursued and answered, will provide much-needed information on the relationships between geology and groundwater occurrence and movement. The following list was compiled on the basis of a perceived need for additional fundamental geologic and geophysical studies that would benefit environmental restoration, waste remediation, land-use planning, and other activities in the future of the ORR. This should not be considered an exhaustive list. Moreover, the list is not completely in order of priority.

Predictions of groundwater contaminant pathways, flow rates, and residence times, as well as the interpretation of hydrologic test results, require an understanding of in situ geologic characteristics. These characteristics include surficial geology and bedrock stratigraphy, sedimentology, structure, rock deformation moduli, and subsurface stress states. Acquiring the needed geological characteristics requires comprehensive studies involving detailed surface mapping, outcrop analysis of mesostructures, drill core analysis, well logging, petrographic analysis, rock mechanics tests, and in situ stress tests. By combining these various approaches, the stratigraphic sequence can be divided into mechanical units that will produce a conceptual geological model to be used as a framework for groundwater flow modeling.

The mechanical response of a stratigraphic sequence under the loading

conditions imposed during basin subsidence, deformation, and uplift will control the type(s) of deformation mechanism(s), their distribution, and relative abundance. Therefore, deciphering the development of mechanically distinct packages of a stratigraphic sequence during the geologic history of a basin will aid in predicting spatial relationships and in modeling mesoscopic structural development. Dividing a stratigraphic sequence into mechanical units involves a variety of methods. Stratigraphic criteria of the rock units include lithology, bed thickness, and petrologic characteristics. Structural criteria include present fracture (density, type, fracture tips) and stylolite characteristics. Rock mechanics criteria include elastic moduli (strength), compressibility, and fracture toughness tests. Another aspect of mechanical stratigraphy that needs consideration is whether mechanical units are transient, that is, does a particular mechanical unit always respond in the same way during progressive deformation (subsidence, folding, thrusting, uplift)? If not, defining mechanical units may require knowledge of the boundary conditions of deformation (P, T, strain rate). The deformational history of the sequence of rocks in the ORR has produced an array of fractures and other structures that, coupled with the large variation in lithologies (fractured soluble carbonates interlayered with fractured relatively insoluble clastic rocks), has produced a very complex hydrologic system that produces multivariate problems for waste remediation and difficulties in assessment for land-use planning.

In situ stress affects nearly all physical properties of rock and hence the measurement and interpretation of (1) geophysical

data; (2) petrophysical properties, such as porosity and permeability; (3) rock strength and ductility; and (4) mechanisms of rock deformation and failure. In fractured controlled groundwater flow systems, the stress influence is even more pronounced with respect to fluid flow through fractures. Lithostatic loads will cause fractures to close at a depth. In situ stress data are also used to model the propagation of hydraulic fractures associated with the Hydrofracture Facility. The best models will require local and regional stress data, geometrical data of mechanical anisotropy's associated with structure and stratigraphy, and information regarding rock unit mechanical characteristics. Therefore, knowledge of in situ stress is important toward a multidisciplinary approach to characterize fractured controlled groundwater flow systems.

9.2 RECOMMENDED FUTURE ACTIVITIES

1. A detailed geologic map of the ORR should be completed.
2. Rock mechanics testing should be conducted (1) to develop realistic mechanical models of fracture propagation during basin subsidence, folding and thrusting, and erosional unloading to consider what might control variations in the characteristics of a mechanical unit through time; (2) to provide data to estimate fracture spacing relationships based on rock type, mechanical unit thickness, and driving stress; (3) to determine different mechanical characteristics of interbedded sedimentary rocks for use in constraining the bedding-perpendicular extent and continuity of fractures; (4) to compare dynamic elastic moduli estimates from sonic logs with static elastic moduli for well-logging calibration purposes; (5) to provide data that can be used to estimate the magnitude of the in situ stresses in the Pumpkin Valley Shale in Melton Valley, when combined with injection pressure records from the hydrofracture site, and for future core strain relaxation experiments of in situ stress; (6) to provide data for use in calculation of bulk compressibility, which is needed to determine in situ matrix porosity under the confining pressure; (7) to provide data that can be used to estimate fracture aperture vs fracture length relationships based on fracture type, bed thickness, and rock type; (8) to study the differences in fracture toughness between brittle materials to correlate with the amount of microcracking at the crack tip, because microcracking has shown to be related to fracture surface roughness, so any future investigations of discrete fracture flow (flow channeling) will require predictions of fracture surface roughness, which can be determined from and correlated with rock mechanics test samples; (9) for use in a microcrack analysis of fracture propagation to determine width of the microcrack zone and fracture connectivity; (10) to compare core sample with outcrop sample mechanical properties; (11) to generate fracture toughness data, a strength measure that can be used to estimate fracture aperture closure as a function of normal stress across the fracture plane, which is primarily controlled by asperity deformation or penetration; and (12) to design tests to document R-curve behavior during crack growth in rock.
3. Perform rigorous integration of hydrologic and geologic data and formulation of structural-hydrologic model for the ORR. Determination of hydrologic flow path(s) should be undertaken.
4. Detailed core analysis should be made (1) to provide detailed, understandable,

and reproducible core descriptions to serve as an important data base for future hydrologic and geologic investigations; (2) to determine the reliability of surface fracture characteristics as a measure of subsurface fracture characteristics; (3) to compare geologic core descriptions with geophysical logs and with hydrologic data (packer tests and flow meter); (4) for calibration of geophysical logs against porosity, density, and gamma radiation of cores; (5) to gain knowledge of core characteristics in packer and flow meter test intervals to aid the interpretation of the hydrologic data; (6) for detailed structural and stratigraphic analysis of particular stratigraphic intervals in each core, along with correlation with other cores for spatial consistency, which will permit the stratigraphy to be divided into mechanical and hydrologic units and which can then be modeled with respect to their deformational response; (7) to provide sample locations for petrographic analysis of fracture and matrix porosity and micro fracture abundance, rock mechanics testing, and core porosity and permeability tests of the matrix, fractures, and stylolites; and (8) to determine the characteristics of drilling- and coring-induced fractures and their potential utility in characterizing the present-day stress field in the area.

5. Detailed investigations of major and minor fault zones (fault rocks, fractures near faults) should be made to determine their role as hydrologic conduits or aquicludes. Major faults in the Oak Ridge area juxtapose noncarbonate and carbonate stratigraphic units that behave as distinct hydrologic units. Because the karstified carbonates are considered potential aquifers, the ability of a fault zone to prevent groundwater flow from the noncarbonate into the carbonate units depends on the mesoscopic structural characteristics of the fault zone, which are

also related to the type of fault. Fluid pathways are created when fault-related fractures are numerous and open, but fluid pathways are blocked where a thick zone of brecciation and cataclasite develops along the fault zone. Although gouge development during fault slip is a function of rock type, confining pressure, temperature, and displacement, the location of gouge development along a fault zone is highly variable. Ascertaining the influence that faults have on the groundwater flow system requires characterizing the change in all mesoscopic structural characteristics near major and minor faults (and folds) and their spatial extent relative to fault dimensions and displacements.

6. Fracture density and orientation maps to relate fracture systems to bedrock geology (structures and lithologies) should be considered. The mechanisms of development of zones of high fracture frequency within a particular fracture set that have no apparent bedding control should be located and determined. A detailed trace study of fracture zone geometry may be useful input to a groundwater model of single vs multiple fracture flow.

Laboratory/computer modeling of hydrologic conditions using known fracture system, fracture density, bedding orientation, lithologic, and other structural data should be developed. Fracture connectivity studies should be made to (1) determine fracture length in the vertical and horizontal dimension, (the vertical length may be constrained by mechanical stratigraphy analysis, and the horizontal length may be constrained from relative fracture aperture width, number of subsidiary fractures, and micro crack density); (2) investigate fracture timing, because the first-formed fracture sets are commonly the most continuous and later-formed fracture sets terminate against them; (3) differentiate between extension

fractures, that tend to be more linear and consist of continuous, single strands, and shear fractures, that may be more sinuous and may consist of a number of anastomosing strands; (4) relate open fracture preference and connectivity to the near-surface stress field; (5) obtain better knowledge of fracture zone characteristics, including continuity, connectivity of fractures in the zone, types of fractures, etc.

Changes in fracture characteristics with depth and relationships to neotectonic fracturing should be conducted on core and coupled with outcrop studies to consider changes in fracture characteristics with depth, such as (1) new sets of different orientation; (2) propagation of existing sets, along with reopening; (3) depth of open fractures (50 to 75 m) as a possible stress break; (4) comparisons of the structural characteristics of similar units at various depths and also at the surface, by setting up a mock drill hole on the outcrop.

Trace-length studies should be made because preliminary fracture spacing studies at the surface indicate that, in well-bedded clastic sequences, systematic fractures have a spacing that is partly controlled by bed thickness. In carbonate sequences, however, the relationship is not so straightforward and a better understanding of mechanical units is required. In order to obtain data useful for groundwater modeling, we need to better quantify fracture frequency relationships in both well-bedded clastic units and carbonates. Probably the most often used and studied statistically are engineering trace length techniques. Trace length methods can be used to quantify three-dimensional relationships between fractures and bedding within a particular mechanical unit. The use of trace length methods will produce a viable data set to analyze statistically and produce estimates of block sizes

and fracture surface areas in a particular volume of rock. Although fracture abundance does increase in outcrop vs core, trace length results may be more applicable to shallow subsurface flow modeling where most of the flow occurs. Accommodation should be made of the mismatch between fracture characteristics that are determined both hydrologically and geologically.

7. Derivative maps (slope and slope condition/hazard, soil stability, karst, flood hazard, foundation conditions, existing waste disposal areas) should be constructed for use in land-use planning, hydrologic investigations, waste remediation, and construction.

8. A detailed map of Quaternary geology of the ORR and a complete soils map of the ORR at 1:12,000 should be constructed.

9. Whole soil analysis should be done for each rock unit that would include chemistry, mineralogy, and particle size.

10. Characteristic weathering profiles should be completed of stratigraphic units and the relationships of both to the water table, as well as to large- and small-diameter auger refusal.

11. Complete map(s) of major and minor (ephemeral) springs and recharge areas in the ORR should be constructed.

12. Seismic reflection profiling of the ORR should be completed.

13. Depth(s) should be determined at which fractures close using a combination of boring, geophysical, hydrologic, and modeling techniques. Less abundant fractures that remain open to greater-than-average depth for closing of fractures should be identified and mapped.

14. Petrographic analysis is needed for (1) detailed study of veins from core and outcrop that should include mineralogy, crystal geometry, strain, and evidence for multiple cracking events to document the opening mode for each fracture set; (2) data on microfracture attributes with respect to the type and characteristics of mesoscopic fractures to correlate micro-crack density change adjacent to a fracture with micro crack density to attempt to estimate the fracture length; (3) examination of fracture tips to study fracture arrest and initiation mechanisms, to look for evidence for subcritical crack growth due to fatigue and corrosion cracking, and to examine fracture tip process zone (micro-crack) development and distribution; (4) matrix analysis for each rock type, including porosity, composition, grain size, strain, and diagenetic history of matrix cements; and (5) relationships of porosity occlusion and enhancement to deformational mechanisms and structural position.

15. Core analysis should be correlated with flowmeter results to determine characteristics of hydraulically active intervals in a hole with the goal of determining whether the intervals contain (1) a single fracture; (2) multiple fractures; (3) a preferred fracture orientation; (4) if the fractured zone extends past the interval; and (5) any evidence from the interval of ground water flow. Once permeable intervals have been established in a core hole, core analysis and knowledge of the mechanical stratigraphy can be used to infer the potential vertical permeability of the units between permeable intervals.

16. Porosity and permeability analysis employing laboratory techniques should be used to determine porosities and permeabilities of nonfriable, coherent rocks that do not appreciably swell or

disintegrate when oven-dried or immersed in water. The techniques include weight reduction, gas saturation, water saturation, mercury porosimetry, neutron logs (very qualitative), and petrography.

17. With the knowledge of mechanical stratigraphy and material properties, a number of different finite element models should be utilized to model fracture growth during basin subsidence, deformation, and uplift. The models could address the relative development of fractures in each mechanical unit in these different stress regimes. Present-day subsurface temperature data are available from the JOY-1 well, which can be used to model the development of unloading fractures. The models could be very specific and show the deformation of a plate with random initial flaw orientations and their interaction during fracture growth. The plate could be either folded, contain a central fault, or be anisotropic to test for by-material effects on fracture propagation.

18. Studies in geochemistry should include the following: (1) continue stable isotope and fluid inclusion work on near-surface veins and matrix to identify zones of active dissolution/precipitation and put this in a spatial context; (2) investigate "secondary" fluid inclusions, because they are the most recent, so they may provide information on conditions during more recent fracturing events; and (3) conduct whole-rock analyses of lithologic units for water-rock interaction modeling.

19. Geological factors influencing karst development should be determined. Carbonate aquifers tend to be heterogeneous and anisotropic where they have been subjected to intensive weathering leading to more mature stages of karst development and where stratigraphic, structural, and topographic interaction

have contributed to the complexity of permeability and porosity development and distribution. (1) The distribution of conduits within the stratigraphic column should be investigated to provide a measure of the amount of solutioning in each type of carbonate and therefore measure the amount of lithologic control exerted on solution development. (2) Once having established that certain carbonate units are less cavernous than others, it is necessary to show what chemical or lithological factors are responsible. (3) Microgravity, electrical resistivity, and electromagnetic methods can be used to locate subsurface conduits.

20. Heterogeneity logging should be employed to investigate how geostatistical methods applied to geophysical well logs can be used to characterize the degree and scale of vertical heterogeneity.

REFERENCES CITED

- Ashworth, J. K. 1982. Depositional environments and paleoecology of Middle Ordovician rocks in Union County, Tennessee. M.S. thesis. The University of Tennessee, Knoxville.
- Ausich, W. I., and D. L. Meyer. 1990. Origin and composition of carbonate buildups and associated facies in the Fort Payne Formation (Lower Mississippian, south-central Kentucky): An integrated sedimentologic and paleoecologic analysis. *Geological Soc. America Bull.* 102:129–46.
- Bahat, D. 1979. Theoretical considerations on mechanical parameters of joint surfaces based on studies on ceramics. *Geology* 116:81–92.
- Bahat, D., and T. Engelder. 1984. Surface morphology on cross fold joints of the Appalachian Plateau, New York and Pennsylvania. *Tectonophysics* 104:299–313.
- Bally, A. W., P. L. Gordy, and G. A. Stewart. 1966. Structure, seismic data and orogenic evolution of southern Canadian Rockies. *Can. Petrol. Geologists Bull.* 14:337–81.
- Bassler, R. S. 1932. The stratigraphy of the Central Basin of Tennessee. *Tenn. Div. Geology Bull.* 38.
- Beets, J. W. 1985. Structural analysis of the Hunter Valley, Wallen Valley, and Whiteoak Mountain fault intersection in northeastern Tennessee. M.S. thesis. The University of Tennessee, Knoxville.
- Belvin, W. M. 1975. Sedimentary environments of the basal Chickamauga Group in a portion of Raccoon Valley, Anderson County, Tennessee. M.S. thesis. The University of Tennessee, Knoxville.
- Berry, W. B. N., and A. J. Boucot. 1970. Correlation of the North American Silurian rocks. *Geological Soc. America Spec. Paper* 102.
- Bogdanov, A. A. 1947. The intensity of cleavage as related to the thickness of the bed. *Sov. Geology* 16:147.
- Borowski, W. S. 1982. Petrology, depositional environments, and stratigraphic analysis of a part of the Middle Ordovician Chickamauga Group limestones near Clinton, Tennessee. M.S. thesis. The University of Tennessee, Knoxville.
- Boyd, G. H. 1955. A geologic study of the Chickamauga formations of Raccoon Valley, Roane County, Tennessee. M.S. thesis. The University of Tennessee, Knoxville.
- Boyer, S. E., and D. Elliott. 1982. Thrust systems. *American Assoc. Petrol. Geologists Bull.* 66:1196–230.
- Bridge, J. 1945. Geologic map and structure sections of the Mascot–Jefferson City zinc mining district, Tennessee, scale 1:31,250. *Tenn. Div. Geology*
- Bridge, J. 1956. Stratigraphy of the Mascot–Jefferson City zinc district, Tennessee. *U. S. Geological Survey Prof. Paper* 277.
- Butts, C. 1926. The Paleozoic rocks. pp. 41–230. In G. I. Adams, C. Butts., L. W. Stephenson, and W. Cooke (eds.), *Geology of Alabama*. Alabama Geological Survey Spec. Rep. 14.
- Butts, C. 1948. Geology and mineral resources of the Paleozoic area in northwest Georgia. *Ga. Dept. of Mines, Min. and Geology Bull.* 54.
- Causey, M. E. 1956. The Chickamauga rocks of a portion of Raccoon Valley, western Knox County, Tennessee. M.S. thesis. The University of Tennessee, Knoxville.

- Christensen, N. I., and D. L. Szymanski. 1991. Seismic properties and the origin of reflectivity from a classic Paleozoic sedimentary sequence, Valley and Ridge province, southern Appalachians. *Geological Soc. America Bull.* 103:277-89.
- Cobb, J. C., and J. L. Kulp. 1960. U-Pb age of the Chattanooga shale. *Geological Soc. America Bull.* 71:223-24.
- Compton, R. N., J. E. Beavers, R. D. Hatcher, Jr., and S. H. Liu. 1991. Corporate Fellows Council report on geosciences at ORNL. Oak Ridge National Laboratory.
- Conant, L. C., and V. E. Swanson. 1961. Chattanooga shale and related rocks of central Tennessee and nearby areas. U. S. Geological Survey Prof. Paper 357.
- Cook, D. C. 1975. Structural style influenced by lithofacies, Rocky Mountain Main Ranges. *Geological Survey Can. Bull.* 33.
- Cooper, B. N. 1945. Industrial limestones and dolomites in Virginia: Clinch Valley district. *Va. Geological Survey Bull.* 66:42-68.
- Cooper, B. N., and G. A. Cooper. 1946. Lower Middle Ordovician stratigraphy of the Shenandoah Valley, Virginia. *Geological Soc. America Bull.* 57:35-114.
- Cooper, B. N., and C. E. Prouty. 1943. Stratigraphy of the Lower Middle Ordovician of Tazewell County, Virginia. *Geological Soc. America Bull.* 54:819-86.
- Cooper, G. A. 1956. Chazy and related brachiopods. *Smithson. Misc. Collect.* 127, Part I.
- Craddock, J. P., and B. A. van der Pluijm. 1989. Late Paleozoic deformation of the cratonic carbonate cover of eastern North America. *Geology* 17:416-19.
- Currie, J. B., H. W. Patnode, and R. P. Trump. 1962. Development of folds in sedimentary strata. *Geological Soc. America Bull.* 73:655-74.
- Dahlstrom, C. D. A. 1969. Balanced cross sections. *Can. J. Earth Sci.* 6:743-57.
- Davis, E. C., D. K. Solomon, R. B. Dreier, S. Y. Lee, P. M. Craig, A. D. Kelmers, and D. A. Lietzke. 1987. Summary of environmental characterization activities at the Oak Ridge National Laboratory Solid Waste Storage Area Six, FY 1986 through 1987. RAP/LTR-87/68. Oak Ridge National Laboratory.
- Davis, G. H. 1984. *Structural Geology of Rocks and Regions*. Wiley, New York.
- Davis, R., R. A. Hopkins, and W. E. Doll. 1992. Seismic refraction survey of the ANS preferred site. TM-11998. Oak Ridge National Laboratory.
- DeBoer, J. Z., J. G. McHone, J. H. Puffer, P. C. Ragland, and D. Whittington. 1988. Mesozoic and Cenozoic magmatism. pp. 217-41. In R. E. Sheridan and J. A. Grow (eds.), *The Atlantic Continental Margin: The Geology of North America*, Vol. I-2. Geological Soc. America, Boulder, Colorado.
- deLaguna W., T. Tamura, N. O. Weeren, E. G. Struxness, W. C. McCain, and R. C. Sexton. 1968. Engineering development of hydraulic fracturing as a method for permanent disposal of radioactive waste. ORNL 4259. Oak Ridge National Laboratory.
- Dennis, J. G. 1972. *Structural Geology*. Ronald Press, New York.
- Diegel, F. A. 1986. Topological constraints on imbricate thrust networks, examples from the Mountain City Window, Tennessee, USA. *J. Struct. Geology* 8:269-80.
- Donath, F. A. and R. B. Parker. 1964. Folds and folding. *Geological Soc. America Bull.* 75: 45-62.
- Douglas, R. J. W. 1950. Callum Creek, Langford Creek, and Gap map-areas, Alberta. *Geological Survey of Can. Mem.* 255.

- Dreier, R. B., and L. E. Toran. 1989. Hydrogeology of Melton Valley determined from hydraulic head measuring station data. ORNL TM-11216. Oak Ridge National Laboratory.
- Dreier, R. B., and R. T. Williams. 1986. Geophysical processing and geological interpretation of seismic line FXY-10, preliminary report. RAP/LTR-86/88. Oak Ridge National Laboratory.
- Dreier, R. B., C. S. Haase, C. M. Beaudoin, H. L. King, and J. Switek. 1987. Summary of geological data in the vicinity of the hydrofracture facilities. ORNL/RAP/LTR-87/26. Oak Ridge National Laboratory.
- Dreier, R. B., P. H. Pollard, and M. B. Leat. 1990. Core barn inventory: Status report. Y/TS 655.
- Dreier, R. B., R. J. Selfridge, and C. M. Beaudoin. 1987. Status report on SWSA 6 geophysical studies. ORNL/RAP/LTR-87/31. Oak Ridge National Laboratory.
- Dreier, R. B., D. K. Solomon, and C. M. Beaudoin. 1987. Fracture characterization in the unsaturated zone of a shallow land burial facility in flow and transport through fractured rock. *American Geophys. Union Monogr.* 40:51-59.
- Driese, S. G. 1988. Depositional history and facies architecture of a Silurian foreland basin, eastern Tennessee. pp. 62-96. In S. G. Driese and D. Walker (eds.), *Depositional History of Paleozoic Sequences, Southern Appalachians*. Univ. Tenn. Dept. Geological Sci. Studies Geology 19.
- Dunne, W. M., and C. P. North. 1990. Orthogonal fracture systems at the limits of thrusting: An example from southwestern Wales. *J. Struct. Geology* 12:207-15.
- Elliott, D. 1976. The energy balance and deformation mechanisms of thrust sheets. *Philos. Trans. R. Soc. London Ser. A*, 283:289-312.
- Elliott, D., and M. R. W. Johnson. 1980. The structural evolution of the northern part of the Moine thrust zone. *Trans. R. Soc. Edinburgh* 71:69-96.
- Engelder, T. 1982. Is there a genetic relationship between selected regional joints and contemporary stress within the lithosphere of North America? *Tectonics* 1:161-77.
- Engelder, T. 1987. Joints and shear fractures in rock. pp. 27-69. In B. K. Atkinson (ed.), *Fracture Mechanics of Rock*. Academic Press, London.
- Engelder, T., and P. Geiser. 1980. On the use of regional joint sets as trajectories of paleostress fields during the development of the Appalachian Plateau, New York. *J. Geophys. Res.* 85:6319-41.
- Eslinger, E. V., S. M. Savin, and H. Yeh. 1979. Oxygen isotope geothermometry of diagenetically altered shales. pp. 13-124. In P. A. Scholle and P. R. Schluger (eds.), *Aspects of Diagenesis*. Soc. Econ. Paleontol. and Mineral. Spec. Publ. 26.
- Fenneman, N. M. 1938. *Physiography of the Eastern United States*. McGraw-Hill, New York.
- Fields, N. E., Jr. 1960. A paleontological study of the Chickamauga rocks in Raccoon Valley, Anderson and Knox Counties, Tennessee. M.S. thesis. The University of Tennessee, Knoxville.
- Fluty, M. J. 1964. The description of folds. *Proc. Geological Assoc.* 75:461-92.
- Foreman, J. L. 1991. Petrologic and geochemical evidence for water-rock interaction in the mixed carbonate-siliciclastic Nolichucky Shale (Upper Cambrian) in East Tennessee. Ph.D. dissertation. The University of Tennessee, Knoxville.

- Foreman, J. L., and W. M. Dunne. 1991. Conditions of vein formation in the southern Appalachian foreland: Constraints from vein geometries and fluid inclusions. *J. Struct. Geology* 13:1173–83.
- Foreman, J. L., K. R. Walker, L. J. Weber, S. L. Driese, and R. B. Dreier. 1991. Slope and basinal carbonate deposition in the Nolichucky Shale (Upper Cambrian), east Tennessee: Effect of Carbonate suppression by siliclastic deposition on basin-margin morphology. ORNL/TM-9326. Oak Ridge National Laboratory.
- Friedman, I., and J. R. O'Neil. 1977. Compilation of stable isotope fractionation factors of geochemical interest. In I. Friedman and J. R. O'Neil (eds.), *Data of Geochemistry*, 6th ed. U. S. Geological Survey Prof. Paper 440-KK.
- Garihan, J. M., W. A. Ranson, K. A. Orlando, and M. S. Preddy. 1990. Kinematic history of Mesozoic faults in northwestern South Carolina and adjacent North Carolina. *S. C. Geology* 33:19–32.
- Ghazizadeh, M. 1987. Petrology, depositional environments, geochemistry, and diagenetic history of lower and middle Chickamauga Group (Middle Ordovician) along Highway 58, East Tennessee. Ph.D. dissertation. The University of Tennessee, Knoxville.
- Haase, C. S., D. M. Rye, and B. K. Butler. 1988. A ^{13}C and ^{18}O stable isotopic study of vein and host rock carbonates in the lower portion of the Copper Creek and Whiteoak Mountain thrust sheets near Oak Ridge, Tennessee. ORNL/TM-10608. Oak Ridge National Laboratory.
- Haase, C. S., E. C. Walls and C. D. Farmer. 1985. Stratigraphic and structural data for the Conasauga Group and the Rome Formation on the Copper Creek fault block near Oak Ridge, Tennessee: Preliminary results from test borehole ORNL-JOY No. 2. ORNL/TM-9159. Oak Ridge National Laboratory.
- Hancock, P.L. 1985. Brittle microtectonics. *J. Struct. Geology* 7:437–57.
- Hancock, P.L., and T. Engelder. 1989. Neotectonic joints. *Geological Soc. America Bull.* 101:1197–208.
- Hancock, P.L., and A. Khadi. 1978. Analysis of mesoscopic fractures in the Dhurma-Nisah segment of the central Arabian graben system. *Geological Soc. London J.* 135:339–47.
- Hardeman, W. D. 1966. Geologic map of Tennessee, scale 1:250,000. *Tenn. Div. Geology*.
- Harris, L. D. 1964. Facies relations of exposed Rome Formation and Conasauga Group of northeastern Tennessee with equivalent rocks in the subsurface of Kentucky and Virginia. U. S. Geological Survey Prof. Paper 501-B:B25–B29.
- Harris, L. D. 1969. Kingsport Formation and Mascot Dolomite (Lower Ordovician) of East Tennessee. *Tenn. Div. Geology Rep. Invest.* 23:1–39.
- Harris, L. D. 1973. Dolomitization model for upper Cambrian and lower Ordovician carbonate rocks in the eastern United States. U. S. Geological Survey *J. Res.* 1:63–78.
- Harris, L. D. 1976. Thin-skinned tectonics and potential hydrocarbon traps illustrated by a seismic profile in the Valley and Ridge province of Tennessee. U. S. Geological Survey *J. Res.* 4:379–86.
- Harris, L. D., and R. L. Milici. 1977. Characteristics of thin-skinned style of deformation in the southern Appalachians, and potential hydrocarbon traps. U. S. Geological Survey Prof. Paper 1018.

- Harvell, G. 1954. A geologic study of the Chickamauga Formation of Raccoon Valley, Anderson County, Tennessee. M.S. thesis. The University of Tennessee, Knoxville.
- Hasson, K. O. 1982. Stratigraphy of the Chattanooga Shale, northeastern Tennessee. *Southeastern Geology* 23:171–85.
- Hasson, K. O., and C. S. Haase. 1988. Lithofacies and paleogeography of the Conasauga Group (Middle and Late Cambrian) in the Valley and Ridge Province of East Tennessee. *Geological Soc. America Bull.* 100:34–246.
- Hatcher, R. D., Jr. 1965. Structure of the northern portion of the Dumplin Valley fault zone in East Tennessee. Ph.D. dissertation. The University of Tennessee, Knoxville.
- Hatcher, R. D., Jr. 1986. Moine thrust zone: A comparison with Appalachian faults and the structure of orogenic belts. pp. 247–257. In D. J. Fettes and A. L. Harris (eds.), *Synthesis of the Caledonian Rocks of Britain*. Reidel Publishing Company, Dordrecht, Netherlands.
- Hatcher, R. D., Jr. 1987. Tectonics of the central and southern Appalachian internides. *Ann. Rev. Earth Planet. Sci.* 15:337–62.
- Hatcher, R. D., Jr., and P. J. Lemiszki. 1991. Contrasts in meso- and map-scale properties of thrusts in the Appalachian foreland fold-thrust belt, Tennessee. *Geological Soc. America Abstr. with Prog.* 23:42.
- Hayes, C. W. 1891. The overthrust faults of the southern Appalachians. *Geological Soc. America Bull.* 2:141–53.
- Hayes, C. W. 1894. Description of the Ringgold folio, scale 1:125,000. U. S. Geological Survey Geological Atlas, Folio No. 2.
- Hayes, C. W., and E. O. Ulrich. 1903. Description of the Columbia quadrangle, Tennessee, scale 1:125,000. U. S. Geological Survey Geological Atlas, Folio No. 95.
- Helton, W. L. 1967. Lithostratigraphy of the Conasauga Group between Rogersville and Kingsport, Tennessee. Ph.D. dissertation. The University of Tennessee, Knoxville.
- Helton, W. L. 1979. The characteristics and origin of thrust slices. *Southeastern Geology* 21:63–74.
- Hester, K., and J. C. S. Long. 1990. Analytical expressions for the permeability of random two-dimensional Poisson fracture networks based on regular lattice percolation and equivalent media theories. *J. Geophys. Res.* 95:21,565–81.
- Hodgson, R. A. 1961. Regional study of jointing in Comb Ridge–Navajo Mountain area, Arizona and Utah. *American Assoc. Petrol. Geologists Bull.* 45:65.
- Ingram, R. L. 1954. Terminology for the thickness of stratification and parting units in sedimentary rocks. *Geological Soc. America Bull.* 65:937–38.
- Johnson, A. M. 1977. *Styles of Folding—Mechanics and Mechanisms of Folding of Natural Elastic Materials*. Elsevier Scientific Publishing Company, Amsterdam.
- Jones, C. K. 1963. Structure along the Whiteoak Mountain fault near Kingston, Roane County, Tennessee. M.S. thesis. The University of Tennessee, Knoxville.
- Kellberg, J. M., and H. C. Harrell. 1964. Foundation experiences at Melton Hill Dam, Tennessee (abstract). *Geological Soc. America Spec. Paper* 76:247–48.
- Kemp, T. O. 1954. A study of the Middle and Lower–Upper Ordovician rocks of the Oak Ridge Valley between Elza Gate and Clinton, Anderson County, Tennessee. M.S. thesis. The University of Tennessee, Knoxville.
- Kilsdonk, B., and D. V. Wiltschko. 1988. Deformation mechanisms in the southeastern ramp region of the Pine Mountain block, Tennessee. *Geological Soc. America Bull.* 100:653–64.

- King, H. L., and C. S. Haase. 1987. Subsurface-controlled geologic maps for the Y-12 plant and adjacent areas of Bear Creek Valley. ORNL/TM-10112. Oak Ridge National Laboratory.
- Klepser, H. J. 1937. The lower Mississippian rocks of the East Highland Rim. Ph.D. dissertation. Ohio State University, Columbus.
- Knipe, R. J. 1985. Footwall geometry and the rheology of thrust sheets. *J. Struct. Geology* 7:1-10.
- Kulander, B. R., C. C. Barton, and S. L. Dean. 1979. The application of fractography to core and outcrop fracture investigation. Paper METC/SP-79/3. U. S. Department of Energy, Government Printing Office, Washington, D.C.
- Kummerle, R. P., and D. A. Benvie. 1987. Exploration, design and excavation of Clinch River Breeder Reactor foundations. pp. 351-57. In I. W. Farmer, J. J. K. Daemen, C. S. Desai, C. E. Glass, and S. P. Neuman (eds.), *Rock Mechanics. Proceedings of the Twenty-Eighth Symposium on Rock Mechanics*. Kluwer Publishing, The Hague.
- Ladeira, F. L., and N. J. Price. 1981. Relationship between fracture spacing and bed thickness. *J. Struct. Geology* 3:179-83.
- Law Engineering. 1975. Preliminary safety analysis report. Docket 50-564. Exxon Nuclear Fuels Recycling RC.
- Lee, R. R., and R. H. Ketelle. 1987. Stratigraphic influence on deep groundwater flow in the Knox Group Copper Ridge Dolomite on the West Chestnut Ridge Site. ORNL/TM-10479. Oak Ridge National Laboratory.
- Lee, R. R., and R. H. Ketelle. 1988. Subsurface geology of the Chickamauga Group at Oak Ridge National Laboratory. ORNL/TM-10749. Oak Ridge National Laboratory.
- Lee, R. R., and R. H. Ketelle. 1989. Geology of the west Bear Creek Valley site. ORNL/TM-10887. Oak Ridge National Laboratory.
- Lee, S.-Y., L. K. Hyder, and P. D. Alley. 1987. Mineralogical characterization of selected shale in support of nuclear waste repository studies. ORNL/TM-10567. Oak Ridge National Laboratory.
- Lee, R. R., R. H. Ketelle, J. M. Bownds, and T. A. Rizk. 1989. Calibration of a groundwater flow and contaminant transport model: Progress toward model validation. ORNL/TM-11294. Oak Ridge National Laboratory.
- Lee, S.-Y., O. C. Kopp, and D. A. Lietzke. 1984. Mineralogical characterization of West Chestnut Ridge soils. ORNL/TM-9361. Oak Ridge National Laboratory.
- Lee, S.-Y., D. A. Lietzke, R. H. Ketelle, and J. T. Ammons. 1988. Soil and surficial geology guidebook to the Oak Ridge Reservation, Oak Ridge, Tennessee. ORNL/TM-10803. Oak Ridge National Laboratory.
- Lietzke, D. A. Soil survey of Walker Branch watershed. ORNL/TM. Oak Ridge National Laboratory (in press).
- Lemiszki, P. J. 1992. Geology of the Bethel Valley quadrangle—Part of the Department of Energy Oak Ridge Reservation in the southern Appalachian Foreland fold-thrust belt and fracture mechanics modeling of extension fracture growth during basin subsidence and buckle folding. Ph.D. dissertation. The University of Tennessee, Knoxville.
- Lomenick, T. F. 1958. The geology of the Chickamauga Group of a portion of Raccoon Valley, Knox County, Tennessee. M.S. thesis. The University of Tennessee, Knoxville.

- Lumsden, D. N. 1988. Origin of the Fort Payne Formation (Lower Mississippian), Tennessee. *Southeastern Geology* 28:167-80.
- Macquown, W. C., and J. H. Perkins. 1982. Stratigraphy and petrology of petroleum-producing Waulsortian-type carbonate mounds in Fort Payne Formation (Lower Mississippian) of north central Tennessee. *American Assoc. Petrol. Geologists Bull.* 66:1055-75.
- Markello, J. R., and J. F. Read. 1981. Carbonate ramp-to-deeper shale shelf transitions of an Upper Cambrian intrashelf basin, Nolichucky Formation, southwest Virginia Appalachians. *Sedimentology* 28:573-97.
- Markello, J. R., and J. F. Read. 1982. Upper Cambrian intrashelf basin, Nolichucky Formation, southwest Virginia Appalachians. *American Assoc. Petrol. Geologists Bull.* 66: 860-78.
- Masuoka, P.M. 1981. Analysis of photogeologic fracture traces and lineaments in the northern portion of the Wartburg basin, Tennessee. M.S. thesis. The University of Tennessee, Knoxville.
- McClay, K. R., and M. W. Insley. 1988. Duplex structures in the Lewis thrust sheet, Crowsnest Pass, Rocky Mountains, Alberta, Canada. *J. Struct. Geology* 8:911-22.
- McMaster, W. M. 1957. The geology of East Fork Ridge and Pilot Knob, Oak Ridge, Anderson County, Tennessee. M.S. thesis. The University of Tennessee, Knoxville.
- McMaster, W. M. 1962. Geologic map of the Oak Ridge Reservation, Tennessee, scale 1:31,680. ORNL/TM-713. U. S. Geological Survey and U. S. Atomic Energy Commission. Oak Ridge National Laboratory.
- McQuillan, H. 1973. Small-scale fracture density in Asmari formation of southwest Iran and its relation to bed thickness and structural setting. *American Assoc. Petrol. Geologists Bull.* 47:2367-85.
- McReynolds, J. A. 1988. Paleoenvironment and facies relations of the Lower Cambrian Rome Formation along Haw Ridge on the U. S. Department of Energy Reservation, Oak Ridge area in Roane and Anderson Counties, Tennessee. M.S. thesis. The University of Tennessee, Knoxville.
- Milici, R. C. 1965. Geology of the Morristown quadrangle, Tennessee, scale 1:24,000. GM-163NE. *Tenn. Div. Geology*.
- Milici, R. C. 1973. The stratigraphy of Knox County, Tennessee. *Tenn. Div. Geology Bull.* 70:9-24
- Milici, R. C. 1975. Structural patterns in the southern Appalachians: Evidence for a gravity glide mechanism for Alleghanian deformation. *Geological Soc. America Bull.* 86:1316-20.
- Milici, R. C., and J. B. Roen. 1981. Stratigraphy of the Chattanooga Shale in the Newman Ridge and Clinch Mountain areas, Tennessee. *Tenn. Div. Geology Rep. Invest. No. 40*.
- Milici, R. C., and J. W. Smith. 1969. Stratigraphy of the Chickamauga supergroup in its type area. pp. 1-36. In *Precambrian-Paleozoic Appalachian problems*. Ga. Dept. of Mines, Min., and Geologists Bull. 80 and *Tenn. Div. Geology Rep. Invest. No. 24*.
- Milici, R. C., and H. Wedow. 1977. Upper Ordovician and Silurian stratigraphy in Sequatchie Valley and parts of the adjacent Valley and Ridge. U. S. Geological Survey Prof. Paper 996.
- Milici, R. C., C. T. Spiker, and J. M. Wilson. 1963. Geologic Map of Virginia, scale 1:500,000. Virginia Division of Mineral Resources.

- Miller, R. L., and J. O. Fuller. 1954. Geology and oil resources of the Rose Hill district—The Fenster area of the Cumberland overthrust block, Lee County, Virginia. Va. Geological Survey Bull. 71.
- Mitra, S. 1986. Duplex structures and imbricate thrust systems: Geometry, structural position, and hydrocarbon potential. *American Assoc. Petrol. Geologists Bull.* 70:1087–112.
- Mitra, S. 1988. Three-dimensional geometry and kinematic evolution of the Pine Mountain thrust system, southern Appalachians. *Geological Soc. America Bull.* 100:72–95.
- Money maker, R. 1981. Soil survey of Anderson County, Tennessee. Government Printing Office, Washington, D.C.
- Moore, G. K. 1989. Groundwater parameters and flow systems near Oak Ridge National Laboratory. ORNL/TM-11368. Oak Ridge National Laboratory.
- Moreno L., C. Tsang, Y. Tsang, and I. Neretnieks. 1990. Some anomalous features of flow and solute transport arising from fracture aperture variability. *Water Resour. Res.* 26:2377–91.
- Norris, D. K. 1958. Structural conditions in Canadian coal mines. *Geological Survey of Can. Bull.* 44.
- Oder, C. R. L. 1934. Preliminary subdivision of the Knox dolomite in East Tennessee. *J. Geology* 42:469–97.
- Oder, C. R. L., and H. W. Miller. 1945. Stratigraphy of the Mascot–Jefferson City zinc district. *American Inst. of Min. and Metall. Eng. Trans.* 178:223–31.
- Olsen, C. R., P. D. Lowry, S.-Y. Lee, I. L. Larsen, and N. H. Cutshall. 1986. Geochemical and environmental processes affecting radionuclide migration from a formerly used seepage trench. *Geochim et Cosmochim. Acta* 50:1–15.
- O'Neil, J. R., R. N. Clayton, and T. K. Mayeda. 1969. Oxygen isotope fractionation in divalent metal carbonates. *J. Chem. Phys.* 51:5547–58.
- Plumb, R. A., and J. W. Cox. 1987. Stress directions in eastern North America determined to 4.5 km from borehole elongation measurements. *J. Geophys. Res.* 92:4805–16.
- Pohn, H. A. 1981. Joint spacing as a method of locating faults. *Geology* 9:258–61.
- Pollard, D. D., and A. Aydin. 1988. Progress in understanding jointing over the past century. *Geological Soc. America Bull.* 100:1181–204.
- Popp, B. N., T. F. Anderson, and P. A. Sandberg. 1986. Brachiopods as indicators of original isotopic compositions in some Paleozoic limestones. *Geological Soc. America Bull.* 97:1262–69.
- Price, N. J. 1966. *Fault and Joint Development in Brittle and Semi-brittle Rock.* Pergamon Press, Oxford.
- Price, N. J., and J. W. Cosgrove. 1990. *Analysis of Geological Structures.* Cambridge University Press.
- Price, R. A., and R. D. Hatcher, Jr. 1983. Geotectonic implications of similarities in the orogenic evolution of the Alabama–Pennsylvania Appalachians and the Alberta–British Columbia Canadian Cordillera. pp. 149–160. In R. D. Hatcher, Jr., H. Williams, and I. Zietz (eds.), *Contributions to the Tectonics and Geophysics of Mountain Chains.* Geological Soc. America Mem. 158.
- Priest, S. D., and J. A. Hudson. 1976. Discontinuity spacings in rock. *Int. J. Rock Mech., Miner. Sci., Geomech. Abstr.* 13:135–48.

- Prouty, C. E. 1943. Lower Middle Ordovician of southwest Virginia and northeast Tennessee. *American Assoc. Petrol. Geologists Bull.* 30:1140–91.
- Rankin, D. W., A. A. Drake, Jr., L. Glover, III, R. Goldsmith, L. M. Hall, D. P. Murray, N. M. Ratcliffe, J. F. Read, D. T. Secor, and R. S. Stanley. 1989. Pre-orogenic terranes. pp. 7–100. In R. D. Hatcher, Jr., W. A. Thomas, and G. W. Viele (eds.), *The Appalachian–Ouachita Orogen in the United States*. Geological Society of America, *The Geology of North America*, F–2.
- Resser, C. E. 1938. Cambrian system (restricted) of the southern Appalachians. *Geological Soc. America Spec. Pap.* 15.
- Rich, J. L. 1934. Mechanics of low angle overthrust faulting as illustrated by Cumberland thrust block, Virginia, Kentucky, and Tennessee. *American Assoc. Petrol. Geologists Bull.* 18:1584–96.
- Rodgers, J. 1943. Geologic map of the Copper Ridge district, Hancock and Grainger Counties, Tennessee. P. N. 31476. U. S. Geological Survey Strat. Miner. Invest., Preliminary Map.
- Rodgers, J. 1953. Geologic map of East Tennessee with explanatory text, scale 1:125,000. *Tenn. Div. Geology Bull.* 58.
- Rodgers, J., and D. F. Kent. 1948. Stratigraphic section at Lee Valley, Hawkins County, Tennessee. *Tenn. Div. Geology Bull.* 55.
- Roeder, D., E. Gilbert, and W. Witherspoon. 1978. Evolution and macroscopic structure of Valley and Ridge thrust belt, Tennessee and Virginia. *Univ. Tenn. Dept. Geological Sci. Studies Geology* 2.
- Royce, F., Jr., M. A. Warner, and D. L. Reese. 1975. Thrust belt structural geometry and related stratigraphic problems, Wyoming–Idaho–northern Utah. pp. 41–54. In D. W. Bolyard (ed.), *Symposium on Drilling Frontiers of the Central Rocky Mountains*. Rocky Mountain Association of Geologists, Denver.
- Ruppel, S. C., and K. R. Walker. 1984. Petrology and depositional history of a Middle Ordovician carbonate platform: Chickamauga Group, northeastern Tennessee. *Geological Soc. America Bull.* 95:568–83.
- Rutherford, E. J., Jr. 1985. Stratigraphic controls of thrust faulting and the structural evolution of the Wartburg Basin, Tennessee. M.S. thesis. The University of Tennessee, Knoxville.
- Sable, E. G., and G. R. Dever, Jr. 1990. Mississippian rocks in Kentucky. U. S. Geological Survey Prof. Paper 1503.
- Safford, J. M. 1851. The Silurian basin of middle Tennessee, with notices of the strata surrounding it. *American J. Sci. Arts*, 2nd series, 12:352–61.
- Safford, J. M. 1869. *Geology of Tennessee*. Mercer, Nashville, Tenn.
- Safford, J. M., and J. B. Killebrew. 1900. *Elements of the Geology of Tennessee*. Foster and Webb, Nashville, Tenn.
- Samman, N. B. 1975. Sedimentation and stratigraphy of the Rome Formation in East Tennessee. Ph.D. dissertation. The University of Tennessee, Knoxville.
- Serra, S. 1977. Styles of deformation in the ramp regions of overthrust faults. pp. 487–98. In E. L. Helsey, D. E. Lawson, E. R. Norwood, P. H. Wach, and L. A. Hale (eds.), *Rocky Mountain Thrust Belt Geology and Resources*. Joint Wyoming–Montana–Utah Geological Associations Guidebook. Laramie, Wyoming Geological Survey.

- Sledz, J. J., and D. D. Huff. 1981. Computer model for determining fracture porosity and permeability in the Conasauga Group. ORNL/TM-7695. Oak Ridge National Laboratory.
- Slusarski, M. L. 1979. Photogeologic fracture traces and lineaments in the Wartburg basin section of the Cumberland Plateau physiographic subprovince, Tennessee. M.S. thesis. The University of Tennessee, Knoxville.
- Smith, E. A. 1890. Geological structure and description of the valley regions adjacent to the Cahaba coal field. Ala. Geological Survey Spec. Rep. (2)2:137-80.
- Smith, E. D., and N. D. Vaughan. 1985. Aquifer test analysis in nonradial flow regimes: A case study. *Ground Water* 23:167-75.
- Soil Survey Staff. 1975. Soil taxonomy: A basic system of soil classification for making and interpreting soil surveys. Agric. Hdbk No. 436. U. S. Dept. Agric., Government Printing Office, Washington, D.C.
- Soil Survey Staff. 1983. National Soils Handbook. Agric. Hdbk No. 430-VI-NSH. U. S. Dept. Agric. Soil Cons. Serv., Government Printing Office, Washington, D.C.
- Soil Survey Staff. 1984. Soil Survey Manual, revised. Agric. Hdbk 430-V-SSM. U. S. Dept. Agric., Soil Cons. Serv., Government Printing Office, Washington, D.C.
- Solomon, D. K., G. K. Moore, L. E. Toran, R. B. Dreier, and W. M. McMaster. 1992. Status report: A hydrologic framework for the Oak Ridge Reservation. ORNL/TM-12026. Oak Ridge National Laboratory.
- Sowers, G. M. 1972. Theory of spacing of extensional fractures in geologic fractures of rapid excavation. *Geological Soc. America Eng. Geology Case Hist.* 9:27-53.
- Spigai, J. J. 1963. A study of the Rome Formation in the Valley and Ridge Province of East Tennessee. M.S. thesis. The University of Tennessee, Knoxville.
- Srivastava, D. C., and T. Engelder. 1990. Crack-propagation sequence and pore fluid conditions during fault-bend folding in the Appalachian Valley and Ridge, central Pennsylvania. *Geological Soc. America Bull.* 102:116-28.
- Staub, W. P., and R. A. Hopkins. 1984. Thickness of Knox Group overburden on central Chestnut Ridge, Oak Ridge Reservation. ORNL/TM-9056. Oak Ridge National Laboratory.
- Stearns, D. W. 1969. Fracture as a mechanism of flow in naturally deformed layered rocks. *Can. Geological Survey Paper* 68-52:79-96.
- Stearns, D. W., and M. Friedman. 1972. Reservoirs in Fractured Rock. *American Assoc. Petrol. Geologists Mem.* 16:82-100.
- Stockdale, P. B. 1951. Geologic conditions at the Oak Ridge National Laboratory (X-10) area relevant to the disposal of radioactive waste. ORO-58. U. S. Atomic Energy Commission, Washington, D.C.
- Swann, M. E., W. Roberts, E. H. Hubbard, and H. C. Porter. 1942. Roane County, Tennessee Soil Survey. U. S. Dept. Agric., Bur. Plant Ind., Supt. Doc., Washington, D.C.
- Swingle, G. D. 1959. Geology, mineral resources, and ground water of the Cleveland area, Tennessee. *Tenn. Div. Geology Bull.* 61.
- Swingle, G. D. 1964. Geologic map and mineral resources summary of the Clinton quadrangle, Tennessee, scale 1:24,000. GM 137-SW. *Tenn. Div. Geology.*
- Tegland, E. R. 1978. Seismic investigations in eastern Tennessee. *Tenn. Div. Geology Bull.* 78.

- Thomas, W. A. 1977. Evolution of Appalachian–Ouachita salients and recesses from reentrants and promontories in the continental margin. *American J. Sci.* 277:1233–78.
- Thompson, A. M. 1970. Tidal-flat deposition and early dolomitization in Upper Ordovician rocks of the Southern Appalachian Valley and Ridge. *J. Sediment. Petrol.* 40:1271–86.
- Thornbury, W. D. 1965. *Regional Geomorphology of the United States*. John Wiley & Sons, New York.
- Troost, G. 1835. Third geological report to the twenty-first general assembly of the state of Tennessee. Mercer, Nashville., Tenn.
- Turner, F. J., and L. E. Weiss. 1963. *Structural Analysis of Metamorphic Tectonites*. McGraw-Hill, New York.
- Turner, J. P., and P. L. Hancock. 1990. Relationships between thrusting and joint systems in the Jaca thrust-top basin, Spanish Pyrenees. *J. Struct. Geology* 12:217–26.
- Ulrich, E. O. 1911. Revision of the Paleozoic systems. *Geological Soc. America Bull.* 22:281–680.
- Ulrich, E. O. 1914. The Ordovician–Silurian boundary. 12th Int. Geologic Congr. *Compte Rendu* 593–667.
- Walker, K. R., T. W. Broadhead, and F. B. Keller. 1980. Middle Ordovician carbonate shelf to deep water basin deposition in the southern Appalachians. Univ. Tenn. Dept. Geological Sci. *Studies Geology* 4.
- Walker, K. R., G. Shanmugan, and S. C. Ruppel. 1983. A model for carbonate to terrigenous clastic sequences. *Geological Soc. America Bull.* 94:700–12.
- Weber, L. J., Jr. 1988. Paleoenvironmental analysis and test of stratigraphic cyclicity in the Nolichucky Shale and Maynardville Limestone (Upper Cambrian) in central east Tennessee. Ph.D. dissertation. The University of Tennessee, Knoxville.
- Weiss, E. A. 1981. Environmental sedimentology of the Middle Ordovician and paleoecology of a portion of the Whitten Formation at Solway, Tennessee. M.S. thesis. The University of Tennessee, Knoxville.
- Wheeler, R. L., and J. M. Dixon. 1980. Intensity of systematic fractures. *Geology* 8:230–33.
- Wheeler, R. L., and S. M. Holland. 1978. Style elements of systematic joints: An analytical procedure with a field example. pp. 393–404. In D. W. O'Leary and J. L. Earle (eds.), 3rd International Conference on the New Basement Tectonics.
- Wheeler, R. L., and J. L. Stubbs, Jr. 1976. Style elements of systematic joints: Statistical analysis of size, spacing and other characteristics. pp. 491–99. In R. A. Hodgson, S. P. Gay, Jr., and J. Y. Benjamin (eds.), 1st Conference on the New Basement Tectonics.
- Wilmarth, M. G. 1938. *Lexicon of geologic names of the United States*. U. S. Geological Survey Bull. 896.
- Wilson, C. W., Jr. 1949. Pre-Chattanooga stratigraphy in central Tennessee. *Tenn. Div. Geology Bull.* 56.
- Wilson, R. L. 1986. Geologic map and mineral resources summary of the Ooltewah quadrangle, Tennessee, scale 1:24,000. GM 112-SE. *Tenn. Div. Geology*.
- Wilschko, D. V., D. A. Medwedeff, and H. E. Milson. 1985. Distribution and mechanisms of strain within rocks on the northwest ramp of Pine Mountain block, southern Appalachian foreland: A field test of theory. *Geological Soc. America Bull.* 96:426–35.

- Wojtal, S. 1986. Deformation within foreland thrust sheets by populations of minor faults. *J. Struct. Geology* 8: 441–56.
- Woodward, N. B. (ed.). 1985. *Balanced structure cross sections in the Appalachians (Pennsylvania to Alabama)*. Univ. Tenn. Dept. Geological Sci. Studies Geology 12.
- Woodward, N. B., K. R. Walker, and C. T. Lutz. 1988. Relationships between early Paleozoic facies patterns and structural trends in the Saltville thrust family, Tennessee Valley and Ridge, southern Appalachians. *Geological Soc. America Bull.* 100:1758–69.
- Zimmer, J. A. 1964. *The geology of the Chamberlain iron deposit, Roane County, Tennessee*. M.S. thesis. The University of Tennessee, Knoxville.
- Zoback, M. L., and M. D. Zoback. 1989. Tectonic stress field in the continental United States. pp. 523–39. In L. C. Pakiser and W. D. Mooney, W. D. (eds.), *Geophysical Framework of the Continental United States*. Geological Soc. America Mem. 172.
- Zucker, C. L. 1987. *Microscopic to macroscopic structural analysis of the lower Rome Formation, Pine Ridge, Tennessee*. Senior thesis. The University of Tennessee, Knoxville.

APPENDIX 1

FIELD TRIP STOPS

The following is a description of a self-guided field trip to localities in and near the Oak Ridge Reservation (ORR) where good exposures of the rock units may be observed on the surface. Most of the localities are within the area of Plate 1 (Fig. A1-1), but the Conasauga Group is poorly exposed on the ORR, hence the description of the very good exposure at Dismal Gap several kilometers along strike to the northeast.

STOP 1. ROME FORMATION AND CONASAUGA GROUP AT DISMAL GAP (POWELL QUADRANGLE)

Dismal Gap, located northeast of the ORR in the Powell 7 1/2-minute quadrangle (Fig. A1-2), exposes an almost complete section of Rome Formation, including the lower Rome (Apison?) shale, and Conasauga Group, with the exception of the Maynardville Limestone. The geology of this area was mapped by Beets (1985), but the Conasauga Group was not subdivided here. This section is the best exposure in the area of the Conasauga and Rome in the same strike belt as Bear Creek Valley in the ORR where most of the Oak Ridge Y-12 Plant burial grounds are located. The stratigraphic section exposed here should also be very similar to that in Melton Valley in the ORR where the burial grounds for Oak Ridge National Laboratory (ORNL) are located.

The Rome Formation exposed here contains the usual variegated red, green, tan, and gray shale; thin-bedded to massive sandstone, siltstone; and some dolomite and limestone. Primary structures (ripple marks, cross bedding, flute casts,

etc.) are common in the upper part of the Rome. A 7-m (20-ft)-thick zone of massive dolomite is present in the upper middle part of the Rome here and may have been observed in the Whiteoak Mountain block in the ORR. The Rome (Apison?) shale here consists of the same lithologies as the shale in the upper part of the Rome Formation.

The lower Pumpkin Valley shale at Dismal Gap consists of reddish-brown and gray to greenish-gray shale with thin interbeds of siltstone and silty, fine-grained sandstone. The sandstones are heavily bioturbated. The upper Pumpkin Valley consists of laminated to thin-bedded, dominantly reddish-brown, reddish-gray, and gray shale with thin wavy and planar-laminated sandstone lenses. Shales are generally fissile and may be massive or thin laminated. Thin partings of fine-grained glauconite pellets are ubiquitous.

The Friendship (formerly Rutledge) formation here consists of light-gray, thin-bedded limestone interbedded with dark-gray or maroon thin-bedded shale. In general, bedding is thicker and lithologies are more homogeneous in the lower Friendship. In contrast to the distinct glauconite partings of the Pumpkin Valley, the frequent incorporation of glauconite throughout the thin limestone beds of the Rutledge is evidence of bioturbation. Note that shale and fine calcareous siltstone are the most common lithologies here.

The Rogersville Shale is the most poorly exposed unit along the road at Dismal Gap. The lower Rogersville consists of dark-gray and greenish-gray shale containing thin-laminated and bioturbated argillaceous limestone lenses. The Craig

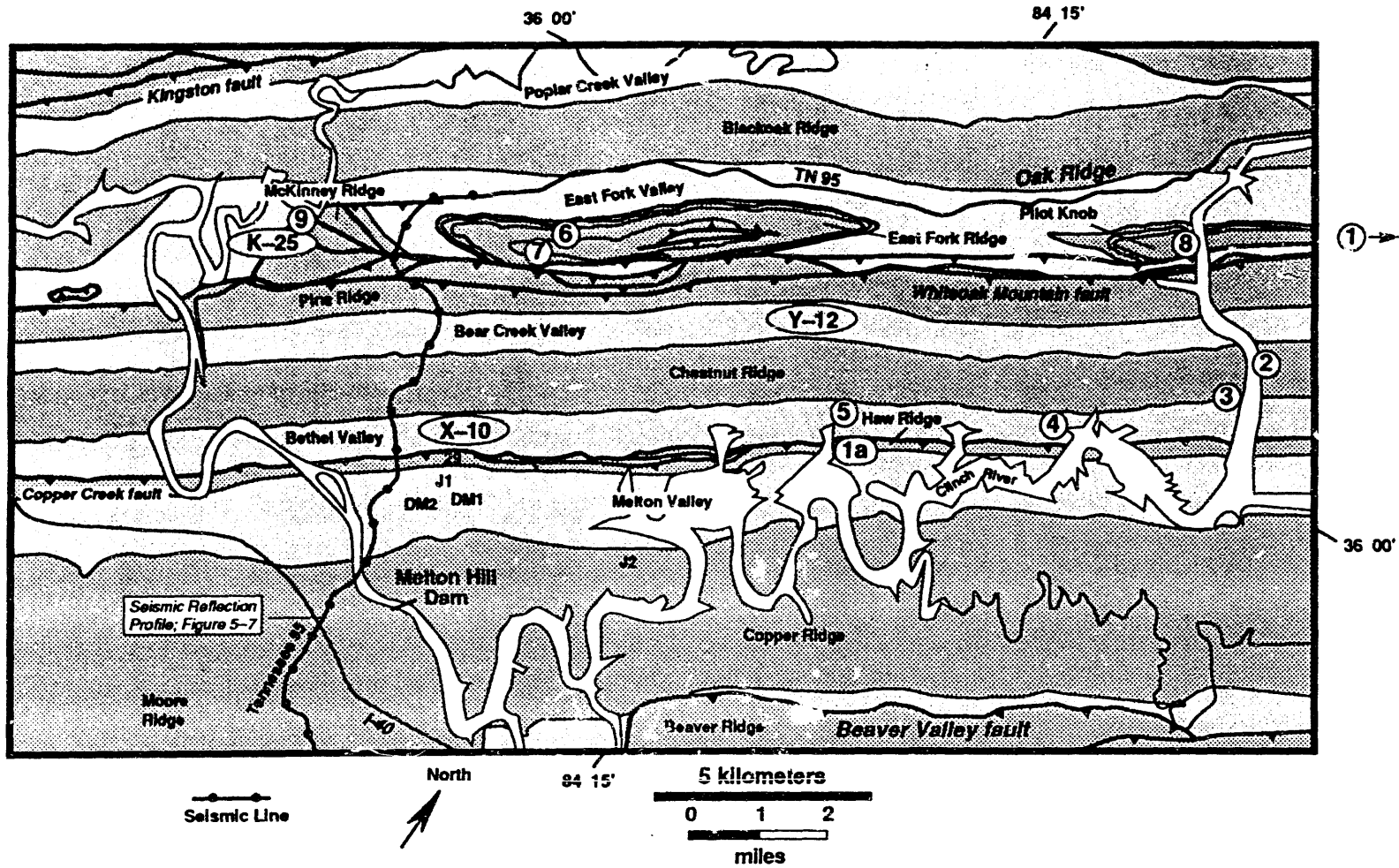


Figure A1-1. Locations of field trip stops.

Limestone Member (Rodgers and Kent 1948) has not been recognized here but may be present in the unexposed interval. The upper Rogersville is dominated by thin-laminated maroon shale containing light-gray calcareous siltstone lenses and glauconitic partings.

The Dismal Gap formation (formerly Maryville Limestone) at Dismal Gap consists of intraclastic, oölitic, and wavy-laminated limestone interbedded with dark-gray shale. Shales typically contain wavy-laminated, coalesced lenses of light-gray limestone and calcareous siltstone. In contrast to the underlying and overlying more shale-rich units, the silty limestone of the Dismal Gap produces a minor ridge here and in Bear Creek and Melton Valleys. This is the type section for the Dismal Gap formation.

The Nolichucky Shale is almost completely exposed at Dismal Gap. The lower Nolichucky is medium- to thick-bedded shale and limestone or calcareous siltstone. Shales are gray, olive gray, and maroon. Limestones are intraclastic or more typically oölitic with glauconite occurring occasionally. The Bradley Creek Member (Helton 1967) may be represented here. The upper Nolichucky is dark-gray shale with planar and wavy-laminated or ribbon-bedded limestone. Several thick (about 1 m) oölitic limestone beds occur in the upper Nolichucky and may be observed here.

The Maynardville Limestone is not well exposed at Dismal Gap, although exposures are present along strike. The contact with the Nolichucky Shale is covered by the road intersection.

The rocks in the Dismal Gap section, particularly those in the lower part, are complexly deformed (Fig. A1-2). Dip of bedding varies from shallow to steep and there are numerous mesoscopic folds and faults (Figs. A1-2 and A1-3). Deformation in the hanging wall of the Whiteoak

Mountain fault may have been sufficient to have produced some repetition of marker layers in the Rome Formation and possibly some apparent thickening in other parts of the Conasauga Group. Folds here are mostly flexural-slip buckle folds, along with some kinks. Thickening is present in the hinge zones of some of the tight buckle folds. This thickening is related to tightening in the hinge zones of folds and not to ductile flow. No cleavage has been observed in any of the rocks here.

STOP 1a (Alternate). Structure in the Copper Creek Thrust Sheet

This stop consists of two exposures (Fig. A1-4): Outcrop 1 contains folds (kink and buckle) and faults developed in thin-bedded siltstone and shale of the Pumpkin Valley Shale. Note that the amount of deformation increases toward the northwest end of the outcrop and the subtle change in overall bed dip that may reflect the geometry of the underlying fault zone. In addition, the largest fold contains a few small, tight folds in the core that are probably due to a material room problem. Between outcrops 1 and 2 a major imbricate fault is inferred, based on stratigraphic duplication evident while mapping along the ridge.

Outcrop 2 exposes folds, faults, and joints in the Rome Formation (Fig. A1-5). Although the exposure is not complete, a number of folds can be seen from the road that involve sandstones, siltstones, and shales. The systematic nature of some of the joint sets is evident on the bedding surfaces (as are nonstructural features such as ripple marks and fossil worm burrows). The tree-covered area contains a number of outstanding small folds and minor faulting in sandstone and shale units. In particular, a thick sandstone sequence contains minor imbricate faults that break

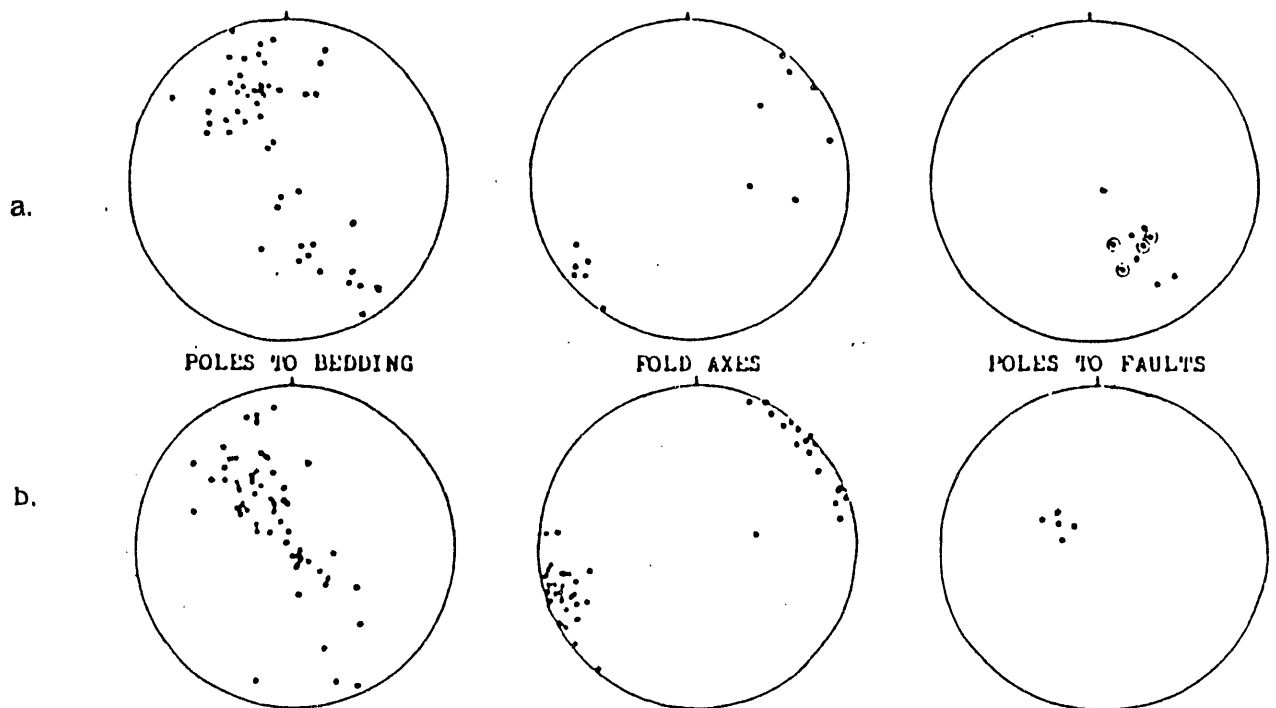


Figure A1-3. Lower hemisphere equal-area plots of structural data for the Rome Formation (a) and Conasauga Group (b) at Dismal Gap. (From Beets 1985.)

base of the Kingsport is well-exposed here. The base of the Longview is recognized by the appearance of white oölitic chert beds, yielding a thickness of ~42 m for the Longview. The base of the Chepultepec is also easily located by the appearance of a 2-m-thick zone of sandstone. The base of the Copper Ridge Dolomite is difficult to locate here because of the subdued topography along the railroad track. Here the top of the Maynardville Limestone is difficult to locate, but the location may be estimated by the disappearance of algal chert.

The uppermost unit consists of gray, olive, and maroonish limestone and calcareous siltstone with occasional fossiliferous and burrowed horizons. This unit is bounded on the southeast by the Copper Creek fault exposed near the bridge above Melton Hill Reservoir.

The rocks here dip uniformly toward the southeast. A number of joints are present that define the usual sets identified in the ORR. A northwest-striking, nearly vertical structure is present here that appears to be caused by pressure solution. This structure may be a spaced cleavage or a set of northwest-striking fractures that were not filled later.

STOP 3. MIDDLE ORDOVICIAN UNCONFORMITY AT EDMOOR ROAD AND MELTON LAKE DRIVE INTERSECTION

The Middle Ordovician (post-Knox) unconformity here consists of erosional debris—hematite-cemented breccia, conglomerate, and carbonate of the Blackford Formation (basal Five Oaks

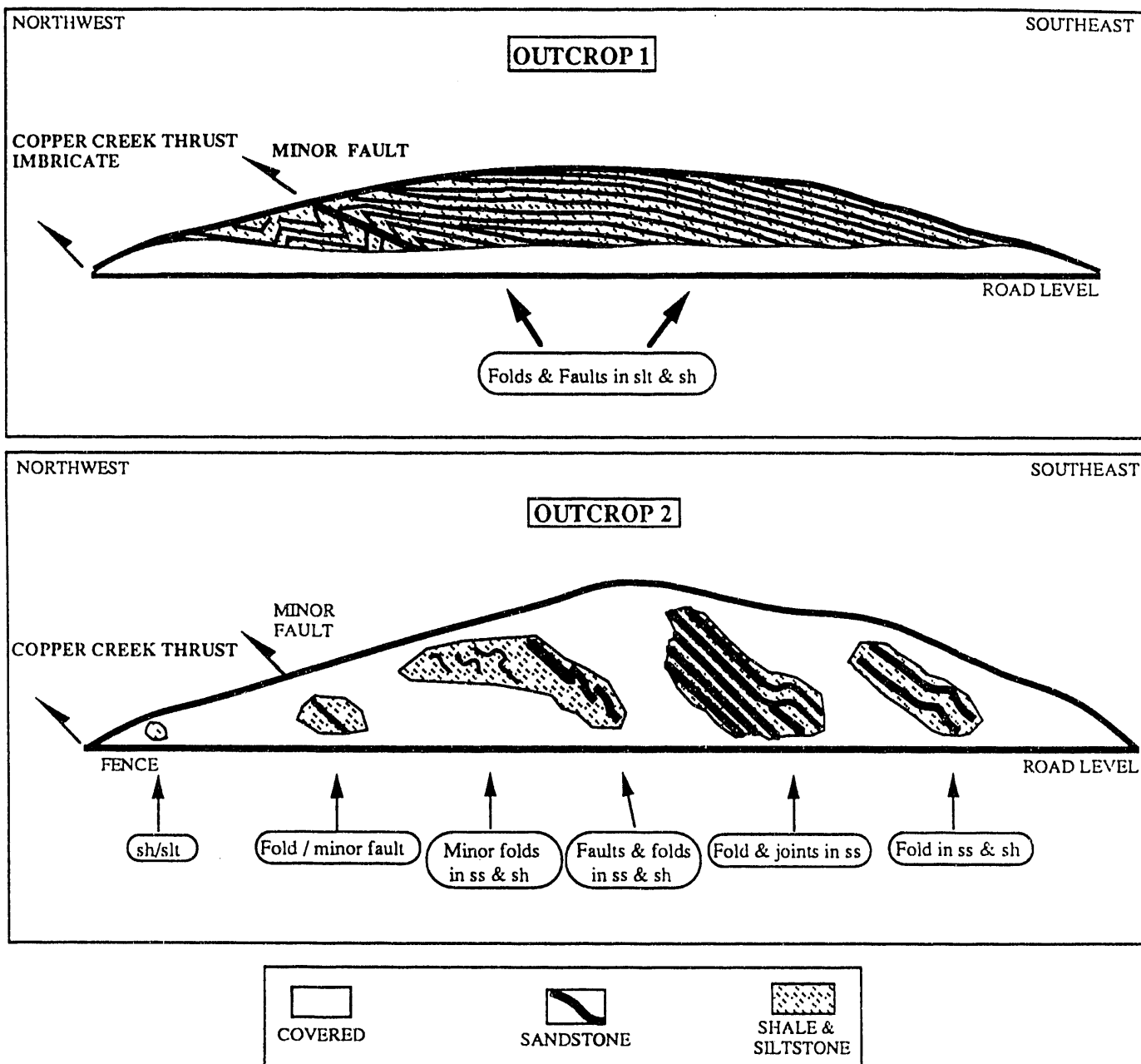


Figure A1-4. Sketch of structural features exposed in the hanging wall of the Copper Creek thrust at Haw Ridge at Stop 1a.

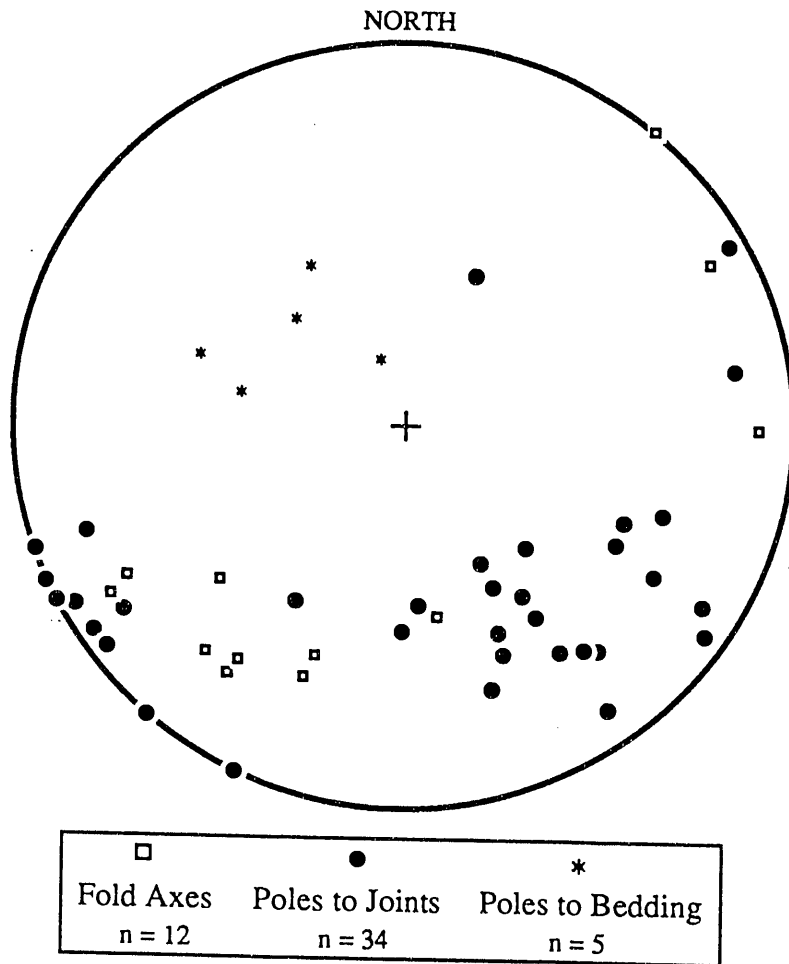


Figure A1-5. Lower hemisphere equal-area plot of structural elements at Stop 1a. Despite the small number of data points, note the presence of two joint sets.

Formation)—resting on Mascot Dolomite. This is one of the best exposures of this boundary in the area.

STOP 4. CHICKAMAUGA GROUP, COPPER CREEK FAULT, AND ROME FORMATION AT SOLWAY BRIDGE

The rocks at Stop 4 dip uniformly toward the southeast. A number of joints are present that define into the usual sets identified in the ORR. A northwest-striking, nearly vertical structure is present here that appears to be caused by pressure solution. This structure may be a spaced cleavage of a set of northwest-striking fractures that were not filled later.

Chickamauga Group rocks exposed at Stop 1 consist of thin- to thick-bedded medium-gray limestone typical of the upper part of the Chickamauga Group in Bethel Valley, and consists of the Witten and Moccasin Formations. One of the redbed units below the Witten (the Bowen Formation) is present but not well-exposed in the cut across the road from the main exposure. Most of the limestone in the Witten and Moccasin is micritic, but frequent zones of fossil hash are also present producing coarsely crystalline biosparite. Burrows are also present here.

Dip slopes in the lower Witten Formation exposed on the northwest side of the road expose an abundant fauna of brachiopods and ostracodes. The unit locally

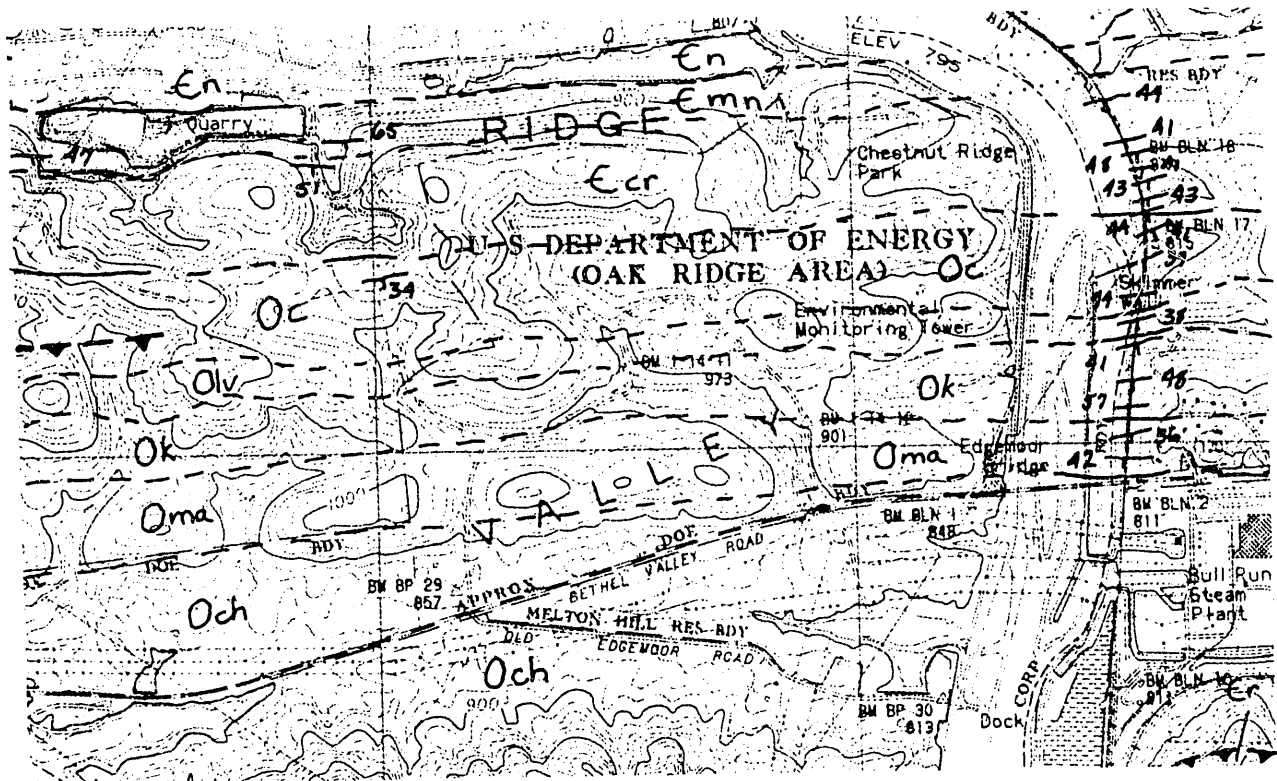


Figure A1-6. Geologic map of the area around Stop 2 at Bull Run Steam Plant.

contains abundant fossils on the southeast side of the road, but the fossils are more difficult to observe or collect because the exposure is not a dip slope.

Most of the Moccasin Formation is present at Stop 1. The Moccasin contains a very thin (4–6 m) but distinctive maroon calcareous siltstone and shale overlain by more than 75 m of limestone, nodular limestone, and calcareous siltstone. The uppermost Moccasin consists of gray, olive, and maroonish limestone and calcareous siltstone with occasional fossiliferous and burrowed horizons.

This unit is truncated on the southeast by the Copper Creek fault, exposed near the bridge above Melton Hill Reservoir. The fault truncates the Moccasin at a low angle and thrusts the Lower Cambrian Rome Formation over the Upper Ordovi-

gian Moccasin. The fault zone contains a thin cataclasite, but no major disturbed zone is present—typical of most faults in foreland fold–thrust belts.

The Rome Formation here consists of interbedded variegated shale and sandstone with minor dolomite.

STOP 5. CHICKAMAUGA GROUP ROCKS AT ROGERS QUARRY IN BETHEL VALLEY

The lower portion of the Chickamauga Group in Bethel Valley consists of more than 60 m (200 ft) of maroon calcareous siltstone and fissile shale with numerous thin limestone beds in the upper part. Vertical burrows commonly occur throughout this unit. The upper part of

this lithology forms the northern face of Rogers Quarry.

The 150-m-thick middle Chickamauga limestone unit consists of a lower, comparatively dense cherty limestone and an upper shaly and fossiliferous lithofacies. It underlies nearly all of ORNL. The lower half of the middle limestone is exposed at Rogers Quarry. These rocks generally consist of nodular and thick-bedded limestone containing nodular and bedded chert and produce a discontinuous low ridge throughout Bethel Valley. The upper half of the middle limestone unit consists of nodular limestone and calcareous siltstone with a distinctive yellow-buff weathered color. This yellowish-buff color can be seen in the soil on the southern edge of Rogers Quarry. Thin beds of shelly and bryozoan-rich fossil hash occur locally and can be seen in numerous small surface exposures.

We will look into Rogers Quarry from a vantage point, then walk across the road into the field to the southeast where the middle units of the Chickamauga are exposed.

STOP 6. ROCKWOOD FORMATION EXPOSED ALONG GLASSBORO DRIVE IN COUNTRY CLUB ESTATES

The Rockwood Formation exposed here consists mostly of tan to medium-brown shale and siltstone. Some fine- to medium-grained sandstone beds may be present. The rocks here dip moderately toward the southeast along the northwest limb of the East Fork Ridge syncline.

STOP 7. ROCKWOOD FORMATION, CHATTANOOGA SHALE, AND FORT PAYNE CHERT EXPOSED AT THE INTERSECTION OF GUM HOLLOW ROAD AND GRACELAND DRIVE IN COUNTRY CLUB ESTATES

It is possible to see the contacts between all three of these units exposed at the corner of Gum Hollow Road and Graceland Drive in Country Club Estates. The rocks here dip gently toward the southeast, and the black Chattanooga Shale is easily recognized separating the light-colored, more siliceous Fort Payne Chert above from the interlayered sandstone and shale of the Rockwood Formation below.

STOP 8. ROCKWOOD FORMATION ALONG MELTON HILL RESERVOIR AT PILOT KNOB

The western (upright) limb of the Pilot Knob syncline exposes Lower Silurian Rockwood Formation above the Upper Ordovician Sequatchie Formation. The southeast limb of the structure has been cut off by a splay of the Whiteoak Mountain fault that brings up part of a large slice (horse) of Middle Ordovician Chickamauga Group rocks.

The Rockwood here is composed of massive orthoquartzite (western tongue of Clinch (Tuscarora) Sandstone—a coarse portion of the Taconic clastic wedge) that grades upward into finer, thin-bedded tan sandstone, siltstone, shale, and several hematite layers high in the section. The top of the unit is not exposed here.

STOP 9. COMPLEX FAULTING IN QUARRY ON BLAIR ROAD NEAR K-25

The Whiteoak Mountain fault splays into the footwall near the Oak Ridge K-25

Site in the ORE, and this faulting may be responsible for the southwest termination of the East Fork Ridge syncline. An abandoned quarry ~1 km northeast of K-25 exposes a steeply dipping fault belonging to the family of splays related to the Whiteoak Mountain fault system. The rocks involved here belong to the Knox Group, probably the Copper Ridge or Chepultepec Dolomite. The fault contact is very sharp, typical of similar structures throughout the Valley and Ridge.

APPENDIX 2

SOIL SERIES

| <u>Soil Series</u> | <u>Geology</u> | <u>Drainage</u> | <u>Hydrology</u> | <u>Depth to Restriction</u> |
|--------------------|----------------------------|------------------|------------------|-----------------------------|
| | (Section Number) | 9.1 (see legend) | 9.2 (see legend) | 9.3 (see legend) |
| 000 | Rome residuum | 2 | R down dip | 50-100 cm (1) |
| 001 | Rome residuum | 1 | R down dip | <50cm (1) |
| 002 | Rome residuum | 2 | R down dip | 50-100 cm (1) |
| 003 | Rome residuum | 1 | R down dip | <50 cm (1) |
| 004 | Rome residuum | 2 | R down dip | 50-100 cm (1) |
| 005 | Whiteoak Mt. fault breccia | 2 | R fault breccia | >200 cm (none) |
| 006 | Whiteoak Mt. Fault Breccia | 2 | R fault breccia | >100 cm (1) |
| 008 | Rome residuum | 2 | R down dip | 50-100 cm (1) |
| 009 | Rome limestone | 2 | R karst | 100-200 cm (4) |
| 010 | Rome colluvium | 2 | R colluvium | >200 cm (none) |
| 011 | Rome colluvium | 2 | R colluvium | >200 cm (none) |
| 012 | Rome colluvium | 2 | R colluvium | >200 cm (none) |
| 013 | Rome colluvium | 2 | R-D colluvium | >200 cm (none) |
| 100 | Pumpkin Valley residuum | 2 | R down dip | 100-150 cm (1) |
| 101 | Pumpkin Valley residuum | 2 | R down dip | 50-100 cm (1) |
| 102 | Pumpkin Valley residuum | 2 | R down dip | 50-75 cm (1) |
| 103 | Pumpkin Valley residuum | 1 | R down dip | <50 cm (1) |
| 104 | Pumpkin Valley residuum | 2 | R down dip | 50-100 cm (1) |
| 105 | Rutledge residuum | 2 | R down dip | 50-100 cm (1) |
| 120 | Pumpkin Valley colluvium | 2 | R colluvium | >200 cm (none) |
| 121 | Pumpkin Valley colluvium | 2 | R-D colluvium | >200 cm (none) |
| 122 | Pumpkin Valley colluvium | 2 | R-D colluvium | >200 cm (none) |
| 123 | Pumpkin Valley colluvium | 2 | R colluvium | >200 cm (none) |
| 200 | Rogersville residuum | 1 | R down dip | < 50 cm (1) |
| 201 | Rogersville residuum | 2 | R down dip | 50 to 100 cm (1) |
| 202 | Rogersville residuum | 2 | R down dip | 75-125 cm (1) |
| 203 | Maryville residuum | 3 | R down dip | 100 to 150 cm (1) |
| 204 | Maryville residuum | 2 | R down dip | 75 to 125 cm (1) |
| 205 | Maryville residuum | 2 | R down dip | 50 to 125 cm (1) |
| 206 | Maryville residuum | 1 | R down dip | < 50 cm (1) |
| 207 | Maryville residuum | 2 | R down dip | 100 to 150 cm (1) |
| 220 | Conasauga Colluvium | 3 | R perched | > 150 cm (3) |
| 221 | Conasauga Colluvium | 2 | R perched | > 150 cm (3) |
| 222 | Conasauga Colluvium | 2 | R-D | 100-150 cm (3) |
| 223 | Conasauga Colluvium | 2 | R perched | > 100 cm (3) |
| 224 | Conasauga Colluvium | 3 | R-D perched | 75-125 cm (3) |
| 225 | Conasauga Colluvium | 2 | R-D | 100-150 cm (3) |
| 300 | Nolichucky residuum | 3-4 | R down dip | 50-125 cm (1) |
| 301 | Nolichucky residuum | 3 | R down dip | 50 to 100 cm (1) |
| 302 | Nolichucky residuum | 2-3 | R down dip | 50-125 cm (1) |
| 303 | Nolichucky residuum | 1-2 | R down dip | 50-100 cm (1) |
| 304 | Maynardville residuum | 2 | R down dip | >150 cm (1) |
| 305 | Maynardville residuum | 2 | R karst | 50-150 cm (4) |
| 306 | Maynardville residuum | 2 | R karst | 0-100 cm (4) |
| 400 | Copper Ridge residuum | 2 | R karst | >200 cm (3) |
| 401 | Copper Ridge residuum | 2 | R karst | >200 (3) |
| 402 | Chepultepec residuum | 2 | R karst | >200 (3) |
| 403 | Longview residuum | 2 | R karst | >200 cm (3) |
| 404 | Mascot residuum | 2 | R karst | >200 cm (3) |
| 405 | Mascot residuum | 2 | R karst | 25->200 cm (4) |
| 406 | Kingsport residuum | 2 | R karst | >200 cm (3) |
| 407 | Kingsport residuum | 2 | R karst | >200 cm (3) |
| 408 | Chepultepec residuum | 2 | R karst | >200 cm (3) |
| 409 | Copper Ridge residuum | 2 | R karst | 0->200 cm (4) |
| 430 | Knox colluvium | 2-3 | R-D colluvium | "75-125 cm (2, 3)" |
| 431 | Knox colluvium | 2-3 | R-D colluvium | 50-150 cm (3) |
| 432 | Knox colluvium | 2 | R-D colluvium | 50-150 cm (3) |
| 433 | Knox colluvium | 2 | R-D colluvium | 50-150 cm (3) |
| 434 | Knox colluvium | 2 | R-D colluvium | 50-150 cm (3) |
| 435 | Knox colluvium | 2 | R-D colluvium | 50-150 cm (3) |

| <u>Soil Series</u> | <u>Geology</u> | <u>Drainage</u> | <u>Hydrology</u> | <u>Depth to Restriction</u> |
|--------------------|-------------------------------------|-----------------|------------------|-----------------------------|
| 436 | Ancient colluvium | 2 | R-D colluvium | 50-150 cm (3) |
| 437 | Doline sediments | 2-3 | R-D doline | "50-125 cm (2, 3)" |
| "438, 438x" | Doline sediments | 2-3 | R dolines | 50-150 cm (3) |
| "439, 439x" | Doline sediments | 4-5 | R dolines | 50-150 cm (3) |
| 500 | Chickamauga Unit B | 2 | R karst | 25-125 cm (4) |
| 501 | Chickamauga Unit C | 1-2 | R karst | 0-50 cm (4) |
| 503 | Chickamauga Unit E | 2-3 | R karst | 50-150 cm (1) |
| 504 | Chickamauga Unit C | 1 | R karst | 0-50 cm (4) |
| 505 | Chickamauga Unit E | 3 | R karst | 50-100 cm (4) |
| 507 | Moccasin Fm. | 2 | R karst | 50-100 cm (4) |
| 540 | Chickamauga colluvium | 2 | R-D perched | "75-125 cm (2, 3)" |
| 541 | Chickamauga colluvium | 2 | R-D perched | "75-125 cm (2, 3)" |
| 600 | Chickamauga Unit A | 2 | R karst | 75-150 cm (1) |
| 601 | Chickamauga Unit A | 2 | R karst | "125->150 cm (1, 4)" |
| 602 | Chickamauga Unit E | 3 | R karst | 100->150 cm (1) |
| 603 | Chickamauga Unit E | 2-3 | R karst | >150 cm (1) |
| 605 | Chickamauga Unit E | 2-3 | R karst | 100-150 cm (1) |
| 606 | Chickamauga Unit D | 2 | R karst | >200 cm (4) |
| 607 | Chickamauga Unit B | 2 | R karst | "100-125 cm (1,4)" |
| 700 | Reedsville and younger residuum | 2 | R down dip | 100-150 cm (1) |
| 750 | Rockwood colluvium | 2 | R-D perched | 50-150 cm (3) |
| 751 | Rockwood colluvium | 2 | R-D perched | 50-150 cm (3) |
| 752 | Rockwood colluvium | 2-3 | R-D perched | 50-100 cm (3) |
| 960 | Rome and Pumpkin Valley alluvium | 2-3 | D | 80-100 cm (3) |
| 961 | Rome and Pumpkin Valley alluvium | 2-3 | D | 80-100 cm (3) |
| 962 | Rome and Pumpkin Valley alluvium | 4-5 | D | 80-100 cm (3) |
| 970 | Conasauga alluvium | 3 and 4 | D | 100 to > 150 cm (3) |
| 971 | Conasauga alluvium | 4 and 5 | D | 100 to > 150 cm (3) |
| 972 | Conasauga alluvium | 4-5 | D | 50-90 cm (3) |
| 980 | Knox alluvium | 2-3 | D | 50-150 cm (3) |
| 981 | Knox alluvium | 2-3 | D | 100-150 cm (3) |
| 982 | Knox alluvium | 4-5 | D | 100-150 cm (3) |
| 983 | Chickamauga alluvium | 2-3 | D | 50-150 cm (3) |
| 984 | Chickamauga alluvium | 4-5 | D | 50-100 cm (3) |
| 985 | Sediments from Dark red alluvium | 2 | R | >200 cm (none) |
| 990 | Ancient dark red alluvium | 2 | R | >200 cm (none) |
| 991 | Ancient loess covered alluvium | 2 | R-D | 50-100 cm (3) |
| 992 | High terrace on Conasauga | 2-3 | R | 100-150 cm (3) |
| 993 | High terrace on Conasauga | 2 | R | 100-150 cm (3) |
| 994 | Ancient alluvium colluvium on Knox | 2 | R | >200 cm (none) |
| 995 | Loess covered alluvium on Conasauga | 2-3 | R | 50-125 cm (3) |
| 996 | Old alluvium on Conasauga | 3 | R perched | 75 to 125 cm (2) |
| 997 | Stranded river terrace | 2 | R | >200 cm (none) |
| 998 | Stranded river terrace | 2 | R | >200 cm (none) |
| 999 | Holocene river terrace | 2 or 3 | R | > 100 cm (3) |

LEGEND

| | | | |
|----------------------|-------------------|--------------|-------------------|
| DRAINAGE | 1 excess | 2 well | 3 mod. well |
| "Drainage, cont." | 4 somewhat poorly | | 5 poorly |
| HYDROLOGY | D = discharge | R = recharge | |
| DEPTH TO RESTRICTION | 1 paralithic | 2 fragipan | 3 change in perm. |
| | 4 lithic | | |

| <u>Soil Series</u> | <u>Disturbed Eros Pot</u> | <u>Undisturbed Eros Pot</u> | <u>Pines</u> | <u>Hardwoods</u> |
|--------------------|---------------------------|-----------------------------|--------------|------------------|
| Section | 9.4 | 9.5 | 9.6 | 9.7 |
| 000 | H | L | F | G |
| 001 | H | L | P-F | F |
| 002 | H | M | P-F | F |
| 003 | H | M | P-F | F |
| 004 | H | L-M | F | F |
| 005 | M | L | G | G |
| 006 | M | L | G | G |
| 008 | H | L | F | F |
| 009 | H | M | G-F | F-G |
| 010 | M | L | G | G |
| 011 | M | L | G | G |
| 012 | H | L | G | G |
| 013 | H | L | G wet | G |
| 100 | M-H | L | G | G |
| 101 | M-H | L | F | F |
| 102 | H | L | F | F |
| 103 | H | L | P-F | F |
| 104 | H | L-M | P-F | F |
| 105 | M-H | M | F | G |
| 120 | M | L | G | G |
| 121 | M | L | G | G |
| 122 | M | L | G | G |
| 123 | M-L | L | G | G |
| 200 | H | M | P | F |
| 201 | H | M | F | G |
| 202 | H | M | G | G |
| 203 | H | M | F | G |
| 204 | M | L-M | F | G |
| 205 | M-H | M | F | F |
| 206 | H | H | P | F |
| 207 | M-H | M | G | G |
| 220 | L-M | L | G | G |
| 221 | L-M | L | G | G |
| 222 | L-M | L | G | G |
| 223 | M | L | G | G |
| 224 | M-H | L-M | F | F |
| 225 | H | L | G | G |
| 300 | H | L-M | G | G |
| 301 | M-H | M | F | F |
| 302 | H | L-M | G | G |
| 303 | H | L-M | F | F |
| 304 | H | L-M | G | G |
| 305 | H | L | G | G |
| 306 | H | L-M | F-P | F-G |
| 400 | M | L | G | G |
| 401 | M | L | G | G |
| 402 | M | L | G | G |
| 403 | M | L | G | G |
| 404 | M | L | G | G |
| 405 | M | L | G | G |
| 406 | M | L | G | G |
| 407 | M | L | G | G |
| 408 | M | L | G | G |
| 409 | M | L | G | G |
| 430 | M | L | G | G |
| 431 | L | L | G | G |
| 432 | M | L | G | G |
| 433 | M | L | G | G |
| 434 | M | L | G | G |
| 435 | M | L | G | G |
| 436 | M | L | G | G |
| 437 | L | L | G | G |
| "438, 438a" | L | L | G | G |
| "439, 439a" | L | L | G | G |
| 500 | H | L | F | F |
| 501 | H | L | P | F-F |
| 503 | H | M | G | G |
| 504 | H | M | P | P |

228

| <u>Soil Series</u> | <u>Disturbed Eros Pot</u> | <u>Undisturbed Eros Pot</u> | <u>Pines</u> | <u>Hardwoods</u> |
|--------------------|---------------------------|-----------------------------|--------------|------------------|
| 505 | H | L - M | P - F | G |
| 507 | H | M - H | P | F - G |
| 540 | M | L | G | G |
| 541 | M | L | F - G | G |
| 600 | H | L | G | G |
| 601 | M - H | L | G | G |
| 602 | H | L | G | G |
| 603 | H | L | G | G |
| 605 | H | L | G | G |
| 606 | M | L | G | G |
| 607 | H | L | G | G |
| 700 | H | L | G | G |
| 750 | M | L | G | G |
| 751 | M | L | G | G |
| 752 | H | L | G | G |
| 960 | M | L | G | G |
| 961 | M | L | G | G |
| 962 | L | L | P - F | G |
| 970 | M | L | F - G | G |
| 971 | L | L | P - F | G |
| 972 | L | L | P - F | G |
| 980 | M - H | L | F - G | G |
| 981 | M | L | F - G | G |
| 982 | L | L | P - F | G |
| 983 | M | L | F - G | G |
| 984 | L | L | P - F | G |
| 985 | L | L | G | G |
| 990 | M - H | L | G | G |
| 991 | H - V H | L | G | G |
| 992 | H | L | G | G |
| 993 | M - H | L | G | G |
| 994 | M - H | L | G | G |
| 995 | V H | L | G | G |
| 996 | V H | L | F - P | F - G |
| 997 | M | L | G | G |
| 998 | M | L | G | G |
| 999 | M | L | G | G |

LEGEND

EROS POT. L - Low M - Medium H - High V H - Very High

| <u>Soil Series</u> | <u>Streets & Roads</u> | <u>Unpaved Roads</u> | <u>Trench Waste Disposal</u> | <u>Tumulus Suitability</u> |
|--------------------|----------------------------|------------------------------|------------------------------|----------------------------|
| See Section | 9.8 | 9.9 | 9.10 | 9.11 |
| 000 | G | V P steep and rock | P too permeable | P |
| 001 | P | V P too steep | P too steep | P too steep |
| 002 | P | "V P steep, unstable" | P too steep | P too steep |
| 003 | G | P too steep | P too steep | P too steep |
| 004 | F | P too steep | P too steep | P too steep |
| 005 | F - P | F too clayey | G | G |
| 006 | F | F steep | G | F - G |
| 008 | F | F steep | F | F - G |
| 009 | P | P rock | P pinnacles | P rock outcrops |
| 010 | F | G | P lateral water | G |
| 011 | F | G | P lateral water | G |
| 012 | P | F - P unstable base | P lateral water | G |
| 013 | F | P unstable and wet | VP high water | F wetness |
| 100 | F | F high clay | F-G | G |
| 101 | F | F high clay | F-G | G |
| 102 | F | P steep | F-G | G |
| 103 | F | V P steep | P | G |
| 104 | P too silty | P too high in silt plus clay | F-P | G |
| 105 | P | "P thin, high silt" | P too steep | P too steep |
| 120 | G | F - G high clay | G | G |
| 121 | G | F - G wetness | P lateral water | F |
| 122 | G | F - G wetness | P lateral water | P wetness |
| 123 | G | F unstable base | P lateral water | G |
| 200 | V P | V P too steep | V P too steep | V P too steep |
| 201 | P too high in silt | P highly variable | P too steep | P too steep |
| 202 | P too clayey | P unstable base | F-G depth to water | G |
| 203 | P too clayey | P unstable base | G | G |
| 204 | F too silty | P too silty | F - G depth to water | G |
| 205 | F | P too silty | F - G depth to water | G |
| 206 | P | P too silty | P too steep | P too steep |
| 207 | P too steep | "P too steep, high silt" | F too steep | P too steep |
| 220 | F | "P wetness, unstable base" | P water | P unstable base |

| <u>Soil Series</u> | <u>Streets & Roads</u> | <u>Unpaved Roads</u> | <u>Trench Waste Disposal</u> | <u>Tumulus Suitability</u> |
|--------------------|----------------------------|---------------------------------------|------------------------------|----------------------------|
| 221 | F | F unstable base | P water | P unstable base |
| 222 | G | F - G | P lateral water | G |
| 223 | F | F too silty at depth | P water | P unstable base |
| 224 | F | "F wetness, unstable base" | P water | F - P |
| 225 | F - P | "P unstable base, too clayey" | P water | F |
| 300 | P | "P wetness, too clayey" | P | F |
| 301 | F | P too clayey | P water | G |
| 302 | P too clayey | P unstable base | F | G |
| 303 | P | P steep | P | P |
| 304 | P too clayey | "P unstable base, high silt and clay" | F | G |
| 305 | P rock | V P variable depth to limestone | P rock | P rock |
| 306 | P too clayey | V P too clayey | P rock | P rock |
| 400 | F - G | "F unstable base, too clayey" | G | G |
| 401 | F - G | "F unstable base, too clayey" | G | G |
| 402 | G | "F unstable base, high silt and clay" | G | |
| 403 | G | F unstable base | G | G |
| 404 | G | F high chert | G | G |
| 405 | P - F rock | "P depth to rock, high clay" | P rock pinnacles | P rock outcrops |
| 406 | G | P high clay and silt | G | G |
| 407 | G | F unstable base | G | G |
| 408 | F large chert | F steep | G | G |
| 409 | P rock outcrops | V P depth to rock | P rock | P rock |
| 430 | G | F perched water | P-F lateral water | G |
| 431 | P | P unstable base | P wetness | P dolines |
| 432 | F - G | F - G | P-F lateral water | G |
| 433 | F - G | "P steep slopes, unstable base" | P-F lateral water | G |
| 434 | F - G | F - G high silt | P-F | G |
| 435 | F - G | F high clay | P-F | G |
| 436 | G | G | P-F lateral water | G |
| 437 | P too silty | "P unstable base, high silt" | "P wetness, dolines" | P dolines |
| "438, 438a" | P too silty | V P very high silt | P dolines | P dolines |
| "439, 439a" | P too silty | V P very high silt | P dolines | P dolines |
| 500 | P rock | P depth to hard rock | P rock | P rock |
| 501 | P rock | V P rock outcrops | P rock | P rock |

| <u>Soil Series</u> | <u>Streets & Roads</u> | <u>Unpaved Roads</u> | <u>Trench Waste Disposal</u> | <u>Tumulus Suitability</u> |
|--------------------|----------------------------|--------------------------------|------------------------------|----------------------------|
| 503 | F | "V P unstable base, high clay" | F | G |
| 504 | P | V P depth to hard rock | P | P |
| 505 | P rock | "V P rock, wet" | "P rock, wet" | "P rock, wet" |
| 507 | P rock | "P clayey, rock" | V P rock | V P rock |
| 540 | F - G | "P - F high silt, wetness" | P water | F - G |
| 541 | F - G | F - G high silt | P water | G |
| 600 | P too clayey | "P high clay, unstable base" | P rock | G |
| 601 | F | F - P. too clayey | P rock | G |
| 602 | P - F | P unstable base | P wetness | G |
| 603 | F - P | P unstable base. | P | G |
| 605 | F - P | "P unstable base, high silt" | P | G |
| 606 | G | F | F | G |
| 607 | F | F high silt | P | G |
| 700 | G | F | P-F | G |
| 750 | F - G | G | P | G |
| 751 | F - G | G | P | G |
| 752 | P - F | P unstable base | P | G |
| 960 | F | P floods frequently | P | P |
| 961 | F | F | P | P |
| 962 | P | V P very freq. flooding | P | P |
| 970 | P | "V P very high silt, floods" | P water | P unstable base |
| 971 | P floods | "V P very freq. floods, wet" | P floods and wetness | P floods |
| 972 | P | "V P very freq. floods, wet" | P | P |
| 980 | F - G | P - F wetness | P | P |
| 981 | F | "F - G wetness, floods" | P | P |
| 982 | P | P very freq. flooding | P | P |
| 983 | F - G | P - F wetness | P | P |
| 984 | P | "V P wetness, high clay" | P | P |
| 985 | P | P high silt | P ponds | P ponds |
| 990 | F - G | G | G | G |
| 991 | F | "P unstable base, high silt" | P lateral water | F unstable base |

| Soil Series | Streets & Roads | Unpaved Roads | Trench Waste Disposal | Tumulus Suitability |
|--------------------|----------------------------|-------------------------------------|------------------------------|----------------------------|
| 992 | F | "P unstable base, high silt" | F-G | F unstable base |
| 993 | F - G | F high silt | P-F lateral water | F-G |
| 994 | F - G | F - G | G | F-G unstable base |
| 995 | P too silty | "V P very unstable base, high silt" | P water | P unstable base |
| 996 | P | V P very high silt | P water | P unstable base |
| 997 | F - G | F - G | G | F |
| 998 | F - G | F - G | G | F |
| 999 | F | F - G | P water | P unstable base |

LEGEND

G Good F Fair P Poor V P Very Poor

| <u>Soil Series</u> | <u>Source of Fill</u> | <u>Source of Cover</u> | <u>Septic Tank Drainfields</u> | <u>Low Buildings</u> |
|--------------------|---------------------------------|------------------------|----------------------------------|----------------------|
| See Section | 9.12 | 9.13 | 9.14 | 9.15 |
| 000 | P thin | P too sandy | V P steep and rock | V P too steep |
| 001 | F thin | P thin | "P Steep, too perm." | V P too steep |
| 002 | "V P too clayey, thin" | P thin | P steep | V P too steep |
| 003 | F thin | P thin | "V P too steep, rock" | V P too steep |
| 004 | "P steep, thin" | P thin | "V P too steep, rock" | P - F steep |
| 005 | P - F high silt plus clay | G | F - G | F - G |
| 006 | F | F - G | F - G | P - F steep |
| 008 | F - P thin | F - G | F depth | P - F steep |
| 009 | "V P too clayey, thin" | P too clayey | P - V P rock | V P rock |
| 010 | G | G | G requires intercept. drain | F steep |
| 011 | G | G | G requires intercept. drain | F - G |
| 012 | P too high in silt and clay | G | "F- P perched water, too clayey" | F - G clayey |
| 013 | F - P wetness | F | P perched water and wetness | F - P wetness |
| 100 | P high clay and silt | G | F - G requires intrcept. drain | P - F steep |
| 101 | P high silt plus clay | G | P depth | V P too steep |
| 102 | "P thin, high clay" | G | V P steep and depth | V P too steep |
| 103 | V P thin | F | V P too steep | V P too steep |
| 104 | "V P thin, high silt plus clay" | F too silty | "V P depth, perched water" | P steep |
| 105 | P thin. high silt | P | V P depth and perched water | P - F dif. sett |
| 120 | F - G high clay | G | F - G requires intercept drain | F steep |
| 121 | F - G wetness | G | F - G requires intercept. drain | F - G |
| 122 | F wetness | G | "P - V P wetness, perched water" | P floods |
| 123 | F - G high silt | G | F - G requires intercept drain | F - G |
| 200 | V P too steep | V P | "V P steep, shallow" | V P too steep |
| 201 | "V P too thin, high silt" | P | "V P depth, perched water" | F diff. sett |
| 202 | "V P too clayey, thin" | P too clayey | "V P depth, perched water" | F - G diff. settl |
| 203 | V P too clayey | P too clayey | "V P perched water, imperm." | F diff. settl. |
| 204 | P too silty | P too silty | F - G depth | F - G |
| 205 | P too silty | P too silty | "V P depth, perched water" | "P - F diff, settl" |
| 206 | "P too silty, thin" | P | "V P too steep, depth" | V P too steep |

| <u>Soil Series</u> | <u>Source of Fill</u> | <u>Source of Cover</u> | <u>Septic Tank Drainfields</u> | <u>Low Buildings</u> |
|--------------------|--------------------------------|------------------------|----------------------------------|----------------------|
| 207 | "P too steep, high silt" | F too silty | P - F too steep | V P too steep |
| 220 | P too clayey | G | V P wetness | F wetness |
| 221 | F too silty | G | F - G requires intercept. drain | F - G |
| 222 | F - G | G | F - G requires intercept. drain | G |
| 223 | F - P too silty at depth | F - G | F requires intercept. drain | F - P unstable |
| 224 | F too silty | F - P | "P perched water, imperm." | P - F wetness |
| 225 | P too clayey | F - P | "P perched water, imperm." | F - G |
| 300 | "P too clayey, thin" | P | "V P depth, wetness" | P wetness |
| 301 | P too clayey | P | "V P depth, perched water" | F - P diff. settl |
| 302 | V P too clayey | P | "V P wetness, imperm." | F clayey |
| 303 | "P steep, thin" | P thin | "V P too steep, depth" | P steep |
| 304 | V P too high in silt and clay | P too silty | P imperm | P clayey |
| 305 | V P too clayey | P thin | "V P depth, floods" | "V P rock, floods" |
| 306 | "V P thin, too clayey" | V P too clayey | V P rock | P |
| 400 | F - P high silt and clay | G | "F - P imperm., steepness" | P - G slopes |
| 401 | "P high silt plus clay, rock" | G | "F - P imperm., steepness" | "P too steep, rock" |
| 402 | P high silt and clay | G | P - F imperm. | P - G slopes |
| 403 | F - P high silt and clay | G large frags. | F - P imperm. | "P - F slopes, sto" |
| 404 | P - F high chert and clay | G | F imperm. | "P - F slopes, sto" |
| 405 | "P high clay, depth" | F-P thin | P - V P depth to limestone | "P rock, slopes" |
| 406 | P high clay and silt | G | P - F imperm. | P - G slopes |
| 407 | F high silt | G | F - G | P slopes |
| 408 | "F high chert, steep" | F large chert | "P - F imperm, steep slopes" | P slopes |
| 409 | "V P high clay, depth to rock" | P thin | V P depth to limestone, V P rock | |
| 430 | F - G high chert | G | F - G requires intercept. drain | F - G slopes |
| 431 | P too silty | G final cover | F - P requires intercept. drain | P - V P dolines |
| 432 | F - G | G | F - G requires intercept. drain | F - G |
| 433 | F high silt | G | F - G steep slopes | V P too steep |
| 434 | F high silt | G | G usually needs intercept. drain | P - G slopes |
| 435 | F - P high clay | G | P imperm. | P steep |
| 436 | "G thin layer, P beneath" | G | F - G | G |
| 437 | V P high silt | P too silty | "P perched water, fragipan" | P unstable |

| <u>Soil Series</u> | <u>Source of Fill</u> | <u>Source of Cover</u> | <u>Septic Tank Drainfields</u> | <u>Low Buildings</u> |
|--------------------|-------------------------------|------------------------|--|----------------------|
| "438, 438a" | V P very high silt | P too silty | V P in depressions | V P dolines |
| "439, 439a" | V P very high silt | P too silty | "V P in depressions, wet" | "V P wet, dolines" |
| 500 | V P thin and depth to rock | P thin | V P shallow to limestone | "V P rock, slopes" |
| 501 | V P very thin | P thin | V P depth to limestone | "V P rock, slopes" |
| 503 | V P high clay and silt | P too silty | "V P imperm, wetness" | "P - F clayey, slo" |
| 504 | V P very shallow to hard rock | P | V P very shallow to limestone | V P rock |
| 505 | V P sticky clay | P | V P wet | P |
| 507 | "V P too clayey, rock" | V P too clayey | V P rock | P |
| 540 | F - G high silt | F-G | "P - F wet, requires intercept. drain" | "P - F wetness, sl" |
| 541 | F - G high clay at depth | G | F requires intercept. drain | "P - F wetness, sl" |
| 600 | V P too clayey | P too clayey | P imperm. | "P - F slopes, roc" |
| 601 | P too clayey | F | F - P imperm | "P - F slopes, roc" |
| 602 | V P high silt and clay | F-P | "V P wetness, imperm." | "F wet, slopes" |
| 603 | V P too high in silt and clay | P too clayey | P - V P imperm. | F clayey |
| 605 | V P too high in silt and clay | F-P too silty | "P - V P wetness, imperm." | F clayey |
| 606 | F high clay and silt | G | F - G imperm. | P - G slopes |
| 607 | P high silt and clay | F thin | "P - F imperm, depth to rock" | "P - F rock, slope" |
| 700 | F | F thin | F - P depth | P slopes |
| 750 | G | G | G requires intrcept. drain | F slopes |
| 751 | G | G | G requires intercept. drain | F slopes |
| 752 | P too clayey | F | F - P requires intercept. drain | P clayey |
| 960 | F | F | P floods frequently | P floods |
| 961 | F high silt | G | F rare flood hazard | F - G |
| 962 | P wetness | P | "V P wetness, very freq. flooding" | "V P. floods, wet" |
| 970 | V P very high silt | P | V P frequent flooding | V P floods |
| 971 | V P floods | P | "V P very freq. floods, very wet" | "V P floods, wet" |
| 972 | V P too silty and clayey | P | "V P very freq. flooding, wetness" | "V P floods, wet" |
| 980 | F - G | G | P - F requires intewrcept. drain | "P floods, wet" |
| 981 | F high chert | P | "V P frequent flooding, wetness" | "V P floods, wet" |
| 982 | F high chert | P | "V P very freq. flooding, wetness" | "V P. floods, wet" |
| 983 | F - G high chert | P | P - F requires intercept. drain | "P slopes, wet" |
| 984 | "V P high clay, wetness" | P | "V P very freq. flooding, wetness" | "V P floods, wet" |

| <u>Soil Series</u> | <u>Source of Fill</u> | <u>Source of Cover</u> | <u>Septic Tank Drainfields</u> | <u>Low Buildings</u> |
|--------------------|-----------------------|------------------------|---------------------------------|----------------------|
| 985 | P too silty | P | P floods | P floods |
| 990 | F high clay | G | G | P - G slopes |
| 991 | P high silt | F too silty | F - G requires intercept. drain | "F slopes, high si" |
| 992 | P high silt | F | F - G imperm. | F high silt |
| 993 | P - F high silt | G | F - G | F slopes |
| 994 | F - G | G | F - G | P - G slopes |
| 995 | V P very high silt | P too silty | F wetness | "V P wet, too silt" |
| 996 | V P very high silt | F - G | "V P perched water, wetness" | "V P wet, too sil" |
| 997 | F - G | G | F - G imper. | P - G slopes |
| 998 | F high silt | G | F - G | F - G slopes |
| 999 | F - G high silt | G | F - G | F - G slopes |

LEGEND

G - Good F - Fair P - Poor V P - Very Poor

APPENDIX 3

OAK RIDGE RESERVATION SOIL CODING LEGEND

A five-digit number system was devised to code all important soil map information for easy computer sorting and manipulation in the soil survey.

The **first digit** codes the important geologic formations.

The **second digit** codes for residuum, colluvium, and alluvium by major geologic formations and for Pleistocene alluvium.

The **third digit** codes for each individual soil.

The **fourth digit** codes each slope gradient class.

The **fifth digit** codes for soil erosion class or other soil or landform properties considered important for planning or utilization.

EXAMPLE OF SOIL MAP CODE

40043 4 _ _ _ _ is the geologic code (Knox Group)
 _ 0 _ _ _ is the geomorphic code (Knox residuum)
 _ _ _ 0 _ is the individual soil code (Copper Ridge Residuum)
 _ _ _ _ 4 _ is the slope code (12 to 25% slopes)
 _ _ _ _ _ 3 is the erosion code (severe)

1st Digit Codes. _0000 Geologic formations

| | |
|---|---|
| 0 | Rome |
| 1 | Conasauga-Pumpkin Valley/Rutledge |
| 2 | Conasauga-Rogersville/Maryville |
| 3 | Conasauga-Nolichucky/Maynardville |
| 4 | Knox-Copper Ridge/Chepultepec/Longview/Kingsport/Mascot |
| 5 | Chickamauga (Lithic within 100 cm) |
| 6 | Chickamauga (deep and paralithic) |
| 7 | Silurian/Devonian/Mississippian |
| 8 | Altered Land (Cut, Cut and Fill, Fill, Burial trenches) |
| 9 | Alluvium |

2nd Digit Codes. 0_000 Geomorphic codes

| | |
|---|-----------------------|
| 0 | residuum |
| 1 | Rome colluvium |
| 2 | Conasauga colluvium |
| 3 | Knox colluvium |
| 4 | Chickamauga colluvium |

- | | |
|---|--|
| 5 | Silurian/Devonian, Mississippian colluvium |
| 6 | Rome alluvium |
| 7 | Conasauga alluvium |
| 8 | Knox/Chickamauga alluvium |
| 9 | Pleistocene-Tertiary alluvium |
-

3rd Digit Codes. 00_00 Individual soil identification numbers, 0 through 9. The first three digits more specifically relates individual soils to their underlying rock types.

4th Digit Codes. 000_0 Slope classes

- | | |
|---|------------------|
| 1 | 0 to 2% slopes |
| 2 | 2 to 5% slopes |
| 3 | 5 to 12% slopes |
| 4 | 12 to 25% slopes |
| 5 | 25 to 45% slopes |
| 6 | >45% slopes |
-

5th Digit codes. 0000_ Past Erosion Classes and Altered Lands

- | | |
|---|--|
| 1 | none to slight accelerated erosion |
| 2 | moderate accelerated erosion |
| 3 | severe accelerated erosion |
| 4 | very severe erosion with few to many gullies |
| 5 | cut land |
| 6 | fill land |
| 7 | cut and fill land |
| 8 | waste burial areas |

The first three digits define each individual member of the soil system in terms of the geology and geomorphology and are shown beneath. The residual and colluvial soils are organized according to geologic parent materials. The alluvial soils are grouped according to age, parent materials, and wetness. The mapping unit descriptions that follow are organized in the same sequence.

Code Classification and [Parent Material(s)]Rome Group residuum

- 000 Typic Hapludults; sandy or coarse-loamy or fine-loamy, mixed, thermic. [Arkosic sandstone.]
- 001 Typic Dystrochrepts; loamy-skeletal, mixed, thermic, shallow, very steep. [Arkosic sandstone and siltstone.]
- 002 Typic Dystrochrepts or Ruptic-Ultic Dystrochrepts or Ochreptic Hapludults; loamy-skeletal, mixed, thermic. [Maroon sandstone and shale, fine and medium grained feldspathic sandstones and siltstones.] Mapped only at 1:1,200 or 1:2,400 scale.
- 003 Typic Dystrochrepts; loamy-skeletal, mixed, thermic, shallow or very shallow. [Pinkish sandstone with mica.]
- 004 Ochreptic Hapludults; clayey or fine-loamy, mixed, thermic (>50 cm to Cr), or Ochreptic Hapludults; clayey or fine-loamy, mixed, thermic, shallow (<50 cm to Cr), or Typic Dystrochrepts; fine-loamy or loamy-skeletal, mixed, thermic, shallow. (These classifications are related to the slope class.) [Red and dark red mudstones with strata of olive shale and siltstone.]
- 005 Typic Hapludults; clayey, mixed, thermic. [Fault breccia of lower Rome.]
- 006 Typic Hapludults; fine-loamy, mixed, thermic. [Highly fractured areas of the Rome.]
- 007 Not used.
- 008 Ochreptic Hapludults; clayey or fine-loamy, mixed, thermic (<100 cm to Cr). [Feldspathic sandstone and siltstone.]
- 009 Typic Hapludults or Hapludalfs, clayey, mixed, thermic. [Rome carbonate unit.]

Rome colluvium

- 010 Typic Hapludults; fine-loamy, mixed, thermic. [Yellowish-brown to yellowish-red from upper Rome.]
- 011 Typic Hapludults; fine-loamy, mixed, thermic. [Reddish from lower Rome.]
- 012 Typic Hapludults; clayey, mixed, thermic. [Rome mudflows on low footslopes.]
- 013 Typic or Aquic Fragiudults; fine-loamy, mixed, thermic. [Rome mudflows on toe slopes.]

CONASAUGA GROUPPumpkin Valley residuum

- 100 Typic Hapludults; clayey, mixed, thermic (>100 cm to Cr). [Lower sandstone and siltstone facies.]
- 101 Typic Hapludults; clayey, mixed, thermic (50-100 cm to Cr). [Lower sandstone and siltstone facies.]
- 102 Ochreptic Hapludults; clayey or fine-loamy, mixed, thermic (<50 cm to Cr). [Lower sandstone and siltstone facies.] Soil of greatest extent.

- 103 Typic Dystrachrepts; loamy–skeletal, glauconitic, thermic, shallow. [Lower sandstone and siltstone facies.]
- 104 Ruptic-Ultic Dystrachrepts; clayey argillic and loamy–skeletal cambic, mixed, thermic. [Violet micaceous and glauconitic facies of upper Pumpkin Valley.]

Friendship residuum

- 105 Ruptic-Ultic Dystrachrepts; clayey argillic and loamy–skeletal cambic, mixed, thermic. [Calcareous siltstone and interbedded limestone member.]

Rogersville residuum

- 200 Typic Dystrachrepts; loamy–skeletal, mixed, thermic, shallow. {Steep slopes.}
- 201 Ruptic-Ultic Dystrachrepts; clayey and fine–loamy argillic and loamy–skeletal cambic, mixed, thermic. {Moderate slopes.}
- 202 Typic or Ochreptic Hapludults; clayey, mixed, thermic. {Slopes less than 6%.}

Dismal Gap residuum

- 203 Typic Hapludults; clayey, mixed, thermic. {Slopes less than 6%.}
- 204 Typic Hapludults; fine–loamy, mixed, thermic. [Siltstone and very fine grained sandstone in Melton Valley SWSA-7 area.]
- 205 Ochreptic Hapludults or Ruptic-Ultic Dystrachrepts; clayey or loamy–skeletal, mixed, thermic. {Moderate slopes.}
- 206 Typic Dystrachrepts; loamy–skeletal, mixed, thermic, shallow. {Steep slopes.}
- 207 Typic Dystrachrepts; loamy–skeletal, mixed, thermic. {Deeply weathered saprolite on steep easterly facing aspects.}

Nolichucky residuum

- 300 Ruptic-Aquultic Dystrachrepts; clayey argillic and loamy–skeletal cambic, mixed, thermic. {Lower sideslopes.}
- 301 Ruptic-Ultic Dystrachrepts; clayey argillic and loamy–skeletal cambic, mixed, thermic. {Moderate slopes.}
- 302 Typic Hapludults; clayey, mixed, thermic. {Slopes less than 6%.}

Maynardville residuum

- 303 Typic Hapludalfs-Ultic Hapludalfs-Rock Ledge Complex.
- 304 Typic Hapludults; clayey, mixed, thermic. [Argillaceous Limestone that forms thick reddish-yellow saprolite.]
- 305 Typic Hapludalfs: fine or very fine, montmorillonitic, thermic. [This member does not form saprolite, but forms a brown sticky clay subsoil with R horizon directly beneath.]
- 306 Rock Ledge-Typic Hapludalfs Complex.

Pumpkin Valley colluvium

- 120 Typic Hapludults; clayey or fine-loamy, mixed (2.5YR hue in the argillic horizon doubly convex toe slopes from landscape inversion). [Pumpkin Valley and some Rome.]
- 121 Typic Hapludults; fine-loamy, mixed, thermic (7.5YR-5YR hue in the argillic horizon). Doubly concave footslopes. [Rome and Pumpkin Valley.]
- 122 Typic Hapludults; fine-loamy or loamy-skeletal, mixed, thermic (10YR hue, gravelly upper argillic with abundant Rome gravels. In drainageways, fans and low toe slopes). [Rome and Pumpkin Valley.]
- 123 Typic Hapludults; fine-loamy, mixed, thermic. [Pumpkin Valley alluvium-colluvium over No. 951 alluvium over Pumpkin Valley saprolite.] Soils of very limited extent.

Rogersville/Dismal Gap/Nolichucky colluvium

- 220 Aquic Hapludults; fine-loamy, mixed, thermic. [Mostly Dismal Gap colluvium.]
- 221 Typic Hapludults; fine-loamy, mixed, thermic. [Rogersville, Dismal Gap, and some Nolichucky colluvium.]
- 222 Typic Hapludults; fine-loamy, mixed, thermic. [Gum Hollow alluvial fan with Rome fragments in Rogersville and Dismal Gap colluvium.]
- 223 Typic Hapludults; fine-loamy, mixed, thermic. [Rogersville-Dismal Gap-Nolichucky colluvium over silty old alluvium over Conasauga residuum.]
- 224 Typic Fragiudults; fine-loamy, mixed, thermic. [Dismal Gap, Nolichucky, and old alluvium.]
- 225 Typic Hapludults; clayey, mixed, thermic. [Rogersville and Dismal Gap colluvium with topographic inversion.]

KNOX GROUPCopper Ridge residuum

- 400 Typic Paleudults; clayey, kaolinitic, thermic (mostly cherty Fullerton with degraded upper Bt).
- 401 Typic Paleudults and Typic Hapludults; clayey, mixed or kaolinitic, thermic (darker surface and only on steep slopes and only on cool aspects of Chestnut Ridge and Melton Hill).
- 409 Hapludalfs-Hapludults-Rock Outcrop complex; fine, mixed, thermic. [Slightly cherty to noncherty.]

Chepultepec residuum

- 402 Typic Paleudults; clayey, kaolinitic, thermic. [Dunmore, cherty and noncherty with 7.5YR and 5YR upper Bt.]
- 408 Typic Hapludults; clayey-skeletal; kaolinitic, thermic. [Chert beds.]

Longview residuum

- 403 Typic Paleudults; clayey or clayey-skeletal, kaolinitic, thermic.

Kingsport residuum

- 406 Typic Paludults; clayey, kaolinitic or mixed, thermic.
 407 Hapludults-Hapludalfs-Rock outcrop complex.

Mascot residuum

- 404 Typic Hapludults; clayey, mixed, thermic.
 405 Hapludalfs-Hapludults-Rock outcrop complex.

Knox Group Colluvium

- 430 Fragric Paleudults; fine-loamy/loamy-skeletal, siliceous, thermic (high chert content throughout).
 432 Typic Paleudults; fine-loamy, siliceous, thermic. [Claiborne series. Has a thick dark epipedon and red clay loam or cherty clay loam argillic horizon and formed in colluvium of fan terraces.]
 433 Typic Paleudults (humic) fine-loamy or loamy skeletal, siliceous, thermic. [Toe slope\Colluvium from A and E horizons of upslope soils, without a red argillic horizon. Has a brown argillic horizon.]
 434 Typic Paleudults; fine-loamy, siliceous, thermic.
 435 Typic Paleudults; clayey, kaolinitic, thermic. [Minvale Clayey Variant on ancient toe slopes.] Only one unit mapped.
 436 Typic Paleudults; fine-loamy, siliceous, thermic. [Ridgetop ancient colluvium.]

Doline soils

- 431 Fluventic Dystrochrepts; fine-loamy, siliceous, thermic.
 437 Typic or Glossic Fragidults; fine-silty/loamy-skeletal, siliceous, thermic. [Loess over old colluvium on uplands and in shallow depressions.]
 438 Typic and Aquic Hapludults; fine-silty/loamy-skeletal, siliceous, thermic. [Loess over colluvium in depressions.]
 439 Typic and Aeris Ochraqults; fine-silty over clayey or clayey-skeletal, siliceous, thermic. [Loess over clayey residuum or cherty colluvium in depressions.]

Chickamauga Group residuumBethel Valley Section

- 500 Typic and Lithic Hapludalfs; fine, mixed, thermic. [Red shaly limestone.] [Unit B.]
 501 Typic Hapludalfs, Lithic Hapludalfs, Rendolls-Rock outcrop complex; fine, mixed, thermic. [Gray limestone and gray shaly limestone.] [Unit C.]
 505 Typic and Aquic Hapludalfs; fine, mixed, thermic (<20 to 40 inches to rock). [Unit E.]
 506 Hapludalfs-Argiudolls-Rendolls-Rock Ledges Complex. [Units F-H.]
 507 Typic Hapludalfs; fine, mixed, thermic. [Moccasin Formation.]
 600 Ultic Hapludalfs; fine, mixed, thermic. (Noncherty maroon unit in lower Chickamauga. Surrounded by No. 601 soils.) [Unit A.]
 601 Typic Paleudults; fine-loamy or clayey, kaolinitic, thermic. [Unit A with brick-like tabular chert fragments.]

- 603 Typic Hapludults or Ultic Hapludalfs; clayey, mixed, thermic. [Low chert.] [Unit E.]
- 606 Typic Hapludults; clayey, kaolinitic, thermic. [Cherty member.] [Unit D.]
- 607 Typic Hapludalfs; fine, mixed, thermic. [Unit B, more than 100 cm to rock.]

Soils below the Whiteoak Mountain Fault.

- 503 Typic or Ultic Hapludalfs; fine or very fine, mixed, thermic. [Hot Yard Hollow Unit E?]
- 504 Gladeville/Rock outcrop complex. [Not Mapped in Bear Creek Area but mapped in the Anderson County area of the Reservation. Unit C, E, F, G, H, and Moccasin.]
- 602 Aquic Hapludalfs or Aquic Hapludults; fine, mixed, thermic. [Hot Yard Hollow Unit E?]
- 605 Typic Hapludults; clayey, mixed, thermic (paralithic < 100 cm). (Brown 10YR and 7.5YR.) [Hot Yard Hollow Unit E?]

Chickamauga Colluvium

- 540 Typic Hapludults or Ultic Hapludalfs; fine-loamy, siliceous, thermic.
- 541 Typic Paleudults; fine-loamy or loamy-skeletal, siliceous, thermic. (Shack or Tassos as mapped in Chickamauga areas.) [Chickamauga and Knox chert sources.]

Reedsville and younger Formations residuum

- 700 Typic Hapludults; clayey, mixed, thermic. [Shale and sandstone residuum.]

Reedsville and younger Formations Colluvium

- 750 Typic Hapludults; fine-loamy, mixed, thermic. [Colluvium from Silurian rocks.] (Buried truncated soil at more than 100 cm.) (Jefferson series.)
- 751 Typic Hapludults; fine-loamy, siliceous, thermic. [Colluvium from Silurian rocks.] (With a buried truncated soil at 50 to 100 cm, also contains some chert.) (Jefferson, Variant.)
- 752 Typic Hapludults; clayey, mixed, thermic. [Colluvium from Reedsville-Sequatchie rock.] (Buried truncated soil horizon at 50 to 100 cm.)

ANCIENT ALLUVIUM

- 990 Rhodic Paleudults; clayey, oxidic, thermic. [Main channel, without chert fragments.]
- 991 Typic Paleudults; fine-silty, siliceous, thermic. [Loess over old local alluvium, not dark red, on Knox uplands.] (Has bisequal profile.)
- 992 Typic Hapludults; fine-loamy, mixed, thermic. Turbeville, Variant. [Mapped on Conasauga Group residuum.]
- 993 Typic Hapludults; fine-loamy, mixed, thermic. [Etowah Variant mapped on Conasauga Group.]
- 994 Typic Paleudults; fine-loamy, siliceous, thermic. [Ancient alluvium mixed with toe-slope cherty colluvium. Mapped on Knox dolostones and associated with No. 722 and No. 90 soils.]

- 995 Typic and Aquic Hapludults; fine-silty, siliceous, thermic. [Loess over silty alluvium over Conasauga Group residuum.]
- 996 Typic and Aquic Fragiudults; fine-loamy, mixed thermic. [Lacustrine/alluvium over Conasauga Group residuum.]
- 997 Typic Paleudults; clayey, mixed, thermic. [Waynesboro on recognizable river terrace landform.]
- 998 Typic Paleudults; fine-loamy-clayey, siliceous, thermic. [Etowah on recognizable river terraces.]

HOLOCENE ALLUVIUM

- 999 Typic Hapludults; fine-loamy, siliceous, thermic. [Sequatchie variant.]

MODERN ALLUVIUM

Rome and Pumpkin Valley.

- 960 Typic and Aquic Udifluvents; coarse-loamy, mixed, thermic.
- 961 Fluventic Dystrochrepts; coarse-loamy, mixed, thermic. [Poplar Creek, has chert fragments.]
- 962 Typic and Aeric Fluvaquents; fine-loamy, mixed, thermic.

Conasauga

- 970 Typic and Aquic Udifluvents; coarse-silty, mixed, thermic.
- 971 Typic and Aeric Fluvaquents; coarse/fine-silty, mixed, thermic.
- 972 Fluvaquents and Ochraqualfs; fine-silty and fine, mixed, thermic. [Bear Creek alluvium over a buried fine Typic Ochraqualf Maynardville soil at <50 to 90 cm.]

Knox

- 980 Udifluvents-Hapludults-Fragiudults complex; loamy-skeletal, siliceous, thermic, acid.
- 981 Typic and Aquic Udifluvents; loamy-skeletal, siliceous, thermic.
- 982 Typic and Aeric Fluvaquents; loamy-skeletal, siliceous thermic.
- 985 Fluventic Umbric Dystrochrepts; fine-loamy, siliceous, thermic [Emory Series.]

Chickamauga

- 983 Udifluvents-Hapludults-Hapludalfs complex; fine-loamy, mixed, thermic, non-acid. [Toe-slope colluvium and alluvium of small drainageways.]
- 984 Typic and Aeric Ochraqualfs; fine, mixed, thermic.

Internal Distribution

- | | | | |
|--------|------------------------------------|----------|---------------------------------|
| 1. | M. J. Aiken, TRI CTY, MS 7606 | 81. | B. McMaster, 9207, MS-8225 |
| 2. | J. E. Beavers, 9207, MS 8083 | 82. | G. K. Moore, 1503, MS-6352 |
| 3. | D. M. Borders, 1503, MS-6352 | 83. | P. J. Mulholland, 1505, MS-6036 |
| 4. | H. L. Boston, 1504, MS-6351 | 84. | J. B. Murphy, 4500N, MS-6198 |
| 5. | J. W. Bownds, 4500N, MS-6185 | 85. | C. E. Nix, 6026-C, MS-6395 |
| 6. | H. M. Braunstein, 130 MIT, MS-6282 | 86. | M. J. Norris, 9207, MS-8225 |
| 7. | R. B. Clapp, 1505, MS-6038 | 87. | D. E. Reichle, 4500N, MS-6253 |
| 8. | A. H. Curtis, 4500N, MS-6185 | 88. | C. T. Rightmire, 1503, MS-6352 |
| 9. | N. H. Cutshall, K-1001, MS-7172 | 89. | M. W. Rosenthal, 4500N, MS-6241 |
| 10. | M. F. P. DeLozier, K-1330, MS-7298 | 90. | T. H. Row, 4500N, MS-6254 |
| 11. | W. E. Doll, 3504, MS-6317 | 91. | P. A. Rubin, 1503, MS-6352 |
| 12-16. | R. B. Dreier, 1503, MS-6352 | 92. | W. E. Sanford, 1503, MS-6352 |
| 17. | T. O. Ear ly, 3504, MS-6317 | 93. | L. A. Shevenell, 1505, MS-6038 |
| 18. | T. A. Fontaine, 1505, MS-6038 | 94. | L. G. Shipe, K-0303-8, MS 7314 |
| 19. | C. W. Francis, 3504, MS-6317 | 95. | E. D. Smith, 1505, MS-6038 |
| 20. | P. L. Goddard, K-1330, MS-7298 | 96. | D. K. Solomon, 1503, MS-6352 |
| 21. | P. M. Goldstrand, 1505, MS-6036 | 97. | S. H. Stow, 1505, MS-6038 |
| 22-46. | R. D. Hatcher, Jr., 1593, MS-6352 | 98. | J. Switek, 3504, MS-6317 |
| 47. | S. G. Hildebrand, 1505, MS-6035 | 99. | L. E. Toran, 1503, MS-6352 |
| 48. | D. D. Huff, 3504, MS-6317 | 100. | J. R. Trabalka, 3047, MS-6020 |
| 49. | R. J. Hunt, 9207, MS 8083 | 101. | R. I. Van Hook, 1505, MS-6037 |
| 50. | W. K. Jago, 9207, MS-8225 | 102. | J. C. Wang, 4500N, MS 6185 |
| 51. | P. M. Jardine, 1505, MS-6038 | 103. | D. R. Watkins, 3504, MS-6317 |
| 52. | S. B. Jones, 9207, MS-8225 | 104. | D. Wesolowski, 4500S, MS 6110 |
| 53. | S. B. Kennedy, 9201-3, MS 8063 | 105. | O. R. West, 1505, MS-6036 |
| 54-58. | R. H. Kettle, 4500N, MS-6185 | 106. | R. K. White, 7509, MS-6383 |
| 59. | B. L. Kimmel, 1505, MS-6038 | 107. | S. Winters, 1503, MS-6352 |
| 60. | A. J. Kuhaida, 7078B, MS-6402 | 108. | T. F. Zondlo, 1503, MS-6352 |
| 61. | D. W. Lee, 4500N, MS 6185 | 109. | Central Research Library |
| 62-66. | R. R. Lee, 4500N, MS-6185 | 110-220. | ESD Library |
| 67-71. | S. Y. Lee, 1505, MS-6038 | 221. | ORNL Y-12 Technical Library |
| 72-76. | P. J. Lemiszki, 1503, MS-6352 | 222-223. | Laboratory Records Department |
| 77. | R. S. Loffman, 4500-OS, MS-6102 | 224. | Laboratory Records, ORNL-RC |
| 78. | T. F. Lomenick, CHINN, MS 6493 | 225. | ORNL Patent Office |
| 79. | R. J. Luxmoore, 1505, MS-6038 | | |
| 80. | L. W. McMahon, 9207, MS-8225 | | |

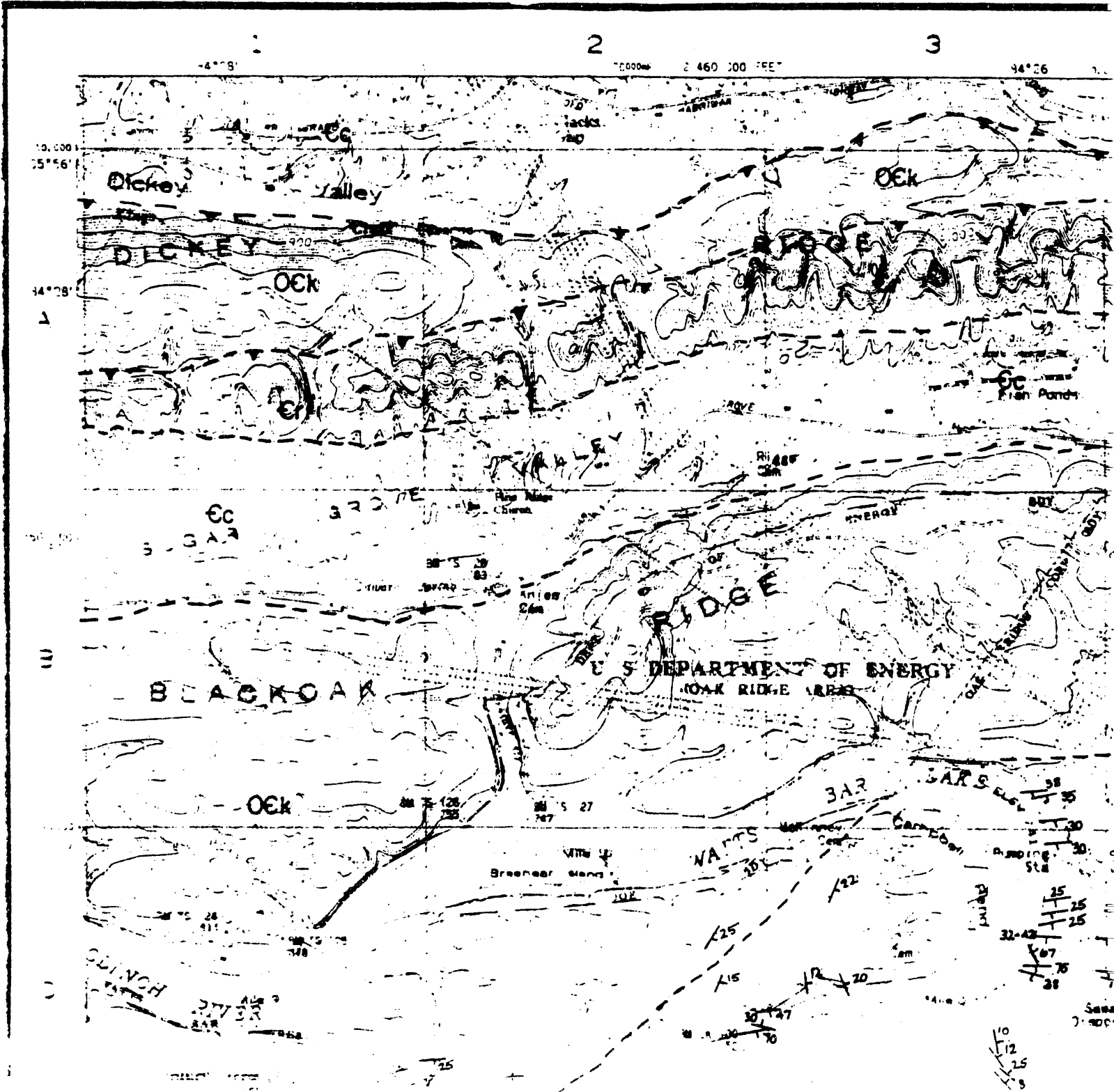
External Distribution

226. Jerry Archer, Geraghty and Miller Inc., 255 S. Tulane Ave., Oak Ridge, TN 37830
227. Richard Arnseth, SAIC, 301 Laboratory Road, Oak Ridge, TN 37830
228. Ernest Beauchamp, C-260 Jackson Plaza, MS 7614, Room 13, Oak Ridge, TN 37830
229. Robert Benfield, TDEC/DOE Oversight, 761 Emory Valley Road, Oak Ridge, TN 37830

230. L. I. Benson, Ogden Environmental Services, 725 Pellissippi Parkway, P. O. Box 22879, Knoxville, TN 37933-0879
231. S. A. Blair, Ogden Environmental Services, 725 Pellissippi Parkway, P. O. Box 22879, Knoxville, TN 37933-0879
232. G. W. Bodenstein, US DOE-OR, Federal Building, Oak Ridge, TN 37830
233. Paul Craig, Environmental Consulting Engineers, P. O. Box 22668, Knoxville, TN 37933
234. S. N. Davis, 6540 Box Canyon Drive, Tucson, AZ 85745
235. R. N. Farvolden, Waterloo Centre for Groundwater Research, University of Waterloo, Waterloo, Ontario N2L 3G1 Canada
236. M. Ebers, Ogden Environmental Services, 725 Pellissippi Parkway, P. O. Box 22879, Knoxville, TN 37933-0879
237. Robert Floyd, 11524 Nassau Drive, Concord, TN 37922
- 238-242. J. L. Foreman, Department of Geological Sciences, University of Tennessee, Knoxville, TN 37996-1410
243. J. F. Franklin, Bloedel Professor of Ecosystem Analysis, College of Forest Resources, University of Washington, Anderson Hall AR-10, Seattle, WA 98195
244. R. E. Fulweiler, Tennessee Division of Geology, 2700 Middlebrook Pike, Knoxville, TN 37921-5602
245. C. S. Haase, 603 School of Mines Road, Socorro, NM 87801
246. Amy Halleran, Department of Geological Sciences, University of Tennessee, Knoxville, TN 37996-1410
247. Jim Harless, TTDEC/DOE Oversight, 761 Emory Valley Road, Oak Ridge, TN 37830
248. R. C. Hariss, Institute for the Study of Earth, Oceans, and Space, Science and Engineering Research Building, University of New Hampshire, Durham, NH 03824
249. G. M. Homberger, Professor, Department of Environmental Sciences, University of Virginia, Charlottesville, VA 22903
250. G. Y. Jordy, Director, Office of Program Analysis, Office of Energy Research, ER-30, G-226. US DOE, Washington, DC 20545
251. Philip E. Lamoreaux and Associates, Inc., P. O. Box 2310, Tuscaloosa, AL 35403
- 252-256. D. A. Lietzke, Lietzke Soil Services, Route 3, Box 607, Rutledge, TN 37861
257. W. C. Luth, ER-15, Division of Engineering and Geosciences, Office of Basic Energy Sciences, DOE, Washington, DC 20585
- 258-262. W. M. McMaster, Dept. of Civil Engineering, University of Tennessee, Knoxville, TN 37996
263. Robert C. Milici, Central U.S. Sedimentary Processes, U.S.G.S., Box 25046, MS 939, Denver Federal Center, Denver, CO 80225

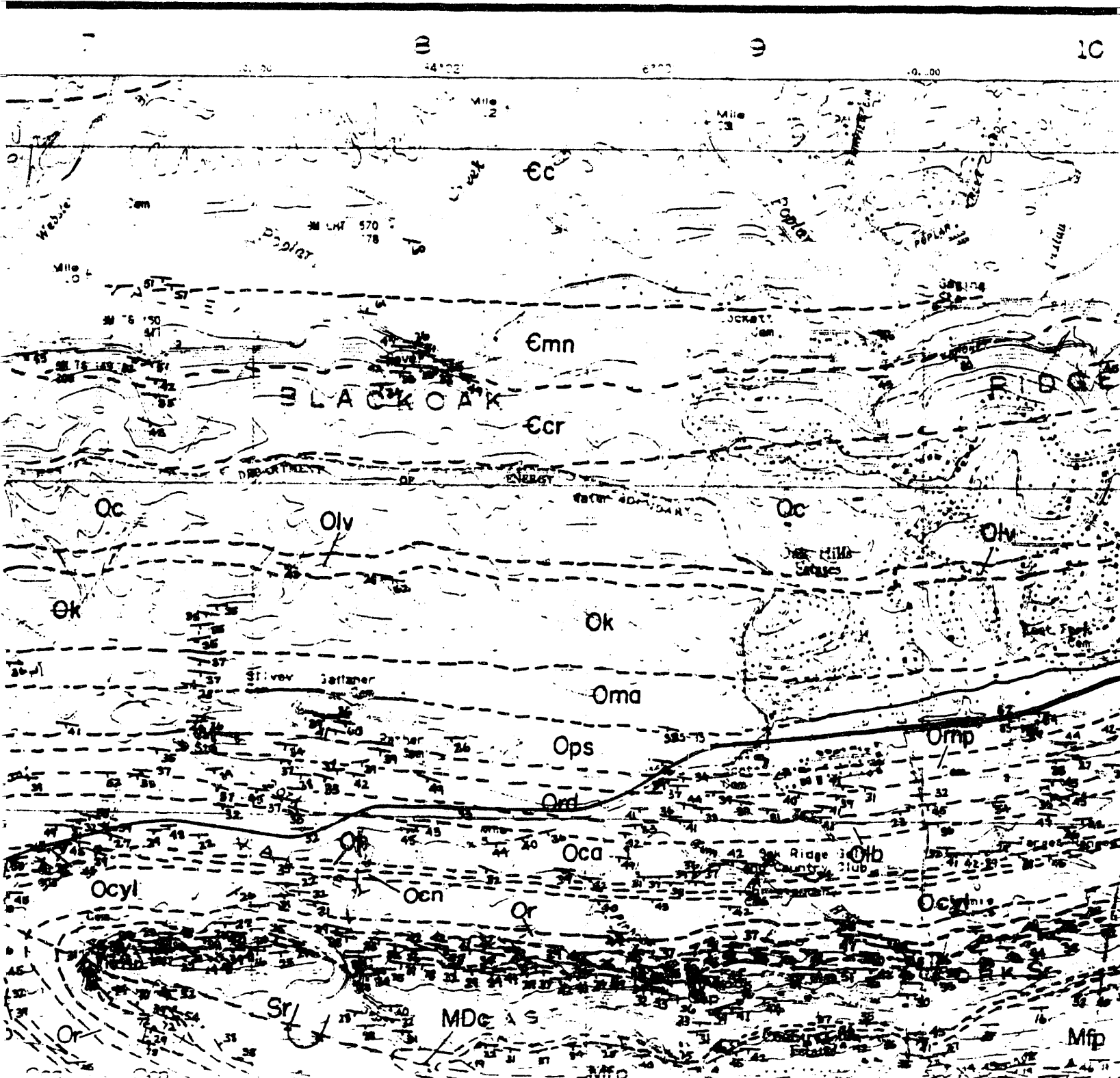
264. R. Native, Department of Soil/Water Sciences, Faculty of Agriculture, Hebrew University of Jerusalem, P. O. Box 12, Rehovot 76100 Israel
265. Chudi Nwangwa, TDEC/DOE Oversight, 761 Emory Valley Road, Oak Ridge, TN 37830
266. Albert E. Ogden, Center for Management, Utilization and Protection of Water Resources, Tennessee Technological University, P. O. Box 5082, Cookeville, TN 38505
267. R. H. Olsen, Professor, Microbiology and Immunology Department, University of Michigan, Medical Sciences II, #5605, 1301 East Catherine Street, Ann Arbor, MI 48109-0620
268. A. Patrinos, Director, Environmental Sciences Division, Office of Health and Environmental Research, ER 74, US DOE, Washington, D. C. 20585
269. James F. Quinlan, Quinlan and Associates, Box 110539, Nashville, TN 37222
270. Fred Quinones, Chief, Tennessee District, WRD, U. S. Geological Survey, A-413 Federal Building, Nashville, TN 37203
271. Radian/Lee Wan Associates, Office Manager, 120 S. Jefferson Circle, Oak Ridge, TN 37830
272. Gregory D. Reed, Chairman, Department of Civil Engineering, University of Tennessee, 62 Perkins Hall, Knoxville, TN 37996-2010
273. Debra Shults, Tennessee Division of Environment and Conservation, Division of Radiological Health, TERRA Building, 150 Ninth Avenue, North, Nashville, TN 37243-1532
274. M. Singer, CH2M Hill Co., 599 Oak Ridge Turnpike, Oak Ridge, TN 37830
275. William C. Sidle, US DOE-OR, Environmental Protection Division, US DOE-OR, P. O. Box 2001, Oak Ridge, TN 37831-8739
276. James Smoot, Department of Civil Engineering, University of Tennessee, 62 Perkins Hall, Knoxville, TN 37996-2010
277. Systematic Management Services, Inc., Office Manager, 673 Emory Valley Road, Oak Ridge, TN 37830
278. Jeff Walker, HSW Environmental Consultants, 687 Emory Valley Road, Suite B, Oak Ridge, TN 37830
279. Steven Wilson, TDEC, Division of Underground Storage Tanks, 2700 Middlebrook Pike, Suite 220, Knoxville, TN 37921
280. F. J. Wobber, Environmental Sciences Division, Office of Health and Environmental Research, Office of Energy Research, ER-74, US DOE, Washington, DC 20585
281. John Young, Camp Dresser & McKee, Suite 500, 800 Oak Ridge Turnpike, Oak Ridge, TN 37830
282. Steven C. Young, TVA Engineering Laboratory, P. O. Box E, Norris, TN 37828
283. Office of Assistant Manager for Energy Research and Development, US DOE, Oak Ridge Field Office, P. O. Box 2001, Oak Ridge, TN 37831-8600
- 284-293. Office of Scientific and Technical Information, P. O. Box 62, Oak Ridge, TN 37831

PLATE 1



PROVISIONAL SEPTEMBER OAK RIDGE

OAK RIDGE, TENN

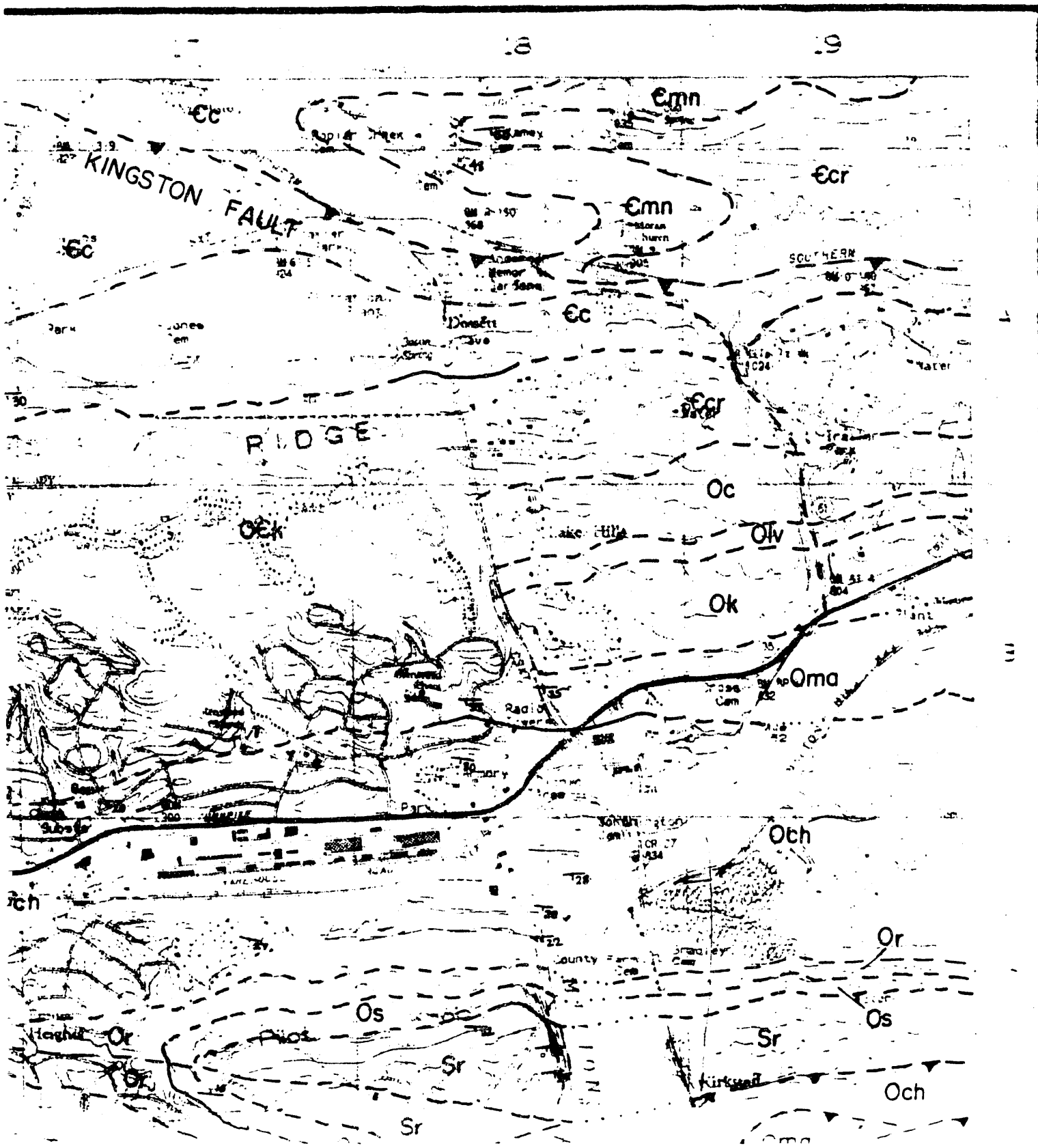


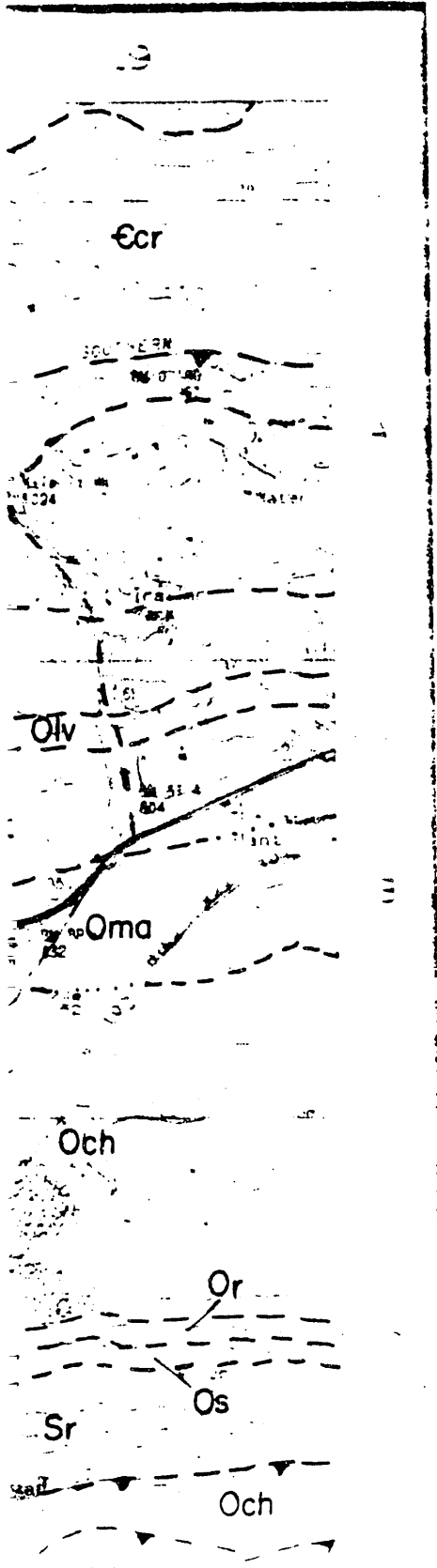
14

15

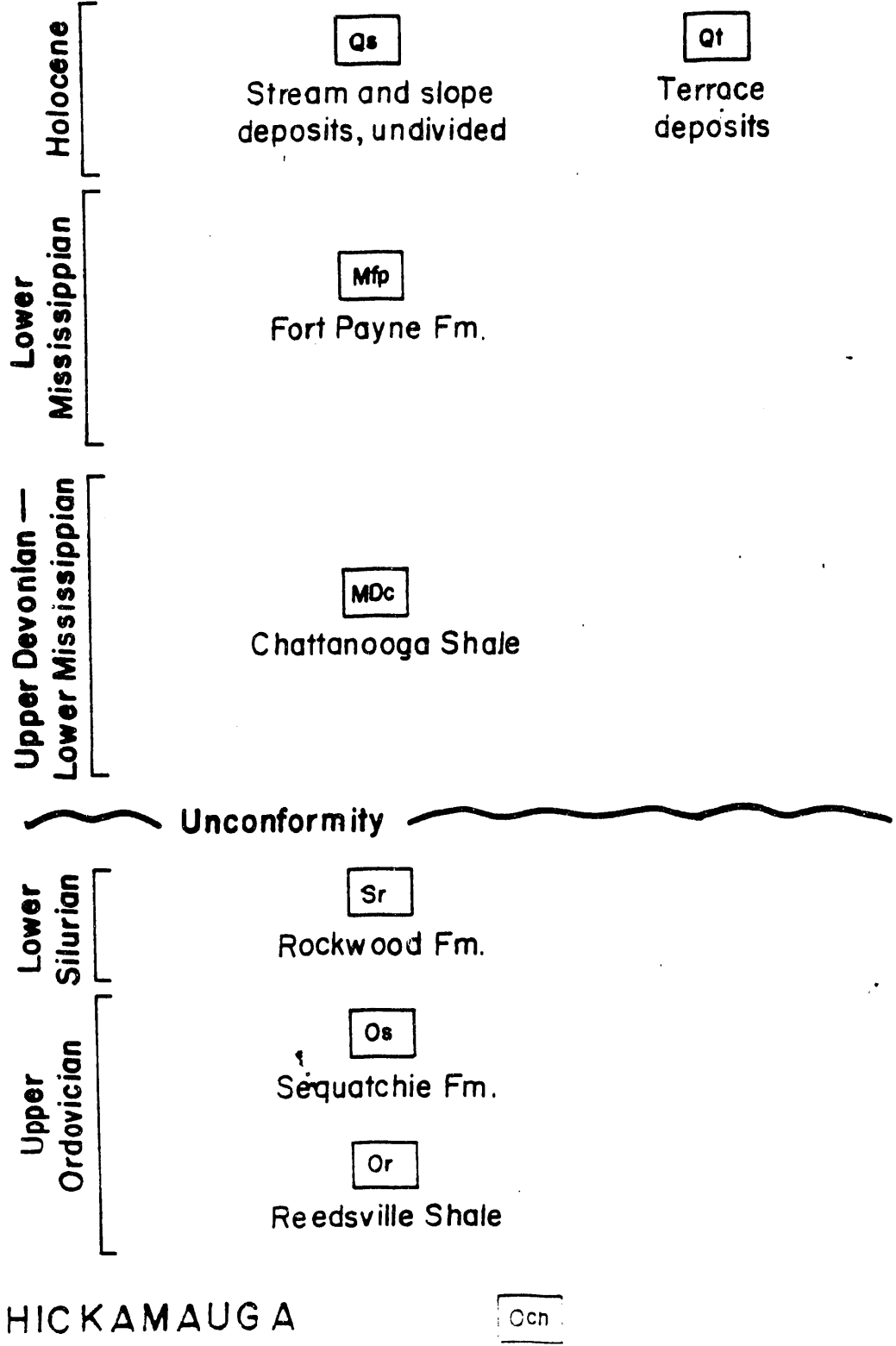
16



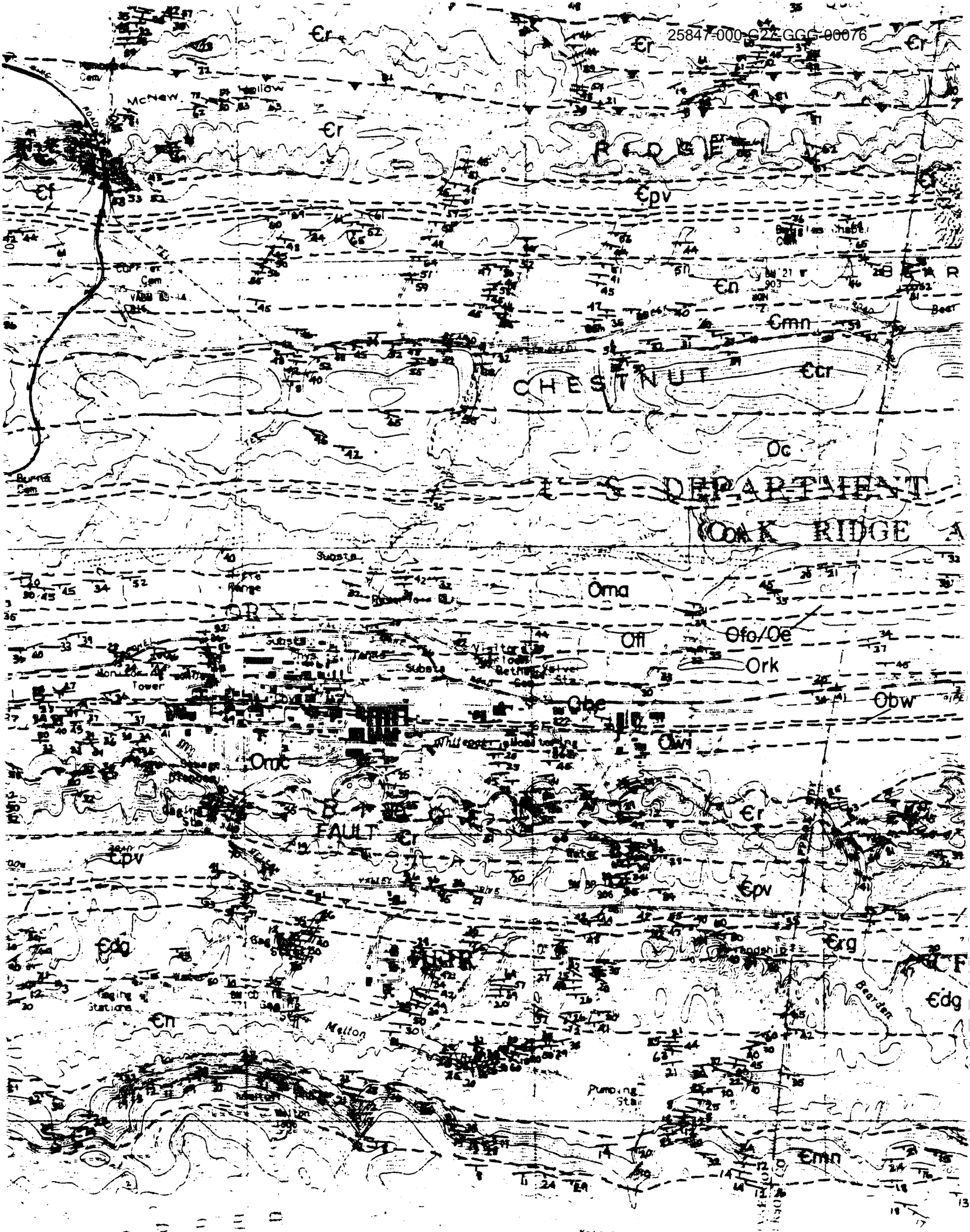




EXPLANATION



CHICKAMAUGA



Er

Cr

Cr

McNEW

Er

Epv

En

Cmn

CHESTNUT

Cr

Oc

DEPARTMENT

COAK RIDGE A

Oma

Off

Ofo/Oe

Ork

Obw

Obe

Owi

Omc

FAULT

Er

Epv

Ecd

Ecg

Ecd

En

Nelson

Pumping Sta

Emn

EA



Lennix
FAULT

PINE

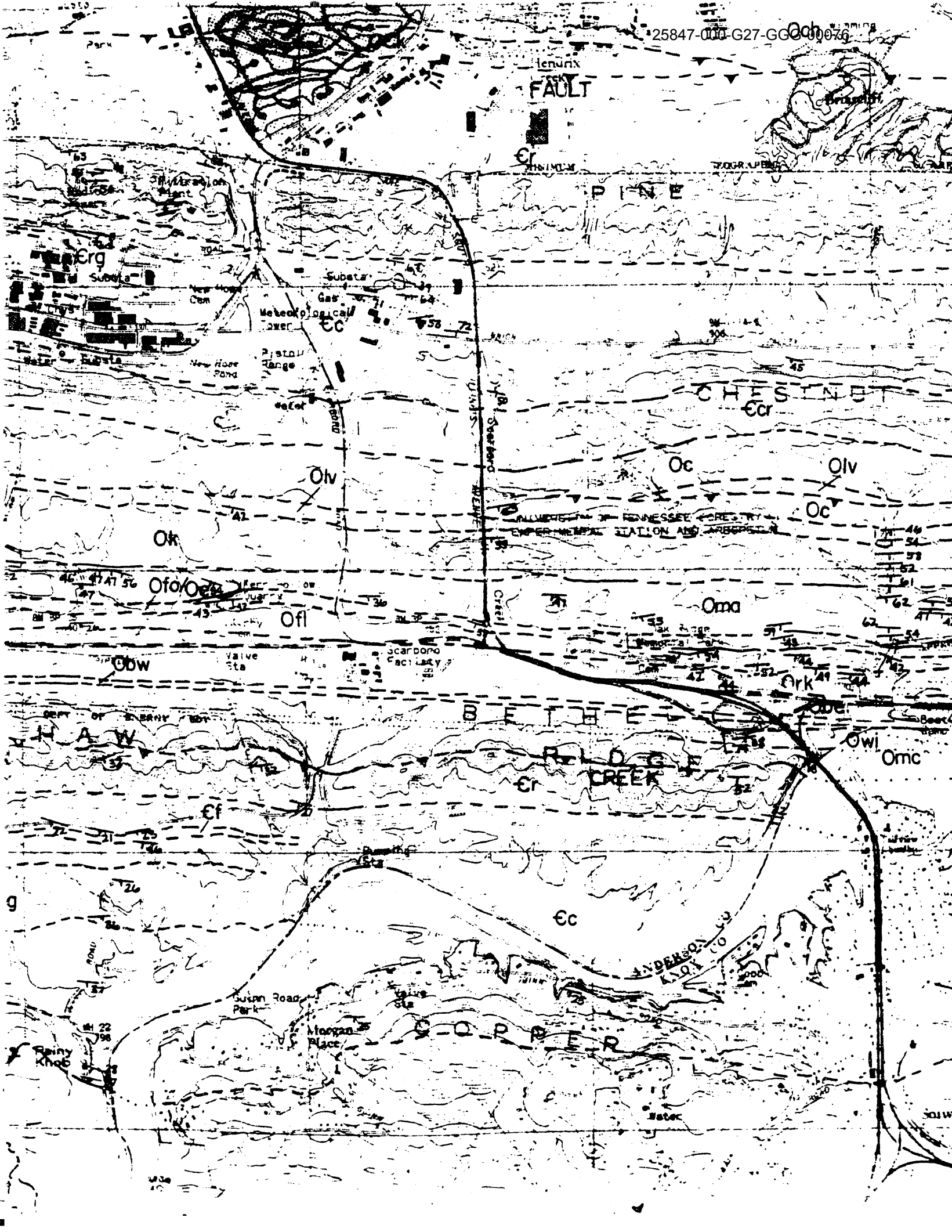
CHESTNUT

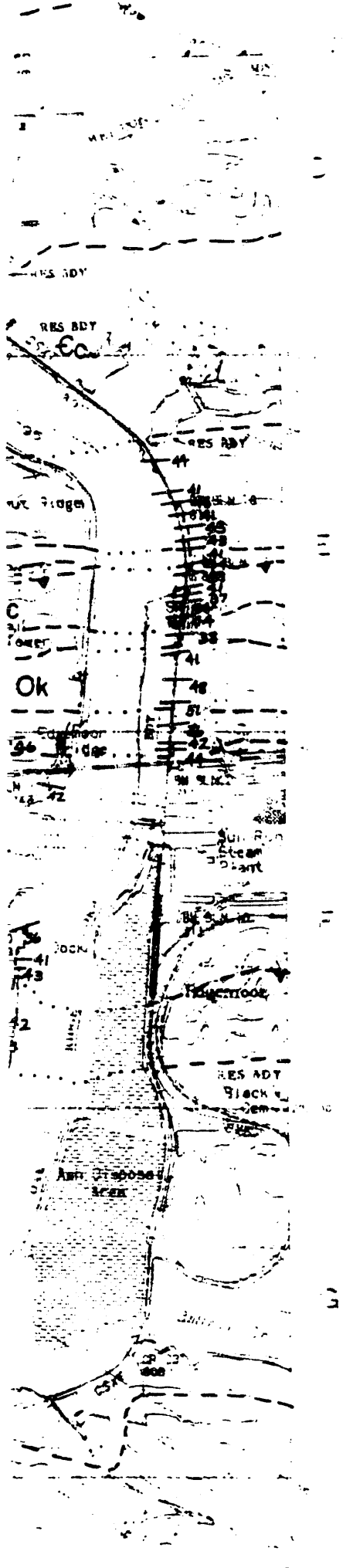
ALUMINUM TENSILE PROPERTY
DEPARTMENT STATION AND LABORATORY

BLAKE
CREEK

COPPER

ANDERSON
KNOX CO





Middle Ordovician

Nashville Group

Stones River Group

OcyI

Catheys Fm. and
Leipers Fm. undivided

Ocn

Cannon Ls.

Oh

Hermitage Fm.

Oca

Carters Ls.

Olb

Lebanon Ls.

Ord

Ridley Ls.

Omp

Pierce Limestone
Murfreesboro Ls.
undivided

Ops

Pond Spring Fm.

Omc

Moccasin Fm.

Owi

Witten Fm.

Obw

Bowen Fm.

Obe

Benbolt Fm.

Ork

Rockdell Fm.

Ofl

Fleanor Shale
Member

Oe

Ofo

Five Oaks Fm./
Eidson Member

Lincolnshire Fm.

Unconformity

KNOX GROUP

Ock

undivided

COPPER

2584 001817 G-00076

Bradbury Community Center

Pumpground 233

Bradbury

Valley

Copper Ridge

Open Cave

Bob Cave

Ock

Cave 1200

Cave 1144

1722

ROANE CO
SOUTH

ROANE CO
SOUTH

5

1

1.00

10

100

1000

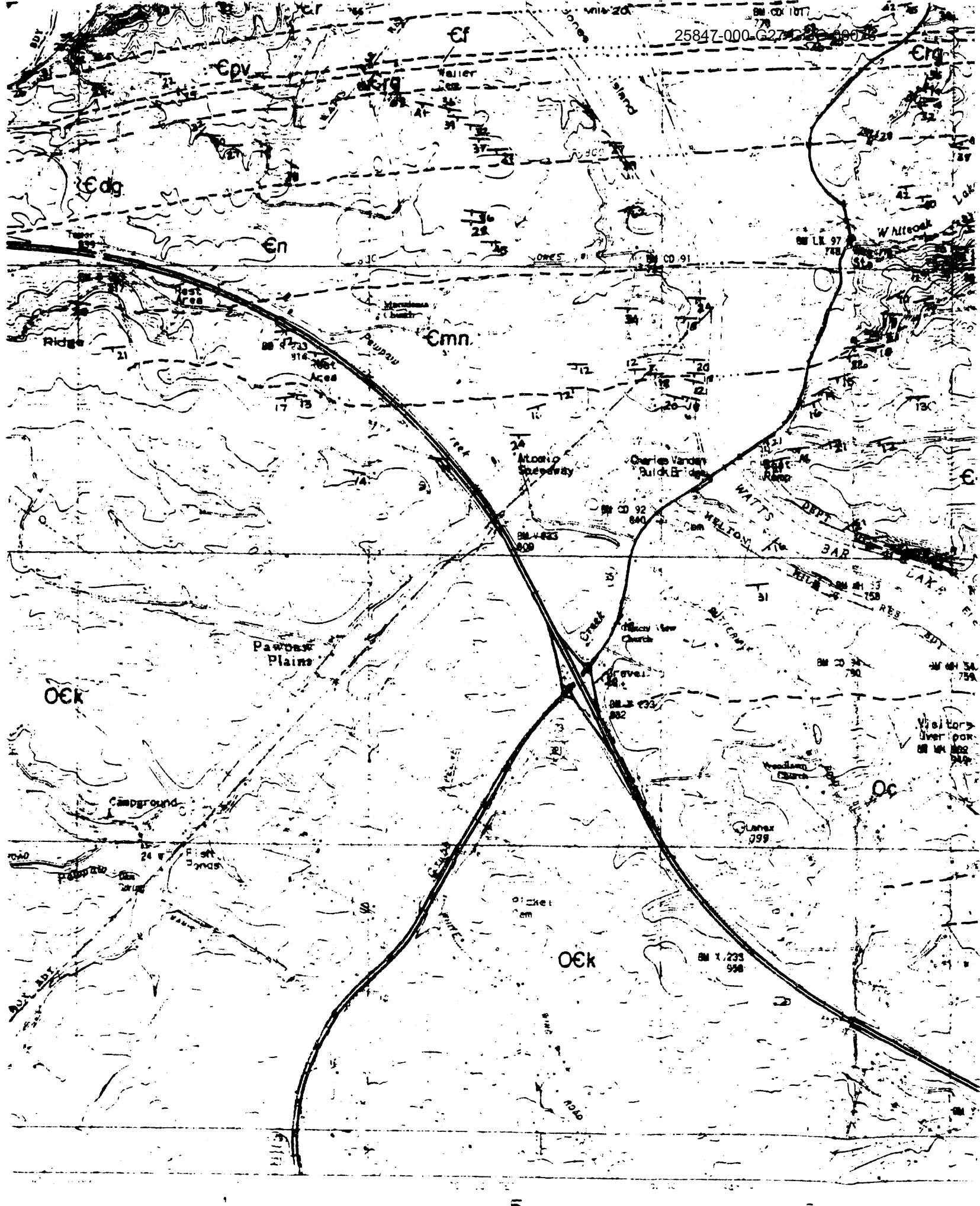
10000

100000

1

3

25847-000 G274 280 890 78



Ock

Ock

Victory Overlook

Clanex 399

BM 1,233 998

BM 1,233 982

BM CD 92 840

BM 1,233 909

BM LN 97 748

BM CD 91

BM CD 107 778

BM 1,233 916

BM 1,233 17

BM 1,233 12

BM 1,233 20

BM 1,233 21

BM 1,233 22

BM 1,233 23

BM 1,233 24

BM 1,233 25

BM 1,233 26

BM 1,233 27

BM 1,233 28

BM 1,233 29

BM 1,233 30

BM 1,233 31

BM 1,233 32

BM 1,233 33

BM 1,233 34

BM 1,233 35

BM 1,233 36

BM 1,233 37

BM 1,233 38

BM 1,233 39

BM 1,233 40

BM 1,233 41

BM 1,233 42

BM 1,233 43

BM 1,233 44

BM 1,233 45

BM 1,233 46

BM 1,233 47

BM 1,233 48

BM 1,233 49

BM 1,233 50

BM 1,233 51

BM 1,233 52

BM 1,233 53

BM 1,233 54

BM 1,233 55

BM 1,233 56

BM 1,233 57

BM 1,233 58

BM 1,233 59

BM 1,233 60

BM 1,233 61

BM 1,233 62

BM 1,233 63

BM 1,233 64

BM 1,233 65

BM 1,233 66

BM 1,233 67

BM 1,233 68

BM 1,233 69

BM 1,233 70

BM 1,233 71

BM 1,233 72

BM 1,233 73

BM 1,233 74

BM 1,233 75

BM 1,233 76

BM 1,233 77

BM 1,233 78

BM 1,233 79

BM 1,233 80

BM 1,233 81

BM 1,233 82

BM 1,233 83

BM 1,233 84

BM 1,233 85

BM 1,233 86

BM 1,233 87

BM 1,233 88

BM 1,233 89

BM 1,233 90

BM 1,233 91

BM 1,233 92

BM 1,233 93

BM 1,233 94

BM 1,233 95

BM 1,233 96

BM 1,233 97

BM 1,233 98

BM 1,233 99

BM 1,233 100

BM 1,233 101

BM 1,233 102

BM 1,233 103

BM 1,233 104

BM 1,233 105

BM 1,233 106

BM 1,233 107

BM 1,233 108

BM 1,233 109

BM 1,233 110

BM 1,233 111

BM 1,233 112

BM 1,233 113

BM 1,233 114

BM 1,233 115

BM 1,233 116

BM 1,233 117

BM 1,233 118

BM 1,233 119

BM 1,233 120

BM 1,233 121

BM 1,233 122

BM 1,233 123

BM 1,233 124

BM 1,233 125

BM 1,233 126

BM 1,233 127

BM 1,233 128

BM 1,233 129

BM 1,233 130

BM 1,233 131

BM 1,233 132

BM 1,233 133

BM 1,233 134

BM 1,233 135

BM 1,233 136

BM 1,233 137

BM 1,233 138

BM 1,233 139

BM 1,233 140

BM 1,233 141

BM 1,233 142

BM 1,233 143

BM 1,233 144

BM 1,233 145

BM 1,233 146

BM 1,233 147

BM 1,233 148

BM 1,233 149

BM 1,233 150

BM 1,233 151

BM 1,233 152

BM 1,233 153

BM 1,233 154

BM 1,233 155

BM 1,233 156

BM 1,233 157

BM 1,233 158

BM 1,233 159

BM 1,233 160

BM 1,233 161

BM 1,233 162

BM 1,233 163

BM 1,233 164

BM 1,233 165

BM 1,233 166

BM 1,233 167

BM 1,233 168

BM 1,233 169

BM 1,233 170

BM 1,233 171

BM 1,233 172

BM 1,233 173

BM 1,233 174

BM 1,233 175

BM 1,233 176

BM 1,233 177

BM 1,233 178

BM 1,233 179

BM 1,233 180

BM 1,233 181

BM 1,233 182

BM 1,233 183

BM 1,233 184

BM 1,233 185

BM 1,233 186

BM 1,233 187

BM 1,233 188

BM 1,233 189

BM 1,233 190

BM 1,233 191

BM 1,233 192

BM 1,233 193

BM 1,233 194

BM 1,233 195

BM 1,233 196

BM 1,233 197

BM 1,233 198

BM 1,233 199

BM 1,233 200

BM 1,233 201

BM 1,233 202

BM 1,233 203

BM 1,233 204

BM 1,233 205

BM 1,233 206

BM 1,233 207

BM 1,233 208

BM 1,233 209

BM 1,233 210

BM 1,233 211

BM 1,233 212

BM 1,233 213

BM 1,233 214

BM 1,233 215

BM 1,233 216

BM 1,233 217

BM 1,233 218

BM 1,233 219

BM 1,233 220

BM 1,233 221

BM 1,233 222

BM 1,233 223

BM 1,233 224

BM 1,233 225

BM 1,233 226

BM 1,233 227

BM 1,233 228

BM 1,233 229

BM 1,233 230

BM 1,233 231

BM 1,233 232

BM 1,233 233

BM 1,233 234

BM 1,233 235

BM 1,233 236

BM 1,233 237

BM 1,233 238

BM 1,233 239

BM 1,233 240

BM 1,233 241

BM 1,233 242

BM 1,233 243

BM 1,233 244

BM 1,233 245

BM 1,233 246

BM 1,233 247

BM 1,233 248

BM 1,233 249

BM 1,233 250

BM 1,233 251

BM 1,233 252

BM 1,233 253

BM 1,233 254

BM 1,233 255

BM 1,233 256

BM 1,233 257

BM 1,233 258

BM 1,233 259

BM 1,233 260

BM 1,233 261

BM 1,233 262

BM 1,233 263

BM 1,233 264

BM 1,233 2





Burchfield Heights

Mile 45

5110

EC

WYVER

Ball...

WELTON HILL RD
3DV
3AT

Mile 3

SOIWAY

MA 58
989

Welford

Cavern in the Ridge

W D G E

OCH

Welford Downs

Edington

MA 10

MA 48

MA 17

961

MA 5

Valley

Welford Court

Och

Welford Court

Reddy

Welford Court

Cr.

Welford Court

Unconformity

KNOX GROUP

Ock

undivided

Lower
Ordovician

Oma

Mascot Dolomite

Ok

Kingsport Fm.

Olv

Longview Dolomite

Oc

Chepultepec Dolomite

Upper
Cambrian

Ecr

Copper Ridge Dolomite

CONASAUGA GROUP

Ec

undivided

Upper
Cambrian

Emn

Maynardville Ls.

En

Nolichucky Shale

Edg

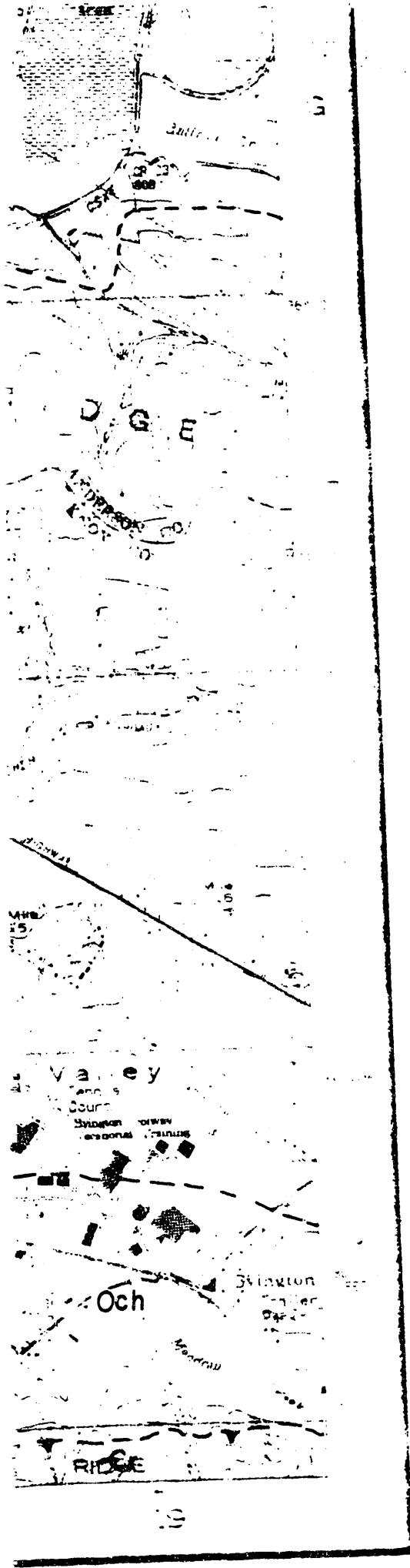
Dismal Gap Fm.
(Provisional name,
Formerly Maryville Ls.)

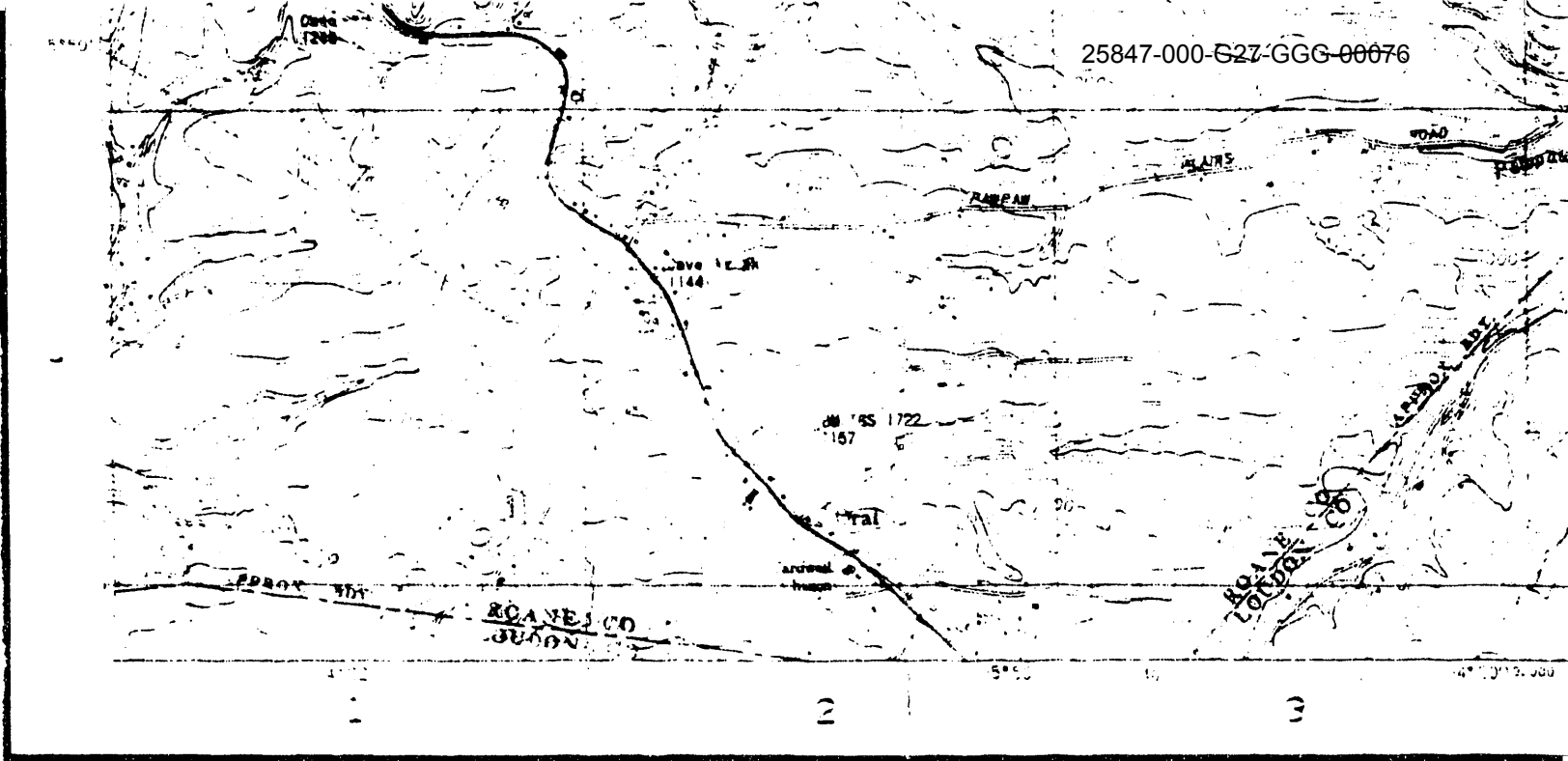
Erg

Rogersville Shale

Middle
Cambrian

Ef





INTERIOR—GEOLOGICAL SURVEY RESTON, VIRGINIA—888

Prepared by Mapping Service Branch, Tennessee Valley Authority,
 for U.S. Department of Energy. Completed by TVA in 1985 by
 photogrammetric methods using aerial photographs taken 1984
 Map field checked by TVA, 1986. Springs not field checked

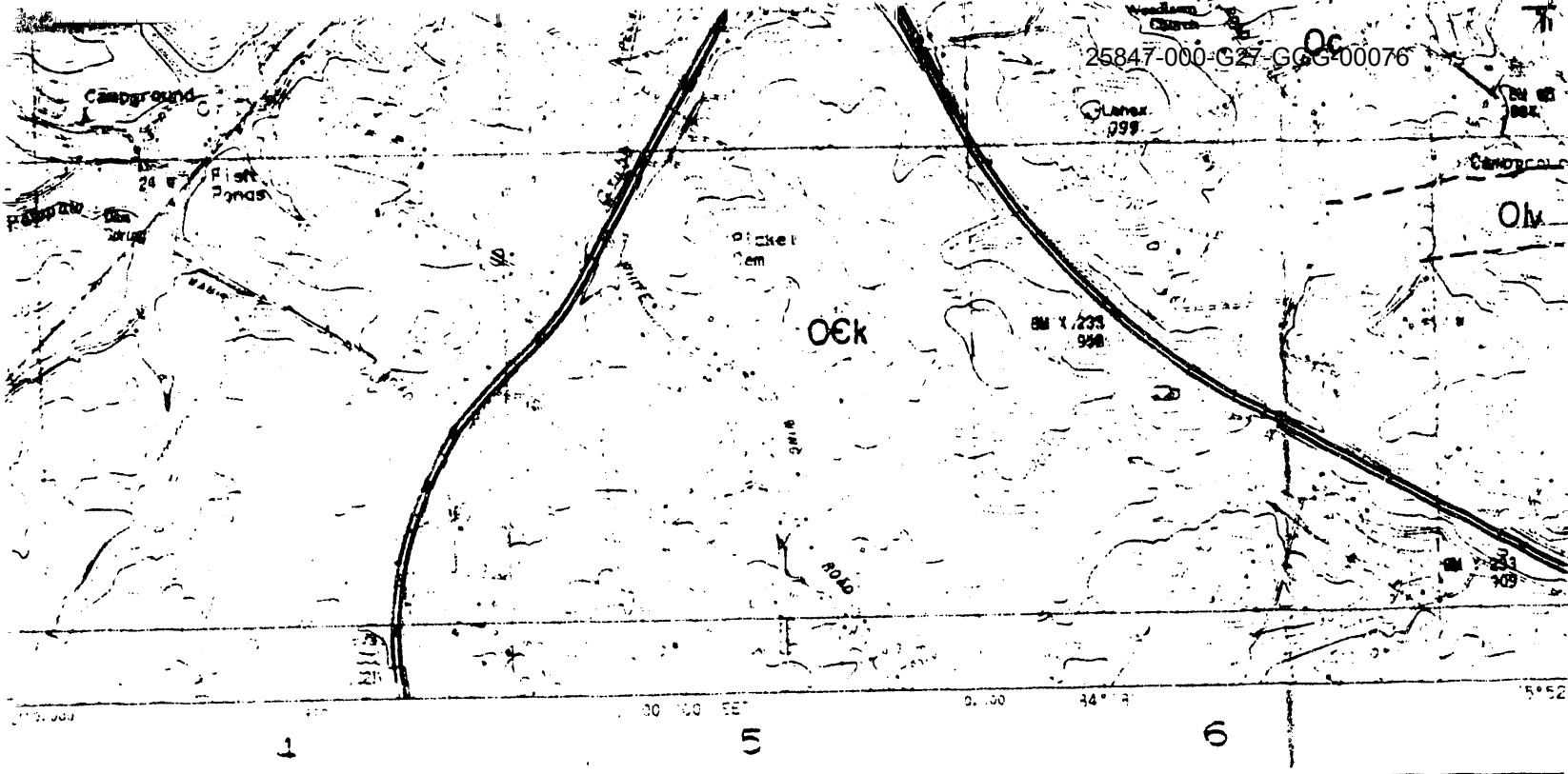
Polyconic Projection, 3,000-foot grid ticks based on Tennessee
 coordinate system, 3,000-meter Universal Transverse Mercator
 Grid ticks. Zone 18 shown. Scale, 3,000-foot (1:62,500)
 Administrative Grid shown in red, 1927 North American Datum

Geology by:

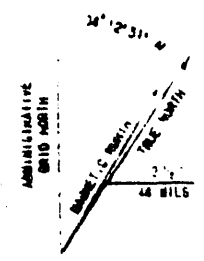
Peter
 Robe
 Rich

with additional c
 from:

McM
 Swin



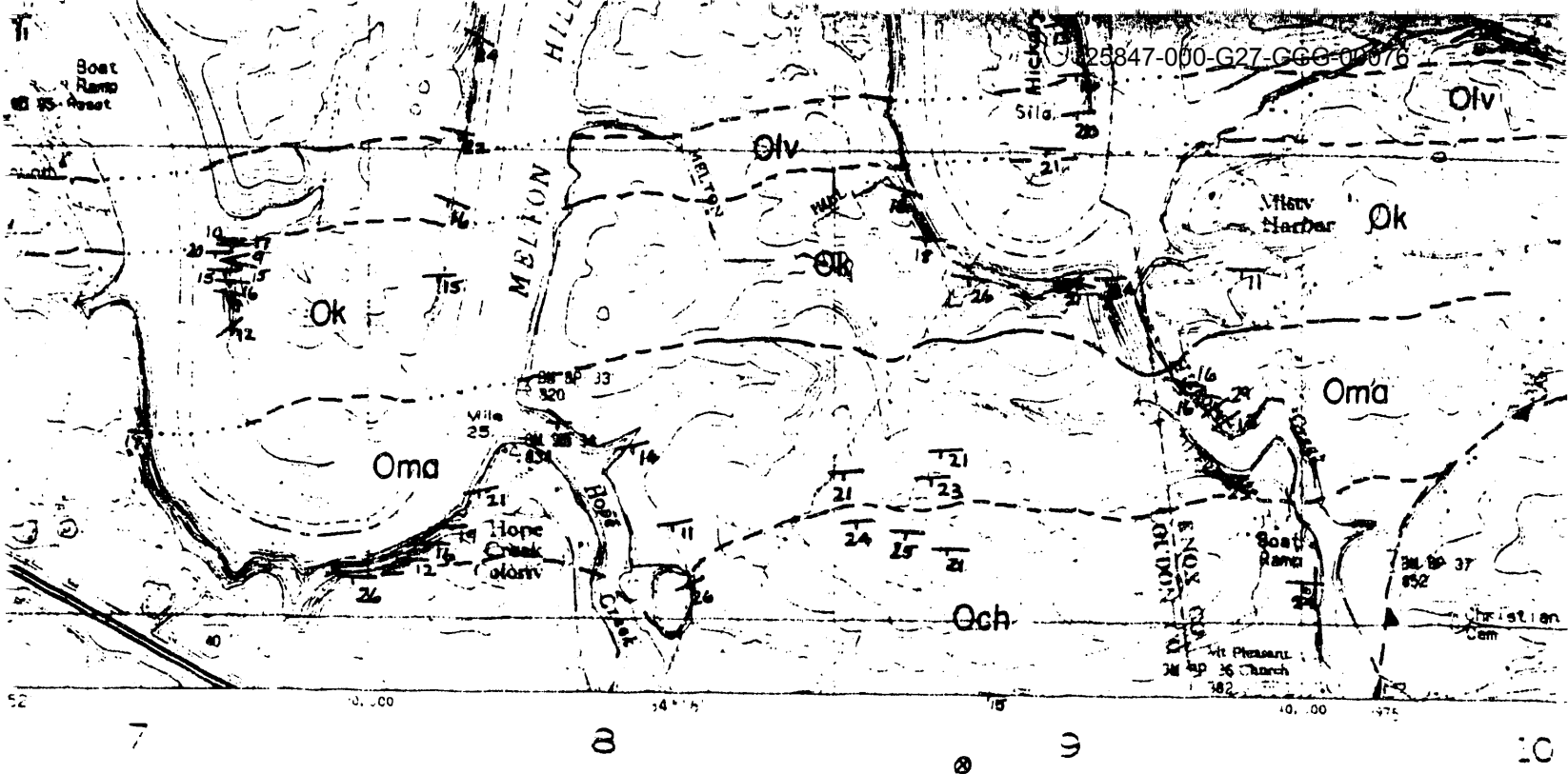
ter J. Lemiszki
 ert D. Hatcher, Jr.
 ichard H. Ketelle



DECLINATION OF GRID 34° 12' 51" W OF TRUE NORTH
 1987 MAGNETIC NORTH DECLINATION AT CENTER OF SHEET

al data compiled
 icMaster (1962)
 wingle (1964)

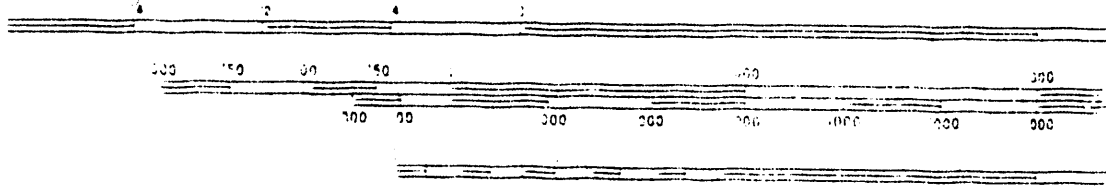
C



OAK RIDGE

OAK RIDGE, TENN

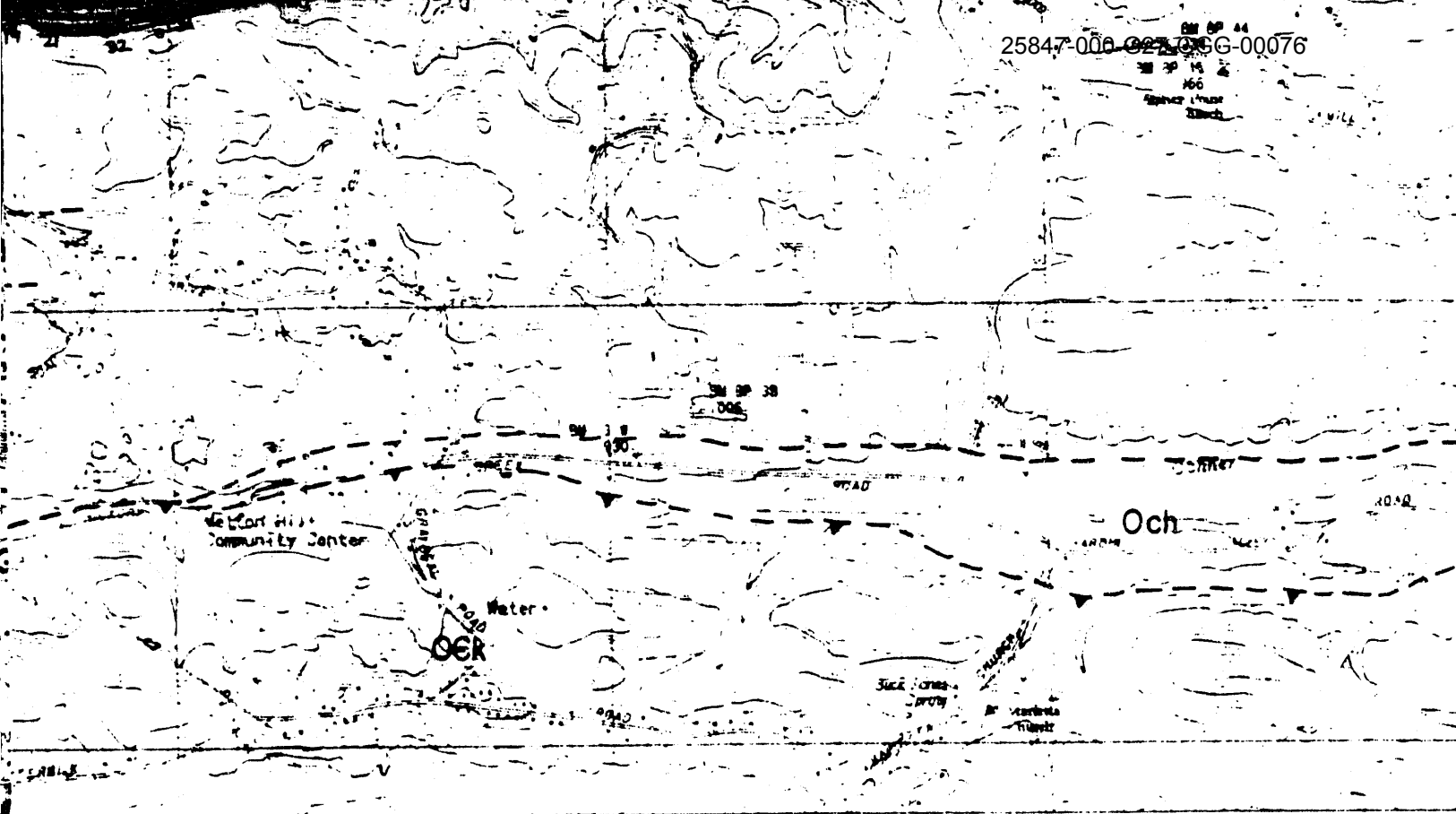
SCALE 1:24,000



CONTOUR INTERVAL
NATIONAL GEODETIC VERTICAL

compilation checked by:
Robert D. Hatcher, Jr.

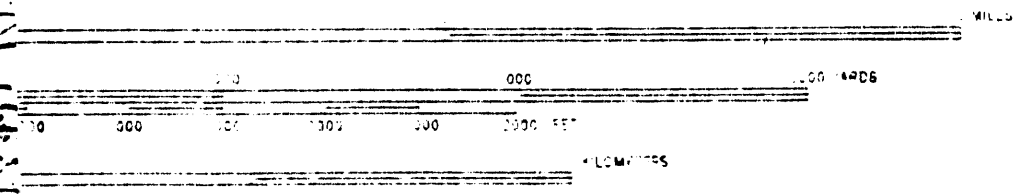
25847-000-027-05G-00076



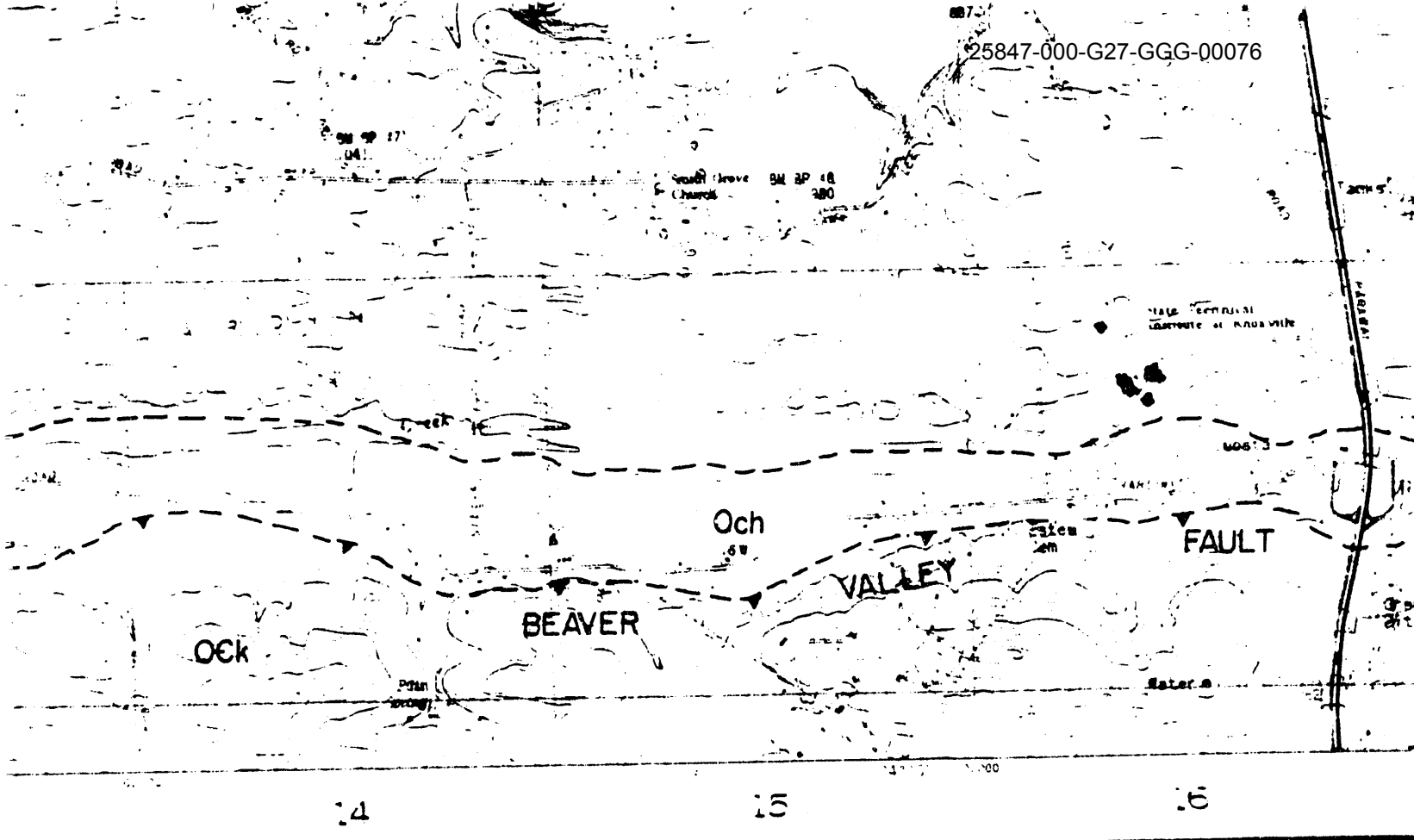
35° 54' 11 12 13

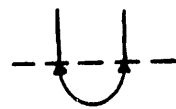
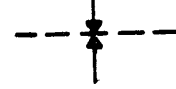
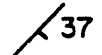
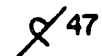
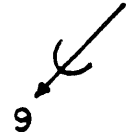
AREA

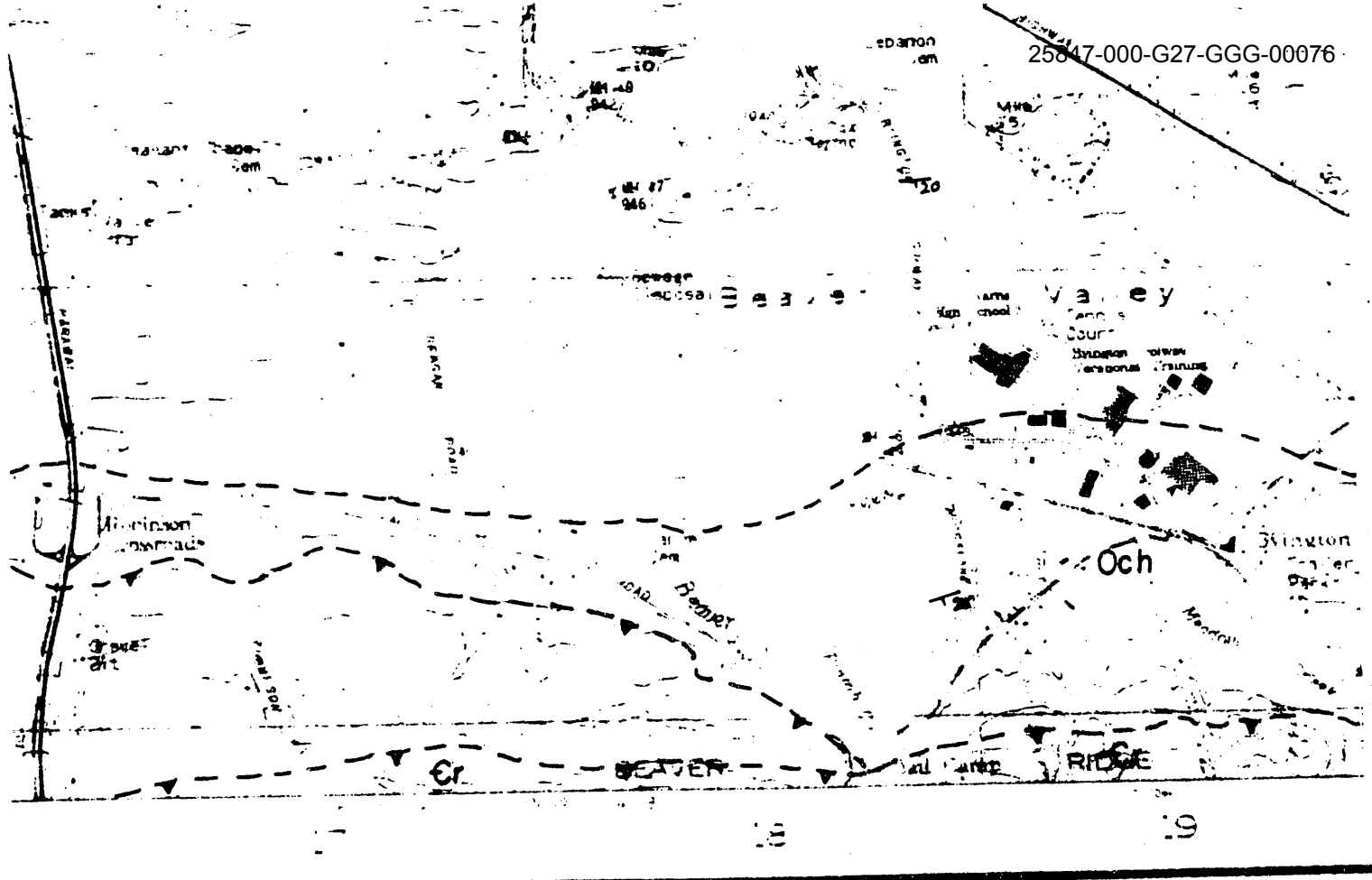
ESSEE



FEET
TLM IF 329



- 
 Lithologic Contact; exact (solid), approxin
- 
 Thrust fault, teeth on hanging wall; exact inferred (dotted).
- 
 Overturned Syncline: Trace of axial surfc
- 
 Syncline: Trace of axial surface
- 
 Strike and dip of bedding
- 
 Strike and dip of overturned bedding
- 
 Strike and dip of cleavage
- 
 Trend and plunge of mesoscopic fold ax



S-16A
NOVEMBER 1967

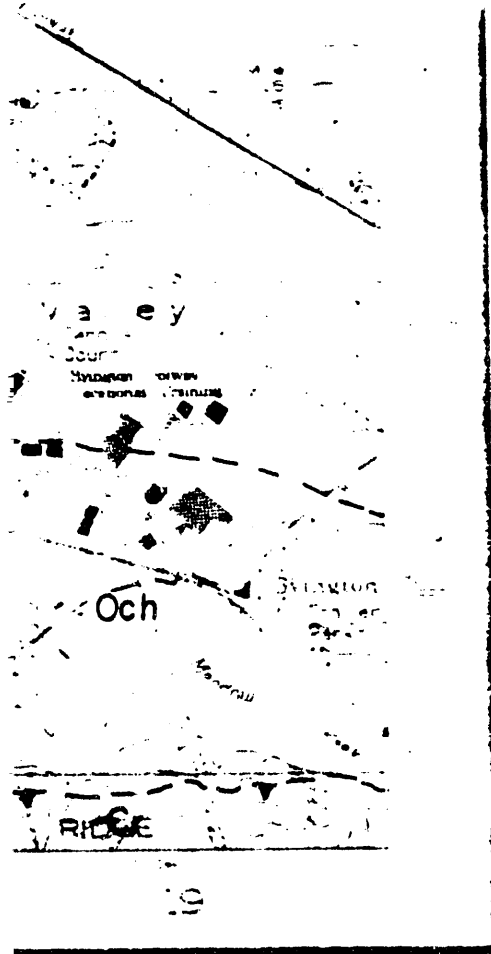
approximate (dashed), inferred (dotted).

II; exact (solid), approximate (dashed),

ial surface

iding

o fold axis



S-16A
 1954

Upper
 Cambrian

€cr
 25847-000-G27-GGG-00076
 Copper Ridge Dolomite

CONASAUGA
 GROUP

€c

undivided

Upper
 Cambrian

€mn

Maynardville Ls.

€n

Nolichucky Shale

€dg

Dismal Gap Fm.
 (Provisional name,
 Formerly Maryville Ls.)

Middle
 Cambrian

€rg

Rogersville Shale

€f

Friendship Fm.
 (Provisional name,
 Formerly Rutledge Ls.)

€pv

Pumpkin Valley Shale

Lower
 Cambrian

€r

Rome Fm.

END

**DATE
FILMED**

6 / 15 / 93

